ISSN 1007-9327 (print)
ISSN 2219-2840 (online)

World Journal of *Gastroenterology*

World J Gastroenterol 2020 July 7; 26(25): 3517-3711

Published by Baishideng Publishing Group Inc

World Journal of Gastroenterology

Contents

Weekly Volume 26 Number 25 July 7, 2020

ABOUT COVER

Editorial board member of *World Journal of Gastroenterology*, Prof. Antonio Biondi is an Associate Editor of *Updates in Surgery*, the official journal of the Italian Society of Surgery, and a Full Professor of surgery at the School of Medicine, University of Catania, Italy. Prof. Biondi obtained his MD degree from the University of Catania in 1993, and his PhD degree in 2001. He was promoted to Full Professor in the School of Medicine, University of Catania, in 2018. His ongoing research interests are colorectal surgery and laparoscopic procedures. He is a member of the editorial boards and a reviewer of several scientific journals, and has published more than 150 peer-reviewed articles. Prof. Biondi served as elected member of the Italian National University Council (CUN). Currently, he is the Chief of the Laparoscopic Surgery Division, Department of General Surgery and Medical-Surgical Specialties, University Hospital Policlinico Vittorio Emanuele, Catania and Director of the Multidisciplinary Research Center for Diagnosis and Treatment of Rare Diseases, University of Catania.

AIMS AND SCOPE

The primary aim of *World Journal of Gastroenterology* (*WJG*, *World J Gastroenterol*) is to provide scholars and readers from various fields of gastroenterology and hepatology with a platform to publish high-quality basic and clinical research articles and communicate their research findings online. *WJG* mainly publishes articles reporting research results and findings obtained in the field of gastroenterology and hepatology and covering a wide range of topics including gastroenterology, hepatology, gastrointestinal endoscopy, gastrointestinal surgery, gastrointestinal oncology, and pediatric gastroenterology.

INDEXING/ABSTRACTING

The *WJG* is now indexed in Current Contents®/Clinical Medicine, Science Citation Index Expanded (also known as SciSearch®), Journal Citation Reports®, Index Medicus, MEDLINE, PubMed, PubMed Central, and Scopus. The 2020 edition of Journal Citation Report® cites the 2019 impact factor for *WJG* as 3.665 (5-year impact factor: 4.048), ranking *WJG* as 35 among 88 journals in gastroenterology and hepatology (quartile in category Q2).

RESPONSIBLE EDITORS FOR THIS ISSUE

NAME OF JOURNAL
World Journal of Gastroenterology

ISSN
ISSN 1007-9327 (print) ISSN 2219-2840 (online)

LAUNCH DATE
October 1, 1995

FREQUENCY
Weekly

EDITORS-IN-CHIEF
Andrzej S Tarnawski, Subrata Ghosh

EDITORIAL BOARD MEMBERS
http://www.wjgnet.com/1007-9327/editorialboard.htm

PUBLICATION DATE
July 7, 2020

INSTRUCTIONS TO AUTHORS
https://www.wjgnet.com/bpg/gerinfo/204

GUIDELINES FOR ETHICS DOCUMENTS
https://www.wjgnet.com/bpg/GerInfo/287

GUIDELINES FOR NON-NATIVE SPEAKERS OF ENGLISH
https://www.wjgnet.com/bpg/gerinfo/240

PUBLICATION ETHICS
https://www.wjgnet.com/bpg/GerInfo/288

PUBLICATION MISCONDUCT
https://www.wjgnet.com/bpg/gerinfo/208

ARTICLE PROCESSING CHARGE
https://www.wjgnet.com/bpg/gerinfo/242

STEPS FOR SUBMITTING MANUSCRIPTS
https://www.wjgnet.com/bpg/GerInfo/239

ONLINE SUBMISSION
https://www.f6publishing.com

E-mail: bpgoffice@wjgnet.com https://www.wjgnet.com

World Journal of Gastroenterology

Submit a Manuscript: https://www.f6publishing.com

World J Gastroenterol 2020 July 7; 26(25): 3517-3527

DOI: 10.3748/wjg.v26.i25.3517

ISSN 1007-9327 (print) ISSN 2219-2840 (online)

GUIDELINES

Chinese expert consensus and practice guideline of totally implantable access port for digestive tract carcinomas

Ke-Cheng Zhang, Lin Chen, Chinese Research Hospital Association Digestive Tumor Committee; Chinese Association of Upper Gastrointestinal Surgeons; Chinese Gastric Cancer Association and Gastrointestinal Surgical Group of Chinese Surgical Society Affiliated to the Chinese Medical Association

ORCID number: Ke-Cheng Zhang 0000-0002-9257-5607; Lin Chen 0000-0002-3507-673X.

Author contributions: Zhang KC designed the study, drafted the article; Chen L conceived and designed the study, and provided critical revision; both authors approved the final version to be published.

Supported by Program of B. Braun Medical, No. CN-0486-AEC-VSE2019169; and Program of Military Medicine for Youth, No. QNF19055.

Conflict-of-interest statement: There is no conflict of interest associated with publication of this manuscript.

Ke-Cheng Zhang, Lin Chen, Department of General Surgery & Institute of General Surgery, The First Medical Centre, Chinese People's Liberation Army General Hospital, Beijing 100853, China

Corresponding author: Lin Chen, MD, PhD, Professor, Chief, Department of General Surgery & Institute of General Surgery, The First Medical Centre, Chinese People's Liberation Army General Hospital, No. 28, Fuxing Road, Beijing 100853, China. chenlin@301hospital.com.cn

Abstract

Totally implantable access port is a fully implantable drug delivery system that is implanted subcutaneously and can be retained for a long time. Advantages of ports include a simple nursing process, low risk of infection and embolism, and high patient comfort. In order to promote the standardized application of ports in the treatment of digestive tract tumors and reduce port-related complications, the Chinese Research Hospital Association Digestive Tumor Committee, the Chinese Association of Upper Gastrointestinal Surgeons, the Chinese Gastric Cancer Association, and the Gastrointestinal Surgical Group of Chinese Surgical Society Affiliated to Chinese Medical Association have organized multidisciplinary expert discussions at the General Hospital of the People's Liberation Army and nation-wide expert letter reviews and on-site seminars, and formulated an expert consensus of the operation guidelines.

Key words: Totally implantable access port; Digestive tract tumor; Consensus and guideline; Venous port; Peritoneal port; Arterial port

Core tip: Totally implantable access port is a fully implantable drug delivery system that is implanted subcutaneously and can be retained for a long time. Advantages of ports include a simple nursing process, low risk of infection and embolism, and high patient comfort. Currently no practice guideline is available. In order to reduce port-related complications, the Chinese Research Hospital Association Digestive Tumor Committee, the Chinese Association of Upper Gastrointestinal Surgeons, the Chinese Gastric Cancer Association,

Manuscript source: Invited manuscript

Received: March 3, 2020
Peer-review started: March 3, 2020
First decision: April 25, 2020
Revised: April 27, 2020
Accepted: June 10, 2020
Article in press: June 10, 2020
Published online: July 7, 2020

P-Reviewer: Muguruma N
S-Editor: Ma RY
L-Editor: MedE-Ma JY
E-Editor: Ma YJ

and the Gastrointestinal Surgical Group of Chinese Surgical Society Affiliated to Chinese Medical Association have, for the first time, organized multidisciplinary expert discussions at the General Hospital of the People's Liberation Army and nation-wide expert letter reviews and on-site seminars, and formulated the present expert consensus of the operation guidelines.

Citation: Zhang KC, Chen L, Chinese Research Hospital Association Digestive Tumor Committee; Chinese Association of Upper Gastrointestinal Surgeons; Chinese Gastric Cancer Association and Gastrointestinal Surgical Group of Chinese Surgical Society Affiliated to the Chinese Medical Association. Chinese expert consensus and practice guideline of totally implantable access port for digestive tract carcinomas. *World J Gastroenterol* 2020; 26(25): 3517-3527
URL: https://www.wjgnet.com/1007-9327/full/v26/i25/3517.htm
DOI: https://dx.doi.org/10.3748/wjg.v26.i25.3517

INTRODUCTION

Totally implantable access port is a fully implantable drug delivery system that is implanted subcutaneously and can be retained for a long time. It can be used for the infusion of various liquids, including chemotherapy drugs, parenteral nutrient solutions, and blood products. Some advantages of ports include a simple nursing process, low risk of infection and embolism, and high patient comfort. According to the infusion route, types of ports include venous[1], peritoneal[2], arterial[3] and intrathecal[4]. Venous access ports are widely used clinically. Therapies, such as chemotherapy and nutritional support, are often needed during the treatment of digestive tract tumors and require a reliable infusion channel. Ports are handled by various clinical personnel[5], and the standard operation needs to be improved. In order to promote the standardized application of ports in the treatment of digestive tract tumors and reduce port-related complications, the Chinese Research Hospital Association Digestive Tumor Committee, the Chinese Association of Upper Gastrointestinal Surgeons, the Chinese Gastric Cancer Association, and the Gastrointestinal Surgical Group of Chinese Surgical Society Affiliated to Chinese Medical Association have successively organized multidisciplinary expert discussions at the General Hospital of the People's Liberation Army and nation-wide expert letter reviews and on-site seminars, and reached an expert consensus of the operation guidelines. The clinical questions included in this expert consensus were taken from the controversial points in the letter review by multidisciplinary experts. Corresponding suggestions are recommended based on the quality of the evidence using the evidence-based Grading of Recommendations, Assessment, Development and Evaluations (GRADE) system[6]. The operation guidelines introduces the venous, peritoneal, and arterial implantation methods as there is a great deal of evidence supporting the use of these methods.

CLINICAL QUESTIONS

Types and selection of port

The main components of a port include the portal and the catheter. There are single-chamber and double-chamber portals[7], with various sizes. Single-chamber ports are used more often clinically[8]. Ports with the smallest number of chamber(s) that can meet the needs of the patient should be selected to reduce the risk of infection[9]. Double-chamber ports can be used for simultaneous infusion of chemotherapy drugs and parenteral nutrient solution[10]. Although some studies support that double-chamber ports do not increase the incidence of sepsis[11], the compatibility of different infusion fluids should be considered during application.

Port catheters are made of two different materials, silica gel and polyurethane, which are considered equally safe. However, silica gel catheters can easily be blocked, and polyurethane catheters can cause venous thrombosis[12,13]. Catheter ends with open and valvular designs are available. Compared with an open-end catheter, a valvular-end catheter can prevent blood from flowing back into the catheter lumen and does

not require heparin washing, but a valvular-end catheter cannot be used to draw blood samples. A prospective randomized controlled study showed that the short-term and long-term complications caused by the two catheters were comparable[14]. Drug-coated catheters can significantly reduce the risk of blood infections[15,16], but there is no evidence of their application in ports.

Recommendation: Single-chamber ports are preferred to reduce the risk of drug interactions that may occur when a double-chamber port infuses liquids simultaneously. Silica gel and polyurethane catheters are safe when used for long-term central venous infusion. (Level of evidence: Medium; degree of recom-mendation: Strong; expert approval rate: 100%).

Implantation modes and routes of venous port

In 1982, Niederhuber *et al*[17] completed the first case of port implantation through the cephalic vein by surgical incision. In 1992, Morris *et al*[18] reported an ultrasound-guided percutaneous port implantation. Presently, the percutaneous puncture route is more commonly applied in clinical practice. The results of a systematic review show that the complications of the percutaneous puncture route are comparable to those after surgical incision, but the success rate of the percutaneous puncture route is higher[19]. The internal jugular vein, subclavian vein, basilic vein, and femoral vein can be selected for the percutaneous puncture route, and the literature reports that the internal jugular vein and subclavian vein are used most often[5]. The selection of the puncture vein should take into account patient-related specific factors (such as whether there is positive pressure ventilation or anatomical dysplasia), relative risks of complications during the operation (hemorrhage, pneumothorax, and thrombosis), and risk of infection. For experienced operators, there is no difference in postoperative complications or patient quality of life between different vein approaches for port implantation[20,21]. A randomized controlled study has confirmed that there are no differences in the incidence of catheter-related thrombotic events or catheter blockage between left-side and right-side port implantation[22]. Percutaneous puncture methods include blind puncture based on anatomical landmarks, real-time ultrasound guidance and venography, and the ultrasound-guided real-time method, which is currently the most common[23]. Research has shown that ultrasound real-time guidance can improve puncture efficiency and reduce venous catheter-related infections[24].

Recommendation: The port is recommended to be implanted through a percutaneous puncture of the internal jugular vein or subclavian vein using real-time ultrasound guidance. (Level of evidence: High; degree of recommendation: Strong; expert approval rate: 96%).

Catheter tip position of the venous port

The position of catheter tip is very important for preventing complications and maintaining a smooth infusion. Data shows that the catheter tip position is an independent risk factor for venous thrombosis[25]. Catheter thrombosis can affect the patency of the infusion. When the catheter tip is located at the lower 1/3 of the superior vena cava, the incidence of venous thrombosis and abnormal catheter patency is the lowest[26]. Positioning the catheter parallel to the vessel wall helps to reduce the risk of catheter movement and the damage to the vessel wall. The position of the catheter tip can be confirmed by intraoperative fluoroscopy and postoperative chest radiograph. A study showed that intracardiac electrocardiogram technology can also accurately and conveniently confirm the position of the catheter tip[27].

Recommendation: The catheter tip is recommended to be placed at the lower 1/3 of the superior vena cava, and the location be confirmed by a postoperative chest radiograph. (Level of evidence: Medium; degree of recommendation: Strong; expert approval rate: 100%).

Timing of the first medication through the venous port

The time interval between the port implantation and first medication may be a risk factor for the occurrence of port-related infections[28]. The results of a prospective cohort study showed that when the intervals between the catheter implantation and first medication were 0-3 d, 4-7 d, and > 7 d, the total incidence rates of complications were 24.4%, 17.1%, and 12.1%, respectively, and the incidence rates of infections were 10.6%, 6.7%, and 2.0%, respectively[29]. The results of a single-center prospective study of 4045 cases also showed that a time interval between port implantation and first medication of > 6 d could significantly reduce the risk of complications and catheter removal rates[30]. However, scholars in China have not found any correlation between the timing of the first medication and complications.

Recommendation: In clinical practice, the timing of first medication should be considered and the first medication should be reasonable according to the regulations of each center. (Level of evidence: Medium; degree of recommendation: Strong; expert approval rate: 94%).

Prophylactic antibiotic use for venous port

The results of a prospective randomized controlled study showed that the prophylactic use of antibiotics did not reduce the postoperative infection complications[31]. Recently, the results of systematic review showed that 5 (1.39%) out of 360 patients receiving prophylactic antibiotics experienced an infection, while 22 (1.23%) out of 1794 patients who did not receive an antibiotic experienced an infection; there were no statistical differences between the two groups. This indicates that prophylactic antibiotics had no effect on postoperative infection complications[32]. Currently, relevant guidelines do not recommend the routine prophylactic use of antibiotics before or during port implantation[33]. Unnecessary use of antibiotics increases the risk of anaphylaxis, leads to the growth of drug-resistant microorganisms, and increases medical expenses[32].

Recommendation: Routine prophylactic use of antibiotics is not recommended. (Level of evidence: High; degree of recommendation: Strong; expert approval rate: 92%).

Flushing and sealing of the venous port

Long-term indwelling catheters can easily be blocked by protein biological films generated by a cross-linking reaction between the biological proteins and the catheter. Flushing and sealing are effective measures to prevent these complications, but the specific protocols vary greatly[34]. To reduce the adhesion of injected substances on the inner surface of the catheter, it is generally recommended to flush the catheter with normal saline, infuse the drug, and flush the catheter with normal saline again[35]. The results of randomized controlled studies confirmed that flushing and sealing the catheter with normal saline is not inferior to using heparin[36,37]. A Cochrane systematic review also does not support any advantage of heparin in reducing catheter blockage[38]. During the non-treatment period, a valvular catheter can be sealed with 10 mL normal saline every 4 wk and an open catheter can be sealed with 10 mL normal saline or 5 mL (100 U/mL) heparin every 4 wk[39,40].

Recommendation: Under normal circumstances, the catheter can be flushed and sealed with normal saline. For maintenance, during the non-treatment period a valvular catheter can be sealed with normal saline every 4 wk and an open catheter can be sealed with normal saline or heparin (100 U/mL) every 4 wk. (Level of evidence: High; degree of recommendation: Strong; expert approval rate: 98%).

Prevention of port-related infections

Port-related infections are caused by various factors. Standardized evidence-based strategies can significantly reduce catheter-related infections[41]. These measures include (operator) hand hygiene, skin disinfection, selection of optimal vascular access, and timely assessment of the necessity of catheter retention. It is not recommended to apply antibacterial ointment to the wound during port implantation[9]. There is no evidence to support the reduction of infections by routine antibiotic catheter sealing, but it is recommended for patients with a history of multiple catheter-related blood infections[42,43]. It is particularly important to provide the necessary training and education for catheter implantation operators and maintenance personnel[44].

Recommendation: The operation and maintenance of the port should be carried out by medical personnel trained on professional standards, and standardized measures should be adopted to prevent port-related infections. (Level of evidence: Medium; degree of recommendation: Strong; expert approval rate: 100%).

PRACTICE GUIDELINES

Indications and contraindications

Indications for a venous port: (1) Long-term repeated infusion of corrosive and/or irritating drugs; (2) Long-term parenteral nutrition support is needed; (3) Long-term intermittent infusion and the transfusion of blood products is required; (4) It is difficult to establish peripheral venous access; (5) Frequent blood collection and

monitoring are required; and (6) Contrast agent bolus injection (high pressure-resistant). Indications for a peritoneal port: Peritoneal metastasis requiring intraperitoneal perfusion chemotherapy[45]. Indications for an arterial port: Hepatic metastasis requiring hepatic artery perfusion chemotherapy[46]. Contraindications: (1) Patients with a massive pleural effusion who cannot tolerate and/or cooperate with surgery; (2) Uncontrolled bacteremia or local infection at the operation site (confirmed or suspected local infection by puncture, bacteremia or symptoms of septicemia); (3) Confirmed or suspected allergies to port materials; (4) Abnormal venous return, such as vena cava compression syndrome; (5) Obvious coagulation dysfunction; (6) No suitable implantable port size for the patient's physique and/or body shape; (7) Severe pulmonary embolism; (8) Those who have received radiotherapy at the site to be punctured; (9) Signs of thrombosis at the site to be used for the catheter insertion or the patient has undergone a surgery; and (10) The puncture site is located on the same side as the only remaining normal lung tissue (there is a risk of fatal pneumothorax).

Preoperative assessment and preparation

Before the port implantation, the patient needs to be evaluated in detail, including the medical history and physical, laboratory, and imaging examinations. The medical history inquiry should include the history of radiotherapy and chemotherapy, the history of central vein catheterization, relevant operation history of the proposed port implantation site, and history of anticoagulant and anti-angiogenic medication use. The physical examination should include an assessment of the anatomy of the proposed portal placement site to assure that it is abnormal and subcutaneous fat thickness/skin condition is acceptable. Laboratory examinations should include routine blood test, immunity and coagulation function. Imaging examinations should include electrocardiogram, erect chest radiograph, and B-mode ultrasonography of the proposed puncture site. The preset catheter insertion length should be estimated according to the chest radiograph.

During preparation for the port implantation operation, it is necessary to communicate with the patients and their family members to inform them of the risks related to the operation, the operation methods and process, as well as matters needing attention after the operation. The informed consent form should be signed and volume expansion should be performed fully before the operation. It is also recommended to take a shower the day before the operation.

Port implantation operation

Implantation should be completed in an operating room that meets aseptic requirements. Before operation, the integrity and patency of the port kit should be checked.

Venous port implantation: Internal jugular vein approach (Figure 1): The patient lies in the supine position with the head turned to the opposite side, exposing the operation area on the neck. The operation plane should be flat and the muscles relaxed. The operator stands on the cranial side of the patient, the B-mode ultrasonography machine is placed on the left side of the patient, and the assistants and console are on the right side of the patient. B-mode ultrasonography is used to probe and locate the internal jugular vein, and to determine the relationship between the carotid arteries and veins and the puncture point. The puncture point, subcutaneous tunnel course, and port pocket position are marked. The skin is disinfected with the collarbone as the center. The disinfection scope includes an area with the upper margin to the level of the ear roots and mandible, the lower margin to the connection line of the bilateral nipples, the margin on the operating side to the posterior axillary line, and the margin on the contralateral side to the clavicle midline. Routine draping is performed. Infiltration with 1% lidocaine is applied for a local anesthesia on the operating region. A small incision of 0.5 cm is made at the puncture site. The puncture needle is guided into the venous lumen layer by layer by holding a B-mode ultrasonography probe, and the needle tip with strong echo light spot in the venous center can be seen after the successful puncture. Blood is drawn to confirm again that the needle tip is in the blood vessel. The guide wire is inserted and slowly fed in by 10-15 cm through the puncture needle. The guide wire is confirmed to enter the superior vena cava by B-mode ultrasonography or fluoroscopy. The peel-away sheath is introduced along the guide wire, and the catheter is introduced through the sheath. The peel-away sheath is sent to the lower 1/3 of the superior vena cava according to the predicted length. Then, the peel-away sheath is removed, blood is drawn to confirm the catheter position, and the rear end of the catheter is clamped. A cutaneous incision is made 2-3 cm below the 1/3 clavicle on the same side. The

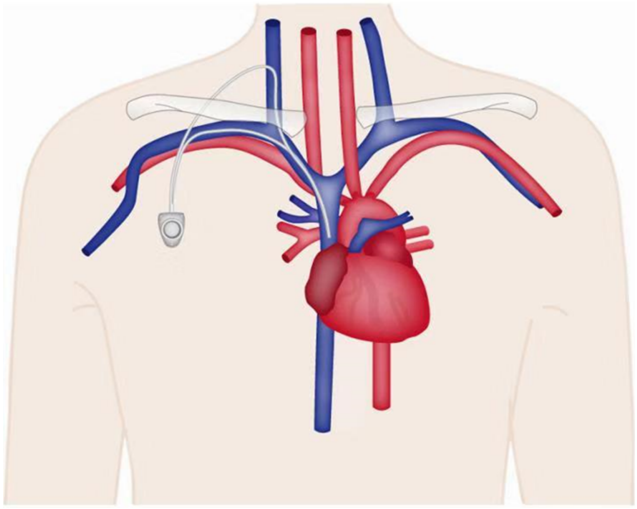

Figure 1 A schematic diagram for venous port implantation.

incision is about 2-3 cm long. A blunt dissection is performed to reach the subcutaneous tissue. A port pocket with a depth of 0.5-1.0 cm is made according to the size of the portal. The upper edge of the portal body is about 1 cm away from the surgical incision site to prevent the atraumatic needle from puncturing on the incision. The tip of the tunneling needle is pushed from the puncture point to the incision of the port pocket to form a subcutaneous tunnel, and the catheter is slowly pulled through the subcutaneous tunnel. The catheter is trimmed to a suitable length and ensured that the trimming edge is flat. The catheter is connected to the portal. The portal is placed into the port pocket and the course and radian of the catheter are adjusted on the neck and in the subcutaneous tunnel to avoid corner folding. A 2-0 non-absorbable suture is used to fix the portal and the surrounding tissues, and suture the neck and port pocket incision, and finally the wound is bound with dressing.

Subclavian vein approach: The patient lies in a supine position with the neck and shoulders elevated with a pad, the head tilted back and turned to the opposite side. The implantation process is roughly the same as that of the internal jugular vein approach, with the following differences: The puncture point is 1-2 cm below the mid-point of the clavicle. The position of the port pocket can be selected by a transverse incision at the needle insertion point without the establishment of a tunnel. The port pocket can also be placed in other positions using tunneling technology. During the puncture, the puncture needle faces the sternoclavicular joint or suprasternal fossa. The insertion angle is horizontal, and the needle is withdrawn while being inserted. Generally, the needle is inserted about 3-4 cm. After blood is seen upon withdrawal, the needle is inserted 1-2 mm further to ensure that the needle tip completely entered the blood vessel. The needle end is fixed, the syringe is disconnected, and the guide wire is sent to the superior vena cava. The other steps are the same as in internal jugular vein implantation.

Peritoneal port implantation: A peritoneal port can be implanted by open surgery, laparoscopy, or ultrasound-guided percutaneous implantation (Figure 2). It is recommended to implant the peritoneal port *via* laparoscope because of its minimal invasiveness, ability to probe the peritoneal cavity to evaluate the lesions, and ability to separate peritoneal adhesions. Under general anesthesia, routine disinfection and draping are performed. Pneumoperitoneum is established through a transumbilical puncture, and the lens are placed in a 10-mm puncture hole. The peritoneal cavity is explored and a 12-mm hole is established to separate peritoneal adhesions if necessary. The catheter is implanted by a method similar to the venous puncture, and the puncture point 5-6 cm laterally of the umbilicus is selected. Under the direct vision of laparoscope, the puncture needle is guided into the peritoneal cavity, the guide wire is introduced, and the puncture needle is removed. The peel-away sheath is fed in along the guide wire and then the guide wire is withdrawn. The catheter is introduced through the sheath. At least 10 cm of the catheter should remain in the peritoneal cavity. Then, the peel-away sheath is removed. The port pocket can be placed near the anterior superior iliac spine on the same side as the puncture point or 2 cm below the costal margin of the medial clavicle on the same side (bony structure support). A

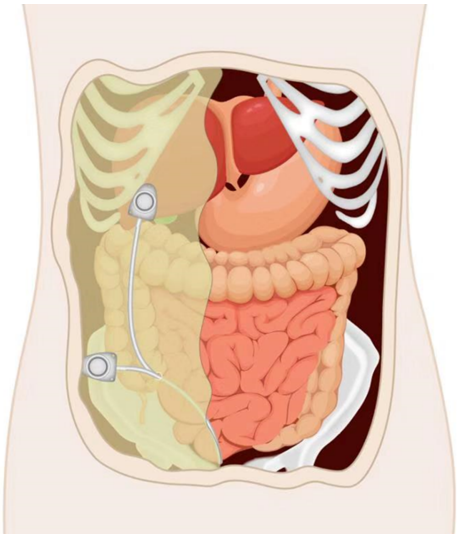

Figure 2 A schematic diagram for peritoneal port.

longitudinal incision of about 3 cm is made near the anterior superior iliac spine and a transverse incision of about 3 cm is made below the costal margin. A tunneling needle is used to establish a subcutaneous tunnel from the puncture point to the port pocket, and the catheter is guided to the port pocket. The catheter is adjusted to the rectovesical or rectouterine pouch in the pelvic cavity via laparoscope. The catheter is trimmed to a suitable length, connected with the portal, and the patency is checked with an atraumatic needle. The edge of the portal is adjusted to about 1 cm away from the incision and the edge of the portal is fixed with a non-absorbable suture. The incision is sutured and the wound is bound with dressing.

Arterial port implantation: An arterial port can be implanted through the left subclavian or the right femoral artery. However, the right femoral artery approach is preferred. In the supine position, the skin on the groin and perineum is prepared, disinfected, draped, and 1% lidocaine is used for local anesthesia. The modified Seldinger method is used to puncture the right femoral artery and insert the appropriate guide wire and catheter. Using the catheter guide wire technology, the catheter is selectively inserted into the celiac trunk for angiography to determine the tumor location, size, and number of arteries that supply blood to the tumor. The catheter is super-selectively inserted into the artery that supplies blood to the tumor, the guide wire is replaced as appropriate along the catheter, the catheter is withdrawn, the guide wire is retained, the port catheter is fed in along the guide wire until reaching the target blood vessel, and the guide wire is slowly withdrawn. The port catheter is fed in along the super-smooth guide wire and then the guide wire is slowly withdrawn. A cavity for the port pocket is created by an incision at the peritoneal wall of the iliac fossa in the superior lateral direction of the puncture point. The catheter is guided to the port pocket cavity by a tunneling needle. The catheter is intercepted at a proper length and connected to the portal interface filled with heparin saline. The portal is embedded in the port pocket. The skin and subcutaneous tissue at the site of the port pocket are sutured layer by layer, and the wound is bound up with local pressure. The lower limb on the puncture side is straightened and strictly immobilized for 12 h.

Prevention of complications

Complications related to the implantation operation: Common complications during port implantation include pneumothorax, hemothorax, arterial injuries, thoracic duct injuries, hematoma, air embolisms, intestinal tract injuries, brachial plexus injuries, arrhythmias, and catheter insertion failure. The keys to prevention and management include: (1) Port implantation should be completed by or under the guidance of trained personnel; (2) The puncture should be guided by an ultrasound or digital subtraction angiography. For blind access without image guidance, the puncture should first be attempted with a fine needle to confirm the direction and depth of the needle insertion; (3) The puncture vessel should remain in a positive-pressure state, *e.g.*, by keeping the head lowered and the feet elevated. Patients should be instructed

to hold their breath and cooperate during the process of transporting the catheter through the sheath. At the same time, care should be taken to prevent the puncture needle and the opening of the peel-away sheath from being exposed to the air. Using a peel-away sheath with a one-way valve can also effectively prevent air embolism; (4) To prevent the catheter from entering too far into the atrium, intraoperative fluoroscopy or a real-time electrocardiogram can be used to accurately evaluate the catheter tip position; and (5) During peritoneal port implantation, the puncture should be performed with a curved puncture needle under the direct vision of the lens to avoid injuring the intestinal tract.

Portal related complications: Complications related to the portal include incision wound dehiscence, inversion of the portal, drug extravasation, port pocket hematoma, and infection. The keys to prevention and management include: (1) When the patient is malnourished or the possibility of cachexia is predicted, the portal can be implanted deeper to reduce the tension at the skin incision. Anti-angiogenic drugs should be avoided before the operation[47] and patients should be educated to avoid strenuous exercises that can increase wound tension after the operation; (2) The port pocket site should be selected as a location receiving relatively little traction from movements and the size should be matched with the portal, which should be sutured and fixed after being placed in the port pocket; (3) An atraumatic needle which is replaced every 7 d should be used to prevent the septum of the portal from being damaged. For peritoneal port implantation, a reinforced suture should be performed, or a catheter cuff should be used for the incision from which the catheter enters the peritoneal cavity. During intraperitoneal chemotherapy, the patient should adopt the supine position to reduce the risk of atraumatic needle prolapse; and (4) When creating the port pocket, bleeding should be minimized by dissection according to the anatomical layers, and the bleeding in the surgical field of view should be stopped completely. Care bundles should be used to prevent infections.

Catheter-related complications: Catheter-related complications include catheter displacement, thrombosis, pinch-off syndrome, breakage/fracture/detachment, deep vein thrombosis, fibrin sheath formation, superior vena cava erosion, and perforation. The prevention and management measures include: (1) Regular X-ray examinations should be performed for patients with a chronic cough or frequent movement of the limbs to eliminate the risk of catheter displacement; (2) The routine use of anticoagulant drugs is not recommended, but the prophylactic use of anticoagulants can be considered for tumor patients with a high risk of thrombosis and low risk of hemorrhage; the catheter flushing and sealing should be standardized to reduce the risk of thrombosis; (3) For a subclavian vein puncture, the lateral 1/3 of the clavicle should be selected as the puncture point to avoid an included angle between the clavicle and the first rib; and (4) Special care should be taken to ensure that the lock connection and catheter are not folded back during operation. If the patient suffers from pain and swelling around the catheter during the infusion, the infusion should be stopped immediately and an X-ray examination should be conducted to identify abnormalities such as catheter breakages as soon as possible. Patients should be instructed to avoid overstretching the catheter indwelling area during daily activities.

Port removal

Most ports can perform their functions without complications, but if complications occur at the initial stage of implantation, it may be necessary to remove the device immediately and attempt to implant a new one during the removal operation. Most complications can be treated without removal, but sometimes removal is the only reasonable choice. The overall removal rate due to complications is 5.5%-18%. Most port-related complications occur after the first chemotherapy session. Common reasons for removal include: (1) Infections: Infections around the portal pocket and along the catheter tunnel can generally be treated with reasonably selected antibiotics, while bacteremia is an indication for port removal; (2) Thrombosis: Thrombosis is the second major cause of port removal; removal can be considered if anticoagulation is ineffective and thrombosis complicated with persistent infection is an absolute indication for port removal; (3) Catheter displacement: There are two path-ophysiological types of catheter displacement. One is the pinch-off sign on a chest radiograph, which indicates that the catheter leakage site is between the first rib and the collarbone; the other type occurs in obese patients when the catheter tip migrates to the periphery due to tissue traction in the upright position; (4) Catheter fragments and embolisms caused by catheter fractures: Detached fragments can be taken out through the femoral vein; the port does not need to be removed if there are no

additional complications; and (5) Skin corrosion on the port surface: This is very rare. It is recommended to ensure that the skin thickness on the surface is 0.5-1 cm when implanting the port. When the port is removed, the catheter tunnel should be closed immediately to avoid an air embolism.

Patient education

Health education for patients can reduce the risk of port-related complications. The specific recommendations include: (1) After the wound heals, patients can take showers or do low-intensity exercise such as walking, while strenuous exercises such as pull-ups should be avoided; (2) After the operation, if symptoms such as chest pain, abdominal discomfort, and fever and chills of an unknown cause occur, medical attention should be sought immediately; (3) Avoid local friction with clothes, bra straps, and knapsack shoulder straps to prevent skin rupture. Patients should go to the hospital every 4 wk for professional port maintenance; (4) During CT or MRI examinations, a contrast agent cannot be injected under high pressure unless a high pressure-resistant port is implanted; and (5) Keep the port maintenance manual.

ACKNOWLEDGEMENTS

We would like to thank the following participants in this study: Xinyu Qin, Yihong Sun, Fenglin Liu, Zhongshan Hospital, Fudan University; Shan Wang, Yinjiang Ye, Kewei Jiang, Peking University People's Hospital; Jiafu Ji, Xiangqian Su, Ziyu Li, Peking University Cancer Hospital & Institute, Beijing, China; Huimian Xu, Zhenning Wang, the First Affiliated Hospital of China Medical University; Zhenggang Zhu, Minhua Zheng, Min Yan, Lu Zang, Shanghai Institute of Digestive Surgery, Shanghai Key Laboratory of Gastric Neoplasm, Ruijing Hospital, Shanghai Jiao Tong University School of Medicine; Xuming Bai, the Second Affiliated Hospital of Soochow University; Hui Cao, Gang Zhao, Renji Hospital; Huanqiu Chen, Jiangsu Province Tumor Hospital; Luchuan Chen, Fujian Cancer Hospital; Xiangdong Chen, the First Affiliated Hospital Zhejiang Chinese Medicine University; Pan Chi, Union Hospital Affiliated to Fujian Medical University; Guanghai Dai, Bo Wei, Jiandong Wang, Zhi Qiao, Niansong Qian, Fengyong Liu, Chaojun Zhang, Chinese PLA General Hospital; Xueyi Dang, Zefeng Gao, Shanxi Provincial Tumor Hospital; Jianhong Dong, Affiliated Tumor Hospital of Shanxi Medical University; Ming Dong, the First Hospital of China Medical University; Fanghai Han, Sun Yat-sen Memorial Hospital; Xianli He, Tangdu Hospital; Yulong He, the First Affiliated Hospital, Sun Yat-sen University; Jiankun Hu, West China Hospital; Hua Huang, Shanghai Cancer Center, Fudan University; Gang Ji, Xijing Hospital; Zhigang Jie, the First Affiliated Hospital of Nanchang Hospital; Leping Li, Changqing Jing, Shandong Provincial Hospital; Guoli Li, Nanjing Medical University; Guoxin Li, Nanfang Hospital; Dongbing Zhao, Xiao Li, Yantao Tian, Qian Liu, Cancer Hospital, Chinese Academy of Medical Sciences; Yong Li, Guangdong General Hospital; Yong Li, Qun Zhao, the Fourth Hospital of Hebei Medical University; Han Liang, Tianjin Medical University Cancer Institute & Hospital; Pin Liang, the First Affiliated Hospital, Dalian Medical University; Jian Suo, Quan Wang, the First Hospital of Jilin University; Liguo Tian, Chinese Journal of Practical Surgery; Jin Wan, Guangdong Provincial Hospital of Chinese Medicien; Xin Wang, Peking University First Hospital; Yi Xiao, Peking Union Medical College Hospital; Zekuan Xu, the First Affiliated Hospital of Nanjing Medical University; Su Yan, Affiliated Hospital of Qinghai University; Zhongtao Zhang, Hongwei Yao, Beijing Friendship Hospital; Jiren Yu, the First Affiliated Hospital of Zhejiang University; Yan Zhao, Zhichao Zheng, Liaoning Cancer Hospital & Institute; Yongliang Zhao, the First Affiliated Hospital of Army Medical University; Yanbing Zhou, Affiliated Hospital of Qingdao University; Jiaming Zhu, the Second Affiliated Hospital of Jilin University.

REFERENCES

1 **Peng JJ**, Peng LF, Chen SL, Xu JB, He YL. Application of totally implantable venous access devices in patients with chemotherapy. *J Digest Oncol (Elect Ver)* 2013; **1**: 56-60

2 **Xue K**, Li ZY, Yan GJ, Gao C, Li SX, Ren H, Ji JF. Safety analysis of implanted peritoneal ports in gastric cancer with peritoneal metastasis. *Chin J Clin Oncol* 2019; **1**: 34-38 [DOI: 10.3969/j.issn.1000-8179.2019.01.901]

3 **Ganeshan A**, Upponi S, Hon LQ, Warakaulle D, Uberoi R. Hepatic arterial infusion of chemotherapy: the role of diagnostic and interventional radiology. *Ann Oncol* 2008; **19**: 847-851 [PMID: 18029972 DOI:

10.1093/annonc/mdm528]
4 **Song L**, Lu F, Liu H. Implantation of intrathecal infusion system for intractable cancer pain therapy. *Chin J Clin Oncol* 2016; **8**: 339-343 [DOI: 10.3969/j.issn.1000-8179.2016.08.153]
5 **Di Carlo I**, Pulvirenti E, Mannino M, Toro A. Increased use of percutaneous technique for totally implantable venous access devices. Is it real progress? A 27-year comprehensive review on early complications. *Ann Surg Oncol* 2010; **17**: 1649-1656 [PMID: 20204533 DOI: 10.1245/s10434-010-1005-4]
6 **Balshem H**, Helfand M, Schünemann HJ, Oxman AD, Kunz R, Brozek J, Vist GE, Falck-Ytter Y, Meerpohl J, Norris S, Guyatt GH. GRADE guidelines: 3. Rating the quality of evidence. *J Clin Epidemiol* 2011; **64**: 401-406 [PMID: 21208779 DOI: 10.1016/j.jclinepi.2010.07.015]
7 **Kim SH**, Oh JS, Chun HJ, Choi BG, Lee HG. Dual-Port versus Mono-Port Implantation for Intra-Arterial Chemoinfusion Therapy for Treatment of Hepatocellular Carcinoma in Patients with Anatomic Hepatic Artery Variation. *J Vasc Interv Radiol* 2019; **30**: 23-30 [PMID: 30297310 DOI: 10.1016/j.jvir.2018.06.006]
8 **Nezami N**, Xing M, Groenwald M, Silin D, Kokabi N, Latich I. Risk Factors of Infection and Role of Antibiotic Prophylaxis in Totally Implantable Venous Access Port Placement: Propensity Score Matching. *Cardiovasc Intervent Radiol* 2019; **42**: 1302-1310 [PMID: 31187229 DOI: 10.1007/s00270-019-02255-0]
9 **Loveday HP**, Wilson JA, Pratt RJ, Golsorkhi M, Tingle A, Bak A, Browne J, Prieto J, Wilcox M, UK Department of Health. epic3: national evidence-based guidelines for preventing healthcare-associated infections in NHS hospitals in England. *J Hosp Infect* 2014; **86** Suppl 1: S1-70 [PMID: 24330862 DOI: 10.1016/S0195-6701(13)60012-2]
10 **Teichgräber UK**, Nagel SN, Kausche S, Streitparth F, Cho CH. Double-lumen central venous port catheters: simultaneous application for chemotherapy and parenteral nutrition in cancer patients. *J Vasc Access* 2010; **11**: 335-341 [PMID: 20954131 DOI: 10.5301/jva.2010.5812]
11 **Johnson BH**, Rypins EB. Single-lumen vs double-lumen catheters for total parenteral nutrition. A randomized, prospective trial. *Arch Surg* 1990; **125**: 990-992 [PMID: 2116119 DOI: 10.1001/archsurg.1990.01410200048007]
12 **Seckold T**, Walker S, Dwyer T. A comparison of silicone and polyurethane PICC lines and postinsertion complication rates: a systematic review. *J Vasc Access* 2015; **16**: 167-177 [PMID: 25634150 DOI: 10.5301/jva.5000330]
13 **Busch JD**, Vens M, Mahler C, Herrmann J, Adam G, Ittrich H. Complication Rates Observed in Silicone and Polyurethane Catheters of Totally Implanted Central Venous Access Devices Implanted in the Upper Arm. *J Vasc Interv Radiol* 2017; **28**: 1177-1183 [PMID: 28549710 DOI: 10.1016/j.jvir.2017.04.024]
14 **Biffi R**, De Braud F, Orsi F, Pozzi S, Arnaldi P, Goldhirsch A, Rotmensz N, Robertson C, Bellomi M, Andreoni B. A randomized, prospective trial of central venous ports connected to standard open-ended or Groshong catheters in adult oncology patients. *Cancer* 2001; **92**: 1204-1212 [PMID: 11571734 DOI: 10.1002/1097-0142(20010901)92:5<1204::aid-cncr1439>3.0.co;2-9]
15 **Maki DG**, Kluger DM, Crnich CJ. The risk of bloodstream infection in adults with different intravascular devices: a systematic review of 200 published prospective studies. *Mayo Clin Proc* 2006; **81**: 1159-1171 [PMID: 16970212 DOI: 10.4065/81.9.1159]
16 **Hockenhull JC**, Dwan K, Boland A, Smith G, Bagust A, Dündar Y, Gamble C, McLeod C, Walley T, Dickson R. The clinical effectiveness and cost-effectiveness of central venous catheters treated with anti-infective agents in preventing bloodstream infections: a systematic review and economic evaluation. *Health Technol Assess* 2008; **12**: iii-iiv, xi-xii, 1-154 [PMID: 18405471 DOI: 10.3310/hta12120]
17 **Niederhuber JE**, Ensminger W, Gyves JW, Liepman M, Doan K, Cozzi E. Totally implanted venous and arterial access system to replace external catheters in cancer treatment. *Surgery* 1982; **92**: 706-712 [PMID: 7123491]
18 **Morris SL**, Jaques PF, Mauro MA. Radiology-assisted placement of implantable subcutaneous infusion ports for long-term venous access. *Radiology* 1992; **184**: 149-151 [PMID: 1609072 DOI: 10.1148/radiology.184.1.1609072]
19 **Hsu CC**, Kwan GN, Evans-Barns H, Rophael JA, van Driel ML. Venous cutdown versus the Seldinger technique for placement of totally implantable venous access ports. *Cochrane Database Syst Rev* 2016; CD008942 [PMID: 27544827 DOI: 10.1002/14651858.CD008942.pub2]
20 **Biffi R**, Orsi F, Pozzi S, Pace U, Bonomo G, Monfardini L, Della Vigna P, Rotmensz N, Radice D, Zampino MG, Fazio N, de Braud F, Andreoni B, Goldhirsch A. Best choice of central venous insertion site for the prevention of catheter-related complications in adult patients who need cancer therapy: a randomized trial. *Ann Oncol* 2009; **20**: 935-940 [PMID: 19179550 DOI: 10.1093/annonc/mdn701]
21 **Biffi R**, Orsi F, Pozzi S, Maldifassi A, Radice D, Rotmensz N, Zampino MG, Fazio N, Peruzzotti G, Didier F. No impact of central venous insertion site on oncology patients' quality of life and psychological distress. A randomized three-arm trial. *Support Care Cancer* 2011; **19**: 1573-1580 [PMID: 20803038 DOI: 10.1007/s00520-010-0984-9]
22 **Lin WY**, Lin CP, Hsu CH, Lee YH, Lin YT, Hsu MC, Shao YY. Right or left? Side selection for a totally implantable vascular access device: a randomised observational study. *Br J Cancer* 2017; **117**: 932-937 [PMID: 28787431 DOI: 10.1038/bjc.2017.264]
23 **Shiono M**, Takahashi S, Takahashi M, Yamaguchi T, Ishioka C. Current situation regarding central venous port implantation procedures and complications: a questionnaire-based survey of 11,693 implantations in Japan. *Int J Clin Oncol* 2016; **21**: 1172-1182 [PMID: 27324107 DOI: 10.1007/s10147-016-1003-z]
24 **Karakitsos D**, Labropoulos N, De Groot E, Patrianakos AP, Kouraklis G, Poularas J, Samonis G, Tsoutsos DA, Konstadoulakis MM, Karabinis A. Real-time ultrasound-guided catheterisation of the internal jugular vein: a prospective comparison with the landmark technique in critical care patients. *Crit Care* 2006; **10**: R162 [PMID: 17112371 DOI: 10.1186/cc5101]
25 **Cadman A**, Lawrance JA, Fitzsimmons L, Spencer-Shaw A, Swindell R. To clot or not to clot? That is the question in central venous catheters. *Clin Radiol* 2004; **59**: 349-355 [PMID: 15041454 DOI: 10.1016/j.crad.2003.11.015]
26 **Caers J**, Fontaine C, Vinh-Hung V, De Mey J, Ponnet G, Oost C, Lamote J, De Greve J, Van Camp B, Lacor P. Catheter tip position as a risk factor for thrombosis associated with the use of subcutaneous infusion ports. *Support Care Cancer* 2005;

13: 325-331 [PMID: 15538639 DOI: 10.1007/s00520-004-0723-1]
27 **Walker G**, Chan RJ, Alexandrou E, Webster J, Rickard C. Effectiveness of electrocardiographic guidance in CVAD tip placement. *Br J Nurs* 2015; **24**: S4, S6, S8-12 [PMID: 26203700 DOI: 10.12968/bjon.2015.24.Sup14.S4]
28 **Pinelli F**, Cecero E, Degl'Innocenti D, Selmi V, Giua R, Villa G, Chelazzi C, Romagnoli S, Pittiruti M. Infection of totally implantable venous access devices: A review of the literature. *J Vasc Access* 2018; **19**: 230-242 [PMID: 29512430 DOI: 10.1177/1129729818758999]
29 **Narducci F**, Jean-Laurent M, Boulanger L, El Bédoui S, Mallet Y, Houpeau JL, Hamdani A, Penel N, Fournier C. Totally implantable venous access port systems and risk factors for complications: a one-year prospective study in a cancer centre. *Eur J Surg Oncol* 2011; **37**: 913-918 [PMID: 21831566 DOI: 10.1016/j.ejso.2011.06.016]
30 **Kakkos A**, Bresson L, Hudry D, Cousin S, Lervat C, Bogart E, Meurant JP, El Bedoui S, Decanter G, Hannebicque K, Regis C, Hamdani A, Penel N, Tresch-Bruneel E, Narducci F. Complication-related removal of totally implantable venous access port systems: Does the interval between placement and first use and the neutropenia-inducing potential of chemotherapy regimens influence their incidence? A four-year prospective study of 4045 patients. *Eur J Surg Oncol* 2017; **43**: 689-695 [PMID: 27889197 DOI: 10.1016/j.ejso.2016.10.020]
31 **Karanlik H**, Kurul S, Saip P, Unal ES, Sen F, Disci R, Topuz E. The role of antibiotic prophylaxis in totally implantable venous access device placement: results of a single-center prospective randomized trial. *Am J Surg* 2011; **202**: 10-15 [PMID: 21601826 DOI: 10.1016/j.amjsurg.2010.05.005]
32 **Johnson E**, Babb J, Sridhar D. Routine Antibiotic Prophylaxis for Totally Implantable Venous Access Device Placement: Meta-Analysis of 2,154 Patients. *J Vasc Interv Radiol* 2016; **27**: 339-43; quiz 344 [PMID: 26776446 DOI: 10.1016/j.jvir.2015.11.051]
33 **Mermel LA**, Allon M, Bouza E, Craven DE, Flynn P, O'Grady NP, Raad II, Rijnders BJ, Sherertz RJ, Warren DK. Clinical practice guidelines for the diagnosis and management of intravascular catheter-related infection: 2009 Update by the Infectious Diseases Society of America. *Clin Infect Dis* 2009; **49**: 1-45 [PMID: 19489710 DOI: 10.1086/599376]
34 **Sona C**, Prentice D, Schallom L. National survey of central venous catheter flushing in the intensive care unit. *Crit Care Nurse* 2012; **32**: e12-e19 [PMID: 22298726 DOI: 10.4037/ccn2012296]
35 **Goossens GA**. Flushing and Locking of Venous Catheters: Available Evidence and Evidence Deficit. *Nurs Res Pract* 2015; **2015**: 985686 [PMID: 26075094 DOI: 10.1155/2015/985686]
36 **Goossens GA**, Jérôme M, Janssens C, Peetermans WE, Fieuws S, Moons P, Verschakelen J, Peerlinck K, Jacquemin M, Stas M. Comparing normal saline versus diluted heparin to lock non-valved totally implantable venous access devices in cancer patients: a randomised, non-inferiority, open trial. *Ann Oncol* 2013; **24**: 1892-1899 [PMID: 23553060 DOI: 10.1093/annonc/mdt114]
37 **Dal Molin A**, Clerico M, Baccini M, Guerretta L, Sartorello B, Rasero L. Normal saline versus heparin solution to lock totally implanted venous access devices: Results from a multicenter randomized trial. *Eur J Oncol Nurs* 2015; **19**: 638-643 [PMID: 25933709 DOI: 10.1016/j.ejon.2015.04.001]
38 **López-Briz E**, Ruiz Garcia V, Cabello JB, Bort-Martí S, Carbonell Sanchis R, Burls A. Heparin versus 0.9% sodium chloride locking for prevention of occlusion in central venous catheters in adults. *Cochrane Database Syst Rev* 2018; **7**: CD008462 [PMID: 30058070 DOI: 10.1002/14651858.CD008462.pub3]
39 **The Nebraska Medical Center**. Standardizing central venous catheter care: hospital to home. National Guideline Clearinghouse 2013. Available from: URL: https://www.nebraskamed.com/central-line
40 **Chinese Nursing Association Venous Infusion Therapy Committee**. Expert consensus on venous catheter maintenance. *Zhonghua Huli Zazhi* 2019; **9**: 1334-1342 [DOI: 10.3761/j.issn.0254-1769.2019.09.011]
41 **Pronovost P**, Needham D, Berenholtz S, Sinopoli D, Chu H, Cosgrove S, Sexton B, Hyzy R, Welsh R, Roth G, Bander J, Kepros J, Goeschel C. An intervention to decrease catheter-related bloodstream infections in the ICU. *N Engl J Med* 2006; **355**: 2725-2732 [PMID: 17192537 DOI: 10.1056/NEJMoa061115]
42 **O'Grady NP**, Alexander M, Burns LA, Dellinger EP, Garland J, Heard SO, Lipsett PA, Masur H, Mermel LA, Pearson ML, Raad II, Randolph AG, Rupp ME, Saint S; Healthcare Infection Control Practices Advisory Committee. Guidelines for the prevention of intravascular catheter-related infections. *Am J Infect Control* 2011; **39**: S1-34 [PMID: 21511081 DOI: 10.1016/j.ajic.2011.01.003]
43 **Gorski LA**. The 2016 Infusion Therapy Standards of Practice. *Home Healthc Now* 2017; **35**: 10-18 [PMID: 27922994 DOI: 10.1097/NHH.0000000000000481]
44 **Kolaček S**, Puntis JWL, Hojsak I; ESPGHAN/ESPEN/ESPR/CSPEN working group on pediatric parenteral nutrition. ESPGHAN/ESPEN/ESPR/CSPEN guidelines on pediatric parenteral nutrition: Venous access. *Clin Nutr* 2018; **37**: 2379-2391 [PMID: 30055869 DOI: 10.1016/j.clnu.2018.06.952]
45 **Chinese Gastric Cancer Association**. Consensus of Chinese experts on prevention and treatment of peritoneal metastasis of gastric cancer. *Zhonghua Weichang Waike Zazhi* 2017; **5**: 481-490 [DOI: 10.3760/cma.j.issn.1671-0274.2017.05.001]
46 **Zhang K**, Chen L. Chinese consensus on the diagnosis and treatment of gastric cancer with liver metastases. *Ther Adv Med Oncol* 2020; **12**: 1758835920904803 [PMID: 32127925 DOI: 10.1177/1758835920904803]
47 **Erinjeri JP**, Fong AJ, Kemeny NE, Brown KT, Getrajdman GI, Solomon SB. Timing of administration of bevacizumab chemotherapy affects wound healing after chest wall port placement. *Cancer* 2011; **117**: 1296-1301 [PMID: 21381016 DOI: 10.1002/cncr.25573]

World Journal of Gastroenterology

Submit a Manuscript: https://www.f6publishing.com

World J Gastroenterol 2020 July 7; 26(25): 3528-3541

DOI: 10.3748/wjg.v26.i25.3528

ISSN 1007-9327 (print) ISSN 2219-2840 (online)

OPINION REVIEW

Management of nonalcoholic fatty liver disease in the Middle East

Faisal M Sanai, Faisal Abaalkhail, Fuad Hasan, Muhammad Hamed Farooqi, Nawal Al Nahdi, Zobair M Younossi

ORCID number: Faisal M Sanai 0000-0002-3830-9236; Faisal Abaalkhail 0000-0003-1287-9887; Fuad Hasan 0000-0002-1980-467X; Muhammad Hamed Farooqi 0000-0001-6489-3715; Nawal Al Nahdi 0000-0002-0002-1085; Zobair M Younossi 0000-0001-9313-577X.

Author contributions: All authors equally contributed to this paper in terms of conception, literature review, drafting, critical revision, editing, and final approval for submission.

Conflict-of-interest statement: None of the authors received any fees for writing this manuscript. Medical writing assistance was funded by Gilead Sciences. No other conflict is declared.

Faisal M Sanai, Gastroenterology Unit, Department of Medicine, King Abdulaziz Medical City, Jeddah 21423, Saudi Arabia

Faisal Abaalkhail, Department of Medicine, Alfaisal University, Riyadh 11533, Saudi Arabia

Faisal Abaalkhail, Department of Liver Transplant, King Fahad Specialist Hospital, Dammam 32253, Saudi Arabia

Fuad Hasan, Department of Internal Medicine, Faculty of Medicine, Kuwait University, Safat 13110, Kuwait

Muhammad Hamed Farooqi, Dubai Diabetes Center, Dubai Health Authority, Dubai 00000, United Arab Emirates

Nawal Al Nahdi, Department of Gastroenterology and Hepatology, Dubai Health Authority, Rashid hospital, Dubai 00000, United Arab Emirates

Zobair M Younossi, Department of Medicine, Inova Fairfax Medical Campus, Falls Church, VA 22042, United States

Corresponding author: Zobair M Younossi, FAASLD, AGAF, FACG, FACP, MD, Chairman, Professor, Department of Medicine, Inova Fairfax Medical Campus, Betty and Guy Beatty Center for Integrated Research, Inova Health System, Claude Moore Health Education and Research Building 3300 Gallows Road, Falls Church, VA 22042, United States. zobair.younossi@inova.org

Abstract

The prevalence of nonalcoholic fatty liver disease (NAFLD) in the Middle East is increasing in parallel to an increase in the prevalence of associated risk factors such as obesity, metabolic syndrome, and type 2 diabetes mellitus. About 20% to 30% of the patients progress to develop nonalcoholic steatohepatitis (NASH), a histological subtype of NAFLD, with features of hepatocyte injury such as hepatocyte ballooning. NASH can progress to fibrosis, cirrhosis, and even hepatocellular carcinoma. NAFLD thus causes a substantial burden on healthcare systems and it is imperative that appropriate strategies are discussed at a regional level to facilitate effective management tailored to the needs of the region. To fulfil this unmet need, expert gastroenterologists, hepatologists, and endocrinologists from the region came together in three advisory board meetings that were conducted in Saudi Arabia, United Arab Emirates, and Kuwait, to

Manuscript source: Unsolicited manuscript

Received: March 5, 2020
Peer-review started: March 5, 2020
First decision: April 8, 2020
Revised: May 15, 2020
Accepted: June 10, 2020
Article in press: June 10, 2020
Published online: July 7, 2020

P-Reviewer: Baffy G, Thompson RR
S-Editor: Zhang L
L-Editor: A
E-Editor: Ma YJ

discuss current local challenges in NAFLD screening and diagnosis, and the different available management options. The experts discussed the disease burden of NAFLD/NASH in the Middle East; screening, diagnosis, and referral patterns in NAFLD; and available treatment options for NAFLD and NASH. This paper summarizes the discussions and opinion of the expert panel on the management of NAFLD/NASH and also presents an extensive literature review on the topic.

Key words: Nonalcoholic fatty liver disease; Nonalcoholic steatohepatitis; Middle East; Expert opinion

Core tip: With the rising prevalence of nonalcoholic fatty liver disease (NAFLD) in the Middle East, there is an unmet need of appropriate strategies to facilitate effective management at a regional level. Therefore, expert gastroenterologists, hepatologists, and endocrinologists from the region came together in three advisory board meetings that were conducted in Saudi Arabia, United Arab Emirates, and Kuwait. Current local challenges in NAFLD screening and diagnosis, and the different available management options were discussed. This paper summarizes the discussions of the expert panel on the management of NAFLD/nonalcoholic steatohepatitis and also presents an extensive literature review on the topic.

Citation: Sanai FM, Abaalkhail F, Hasan F, Farooqi MH, Nahdi NA, Younossi ZM. Management of nonalcoholic fatty liver disease in the Middle East. *World J Gastroenterol* 2020; 26(25): 3528-3541
URL: https://www.wjgnet.com/1007-9327/full/v26/i25/3528.htm
DOI: https://dx.doi.org/10.3748/wjg.v26.i25.3528

INTRODUCTION

Nonalcoholic fatty liver disease (NAFLD) is the most common chronic liver disease worldwide and is characterized by fatty infiltration of the liver in the absence of alcohol abuse or other causes of hepatic steatosis such as medications and viral or autoimmune hepatitis[1]. It encompasses the entire spectrum of manifestations from steatosis, steatohepatitis, and fibrosis to cirrhosis[1]. NAFLD can be categorized as nonalcoholic fatty liver (NAFL) and nonalcoholic steatohepatitis (NASH) based on histopathological criteria. NAFL is defined as the presence of more than 5% of hepatic steatosis without evidence of hepatocellular injury and is generally a nonprogressive condition. On the other hand, NASH implies the presence of hepatic steatosis (> 5%), in conjunction with features of hepatocyte injury (such as hepatocyte ballooning), and can progress to fibrosis, cirrhosis, and even hepatocellular carcinoma (HCC)[1,2]. Although patients with only hepatic steatosis (NAFL) typically do not develop cirrhosis or liver-related complications, about 20% to 30% of NAFLD can be classified as NASH[3,4]. It is important to distinguish between the different types of NAFLD as it has an impact on prognosis and management[5].

The estimated prevalence of NAFLD varies worldwide, ranging from 6% to 35%[6,7]. In a recent meta-analysis on the global epidemiology of NAFLD, Younossi *et al*[8] reported its prevalence to be highest (32%) in the Middle East. Also, with an increase in the risk factors of NAFLD and NASH such as obesity, metabolic syndrome (MetS), and type 2 diabetes mellitus (T2DM), the prevalence is estimated to grow further[6]. Alswat *et al*[9] conducted an analysis to estimate the burden of NAFLD in Saudi Arabia and United Arab Emirates (UAE) by the year 2030[9]. The analysis projected that by 2030 there will be over 12 million individuals (an increase by 48% from 2017) with NAFLD in Saudi Arabia and 372000 (an increase by 46% from 2017) in UAE[9]. This projected NAFLD prevalence corresponds to predicted increase in the burden of obesity and T2DM. Furthermore, NASH prevalence, which was 4.2% and 4.1% of the total population in Saudi Arabia and UAE, respectively, in 2017, is expected to rise by 96% and 87%, respectively, by 2030. This model also predicts that the percentage of patients with F3/F4 fibrosis or advanced liver disease (decompensated cirrhosis or HCC) is anticipated to increase to 21.8% (13.5% in 2017) and 21.1% (13.6% in 2017) of

the NASH cases in Saudi Arabia and UAE, respectively, by 2030. In Saudi Arabia, incident decompensated cirrhosis is expected to rise by 273% with almost seven thousand cases in 2030. In UAE, the incident decompensation is anticipated to rise by 241%. NAFLD related HCC cases are projected to increase by 209% (580 to 1790) in Saudi Arabia and by 181% (18 to 51) in UAE. By 2030, annual liver-related deaths are estimated to rise by 295% in Saudi Arabia and by 270% in UAE[9].

It is important to note that the clinical outcomes of NAFLD can vary across the globe. In a recent study of the Global NASH Registry™, NAFLD subjects enrolled from 14 different countries showed some clinical similarities but also a number of differences[10]. These data suggest that the epidemiology of NAFLD must be considered in the context of regional and country-specific factors that impact the incidence, prevalence, and natural history of NAFLD.

NAFLD and NASH pose major challenges in both diagnosis and treatment. There is an ongoing debate as to whether at-risk patients should be screened for NAFLD/NASH in the absence of effective, approved pharmacological treatment options[2,11]. In such a scenario, screening of high-risk groups could be a more practical option. Also, there are uncertainties regarding appropriate referral, management, and follow-up of these patients. With the rising prevalence of NAFLD and NASH in the Middle East, it is imperative that these concerns are discussed at a regional level to facilitate effective strategies tailored to the needs of the region.

With this objective, advisory board meetings were conducted between May 2018 and February 2019 in Saudi Arabia, UAE, and Kuwait, to discuss current local challenges in NASH screening and diagnosis and the different available management options. These meetings were attended by expert gastroenterologists, hepatologists, and endocrinologists from the region. This paper summarizes the discussions in the meetings, along with a comprehensive literature review on the topic. For the review, PubMed and Google Scholar were searched employing the Boolean operators, "AND" and "OR", and using the following search terms: "nonalcoholic fatty liver disease", "NAFLD", "nonalcoholic steatohepatitis", "NASH", "type 2 diabetes mellitus", "T2DM", "metabolic syndrome", "obesity", "guidelines". The bibliographies of the key references were also searched manually for additional relevant references.

During the meetings, the experts discussed the following topics: (1) Disease burden of NAFLD/NASH in the Middle East; (2) Screening, diagnosis, and referral patterns in NAFLD; and (3) Available treatment options for NAFL and NASH.

DISEASE BURDEN OF NONALCOHOLIC FATTY LIVER DISEASE/ NONALCOHOLIC STEATOHEPATITIS IN THE MIDDLE EAST

NAFLD/NASH burden in the Middle East countries is growing with the increase in the prevalence of risk factors such as obesity, MetS, and T2DM

A population-wide screening program in UAE found that 35% of the population had obesity, 32% were overweight, 55% had central obesity, 18% had diabetes, 27% were prediabetic, and 44% had dyslipidemia[12] (Table 1). Further, Radwan *et al*[13] reported a two to three-fold increase in the prevalence of obesity in the UAE between 1989 and 2017[13]. In a survey conducted in 2013 in Saudi Arabia, 28.7% of the 10735 participants were obese (body mass index, ≥ 30 kg/m^2)[14]. Moreover, Al-Quwaidhi *et al*[15] projected an increase in the overall prevalence of obesity in Saudi Arabia to 41% in men, and 78% in women by 2022[15]. Obesity has been strongly linked with NAFLD and is known to be associated with the entire histological spectrum from steatosis, hepatocellular injury, fibrosis, cirrhosis, and even HCC[16]. In a study (n = 296), Alqahtani *et al*[17] found that 65% of severely obese young children in Saudi Arabia had NASH and 60% had clinically significant liver fibrosis[17].

Similarly, regional disease burden from diabetes has been steadily increasing. As per the World Health Organization, in the Middle East and North Africa region, a 72% increase in the prevalence of diabetes from 39 million adults in 2017 to 85 million in 2045 is estimated[18]. In Saudi Arabia, the prevalence of diabetes has risen almost 10 fold over the past three decades[19]. There are several contributors to this, including rapid urbanization, unhealthy eating habits, and sedentary lifestyle[18]. Patients with T2DM have a high prevalence of NAFLD and advanced fibrosis. In a meta-analysis of 24 studies, the pooled prevalence of NAFLD in T2DM patients was almost 60%[20]. In another more recent (2019) meta-analysis, the global prevalence of NAFLD among T2DM patients was 55.5%[21]. Similarly, a meta-analysis that included 17 studies with T2DM patients found the prevalence of NAFLD to be 54%[22]. All these studies may

Table 1 Prevalence and Estimation Studies of Risk Factors of nonalcoholic fatty liver disease in United Arab Emirates, Kingdom of Saudi Arabia, and Kuwait

Place of study	Study	Main findings	Ref.
Dubai, UAE	Cross-sectional study to access prevalence of MetS and its associated risk factors among children and adolescents (596 students)	Prevalence of MetS was 3.7%; was more common among boys than girls (12 boys versus 10 girls); 18.6% were overweight; 21.2% were obese; MetS was more commonly found in obese (16%) compared to overweight students (2%)	Haroun *et al*[81], 2018
Abu Dhabi, UAE	Multicenter cohort study to determine cardiovascular risk factor prevalence rates (50138 participants)	35% were obese, 32% were overweight, 55% had central obesity, 18% were diabetic, 27% were prediabetic; Age-standardized diabetes and prediabetes rates were 25% and 30%, respectively; Age-standardized obesity and overweight rates were 41% and 34%, respectively	Hajat *et al*[12], 2012
UAE	Systematic review and qualitative synthesis of prevalence, incidence rates, trends, and Economic Burden of Obesity and cardiometabolic disorder (36 studies)	All studies reported high prevalence rates for obesity, diabetes, hypertension, and MetS; Obesity and related cardiometabolic disorders seem highly prevalent in the UAE but estimating an accurate occurrence is challenging due to methodological heterogeneity of the epidemiological studies addressing them; Frequency of overweight and obesity was reported to increase by 2-3-fold between 1989 and 2017	Radwan *et al*[13], 2018
Saudi Arabia	Survey to determine obesity prevalence and associated factors (n = 10293)	28.7% of the population evaluated were obese; Obesity prevalence was higher among women (33.5%) than men (24.1%)	Memish *et al*[14], 2014
Saudi Arabia	Secondary analysis to estimate the trends in the prevalence of adult obesity over the period 1992–2022 (5 studies)	Obesity trend from 1992-2005: In men, the prevalence increased from (1) 10.1% to 27.1% in age-group 25-34 yr; and (2) 12.9% to 31.0% in age group 55-64 yr. In women, obesity prevalence was higher; increased from (1) 16.1% to 39.5% in age group 25-34 yr; and (2) 22.8% to 53.2% in age group 55-64 yr. Obesity projection from 1992-2022: The future obesity prevalence was estimated to increase from (1) 12% to 41% in men; and (2) 21% to 78% in women	Al-Quwaidhi *et al*[15], 2014
Saudi Arabia	Cross sectional study to evaluate the prevalence of MetS	The prevalence of MetS in Saudi Arabia was found to be 39.8% (34.4% in men and 29.2% in women) as per the NCEP ATP III and 31.6% (45.0% in men and 35.4% in women) as per IDF criteria	Al-Rubeaan *et al*[26], 2018
Kuwait	Observational study (multicenter) to examine the prevalence of MetS and its components (992 adults ≥ 20 yr)	Obesity percentage was significantly greater in females (54.7%) compared to males (32.3%); Abdominal obesity was the most predominant MetS abnormality; Prevalence of MetS increased with age and was higher in females than males	Al Zenki *et al*[82], 2012
Kuwait	Cross-sectional survey to estimate prevalence of overweight, obesity, and various types of adiposity (3589 adults, 18-69 yr)	Overall obesity prevalence was 40.3% (men, 36.5%; women, 44.0%); The prevalence of Class I, Class II, and Class III obesity was 24.9%, 9.9%, and 5.5%, respectively	Weiderpass *et al*[83], 2019
Kuwait	Descriptive, cross-sectional survey (multicenter) to understand the prevalence of MetS, and estimation of the 10-year risk for developing T2DM and CHD (n = 1610)	4% subjects were found to have screen detected T2DM. A history of high blood glucose levels was reported by 18.0% subjects; 35.5% of the participants were obese; MetS was present in about 32% of the participants; Almost 30% of participants were found to be at moderate/high/very high risk of developing T2DM within the next 10 yr; 8.45% were found to be at moderate/high/very high risk of developing both T2DM/CHD within the next 10 yr	Awad *et al*[84], 2014

IDF: International Diabetes Federation; MetS: Metabolic syndrome; NCEP ATP III: National Cholesterol Education Program and Adult Treatment Panel III; T2DM: Type 2 diabetes mellitus; UAE: United Arab Emirates.

have slightly different methodology but, as is evident, prevalence of NAFLD in individuals with T2DM was quite high. Moreover, presence of NAFLD has been reported to be associated with a twofold increased risk of incident diabetes[23]. Further, the prevalence of NASH in diabetic patients with NAFLD has also been evaluated. In a recent meta-analysis by Younossi *et al*[21], while the global prevalence of NASH in patients with T2DM was found to be 37.3%, the prevalence of advanced fibrosis was 17%[21]. In a study derived from the NASH Clinical Research Network, of 346 patients with diabetes and NAFLD, the prevalence of NASH and advanced fibrosis was 69.2%

and 41%, respectively[24].

Similar to T2DM, the prevalence of MetS (*i.e*., abdominal obesity, hypertension, atherogenic dyslipidemia, and hyperglycemia) in the Middle East is also on the rise. A meta-analysis of cross-sectional studies from the Middle East countries reported the prevalence of MetS to be 16%-41% in Saudi-Arabia, 9%-36% in Kuwait, and 22%-50% in UAE[25]. A recent study found the prevalence of MetS in Saudi Arabia to be about 40%[26]. A strong association between MetS and NAFLD has been reported previously. In a study conducted on 304 patients with NAFLD without overt diabetes, 88% of patients who had NASH on liver biopsy had MetS. Further, the study showed that MetS was associated with a high risk of NASH among NAFLD patients [odds ratio (OR), 3.2; 95%CI: 1.2-8.9; P = 0.026][27]. Furthermore, in the NASH Clinical Research Network data, presence of NASH was significantly associated with MetS (OR: 1.43; 95%CI: 1.09-1.98; P = 0.009)[28]. In a regional study from Kuwait, T2DM (P = 0.02) and obesity (P < 0.004) were again significantly associated with NAFLD[29].

In summary, obesity, MetS, T2DM, and NAFLD are all associated with each other. Emerging data also appears to show that the prevalence of NAFLD is growing in parallel with that of obesity, MetS, and T2DM, worldwide, with Middle East being no exception[11,30,31].

SCREENING, DIAGNOSIS, AND REFERRAL PATTERNS IN NONALCOHOLIC FATTY LIVER DISEASE

Patients with risk factors, namely obesity, MetS, and T2DM should be screened for NAFLD

Given the high prevalence of NAFLD in high-risk groups, most international guidelines including European, Asia-Pacific, and National Institute for Health and Care Excellence recommend routine screening in these patients with liver enzymes, ultrasonography, and transient elastography, where available[2,32,33]. European guidelines also recommend case finding of advanced disease (*i.e*. NASH with fibrosis) in high risk individuals (age > 50 years, T2DM, MetS)[2]. However, the American Association for the Study of Liver Diseases (AASLD) guidelines currently do not recommend routine screening for NAFLD given the uncertainties regarding performance characteristics of diagnostic tests and available treatment options[1]. Nevertheless, they urge clinicians to have a high index of suspicion for NAFLD and NASH in patients with diabetes even if liver enzymes are normal[1]. European guideline also recommends that individuals with persistently abnormal liver enzymes be screened for NAFLD and all those with steatosis be screened for MetS independent of liver enzymes[2]. Obtaining a random aspartate transaminase and alanine transaminase (ALT) level in individuals with obesity, MetS, and T2DM may be a reasonable approach[34]. However, as it is known that liver enzymes may not always be elevated in NAFLD, an ultrasound can be done on patients suspected to have NAFLD. Other tests can be used for screening based on availability and feasibility.

Definite diagnosis of NASH can only be made by liver biopsy. Candidates for liver biopsy should be chosen carefully based on the results of noninvasive tests.

The diagnosis of NAFLD involves clinical history to rule out secondary causes of fatty liver and to obtain information on risk factors such as age (≥ 50 years) and the presence of T2DM and MetS[35] (Figure 1). Further, biochemical investigations and radiological findings aid in making the diagnosis. Patients often do not experience overt symptoms but their quality of life is impaired[36]. In most cases, the diagnosis of NAFLD is made when elevated liver enzymes are found incidentally. Also, it is important to note that liver enzymes can be within the normal range in NASH and a definitive diagnosis can only be made by histology[30].

Although liver biopsy is considered as the gold standard for establishing NASH and for staging of fibrosis, it is associated with the risk of complications such as pain, intraperitoneal bleeding, and pneumothorax[35]. Noninvasive methods of diagnosis include serum biomarkers, routine radiologic tests such as ultrasound, computed tomography, magnetic resonance imaging, and assessment of liver stiffness by transient elastography (FibroScan®) and magnetic resonance elastography[37]. Validated laboratory-based scoring systems for estimating the stage of hepatic fibrosis are also available, such as NAFLD fibrosis score, FibroMeter, and Fibrosis-4[35]. The advantages and limitations of some of the available diagnostic modalities are listed in Table 2.

In addition to these tests, a number of serum fibrosis tests are being evaluated for

Table 2 Key diagnostic modalities for nonalcoholic fatty liver disease and nonalcoholic steatohepatitis[11,35,85,86]

Diagnostic Tests	Advantages	Limitations
Liver enzymes and other blood tests for fibrosis		
Platelet count; APRI; AST; ALT; AST/ALT ratio; Hyaluronic acid; ELF; Hepascore; FibroSpect; FibroTest/FibroSure	Simple and easy; AST/ALT of > 1 is predictive of fibrosis; ELF can predict stage of fibrosis and outcomes	AST and ALT can be normal in some patients with NAFLD; ELF is not widely available; Some tests initially developed for HCV; Limited published data on external validation
Radiology		
Ultrasonography	Easily available; Safe; Overall scanning of abdominal organs	Cannot detect mild degree of steatosis (< 30% of hepatocytes); Does not distinguish between steatosis and NASH; Operator dependent
MRI	More sensitive than ultrasonography	Cost and availability; Does not distinguish between steatosis and NASH
Transient; Elastography	Can detect fibrosis	Cost and availability
MRE	Can detect fibrosis and MRI-PDFF can quantify steatosis	Cost and availability
Fibrosis scoring systems		
NAFLD fibrosis score (NFS), Fibro Meter Fibrosis-4 (FIB-4)	Allow a more targeted use of liver biopsy by reliably excluding advanced fibrosis in a high proportion of NAFLD patients; Potentially predict liver-related and cardiovascular complications and death	Significant number with indeterminate scores; Limited external validation in NASH
Liver biopsy	Gold standard for diagnosis of NAFLD and NASH; Allows staging of the disease	Invasive; Associated with complications – pain, intraperitoneal bleeding; Cost

ALT: Alanine aminotransferase; AST: Aspartate aminotransferase; APRI: AST-to-platelet ratio index; CT: Computerized tomographic; ELF: Enhanced liver fibrosis; MRE: Magnetic resonance elastography; MRI: Magnetic resonance imaging; MRI-PDFF: MRI-based proton density fat fraction; NAFLD: Nonalcoholic fatty liver disease; NASH: Nonalcoholic steatohepatitis.

risk-stratifying patients with NASH. Of these, Enhanced Liver Fibrosis (ELF™) is available in Europe and seems to be a promising non-invasive test for risk assessment in patients with NASH[38].

Since none of the noninvasive tests can confirm a diagnosis of NASH, the only available option for definitive diagnosis is liver biopsy. However, it has been found that the combination or sequential use of different noninvasive methods or different scoring systems can increase overall diagnostic accuracy with consequent decrease in the need for liver biopsy[39-41]. In summary, diagnosis of NASH is complex and needs careful consideration of available non-invasive diagnostic tools. It is advisable to use these various modalities based on availability and carefully select the subset of patients, who will benefit from liver biopsy, based on the results of the noninvasive methods.

Liver biopsy also plays an important role in staging and risk-stratification of the disease. NASH fibrosis is divided into four stages based on severity, ranging from the less severe stages (F1 and F2) to F3 and F4 (bridging fibrosis and cirrhosis, respectively)[42]. The presence and degree of fibrosis has been shown to be the most

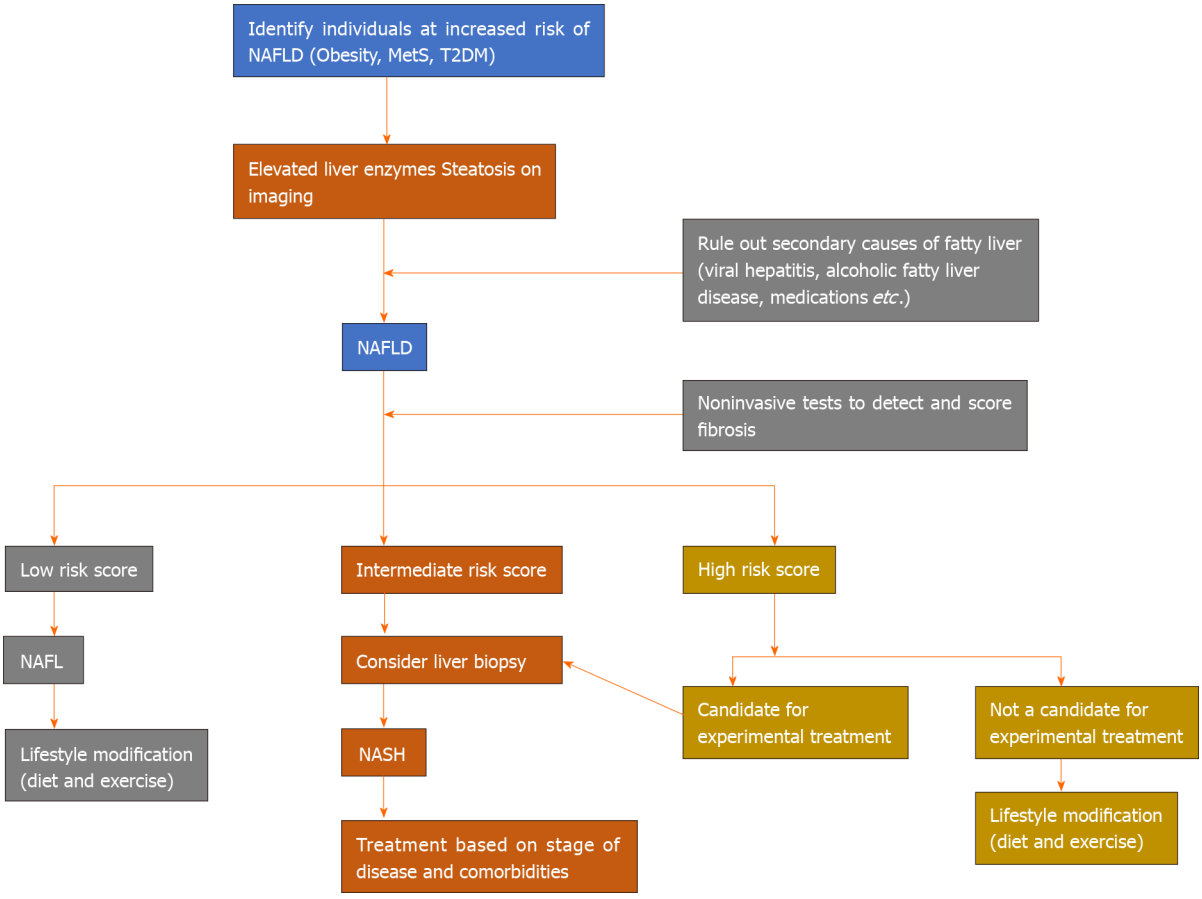

Figure 1 Basic algorithm for diagnosis and treatment of nonalcoholic fatty liver disease/nonalcoholic steatohepatitis. MetS: Metabolic syndrome; NAFL: Nonalcoholic fatty liver; NAFLD: Nonalcoholic fatty liver disease; NASH: Nonalcoholic steatohepatitis; T2DM: Type 2 diabetes mellitus.

important prognostic marker in NASH[43-46]. In a study, during a follow-up of mean 20 years (range 0-40) equivalent to 139163 person-years, the risk of severe liver disease increased per stage of fibrosis (hazard ratio ranging from 1.9 in F0 to 104.9 in F4) compared to controls[44]. In another study, features of liver biopsies significantly associated with death or liver transplantation included fibrosis stage 1 (HR: 1.88; 95%CI: 1.28-2.77), stage 2 (HR: 2.89; 95%CI: 1.93-4.33), stage 3 (HR: 3.76; 95%CI: 2.40-5.89), and stage 4 (HR: 10.9; 95%CI: 6.06-19.62) compared with stage 0[43].

Referral of patients should be done promptly once NASH is suspected and NASH should be managed by multidisciplinary teams

Currently, NAFLD is underdiagnosed[47]. It is crucial to increase awareness regarding NAFLD and NASH *via* effective multi-disciplinary collaboration among healthcare professionals. Education of primary care physicians as well as diabetologists is important. Diabetologists and primary care physicians should be encouraged to screen at-risk patients for NAFLD, followed by time-sensitive referral, especially in patients with suspected NASH. In view of the co-morbid conditions often associated with NAFLD, a multidisciplinary management approach that includes primary care physicians, gastroenterologists, endocrinologists/diabetologists, cardiologists, and nutritionists is warranted.

AVAILABLE TREATMENT OPTIONS FOR NONALCOHOLIC FATTY LIVER AND NONALCOHOLIC STEATOHEPATITIS

Patients with NAFL should be advised lifestyle modifications only. Patients with NASH should be considered for therapy based on the stage of the disease and the presence of comorbidities

Once NAFLD/NASH is diagnosed, the next step is to consider appropriate therapeutic intervention. This is currently limited by lack of effective treatment options

to prevent or reduce progression to cirrhosis and HCC. Although all patients with NAFLD are candidates for lifestyle intervention to optimize their cardiovascular risks, only patients with NASH are candidates for pharmacotherapy. Therefore, the current treatment options for NASH include lifestyle interventions, pharmacotherapy (mostly off-label), and consideration for bariatric surgery in the context of metabolic indication for weight loss surgery. Importantly, treatment should also involve the management of comorbidities[1,2].

Patients with NAFL usually have a favorable liver-related prognosis and require management of their cardiovascular risks. In this context, NAFL patients do not require consideration of pharmacotherapy for liver disease and this treatment option should be reserved for patients diagnosed with NASH. Intervention in patients with NAFL should be limited to encouragement of appropriate lifestyle modifications[1,2]. Lifestyle interventions, including diet and exercise, have been found to be effective when adequate weight loss is achieved. In a meta-analysis that included 20 studies and 1073 NAFLD patients, exercise significantly improved aspartate transaminase and ALT ($P < 0.05$). Additionally, combined exercise and diet decreased ALT ($P < 0.01$) and improved NAFLD activity score (standardized mean difference -0.61, 95%CI: -1.09 to -0.13)[48]. Bradford *et al*[49] reviewed 30 studies that used diet and/or exercise as an intervention for patients with NAFLD[49]. A total of 14 studies that included both diet and exercise showed improvement in the various outcome measures evaluated. Of the nine studies that included only exercise as an intervention, eight studies showed a positive outcome. Furthermore, all seven studies that used only diet as an intervention also showed improvement in markers of hepatic steatosis, leading the authors to conclude that lifestyle intervention is a critical component of management of patients with NAFLD[49].

European Association for the Study of the Liver, European Association for the Study of Diabetes, and European Association for the Study of Obesity and AASLD guidelines recommend a combination of daily reduction in caloric intake by 500 to 1000 kcal and moderate-intensity exercise for sustaining weight loss over time[1,2]. A systematic review and meta-analysis reported improved hepatic steatosis with ≥ 5% weight loss and improvement in NASH with a weight loss of ≥ 7%[50]. As per the AASLD guidelines, weight loss of 3%-5% of total body weight is required to improve steatosis and weight loss of 7%-10% is necessary to improve histopathological features of NASH[1]. It has also been suggested that weight loss of more than 10% may improve fibrosis[51,52].

It is important to note that currently, there are no pharmacotherapies approved for the treatment of NASH. This underscores the need for clinicians to make treatment decisions based on individual patient circumstances, taking into account the stage of NASH and safety, expected benefit, pricing, and evidence base of available off-label pharmacological treatment options. Although metformin has been widely studied in patients with NASH, it was not found to have beneficial effects on liver histology[53-55] and is therefore not recommended in patients with NASH[1,2,32]. On the other hand, the thiazolidinedione, pioglitazone has been shown to be promising in improving liver histology in NASH patients with or without T2DM[56-58]. Pioglitazone could be considered in these patients although currently AASLD guidelines recommend consideration of its use in biopsy-proven NASH only[1]. Vitamin E has also been used in patients with NAFLD and NASH. In a meta-analysis, vitamin E supplementation was associated with significant ($P < 0.05$) improvement in all histological parameters including steatosis, ballooning, lobular inflammation, and fibrosis in nondiabetic individuals with NASH[59]. Similar results were found in another meta-analysis, where vitamin E significantly reduced liver enzymes and improved liver histology[60]. However, concerns have been raised about the safety of vitamin E supplementation, including increased all-cause mortality with dose of > 800 IU/d and an observed association with prostate cancer[61,62]. Nevertheless, a large meta-analysis that included 57 studies including 246371 patients, who were followed for up to 10 years, did not show any association between vitamin E and all-cause mortality[63]. Consequently, it is recommended that vitamin E at a dose of 800 IU/d be considered in nondiabetic adults with biopsy-proven NASH[1]. A meta-analysis that included nine clinical trials (three with thiazolidinedione, three with metformin, two with vitamin E and one with both thiazolidinedione and vitamin E), found that thiazolidinedione and vitamin E improved liver histologic scores, but metformin did not. None of the agents improved fibrosis[64].

NAFLD has been shown to be associated with an increased risk of cardiovascular events, regardless of the presence of coexisting metabolic syndrome, mandating consideration of interventions to treat cardiovascular risk factors[65]. Concerns persist amongst clinicians regarding statin use in patients with liver disease. However, statins

can be used to treat dyslipidemia in patients with NAFLD and NASH without any concern regarding liver toxicity[1,66]. Statins have also been studied for the treatment of NAFLD and NASH but their efficacy for this indication is debated due to inconsistent results in clinical trials[66].

Sustained weight loss is indeed the most effective way to treat NAFLD and NASH. Unfortunately, this is difficult to achieve utilizing lifestyle modifications alone. Bariatric surgery, therefore, has an important role in the management of obese NASH patients. In one study, 85% of 109 morbidly obese patients with biopsy-proven NASH showed resolution of disease one year after bariatric surgery and the likelihood of improvement correlated with liver disease severity prior to surgery and degree of weight loss achieved[67]. A third of patients were also observed to have improvement in hepatic fibrosis[67]. In a systematic review and meta-analysis, bariatric surgery was associated with a significant reduction in the weighted incidence of a number of histological features of NAFLD including steatosis (50.2%), fibrosis (11.9%), hepatocyte ballooning (67.7%), and lobular inflammation (50.7%)[68]. A study conducted in the United States found bariatric surgery to be not just effective but also cost-effective in the treatment of obese patients with NASH[69].

In a study conducted in the UAE, 80 patients underwent bariatric surgery, either laparoscopic sleeve gastrectomy (n = 53) or mini-gastric bypass (n = 27). There was significant reduction in mean body weight at 3, 6, 12, and 24 mo (P < 0.001 for each time point). Of the 61.3% who had NAFLD, 22.4% showed improvement in sonographic features of hepatic steatosis with normalization of ALT[70]. In another study (n = 27) conducted in Saudi Arabia, after 3 mo of bariatric surgery, 66.6% of the patients with preoperative steatosis (median score 2) had reduced steatosis scores postoperatively (P = 0.025) and 68% of the patients had reduced fibrosis (median score 1) (P = 0.012). Also, NAFLD activity score was decreased from 4 (3-5) to 2 (1-3) (P = 0.004)[71]. However, it is also important to note that the use of bariatric surgery is limited by its cost and complications that are associated with any surgical procedure. As such, any advocacy for bariatric surgery must be tempered with a parallel education of its associated complications, which remains suboptimal in the region[72].

NASH-related cirrhosis is growing as an indication for liver transplantation

NASH is projected to become the most common indication for liver transplantation in near future[73]. With the availability of highly effective treatment options for hepatitis C virus (HCV)-related cirrhosis, NASH-related cirrhosis is emerging as the leading indication for liver transplantation worldwide.

In a study conducted in Saudi Arabia, over the course of the time period from January 2001 to December 2006, 50%, 17%, and 12% of the patients underwent liver transplant for HCV-induced cirrhosis, HBV-induced cirrhosis, and NASH-related cirrhosis, respectively. On the other hand, from January 2007 to January 2012, 35%, 16%, and 20% of the patients underwent transplantation for HCV-, HBV-, and NASH-induced cirrhosis, respectively, underscoring the evolving trends in the indications for liver transplantation[74].

Being a complex procedure, liver transplantation is associated with several limitations. Another important aspect to consider is that liver transplantation does not treat the comorbidities of NASH and therefore interventions to address the accompanying metabolic diseases is important, before and after transplantation[73].

Emerging therapies for NASH are awaited for more effective management of this disease

Currently, many new drugs are being developed with varying mechanisms of action, with the goal of improving hepatic steatosis, inflammation, liver cell injury, and fibrosis in patients with NAFLD[75]. Some of these include obeticholic acid (farnesoid X receptor agonist), elafibranor (a dual receptor peroxisome proliferator activated alpha/delta agonist), GS-9674 (farnesoid X receptor agonist), and GS-0976 (Acetyl-CoA carboxylase inhibitor). Future treatment options may also include combination therapies[75,76].

ADDRESSING NONALCOHOLIC FATTY LIVER DISEASE BURDEN IN THE MIDDLE EAST

Despite the high burden of NAFLD, there are no proper epidemiological studies or regional clinical guidelines that are relevant to these countries. The lack of properly

carried out community-based epidemiological studies is a particular concern, and has obvious fallouts on resource planning and allocation, and poses considerable difficulties to these countries' healthcare systems. To some extent, regional prevalence numbers remain best guess estimates, based in part on modeling analyses or otherwise on indirect markers of NAFLD such as obesity and T2DM[9]. This stresses an immediate need for adequately sampled, large-scale, nationwide surveys for NAFLD, where the prevalence across all population sectors, age groups, and geographic distributions is properly estimated. The relevant health authorities and ministries of these countries would be best positioned to lead such an initiative, executing it jointly with regional scientists and public health experts. Part of the epidemiological equation entails understanding the demographics and evolution of the disease, and towards this an access to a national registry for NASH is crucial.

There must be an urgent commitment to address the factors contributing to obesity in the Middle East, including dietary factors and inactivity, with particular focus on childhood obesity[77]. Dietary and lifestyle changes have a substantial impact on the natural course of the disease. As such, from a public health perspective, one of the most crucial aspects to focus on is to modify risk factors that are geared towards reducing obesity rates and achieving better dietary habits. Targeted measures such as taxation of beverages, marketing regulation, improving nutritional labeling, conducting awareness campaigns, and allocating subsidies to improve healthy eating could be implemented[78].

The dearth of algorithms for primary care referral is worrisome in view of the high prevalence of NAFLD in the Middle East. Primary health care should play a key role in the management of NAFLD, not only because of its pivotal role in health promotion and community care but also because specialized liver care is generally not prepared to receive such a large number of patients. Simple and affordable algorithms to identify patients at high risk of complications could be implemented in primary care to determine patients needing specialized care. A broad availability of transient elastography in primary healthcare centers must be envisioned in any NAFLD national plan, since significant hepatic disease may exist in non-obese individuals, and in those with normal liver enzymes[79]. This approach would contribute substantially to managing the intricacies of NAFLD-related disease burden within a healthcare system that provides early detection while preserving economic sustainability and equity[78].

Therefore, continuing education programs and awareness campaigns are crucial, as well as development and adaptation of clinical guidelines to protocols that identify patients who need specialist referral. Potential factors that need to be assessed include the role of non-liver specialists, and the implementation of community-based initiatives and civil society involvement aimed at NAFLD education, prevention, detection, and care.

This huge challenge facing our medical community must be effectively tackled with comprehensive, widely adopted, national (or regional) NAFLD plans, that start from awareness and education, emphasize prevention, set up early detection programs, and provide the recommended algorithms of care in a cost-effective and evidence-based manner. Such efforts should be led by robust research machinery that is able to predict, rationalize, and assess the effectiveness of hereupon-adopted strategies. Alliances will require to be forged not just across different institutes and affiliations, but also involving patients and community partners. However, most importantly, such plans would demand unprecedented attention to public health and can only succeed if they are coupled with an enforcement power that can guarantee their implementation[80].

CONCLUSION

The prevalence of NAFLD in the Middle East is increasing, along with its known associations of obesity, MetS, and T2DM, thereby placing a substantial burden on healthcare systems in the region. Suggested interventions to mitigate this challenge include education and awareness of patients and primary care providers regarding NAFLD; management of the risk factors and comorbidities; appropriate screening, evaluation, and diagnosis; and timely referral to hepatologists. This calls for a multidisciplinary approach involving primary care providers, gastroenterologists, endocrinologists, diabetologists, cardiologists, and hepatologists. There remains a need for clinical care pathways to help guide clinicians involved in the care of these patients[81-86].

Many challenges and unmet needs remain in the diagnosis and management of

NAFLD. There is a lack of reliable noninvasive tests for the accurate diagnosis of NASH. Also, there is no approved therapy for the treatment of NASH and current management is largely dependent on lifestyle modifications, which are challenging to initiate and sustain, resulting in inadequate weight reduction. Many therapies are currently under development and are keenly awaited. The availability of effective pharmacotherapy holds significant promise to improve the current landscape of available treatment options in NAFLD.

REFERENCES

1 **Chalasani N**, Younossi Z, Lavine JE, Charlton M, Cusi K, Rinella M, Harrison SA, Brunt EM, Sanyal AJ. The diagnosis and management of nonalcoholic fatty liver disease: Practice guidance from the American Association for the Study of Liver Diseases. *Hepatology* 2018; **67**: 328-357 [PMID: 28714183 DOI: 10.1002/hep.29367]

2 **European Association for the Study of the Liver (EASL)**. European Association for the Study of Diabetes (EASD); European Association for the Study of Obesity (EASO). EASL-EASD-EASO Clinical Practice Guidelines for the management of non-alcoholic fatty liver disease. *J Hepatol* 2016; **64**: 1388-1402 [PMID: 27062661 DOI: 10.1016/j.jhep.2015.11.004]

3 **Wong VW**, Wong GL, Choi PC, Chan AW, Li MK, Chan HY, Chim AM, Yu J, Sung JJ, Chan HL. Disease progression of non-alcoholic fatty liver disease: a prospective study with paired liver biopsies at 3 years. *Gut* 2010; **59**: 969-974 [PMID: 20581244 DOI: 10.1136/gut.2009.205088]

4 **Pais R**, Charlotte F, Fedchuk L, Bedossa P, Lebray P, Poynard T, Ratziu V; LIDO Study Group. A systematic review of follow-up biopsies reveals disease progression in patients with non-alcoholic fatty liver. *J Hepatol* 2013; **59**: 550-556 [PMID: 23665288 DOI: 10.1016/j.jhep.2013.04.027]

5 **Vuppalanchi R**, Chalasani N. Screening Strategies for Nonalcoholic Steatohepatitis in High-Risk Individuals: Trimming Away the Fat. *Dig Dis Sci* 2016; **61**: 1790-1792 [PMID: 27010545 DOI: 10.1007/s10620-016-4134-1]

6 **Sayiner M**, Koenig A, Henry L, Younossi ZM. Epidemiology of Nonalcoholic Fatty Liver Disease and Nonalcoholic Steatohepatitis in the United States and the Rest of the World. *Clin Liver Dis* 2016; **20**: 205-214 [PMID: 27063264 DOI: 10.1016/j.cld.2015.10.001]

7 **Bellentani S**. The epidemiology of non-alcoholic fatty liver disease. *Liver Int* 2017; **37** Suppl 1: 81-84 [PMID: 28052624 DOI: 10.1111/liv.13299]

8 **Younossi ZM**, Koenig AB, Abdelatif D, Fazel Y, Henry L, Wymer M. Global epidemiology of nonalcoholic fatty liver disease-Meta-analytic assessment of prevalence, incidence, and outcomes. *Hepatology* 2016; **64**: 73-84 [PMID: 26707365 DOI: 10.1002/hep.28431]

9 **Alswat K**, Aljumah AA, Sanai FM, Abaalkhail F, Alghamdi M, Al Hamoudi WK, Al Khathlan A, Al Quraishi H, Al Rifai A, Al Zaabi M, Babatin MA, Estes C, Hashim A, Razavi H. Nonalcoholic fatty liver disease burden - Saudi Arabia and United Arab Emirates, 2017-2030. *Saudi J Gastroenterol* 2018; **24**: 211-219 [PMID: 29956688 DOI: 10.4103/sjg.SJG_122_18]

10 **Younossi ZM**, Yu ML, El Kassas M, Esmat G, Yilmaz Y, Fernandez MC, Duseja AK, Isakov VA, Buti M, Mendez□Sanchez N, Papatheodoridis GV, Chan WK, George J, Bugianesi E, Romero□Gomez M, Roberts SK, Younes Z, Wai□Sun Wong V, Fan JG, Eguchi Y, Gordon SC, Ahmed A, Ong J, Jacobson IM, Rinella ME, Hamid SS, Ziayee M, Younossi I, Lam BP, Arrese M, Nader F, Racila A, Henry L, Stepanova M on behalf of the Global NASH Council. Clinical and Patient□Reported Outcomes Data for Patients with Non□Alcoholic Fatty Liver Disease (NAFLD) and Non□Alcoholic Steatohepatitis (NASH) Across the World: Data from the Global NASH Registry. *Hepatology* 2019; **70**: i-ii, 1-1476 Available from: https://aasldpubs.onlinelibrary.wiley.com/doi/10.1002/hep.30941

11 **Lonardo A**, Nascimbeni F, Maurantonio M, Marrazzo A, Rinaldi L, Adinolfi LE. Nonalcoholic fatty liver disease: Evolving paradigms. *World J Gastroenterol* 2017; **23**: 6571-6592 [PMID: 29085206 DOI: 10.3748/wjg.v23.i36.6571]

12 **Hajat C**, Harrison O, Al Siksek Z. Weqaya: a population-wide cardiovascular screening program in Abu Dhabi, United Arab Emirates. *Am J Public Health* 2012; **102**: 909-914 [PMID: 21940918 DOI: 10.2105/AJPH.2011.300290]

13 **Radwan H**, Ballout RA, Hasan H, Lessan N, Karavetian M, Rizk R. The Epidemiology and Economic Burden of Obesity and Related Cardiometabolic Disorders in the United Arab Emirates: A Systematic Review and Qualitative Synthesis. *J Obes* 2018; **2018**: 2185942 [PMID: 30652030 DOI: 10.1155/2018/2185942]

14 **Memish ZA**, El Bcheraoui C, Tuffaha M, Robinson M, Daoud F, Jaber S, Mikhitarian S, Al Saeedi M, AlMazroa MA, Mokdad AH, Al Rabeeah AA. Obesity and associated factors--Kingdom of Saudi Arabia, 2013. *Prev Chronic Dis* 2014; **11**: E174 [PMID: 25299980 DOI: 10.5888/pcd11.140236]

15 **Al-Quwaidhi AJ**, Pearce MS, Critchley JA, Sobngwi E, O'Flaherty M. Trends and future projections of the prevalence of adult obesity in Saudi Arabia, 1992-2022. *East Mediterr Health J* 2014; **20**: 589-595 [PMID: 25356689 DOI: 10.26719/2014.20.10.589]

16 **Polyzos SA**, Kountouras J, Mantzoros CS. Obesity and nonalcoholic fatty liver disease: From pathophysiology to therapeutics. *Metabolism* 2019; **92**: 82-97 [PMID: 30502373 DOI: 10.1016/j.metabol.2018.11.014]

17 **Alqahtani A**, Elahmedi M, Alswat K, Arafah M, Fagih M, Lee J. Features of nonalcoholic steatohepatitis in severely obese children and adolescents undergoing sleeve gastrectomy. *Surg Obes Relat Dis* 2017; **13**: 1599-1609 [PMID: 28600116 DOI: 10.1016/j.soard.2017.04.005]

18 **International Diabetes Federation**, Diabetes Atlas. Eighth Edition 2017. [accessed 2019 Nov 07]. In: idf.org [Internet]. Available from: https://www.idf.org/our-network/regions-members/middle-east-and-

north-africa/diabetes-in-mena.html
19 **Alzaid A**. Diabetes: A tale of two cultures. 2012; **12**: 57-59
20 **Dai W**, Ye L, Liu A, Wen SW, Deng J, Wu X, Lai Z. Prevalence of nonalcoholic fatty liver disease in patients with type 2 diabetes mellitus: A meta-analysis. *Medicine (Baltimore)* 2017; **96**: e8179 [PMID: 28953675 DOI: 10.1097/MD.0000000000008179]
21 **Younossi ZM**, Golabi P, de Avila L, Paik JM, Srishord M, Fukui N, Qiu Y, Burns L, Afendy A, Nader F. The global epidemiology of NAFLD and NASH in patients with type 2 diabetes: A systematic review and meta-analysis. *J Hepatol* 2019; **71**: 793-801 [PMID: 31279902 DOI: 10.1016/j.jhep.2019.06.021]
22 **Amiri Dash Atan N**, Koushki M, Motedayen M, Dousti M, Sayehmiri F, Vafaee R, Norouzinia M, Gholami R. Type 2 diabetes mellitus and non-alcoholic fatty liver disease: a systematic review and meta-analysis. *Gastroenterol Hepatol Bed Bench* 2017; **10**: S1-S7 [PMID: 29511464]
23 **Mantovani A**, Byrne CD, Bonora E, Targher G. Nonalcoholic Fatty Liver Disease and Risk of Incident Type 2 Diabetes: A Meta-analysis. *Diabetes Care* 2018; **41**: 372-382 [PMID: 29358469 DOI: 10.2337/dc17-1902]
24 **Bazick J**, Donithan M, Neuschwander-Tetri BA, Kleiner D, Brunt EM, Wilson L, Doo E, Lavine J, Tonascia J, Loomba R. Clinical Model for NASH and Advanced Fibrosis in Adult Patients With Diabetes and NAFLD: Guidelines for Referral in NAFLD. *Diabetes Care* 2015; **38**: 1347-1355 [PMID: 25887357 DOI: 10.2337/dc14-1239]
25 **Ansarimoghaddam A**, Adineh HA, Zareban I, Iranpour S, HosseinZadeh A, Kh F. Prevalence of metabolic syndrome in Middle-East countries: Meta-analysis of cross-sectional studies. *Diabetes Metab Syndr* 2018; **12**: 195-201 [PMID: 29203060 DOI: 10.1016/j.dsx.2017.11.004]
26 **Al-Rubeaan K**, Bawazeer N, Al Farsi Y, Youssef AM, Al-Yahya AA, AlQumaidi H, Al-Malki BM, Naji KA, Al-Shehri K, Al Rumaih FI. Prevalence of metabolic syndrome in Saudi Arabia - a cross sectional study. *BMC Endocr Disord* 2018; **18**: 16 [PMID: 29506520 DOI: 10.1186/s12902-018-0244-4]
27 **Marchesini G**, Bugianesi E, Forlani G, Cerrelli F, Lenzi M, Manini R, Natale S, Vanni E, Villanova N, Melchionda N, Rizzetto M. Nonalcoholic fatty liver, steatohepatitis, and the metabolic syndrome. *Hepatology* 2003; **37**: 917-923 [PMID: 12668987 DOI: 10.1053/jhep.2003.50161]
28 **Brunt EM**, Kleiner DE, Wilson LA, Belt P, Neuschwander-Tetri BA; NASH Clinical Research Network (CRN). Nonalcoholic fatty liver disease (NAFLD) activity score and the histopathologic diagnosis in NAFLD: distinct clinicopathologic meanings. *Hepatology* 2011; **53**: 810-820 [PMID: 21319198 DOI: 10.1002/hep.24127]
29 **Babusik P**, Bilal M, Duris I. Nonalcoholic fatty liver disease of two ethnic groups in Kuwait: comparison of prevalence and risk factors. *Med Princ Pract* 2012; **21**: 56-62 [PMID: 22024606 DOI: 10.1159/000331591]
30 **Iqbal U**, Perumpail BJ, Akhtar D, Kim D, Ahmed A. The Epidemiology, Risk Profiling and Diagnostic Challenges of Nonalcoholic Fatty Liver Disease. *Medicines (Basel)* 2019; 6 [PMID: 30889791 DOI: 10.3390/medicines6010041]
31 **Tesfay M**, Goldkamp WJ, Neuschwander-Tetri BA. NASH: The Emerging Most Common Form of Chronic Liver Disease. *Mo Med* 2018; **115**: 225-229 [PMID: 30228727]
32 **National Guideline Centre (UK)**. 2016 [PMID: 27441333]
33 **Wong VW**, Chan WK, Chitturi S, Chawla Y, Dan YY, Duseja A, Fan J, Goh KL, Hamaguchi M, Hashimoto E, Kim SU, Lesmana LA, Lin YC, Liu CJ, Ni YH, Sollano J, Wong SK, Wong GL, Chan HL, Farrell G. Asia-Pacific Working Party on Non-alcoholic Fatty Liver Disease guidelines 2017-Part 1: Definition, risk factors and assessment. *J Gastroenterol Hepatol* 2018; **33**: 70-85 [PMID: 28670712 DOI: 10.1111/jgh.13857]
34 **Spengler EK**, Loomba R. Recommendations for Diagnosis, Referral for Liver Biopsy, and Treatment of Nonalcoholic Fatty Liver Disease and Nonalcoholic Steatohepatitis. *Mayo Clin Proc* 2015; **90**: 1233-1246 [PMID: 26219858 DOI: 10.1016/j.mayocp.2015.06.013]
35 **Tsai E**, Lee TP. Diagnosis and Evaluation of Nonalcoholic Fatty Liver Disease/Nonalcoholic Steatohepatitis, Including Noninvasive Biomarkers and Transient Elastography. *Clin Liver Dis* 2018; **22**: 73-92 [PMID: 29128062 DOI: 10.1016/j.cld.2017.08.004]
36 **Younossi ZM**, Stepanova M, Lawitz EJ, Reddy KR, Wai-Sun Wong V, Mangia A, Muir AJ, Jacobson I, Djedjos CS, Gaggar A, Myers RP, Younossi I, Nader F, Racila A. Patients With Nonalcoholic Steatohepatitis Experience Severe Impairment of Health-Related Quality of Life. *Am J Gastroenterol* 2019; **114**: 1636-1641 [PMID: 31464743 DOI: 10.14309/ajg.0000000000000375]
37 **Neuschwander-Tetri BA**. Non-alcoholic fatty liver disease. *BMC Med* 2017; **15**: 45 [PMID: 28241825 DOI: 10.1186/s12916-017-0806-8]
38 **Day J**, Patel P, Parkes J, Rosenberg W. Derivation and Performance of Standardized Enhanced Liver Fibrosis (ELF) Test Thresholds for the Detection and Prognosis of Liver Fibrosis. *J Appl Lab Med* 2019; **3**: 815-826 [PMID: 31639756 DOI: 10.1373/jalm.2018.027359]
39 **Festi D**, Schiumerini R, Marzi L, Di Biase AR, Mandolesi D, Montrone L, Scaioli E, Bonato G, Marchesini-Reggiani G, Colecchia A. Review article: the diagnosis of non-alcoholic fatty liver disease -- availability and accuracy of non-invasive methods. *Aliment Pharmacol Ther* 2013; **37**: 392-400 [PMID: 23278163 DOI: 10.1111/apt.12186]
40 **Demir M**, Lang S, Nierhoff D, Drebber U, Hardt A, Wedemeyer I, Schulte S, Quasdorff M, Goeser T, Töx U, Steffen HM. Stepwise combination of simple noninvasive fibrosis scoring systems increases diagnostic accuracy in nonalcoholic fatty liver disease. *J Clin Gastroenterol* 2013; **47**: 719-726 [PMID: 23442837 DOI: 10.1097/MCG.0b013e3182819a89]
41 **Petta S**, Vanni E, Bugianesi E, Di Marco V, Cammà C, Cabibi D, Mezzabotta L, Craxì A. The combination of liver stiffness measurement and NAFLD fibrosis score improves the noninvasive diagnostic accuracy for severe liver fibrosis in patients with nonalcoholic fatty liver disease. *Liver Int* 2015; **35**: 1566-1573 [PMID: 24798049 DOI: 10.1111/liv.12584]
42 **Benedict M**, Zhang X. Non-alcoholic fatty liver disease: An expanded review. *World J Hepatol* 2017; **9**: 715-732 [PMID: 28652891 DOI: 10.4254/wjh.v9.i16.715]
43 **Angulo P**, Kleiner DE, Dam-Larsen S, Adams LA, Bjornsson ES, Charatcharoenwitthaya P, Mills PR,

Keach JC, Lafferty HD, Stahler A, Haflidadottir S, Bendtsen F. Liver Fibrosis, but No Other Histologic Features, Is Associated With Long-term Outcomes of Patients With Nonalcoholic Fatty Liver Disease. *Gastroenterology* 2015; **149**: 389-397.e10 [PMID: 25935633 DOI: 10.1053/j.gastro.2015.04.043]

44 **Hagström H**, Nasr P, Ekstedt M, Hammar U, Stål P, Hultcrantz R, Kechagias S. Fibrosis stage but not NASH predicts mortality and time to development of severe liver disease in biopsy-proven NAFLD. *J Hepatol* 2017; **67**: 1265-1273 [PMID: 28803953 DOI: 10.1016/j.jhep.2017.07.027]

45 **Younossi ZM**, Stepanova M, Rafiq N, Makhlouf H, Younoszai Z, Agrawal R, Goodman Z. Pathologic criteria for nonalcoholic steatohepatitis: interprotocol agreement and ability to predict liver-related mortality. *Hepatology* 2011; **53**: 1874-1882 [PMID: 21360720 DOI: 10.1002/hep.24268]

46 **Dulai PS**, Singh S, Patel J, Soni M, Prokop LJ, Younossi Z, Sebastiani G, Ekstedt M, Hagstrom H, Nasr P, Stal P, Wong VW, Kechagias S, Hultcrantz R, Loomba R. Increased risk of mortality by fibrosis stage in nonalcoholic fatty liver disease: Systematic review and meta-analysis. *Hepatology* 2017; **65**: 1557-1565 [PMID: 28130788 DOI: 10.1002/hep.29085]

47 **Alexander M**, Loomis AK, Fairburn-Beech J, van der Lei J, Duarte-Salles T, Prieto-Alhambra D, Ansell D, Pasqua A, Lapi F, Rijnbeek P, Mosseveld M, Avillach P, Egger P, Kendrick S, Waterworth DM, Sattar N, Alazawi W. Real-world data reveal a diagnostic gap in non-alcoholic fatty liver disease. *BMC Med* 2018; **16**: 130 [PMID: 30099968 DOI: 10.1186/s12916-018-1103-x]

48 **Katsagoni CN**, Georgoulis M, Papatheodoridis GV, Panagiotakos DB, Kontogianni MD. Effects of lifestyle interventions on clinical characteristics of patients with non-alcoholic fatty liver disease: A meta-analysis. *Metabolism* 2017; **68**: 119-132 [PMID: 28183444 DOI: 10.1016/j.metabol.2016.12.006]

49 **Bradford V**, Dillon J, Miller M. Lifestyle interventions for the treatment of non-alcoholic fatty liver disease. *Hepat Med* 2014; **6**: 1-10 [PMID: 24826079 DOI: 10.2147/HMER.S34472]

50 **Musso G**, Cassader M, Rosina F, Gambino R. Impact of current treatments on liver disease, glucose metabolism and cardiovascular risk in non-alcoholic fatty liver disease (NAFLD): a systematic review and meta-analysis of randomised trials. *Diabetologia* 2012; **55**: 885-904 [PMID: 22278337 DOI: 10.1007/s00125-011-2446-4]

51 **Hannah WN Jr**, Harrison SA. Lifestyle and Dietary Interventions in the Management of Nonalcoholic Fatty Liver Disease. *Dig Dis Sci* 2016; **61**: 1365-1374 [PMID: 27052013 DOI: 10.1007/s10620-016-4153-y]

52 **Glass LM**, Dickson RC, Anderson JC, Suriawinata AA, Putra J, Berk BS, Toor A. Total body weight loss of ≥ 10 % is associated with improved hepatic fibrosis in patients with nonalcoholic steatohepatitis. *Dig Dis Sci* 2015; **60**: 1024-1030 [PMID: 25354830 DOI: 10.1007/s10620-014-3380-3]

53 **Haukeland JW**, Konopski Z, Eggesbø HB, von Volkmann HL, Raschpichler G, Bjøro K, Haaland T, Løberg EM, Birkeland K. Metformin in patients with non-alcoholic fatty liver disease: a randomized, controlled trial. *Scand J Gastroenterol* 2009; **44**: 853-860 [PMID: 19811343 DOI: 10.1080/00365520902845268]

54 **Shields WW**, Thompson KE, Grice GA, Harrison SA, Coyle WJ. The Effect of Metformin and Standard Therapy versus Standard Therapy alone in Nondiabetic Patients with Insulin Resistance and Nonalcoholic Steatohepatitis (NASH): A Pilot Trial. *Therap Adv Gastroenterol* 2009; **2**: 157-163 [PMID: 21180541 DOI: 10.1177/1756283X09105462]

55 **Nair S**, Diehl AM, Wiseman M, Farr GH Jr, Perrillo RP. Metformin in the treatment of non-alcoholic steatohepatitis: a pilot open label trial. *Aliment Pharmacol Ther* 2004; **20**: 23-28 [PMID: 15225167 DOI: 10.1111/j.1365-2036.2004.02025.x]

56 **Belfort R**, Harrison SA, Brown K, Darland C, Finch J, Hardies J, Balas B, Gastaldelli A, Tio F, Pulcini J, Berria R, Ma JZ, Dwivedi S, Havranek R, Fincke C, DeFronzo R, Bannayan GA, Schenker S, Cusi K. A placebo-controlled trial of pioglitazone in subjects with nonalcoholic steatohepatitis. *N Engl J Med* 2006; **355**: 2297-2307 [PMID: 17135584 DOI: 10.1056/NEJMoa060326]

57 **Cusi K**, Orsak B, Bril F, Lomonaco R, Hecht J, Ortiz-Lopez C, Tio F, Hardies J, Darland C, Musi N, Webb A, Portillo-Sanchez P. Long-Term Pioglitazone Treatment for Patients With Nonalcoholic Steatohepatitis and Prediabetes or Type 2 Diabetes Mellitus: A Randomized Trial. *Ann Intern Med* 2016; **165**: 305-315 [PMID: 27322798 DOI: 10.7326/M15-1774]

58 **Aithal GP**, Thomas JA, Kaye PV, Lawson A, Ryder SD, Spendlove I, Austin AS, Freeman JG, Morgan L, Webber J. Randomized, placebo-controlled trial of pioglitazone in nondiabetic subjects with nonalcoholic steatohepatitis. *Gastroenterology* 2008; **135**: 1176-1184 [PMID: 18718471 DOI: 10.1053/j.gastro.2008.06.047]

59 **Xu R**, Tao A, Zhang S, Deng Y, Chen G. Association between vitamin E and non-alcoholic steatohepatitis: a meta-analysis. *Int J Clin Exp Med* 2015; **8**: 3924-3934 [PMID: 26064294]

60 **Sato K**, Gosho M, Yamamoto T, Kobayashi Y, Ishii N, Ohashi T, Nakade Y, Ito K, Fukuzawa Y, Yoneda M. Vitamin E has a beneficial effect on nonalcoholic fatty liver disease: a meta-analysis of randomized controlled trials. *Nutrition* 2015; **31**: 923-930 [PMID: 26059365 DOI: 10.1016/j.nut.2014.11.018]

61 **Miller ER 3rd**, Pastor-Barriuso R, Dalal D, Riemersma RA, Appel LJ, Guallar E. Meta-analysis: high-dosage vitamin E supplementation may increase all-cause mortality. *Ann Intern Med* 2005; **142**: 37-46 [PMID: 15537682 DOI: 10.7326/0003-4819-142-1-200501040-00110]

62 **Klein EA**, Thompson IM Jr, Tangen CM, Crowley JJ, Lucia MS, Goodman PJ, Minasian LM, Ford LG, Parnes HL, Gaziano JM, Karp DD, Lieber MM, Walther PJ, Klotz L, Parsons JK, Chin JL, Darke AK, Lippman SM, Goodman GE, Meyskens FL Jr, Baker LH. Vitamin E and the risk of prostate cancer: the Selenium and Vitamin E Cancer Prevention Trial (SELECT). *JAMA* 2011; **306**: 1549-1556 [PMID: 21990298 DOI: 10.1001/jama.2011.1437]

63 **Abner EL**, Schmitt FA, Mendiondo MS, Marcum JL, Kryscio RJ. Vitamin E and all-cause mortality: a meta-analysis. *Curr Aging Sci* 2011; **4**: 158-170 [PMID: 21235492 DOI: 10.2174/1874609811104020158]

64 **Said A**, Akhter A. Meta-Analysis of Randomized Controlled Trials of Pharmacologic Agents in Non-alcoholic Steatohepatitis. *Ann Hepatol* 2017; **16**: 538-547 [PMID: 28611274 DOI: 10.5604/01.3001.0010.0284]

65 **Patil R**, Sood GK. Non-alcoholic fatty liver disease and cardiovascular risk. *World J Gastrointest Pathophysiol* 2017; **8**: 51-58 [PMID: 28573067 DOI: 10.4291/wjgp.v8.i2.51]

66 **Pastori D**, Polimeni L, Baratta F, Pani A, Del Ben M, Angelico F. The efficacy and safety of statins for the treatment of non-alcoholic fatty liver disease. *Dig Liver Dis* 2015; **47**: 4-11 [PMID: 25224698 DOI: 10.1016/j.dld.2014.07.170]

67 **Lassailly G**, Caiazzo R, Buob D, Pigeyre M, Verkindt H, Labreuche J, Raverdy V, Leteurtre E, Dharancy S, Louvet A, Romon M, Duhamel A, Pattou F, Mathurin P. Bariatric Surgery Reduces Features of Nonalcoholic Steatohepatitis in Morbidly Obese Patients. *Gastroenterology* 2015; **149**: 379-88; quiz e15-6 [PMID: 25917783 DOI: 10.1053/j.gastro.2015.04.014]

68 **Bower G**, Toma T, Harling L, Jiao LR, Efthimiou E, Darzi A, Athanasiou T, Ashrafian H. Bariatric Surgery and Non-Alcoholic Fatty Liver Disease: a Systematic Review of Liver Biochemistry and Histology. *Obes Surg* 2015; **25**: 2280-2289 [PMID: 25917981 DOI: 10.1007/s11695-015-1691-x]

69 **Klebanoff MJ**, Corey KE, Chhatwal J, Kaplan LM, Chung RT, Hur C. Bariatric surgery for nonalcoholic steatohepatitis: A clinical and cost-effectiveness analysis. *Hepatology* 2017; **65**: 1156-1164 [PMID: 27880977 DOI: 10.1002/hep.28958]

70 **Alnageeb H**, Abdelgadir E, Khalifa A, Suliman M, Gautam SC, Layani L, Subramaniam S, Bashier A. Efficacy of bariatric surgery in improving metabolic outcomes in patients with diabetes. A 24-month follow-up study from a single center in the UAE. *Diabetes Metab Syndr Obes* 2018; **11**: 459-467 [PMID: 30214265 DOI: 10.2147/DMSO.S176761]

71 **Aldoheyan T**, Hassanain M, Al-Mulhim A, Al-Sabhan A, Al-Amro S, Bamehriz F, Al-Khalidi H. The effects of bariatric surgeries on nonalcoholic fatty liver disease. *Surg Endosc* 2017; **31**: 1142-1147 [PMID: 27405478 DOI: 10.1007/s00464-016-5082-8]

72 **Alamri AA**, Alsadiqi AI, Dahlawi A, Alghamdi A, Alnefaie M, Alhazmi M, Tewfik O, Almaymuni A, Al-Abbadi H, Mosli M. Are patients aware of potential risks of weight reduction surgery? An internet based survey. *Saudi J Gastroenterol* 2019; **25**: 97-100 [PMID: 30479318 DOI: 10.4103/sjg.SJG_232_18]

73 **Bzowej NH**. Nonalcoholic steatohepatitis: the new frontier for liver transplantation. *Curr Opin Organ Transplant* 2018; **23**: 169-174 [PMID: 29356708 DOI: 10.1097/MOT.0000000000000502]

74 **Al-Hamoudi W**, Elsiesy H, Bendahmash A, Al-Masri N, Ali S, Allam N, Al Sofayan M, Al Bahili H, Al Sebayel M, Broering D, Saab S, Abaalkhail F. Liver transplantation for hepatitis B virus: Decreasing indication and changing trends. *World J Gastroenterol* 2015; **21**: 8140-8147 [PMID: 26185387 DOI: 10.3748/wjg.v21.i26.8140]

75 **Younossi ZM**, Loomba R, Rinella ME, Bugianesi E, Marchesini G, Neuschwander-Tetri BA, Serfaty L, Negro F, Caldwell SH, Ratziu V, Corey KE, Friedman SL, Abdelmalek MF, Harrison SA, Sanyal AJ, Lavine JE, Mathurin P, Charlton MR, Chalasani NP, Anstee QM, Kowdley KV, George J, Goodman ZD, Lindor K. Current and future therapeutic regimens for nonalcoholic fatty liver disease and nonalcoholic steatohepatitis. *Hepatology* 2018; **68**: 361-371 [PMID: 29222911 DOI: 10.1002/hep.29724]

76 **Connolly JJ**, Ooka K, Lim JK. Future Pharmacotherapy for Non-alcoholic Steatohepatitis (NASH): Review of Phase 2 and 3 Trials. *J Clin Transl Hepatol* 2018; **6**: 264-275 [PMID: 30271738 DOI: 10.14218/JCTH.2017.00056]

77 **Al-Hussaini A**, Bashir MS, Khormi M, AlTuraiki M, Alkhamis W, Alrajhi M, Halal T. Overweight and obesity among Saudi children and adolescents: Where do we stand today? *Saudi J Gastroenterol* 2019; **25**: 229-235 [PMID: 31187784 DOI: 10.4103/sjg.SJG_617_18]

78 **Lazarus JV**, Ekstedt M, Marchesini G, Mullen J, Novak K, Pericàs JM, Roel E, Romero-Gómez M, Ratziu V, Tacke F, Cortez-Pinto H, Anstee QM; EASL International Liver Foundation NAFLD Policy Review Collaborators. A cross-sectional study of the public health response to non-alcoholic fatty liver disease in Europe. *J Hepatol* 2020; **72**: 14-24 [PMID: 31518646 DOI: 10.1016/j.jhep.2019.08.027]

79 **Alsaif FA**, Alqahtani SH, Alsadoon AM, Alswat KA, Abdo AA, Hassanain MM, Alsharabi AB, Aljuhani GR, Alkhalidi HM, Elsharkawy MS, Alotaibi MA, Sanai FM, Al-Hamoudi WK. Prevalence of biopsy-proven nonalcoholic fatty liver among patients with gallstone disease. *Saudi J Gastroenterol* 2020 [PMID: 32341228 DOI: 10.4103/sjg.SJG_29_20]

80 **Alaama T**. Nonalcoholic fatty liver disease: One more reason to strengthen public health. *Saudi J Gastroenterol* 2018; **24**: 199-200 [PMID: 30052238 DOI: 10.4103/sjg.SJG_266_18]

81 **Haroun D**, Mechli R, Sahuri R, AlKhatib S, Obeid O, El Mallah C, Wood L, AlSuwaidi K. Metabolic syndrome among adolescents in Dubai, United Arab Emirates, is attributable to the high prevalence of low HDL levels: a cross-sectional study. *BMC Public Health* 2018; **18**: 1284 [PMID: 30463538 DOI: 10.1186/s12889-018-6215-x]

82 **Al Zenki S**, Al Omirah H, Al Hooti S, Al Hamad N, Jackson RT, Rao A, Al Jahmah N, Al Obaid I, Al Ghanim J, Al Somaie M, Zaghloul S, Al Othman A. High prevalence of metabolic syndrome among Kuwaiti adults--a wake-up call for public health intervention. *Int J Environ Res Public Health* 2012; **9**: 1984-1996 [PMID: 22754486 DOI: 10.3390/ijerph9051984]

83 **Weiderpass E**, Botteri E, Longenecker JC, Alkandari A, Al-Wotayan R, Al Duwairi Q, Tuomilehto J. The Prevalence of Overweight and Obesity in an Adult Kuwaiti Population in 2014. *Front Endocrinol (Lausanne)* 2019; **10**: 449 [PMID: 31338067 DOI: 10.3389/fendo.2019.00449]

84 **Awad AI**, Alsaleh FM. 10-year risk estimation for type 2 diabetes mellitus and coronary heart disease in Kuwait: a cross-sectional population-based study. *PLoS One* 2015; **10**: e0116742 [PMID: 25629920 DOI: 10.1371/journal.pone.0116742]

85 **Cobbina E**, Akhlaghi F. Non-alcoholic fatty liver disease (NAFLD) - pathogenesis, classification, and effect on drug metabolizing enzymes and transporters. *Drug Metab Rev* 2017; **49**: 197-211 [PMID: 28303724 DOI: 10.1080/03602532.2017.1293683]

86 **Leung JC**, Loong TC, Pang J, Wei JL, Wong VW. Invasive and non-invasive assessment of portal hypertension. *Hepatol Int* 2018; **12**: 44-55 [PMID: 28361299 DOI: 10.1007/s12072-017-9795-0]

World Journal of Gastroenterology

Submit a Manuscript: https://www.f6publishing.com

World J Gastroenterol 2020 July 7; 26(25): 3542-3561

DOI: 10.3748/wjg.v26.i25.3542

ISSN 1007-9327 (print) ISSN 2219-2840 (online)

REVIEW

Practical review for diagnosis and clinical management of perihilar cholangiocarcinoma

Daniele Dondossola, Michele Ghidini, Francesco Grossi, Giorgio Rossi, Diego Foschi

ORCID number: Daniele Dondossola 0000-0002-4374-3184; Michele Ghidini 0000-0001-5435-1218; Francesco Grossi 0000-0001-8412-3136; Giorgio Rossi 0000-0002-5588-1306; Diego Foschi 0000-0002-7702-8226.

Author contributions: Dondossola D and Ghidini M drafted the paper; Dondossola D and Foschi D conceptualized the study; Grossi F reviewed the paper; Rossi G and Foschi D approved the final manuscript.

Conflict-of-interest statement: Authors declare no conflict of interests for this article.

Manuscript source: Invited manuscript

Daniele Dondossola, Giorgio Rossi, General and Liver Transplant Surgery Unit, Fondazione IRCCS Ca' Granda, Ospedale Maggiore Policlinico, Milan 20122, Italy

Daniele Dondossola, Giorgio Rossi, Department of Pathophysiology and Transplantation, Università degli Studi of Milan, Milan 20122, Italy

Michele Ghidini, Francesco Grossi, Medical Oncology Unit, Fondazione IRCCS Ca' Granda Ospedale Maggiore Policlinico, Milan 20122, Italy

Diego Foschi, Department of Biomedical and Clinical Sciences "Luigi Sacco", L. Sacco Hospital, Università degli Studi of Milan, Milan 20157, Italy

Corresponding author: Dondossola Daniele, MD, Postdoctoral Fellow, Surgeon, General and Liver Transplant Surgery Unit, Fondazione IRCCS Ca' Granda Ospedale Maggiore Policlinico, Via Franscesco Sforza, 35, Milan 20122, Italy. dondossola.daniele@gmail.com

Abstract

Cholangiocarcinoma (CCC) is the most aggressive malignant tumor of the biliary tract. Perihilar CCC (pCCC) is the most common CCC and is burdened by a complicated diagnostic iter and its anatomical location makes surgical approach burden by poor results. Besides its clinical presentation, a multimodal diagnostic approach should be carried on by a tertiary specialized center to avoid miss-diagnosis. Preoperative staging must consider the extent of liver resection to avoid post-surgical hepatic failure. During staging iter, magnetic resonance can obtain satisfactory cholangiographic images, while invasive techniques should be used if bile duct samples are needed. Consistently, to improve diagnostic potential, bile duct drainage is not necessary in jaundice, while it is indicated in refractory cholangitis or when liver hypertrophy is needed. Once resecability criteria are identified, the extent of liver resection is secondary to the longitudinal spread of CCC. While in the past type IV pCCC was not considered resectable, some authors reported good results after their treatment. Conversely, in selected unresectable cases, liver transplantation could be a valuable option. Adjuvant chemotherapy is the standard of care for resected patients, while neoadjuvant approach has growing evidences. If curative resection is not achieved, radiotherapy can be added to chemotherapy. This multistep curative iter must be carried on in specialized centers. Hence, the aim of this review is to highlight the main steps and pitfalls of the diagnostic and therapeutic approach to pCCC with a peculiar attention to type IV pCCC.

Received: December 31, 2019
Peer-review started: December 31, 2019
First decision: January 16, 2020
Revised: June 5, 2020
Accepted: June 19, 2020
Article in press: June 19, 2020
Published online: July 7, 2020

P-Reviewer: Yi PS, Zeng YY
S-Editor: Zhang H
L-Editor: A
E-Editor: Ma YJ

Key words: Perihilar cholangiocarncioma; Liver resection; Biliary drainage; Neo-adjuvant therapy; Type IV cholangiocarcinoma; Klatskin tumor

Core tip: Perihilar cholangiocarncioma (pCCC) is burdened by a complicated diagnostic iter and, due to its anatomical location and biological characteristics, is affected by poor results. Confounding factors, such as biliary decompression, must be avoided during diagnosis and evaluation of longitudinal extension of the tumor. While surgical advances allows the extension of surgical indication (especially for type IV pCCC and portal invasion), adjuvant chemotherapy should be administered to improve post-surgical results. Herein, a highlight on diagnostic and therapeutic management is here provided.

Citation: Dondossola D, Ghidini M, Grossi F, Rossi G, Foschi D. Practical review for diagnosis and clinical management of perihilar cholangiocarcinoma. *World J Gastroenterol* 2020; 26(25): 3542-3561
URL: https://www.wjgnet.com/1007-9327/full/v26/i25/3542.htm
DOI: https://dx.doi.org/10.3748/wjg.v26.i25.3542

INTRODUCTION

Cholangiocarcinoma (CCC) is the most frequent and aggressive malignant tumor of the biliary tract. It arises from the epithelial cells of a bile duct and from their progenitor cells (a group of heterogeneous dynamic cells lining the biliary tree). CCC develops either within the duct or shaping a mass infiltrating the adjacent tissue (mass forming cholangiocarcinoma)[1].

CCC is commonly classified according to the site of invasion into intrahepatic and extrahepatic, itself divided into hilar/perihilar [or Klatskin tumor, perihilar CCC (pCCC)] and distal. Extrahepatic CCC are the most common among CCC[2]. pCCC is defined as CCC located in the extrahepatic biliary tree proximal to the origin of the cystic duct[3,4]. It is burdened by a complicated diagnostic iter and its anatomical location makes the surgical site less accessible, causing higher unresectable rates[5].

In this review, we will focus our attention on diagnostic and surgical approach to pCCC in order to underline the key points in its management.

EPIDEMIOLOGY AND ETIOPATHOGENESIS

CCC is a heterogeneous group of malignancies that represent the 3% of all gastrointestinal tumors[6]. Among CCC, 75% are extrahepatic CCC and half of them pCCC. The incidence of extrahepatic CCC varies worldwide from 0.3-3.5 per 100000 inhabitants/year in North America to 90/100000 inhabitants/year in Thailand. Among Mediterranean region, the incidence is fixed around 7.5/10000 inhabitants/year[7,8]. In Italy 5400 new cases/year are expected[9]. Extrahepatic CCC represent 1% of new neoplastic diagnosis in male and 1.4% in female, with a reduction in the female sex during the last few years[10]. The median age at diagnosis is 50 years; almost null risk is reported before 40 years, while a peak is registered around 70 years[9].

The identification of risk factors for pCCC is some-like difficult due to many reasons; first of all, papers do not often distinguish CCC into intrahepatic or extrahepatic and merge CCC with gallbladder carcinomas. Furthermore, cases are frequently isolated with no identifiable risk factors. The published risk factors can be divided in[11,12]: Known: Hepato/choledocholithiasis, hepatitis B and C infection, obesity, diabetes mellitus, congenital hepatic fibrosis, Caroli's disease or choledocal cyst, primary sclerosing cholangitis (PSC), liver fluke infections (Opisthorchis viverrini and Clonorchis sinensis), intrahepatic litiasis and recurrent pyogenic cholangitis; suspect: Inflammatory bowel disease, smoke, asbestos, genetic polymorphisms, diabetes.

According to these data, a surveillance program can be settled in selected patients using magnetic resonance or endoscopic-retrograde-pancreatoduodenoscopy (ERCP)

(Table 1)[13-16].

The highest relative risk is identified in liver fluke infections (Opisthorchis viverrini and Clonorchis sinensis), endemic in South-East Asia[17]. Infection spreads after the ingestion of contaminated fish; and then the flukes colonize biliary tree causing chronic infection and inflammation.

Even if the mechanisms causing the transformation of cholangiocyte into neoplastic cells are nowadays unknown, CCC development in PSC is widely investigated. The risk for patients affected by PSC (as well as other diseases of biliary plate, *e.g.* Caroli's disease) to develop CCC in their lifetime is around 3%-30%[15]. Pancreatic enzymes reflux, cholestasis and chronic inflammation leads to cholangiocyte activation, apoptosis, progression of senescence pathways and increased cellular turnover. All these mechanisms are involved in carcinogenesis: Some studies underline a common pathway (interleukin 6, cyclooxygenase-2, nitric oxide, *etc.*) between inflammation and malignant cellular proliferation acting on hepatic progenitor cells[18-20]. Together with this pathogenetic theory, an alternative carcinogenetic mechanism has been introduced: It is based on mitogenic pathway activation with a consequent multistep tumoral development[21]. These two mechanisms cannot be considered mutually exclusive. Indeed, in PSC patients the presence of cholangiocyte dysplasia was demonstrated together with CCC. The analyses of CCC specimens underlined a wide heterogeneity of gene mutations, however they seem to be polled according to a geographical distribution[22].

CLASSIFICATION AND STAGING

Macrosopic classification

The Bismuth classification, after modified by Corlette, is well known between general surgeons (Figure 1)[23]. It is used to try to define the correct surgical approach and it is based on macroscopic tumor appearance at the pre-surgical imaging. Although this classification is largely used in literature, it has different limits: The absence of longitudinal description of the cancer extension, no relation with prognostic data, and no clearly defined resectability criteria[24,25]. Other classifications have been proposed (*e.g.*, Memorial Sloan-kattering Cancer Centre) but none of them supplanted the use of the Bismuth-Corlette one.

On the other hand, tumor-node-metastasis (TNM) classification is worldwide accepted to define the prognosis[4]. Since the 7th edition of America Joint Commission on Cancer (AJCC) classification, pCCC has been recognized as a separate disease from the distal CCC. Unfortunately, hystopathological evaluation of surgical specimen, together with pre-operative imaging data is needed to define the correct TMN classification. For these reasons, it cannot be used to define resectability during diagnostic iter.

At the end of 2016, AJCC was revised and the 8th edition of TNM classification was published. Some main changes were introduced in the 8th edition to better depict pCCC prognosis[3,26,27]. T4 stage is no longer linked to Bismuth-Corlette type IV pCCC, as underlined by Ebata *et al*. T4 pCCC is now defined as a tumor invading the main portal vein or its branches bilaterally, or the common hepatic artery, or unilateral second order biliary radicals with contralateral portal or hepatic artery involvement. According to the current TNM classification, N stage depends on the number of loco-regional lymph nodes involved. Furthermore, stage IIIC category was introduced in TNM staging.

Beside these changings, some comments can be pointed out: Liver parenchymal invasion does not define a metastatic disease (T2b) and represent a more favorable prognostic factor than omolateral vascular invasion (T3); the main portal vein invasion (T4) is not a surgical contraindication, but requires vascular reconstruction. A proper N stage can be achieved, according to the 8th edition, only if at least 15 lymph nodes are detected on surgical specimen. A recent paper by Ruzzente *et al*[26], tried to evaluate the performance of the new TNM classification in a Western setting. Surprisingly, in this publication, the T4-staged patients had no increased risk of death compared to T1. Furthermore, the ability to predict prognosis of 8th edition N stage was not improved compared to the previous edition. These differences are probably explained by the biological behavior and surgical approach to pCCC in Western and Eastern countries[28,29].

Microsopic morphology

Along with the macroscopic and staging classification, pCCC can be grouped in four

Table 1 Patients that should undergo to screening programs and the techniques that should be applied

Predisposing factors	Diagnostic technique	Worrisome features
Intrahepatic lithiasis and recurrent pyogenic cholangitis	MR	Stenosis progression, distal bile duct dilatation, intraductal polypoid mass > 1 cm.
PSC	MR + ERCP	Irregular bile duct stenosis, bilateral bile duct dilatation, ipsilateral lobar atrophy. ERCP bile duct sampling can simplify differential diagnosis.
Intrahepatic fluke	US/MR	Central intrahepatic and main bile duct dilation with stenosis identification[a].

MR: Magnetic resonance; PSC: Primary sclerosing cholangitis; ERCP: Endoscopic retrograde pacreatoduodenoscopy; US: Ultrasound.

[a]: Ultrasound, computed tomography and magnetic resonance findings for intrahepatic fluke are diffuse and uniform dilatation of peripheral intrahepatic bile ducts with no dilatation of central intrahepatic and main bile ducts, without focal obstruction lesions, with increased echogenity of bile ducts and non-shadowing echogenic foci within bile ducts (eggs or flukes).

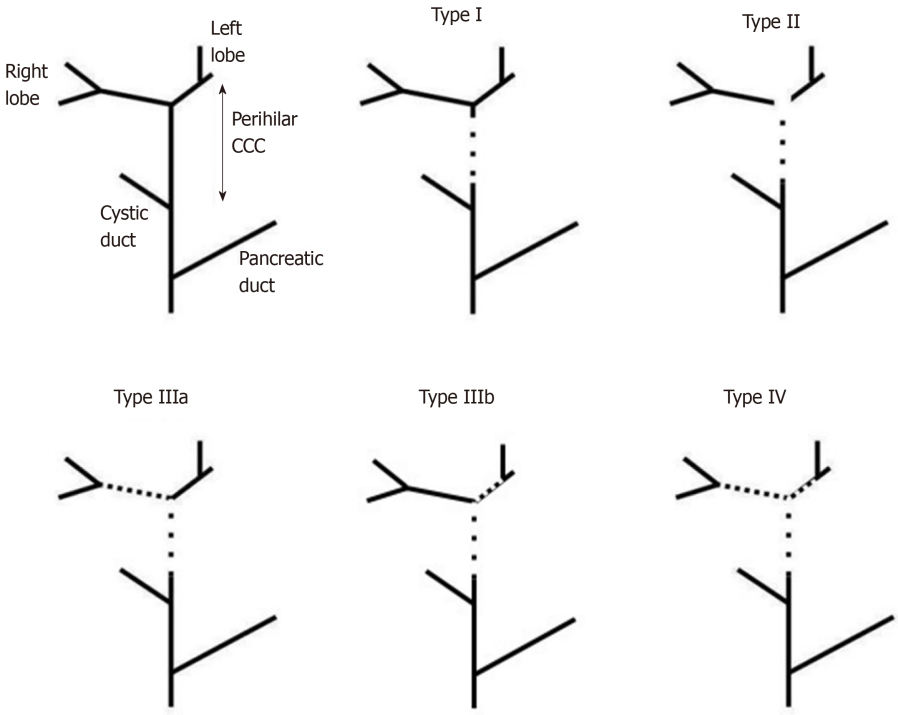

Figure 1 Schematic representation of extrahepatic and intrahepatic bile ducts (until second order) showing Bismuth-Corlette classification. CCC: Cholangiocarncioma.

patterns according to its microscopic morphology[5,20]: (1) Periductal infiltrating: The most common pattern, characterized by an undefined annular thickening of the duct, is frequently associated to perineural and lymphatic invasion; (2) Mixed: Periductal infiltrating associated with a mass forming tumor involving biliary ducts; (3) Intraductal: Mucosal growth associated to segmental bile duct dilatation. biliary-intrapapillary mucinosus neoplasm are included in this pattern; and (4) Papillary-mucinosus: This class is characterized by rich mucina secretion that clutter bile ducts. Their diagnosis is frequently associated to liver abscess.

DIAGNOSIS

Literature identifies the characteristics of an ideal diagnostic iter for pCCC: Non-invasive imaging and characterization of pCCC, correct localization of the tumor, pre-surgical stadiation and resectability evaluation (vascular invasion and biliary spread)[30]. Once CCC is suspected, patients must be referred to specialized surgical centers to complete diagnosis and settle a correct treatment. An incorrect diagnostic pathway exposes patients to delayed diagnosis or repetition of invasive and useless

examinations[31].

The onset of symptoms is not specific and most of the patients (> 65%-80%) are not resectable at the time of diagnosis[32-34]. pCCC identification can be anticipated by jaundice (90%) or cholangitis (10%). Almost patients subjected to screening are found asymptomatic[5]. A proposed diagnostic flow chart for pCCC is showed in Figure 2.

Non-invasive diagnosis

Ultrasound (US) is considered the first line examination. Even if it is weighted by operator-dependent sensitivity and specificity (55%-95% and 71%-96% respectively) in stenosis visualization, US offers valuable information (also using color-doppler) to establish the future diagnostic plan[35-37].

Computer tomography (CT) and magnetic resonance cholangiographic sequences (MRCP) provide complementary information. CT allows a better definition of local tumor extension, vascular invasion and metastatic disease, but only small details about intraductal extension of pCCC (sensitivity and accuracy of 60% and 92% respectively). However, the introduction of multidetector-row CT (high-resolution) has increased the ability to predict intraductal biliary spread of pCCC[38], in particular when bile ducts are dilated[31].

MRCP has the best sensitivity and accuracy (92% and 76% respectively) in identifying the extension of pCCC, but alone is not enough to establish a correct surgical strategy (*e.g.*, lack in vascular invasion)[39,40]. The importance of a correct MRCP execution is highlighted in Zhang *et al*[41] review. Indeed, they demonstrated that inadequate MRCP image leads to the re-execution of the exam and up to 60% of MRCP were found incomplete or inadequate if performed in non-specialized centers.

Positron-emissions-tomography has a marginal role in pCCC staging. It can be used to identify metastatic lymph nodes, distant metastases or clarify indeterminate lesions, especially in PSC patients[42,43]. Due to its low sensitivity (< 70%), it can be considered only in selected cases: In fact, distant metastasis are better identified using CT, while EUS is the gold standard in lymphnode staging[37].

Invasive diagnosis

In selected pCCC cases, diagnosis should rely on invasive examinations: ERCP, percutaneous transhepatic colangiography (PTC), endoscopic ultrasound (EUS). They should be addressed to clarify the nature of a stenosis (biopsy) or to drain bile ducts[5,32,44,45]. Indded, ERCP and PTC are not more relevant than MRCP images in visualizing biliary tree[46,47]. Park *et al*[48] showed an accuracy for predicting biliary confluence and intrahepatic bile duct involvement of 91%-87% for MRCP and 85%-87% for CT combined with invasive cholangiography.

Nowadays, PTC is considered a second choice compared to ERCP due to its increased number of complications. However, Zhimin *et al*[49] described an increased accuracy of PTC (> 90%) in identifying the cranial border of pCCC (especially in pCCC with a proximal localization) compared to ERCP and MRCP.

Endoscopic ultrasound has a controversial role in pCCC diagnosis and management. It provides accurate information about localization of biliary lesions, peribilary tissue involvement, visualization of lymph nodes, hepatic vessels involvement, and it ultimately allows a proper preoperative staging[5,16,32,44,45,50]. However, EUS and EUS fine-needle-aspiration (FNA) sensitivity is reduced from distal to proximal lesions (100% and 83% respectively)[51]. Definition of N staging using EUS needs further studies: Clinical trials are ongoing to identify the role of lymph nodes FNA in predicting pre-operative N stage[52].

Cytological sampling can be obtained through brushing or FNA. It is usefull in non-resectable pCCC or before surgery when diagnosis is not confirmed by non-invaisve techiniques[5,44]. EUS-FNA could also be usefull for cases with negative ERCP-examination[53]. The brushing sensitivity ranges from 20%-40%[54,55] while 79%-83% for FNA[51]. Overall specificity is 92%-100% (the number of cases performed in a hospital highly increase specificity and sensitivity)[16,56]. The low global negative predictive value of cytological sampling using ERCP, PTC and EUS does not exclude the presence of pCCC when a non-neoplastic report is given. It is worth highlighting that, although FNA or brushing allows a proper diagnosis, they are charged by an increased risk of seeding. Only small data are reported on this topic[7,52]. Seeding is a major concern especially during EUS FNA: Indeed, the fine-needle crosses duodenal bulb and peritoneal cavity to sample the pCCC. For these reasons, EUS FNA is contraindicated before liver transplantation[16,52].

A further improvement in endoscopic diagnosis is intraductal-EUS. Even if it has almost 91% accuracy[57], it has a lack in tissue sampling and a reduced radial visualization (max 2 cm). Cholangioscopy allows direct visualization of bile duct

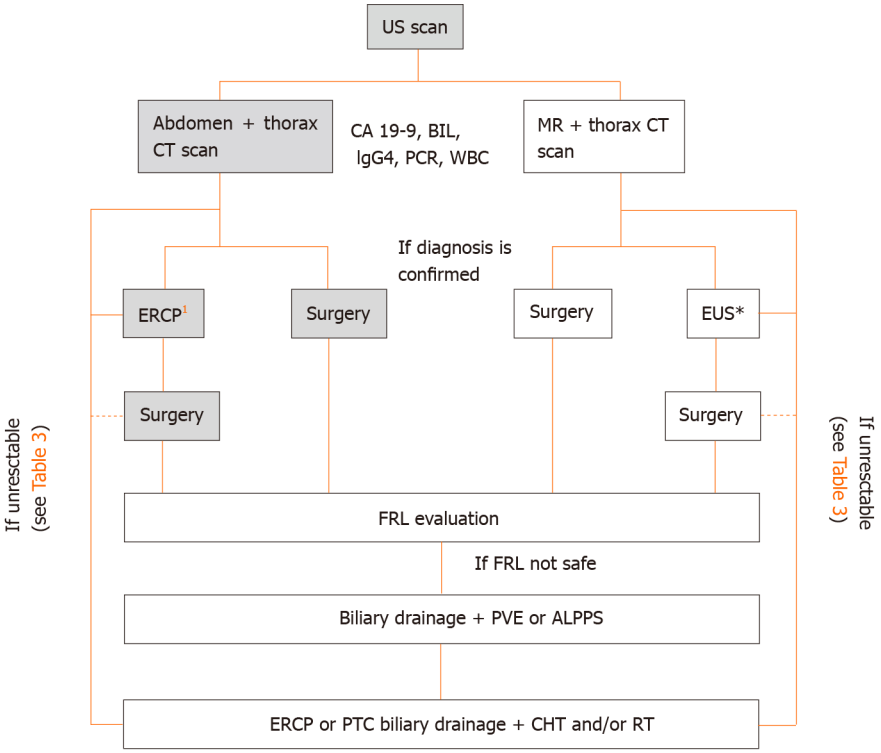

Figure 2 Diagnostic and therapeutic work-flow for perihilar cholangiocarncioma.[1]If cytological confirmation is needed (negative carbohydrate antigen 19-9, positive immunoglobulin G4, and confounding diagnosis at imaging); interrupted line, consider neo-adjuvant therapies. US: Ultrasound; CT: Computed tomography; MR: Magnetic resonance; CA 19-9: Carbohydrate antigen 19-9; BIL: Bilirubin; IgG4: Immunoglobulin G4; ERCP: Endoscopic-retrograde-pancreatoduodenoscopy; EUS: Endoscopic ultrasound; FRL: Future remnant liver; PVE: Portal vein embolization; ALPPS: Associated liver partition to portal vein ligation for staged hepatectomy; PTC: Percutaneous transhepatic colangiography; CHT: Chemotherapy; RT: Radiotherapy.

epithelium and FNA execution and has a sensitivity and specificity of 90% and 96%, and 85% and 100%, respectively[58]. Confocal laser endomicroscopy has high sensitivity, specificity and accuracy (89%-71%-82%[59]). However, many concerns are reported concerning standardization and reproducibility of this diagnostic tool, for this reason it is not suggested for a routine use[16].

Serum markers

Carbohydrate antigen (CA) 19-9 is elevated in 85% of pCCC, but it has a variable sensitivity (33%-93%) and specificity (67%-98%) with low positive predictive value (16%-40%). A CA 19-9 cut-off of 129 ng/dL should raise specificity at 70%[2,7,56,60-62]. The main confounding factor is jaundice: A re-evaluation after biliary decompression (BD) is suggested. Another tumor marker is CA-125, but it is seldom used outside clinical trials[7]. Immunoglobulin G4 (IgG4) are specific immunoglobulines produced during IgG4 cholangiopathy, a rare autoimmune disease associated with pancreatitis. The presence of IgG4 suggests IgG4 cholangiopathy, susceptible to steroids' treatment rather than surgery[63]. New diagnostic approaches are based on liquid biopsy: Detection of cholangiocarcinoma cell-free DNA and circulating tumor cells. Even if some authors reported a usefulness of miRNA measured in bile and blood in pCCC diagnosis, further studies are needed and it probably has a prognostic, more than a diagnostic, role[64-66].

TO DRAIN OR NOT TO DRAIN

BD is a key point during diagnostic and therapeutic management of the pCCC patients. A wide debate is open in literature about this topic and BD must be evaluated according to patient clinical conditions.

Diagnosis and staging in patients with a suspected pCCC are better obtained in absence of foreign bodies in biliary tree. Incorrect indication to BD is one of the most frequent causes of delayed or miss-diagnosis, especially as regards the intraductal extension of the tumor. Hosokawa and colleagues[31] demonstrated that biliary

drainage placed before proper diagnosis and staging leads to a higher rate of non-R0 resections. They hypothesized a confounding factor due to artifacts and reduction of the bile duct dilatation.

Sepsis secondary to cholangitis non-responsive to pharmacological treatment is the only absolute indication to BD. Jaundice, itching or cholangitis are not indications to drain the biliary tree during diagnostic time if the patient is a candidate for liver resection. The use of plastic stents or naso-biliary drainages is more suitable than the use of metallic stents. Indeed the fisrt are easily removed to obtain a correct diagnosis[11,5].

Once surgical indication is established, biliary decompression is anyway debated. Wide accordance on drainage is achieved when a two-step procedure (two-setp hepatectomy or portal vein embolization followed by hepatectomy) is needed to increase the future remnant liver (FRL) volume. Indeed, standard surgical procedure in pCCC requires the resection of a large portion of "healthy" liver parenchyma and liver hypertrophy could be needed before surgery. When a two-step procedure is programmed, whilst the risk of bacterial colonization is increased, BD can improve FRL hypertrophy[67] and could reduce morbidity and mortality[68,69]. In this setting, Eastern surgeons are more likely to use a naso-biliary drainage[31], while Western specialists prefer endoscopic stents[29].

Once a one-step hepatectomy is programmed, BD is associated to high risk of septic shock secondary to retrograde cholangitis that could exclude resectable patient from surgery[70]. In a multicenter study, Farges and colleagues[71] reported an increased mortality after BD in patients that underwent left hepatectomy (mainly due to post-operative septic shock) (adjusted OR 4.06, 95%CI 1.01 to 16.3; P = 0.035), while a decreased mortality rate, due to reduction of post-operative liver failure, was observed after right-side hepatectomy (adjusted OR 0.29, 95%CI: 0.11-0.77; P = 0.013). According to their data, the authors suggested that when a right-side hepatectomy is planned in jaundiced patients, BD should be performed and surgery scheduled when bilirubin < 3 mg/dL. Conversely, Celotti *et al*[72], in their meta-analyses, underlined that patients that underwent pre-operative BD had an increased rate of morbidity and wound infections with no advantages on post-operative mortality. While only a selective use of pre-operative BD is suggested (*e.g.*, patients affected by cholangitis) if one-step hepatectomy is planned, randomized prospective studies are needed to better depict the indications for BD.

BD can be achieved through percutaneous [Percutaneous Transhepatic Biliary Drainage (PTBD)] or endoscopic (plastic or metallic stent or naso-gastic tube) approach according to hospital expertise. No definitive data are published on the best technique for BD[67]. Table 2 summarizes pros and cons of the two techniques. A recent paper by Higuchi *et al*[73] estimated a comparable patient survival and morbidity in patients undergoing PTC or ERCP. While increased post-operative tumor dissemination in PTC group is reported, an increased rate of infection is highlighted in ERCP patients[74,75]. Even if some authors reported the overall superiority of PTC on ERCP[74-76], a recent randomized control[77] trial was prematurely stopped due to the higher rate of pre-surgical mortality among PTC patients (PTC *vs* ERCP: 41% *vs* 11%). Until PTBD the superiority of a technique will be demonstrated, ERCP with endoscopic stent placement should be considered the first line technique to obtain BD[78]. When curative intent resection is not feasible, ERCP must be pursued in a patient oriented approach.

TREATMENT

Patient and resecability assessment

Due to the late onset of symptoms and the aggressive nature of pCCC, less than 50% of the patients are surgically resectable at diagnosis[5]. The main criteria involved in resecability evaluation are highlighted in Table 3.

A recent paper provides a pre-operative risk score designed to predict the risk of intraoperative metastatic disease or locally advanced pCCC (*i.e.* unresectable) and the post-operative mortality[79]. Through the evaluation of 566 resected pCCC, the authors identified 5 objective criteria (bilirubin > 2 mg/dL; Bismuth classification at imaging; portal vein and hepatic artery involvement at imaging; suspicious lymph node on imaging) that allow the definition of 4 risk categories. An interesting perspective can be the adoption of this score to define the need for up-front neo-adjuvant chemotherapies in high-risk patients.

According to the complexity of surgical approach, resectability decision is strictly connected to a careful evaluation of the patient's performance status, liver, cardiac,

Table 2 Main advantages of two the two techniques available to obtain bile duct drainage

ERCP	PTC
Internal stent: Less patient discomfort[5]	External drainage: Increased patient discomfort[5]
Reduced risk of seeding[73]	Higher expertise needed[108]
Higher rate of bacterial contamination/cholangitis[76]	Higher rate of hemorrhage[76]
"One shot" microbiological examination	Never cross the malignant bile duct stenosis[5]
Removed during surgery	Repeated cholangiography and microbiological samples
	Useful during and after surgery

ERCP: Endoscopic retrograde pacreatoduodenoscopy; PTC: Percutaneous transhepatic colangiography.

Table 3 Criteria that can be used to identify non-resectable patients

Absolute criteria	Relative criteria	
	Criteria	Suggestions
Presence of distant metastasis (especially liver, lung, peritoneum)	Longitudinal and lateral dissemination	Consider adequate staging (avoid R1-2)
Extra-regional lymphnode involvement (para-aortic and extraperitoneal)		
Bilateral intrahepatic involvement of biliary tree that exclude bilio-enteric anastomosis	Portal infiltration < 2 cm	Portal vein resection needed
Infiltration or occlusion of the main portal trunk proximal to bifurcation		
Right lobe atrophy associated to contralateral portal vein infiltration or portal occlusion > 2 cm	Low remant liver	Consider liver hypertrophy techniques
Right lobe atrophy associated to contralateral tumor extension more than to 2 cm from hepatic hilum		
Contralateral invasion of hepatic artery	Type IV pCCC	High expertise; consider en-bloc resection
Unilobar secondary bile ducts invasion associated to contralateral infiltration or collusion of portal vein		

pCCC: Perihilar cholangiocarncioma.

respiratory and kidney function[45]. Nutritional status must be evaluated before surgery and all efforts should be directed towards counterbalancing malnutrition progression. Poor nutritional condition leads to reduced survival, increased post-operative complications and prolonged hospital stay[80-82].

Advanced age was identified as one of the main changings in the characteristics of pCCC population. Despite the advanced age, the rate of resectable patients (70%) was similar in octogenarian and non-octogenarian patients. Post-surgical overall survival was not reduced by age even if a carefully selection of patients is needed. Indeed, 30% of octogenarians (*vs* 6% of under 60 years) were excluded to surgery for poor performance status and poor liver function[83].

Surgical resection

Curative approach to pCCC relies on free surgical margins. Indeed, after R0 resection, 5-year survival reaches 20%-42% in association or not with chemotherapy[8,5,45,67]. The localization of pCCC is one of the most important factors influencing surgical strategy: Isolated bile duct resection is applicable in Bismuth Corlette type I pCCC, while resection of the bile duct confluence is associated to major hepatectomies in the other types. The quantity of liver parenchyma and the number of segments resected depend on the localization of the cranial border of pCCC: Right hepatectomy + S4 in Bismuth-Corlette type IIIa and left hepatectomy in type IIIb. As surgical procedures (especially in type IIIa) require the resection of more than 50% of the liver, post-surgical hepatic failure must be avoided. FRL and liver functional reserve need to be carefully evaluated through liver functional tests (*e.g.*, indocyanine green clearance), imaging techniques and, if possible, liver biopsy. If the predicted FRL is less than the necessary

(< 40% in hepatopatic patients, < 30% in normal liver), a single step hepatectomy is related to an increased risk of liver failure and death[84,85]. A two-step procedure (associated liver partition to portal vein ligation for staged hepatectomy or simple portal vein ligation) or pre-operative portal vein embolization (PVE) must be settled. PVE is largely adopted in the Eastern Countries (55% of the cases compared to the 7% of Western Countries)[29]. A recent study by Lee *et al*[86] developed a score to evaluate the risk of "small for size" after resection. They included in their analyses FRL, intraoperative blood loss and prothrombine time > 1.2. Olthof *et al*[69], in the same year, proposed their own score based on FRL, jaundice at presentation, preoperative cholangitis and immediate post-operative bilirubin > 2.9 mg/dL. While the authors underlined that pre-operative BD increases FRL hypertrophy, post-BD cholangitis reduced the positive effect of biliary decompression on post-operative liver failure rate. Even if PVE is more frequently used in Eastern countries, the rate of post-surgical liver failure is similar to Western ones. A more aggressive approach to liver vascular pedicle, a larger lymphadenectomy and an increased rate of intraoperative trans-hepatic biliary drainage in the Eastern Countries can counterbalance the effect of PVE hypertrophy[87].

Regardless of the type of hepatectomies, resection of caudate lobe is considered the gold standard. Caudate lobe's bile ducts open out at bile duct bifurcation and are frequently infiltrated by pCCC. Its removal increases the percentage of R0 resections (59%-87%) with better results in long-term survival (5 years survival from 33% to 44%, resection S1 *vs* non-resection HR 3.03)[88,89].

Curative surgical strategies cannot leave aside from a histological intraoperative evaluation of bile duct margins (cranial and caudal). Bile duct R0 resection is one of the most important factors influencing long-term follow-up. If neoplastic cells are detected at frozen section, surgical resection will be enlarged till feasible to obtain R0 (60% of the cases[90]). The growth of pCCC is intraluminal and the perineural spread is frequent. A resection of 1 cm above pCCC localization must be considered in the infiltrative type[91], as well as 2 cm in the papillary/mass-forming[92]. A debate in literature is open to understand the results of high-grade dysplasia detection on bile duct margins. While some studies reported comparable patients'- but reduced disease free – survival, other studies showed a reduced 2 and 5-year disease specific survival in N0 R1-high grade-dysplasia patients (2-year, 76.7% *vs* 84.3%; 5-year, 37.5% *vs* 69.3%)[73,93].

Portal vein resection can be headed if focal portal invasion (< 2 cm) of the main trunk is demonstrated. Indeed, portal vein resection does not affect post-resection outcome[4,90,94]. Conversely, hepatic artery resection is related to an increased surgical risk, without a demonstrated positive influence on long-term results[95,96].

In 2012 Neuhaus *et al*[91] proposed a new approach to liver resection in type IIIa pCCC, called "en bloc resection". In his paper, Neuhaus presented a series of 100 type IIIa pCCC patients that received two different surgical treatements according to the tumor localization: "en bloc resection" in tumors located close to hepatic hilum (n = 50) and standard resection in the others (n = 50). "En bloc resection" consisted in right enlarged hepatectomy + S1, lymphadenectomy and en bloc resection of biliary confluence, extrahepatic bile duct, portal vein bifurcation and right hepatic artery (portal vein reconstruction is needed). 3 and 5-year survival was superior in "en bloc" group (35% and 25% *vs* 65% and 58% respectively) without an increase in surgical complications. Other authors adopted this approach with reported comparable results[97]. The "en bloc resection" is not feasible in left hepatectomy because the no touch approach on hilum is impossible, unless resection and reconstruction of the right hepatic artery are being considered.

In 2017, Kawabata *et al*[98] proposed their own surgical technique based on reduced liver manipulation and tumor spread. They described an ab-initio parenchymal transection prior to liver mobilization. Two-year survival was increased in the study group (95% *vs* 58%) with a decrease in surgical complications.

Bismuth-Corlette Type IV pCCC deserves a peculiar consideration (Table 4). It was considered a surgical contraindication for several years due to the bilateral bile duct invasion. However, in the last few years, the surgical approach to this type of pCCC changed due to the Japanese group's contributions. In 2018, they published[99] a series of 216 patients with Bismuth Corlette type IV pCCC that underwent surgical resection: R0 resection was achieved in 76.2% of the cases, post-surgical morbidity was 41.6% and the 5-year survival was superior in the resected patients (32.8% *vs* 1.5%). Even if the resection of type IV pCCC is feasible and the results are promising, two main concerns are emerging: An undiagnosed vascular invasion often detected at histopathological evaluation and the high rate of N positive specimens[100,101]. The adoption of an en-bloc approach can be suggested in this type of pCCC to avoid

Table 4 Articles reporting resection of type IV perihilar cholangiocarncioma according di bismuth

Author	Publication year	Resection rate (%)	Resected cases (*n*)	Vascular resection (*n*)	Vascular reconstruction (*n*)	Vascular invasion at histological evaluation (*n*)	Complications (%)	N+ (%)	R0 (%)	Patient survival 1-3-5 yr (%)
Hu HJ	2018	NA	69	52	14	63	39	57	86	76-44-22
Li B	2017	NA	142	42	NA	NA	NA	37	75	35-12-3
Ebata T	2018	50	216	131	NA	136 PV + 53 HA	19	20	72	68-34-22
Ji GW	2017	NA	25	4	4	13	13	76	95	NA
Hoffman K	2015	NA	31 (+29 tipo II e III)	31[12]	21[1]	19	52	36	60	84-38-18[1]
Han IW	2014	21	33	6	NA	12 PV + 13 HA	NA	36	54	NA-28-NA
Cheng QB	2012	61	101 (+75 tipo III)	NA	NA	NA	25	40	76	89-38-13[3]

We selected only the series were data on type IV resection can be extract.

[1]Added type II and III cases.

[2]All cases with presumed vascular infiltration had vascular resection, while only 19 cases had histological proven vascular infiltration.

[3]Added type III cases. PV: Portal vein; HA: Hepatic artery. NA: Not applicable.

unexpected vascular invasion diagnosis. Furthermore, neoadjuvant chemotherapy can be useful in type IV pCCC to select chemo-responsive tumors, reduce the possible futile resections and improve the extent of R0 rate.

Liver transplantation

In unresectable pCCC, liver transplantation (LT) can be considered within research protocols and with strict inclusion criteria[102]. These criteria are: Tumor smaller than 3 cm, no evidence of lymph node involvement or metastatic disease, and no prior percutaneous or endoscopic biopsy[103]. The initial results of LT for pCCC were poor. Indeed, overall survival (OS) following LT alone for incidentally diagnosed pCCC in PSC are < 40% at 3-year[104]. LT for pCCC gained new enthusiasm with the publication of Mayo Clinic results: In their studies they identified the risks for disease progression and recurrence, and a multimodal therapy (neoadjuvant chemoradiation therapy is mandatory prior to listing) was successfully applied. In the published series of LT performed at Mayo Clinic, the LT group with neoadjuvant chemoradiation (38 patients) achieved better 1 year (92% *vs* 82%), 3 years (82% *vs* 48%), and 5 years (82% *vs* 21%) overall survival (OS) when compared with the resection group (26 patients). Consistently, the LT group experienced lower post-transplant recurrence (13% *vs* 27%) [105]. Ethun *et al*[106] compared 191 patients that underwent curative resection with 41 patients that received LT (with Mayo Clinic Protocol) for pCCC. In LT group, 38% of the patients were excluded. Patients who underwent transplant for pCCC showed improved OS compared with resection (5-year: 64% *vs* 18%; $P < 0.001$). The same results were obtained if patients with tumors < 3 cm with lymph-node negative disease and without PSC patients from resection group (5-year: 54% *vs* 29%; $P = 0.03$).

Resective surgery in pCCC is the standard of care for suitable patients outside the setting of PSC[107]. To date, even if there are no randomized controlled trials, LT after aggressive neoadjuvant therapy (including external beam and transluminal radiation, as well as systemic chemotherapy) seems like an adequate treatment for both unresectable pCCC, as well as pCCC arising in the setting of PSC[108].

Laparoscopic exploration

The role of laparoscopic exploration (LE) decreased over time together with the increase of sensibility and specificity of imaging techniques. Routine LE is not recommended, but it can be useful in T2/T3 pCCC according to AJCC classification or type III and IV according to Bismuth-Corlette[92,109]. LE is the only way to detect peritoneal metastasis prior to laparotomy, due to the low predictive value of non-invasive technique. Furthermore, routine opening of the lesser sac during LE can help in detecting metastatic lymphnode of hepatic artery (N2 stage)[110]. A recent meta-analysis[111] collected 8 studies evaluating the role of LE: 32.4% of the patients

were found unresectable at exploration with a sensitivity of 56% and a specificity of 100%. In another study, sensitivity of LE increased from 24% to 41% using intraoperative ultrasound[112].

Lymphadenectomy

Lymphadenectomy is an essential part of the surgical intervention, as well as bile duct and liver resection. In pCCC, hilar, hepatic artery, portal vein, bile duct, celiac trunk and retroduodenal lymph nodes must be resected. The role of lymphadenectomy is to obtain an adequate post-surgical staging, even if some authors reported a survival benefit[88,113,114]. The 8th edition of TNM classification identifies 15 lymph nodes as the minimum number to obtain an adequate N staging (N1 when 1 to 3 regional lymph nodes are positive, N2 when more than 4 regional lymph nodes are positive)[4]. Regional lymph nodes are located in the hepatic hilum and in the hepatoduodenal ligament (pericholedochal nodes). The first systematic review on lymphadenectomy was published in 2015[115]. Beside AJCC classification, Kambakamba *et al*[115] rose criticism about the minimum number of dissected nodes. Indeed, in their review, only 9% of the series reported a number of dissected lymph nodes > 15, while N positivity ranged from 31% to 58%[116,117]. Their analyses showed that 7 is the number of lymph nodes that ensures the highest detection rate of N1 and the lowest rate of potentially understated N0 patients. The impact on survival of extended lymphadenectomy (> 15 lymph nodes) is debated, because it does not improve 5-year survival and median OS with an increased rate of surgical complications[5]. The presence of malignant cells within dissected lymph nodes (N1) has a detrimental impact on patient survival: 3-year survival 35% *vs* 10% in N0 *vs* N1 patients[115]. It was recently suggested that the presence of a small number of metastatic lymph nodes (lymph nodal ratio < 0.2 or number of lymph node < 4) does not exclude good long-term survival[114,118].

Chemotherapy, radiotherapy and palliative treatments

The role of neo-adjuvant chemotherapy in pCCC is not clearly identified and it is mostly adopted in clinical studies.

The Mayo Clinic protocol combined neoadjuvant chemosensitization with 5-fluorouracil, external beam radiotherapy plus brachytherapy boost and orthotopic liver transplantation for patients with stage I and II pCCC. In a retrospective series, thirty-eight patients underwent liver transplantation while 54 patients were explored for resection. Patients receiving transplantation had better one-, three- and five-year survival (92%, 82% and 82%) compared to resection (82%, 48% and 21%, P = 0.022). Transplanted patients had fewer recurrences compared to resection (13% *vs* 27%)[105]. The ongoing phase III TRANSPHIL trial is comparing resection with neoadjuvant chemoradiotherapy capecitabine-based and orthotopic liver transplantation[102].

Resected patients, except the R0 pT1N0M0 ones, as well as non-resected patients must undertake chemotherapy with adjuvant intent. The role of adjuvant chemoradiotherapy is not well defined due to the lack of data from randomized trial[8]. On the contrary, the phase III randomized BILCAP trial, comparing adjuvant capecitabine with observation in resected biliary tract cancers, showed an increased OS for the experimental arm in the protocol-specified sensitivity analysis (adjusting for minimisation factors, nodal status, grade and gender). Specifically, median OS in the capecitabine arm was 53 mo *vs* 36 mo in the observation group (P = 0.028)[119]. Diversely, the phase III Prodige 12-Accord 18 trial, comparing chemotherapy with oxaliplatin and gemcitabine *vs* observation after resection, failed to show an increase in OS (P = 0.74)[120].

A further phase III study, comparing cisplatin and gemcitabine treatment *vs* observation (ACTICCA-1) is open and recruiting patients[121].

A meta-analysis evaluating studies of adjuvant chemotherapy, chemoradiotherapy or radiotherapy in biliary tract cancers found a nonsignificant improvement in OS compared with adjuvant treatment compared with surgery alone (P = 0.06). However, patients treated with chemoradiotherapy (OR 0.61) or chemotherapy (OR 0.39) had greater benefit with compared to radiotherapy alone (OR 0.98, P = 0.02) and, specifically, the greatest benefit was in those patients with nodes positive (OR 0.49, P = 0.004) and R1 disease (OR 0.36, P = 0.002)[122]. Another meta-analysis of randomized and non-randomized studies confirmed the improvement in OS given by adjuvant chemotherapy, with a 41% of risk of death reduction compared with observation after resection (HR 0.59, P < 0.0001)[123]. In contrast, a meta-analysis of randomized clinical trials showed no effect of adjuvant treatment on OS improvement (HR 0.91) and a mild improvement in recurrence-free survival (HR 0.83). Neither the lymph-node positive (HR 0.84) nor the surgical margin positive subgroups (HR 0.95) had an OS prolongation with adjuvant treatment[124]. Nassour *et al*[125] retrospectively analyzed the

National Cancer Database to evaluate the role of adjuvant chemotherapy (AT) on pCCC. They found the patients that received AT were younger, with a higher pathological T and N staging, a higher rate of non-R0 resections and a longer hospital stay than patients that did not undergo AT. After a propensity match analyses, they found that AT had a beneficial role on 5-year survival in all resected patients, especially in high risk (non-R0 resection) ones. Furthermore, an advantage on 5-year survival was showed for patient that underwent chemo-radiotherapy compared to chemotherapy alone.

In case of locally-advanced unresectable disease, the role of radiation therapy remains unclear[8]. A phase II trial compared gemcitabine plus oxaliplatin *vs* chemoradiotherapy with 5-fluorouracil and cisplatin. The trial closed before completion due to slow recruitment, showing an increased median OS (19.9 mo *vs* 13.5 mo, HR 0.69) and progression free survival (11.0 mo *vs* 5.8 mo, HR 0.65) for the chemotherapy arm[126]. A small series using image-guided intensity-modulated radiation therapy both in gallbladder and extrahepatic bile ducts cancers demonstrated the feasibility of the procedure, allowing safe dose escalation[127].

Exclusive chemotherapy remains a suitable option in case of unresectable disease. The phase III UK ABC-02 study has established the cisplatin/gemcitabine chemotherapy as the new standard of care in patients with advanced biliary tract cancer. Median survival was 11.7 for the combination therapy compared with 8.1 mo for the gemcitabine only comparator arm ($P < 0.001$)[128]. The benefit of the combination was present independent of age (inferior *vs* superior to 65 years), gender, primary tumour site (intra *vs* extrahepatic *vs* gallbladder *vs* ampullary), stage of disease (locally advanced *vs* metastatic) and previous therapy (surgery *vs* stenting)[129]. In case of altered renal function, oxaliplatin may be used instead of cisplatin, while in case of poorer clinical conditions, gemcitabine monotherapy may be a choice[8].

Beyond failure of first line treatment, evidence is scarce. A recent systematic review of the literature gathering 25 non-randomized prospective and retrospective studies reported a median progression-free survival (mPFS) and median overall-survival (mOS) of 3.2 and 7.2 mo, respectively[130]. A large multicenter Italian survey and pooled analysis with published data found a mPFS of 3.1 and median OS of 6.3 mo[131]. Recently, the results of a phase III trial (ABC-06) comparing modified FOLFOX to best supportive care found an advantage in mOS (6.2 mo *vs* 5.3 mo) with adjusted hazard ratio (HR) 0.69. Patients treated with FOLFOX had a prolongation of median radiological PFS or 4 mo. Moreover, the study showed a 1% rate of complete responses, 4% of partial responses and a 28% of cases had disease stabilization. The overall disease control rate was 33%. Due to the results of this trial, modified FOLFOX should be considered the standard of care in the second-line treatment of BTCs[132].

Isocitrate dehydrogenase isoenzyme 1 (IDH1) mutations are present in 15% of patients with CCC. Recently, the results of treatment with ivosedinib, an oral small-molecule inhibitor of mutant IDH1 (mIDH1), have been presented. In patients with mIDH1 progressed to first line treatment, mPFS was 2.7 mo with ivosedinib *vs* 1.4 mo for placebo (HR 0.37, $P < 0.001$). MOS was 10.8 mo for ivosedinib *vs* 9.7 mo for placebo (10.8 mo *vs* 9.7 mo for placebo, HR 0.69, $P = 0.06$). However, mOS for placebo decreased to 6 mo after considering a 57% crossover-rate from placebo to experimental treatment and the difference in mOS between ivosedinib and placebo became statistically significant (HR 0.46, $P = 0.0008$)[133]. Ivosedinib is the first targeted molecular agent showing efficacy in the treatment of advanced CCC and its use will probably become a standard in the second-line treatment of mIDH1 CCC.

In patients with an estimated survival longer than 3 mo, bile duct decompression should be reached. Percutaneous or endoscopic approaches are both possibile. ERCP has the advantage of a totally internal stent, without the discomfort of PTBD (less pain and aesthetic impact). On the other hand, endoscopic stents are not easy to arrange in type III and IV pCCC. Percutaneous transhepatic biliary stent placement is an effective alternative to endoscopic stent to relieve cholestasis[77]. Combined seed intracavitary irradiation with ^{125}I can be applied to obtain a better stent patency and survival[134,135].

OUTCOME AND RESULTS

Survival after pCCC diagnosis is poor and frequently accompanied by a prolonged hospitalization and a wide use of diagnostic and therapeutic techniques. Median survival is 12 mo in patients not susceptible to surgery and 38 (range 25-40) mo in radically resected patients. Koerkamp and colleagues in 2015[136] evaluated a population of 306 patients that underwent surgical resection for pCCC: Overall 5-year

survival was 35%, while it increased to 50% in the 122 (42%) patients N0R0 resection. Excluding R2 patients and patients with intra-hospital death, the median time to recurrence was 31 mo with a 3-year survival after recurrence of 18%. Eastern post-operative survival is slightly better that Western one (median OS of 56 mo *vs* 43 mo respectively, $P = 0.028$), depicting a possible more aggressive behavior of pCCC in Western world[29].

In literature, many variables influence 3 and 5-year survival: Resection margins, type of resection, T stage, N stage, staging, lymphovascular invasion and caudate lobe invasion[88,137,138]. T stage and N positivity are burdened by the highest Hazard Ratios: N1 HR 2.32 (5-year survival N1 *vs* N0 11% *vs* 35%) and T3-4 HR 1.86 (5-year survival T1-2 *vs* T3-4 47% *vs* 19%)[137]. R0 resection was recently underlined as the main factor influencing the outcome, irrespective of the tumor staging[31,139]. Three and five-year recurrence-free survival was 57% and 49% in R0 resection, while 31% and 16% in R1 resection. In stage I, II and III, R0 resection was directly related to segment 1 resection and age > 56 year[31]. Lymphovascular invasion was identified as one of the detrimental prognostic factors on patient and disease free survival. Its role was investigated in lymph nodes positive and negative patients and in both was identified as a detrimental factor[138]. Furthermore, lymphovascular invasion resulted in an increased percentage of patients with lymph nodes metastasis, but not with a decrease in R0 rate, also in Bismuth-Corlette tipe IV pCCC[101,137,140].

In 2017, van Vugt *et al*[95] evaluated the impact of vascular invasion on 674 patients affected by pCCC. Median OS was considered independently from curative resection. They found that any hepatic artery involvement is related to poor prognosis (median OS: 16.9 (13.2-20.5) mo *vs* 10.3 (8.9-11.7) mo, $P < 0.001$), while unilateral or main portal vein involvement was not related to reduced median OS [14.7 (11.7-17.6) mo *vs* 13.3 (11.0-15.7) mo, $P = 0.116$]. This paper confirmed the results provided by other authors and highlighted the necessity of a further modification of the 8th AJCC classification. Indeed, the T4 classification does not discriminate arterial or main portal vein infiltration with a reduced ability to predict patient outcome[26].

The resection benefits have to deal with the high surgical morbidity and mortality of pCCC. In both Western and Eastern Centre, 90-d surgical mortality ranges around 10%.

The 5-year survival rate for perihilar cholangiocarcinoma in patients receiving a liver transplant is greater than 70%[105], although these data are affected by selection bias. A number of factors were identified as predictors of outcomes in pCCC liver transplantation: Elevated CA 19-9, portal vein encasement, perineural invasion and absence of vital tumor at explant histopathological examination[140-142]. Recent evidence showed that overall survival is affected by the amount of necrotic tumor after neo-adjuvant therapy (patients with minimal response were 9.0 times more likely to die than patients with a complete tumor necrosis) and by lymphovascular invasion[140].

CONCLUSION

In conclusion, perihilar cholangiocarcinoma is characterized by high mortality and low rate of resectable patients. The main issue for surgeons is to obtain the most rapid and accurate diagnosis. For this reason, patients must be referred to specialized centers after a suspect diagnosis. Biliary drainage is an important tool in non-resectable patients and in those that are candidate to two-stage hepatectomy. It must be obtained after a definitive diagnosis. Even if surgery represents the only curative option, it is still charged by reduced long-term survival.

ACKNOWLEDGEMENTS

Authors would like to thank "Associazione Italiana Copev per la prevenzione e cura dell'epatite virale Beatrice Vitiello- ONLUS" for the valuable support and Erica Bosco for langue review.

REFERENCES

1 **Doherty B**, Nambudiri VE, Palmer WC. Update on the Diagnosis and Treatment of Cholangiocarcinoma. *Curr Gastroenterol Rep* 2017; **19**: 2 [PMID: 28110453 DOI: 10.1007/s11894-017-0542-4]

2 **Kondo S**, Takada T, Miyazaki M, Miyakawa S, Tsukada K, Nagino M, Furuse J, Saito H, Tsuyuguchi T, Yamamoto M, Kayahara M, Kimura F, Yoshitomi H, Nozawa S, Yoshida M, Wada K, Hirano S, Amano H, Miura F; Japanese Association of Biliary Surgery; Japanese Society of Hepato-Biliary-Pancreatic Surgery; Japan Society of Clinical Oncology. Guidelines for the management of biliary tract and ampullary carcinomas: surgical treatment. *J Hepatobiliary Pancreat Surg* 2008; **15**: 41-54 [PMID: 18274843 DOI: 10.1007/s00534-007-1279-5]

3 **Meng ZW**, Pan W, Hong HJ, Chen JZ, Chen YL. Macroscopic types of intrahepatic cholangiocarcinoma and the eighth edition of AJCC/UICC TNM staging system. *Oncotarget* 2017; **8**: 101165-101174 [PMID: 29254154 DOI: 10.18632/oncotarget.20932]

4 **Brierley JD**, Gospodarowicz MK, Wittekind C. TNM Classification of Malignant Tumours, 8th Edition. John Wiley & Sons, 2017. Available from: https://play.google.com/store/books/details?id=642GDQAAQBAJ

5 **AI di Oncologia Medica**. Linee guida TUMORI DELLE VIE BILIARI. Available from: http://media.aiom.it/userfiles/files/doc/LG/2016_LG_AIOM_Vie_biliari.pdf

6 **Bergquist A**, von Seth E. Epidemiology of cholangiocarcinoma. *Best Pract Res Clin Gastroenterol* 2015; **29**: 221-232 [PMID: 25966423 DOI: 10.1016/j.bpg.2015.02.003]

7 **Khan SA**, Davidson BR, Goldin RD, Heaton N, Karani J, Pereira SP, Rosenberg WM, Tait P, Taylor-Robinson SD, Thillainayagam AV, Thomas HC, Wasan H; British Society of Gastroenterology. Guidelines for the diagnosis and treatment of cholangiocarcinoma: an update. *Gut* 2012; **61**: 1657-1669 [PMID: 22895392 DOI: 10.1136/gutjnl-2011-301748]

8 **Valle JW**, Borbath I, Khan SA, Huguet F, Gruenberger T, Arnold D; ESMO Guidelines Committee. Biliary cancer: ESMO Clinical Practice Guidelines for diagnosis, treatment and follow-up. *Ann Oncol* 2016; **27**: v28-v37 [PMID: 27664259 DOI: 10.1093/annonc/mdw324]

9 **AI di Oncologia Medica**. I Numeri del Cancro in Italia. [accessed 2019 March 5]. Associazione Italiana dei Registri Tumori, Istituto Superiore di Sanità. Available from: https://www.aiom.it/wp-content/uploads/2018/10/2018_ NumeriCancro-operatori.pdf

10 **Deoliveira ML**, Schulick RD, Nimura Y, Rosen C, Gores G, Neuhaus P, Clavien PA. New staging system and a registry for perihilar cholangiocarcinoma. *Hepatology* 2011; **53**: 1363-1371 [PMID: 21480336 DOI: 10.1002/hep.24227]

11 **European Association for the Study of the Liver**. EASL Clinical Practice Guidelines: management of cholestatic liver diseases. *J Hepatol* 2009; **51**: 237-267 [PMID: 19501929 DOI: 10.1016/j.jhep.2009.04.009]

12 **Sierra H**, Cordova M, Chen CJ, Rajadhyaksha M. Confocal imaging-guided laser ablation of basal cell carcinomas: an ex vivo study. *J Invest Dermatol* 2015; **135**: 612-615 [PMID: 25178106 DOI: 10.1038/jid.2014.371]

13 **Jarnagin W**, Winston C. Hilar cholangiocarcinoma: diagnosis and staging. *HPB (Oxford)* 2005; **7**: 244-251 [PMID: 18333200 DOI: 10.1080/13651820500372533]

14 **Blechacz B**, Gores GJ. Cholangiocarcinoma: advances in pathogenesis, diagnosis, and treatment. *Hepatology* 2008; **48**: 308-321 [PMID: 18536057 DOI: 10.1002/hep.22310]

15 **Sierra H**, Cordova M, Chen CJ, Rajadhyaksha M. Confocal imaging-guided laser ablation of basal cell carcinomas: an ex vivo study. *J Invest Dermatol* 2015; **135**: 612-615 [PMID: 25178106 DOI: 10.1038/jid.2014.371]

16 **Rizvi S**, Eaton J, Yang JD, Chandrasekhara V, Gores GJ. Emerging Technologies for the Diagnosis of Perihilar Cholangiocarcinoma. *Semin Liver Dis* 2018; **38**: 160-169 [PMID: 29871021 DOI: 10.1055/s-0038-1655775]

17 **Sripa B**, Pairojkul C. Cholangiocarcinoma: lessons from Thailand. *Curr Opin Gastroenterol* 2008; **24**: 349-356 [PMID: 18408464 DOI: 10.1097/MOG.0b013e3282fbf9b3]

18 **Tabibian JH**, O'Hara SP, Splinter PL, Trussoni CE, LaRusso NF. Cholangiocyte senescence by way of N-ras activation is a characteristic of primary sclerosing cholangitis. *Hepatology* 2014; **59**: 2263-2275 [PMID: 24390753 DOI: 10.1002/hep.26993]

19 **Chung BK**, Karlsen TH, Folseraas T. Cholangiocytes in the pathogenesis of primary sclerosing cholangitis and development of cholangiocarcinoma. *Biochim Biophys Acta Mol Basis Dis* 2018; **1864**: 1390-1400 [PMID: 28844951 DOI: 10.1016/j.bbadis.2017.08.020]

20 **Lendvai G**, Szekerczés T, Illyés I, Dóra R, Kontsek E, Gógl A, Kiss A, Werling K, Kovalszky I, Schaff Z, Borka K. Cholangiocarcinoma: Classification, Histopathology and Molecular Carcinogenesis. *Pathol Oncol Res* 2020; **26**: 3-15 [PMID: 30448973 DOI: 10.1007/s12253-018-0491-8]

21 **Sia D**, Hoshida Y, Villanueva A, Roayaie S, Ferrer J, Tabak B, Peix J, Sole M, Tovar V, Alsinet C, Cornella H, Klotzle B, Fan JB, Cotsoglou C, Thung SN, Fuster J, Waxman S, Garcia-Valdecasas JC, Bruix J, Schwartz ME, Beroukhim R, Mazzaferro V, Llovet JM. Integrative molecular analysis of intrahepatic cholangiocarcinoma reveals 2 classes that have different outcomes. *Gastroenterology* 2013; **144**: 829-840 [PMID: 23295441 DOI: 10.1053/j.gastro.2013.01.001]

22 **Marino D**, Leone F, Cavalloni G, Cagnazzo C, Aglietta M. Biliary tract carcinomas: from chemotherapy to targeted therapy. *Crit Rev Oncol Hematol* 2013; **85**: 136-148 [PMID: 22809696 DOI: 10.1016/j.critrevonc.2012.06.006]

23 **Paul A**, Kaiser GM, Molmenti EP, Schroeder T, Vernadakis S, Oezcelik A, Baba HA, Cicinnati VR, Sotiropoulos GC. Klatskin tumors and the accuracy of the Bismuth-Corlette classification. *Am Surg* 2011; **77**: 1695-1699 [PMID: 22273233]

24 **Zervos EE**, Osborne D, Goldin SB, Villadolid DV, Thometz DP, Durkin A, Carey LC, Rosemurgy AS. Stage does not predict survival after resection of hilar cholangiocarcinomas promoting an aggressive operative approach. *Am J Surg* 2005; **190**: 810-815 [PMID: 16226963 DOI: 10.1016/j.amjsurg.2005.07.025]

25 **Park J**, Kim MH, Kim KP, Park DH, Moon SH, Song TJ, Eum J, Lee SS, Seo DW, Lee SK. Natural History and Prognostic Factors of Advanced Cholangiocarcinoma without Surgery, Chemotherapy, or Radiotherapy: A Large-Scale Observational Study. *Gut Liver* 2009; **3**: 298-305 [PMID: 20431764 DOI: 10.5009/gnl.2009.3.4.298]

26 **Ruzzenente A**, Bagante F, Ardito F, Campagnaro T, Scoleri I, Conci S, Iacono C, Giuliante F, Guglielmi A.

Comparison of the 7th and 8th editions of the American Joint Committee on Cancer Staging Systems for perihilar cholangiocarcinoma. *Surgery* 2018; **164**: 244-250 [PMID: 29801730 DOI: 10.1016/j.surg.2018.03.012]

27 **Ebata T**, Kosuge T, Hirano S, Unno M, Yamamoto M, Miyazaki M, Kokudo N, Miyagawa S, Takada T, Nagino M. Proposal to modify the International Union Against Cancer staging system for perihilar cholangiocarcinomas. *Br J Surg* 2014; **101**: 79-88 [PMID: 24375300 DOI: 10.1002/bjs.9379]

28 **Young AL**, Prasad KR, Toogood GJ, Lodge JP. Surgical treatment of hilar cholangiocarcinoma in a new era: comparison among leading Eastern and Western centers, Leeds. *J Hepatobiliary Pancreat Sci* 2010; **17**: 497-504 [PMID: 19859651 DOI: 10.1007/s00534-009-0203-6]

29 **Olthof PB**, Miyasaka M, Koerkamp BG, Wiggers JK, Jarnagin WR, Noji T, Hirano S, van Gulik TM. A comparison of treatment and outcomes of perihilar cholangiocarcinoma between Eastern and Western centers. *HPB (Oxford)* 2019; **21**: 345-351 [PMID: 30087051 DOI: 10.1016/j.hpb.2018.07.014]

30 **Sainani NI**, Catalano OA, Holalkere NS, Zhu AX, Hahn PF, Sahani DV. Cholangiocarcinoma: current and novel imaging techniques. *Radiographics* 2008; **28**: 1263-1287 [PMID: 18794305 DOI: 10.1148/rg.285075183]

31 **Hosokawa I**, Shimizu H, Yoshitomi H, Furukawa K, Takayashiki T, Miyazaki M, Ohtsuka M. Impact of Biliary Drainage on Multidetector-Row Computed Tomography on R0 Resection of Perihilar Cholangiocarcinoma. *World J Surg* 2018; **42**: 3676-3684 [PMID: 29752510 DOI: 10.1007/s00268-018-4654-2]

32 **Brandi G**, Venturi M, Pantaleo MA, Ercolani G; GICO. Cholangiocarcinoma: Current opinion on clinical practice diagnostic and therapeutic algorithms: A review of the literature and a long-standing experience of a referral center. *Dig Liver Dis* 2016; **48**: 231-241 [PMID: 26769568 DOI: 10.1016/j.dld.2015.11.017]

33 **Regimbeau JM**, Fuks D, Le Treut YP, Bachellier P, Belghiti J, Boudjema K, Baulieux J, Pruvot FR, Cherqui D, Farges O; AFC-HC study group. Surgery for hilar cholangiocarcinoma: a multi-institutional update on practice and outcome by the AFC-HC study group. *J Gastrointest Surg* 2011; **15**: 480-488 [PMID: 21249527 DOI: 10.1007/s11605-011-1414-0]

34 **Nagino M**. Surgical Treatment of Perihilar Cholangiocarcinoma: Resection or Transplant? *Ann Surg* 2018; **267**: 806-807 [PMID: 29206670 DOI: 10.1097/SLA.0000000000002624]

35 **Bloom CM**, Langer B, Wilson SR. Role of US in the detection, characterization, and staging of cholangiocarcinoma. *Radiographics* 1999; **19**: 1199-1218 [PMID: 10489176 DOI: 10.1148/radiographics.19.5.g99se081199]

36 **Chung YE**, Kim MJ, Park YN, Choi JY, Pyo JY, Kim YC, Cho HJ, Kim KA, Choi SY. Varying appearances of cholangiocarcinoma: radiologic-pathologic correlation. *Radiographics* 2009; **29**: 683-700 [PMID: 19448110 DOI: 10.1148/rg.293085729]

37 **Joo I**, Lee JM, Yoon JH. Imaging Diagnosis of Intrahepatic and Perihilar Cholangiocarcinoma: Recent Advances and Challenges. *Radiology* 2018; **288**: 7-13 [PMID: 29869969 DOI: 10.1148/radiol.2018171187]

38 **Senda Y**, Nishio H, Oda K, Yokoyama Y, Ebata T, Igami T, Sugiura T, Shimoyama Y, Nimura Y, Nagino M. Value of multidetector row CT in the assessment of longitudinal extension of cholangiocarcinoma: correlation between MDCT and microscopic findings. *World J Surg* 2009; **33**: 1459-1467 [PMID: 19381719 DOI: 10.1007/s00268-009-0025-3]

39 **Masselli G**, Manfredi R, Vecchioli A, Gualdi G. MR imaging and MR cholangiopancreatography in the preoperative evaluation of hilar cholangiocarcinoma: correlation with surgical and pathologic findings. *Eur Radiol* 2008; **18**: 2213-2221 [PMID: 18463877 DOI: 10.1007/s00330-008-1004-z]

40 **Sun HY**, Lee JM, Park HS, Yoon JH, Baek JH, Han JK, Choi BI. Gadoxetic acid-enhanced MRI with MR cholangiography for the preoperative evaluation of bile duct cancer. *J Magn Reson Imaging* 2013; **38**: 138-147 [PMID: 23281093 DOI: 10.1002/jmri.23957]

41 **Zhang H**, Zhu J, Ke F, Weng M, Wu X, Li M, Quan Z, Liu Y, Zhang Y, Gong W. Radiological Imaging for Assessing the Respectability of Hilar Cholangiocarcinoma: A Systematic Review and Meta-Analysis. *Biomed Res Int* 2015; **2015**: 497942 [PMID: 26448940 DOI: 10.1155/2015/497942]

42 **Naser B**. [Removable dentures for children]. *Cah Prothese* 1991; **76**: 20-26 [PMID: 1817745 DOI: 10.1111/j.1572-0241.2007.01710.x]

43 **Jiang L**, Tan H, Panje CM, Yu H, Xiu Y, Shi H. Role of 18F-FDG PET/CT Imaging in Intrahepatic Cholangiocarcinoma. *Clin Nucl Med* 2016; **41**: 1-7 [PMID: 26402131 DOI: 10.1097/RLU.0000000000000998]

44 **Miyazaki M**, Yoshitomi H, Miyakawa S, Uesaka K, Unno M, Endo I, Ota T, Ohtsuka M, Kinoshita H, Shimada K, Shimizu H, Tabata M, Chijiiwa K, Nagino M, Hirano S, Wakai T, Wada K, Isayama H, Okusaka T, Tsuyuguchi T, Fujita N, Furuse J, Yamao K, Murakami K, Yamazaki H, Kijima H, Nakanuma Y, Yoshida M, Takayashiki T, Takada T. Clinical practice guidelines for the management of biliary tract cancers 2015: the 2nd English edition. *J Hepatobiliary Pancreat Sci* 2015; **22**: 249-273 [PMID: 25787274 DOI: 10.1002/jhbp.233]

45 **Ruzzenente A**, Fassan M, Conci S, Simbolo M, Lawlor RT, Pedrazzani C, Capelli P, D'Onofrio M, Iacono C, Scarpa A, Guglielmi A. Cholangiocarcinoma Heterogeneity Revealed by Multigene Mutational Profiling: Clinical and Prognostic Relevance in Surgically Resected Patients. *Ann Surg Oncol* 2016; **23**: 1699-1707 [PMID: 26717940 DOI: 10.1245/s10434-015-5046-6]

46 **Vogl TJ**, Schwarz WO, Heller M, Herzog C, Zangos S, Hintze RE, Neuhaus P, Hammerstingl RM. Staging of Klatskin tumours (hilar cholangiocarcinomas): comparison of MR cholangiography, MR imaging, and endoscopic retrograde cholangiography. *Eur Radiol* 2006; **16**: 2317-2325 [PMID: 16622690 DOI: 10.1007/s00330-005-0139-4]

47 **Jorgensen JE**, Waljee AK, Volk ML, Sonnenday CJ, Elta GH, Al-Hawary MM, Singal AG, Taylor JR, Elmunzer BJ. Is MRCP equivalent to ERCP for diagnosing biliary obstruction in orthotopic liver transplant recipients? A meta-analysis. *Gastrointest Endosc* 2011; **73**: 955-962 [PMID: 21316670 DOI: 10.1016/j.gie.2010.12.014]

48 **Park HS**, Lee JM, Choi JY, Lee MW, Kim HJ, Han JK, Choi BI. Preoperative evaluation of bile duct cancer: MRI combined with MR cholangiopancreatography versus MDCT with direct cholangiography. *AJR Am J Roentgenol* 2008;

190: 396-405 [PMID: 18212225 DOI: 10.2214/AJR.07.2310]
49 **Zhimin G**, Noor H, Jian-Bo Z, Lin W, Jha RK. Advances in diagnosis and treatment of hilar cholangiocarcinoma -- a review. *Med Sci Monit* 2013; **19**: 648-656 [PMID: 23921971 DOI: 10.12659/MSM.889379]
50 **Song J**, Li Y, Bowlus CL, Yang G, Leung PSC, Gershwin ME. Cholangiocarcinoma in Patients with Primary Sclerosing Cholangitis (PSC): a Comprehensive Review. *Clin Rev Allergy Immunol* 2020; **58**: 134-149 [PMID: 31463807 DOI: 10.1007/s12016-019-08764-7]
51 **Mohamadnejad M**, DeWitt JM, Sherman S, LeBlanc JK, Pitt HA, House MG, Jones KJ, Fogel EL, McHenry L, Watkins JL, Cote GA, Lehman GA, Al-Haddad MA. Role of EUS for preoperative evaluation of cholangiocarcinoma: a large single-center experience. *Gastrointest Endosc* 2011; **73**: 71-78 [PMID: 21067747 DOI: 10.1016/j.gie.2010.08.050]
52 **Levy MJ**, Heimbach JK, Gores GJ. Endoscopic ultrasound staging of cholangiocarcinoma. *Curr Opin Gastroenterol* 2012; **28**: 244-252 [PMID: 22274618 DOI: 10.1097/MOG.0b013e32835005bc]
53 **Ohshima Y**, Yasuda I, Kawakami H, Kuwatani M, Mukai T, Iwashita T, Doi S, Nakashima M, Hirose Y, Asaka M, Moriwaki H. EUS-FNA for suspected malignant biliary strictures after negative endoscopic transpapillary brush cytology and forceps biopsy. *J Gastroenterol* 2011; **46**: 921-928 [PMID: 21526370 DOI: 10.1007/s00535-011-0404-z]
54 **Barr Fritcher EG**, Voss JS, Brankley SM, Campion MB, Jenkins SM, Keeney ME, Henry MR, Kerr SM, Chaiteerakij R, Pestova EV, Clayton AC, Zhang J, Roberts LR, Gores GJ, Halling KC, Kipp BR. An Optimized Set of Fluorescence In Situ Hybridization Probes for Detection of Pancreatobiliary Tract Cancer in Cytology Brush Samples. *Gastroenterology* 2015; **149**: 1813-1824.e1 [PMID: 26327129 DOI: 10.1053/j.gastro.2015.08.046]
55 **Trikudanathan G**, Navaneethan U, Njei B, Vargo JJ, Parsi MA. Diagnostic yield of bile duct brushings for cholangiocarcinoma in primary sclerosing cholangitis: a systematic review and meta-analysis. *Gastrointest Endosc* 2014; **79**: 783-789 [PMID: 24140129 DOI: 10.1016/j.gie.2013.09.015]
56 **Rizvi S**, Khan SA, Hallemeier CL, Kelley RK, Gores GJ. Cholangiocarcinoma - evolving concepts and therapeutic strategies. *Nat Rev Clin Oncol* 2018; **15**: 95-111 [PMID: 28994423 DOI: 10.1038/nrclinonc.2017.157]
57 **Meister T**, Heinzow HS, Woestmeyer C, Lenz P, Menzel J, Kucharzik T, Domschke W, Domagk D. Intraductal ultrasound substantiates diagnostics of bile duct strictures of uncertain etiology. *World J Gastroenterol* 2013; **19**: 874-881 [PMID: 23430958 DOI: 10.3748/wjg.v19.i6.874]
58 **Navaneethan U**, Hasan MK, Kommaraju K, Zhu X, Hebert-Magee S, Hawes RH, Vargo JJ, Varadarajulu S, Parsi MA. Digital, single-operator cholangiopancreatoscopy in the diagnosis and management of pancreatobiliary disorders: a multicenter clinical experience (with video). *Gastrointest Endosc* 2016; **84**: 649-655 [PMID: 26995690 DOI: 10.1016/j.gie.2016.03.789]
59 **Slivka A**, Gan I, Jamidar P, Costamagna G, Cesaro P, Giovannini M, Caillol F, Kahaleh M. Validation of the diagnostic accuracy of probe-based confocal laser endomicroscopy for the characterization of indeterminate biliary strictures: results of a prospective multicenter international study. *Gastrointest Endosc* 2015; **81**: 282-290 [PMID: 25616752 DOI: 10.1016/j.gie.2014.10.009]
60 **Viterbo D**, Gausman V, Gonda T. Diagnostic and therapeutic biomarkers in pancreaticobiliary malignancy. *World J Gastrointest Endosc* 2016; **8**: 128-142 [PMID: 26862363 DOI: 10.4253/wjge.v8.i3.128]
61 **Kondo N**, Murakami Y, Uemura K, Sudo T, Hashimoto Y, Sasaki H, Sueda T. Elevated perioperative serum CA 19-9 levels are independent predictors of poor survival in patients with resectable cholangiocarcinoma. *J Surg Oncol* 2014; **110**: 422-429 [PMID: 24889968 DOI: 10.1002/jso.23666]
62 **Charatcharoenwitthaya P**, Enders FB, Halling KC, Lindor KD. Utility of serum tumor markers, imaging, and biliary cytology for detecting cholangiocarcinoma in primary sclerosing cholangitis. *Hepatology* 2008; **48**: 1106-1117 [PMID: 18785620 DOI: 10.1002/hep.22441]
63 **Oseini AM**, Chaiteerakij R, Shire AM, Ghazale A, Kaiya J, Moser CD, Aderca I, Mettler TA, Therneau TM, Zhang L, Takahashi N, Chari ST, Roberts LR. Utility of serum immunoglobulin G4 in distinguishing immunoglobulin G4-associated cholangitis from cholangiocarcinoma. *Hepatology* 2011; **54**: 940-948 [PMID: 21674559 DOI: 10.1002/hep.24487]
64 **Nakaoka T**, Saito Y, Saito H. Aberrant DNA Methylation as a Biomarker and a Therapeutic Target of Cholangiocarcinoma. *Int J Mol Sci* 2017; **18**: 1111 [PMID: 28545228 DOI: 10.3390/ijms18061111]
65 **Ghidini M**, Pizzo C, Botticelli A, Hahne JC, Passalacqua R, Tomasello G, Petrelli F. Biliary tract cancer: current challenges and future prospects. *Cancer Manag Res* 2019; **11**: 379-388 [PMID: 30643463 DOI: 10.2147/CMAR.S157156]
66 **Li L**, Masica D, Ishida M, Tomuleasa C, Umegaki S, Kalloo AN, Georgiades C, Singh VK, Khashab M, Amateau S, Li Z, Okolo P, Lennon AM, Saxena P, Geschwind JF, Schlachter T, Hong K, Pawlik TM, Canto M, Law J, Sharaiha R, Weiss CR, Thuluvath P, Goggins M, Shin EJ, Peng H, Kumbhari V, Hutfless S, Zhou L, Mezey E, Meltzer SJ, Karchin R, Selaru FM. Human bile contains microRNA-laden extracellular vesicles that can be used for cholangiocarcinoma diagnosis. *Hepatology* 2014; **60**: 896-907 [PMID: 24497320 DOI: 10.1002/hep.27050]
67 **Rassam F**, Roos E, van Lienden KP, van Hooft JE, Klümpen HJ, van Tienhoven G, Bennink RJ, Engelbrecht MR, Schoorlemmer A, Beuers UHW, Verheij J, Besselink MG, Busch OR, van Gulik TM. Modern work-up and extended resection in perihilar cholangiocarcinoma: the AMC experience. *Langenbecks Arch Surg* 2018; **403**: 289-307 [PMID: 29350267 DOI: 10.1007/s00423-018-1649-2]
68 **Ratti F**, Cipriani F, Fiorentini G, Hidalgo Salinas C, Catena M, Paganelli M, Aldrighetti L. Management of hilum infiltrating tumors of the liver: The impact of experience and standardization on outcome. *Dig Liver Dis* 2019; **51**: 135-141 [PMID: 30115572 DOI: 10.1016/j.dld.2018.07.006]
69 **Olthof PB**, Wiggers JK, Groot Koerkamp B, Coelen RJ, Allen PJ, Besselink MG, Busch OR, D'Angelica MI, DeMatteo RP, Kingham TP, van Lienden KP, Jarnagin WR, van Gulik TM. Postoperative Liver Failure Risk Score: Identifying Patients with Resectable Perihilar Cholangiocarcinoma Who Can Benefit from Portal Vein Embolization. *J Am Coll Surg* 2017; **225**: 387-394 [PMID: 28687509 DOI: 10.1016/j.jamcollsurg.2017.06.007]

70 **Ebata T**, Yokoyama Y, Igami T, Sugawara G, Takahashi Y, Nagino M. Portal vein embolization before extended hepatectomy for biliary cancer: current technique and review of 494 consecutive embolizations. *Dig Surg* 2012; **29**: 23-29 [PMID: 22441616 DOI: 10.1159/000335718]

71 **Farges O**, Regimbeau JM, Fuks D, Le Treut YP, Cherqui D, Bachellier P, Mabrut JY, Adham M, Pruvot FR, Gigot JF. Multicentre European study of preoperative biliary drainage for hilar cholangiocarcinoma. *Br J Surg* 2013; **100**: 274-283 [PMID: 23124720 DOI: 10.1002/bjs.8950]

72 **Celotti A**, Solaini L, Montori G, Coccolini F, Tognali D, Baiocchi G. Preoperative biliary drainage in hilar cholangiocarcinoma: Systematic review and meta-analysis. *Eur J Surg Oncol* 2017; **43**: 1628-1635 [PMID: 28477976 DOI: 10.1016/j.ejso.2017.04.001]

73 **Higuchi R**, Yazawa T, Uemura S, Izumo W, Chaudhary RJ, Furukawa T, Yamamoto M. ENBD is Associated with Decreased Tumor Dissemination Compared to PTBD in Perihilar Cholangiocarcinoma. *J Gastrointest Surg* 2017; **21**: 1506-1514 [PMID: 28721561 DOI: 10.1007/s11605-017-3492-0]

74 **Kloek JJ**, van der Gaag NA, Aziz Y, Rauws EA, van Delden OM, Lameris JS, Busch OR, Gouma DJ, van Gulik TM. Endoscopic and percutaneous preoperative biliary drainage in patients with suspected hilar cholangiocarcinoma. *J Gastrointest Surg* 2010; **14**: 119-125 [PMID: 19756881 DOI: 10.1007/s11605-009-1009-1]

75 **Kawakami H**, Kuwatani M, Onodera M, Haba S, Eto K, Ehira N, Yamato H, Kudo T, Tanaka E, Hirano S, Kondo S, Asaka M. Endoscopic nasobiliary drainage is the most suitable preoperative biliary drainage method in the management of patients with hilar cholangiocarcinoma. *J Gastroenterol* 2011; **46**: 242-248 [PMID: 20700608 DOI: 10.1007/s00535-010-0298-1]

76 **Tang Z**, Yang Y, Meng W, Li X. Best option for preoperative biliary drainage in Klatskin tumor: A systematic review and meta-analysis. *Medicine (Baltimore)* 2017; **96**: e8372 [PMID: 29069029 DOI: 10.1097/MD.0000000000008372]

77 **Coelen RJS**, Roos E, Wiggers JK, Besselink MG, Buis CI, Busch ORC, Dejong CHC, van Delden OM, van Eijck CHJ, Fockens P, Gouma DJ, Koerkamp BG, de Haan MW, van Hooft JE, IJzermans JNM, Kater GM, Koornstra JJ, van Lienden KP, Moelker A, Damink SWMO, Poley JW, Porte RJ, de Ridder RJ, Verheij J, van Woerden V, Rauws EAJ, Dijkgraaf MGW, van Gulik TM. Endoscopic versus percutaneous biliary drainage in patients with resectable perihilar cholangiocarcinoma: a multicentre, randomised controlled trial. *Lancet Gastroenterol Hepatol* 2018; **3**: 681-690 [PMID: 30122355 DOI: 10.1016/S2468-1253(18)30234-6]

78 **Jo JH**, Chung MJ, Han DH, Park JY, Bang S, Park SW, Song SY, Chung JB. Best options for preoperative biliary drainage in patients with Klatskin tumors. *Surg Endosc* 2017; **31**: 422-429 [PMID: 27287904 DOI: 10.1007/s00464-016-4993-8]

79 **Wiggers JK**, Groot Koerkamp B, van Klaveren D, Coelen RJ, Nio CY, Allen PJ, Besselink MG, Busch OR, D'Angelica MI, DeMatteo RP, Kingham TP, van Gulik TM, Jarnagin WR. Preoperative Risk Score to Predict Occult Metastatic or Locally Advanced Disease in Patients with Resectable Perihilar Cholangiocarcinoma on Imaging. *J Am Coll Surg* 2018; **227**: 238-246.e2 [PMID: 29627334 DOI: 10.1016/j.jamcollsurg.2018.03.041]

80 **Schwegler I**, von Holzen A, Gutzwiller JP, Schlumpf R, Mühlebach S, Stanga Z. Nutritional risk is a clinical predictor of postoperative mortality and morbidity in surgery for colorectal cancer. *Br J Surg* 2010; **97**: 92-97 [PMID: 20013933 DOI: 10.1002/bjs.6805]

81 **Beier-Holgersen R**, Boesby S. Influence of postoperative enteral nutrition on postsurgical infections. *Gut* 1996; **39**: 833-835 [PMID: 9038665 DOI: 10.1136/gut.39.6.833]

82 **Saha SK**, Lee SB, Won J, Choi HY, Kim K, Yang GM, Dayem AA, Cho SG. Correlation between Oxidative Stress, Nutrition, and Cancer Initiation. *Int J Mol Sci* 2017; **18**: 1544 [PMID: 28714931 DOI: 10.3390/ijms18071544]

83 **Akashi K**, Ebata T, Mizuno T, Yokoyama Y, Igami T, Yamaguchi J, Onoe S, Nagino M. Surgery for perihilar cholangiocarcinoma from a viewpoint of age: Is it beneficial to octogenarians in an aging society? *Surgery* 2018; **164**: 1023-1029 [PMID: 30082134 DOI: 10.1016/j.surg.2018.05.051]

84 **Pulitano C**, Crawford M, Joseph D, Aldrighetti L, Sandroussi C. Preoperative assessment of postoperative liver function: the importance of residual liver volume. *J Surg Oncol* 2014; **110**: 445-450 [PMID: 24962104 DOI: 10.1002/jso.23671]

85 **Van Der Walt AM**. Patient classification in the Groote Schuur Hospital region, Republic of South Africa. *Nurs Adm Q* 1992; **16**: 43-46 [PMID: 1738490 DOI: 10.1007/s00534-006-1125-1]

86 **Lee EC**, Park SJ, Han SS, Shim JR, Park HM, Lee SD, Kim SH. Risk prediction of post-hepatectomy liver failure in patients with perihilar cholangiocarcinoma. *J Gastroenterol Hepatol* 2018; **33**: 958-965 [PMID: 28843035 DOI: 10.1111/jgh.13966]

87 **Sultana A**, Brooke-Smith M, Ullah S, Figueras J, Rees M, Vauthey JN, Conrad C, Hugh TJ, Garden OJ, Fan ST, Crawford M, Makuuchi M, Yokoyama Y, Büchler M, Padbury R. Prospective evaluation of the International Study Group for Liver Surgery definition of post hepatectomy liver failure after liver resection: an international multicentre study. *HPB (Oxford)* 2018; **20**: 462-469 [PMID: 29287736 DOI: 10.1016/j.hpb.2017.11.007]

88 **Nuzzo G**, Giuliante F, Ardito F, Giovannini I, Aldrighetti L, Belli G, Bresadola F, Calise F, Dalla Valle R, D'Amico DF, Gennari L, Giulini SM, Guglielmi A, Jovine E, Pellicci R, Pernthaler H, Pinna AD, Puleo S, Torzilli G, Capussotti L; Italian Chapter of the International Hepato-Pancreato-Biliary Association, Cillo U, Ercolani G, Ferrucci M, Mastrangelo L, Portolani N, Pulitanò C, Ribero D, Ruzzenente A, Scuderi V, Federico B. Improvement in perioperative and long-term outcome after surgical treatment of hilar cholangiocarcinoma: results of an Italian multicenter analysis of 440 patients. *Arch Surg* 2012; **147**: 26-34 [PMID: 22250108 DOI: 10.1001/archsurg.2011.771]

89 **Hoyos S**, Navas MC, Restrepo JC, Botero RC. Current controversies in cholangiocarcinoma. *Biochim Biophys Acta Mol Basis Dis* 2018; **1864**: 1461-1467 [PMID: 28756216 DOI: 10.1016/j.bbadis.2017.07.027]

90 **Molina V**, Sampson J, Ferrer J, Díaz A, Ayuso JR, Sánchez-Cabús S, Fuster J, García-Valdecasas JC. Surgical treatment of perihilar cholangiocarcinoma: early results of en bloc portal vein resection. *Langenbecks Arch Surg* 2017; **402**: 95-104 [PMID: 28012034 DOI: 10.1007/s00423-016-1542-9]

91 **Neuhaus P**, Thelen A, Jonas S, Puhl G, Denecke T, Veltzke-Schlieker W, Seehofer D. Oncological

superiority of hilar en bloc resection for the treatment of hilar cholangiocarcinoma. *Ann Surg Oncol* 2012; **19**: 1602-1608 [PMID: 21964888 DOI: 10.1245/s10434-011-2077-5]

92 **Benson AB 3rd**, D'Angelica MI, Abrams TA, Are C, Bloomston PM, Chang DT, Clary BM, Covey AM, Ensminger WD, Iyer R, Kelley RK, Linehan D, Malafa MP, Meranze SG, Park JO, Pawlik T, Posey JA, Scaife C, Schefter T, Sigurdson ER, Tian GG, Vauthey JN, Venook AP, Yen Y, Zhu AX, Hoffmann KG, McMillian NR, Sundar H. Hepatobiliary cancers, version 2.2014. *J Natl Compr Canc Netw* 2014; **12**: 1152-1182 [PMID: 25099447 DOI: 10.6004/jnccn.2014.0112]

93 **Park Y**, Hwang DW, Kim JH, Hong SM, Jun SY, Lee JH, Song KB, Jun ES, Kim SC, Park KM. Prognostic comparison of the longitudinal margin status in distal bile duct cancer: R0 on first bile duct resection versus R0 after additional resection. *J Hepatobiliary Pancreat Sci* 2019; **26**: 169-178 [PMID: 30849218 DOI: 10.1002/jhbp.619]

94 **Nakanishi Y**, Tsuchikawa T, Okamura K, Nakamura T, Tamoto E, Murakami S, Ebihara Y, Kurashima Y, Noji T, Asano T, Shichinohe T, Hirano S. Prognostic impact of the site of portal vein invasion in patients with surgically resected perihilar cholangiocarcinoma. *Surgery* 2016; **159**: 1511-1519 [PMID: 26948498 DOI: 10.1016/j.surg.2016.01.012]

95 **van Vugt JLA**, Gaspersz MP, Coelen RJS, Vugts J, Labeur TA, de Jonge J, Polak WG, Busch ORC, Besselink MG, IJzermans JNM, Nio CY, van Gulik TM, Willemssen FEJA, Groot Koerkamp B. The prognostic value of portal vein and hepatic artery involvement in patients with perihilar cholangiocarcinoma. *HPB (Oxford)* 2018; **20**: 83-92 [PMID: 28958483 DOI: 10.1016/j.hpb.2017.08.025]

96 **Groot Koerkamp B**, Jarnagin WR. Surgery for perihilar cholangiocarcinoma. *Br J Surg* 2018; **105**: 771-772 [PMID: 29756647 DOI: 10.1002/bjs.10875]

97 **Perini MV**, Coelho FF, Kruger JA, Rocha FG, Herman P. Extended right hepatectomy with caudate lobe resection using the hilar "en bloc" resection technique with a modified hanging maneuver. *J Surg Oncol* 2016; **113**: 427-431 [PMID: 26776500 DOI: 10.1002/jso.24154]

98 **Kawabata Y**, Hayashi H, Yano S, Tajima Y. Liver parenchyma transection-first approach in hemihepatectomy with en bloc caudate lobectomy for hilar cholangiocarcinoma: A safe technique to secure favorable surgical outcomes. *J Surg Oncol* 2017; **115**: 963-970 [PMID: 28334429 DOI: 10.1002/jso.24612]

99 **Ebata T**, Mizuno T, Yokoyama Y, Igami T, Sugawara G, Nagino M. Surgical resection for Bismuth type IV perihilar cholangiocarcinoma. *Br J Surg* 2018; **105**: 829-838 [PMID: 28488733 DOI: 10.1002/bjs.10556]

100 **Hu HJ**, Jin YW, Zhou RX, Shrestha A, Ma WJ, Yang Q, Wang JK, Liu F, Cheng NS, Li FY. Hepatic Artery Resection for Bismuth Type III and IV Hilar Cholangiocarcinoma: Is Reconstruction Always Required? *J Gastrointest Surg* 2018; **22**: 1204-1212 [PMID: 29512002 DOI: 10.1007/s11605-018-3711-3]

101 **Li B**, Xiong XZ, Zhou Y, Wu SJ, You Z, Lu J, Cheng NS. Prognostic value of lymphovascular invasion in Bismuth-Corlette type IV hilar cholangiocarcinoma. *World J Gastroenterol* 2017; **23**: 6685-6693 [PMID: 29085213 DOI: 10.3748/wjg.v23.i36.6685]

102 **Rosen CB**. Transplantation Versus Resection for Hilar Cholangiocarcinoma: An Argument for Shifting Paradigms for Resectable Disease in Annals of Surgery 2018. *Ann Surg* 2018; **267**: 808-809 [PMID: 29465456 DOI: 10.1097/SLA.0000000000002716]

103 **Rizvi S**, Gores GJ. Pathogenesis, diagnosis, and management of cholangiocarcinoma. *Gastroenterology* 2013; **145**: 1215-1229 [PMID: 24140396 DOI: 10.1053/j.gastro.2013.10.013]

104 **Heimbach JK**, Haddock MG, Alberts SR, Nyberg SL, Ishitani MB, Rosen CB, Gores GJ. Transplantation for hilar cholangiocarcinoma. *Liver Transpl* 2004; **10**: S65-S68 [PMID: 15382214 DOI: 10.1002/lt.20266]

105 **Rea DJ**, Heimbach JK, Rosen CB, Haddock MG, Alberts SR, Kremers WK, Gores GJ, Nagorney DM. Liver transplantation with neoadjuvant chemoradiation is more effective than resection for hilar cholangiocarcinoma. *Ann Surg* 2005; **242**: 451-8; discussion 458-61 [PMID: 16135931 DOI: 10.1097/01.sla.0000179678.13285.fa]

106 **Ethun CG**, Lopez-Aguiar AG, Anderson DJ, Adams AB, Fields RC, Doyle MB, Chapman WC, Krasnick BA, Weber SM, Mezrich JD, Salem A, Pawlik TM, Poultsides G, Tran TB, Idrees K, Isom CA, Martin RCG, Scoggins CR, Shen P, Mogal HD, Schmidt C, Beal E, Hatzaras I, Shenoy R, Cardona K, Maithel SK. Transplantation Versus Resection for Hilar Cholangiocarcinoma: An Argument for Shifting Treatment Paradigms for Resectable Disease. *Ann Surg* 2018; **267**: 797-805 [PMID: 29064885 DOI: 10.1097/SLA.0000000000002574]

107 **Goldaracena N**, Gorgen A, Sapisochin G. Current status of liver transplantation for cholangiocarcinoma. *Liver Transpl* 2018; **24**: 294-303 [PMID: 29024405 DOI: 10.1002/lt.24955]

108 **Mansour JC**, Aloia TA, Crane CH, Heimbach JK, Nagino M, Vauthey JN. Hilar cholangiocarcinoma: expert consensus statement. *HPB (Oxford)* 2015; **17**: 691-699 [PMID: 26172136 DOI: 10.1111/hpb.12450]

109 **Rotellar F**, Pardo F. Laparoscopic staging in hilar cholangiocarcinoma: Is it still justified? *World J Gastrointest Oncol* 2013; **5**: 127-131 [PMID: 23919106 DOI: 10.4251/wjgo.v5.i7.127]

110 **Coelen RJ**, Ruys AT, Wiggers JK, Nio CY, Verheij J, Gouma DJ, Besselink MG, Busch OR, van Gulik TM. Development of a Risk Score to Predict Detection of Metastasized or Locally Advanced Perihilar Cholangiocarcinoma at Staging Laparoscopy. *Ann Surg Oncol* 2016; **23**: 904-910 [PMID: 27586005 DOI: 10.1245/s10434-016-5531-6]

111 **Tian Y**, Liu L, Yeolkar NV, Shen F, Li J, He Z. Diagnostic role of staging laparoscopy in a subset of biliary cancers: a meta-analysis. *ANZ J Surg* 2017; **87**: 22-27 [PMID: 27647697 DOI: 10.1111/ans.13762]

112 **Connor S**, Barron E, Wigmore SJ, Madhavan KK, Parks RW, Garden OJ. The utility of laparoscopic assessment in the preoperative staging of suspected hilar cholangiocarcinoma. *J Gastrointest Surg* 2005; **9**: 476-480 [PMID: 15797226 DOI: 10.1016/j.gassur.2004.10.009]

113 **Ramacciato G**, Nigri G, Bellagamba R, Petrucciani N, Ravaioli M, Cescon M, Del Gaudio M, Ercolani G, Di Benedetto F, Cautero N, Quintini C, Cucchetti A, Lauro A, Miller C, Pinna AD. Univariate and multivariate analysis of prognostic factors in the surgical treatment of hilar cholangiocarcinoma. *Am Surg* 2010; **76**: 1260-1268 [PMID: 21140696]

114 **Aoba T**, Ebata T, Yokoyama Y, Igami T, Sugawara G, Takahashi Y, Nimura Y, Nagino M. Assessment of nodal status for perihilar cholangiocarcinoma: location, number, or ratio of involved nodes. *Ann Surg* 2013; **257**: 718-725 [PMID: 23407295 DOI: 10.1097/SLA.0b013e3182822277]

115 **Kambakamba P**, Linecker M, Slankamenac K, DeOliveira ML. Lymph node dissection in resectable perihilar cholangiocarcinoma: a systematic review. *Am J Surg* 2015; **210**: 694-701 [PMID: 26212390 DOI: 10.1016/j.amjsurg.2015.05.015]

116 **Kow AW**, Wook CD, Song SC, Kim WS, Kim MJ, Park HJ, Heo JS, Choi SH. Role of caudate lobectomy in type III A and III B hilar cholangiocarcinoma: a 15-year experience in a tertiary institution. *World J Surg* 2012; **36**: 1112-1121 [PMID: 22374541 DOI: 10.1007/s00268-012-1497-0]

117 **Hakeem AR**, Marangoni G, Chapman SJ, Young RS, Nair A, Hidalgo EL, Toogood GJ, Wyatt JI, Lodge PA, Prasad KR. Does the extent of lymphadenectomy, number of lymph nodes, positive lymph node ratio and neutrophil-lymphocyte ratio impact surgical outcome of perihilar cholangiocarcinoma? *Eur J Gastroenterol Hepatol* 2014; **26**: 1047-1054 [PMID: 25051217 DOI: 10.1097/MEG.0000000000000162]

118 **Kiriyama M**, Ebata T, Aoba T, Kaneoka Y, Arai T, Shimizu Y, Nagino M; Nagoya Surgical Oncology Group. Prognostic impact of lymph node metastasis in distal cholangiocarcinoma. *Br J Surg* 2015; **102**: 399-406 [PMID: 25611179 DOI: 10.1002/bjs.9752]

119 **Primrose JN**, Fox RP, Palmer DH, Malik HZ, Prasad R, Mirza D, Anthony A, Corrie P, Falk S, Finch-Jones M, Wasan H, Ross P, Wall L, Wadsley J, Evans JTR, Stocken D, Praseedom R, Ma YT, Davidson B, Neoptolemos JP, Iveson T, Raftery J, Zhu S, Cunningham D, Garden OJ, Stubbs C, Valle JW, Bridgewater J; BILCAP study group. Capecitabine compared with observation in resected biliary tract cancer (BILCAP): a randomised, controlled, multicentre, phase 3 study. *Lancet Oncol* 2019; **20**: 663-673 [PMID: 30922733 DOI: 10.1016/S1470-2045(18)30915-X]

120 **Edeline J**, Benabdelghani M, Bertaut A, Watelet J, Hammel P, Joly JP, Boudjema K, Fartoux L, Bouhier-Leporrier K, Jouve JL, Faroux R, Guerin-Meyer V, Kurtz JE, Assénat E, Seitz JF, Baumgaertner I, Tougeron D, de la Fouchardière C, Lombard-Bohas C, Boucher E, Stanbury T, Louvet C, Malka D, Phelip JM. Gemcitabine and Oxaliplatin Chemotherapy or Surveillance in Resected Biliary Tract Cancer (PRODIGE 12-ACCORD 18-UNICANCER GI): A Randomized Phase III Study. *J Clin Oncol* 2019; **37**: 658-667 [PMID: 30707660 DOI: 10.1200/JCO.18.00050]

121 **Stein A**, Arnold D, Bridgewater J, Goldstein D, Jensen LH, Klümpen HJ, Lohse AW, Nashan B, Primrose J, Schrum S, Shannon J, Vettorazzi E, Wege H. Adjuvant chemotherapy with gemcitabine and cisplatin compared to observation after curative intent resection of cholangiocarcinoma and muscle invasive gallbladder carcinoma (ACTICCA-1 trial) - a randomized, multidisciplinary, multinational phase III trial. *BMC Cancer* 2015; **15**: 564 [PMID: 26228433 DOI: 10.1186/s12885-015-1498-0]

122 **Horgan AM**, Amir E, Walter T, Knox JJ. Adjuvant therapy in the treatment of biliary tract cancer: a systematic review and meta-analysis. *J Clin Oncol* 2012; **30**: 1934-1940 [PMID: 22529261 DOI: 10.1200/JCO.2011.40.5381]

123 **Ghidini M**, Tomasello G, Botticelli A, Barni S, Zabbialini G, Seghezzi S, Passalacqua R, Braconi C, Petrelli F. Adjuvant chemotherapy for resected biliary tract cancers: a systematic review and meta-analysis. *HPB (Oxford)* 2017; **19**: 741-748 [PMID: 28684194 DOI: 10.1016/j.hpb.2017.05.010]

124 **Messina C**, Merz V, Frisinghelli M, Trentin C, Grego E, Veccia A, Salati M, Messina M, Carnaghi C, Caffo O. Adjuvant chemotherapy in resected bile duct cancer: A systematic review and meta-analysis of randomized trials. *Crit Rev Oncol Hematol* 2019; **143**: 124-129 [PMID: 31563828 DOI: 10.1016/j.critrevonc.2019.09.002]

125 **Nassour I**, Mokdad AA, Porembka MR, Choti MA, Polanco PM, Mansour JC, Minter RM, Wang SC, Yopp AC. Adjuvant Therapy Is Associated With Improved Survival in Resected Perihilar Cholangiocarcinoma: A Propensity Matched Study. *Ann Surg Oncol* 2018; **25**: 1193-1201 [PMID: 29488187 DOI: 10.1245/s10434-018-6388-7]

126 **Phelip JM**, Vendrely V, Rostain F, Subtil F, Jouve JL, Gasmi M, Michel P, Le Malicot K, Smith D, Seitz JF, Fauchart JP, Martin P, Bennouna J, Morin T, Bonnet I, Maingon P, Lepage C, Chauffert B. Gemcitabine plus cisplatin versus chemoradiotherapy in locally advanced biliary tract cancer: Fédération Francophone de Cancérologie Digestive 9902 phase II randomised study. *Eur J Cancer* 2014; **50**: 2975-2982 [PMID: 25241229 DOI: 10.1016/j.ejca.2014.08.013]

127 **Fuller CD**, Dang ND, Wang SJ, Desai P, Choi M, Thomas CR Jr, Fuss M. Image-guided intensity-modulated radiotherapy (IG-IMRT) for biliary adenocarcinomas: Initial clinical results. *Radiother Oncol* 2009; **92**: 249-254 [PMID: 19324442 DOI: 10.1016/j.radonc.2009.02.015]

128 **Valle J**, Wasan H, Palmer DH, Cunningham D, Anthoney A, Maraveyas A, Madhusudan S, Iveson T, Hughes S, Pereira SP, Roughton M, Bridgewater J; ABC-02 Trial Investigators. Cisplatin plus gemcitabine versus gemcitabine for biliary tract cancer. *N Engl J Med* 2010; **362**: 1273-1281 [PMID: 20375404 DOI: 10.1056/NEJMoa0908721]

129 **Valle JW**, Furuse J, Jitlal M, Beare S, Mizuno N, Wasan H, Bridgewater J, Okusaka T. Cisplatin and gemcitabine for advanced biliary tract cancer: a meta-analysis of two randomised trials. *Ann Oncol* 2014; **25**: 391-398 [PMID: 24351397 DOI: 10.1093/annonc/mdt540]

130 **Lamarca A**, Hubner RA, David Ryder W, Valle JW. Second-line chemotherapy in advanced biliary cancer: a systematic review. *Ann Oncol* 2014; **25**: 2328-2338 [PMID: 24769639 DOI: 10.1093/annonc/mdu162]

131 **Fornaro L**, Vivaldi C, Cereda S, Leone F, Aprile G, Lonardi S, Silvestris N, Santini D, Milella M, Caparello C, Musettini G, Pasquini G, Falcone A, Brandi G, Sperduti I, Vasile E; GICO group (Gruppo Italiano COlangiocarcinoma). Second-line chemotherapy in advanced biliary cancer progressed to first-line platinum-gemcitabine combination: a multicenter survey and pooled analysis with published data. *J Exp Clin Cancer Res* 2015; **34**: 156 [PMID: 26693938 DOI: 10.1186/s13046-015-0267-x]

132 **Lamarca A**, Palmer DH, Singh Wasan H, Ross PJ, Ma YT, Arora A, Falk S, Gillmore R, Wadsley J, Patel K, Anthoney A, Maraveyas A, Waters JS, Hobbs C, Barber S, Ryder D, Ramage J, Davies LM, Bridgewater JA, Valle JW. ABC-06 | A randomised phase III, multi-centre, open-label study of active symptom control (ASC) alone or ASC with oxaliplatin / 5-FU chemotherapy (ASC+mFOLFOX) for patients (pts) with locally advanced / metastatic biliary tract cancers (ABC) previously-treated with cisplatin/gemcitabine (CisGem) chemotherapy. *J Clin Oncol* 2019; **37**: 4003 [DOI: 10.1200/JCO.2019.37.15_suppl.4003]

133 **Abou-Alfa GK**, Mercade TM, Javle M, Kelley RK, Lubner S, Adeva J, Cleary JM, Catenacci DV, Borad MJ, Bridgewater JA, Harris WP, Murphy AG, Oh DY, Whisenant J, Wu B, Jiang L, Gliser C, Pandya SS,

Valle JW, Zhu AX. LBA10_PR - ClarIDHy: A global, phase III, randomized, double-blind study of ivosidenib (IVO) vs placebo in patients with advanced cholangiocarcinoma (CC) with an isocitrate dehydrogenase 1 (IDH1) mutation. *Ann Oncol* 2019; **30**: v872-v873 [DOI: 10.1093/annonc/mdz394.027]

134 **Indar AA**, Lobo DN, Gilliam AD, Gregson R, Davidson I, Whittaker S, Doran J, Rowlands BJ, Beckingham IJ. Percutaneous biliary metal wall stenting in malignant obstructive jaundice. *Eur J Gastroenterol Hepatol* 2003; **15**: 915-919 [PMID: 12867803 DOI: 10.1097/00042737-200308000-00013]

135 **Cui P**, Pang Q, Wang Y, Qian Z, Hu X, Wang W, Li Z, Zhou L, Man Z, Yang S, Jin H, Liu H. Nutritional prognostic scores in patients with hilar cholangiocarcinoma treated by percutaneous transhepatic biliary stenting combined with 125I seed intracavitary irradiation: A retrospective observational study. *Medicine (Baltimore)* 2018; **97**: e11000 [PMID: 29851859 DOI: 10.1097/MD.0000000000011000]

136 **Groot Koerkamp B**, Wiggers JK, Allen PJ, Besselink MG, Blumgart LH, Busch OR, Coelen RJ, D'Angelica MI, DeMatteo RP, Gouma DJ, Kingham TP, Jarnagin WR, van Gulik TM. Recurrence Rate and Pattern of Perihilar Cholangiocarcinoma after Curative Intent Resection. *J Am Coll Surg* 2015; **221**: 1041-1049 [PMID: 26454735 DOI: 10.1016/j.jamcollsurg.2015.09.005]

137 **Buettner S**, van Vugt JL, Gani F, Groot Koerkamp B, Margonis GA, Ethun CG, Poultsides G, Tran T, Idrees K, Isom CA, Fields RC, Krasnick B, Weber SM, Salem A, Martin RC, Scoggins C, Shen P, Mogal HD, Schmidt C, Beal E, Hatzaras I, Shenoy R, Maithel SK, Guglielmi A, IJzermans JN, Pawlik TM. A Comparison of Prognostic Schemes for Perihilar Cholangiocarcinoma. *J Gastrointest Surg* 2016; **20**: 1716-1724 [PMID: 27412318 DOI: 10.1007/s11605-016-3203-2]

138 **Lurje G**, Bednarsch J, Czigany Z, Lurje I, Schlebusch IK, Boecker J, Meister FA, Tacke F, Roderburg C, Den Dulk M, Gaisa NT, Bruners P, Neumann UP. The prognostic role of lymphovascular invasion and lymph node metastasis in perihilar and intrahepatic cholangiocarcinoma. *Eur J Surg Oncol* 2019; **45**: 1468-1478 [PMID: 31053477 DOI: 10.1016/j.ejso.2019.04.019]

139 **Natsume S**, Ebata T, Yokoyama Y, Igami T, Sugawara G, Shimoyama Y, Nagino M. Clinical significance of left trisectionectomy for perihilar cholangiocarcinoma: an appraisal and comparison with left hepatectomy. *Ann Surg* 2012; **255**: 754-762 [PMID: 22367444 DOI: 10.1097/SLA.0b013e31824a8d82]

140 **Lehrke HD**, Heimbach JK, Wu TT, Jenkins SM, Gores GJ, Rosen CB, Mounajjed T. Prognostic Significance of the Histologic Response of Perihilar Cholangiocarcinoma to Preoperative Neoadjuvant Chemoradiation in Liver Explants. *Am J Surg Pathol* 2016; **40**: 510-518 [PMID: 26752544 DOI: 10.1097/PAS.0000000000000588]

141 **Darwish Murad S**, Kim WR, Harnois DM, Douglas DD, Burton J, Kulik LM, Botha JF, Mezrich JD, Chapman WC, Schwartz JJ, Hong JC, Emond JC, Jeon H, Rosen CB, Gores GJ, Heimbach JK. Efficacy of neoadjuvant chemoradiation, followed by liver transplantation, for perihilar cholangiocarcinoma at 12 US centers. *Gastroenterology* 2012; **143**: 88-98.e3 [PMID: 22504095 DOI: 10.1053/j.gastro.2012.04.008]

142 **Darwish Murad S**, Kim WR, Therneau T, Gores GJ, Rosen CB, Martenson JA, Alberts SR, Heimbach JK. Predictors of pretransplant dropout and posttransplant recurrence in patients with perihilar cholangiocarcinoma. *Hepatology* 2012; **56**: 972-981 [PMID: 22290335 DOI: 10.1002/hep.25629]

World Journal of Gastroenterology

Submit a Manuscript: https://www.f6publishing.com

World J Gastroenterol 2020 July 7; 26(25): 3562-3576

DOI: 10.3748/wjg.v26.i25.3562

ISSN 1007-9327 (print) ISSN 2219-2840 (online)

REVIEW

Development of innovative tools for investigation of nutrient-gut interaction

Wei-Kun Huang, Cong Xie, Richard L Young, Jiang-Bo Zhao, Heike Ebendorff-Heidepriem, Karen L Jones, Christopher K Rayner, Tong-Zhi Wu

ORCID number: Wei-Kun Huang 0000-0001-9400-3840; Cong Xie 0000-0002-0054-9269; Richard L Young 0000-0001-5116-4951; Jiang-Bo Zhao 0000-0002-5883-6017; Heike Ebendorff-Heidepriem 0000-0002-4877-7770; Karen L Jones 0000-0002-1155-5816; Christopher K Rayner 0000-0002-5527-256X; Tong-Zhi Wu 0000-0003-1656-9210.

Author contributions: Huang WK and Wu TZ designed the study; Huang WK and Xie C provided input into the writing of the paper; Xie C contributed to preparation of the figures; Huang WK, Wu TZ, Young RL, Zhao JB, Ebendorff-Heidepriem H, Jones KL and Rayner CK revised the manuscript.

Supported by the National Health and Medical Research Council (NHMRC) of Australia, No. APP1147333; the National Nature Science Foundation of China, No. 81870561; the Hospital Research Foundation of Australia; and the Australian Research Council Centre of Excellence for Nanoscale BioPhotonics, No. CE140100003.

Conflict-of-interest statement: Jones KL has received research funding from Sanofi and AstraZeneca; Rayner CK has received research funding from AstraZeneca, Merck Sharp & Dohme, Eli Lilly, Novartis, and

Wei-Kun Huang, Cong Xie, Richard L Young, Karen L Jones, Christopher K Rayner, Tong-Zhi Wu, Adelaide Medical School, Centre of Research Excellence in Translating Nutritional Science to Good Health, the University of Adelaide, Adelaide, SA 5005, Australia

Wei-Kun Huang, Jiang-Bo Zhao, Heike Ebendorff-Heidepriem, Institute for Photonics and Advanced Sensing, School of Physical Sciences, University of Adelaide, Adelaide, SA 5005, Australia

Wei-Kun Huang, Jiang-Bo Zhao, Heike Ebendorff-Heidepriem, The ARC Centre of Excellence for Nanoscale BioPhotonics, Adelaide, SA 5005, Australia

Richard L Young, Diabetes, Nutrition and Gut Health, Lifelong Health, South Australia Health and Medical Research Institute, Adelaide, SA 5005, Australia

Christopher K Rayner, Department of Gastroenterology and Hepatology, Royal Adelaide Hospital, Adelaide, SA 5000, Australia

Tong-Zhi Wu, Department of Endocrinology, Zhongda Hospital, Institute of Diabetes, School of Medicine, Southeast University, Nanjing 210009, Jiangsu Province, China

Corresponding author: Tong-Zhi Wu, MD, PhD, Doctor, Senior Research Fellow, Adelaide Medical School, Centre of Research Excellence in Translating Nutritional Science to Good Health, the University of Adelaide, Level 6 Adelaide Health and Medical Sciences (AHMS) building, North Terrace, Adelaide, SA 5005, Australia. tongzhi.wu@adelaide.edu.au

Abstract

The gastrointestinal tract is the key interface between the ingesta and the human body. There is wide recognition that the gastrointestinal response to nutrients or bioactive compounds, particularly the secretion of numerous hormones, is critical to the regulation of appetite, body weight and blood glucose. This concept has led to an increasing focus on "gut-based" strategies for the management of metabolic disorders, including type 2 diabetes and obesity. Understanding the underlying mechanisms and downstream effects of nutrient-gut interactions is fundamental to effective translation of this knowledge to clinical practice. To this end, an array of research tools and platforms have been developed to better understand the mechanisms of gut hormone secretion from enteroendocrine cells. This review discusses the evolution of *in vitro* and *in vivo* models and the integration of

Sanofi; Wu TZ has received research funding from Novartis and AstraZeneca; None of the other authors has any personal or financial conflict of interest to declare.

Manuscript source: Invited manuscript

Received: March 15, 2020
Peer-review started: March 15, 2020
First decision: March 21, 2020
Revised: May 29, 2020
Accepted: June 18, 2020
Article in press: June 18, 2020
Published online: July 7, 2020

P-Reviewer: Jamali R, Kung WM, Qin R, Wada R
S-Editor: Yan JP
L-Editor: A
E-Editor: Wang LL

innovative techniques that will ultimately enable the development of novel therapies for metabolic diseases.

Key words: Nutrient-gut interaction; Metabolic disorders; Incretin hormones; Enteroendocrine cells; Enteroids; Intestinal intubation; Intestine-on-a-chip

Core tip: The development of platforms for investigating nutrient-gut interactions is critical to understanding how nutrients trigger the release of gut hormones and has the potential to yield novel targets for improved management of metabolic disorders. In addition to the use of endoscopic or surgical gut tissues or primary enteroendocrine cells, *in vitro* models now include enteroendocrine cell lines originating from rodent (STC-1 and GLUTag) or human (NCI-H716 and HuTo-80) intestinal tumours, and intestinal organoids differentiated from intestinal stem cells. The physiological relevance of these models has been challenged, but may be improved substantially by incorporating advanced biomedical techniques (*e.g.*, microfluidic devices) into the culture system. These approaches have complemented clinical studies utilising intestinal intubation, often with integrated manometry and impedance recording, which have revealed gut region-specific responses to intraluminal contents. Newer clinical developments include the use of novel ingestible sensors.

Citation: Huang WK, Xie C, Young RL, Zhao JB, Ebendorff-Heidepriem H, Jones KL, Rayner CK, Wu TZ. Development of innovative tools for investigation of nutrient-gut interaction. *World J Gastroenterol* 2020; 26(25): 3562-3576
URL: https://www.wjgnet.com/1007-9327/full/v26/i25/3562.htm
DOI: https://dx.doi.org/10.3748/wjg.v26.i25.3562

INTRODUCTION

It is now widely appreciated that the gastrointestinal (GI) tract not only serves to process food, but also represents the largest endocrine organ in the body, releasing a wide array of peptide hormones to orchestrate metabolic homeostasis[1]. Ghrelin, for example, is released from gastric Gr-cells into the circulation during fasting or periods of negative energy balance and triggers hunger to drive food intake[2]; ghrelin levels in circulation are subsequently suppressed upon feeding[3]. The interaction of nutrients and digestive juices with the intestinal mucosa triggers the secretion of a number of postprandial hormones, including cholecystokinin (CCK) from enteroendocrine (EE) I-cells[4] and glucose-dependent insulinotropic polypeptide (GIP) from K-cells in the upper small intestine, and glucagon-like peptide-1 (GLP-1) and peptide YY (PYY) from L-cells located predominantly in the distal small and large intestine[5,6]. A subset of EE cells in the proximal small intestine have also been shown to secrete both GLP-1 and GIP[7]. GLP-1 and GIP are known as the incretin hormones; both stimulate insulin secretion in a glucose-dependent manner[8,9]. GLP-1 also suppresses glucagon and acts with CCK and PYY to inhibit appetite, slow the delivery of nutrients from the stomach into the small intestine and retard their subsequent absorption[10]. Accordingly, the integrated responses of GI hormones to meal ingestion is a critical determinant of energy balance and postprandial glycaemia.

That plasma concentrations of GI hormones are typically increased after enteral, but not intravenous, nutrient administration attests to the importance of nutrient-gut interactions to the release of these hormones[11]. Accordingly, improved understanding of the sensor and actuator mechanisms through which nutrients or bioactive compounds interact with EE cells, has the potential to yield novel "gut-based" approaches for the management of metabolic diseases. In the last few decades, a broad range of preclinical and clinical models have been developed to study nutrient-gut interactions, with increasing efforts to achieve clinically relevant outcomes. To this end, *ex vivo* studies have extended from the use of EE cell lines towards primary intestinal tissues and organoids, and have increasingly incorporated sophisticated culture conditions to mimic normal physiology. Clinical studies employing customised intestinal perfusion catheters for targeted delivery of nutrients or therapeutic compounds, or novel ingestible sensors, have attempted to better characterise the

regional specificity of GI responses. In this review, we summarise the research tools and models used to investigate nutrient-gut interactions, and discuss their advantages and limitations for clinical translation of findings (Table 1).

CELLULAR MODELS

The GI mucosa incorporates a monolayer of columnar epithelium with region-specific architecture and EE cell composition that is uniquely tuned to secrete specific gut hormones and absorb nutrients to fulfil specific metabolic functions. EE cells account for less than 1% of all epithelial cells, and their distribution varies substantially along the GI tract (Figure 1)[12]. Immortalised cell lines derived from murine and human intestinal tumours have been developed for *in vitro* studies, and retain the capacity to secrete GI hormones in response to nutrient stimuli (Table 2).

STC-1 cells are a heterogeneous and poorly differentiated EE cell line derived from intestinal secretin-producing tumours in mice. They have a high immunoreactivity to anti-proglucagon sera and are capable of releasing glucagon-like immuno-reactants[13]. STC-1 cells were subsequently shown to secrete multiple gut hormones, including CCK[14], GLP-1[15,16], GIP[17], and PYY[18,19], in a similar manner to native murine EE cells, when stimulated by glucose[20], amino acids and fatty acids. As a result, STC-1 cells have been a popular model to screen for gut hormone-releasing stimuli. However, the clinical relevance of this model has been frequently questioned. For example, treatment with potato protease inhibitor concentrate (PPIC) or whey protein does not induce CCK secretion from STC-1 cells[21,22]. By contrast, oral administration of PPIC (100 mg/kg per day) stimulates CCK secretion in rodents[21], while ingestion of whey protein (55 g) increases plasma CCK levels in humans[23].

GLUTag cell line is a subcloned homogeneous EE cell model developed by the Drucker group from an endocrine carcinoma of the large bowel in transgenic mice[24]. These cells express both proglucagon and CCK genes[25] but produce primarily GLP1(7-36)-amide. GLUTag cells are equipped with a wide repertoire of nutrient sensors and transporters, including G-protein coupled receptors (GPCRs)[26], glucokinase[27] and the sodium-glucose linked transporter 1 (SGLT1)[28] involved in nutrient-induced GLP-1 secretion. In agreement with *in vivo* findings, GLUTag cells exhibit robust release of GLP-1 in response to glucose[29], bile acids[30], fatty acids[31] and amino acids[32]. These observations have promoted GLUTag cells as a frontline model of L cells, leading to a wide application for studying the mechanisms underlying GLP-1 secretion and for screening potential GLP-1 secretagogues. However, clinical studies are still required to validate *in vitro* findings. For example, the treatment of glutamine (10 mmol/L) was shown to markedly increase GLP-1 secretion (7-fold) from GLUTag cells[32]. However, oral administration of encapsulated ileal-release glutamine (6 g) or intra-duodenal glutamine infusion (7.5-15 g) evoked only modest increases in plasma GLP-1 levels in healthy subjects and patients with type 2 diabetes[33,34].

The human cell lines NCI-H716 and HuTu-80 have also been used widely to characterise nutrient-evoked GLP-1 release. The NCI-H716 cell line was first reported by Park *et al*[35] from human colorectal carcinoma. It contains dense-core granules, expresses chromogranin A, and secretes GLP-1 in response to glucose, fatty acids and protein hydrolysates[36]. Studies incorporating the NCI-H716 cell line have revealed critical roles of amino acid transporters[37], type 1 taste receptors[38] and monoacylglycerol-sensing GPCR[31] in GLP-1 secretion. However, the secretory profile of NCI-H716 cells is more limited compared to murine STC-1 or GLUTag cells. For example, NCI-H716 cells secrete GLP-1 and GLP-2 but not GIP, PYY or CCK in response to 50 mmol/L KCl, or combined glucose (10 mmol/L), forskolin and phosphodiesterase inhibitor (10 μmol/L)[39]. That NCI-H716 cells do not secrete PYY reflects their limited resemblance to native L-cells.

The HuTu-80 cell line is an alternative EE cell model of human origin that secretes GLP-1, GIP, PYY and CCK[40] and was developed initially to study the biology of GI cancers[41]. Sweet and bitter taste receptors are abundantly expressed in HuTo-80 cells as in native human L-cells, making them a potential model to investigate tastant-induced gut hormone secretion[42,43]. However, unlike native L-cells, bitter tastants, including quinine, denatonium benzoate and phenylthiocarbamide fail to trigger GLP-1 secretion from HuTu-80 cells[44]. Relative to the three aforementioned cell lines, HuTu-80 cells have been less frequently employed to study nutrient-gut interactions.

Table 1 Available tools used for investigation of nutrient-gut interactions

Tools		Advantages	Disadvantages/challenges
Cellular models	EE cell lines	Established secretion profiles; genetically modifiable; readily accessible	Limited resemblance to native l-cells; lack of inter-organ interaction; limited success in clinical translation
Tissue-based approaches	Intestinal organoids	Preserved native architecture; region-specific functions; high plasticity for oriented differentiation	Undefined secretion profiles; lack of integrated nervous or immune systems; inconsistent culture outcomes
	Isolated intestinal tissues	Preserved native intestinal structure; access to luminal and basolateral surface; high physiological relevance	Short viable period; lack of inter-organ interaction; limited access to human tissue; low EE cell density
Intestinal intubation	*In vivo* infusion in gut	Region-specific delivery; direct insights into human (patho-)physiology	Technically demanding; restricted to specialised research centre
Novel techniques	3D culture	Enhanced anatomical complexity; compatibility with co-culture system	Limited cellular variety; static culture environment
	Intestine-on-a-chip	Dynamic culture environment; recapitulation of luminal events	Sophisticated validation of the system; partial resemblance to luminal physiology
	Ingestible sensors	A broad range of application; high potential for multi-purposed *in vivo* investigation	Difficulty in signal interpretation; lack of stability; High cost

EE: Enteroendocrine.

Table 2 Enteroendocrine cell models

Species	Model	Origin	Hormones	Features
Mouse	STC-1	Duodenal secretin tumour cells	GLP-1, GLP-2, CCK, GIP, PYY,	Heterogeneous cell population; respond to glucose, amino acids, fatty acids and neural stimuli; poor expression of CaSR
	GLUTag	Colonic tumour	GLP-1, GLP-2, CCK	Subcloned homogenous cells; respond to glucose, bile acids, fatty acids, amino acids
Human	NCI-H716	Colorectal carcinoma	GLP-1, GLP-2	Heterogeneous cell population; poorly differentiated; respond to glucose, fatty acids, protein hydrolysates
	HuTu-80	Duodenal carcinoma	GLP-1, PYY, GIP, CCK	Respond to antioxidant compounds, sweet and bitter substances

CCK: Cholecystokinin; GLP-1: Glucagon-like peptide 1; GIP: Glucose-dependent insulinotropic polypeptide; PYY: Peptide YY; CaSR: Ca^{2+}-sensing receptor.

TISSUE-BASED GUT HORMONE RELEASE *EX VIVO*

The major functional differences between immortalised intestinal cell lines and primary EE cells have led to an increased research focus on primary intestinal models to study the endocrine function of the gut. These have included the isolation and use of primary EE cells[45-47] and use of *ex vivo* intestinal tissue preparations from animals[48-51] and humans[52,53]. These tissue-based approaches maintain native cell-cell connections and polarity, and have hitherto yielded a deep understanding of the mechanisms governing nutrient and drug-evoked 5-hydroxytryptamine and GLP-1 release[54,55]. However, clinical access to gut endoscopic, colonoscopic or surgical tissues, tissue viability and potentially low EE cell density can limit these primary models. The purification of primary EE cells is also technically demanding. The recent development of intestinal organoids holds the promise to overcome some of these limitations.

INTESTINAL ORGANOIDS

Intestinal organoids, also known as "mini-guts", are miniaturised intestinal units that display many features of gut tissue architecture and function. In 2007, Barker and colleagues identified leucine-rich repeat-containing GPCRG-5 (Lgr5) -positive cells as stem cells in the small intestine and colon via genetic lineage tracing experiments[56]. Subsequently, a single Lgr5-positive stem cell was shown to differentiate into crypt-

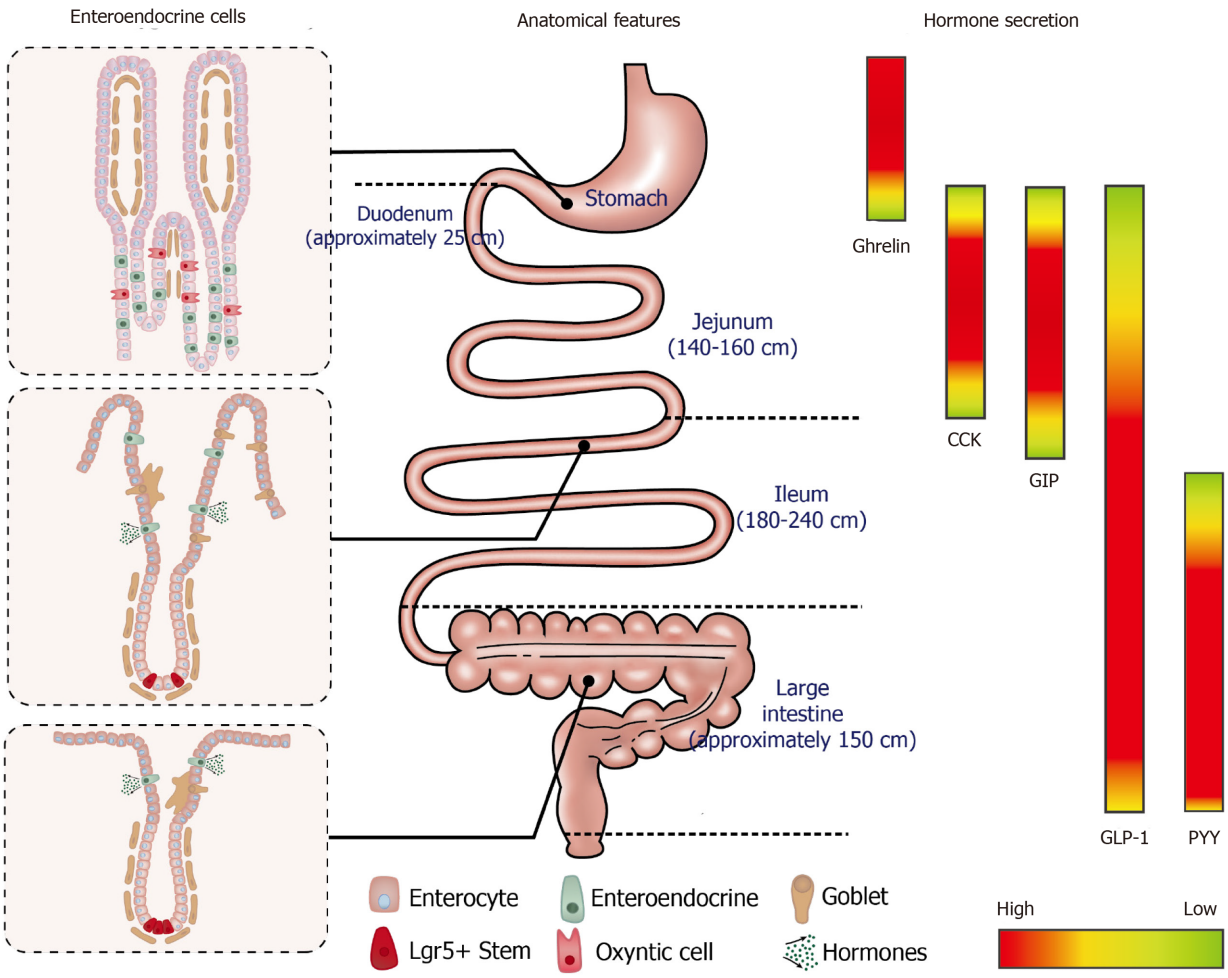

Figure 1 The composition of intestinal epithelial cells along the gastrointestinal tract (left); anatomical features and typical length of different sections of gastrointestinal tract (middle); regionally specific secretion profile of different gut hormones, including ghrelin, cholecystokinin, glucose-dependent insulinotropic polypeptide, glucagon-like peptide 1 and peptide YY (right). CCK: Cholecystokinin; GLP-1: Glucagon-like peptide 1; GIP: Glucose-dependent insulinotropic polypeptide; PYY: Peptide YY.

villus organoids, namely enteroids, that are inclusive of all cell types present in the native intestinal epithelium[57]. Of note, enteroids can be developed from Lgr5-positive cells originating from any section of the gut. *Ex vivo* characterisation has shown that these enteroids display the basal-apical polarity of mature epithelial cells[58,59]. Moreover, they retain many region-specific functions of the original location from which the stem cells were taken[60].

Intestinal organoids can also be developed from human pluripotent stem cells, which are referred to as human intestinal organoids (HIOs)[61,62]. HIOs have similar morphology as enteroids and display crypt-villus structures inclusive of all intestinal cell types. By contrast, HIOs contain a mesenchyme layer that is composed of myofibroblasts, endothelial cells and smooth muscle[63]. Moreover, HIOs do not show region-specific features and eventually grow into an unselective population of EE cells[61]. The differentiation process has been shown to be enhanced by the Happy Cell Advanced Suspension Medium[64] and by activation of the bone morphogenetic protein signalling pathway[65].

In contrast to primary intestinal epithelium, intestinal organoids remain viable for over 1-year *ex vivo* and show plasticity in cellular composition in response to changes in the culture environment or modified gene expression. Accumulating evidence suggests that the density of EE cells in organoids is subject to the expression of several translational factors, including Neurogenin 3 and *Aristaless*-related homobox[61,66,67], raising the prospect that EE cells can be customised in an organoid. Indeed, exposure of mouse or human enteroids to short-chained fatty acids (SCFAs) increases the number of L cells, and hence GLP-1 secretion, over 48 h of SCFA treatment[68]. Similar trends in differentiation have also been observed with enteroids treated with dibenzazepine or bile acids[69,70]. However, the secretory profile of intestinal organoids

in response to nutrients or non-nutritive compounds has not been well characterised. It should also be noted that delivery of stimuli to the lumen of the organoids requires individual microinjection, which is both labour-intensive and technically demanding due to their small size[71]. Moreover, the culture of organoids in conventional platforms makes it difficult to mimic the continuous movement of luminal contents and constantly changing nature of the extracellular fluid. Finally, it is not yet possible to recreate the architectural complexity of the GI tract, including its vascular, nervous, immune, mucous elements and the microbiome, in any organoid preparation.

INTESTINAL PERFUSION *IN VIVO*

The development of intestinal perfusion techniques and analytic methods capable of measuring GI hormones released into the peripheral circulation has allowed the evaluation of nutrient-gut interactions *in vivo*. In rodents, dietary effects on gut hormone secretion have been investigated in models of isolated intestinal perfusion[72,73]. In humans, it is also possible to characterise the responses of various regions of the gut to intraluminal stimuli, and to examine the underlying mechanisms.

A rubber feeding tube was initially designed to deliver medication to the intestine and to examine luminal contents in paediatric patients[74]. This early design incorporated 1-2 cm wide lateral window(s) for infusion/aspiration of liquids and a weighted terminal bulb to facilitate passage of the catheter by peristalsis. Subsequently, intestinal catheters have been increasingly customised to study gut function. For example, the integration of an inflatable balloon at the distal end of the catheter was employed to evaluate the perception of distension or control the position of the catheter[75]. Use of a multi-lumen catheter has allowed for multiple inflatable balloons, making it possible to isolate segments of the lumen[76], within which nutrient absorption can be carefully characterised[77-79]. Incorporation of manometry and impedance sensors into the catheter design has further facilitated concurrent recording of gut motility[34] and flow events[80]. Positioning these catheters has relied on fluoroscopy, for which radiation exposure represents a major limitation. To overcome this, Andersson and Grossman established an alternative method of monitoring catheter position by measuring transmucosal potential difference (TMPD) between skin or blood and the intestinal lumen[81]. Corresponding to the differences in pH between the stomach and the duodenum, TMPD in the distal antral channel and the proximal duodenal channel record around -40 mV and 0 mV, respectively[82,83]. Accordingly, a change of TMPD from -40 mV to 0 mV reflects passage of channels through the transpyloric area (Figure 2).

Relative to oral administration, intestinal perfusion of nutrients or investigational compounds circumvents the impact of inter-individual variations in the rate of gastric emptying – which can be substantial[84-86] – such that the exposure of the small intestine to nutrients can be standardised. Studies employing intraduodenal infusion of nutrients spanning the normal range of gastric emptying (1-4 kcal/min) have established that the stimulation of gut hormones, including CCK, GIP, GLP-1 and PYY, is dependent on the rate of nutrient entry into the small intestine. In line with the biological distribution of respective EE cells, the secretion of CCK and GIP appears to be proportional to the load of glucose, lipid or protein, whereas GLP-1 and PPY responses are non-linear, being modest at 1-2 kcal/min and substantially greater at 3-4 kcal/min[87]. Moreover, when glucose and fat are infused intraduodenally at an identical rate of 2 kcal/min, it is observed that fat is significantly more potent than glucose at stimulating GLP-1 and GIP secretion[88].

A multi-lumen catheter of adequate length can also be positioned over a long length of small intestine to allow targeted delivery of nutrients or investigational compounds into proximal or distal sites, to determine the regional specificity of nutrient-gut interactions. In this way, infusion of glucose (2 kcal/min) into jejunum (50 cm distal to pylorus) was shown to elicit more GLP-1 and GIP release compared to equivalent duodenal infusion (12 cm distal to pylorus) in healthy men[89]. Furthermore, ileal glucose infusion (2 kcal/min, 190 cm distal to pylorus) resulted in markedly greater GLP-1 and lower (but more sustained) GIP responses compared to intraduodenal infusion, and was associated with a greater incretin effect and GI-mediated glucose disposal in both healthy subjects and patients with type 2 diabetes (Figure 3)[90]. Administration of compounds into the rectum can similarly be undertaken using a soft tube with minimal discomfort[91,92]. Characterisation of the region-specific profile of gut hormone release has shed light on the mechanisms by which Roux-en-Y gastric bypass surgery improves blood glucose control in type 2 diabetes[93]. In addition, this

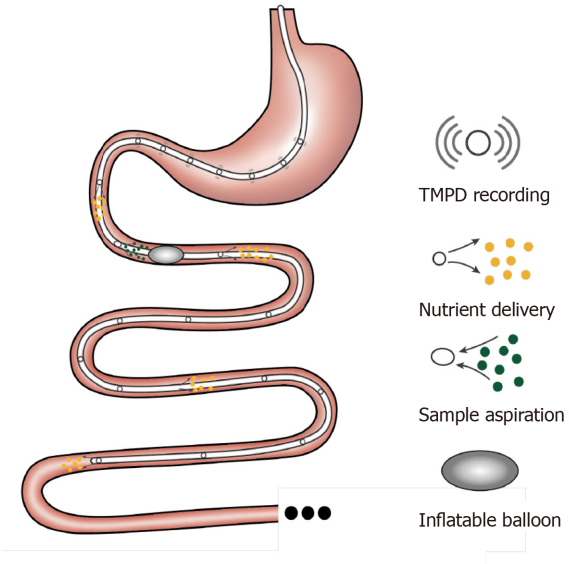

Figure 2 Schematic of a multichannel intestinal catheter to study regional specificity of nutrient-gut interactions. Multiple channels are opened on the catheter to record the transmucosal potential difference and monitor its position. These channels can also deliver investigational compounds of aspirate luminal samples in a specific region of intestine. The balloon is generally designed to create physical restriction to prevent the fluid flow or the movement of the catheter. TMPD: Transmucosal potential difference.

knowledge has directed the precise delivery of stimuli to optimise gut hormone response for therapeutic gain. For example, enteric coating of a small dose of lauric acid to allow targeted release in the ileum and colon was shown to be effective at stimulating GLP-1 secretion and lowering blood glucose in patients with type 2 diabetes[94].

Access to the intestines via endoscopy and colonoscopy has provided an additional means for targeting intestinal perfusion to a specific region, while also allowing for the collection of mucosal biopsies to study anatomical and molecular mechanisms underlying nutrient-gut interactions (discussed in earlier section). In this way, sweet taste receptors (STRs) (heterodimeric T1R2 and T1R3) were found to be involved in intestinal glucose sensing and linked to regulation of glucose absorption in both health and type 2 diabetes; in patients with type 2 diabetes, a defect in the downregulation of STRs in the face of hyperglycaemia was shown to contribute to excessive postprandial glycaemic excursions[95]. Moreover, *ex vivo* studies using human intestinal biopsies have revealed a critical role for both SGLT1 and the facilitative glucose transporter 2 in mediating glucose-induced GLP-1 secretion[55].

NOVEL TECHNIQUES TO STUDY GUT HORMONE SECRETION

Several novel techniques are emerging to evaluate nutrient-gut interactions with improved physiological or therapeutic relevance, while overcoming limitations of clinical studies.

Recent development of culture engineering techniques has allowed integration of advanced culture interfaces into the conventional 2D culture platforms of intestinal organoids and primary epithelial cells. This has enabled the provision of culture frameworks that support the growth of intestinal cells and facilitate the assessment of tissue function in a more physiologically relevant environment[96,97]. For example, culturing intestinal cells on a porous polyester membrane provides access to both basolateral and apical sides of the polarised epithelial cells, which is of particular importance for the investigation of the intestinal function in response to luminal stimuli (Figure 4A). In addition, the membrane can be coated with an extracellular matrix containing growth factors to induce growth and differentiation of organoids. This experimental platform is being increasingly used to study intestinal barrier function[98,99], immune responses[100], and drug metabolism[101,102], with a handful of studies focusing on nutrient-gut interactions. Kozuka *et al*[103] developed an intestinal monolayer culture platform utilising Transwell (a culture plate with an inserted membrane) with a 0.4 μm or 1 μm pore membrane and successfully cultured murine

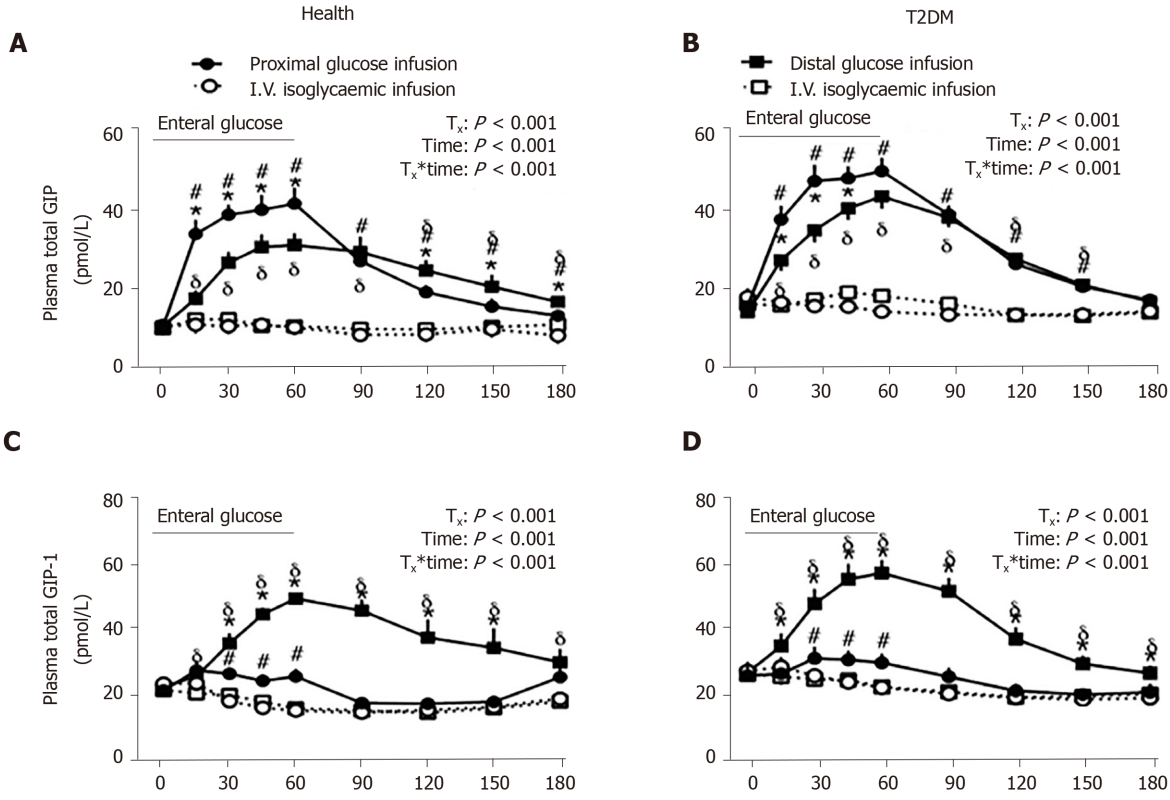

Figure 3 Comparison of the effect of enteral (proximal or distal) and intravenous (i.v.) isoglycemic glucose administrations on plasma incretin hormone, glucose-dependent insulinotropic polypeptide and glucagon-like peptide-1 secretions in healthy subjects and subjects with type 2 diabetes mellitus. A and B: Glucose-dependent insulinotropic polypeptide; C and D: Glucagon-like peptide-1. Asterisk represents P < 0.05 for proximal *vs* distal enteral glucose infusion; Numbersign represents P < 0.05 for proximal enteral *vs* corresponding i.v. glycemic glucose infusion; Delta represents P < 0.05 for distal enteral *vs* corresponding i.v. glycemic glucose infusion. Data are presented as mean ± SEM. GLP-1: Glucagon-like peptide 1; GIP: Glucose-dependent insulinotropic polypeptide; T2DM: Type 2 diabetes mellitus. Citation: Zhang X, Young RL, Bound M, Hu S, Jones KL, Horowitz M, Rayner CK, Wu T. Comparative Effects of Proximal and Distal Small Intestinal Glucose Exposure on Glycemia, Incretin Hormone Secretion, and the Incretin Effect in Health and Type 2 Diabetes. Diabetes Care 2019; 42: 520-528. Copyright© The Authors 2019. Published by American Diabetes Association.

and human intestinal enteroids. Treatment with forskolin (100 μM) in the apical chamber stimulated GLP-1 release into the basolateral chamber, consistent with the presence of functional L-cells and GLP-1 deployment mechanisms. With this compartmental culture system, it is possible to model the interaction between the intestinal epithelium and luminal content and monitor the hormonal response in the downstream chamber.

More advanced and complex intestine models have been achieved by applying microfluidic devices in gut function studies, also known as "intestine-on-a-chip". These microfluidic devices have the capacity to provide a dynamic culture environment, including continuously refreshed culture media and biomimetic mechanical strain, to more accurately resemble physiological conditions (Figure 4B). Current *in vitro* gut models on microfluidic devices have mainly been used to investigate drug metabolism[104] and gut-liver interactions[105]. The application of the "intestine-on-a-chip" model for gut hormone secretion study is in its infancy. In 2016, Hsiao *et al*[106] developed a high-throughput automated microfluidic platform to assess the response of NCL-H716 cells to sweet and bitter stimuli. Although gut hormones were not measured in the study, the microfluidic system recorded the dynamic changes in intracellular Ca^{2+} in over 500 single NCI-H716 cells trapped in each micro-well. In another study, Park and his colleagues established a co-culture of GLUTag cells and the β cell line INS-1 to screen compounds of anti-diabetic potential[107]. Relative to the use of intestinal cancer cell line, intestinal organoids cultured on a microfluidic device display a high resemblance to the native intestine transcriptome, including the expression of genes related to cell proliferation, digestion and responses to nutrients[108], and may prove to be a useful *ex vivo* model for studying GI hormone secretion.

Ingestible sensors are under rapid development in clinical settings. These are typically capsule devices of up to 11 mm in diameter and 28 mm in length, to allow

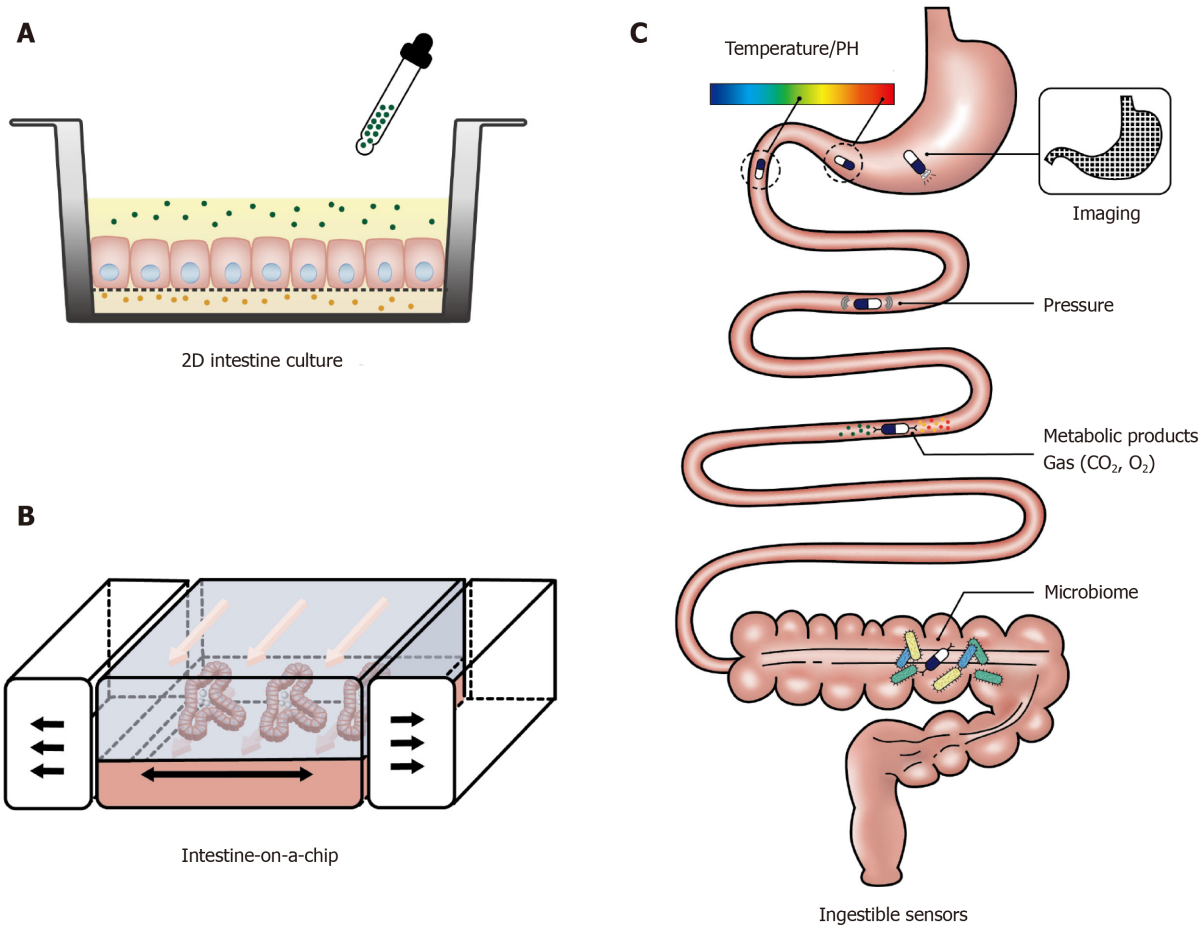

Figure 4 Emerging advanced techniques to study nutrient-gut interaction. A: 2D culture of intestinal epithelium on a porous membrane; B: intestine-on-a-chip model with intestinal organoids cultured in a microfluidic device, where constant perfusion and periodic mechanical strain can be applied on the system; C: ingestible sensors for measuring various parameters relevant to gut functions.

easy transit through the gut while measuring biomedical parameters (Figure 4C). To date, ingestible sensors have been developed for imaging[109-112] and measurements of gases[113], pH, temperature[114-117], pressure[118] and luminal contents[119-121]. The pH sensors have been used to assess gastric emptying and small intestinal transit, marked by abrupt pH changes between the stomach and duodenum (> 3 units) and between the ileum and colon (> 1 unit)[122,123]. The wide application of ingestible sensors will require further technical development to improve stability, signal interpretation and reduce costs, but offer an exciting glimpse into the future of GI surveillance.

CONCLUSION

A better understanding of the mechanisms underlying nutrient-gut interactions is fundamental to the development of gut-based therapies for major metabolic disorders. For this purpose, the development of *in vitro* EE cell models, and techniques suitable for *in vivo* studies, particularly in humans, is of critical importance. EE cell lines of both murine (STC-1 and GLUTag) and human (NCI-H716 and HuTo-80) origin are useful for early studies on gut hormone secretion, but have had limited translational success. This necessitates the development of more physiologically relevant *in vitro* gut models. The emergence of intestinal organoids and novel co-culture systems represents a major advance in this area. In particular, the combination of intestinal organoids and microfluidics will provide an unprecedented opportunity to study the dynamic hormonal response to stimuli under various conditions. *In vivo* validation of research outcomes derived from these models remains critical. In clinical studies, intestinal intubation and the application of novel ingestible sensors, have provided deep knowledge of the region-specific nature of nutrient-gut interactions, and ensuing hormonal and metabolic responses. Further development of non-invasive techniques

suitable for use in humans will expand opportunities to translate research findings from the bench to bedside.

REFERENCES

1 **Steinert RE**, Feinle-Bisset C, Asarian L, Horowitz M, Beglinger C, Geary N. Ghrelin, CCK, GLP-1, and PYY(3-36): Secretory Controls and Physiological Roles in Eating and Glycemia in Health, Obesity, and After RYGB. *Physiol Rev* 2017; **97**: 411-463 [PMID: 28003328 DOI: 10.1152/physrev.00031.2014]

2 **Shiiya T**, Nakazato M, Mizuta M, Date Y, Mondal MS, Tanaka M, Nozoe S, Hosoda H, Kangawa K, Matsukura S. Plasma ghrelin levels in lean and obese humans and the effect of glucose on ghrelin secretion. *J Clin Endocrinol Metab* 2002; **87**: 240-244 [PMID: 11788653 DOI: 10.1210/jcem.87.1.8129]

3 **Spiegel K**, Tasali E, Leproult R, Scherberg N, Van Cauter E. Twenty-four-hour profiles of acylated and total ghrelin: relationship with glucose levels and impact of time of day and sleep. *J Clin Endocrinol Metab* 2011; **96**: 486-493 [PMID: 21106712 DOI: 10.1210/jc.2010-1978]

4 **Polak JM**, Bloom SR, Rayford PL, Pearse AG, Buchan AM, Thompson JC. Identification of cholecystokinin-secreting cells. *Lancet* 1975; **2**: 1016-1018 [PMID: 53500 DOI: 10.1016/S0140-6736(75)90297-4]

5 **Buffa R**, Capella C, Fontana P, Usellini L, Solcia E. Types of endocrine cells in the human colon and rectum. *Cell Tissue Res* 1978; **192**: 227-240 [PMID: 699014 DOI: 10.1007/BF00220741]

6 **Svendsen B**, Pedersen J, Albrechtsen NJ, Hartmann B, Toräng S, Rehfeld JF, Poulsen SS, Holst JJ. An analysis of cosecretion and coexpression of gut hormones from male rat proximal and distal small intestine. *Endocrinology* 2015; **156**: 847-857 [PMID: 25535831 DOI: 10.1210/en.2014-1710]

7 **Theodorakis MJ**, Carlson O, Michopoulos S, Doyle ME, Juhaszova M, Petraki K, Egan JM. Human duodenal enteroendocrine cells: source of both incretin peptides, GLP-1 and GIP. *Am J Physiol Endocrinol Metab* 2006; **290**: E550-E559 [PMID: 16219666 DOI: 10.1152/ajpendo.00326.2004]

8 **Mojsov S**, Weir GC, Habener JF. Insulinotropin: glucagon-like peptide I (7-37) co-encoded in the glucagon gene is a potent stimulator of insulin release in the perfused rat pancreas. *J Clin Invest* 1987; **79**: 616-619 [PMID: 3543057 DOI: 10.1172/JCI112855]

9 **Kreymann B**, Williams G, Ghatei MA, Bloom SR. Glucagon-like peptide-1 7-36: a physiological incretin in man. *Lancet* 1987; **2**: 1300-1304 [PMID: 2890903 DOI: 10.1016/S0140-6736(87)91194-9]

10 **Näslund E**, Barkeling B, King N, Gutniak M, Blundell JE, Holst JJ, Rössner S, Hellström PM. Energy intake and appetite are suppressed by glucagon-like peptide-1 (GLP-1) in obese men. *Int J Obes Relat Metab Disord* 1999; **23**: 304-311 [PMID: 10193877 DOI: 10.1038/sj.ijo.0800818]

11 **Perley MJ**, Kipnis DM. Plasma insulin responses to oral and intravenous glucose: studies in normal and diabetic sujbjects. *J Clin Invest* 1967; **46**: 1954-1962 [PMID: 6074000 DOI: 10.1172/JCI105685]

12 **McLaughlin JT**, Lomax RB, Hall L, Dockray GJ, Thompson DG, Warhurst G. Fatty acids stimulate cholecystokinin secretion via an acyl chain length-specific, Ca2+-dependent mechanism in the enteroendocrine cell line STC-1. *J Physiol* 1998; **513**: 11-18 [PMID: 9782155 DOI: 10.1111/j.1469-7793.1998.011by.x]

13 **Rindi G**, Grant SG, Yiangou Y, Ghatei MA, Bloom SR, Bautch VL, Solcia E, Polak JM. Development of neuroendocrine tumors in the gastrointestinal tract of transgenic mice. Heterogeneity of hormone expression. *Am J Pathol* 1990; **136**: 1349-1363 [PMID: 2162628 DOI: 10.1097/00000433-199006000-00018]

14 **Wang Y**, Prpic V, Green GM, Reeve JR Jr, Liddle RA. Luminal CCK-releasing factor stimulates CCK release from human intestinal endocrine and STC-1 cells. *Am J Physiol Gastrointest Liver Physiol* 2002; **282**: G16-G22 [PMID: 11751153 DOI: 10.1152/ajpgi.2002.282.1.G16]

15 **Cordier-Bussat M**, Bernard C, Levenez F, Klages N, Laser-Ritz B, Philippe J, Chayvialle JA, Cuber JC. Peptones stimulate both the secretion of the incretin hormone glucagon-like peptide 1 and the transcription of the proglucagon gene. *Diabetes* 1998; **47**: 1038-1045 [PMID: 9648826 DOI: 10.2337/diabetes.47.7.1038]

16 **Hirasawa A**, Tsumaya K, Awaji T, Katsuma S, Adachi T, Yamada M, Sugimoto Y, Miyazaki S, Tsujimoto G. Free fatty acids regulate gut incretin glucagon-like peptide-1 secretion through GPR120. *Nat Med* 2005; **11**: 90-94 [PMID: 15619630 DOI: 10.1038/nm1168]

17 **Hand KV**, Giblin L, Green BD. Hormone profiling in a novel enteroendocrine cell line pGIP/neo: STC-1. *Metabolism* 2012; **61**: 1683-1686 [PMID: 22768997 DOI: 10.1016/j.metabol.2012.05.017]

18 **Geraedts MC**, Troost FJ, Saris WH. Peptide-YY is released by the intestinal cell line STC-1. *J Food Sci* 2009; **74**: H79-H82 [PMID: 19323755 DOI: 10.1111/j.1750-3841.2009.01074.x]

19 **Hand KV**, Bruen CM, O'Halloran F, Panwar H, Calderwood D, Giblin L, Green BD. Examining acute and chronic effects of short- and long-chain fatty acids on peptide YY (PYY) gene expression, cellular storage and secretion in STC-1 cells. *Eur J Nutr* 2013; **52**: 1303-1313 [PMID: 22926626 DOI: 10.1007/s00394-012-0439-9]

20 **Mangel AW**, Prpic V, Scott L, Liddle RA. Inhibitors of ATP-sensitive potassium channels stimulate intestinal cholecystokinin secretion. *Peptides* 1994; **15**: 1565-1566 [PMID: 7700857 DOI: 10.1016/0196-9781(94)90134-1]

21 **Komarnytsky S**, Cook A, Raskin I. Potato protease inhibitors inhibit food intake and increase circulating cholecystokinin levels by a trypsin-dependent mechanism. *Int J Obes (Lond)* 2011; **35**: 236-243 [PMID: 20820171 DOI: 10.1038/ijo.2010.192]

22 **Foltz M**, Ansems P, Schwarz J, Tasker MC, Lourbakos A, Gerhardt CC. Protein hydrolysates induce CCK release from enteroendocrine cells and act as partial agonists of the CCK1 receptor. *J Agric Food Chem* 2008; **56**: 837-843 [PMID: 18211011 DOI: 10.1021/jf072611h]

23 **Ma J**, Stevens JE, Cukier K, Maddox AF, Wishart JM, Jones KL, Clifton PM, Horowitz M, Rayner CK. Effects of a protein preload on gastric emptying, glycemia, and gut hormones after a carbohydrate meal in diet-controlled type 2 diabetes. *Diabetes Care* 2009;

32: 1600-1602 [PMID: 19542012 DOI: 10.2337/dc09-0723]
24 **Lee YC**, Asa SL, Drucker DJ. Glucagon gene 5'-flanking sequences direct expression of simian virus 40 large T antigen to the intestine, producing carcinoma of the large bowel in transgenic mice. *J Biol Chem* 1992; **267**: 10705-10708 [PMID: 1587847]
25 **Drucker DJ**, Jin T, Asa SL, Young TA, Brubaker PL. Activation of proglucagon gene transcription by protein kinase-A in a novel mouse enteroendocrine cell line. *Mol Endocrinol* 1994; **8**: 1646-1655 [PMID: 7535893 DOI: 10.1210/mend.8.12.7535893]
26 **Oya M**, Kitaguchi T, Pais R, Reimann F, Gribble F, Tsuboi T. The G protein-coupled receptor family C group 6 subtype A (GPRC6A) receptor is involved in amino acid-induced glucagon-like peptide-1 secretion from GLUTag cells. *J Biol Chem* 2013; **288**: 4513-4521 [PMID: 23269670 DOI: 10.1074/jbc.M112.402677]
27 **Parker HE**, Adriaenssens A, Rogers G, Richards P, Koepsell H, Reimann F, Gribble FM. Predominant role of active versus facilitative glucose transport for glucagon-like peptide-1 secretion. *Diabetologia* 2012; **55**: 2445-2455 [PMID: 22638549 DOI: 10.1007/s00125-012-2585-2]
28 **Gribble FM**, Williams L, Simpson AK, Reimann F. A novel glucose-sensing mechanism contributing to glucagon-like peptide-1 secretion from the GLUTag cell line. *Diabetes* 2003; **52**: 1147-1154 [PMID: 12716745 DOI: 10.2337/diabetes.52.5.1147]
29 **Reimann F**, Gribble FM. Glucose-sensing in glucagon-like peptide-1-secreting cells. *Diabetes* 2002; **51**: 2757-2763 [PMID: 12196469 DOI: 10.2337/diabetes.51.9.2757]
30 **Parker HE**, Wallis K, le Roux CW, Wong KY, Reimann F, Gribble FM. Molecular mechanisms underlying bile acid-stimulated glucagon-like peptide-1 secretion. *Br J Pharmacol* 2012; **165**: 414-423 [PMID: 21718300 DOI: 10.1111/j.1476-5381.2011.01561.x]
31 **Lauffer LM**, Iakoubov R, Brubaker PL. GPR119 is essential for oleoylethanolamide-induced glucagon-like peptide-1 secretion from the intestinal enteroendocrine L-cell. *Diabetes* 2009; **58**: 1058-1066 [PMID: 19208912 DOI: 10.2337/db08-1237]
32 **Reimann F**, Williams L, da Silva Xavier G, Rutter GA, Gribble FM. Glutamine potently stimulates glucagon-like peptide-1 secretion from GLUTag cells. *Diabetologia* 2004; **47**: 1592-1601 [PMID: 15365617 DOI: 10.1007/s00125-004-1498-0]
33 **Meek CL**, Lewis HB, Vergese B, Park A, Reimann F, Gribble F. The effect of encapsulated glutamine on gut peptide secretion in human volunteers. *Peptides* 2016; **77**: 38-46 [PMID: 26541888 DOI: 10.1016/j.peptides.2015.10.008]
34 **Chang J**, Wu T, Greenfield JR, Samocha-Bonet D, Horowitz M, Rayner CK. Effects of intraduodenal glutamine on incretin hormone and insulin release, the glycemic response to an intraduodenal glucose infusion, and antropyloroduodenal motility in health and type 2 diabetes. *Diabetes Care* 2013; **36**: 2262-2265 [PMID: 23564914 DOI: 10.2337/dc12-1663]
35 **Park JG**, Oie HK, Sugarbaker PH, Henslee JG, Chen TR, Johnson BE, Gazdar A. Characteristics of cell lines established from human colorectal carcinoma. *Cancer Res* 1987; **47**: 6710-6718 [PMID: 3479249]
36 **Reimer RA**, Darimont C, Gremlich S, Nicolas-Métral V, Rüegg UT, Macé K. A human cellular model for studying the regulation of glucagon-like peptide-1 secretion. *Endocrinology* 2001; **142**: 4522-4528 [PMID: 11564718 DOI: 10.1210/endo.142.10.8415]
37 **Reimer RA**. Meat hydrolysate and essential amino acid-induced glucagon-like peptide-1 secretion, in the human NCI-H716 enteroendocrine cell line, is regulated by extracellular signal-regulated kinase1/2 and p38 mitogen-activated protein kinases. *J Endocrinol* 2006; **191**: 159-170 [PMID: 17065399 DOI: 10.1677/joe.1.06557]
38 **Jang HJ**, Kokrashvili Z, Theodorakis MJ, Carlson OD, Kim BJ, Zhou J, Kim HH, Xu X, Chan SL, Juhaszova M, Bernier M, Mosinger B, Margolskee RF, Egan JM. Gut-expressed gustducin and taste receptors regulate secretion of glucagon-like peptide-1. *Proc Natl Acad Sci USA* 2007; **104**: 15069-15074 [PMID: 17724330 DOI: 10.1073/pnas.0706890104]
39 **Kuhre RE**, Wewer Albrechtsen NJ, Deacon CF, Balk-Møller E, Rehfeld JF, Reimann F, Gribble FM, Holst JJ. Peptide production and secretion in GLUTag, NCI-H716, and STC-1 cells: a comparison to native L-cells. *J Mol Endocrinol* 2016; **56**: 201-211 [PMID: 26819328 DOI: 10.1530/JME-15-0293]
40 **Rozengurt N**, Wu SV, Chen MC, Huang C, Sternini C, Rozengurt E. Colocalization of the alpha-subunit of gustducin with PYY and GLP-1 in L cells of human colon. *Am J Physiol Gastrointest Liver Physiol* 2006; **291**: G792-G802 [PMID: 16728727 DOI: 10.1152/ajpgi.00074.2006]
41 **Schmidt M**, Deschner EE, Thaler HT, Clements L, Good RA. Gastrointestinal cancer studies in the human to nude mouse heterotransplant system. *Gastroenterology* 1977; **72**: 829-837 [PMID: 321290 DOI: 10.1016/S0016-5085(77)80195-9]
42 **Ohtsu Y**, Nakagawa Y, Nagasawa M, Takeda S, Arakawa H, Kojima I. Diverse signaling systems activated by the sweet taste receptor in human GLP-1-secreting cells. *Mol Cell Endocrinol* 2014; **394**: 70-79 [PMID: 25017733 DOI: 10.1016/j.mce.2014.07.004]
43 **Pham H**, Hui H, Morvaridi S, Cai J, Zhang S, Tan J, Wu V, Levin N, Knudsen B, Goddard WA 3rd, Pandol SJ, Abrol R. A bitter pill for type 2 diabetes? The activation of bitter taste receptor TAS2R38 can stimulate GLP-1 release from enteroendocrine L-cells. *Biochem Biophys Res Commun* 2016; **475**: 295-300 [PMID: 27208775 DOI: 10.1016/j.bbrc.2016.04.149]
44 **Le Nevé B**, Foltz M, Daniel H, Gouka R. The steroid glycoside H.g.-12 from Hoodia gordonii activates the human bitter receptor TAS2R14 and induces CCK release from HuTu-80 cells. *Am J Physiol Gastrointest Liver Physiol* 2010; **299**: G1368-G1375 [PMID: 20930049 DOI: 10.1152/ajpgi.00135.2010]
45 **Buchan AM**, Barber DL, Gregor M, Soll AH. Morphologic and physiologic studies of canine ileal enteroglucagon-containing cells in short-term culture. *Gastroenterology* 1987; **93**: 791-800 [PMID: 2887480 DOI: 10.1016/0016-5085(87)90442-2]
46 **Koop I**, Buchan AM. Cholecystokinin release from isolated canine epithelial cells in short-term culture. *Gastroenterology* 1992; **102**: 28-34 [PMID: 1727760 DOI: 10.1016/0016-5085(92)91780-8]
47 **Brubaker PL**, Vranic M. Fetal rat intestinal cells in monolayer culture: a new in vitro system to study the glucagon-like immunoreactive peptides. *Endocrinology* 1987; **120**: 1976-1985 [PMID: 3552626 DOI:

10.1210/endo-120-5-1976]
48 **Drucker DJ**, Brubaker PL. Proglucagon gene expression is regulated by a cyclic AMP-dependent pathway in rat intestine. *Proc Natl Acad Sci USA* 1989; **86**: 3953-3957 [PMID: 2542959 DOI: 10.1073/pnas.86.11.3953]
49 **Shima K**, Suda T, Nishimoto K, Yoshimoto S. Relationship between molecular structures of sugars and their ability to stimulate the release of glucagon-like peptide-1 from canine ileal loops. *Acta Endocrinol (Copenh)* 1990; **123**: 464-470 [PMID: 2239092 DOI: 10.1530/acta.0.1230464]
50 **Orskov C**, Holst JJ, Knuhtsen S, Baldissera FG, Poulsen SS, Nielsen OV. Glucagon-like peptides GLP-1 and GLP-2, predicted products of the glucagon gene, are secreted separately from pig small intestine but not pancreas. *Endocrinology* 1986; **119**: 1467-1475 [PMID: 3530719 DOI: 10.1210/endo-119-4-1467]
51 **Dumoulin V**, Moro F, Barcelo A, Dakka T, Cuber JC. Peptide YY, glucagon-like peptide-1, and neurotensin responses to luminal factors in the isolated vascularly perfused rat ileum. *Endocrinology* 1998; **139**: 3780-3786 [PMID: 9724030 DOI: 10.1210/endo.139.9.6202]
52 **Sun EW**, Martin AM, Wattchow DA, de Fontgalland D, Rabbitt P, Hollington P, Young RL, Keating DJ. Metformin Triggers PYY Secretion in Human Gut Mucosa. *J Clin Endocrinol Metab* 2019; **104**: 2668-2674 [PMID: 30759215 DOI: 10.1210/jc.2018-02460]
53 **Young RL**, Sutherland K, Pezos N, Brierley SM, Horowitz M, Rayner CK, Blackshaw LA. Expression of taste molecules in the upper gastrointestinal tract in humans with and without type 2 diabetes. *Gut* 2009; **58**: 337-346 [PMID: 19039089 DOI: 10.1136/gut.2008.148932]
54 **Lumsden AL**, Martin AM, Sun EW, Schober G, Isaacs NJ, Pezos N, Wattchow DA, de Fontgalland D, Rabbitt P, Hollington P, Sposato L, Due SL, Rayner CK, Nguyen NQ, Liou AP, Jackson VM, Young RL, Keating DJ. Sugar Responses of Human Enterochromaffin Cells Depend on Gut Region, Sex, and Body Mass. *Nutrients* 2019; **11**: 234 [PMID: 30678223 DOI: 10.3390/nu11020234]
55 **Sun EW**, de Fontgalland D, Rabbitt P, Hollington P, Sposato L, Due SL, Wattchow DA, Rayner CK, Deane AM, Young RL, Keating DJ. Mechanisms Controlling Glucose-Induced GLP-1 Secretion in Human Small Intestine. *Diabetes* 2017; **66**: 2144-2149 [PMID: 28385801 DOI: 10.2337/db17-0058]
56 **Barker N**, van Es JH, Kuipers J, Kujala P, van den Born M, Cozijnsen M, Haegebarth A, Korving J, Begthel H, Peters PJ, Clevers H. Identification of stem cells in small intestine and colon by marker gene Lgr5. *Nature* 2007; **449**: 1003-1007 [PMID: 17934449 DOI: 10.1038/nature06196]
57 **Sato T**, Vries RG, Snippert HJ, van de Wetering M, Barker N, Stange DE, van Es JH, Abo A, Kujala P, Peters PJ, Clevers H. Single Lgr5 stem cells build crypt-villus structures in vitro without a mesenchymal niche. *Nature* 2009; **459**: 262-265 [PMID: 19329995 DOI: 10.1038/nature07935]
58 **Matano M**, Date S, Shimokawa M, Takano A, Fujii M, Ohta Y, Watanabe T, Kanai T, Sato T. Modeling colorectal cancer using CRISPR-Cas9-mediated engineering of human intestinal organoids. *Nat Med* 2015; **21**: 256-262 [PMID: 25706875 DOI: 10.1038/nm.3802]
59 **Sugimoto S**, Sato T. Establishment of 3D Intestinal Organoid Cultures from Intestinal Stem Cells. *Methods Mol Biol* 2017; **1612**: 97-105 [PMID: 28634937 DOI: 10.1007/978-1-4939-7021-6_7]
60 **Middendorp S**, Schneeberger K, Wiegerinck CL, Mokry M, Akkerman RD, van Wijngaarden S, Clevers H, Nieuwenhuis EE. Adult stem cells in the small intestine are intrinsically programmed with their location-specific function. *Stem Cells* 2014; **32**: 1083-1091 [PMID: 24496776 DOI: 10.1002/stem.1655]
61 **Spence JR**, Mayhew CN, Rankin SA, Kuhar MF, Vallance JE, Tolle K, Hoskins EE, Kalinichenko VV, Wells SI, Zorn AM, Shroyer NF, Wells JM. Directed differentiation of human pluripotent stem cells into intestinal tissue in vitro. *Nature* 2011; **470**: 105-109 [PMID: 21151107 DOI: 10.1038/nature09691]
62 **McCracken KW**, Howell JC, Wells JM, Spence JR. Generating human intestinal tissue from pluripotent stem cells in vitro. *Nat Protoc* 2011; **6**: 1920-1928 [PMID: 22082986 DOI: 10.1038/nprot.2011.410]
63 **Watson CL**, Mahe MM, Múnera J, Howell JC, Sundaram N, Poling HM, Schweitzer JI, Vallance JE, Mayhew CN, Sun Y, Grabowski G, Finkbeiner SR, Spence JR, Shroyer NF, Wells JM, Helmrath MA. An in vivo model of human small intestine using pluripotent stem cells. *Nat Med* 2014; **20**: 1310-1314 [PMID: 25326803 DOI: 10.1038/nm.3737]
64 **Takahashi Y**, Sato S, Kurashima Y, Yamamoto T, Kurokawa S, Yuki Y, Takemura N, Uematsu S, Lai CY, Otsu M, Matsuno H, Osawa H, Mizushima T, Nishimura J, Hayashi M, Yamaguchi T, Kiyono H. A Refined Culture System for Human Induced Pluripotent Stem Cell-Derived Intestinal Epithelial Organoids. *Stem Cell Reports* 2018; **10**: 314-328 [PMID: 29233552 DOI: 10.1016/j.stemcr.2017.11.004]
65 **Múnera JO**, Sundaram N, Rankin SA, Hill D, Watson C, Mahe M, Vallance JE, Shroyer NF, Sinagoga KL, Zarzoso-Lacoste A, Hudson JR, Howell JC, Chatuvedi P, Spence JR, Shannon JM, Zorn AM, Helmrath MA, Wells JM. Differentiation of Human Pluripotent Stem Cells into Colonic Organoids via Transient Activation of BMP Signaling. *Cell Stem Cell* 2017; **21**: 51-64.e6 [PMID: 28648364 DOI: 10.1016/j.stem.2017.05.020]
66 **Chang-Graham AL**, Danhof HA, Engevik MA, Tomaro-Duchesneau C, Karandikar UC, Estes MK, Versalovic J, Britton RA, Hyser JM. Human Intestinal Enteroids With Inducible Neurogenin-3 Expression as a Novel Model of Gut Hormone Secretion. *Cell Mol Gastroenterol Hepatol* 2019; **8**: 209-229 [PMID: 31029854 DOI: 10.1016/j.jcmgh.2019.04.010]
67 **Du A**, McCracken KW, Walp ER, Terry NA, Klein TJ, Han A, Wells JM, May CL. Arx is required for normal enteroendocrine cell development in mice and humans. *Dev Biol* 2012; **365**: 175-188 [PMID: 22387004 DOI: 10.1016/j.ydbio.2012.02.024]
68 **Petersen N**, Reimann F, Bartfeld S, Farin HF, Ringnalda FC, Vries RG, van den Brink S, Clevers H, Gribble FM, de Koning EJ. Generation of L cells in mouse and human small intestine organoids. *Diabetes* 2014; **63**: 410-420 [PMID: 24130334 DOI: 10.2337/db13-0991]
69 **Petersen N**, Reimann F, van Es JH, van den Berg BM, Kroone C, Pais R, Jansen E, Clevers H, Gribble FM, de Koning EJ. Targeting development of incretin-producing cells increases insulin secretion. *J Clin Invest* 2015; **125**: 379-385 [PMID: 25500886 DOI: 10.1172/JCI75838]
70 **Lund ML**, Sorrentino G, Egerod KL, Kroone C, Mortensen B, Knop FK, Reimann F, Gribble FM, Drucker DJ, de Koning EJP, Schoonjans K, Bäckhed F, Schwartz TW, Petersen N. L-Cell Differentiation Is Induced by Bile Acids Through GPBAR1 and Paracrine GLP-1 and Serotonin Signaling. *Diabetes* 2020; **69**: 614-623

[PMID: 32041793 DOI: 10.2337/db19-0764]
71 **Bartfeld S**, Bayram T, van de Wetering M, Huch M, Begthel H, Kujala P, Vries R, Peters PJ, Clevers H. In vitro expansion of human gastric epithelial stem cells and their responses to bacterial infection. *Gastroenterology* 2015; **148**: 126-136.e6 [PMID: 25307862 DOI: 10.1053/j.gastro.2014.09.042]
72 **Svendsen B**, Holst JJ. Regulation of gut hormone secretion. Studies using isolated perfused intestines. *Peptides* 2016; **77**: 47-53 [PMID: 26275337 DOI: 10.1016/j.peptides.2015.08.001]
73 **Cheung GW**, Kokorovic A, Lam CK, Chari M, Lam TK. Intestinal cholecystokinin controls glucose production through a neuronal network. *Cell Metab* 2009; **10**: 99-109 [PMID: 19656488 DOI: 10.1016/j.cmet.2009.07.005]
74 **Scheltema G**. Permeation in the examination and treatment of the stomach and intestines. *Arch Roentg Ray* 1908; **13**: 144-149 [DOI: 10.1259/arr.1908.0072]
75 **Miller G**, Abbott W. Intestinal intubation: a practical technique. *Am J Med Sci* 1934; **187**: 595-598 [DOI: 10.1097/00000441-193405000-00002]
76 **Abbott WO**, Miller TG. Intubation Studies of the human small intestine: III. A technic for the collection of pure intestinal secretion and for the study of intestinal absorption. *JAMA* 1936; **106**: 16-18 [DOI: 10.1001/jama.1936.02770010018004]
77 **Abbott WO**, Karr WG, Miller TG. Intubation studies of the human small intestine: VII. Factors concerned in absorption of glucose from the jejunum and ileum. *Am J Dig Dis* 1937; **4**: 742-752 [DOI: 10.1007/BF03000444]
78 **Groen J**. THE ABSORPTION OF HEXOSES FROM THE UPPER PART OF THE SMALL INTESTINE IN MAN. *J Clin Invest* 1937; **16**: 245-255 [PMID: 16694475 DOI: 10.1172/JCI100854]
79 **Shay H**, Gershon-Cohen J, Fels SS, Munro FL, Siplet H. The absorption and dilution of glucose solutions in the human stomach and duodenum. *Am J Dig Dis* 1939; **6**: 535-544 [DOI: 10.1007/BF02997033]
80 **Silny J**. Intraluminal multiple electric impedance procedure for measurement of gastrointestinal motility. *Neurogastroenterol Motil* 1991; **3**: 151-162 [DOI: 10.1111/j.1365-2982.1991.tb00061.x]
81 **Andersson S**, Grossman MI. Profile of pH, pressure, and potential difference at gastroduodenal junction in man. *Gastroenterology* 1965; **49**: 364-371 [PMID: 5831780 DOI: 10.1016/S0016-5085(19)34511-1]
82 **Veedfald S**, Wu T, Bound M, Grivell J, Hartmann B, Rehfeld JF, Deacon CF, Horowitz M, Holst JJ, Rayner CK. Hyperosmolar Duodenal Saline Infusion Lowers Circulating Ghrelin and Stimulates Intestinal Hormone Release in Young Men. *J Clin Endocrinol Metab* 2018; **103**: 4409-4418 [PMID: 30053031 DOI: 10.1210/jc.2018-00699]
83 **Wu T**, Trahair LG, Little TJ, Bound MJ, Zhang X, Wu H, Sun Z, Horowitz M, Rayner CK, Jones KL. Effects of Vildagliptin and Metformin on Blood Pressure and Heart Rate Responses to Small Intestinal Glucose in Type 2 Diabetes. *Diabetes Care* 2017; **40**: 702-705 [PMID: 28258090 DOI: 10.2337/dc16-2391]
84 **Hutson WR**, Roehrkasse RL, Wald A. Influence of gender and menopause on gastric emptying and motility. *Gastroenterology* 1989; **96**: 11-17 [PMID: 2909416 DOI: 10.1016/0016-5085(89)90758-0]
85 **Watson LE**, Xie C, Wang X, Li Z, Phillips LK, Sun Z, Jones KL, Horowitz M, Rayner CK, Wu T. Gastric Emptying in Patients With Well-Controlled Type 2 Diabetes Compared With Young and Older Control Subjects Without Diabetes. *J Clin Endocrinol Metab* 2019; **104**: 3311-3319 [PMID: 30933282 DOI: 10.1210/jc.2018-02736]
86 **Cecil JE**, Francis J, Read NW. Comparison of the effects of a high-fat and high-carbohydrate soup delivered orally and intragastrically on gastric emptying, appetite, and eating behaviour. *Physiol Behav* 1999; **67**: 299-306 [PMID: 10477062 DOI: 10.1016/S0031-9384(99)00069-4]
87 **Wu T**, Rayner CK, Young RL, Horowitz M. Gut motility and enteroendocrine secretion. *Curr Opin Pharmacol* 2013; **13**: 928-934 [PMID: 24060702 DOI: 10.1016/j.coph.2013.09.002]
88 **Wu T**, Rayner CK, Watson LE, Jones KL, Horowitz M, Little TJ. Comparative effects of intraduodenal fat and glucose on the gut-incretin axis in healthy males. *Peptides* 2017; **95**: 124-127 [PMID: 28800948 DOI: 10.1016/j.peptides.2017.08.001]
89 **Wu T**, Thazhath SS, Marathe CS, Bound MJ, Jones KL, Horowitz M, Rayner CK. Comparative effect of intraduodenal and intrajejunal glucose infusion on the gut-incretin axis response in healthy males. *Nutr Diabetes* 2015; **5**: e156 [PMID: 25985092 DOI: 10.1038/nutd.2015.6]
90 **Zhang X**, Young RL, Bound M, Hu S, Jones KL, Horowitz M, Rayner CK, Wu T. Comparative Effects of Proximal and Distal Small Intestinal Glucose Exposure on Glycemia, Incretin Hormone Secretion, and the Incretin Effect in Health and Type 2 Diabetes. *Diabetes Care* 2019; **42**: 520-528 [PMID: 30765429 DOI: 10.2337/dc18-2156]
91 **Wu T**, Bound MJ, Standfield SD, Gedulin B, Jones KL, Horowitz M, Rayner CK. Effects of rectal administration of taurocholic acid on glucagon-like peptide-1 and peptide YY secretion in healthy humans. *Diabetes Obes Metab* 2013; **15**: 474-477 [PMID: 23181598 DOI: 10.1111/dom.12043]
92 **Lennernäs H**, Fagerholm U, Raab Y, Gerdin B, Hällgren R. Regional rectal perfusion: a new in vivo approach to study rectal drug absorption in man. *Pharm Res* 1995; **12**: 426-432 [PMID: 7617532 DOI: 10.1023/A:1016216905197]
93 **Laferrère B**, Heshka S, Wang K, Khan Y, McGinty J, Teixeira J, Hart AB, Olivan B. Incretin levels and effect are markedly enhanced 1 month after Roux-en-Y gastric bypass surgery in obese patients with type 2 diabetes. *Diabetes Care* 2007; **30**: 1709-1716 [PMID: 17416796 DOI: 10.2337/dc06-1549]
94 **Ma J**, Checklin HL, Wishart JM, Stevens JE, Jones KL, Horowitz M, Meyer JH, Rayner CK. A randomised trial of enteric-coated nutrient pellets to stimulate gastrointestinal peptide release and lower glycaemia in type 2 diabetes. *Diabetologia* 2013; **56**: 1236-1242 [PMID: 23471488 DOI: 10.1007/s00125-013-2876-2]
95 **Young RL**, Chia B, Isaacs NJ, Ma J, Khoo J, Wu T, Horowitz M, Rayner CK. Disordered control of intestinal sweet taste receptor expression and glucose absorption in type 2 diabetes. *Diabetes* 2013; **62**: 3532-3541 [PMID: 23761104 DOI: 10.2337/db13-0581]
96 **Wang Y**, Gunasekara DB, Reed MI, DiSalvo M, Bultman SJ, Sims CE, Magness ST, Allbritton NL. A microengineered collagen scaffold for generating a polarized crypt-villus architecture of human small intestinal epithelium. *Biomaterials* 2017; **128**: 44-55 [PMID: 28288348 DOI: 10.1016/j.biomaterials.2017.03.005]
97 **Chen Y**, Zhou W, Roh T, Estes MK, Kaplan DL. In vitro enteroid-derived three-dimensional tissue model

of human small intestinal epithelium with innate immune responses. *PLoS One* 2017; **12**: e0187880 [PMID: 29186150 DOI: 10.1371/journal.pone.0187880]

98 **Eaton AD**, Zimmermann C, Delaney B, Hurley BP. Primary human polarized small intestinal epithelial barriers respond differently to a hazardous and an innocuous protein. *Food Chem Toxicol* 2017; **106**: 70-77 [PMID: 28533127 DOI: 10.1016/j.fct.2017.05.038]

99 **Bhatt AP**, Gunasekara DB, Speer J, Reed MI, Peña AN, Midkiff BR, Magness ST, Bultman SJ, Allbritton NL, Redinbo MR. Nonsteroidal Anti-Inflammatory Drug-Induced Leaky Gut Modeled Using Polarized Monolayers of Primary Human Intestinal Epithelial Cells. *ACS Infect Dis* 2018; **4**: 46-52 [PMID: 29094594 DOI: 10.1021/acsinfecdis.7b00139]

100 **Graves CL**, Harden SW, LaPato M, Nelson M, Amador B, Sorenson H, Frazier CJ, Wallet SM. A method for high purity intestinal epithelial cell culture from adult human and murine tissues for the investigation of innate immune function. *J Immunol Methods* 2014; **414**: 20-31 [PMID: 25193428 DOI: 10.1016/j.jim.2014.08.002]

101 **Speer JE**, Wang Y, Fallon JK, Smith PC, Allbritton NL. Evaluation of human primary intestinal monolayers for drug metabolizing capabilities. *J Biol Eng* 2019; **13**: 82 [PMID: 31709009 DOI: 10.1186/s13036-019-0212-1]

102 **Takayama K**, Negoro R, Yamashita T, Kawai K, Ichikawa M, Mori T, Nakatsu N, Harada K, Ito S, Yamada H, Yamaura Y, Hirata K, Ishida S, Mizuguchi H. Generation of Human iPSC-Derived Intestinal Epithelial Cell Monolayers by CDX2 Transduction. *Cell Mol Gastroenterol Hepatol* 2019; **8**: 513-526 [PMID: 31228606 DOI: 10.1016/j.jcmgh.2019.06.004]

103 **Kozuka K**, He Y, Koo-McCoy S, Kumaraswamy P, Nie B, Shaw K, Chan P, Leadbetter M, He L, Lewis JG, Zhong Z, Charmot D, Balaa M, King AJ, Caldwell JS, Siegel M. Development and Characterization of a Human and Mouse Intestinal Epithelial Cell Monolayer Platform. *Stem Cell Reports* 2017; **9**: 1976-1990 [PMID: 29153987 DOI: 10.1016/j.stemcr.2017.10.013]

104 **Kimura H**, Sakai Y, Fujii T. Organ/body-on-a-chip based on microfluidic technology for drug discovery. *Drug Metab Pharmacokinet* 2018; **33**: 43-48 [PMID: 29175062 DOI: 10.1016/j.dmpk.2017.11.003]

105 **Choe A**, Ha SK, Choi I, Choi N, Sung JH. Microfluidic Gut-liver chip for reproducing the first pass metabolism. *Biomed Microdevices* 2017; **19**: 4 [PMID: 28074384 DOI: 10.1007/s10544-016-0143-2]

106 **Hsiao YH**, Hsu CH, Chen C. A High-Throughput Automated Microfluidic Platform for Calcium Imaging of Taste Sensing. *Molecules* 2016; **21**: 896 [PMID: 27399663 DOI: 10.3390/molecules21070896]

107 **Nguyen DT**, van Noort D, Jeong IK, Park S. Endocrine system on chip for a diabetes treatment model. *Biofabrication* 2017; **9**: 015021 [PMID: 28222044 DOI: 10.1088/1758-5090/aa5cc9]

108 **Kasendra M**, Tovaglieri A, Sontheimer-Phelps A, Jalili-Firoozinezhad S, Bein A, Chalkiadaki A, Scholl W, Zhang C, Rickner H, Richmond CA, Li H, Breault DT, Ingber DE. Development of a primary human Small Intestine-on-a-Chip using biopsy-derived organoids. *Sci Rep* 2018; **8**: 2871 [PMID: 29440725 DOI: 10.1038/s41598-018-21201-7]

109 **Gluck N**, Shpak B, Brun R, Rösch T, Arber N, Moshkowitz M. A novel prepless X-ray imaging capsule for colon cancer screening. *Gut* 2016; **65**: 371-373 [PMID: 26628510 DOI: 10.1136/gutjnl-2015-310893]

110 **Becker D**, Zhang J, Heimbach T, Penland RC, Wanke C, Shimizu J, Kulmatycki K. Novel orally swallowable IntelliCap(®) device to quantify regional drug absorption in human GI tract using diltiazem as model drug. *AAPS PharmSciTech* 2014; **15**: 1490-1497 [PMID: 25023947 DOI: 10.1208/s12249-014-0172-1]

111 **Gora MJ**, Sauk JS, Carruth RW, Gallagher KA, Suter MJ, Nishioka NS, Kava LE, Rosenberg M, Bouma BE, Tearney GJ. Tethered capsule endomicroscopy enables less invasive imaging of gastrointestinal tract microstructure. *Nat Med* 2013; **19**: 238-240 [PMID: 23314056 DOI: 10.1038/nm.3052]

112 **Abramson A**, Caffarel-Salvador E, Khang M, Dellal D, Silverstein D, Gao Y, Frederiksen MR, Vegge A, Hubálek F, Water JJ, Friderichsen AV, Fels J, Kirk RK, Cleveland C, Collins J, Tamang S, Hayward A, Landh T, Buckley ST, Roxhed N, Rahbek U, Langer R, Traverso G. An ingestible self-orienting system for oral delivery of macromolecules. *Science* 2019; **363**: 611-615 [PMID: 30733413 DOI: 10.1126/science.aau2277]

113 **Kalantar-Zadeh K**, Berean KJ, Ha N, Chrimes AF, Xu K, Grando D, Ou JZ, Pillai N, Campbell JL, Brkljača R, Taylor KM, Burgell RE, Yao CK, Ward SA, McSweeney CS, Muir JG, Gibson PR. A human pilot trial of ingestible electronic capsules capable of sensing different gases in the gut. *Nat Electron* 2018; **1**: 79-87 [DOI: 10.1038/s41928-017-0004-x]

114 **van der Schaar PJ**, Dijksman JF, Broekhuizen-de Gast H, Shimizu J, van Lelyveld N, Zou H, Iordanov V, Wanke C, Siersema PD. A novel ingestible electronic drug delivery and monitoring device. *Gastrointest Endosc* 2013; **78**: 520-528 [PMID: 23684148 DOI: 10.1016/j.gie.2013.03.170]

115 **Sarosiek I**, Selover KH, Katz LA, Semler JR, Wilding GE, Lackner JM, Sitrin MD, Kuo B, Chey WD, Hasler WL, Koch KL, Parkman HP, Sarosiek J, McCallum RW. The assessment of regional gut transit times in healthy controls and patients with gastroparesis using wireless motility technology. *Aliment Pharmacol Ther* 2010; **31**: 313-322 [PMID: 19814743 DOI: 10.1111/j.1365-2036.2009.04162.x]

116 **Koziolek M**, Grimm M, Becker D, Iordanov V, Zou H, Shimizu J, Wanke C, Garbacz G, Weitschies W. Investigation of pH and Temperature Profiles in the GI Tract of Fasted Human Subjects Using the Intellicap(®) System. *J Pharm Sci* 2015; **104**: 2855-2863 [PMID: 25411065 DOI: 10.1002/jps.24274]

117 **Maurer JM**, Schellekens RC, van Rieke HM, Wanke C, Iordanov V, Stellaard F, Wutzke KD, Dijkstra G, van der Zee M, Woerdenbag HJ, Frijlink HW, Kosterink JG. Gastrointestinal pH and Transit Time Profiling in Healthy Volunteers Using the IntelliCap System Confirms Ileo-Colonic Release of ColoPulse Tablets. *PLoS One* 2015; **10**: e0129076 [PMID: 26177019 DOI: 10.1371/journal.pone.0129076]

118 **Rao SS**, Kuo B, McCallum RW, Chey WD, DiBaise JK, Hasler WL, Koch KL, Lackner JM, Miller C, Saad R, Semler JR, Sitrin MD, Wilding GE, Parkman HP. Investigation of colonic and whole-gut transit with wireless motility capsule and radiopaque markers in constipation. *Clin Gastroenterol Hepatol* 2009; **7**: 537-544 [PMID: 19418602 DOI: 10.1016/j.cgh.2009.01.017]

119 **Demosthenous P**, Pitris C, Georgiou J. Infrared Fluorescence-Based Cancer Screening Capsule for the Small Intestine. *IEEE Trans Biomed Circuits Syst* 2016; **10**: 467-476 [PMID: 26302520 DOI:

10.1109/TBCAS.2015.2449277]

120 **Qiao P**, Liu H, Yan X, Jia Z, Pi X. A Smart Capsule System for Automated Detection of Intestinal Bleeding Using HSL Color Recognition. *PLoS One* 2016; **11**: e0166488 [PMID: 27902728 DOI: 10.1371/journal.pone.0166488]

121 **Mimee M**, Nadeau P, Hayward A, Carim S, Flanagan S, Jerger L, Collins J, McDonnell S, Swartwout R, Citorik RJ, Bulović V, Langer R, Traverso G, Chandrakasan AP, Lu TK. An ingestible bacterial-electronic system to monitor gastrointestinal health. *Science* 2018; **360**: 915-918 [PMID: 29798884 DOI: 10.1126/science.aas9315]

122 **Kuo B**, Maneerattanaporn M, Lee AA, Baker JR, Wiener SM, Chey WD, Wilding GE, Hasler WL. Generalized transit delay on wireless motility capsule testing in patients with clinical suspicion of gastroparesis, small intestinal dysmotility, or slow transit constipation. *Dig Dis Sci* 2011; **56**: 2928-2938 [PMID: 21625964 DOI: 10.1007/s10620-011-1751-6]

123 **Maqbool S**, Parkman HP, Friedenberg FK. Wireless capsule motility: comparison of the SmartPill GI monitoring system with scintigraphy for measuring whole gut transit. *Dig Dis Sci* 2009; **54**: 2167-2174 [PMID: 19655250 DOI: 10.1007/s10620-009-0899-9]

World Journal of Gastroenterology

Submit a Manuscript: https://www.f6publishing.com

World J Gastroenterol 2020 July 7; 26(25): 3577-3585

DOI: 10.3748/wjg.v26.i25.3577

ISSN 1007-9327 (print) ISSN 2219-2840 (online)

MINIREVIEWS

Monoacylglycerol lipase reprograms lipid precursors signaling in liver disease

Matteo Tardelli

ORCID number: Matteo Tardelli 0000-0003-2232-7779.

Author contributions: Tardelli M wrote, ideated, and proofread this manuscript.

Conflict-of-interest statement: There is no conflict of interest associated with any of the senior author or other coauthors contributed their efforts in this manuscript.

Manuscript source: Invited manuscript

Received: March 18, 2020
Peer-review started: March 18, 2020
First decision: May 15, 2020
Revised: June 18, 2020

Matteo Tardelli, Division of Gastroenterology and Hepatology, Joan and Sanford I Weill Cornell Department of Medicine, Weill Cornell Medical College, New York, NY 10021, United States

Matteo Tardelli, Hans Popper Laboratory of Molecular Hepatology, Division of Gastroenterology and Hepatology, Internal Medicine III, Medical University of Vienna, Vienna 1040, Austria

Corresponding author: Matteo Tardelli, MSc, PhD, Lecturer, Postdoctoral Fellow, Division of Gastroenterology and Hepatology, Joan and Sanford I Weill Department of Medicine, Weill Cornell Medical College, 413 E. 69th Street, New York, NY 10021, United States. mat4005@med.cornell.edu

Abstract

Dietary oversupply of triglycerides represent the hallmark of obesity and connected complications in the liver such as non-alcoholic fatty liver disease and non-alcoholic steatohepatitis, which eventually progress to cirrhosis and hepatocellular carcinoma. Monoacylglycerol lipase is the last enzymatic step in the hydrolysis of triglycerides, generating glycerol and fatty acids (FAs), which are signaling precursors in physiology and disease. Notably, monoacylglycerol lipase (MGL) also hydrolyzes 2-arachidonoylglycerol, which is a potent ligand within the endocannabinoid system, into arachidonic acid - a precursor for prostaglandin synthesis; thus representing a pivotal substrates provider in multiple organs for several intersecting biological pathways ranging from FA metabolism to inflammation, pain and appetite. MGL inhibition has been shown protective in limiting several liver diseases as FAs may drive hepatocyte injury, fibrogenesis and de- activate immune cells, however the complexity of MGL network system still needs further and deeper understanding. The present review will focus on MGL function and FA partitioning in the horizons of liver disease.

Key words: Lipid metabolism; Monoacylglycerol lipase; Non-alcoholic steatohepatitis; Non-alcoholic fatty liver disease; Cannabinoid; Nuclear receptors

Core tip: Monoacylglycerol lipase inhibition/modulation is yet unappreciated however

Accepted: June 23, 2020
Article in press: June 23, 2020
Published online: July 7, 2020

P-Reviewer: Balaban YH, Chiu KW, Gassler N, Hashimoto N, Li YY, Makishima M, Niu ZS, Shimizu Y
S-Editor: Zhang L
L-Editor: A
E-Editor: Ma YJ

attractive therapeutic concept to limit liver disease as fatty acids may drive hepatocyte injury, fibrogenesis and change immune cells phenotype.

Citation: Tardelli M. Monoacylglycerol lipase reprograms lipid precursors signaling in liver disease. *World J Gastroenterol* 2020; 26(25): 3577-3585
URL: https://www.wjgnet.com/1007-9327/full/v26/i25/3577.htm
DOI: https://dx.doi.org/10.3748/wjg.v26.i25.3577

INTRODUCTION

Dietary lipids are major sources of energy in the body and serve a variety of vital functions[1]. They represent pivotal substrates for beta oxidation, fueling the production of cellular energy as well as being precursors of all lipid classes, including prostaglandins, steroid hormones and those that form biological membranes[1]. Notwithstanding their key roles, aberrant lipid metabolism may become harmful to cells, as free fatty acids (FAs) are known to be powerful signaling molecules[2,3]. FAs and their metabolites regulate several intracellular processes such as gene transcription and expression, post-transcriptional/translational modification of proteins, also directly modulating an array of enzyme activities as co-activators[4,5]. Fat stores in the adipose tissue (AT) are the major energy reserves in mammals. Upon food intake, lipid species are absorbed in the intestine and delivered to the circulation; the surplus of dietary non-esterified fatty acids (NEFAs) which are not immediately needed by the body, are re-esterified into triglycerides (TG) that are subsequently stored in cytosolic lipid droplets of the adipocytes[3]. During fasting for instance, these TG stores in the AT can be released by hydrolytic cleavage, and the resulting NEFAs reach peripheral tissues such as liver and muscle to be processed for β-oxidation and therefore energy/ATP production[6]. Of interest, also non-adipose organs can effectively esterify NEFAs into TG and re-hydrolyze them back into NEFAs according to the energy demands[6]. Excessive amounts of TGs store into AT and other organs such as liver leading to lipotoxicity as well as non-alcoholic fatty liver disease and type 2 diabetes[7]. The cleavage of primary/secondary ester bonds between long chain FAs and glycerol backbone that form TGs, depends on specific hydrolases commonly called neutral lipases (to be differentiated from lysosomal acid lipases)[3,8]. Three main enzymes are involved in the thorough hydrolysis of TGs in cellular lipid stores: adipose triglyceride lipase exclusively performs the first step hydrolyzing TGs to generate diacylglycerols (DGs) and FAs[3]. Hormone-sensitive lipase instead is capable of hydrolyzing several acylesters including TGs, DGs, and monoacylglycerols (MGs)[3,6]. Finally, monoacylglycerol lipase (MGL) efficiently cleaves MGs into glycerol and FAs[9](Figure 1). This process is aided by comparative gene identification-58 (CGI-58, also known as ABHD5), which interacts with perilipin, protecting or exposing the TG core of a lipid droplet to lipases (mainly adipose triglyceride lipase)[10] and therefore enhancing their activity[11]. Hydrolysis is finely balanced by concomitant re-esterification of MGs/DGs into TGs, which is performed by monoacylglycerol acyltransferases (MGAT) and diacylglycerol acyltransferase (DGAT) respectively, as shown in Figure 1.

MGL is a particularly interesting enzyme as substantially bridges organ-specific nutrient metabolism to central and peripheral endocannabinoid and eicosanoid systems[12]. The fact that the latter holds such a multipurpose and promiscuous role in several physiological processes is driving a resurgence of interest in this lipase as putative drug target for several different disorders[13]. Although, very well characterized in behavioral studies and central nervous system disease models[14-16] (in connection to the endocannabinoids and prostaglandins network), the contribution of MGL to metabolic liver disease, cholestasis, inflammation, and fibrosis is surprisingly unknown.

PRE-CLINICAL STUDIES ON MONOACYLGLYCEROL LIPASE DELETION/INHIBITION

MGL is the rate-limiting enzyme of MG degradation that derive from intra- /extra-

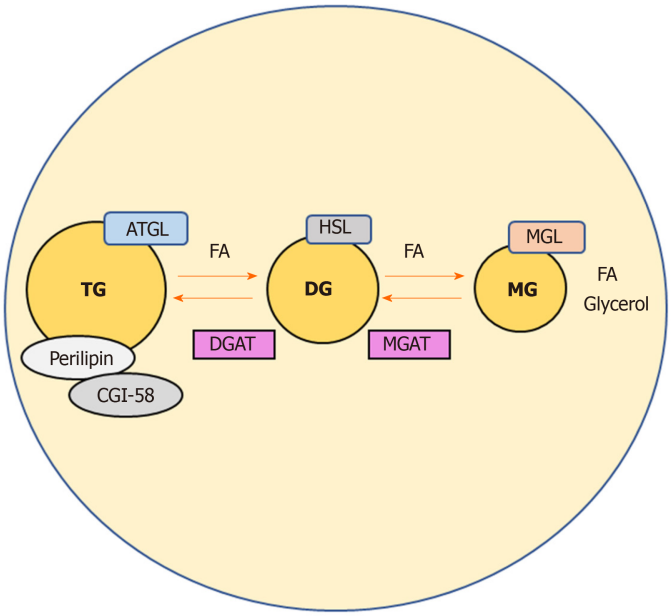

Figure 1 Catabolic pathways regulating triglycerides levels in adipocytes. Adipose triglyceride lipase, hormone sensitive lipase, and monoacylglycerol lipase act on triglycerides in a series of subsequent reactions in order to generate glycerol and fatty acids. Comparative gene identification-58 binds to perilipin facilitating lipolysis, as a known activator of adipose triglyceride lipase. Intermediates of this catabolic pathway may also be re-esterified to phospholipids and triglycerides by the enzymes monoacylglycerol acyltransferases and diacylglycerol acyltransferase. ATGL: Adipose triglyceride lipase; HSL: Hormone sensitive lipase; MGL: Monoacylglycerol lipase; TGs: Triglycerides; FAs: Fatty acids; CGI-58: Comparative gene identification-58; MGAT: Monoacyglycerol acyltransferases; DGAT: Diacylglycerol acyltransferase.

cellular phospholipids or TGs[17]. The extracellular most important source of MGs is TG-rich lipoproteins such as the liver-derived very low density lipoproteins[18]. TGs are released from circulating very low density lipoproteins by the action of the endothelial lipoprotein lipase that generates FAs, hydrolyzing TGs in positions sn-1- and sn-3, thus generating MG species[19]. Digestion of dietary TG is also aided by pancreatic lipase that can generate in addition fair amounts of MGs[20]. Extracellular derived MGs are internalized by cells and may be further degraded by MGL or alternatively re-esterified to TGs by the enzymatic activities of MGAT and DGAT (Figure 1). In fact, MGAT and DGAT are key players in enterocytes and particularly in the small intestine, where they are thought of synthesizing up to 80% of the TG incorporated into chylomicrons[21]. In addition, another source of MGs can directly originate from the intracellular TGs storage in cytosolic lipid droplets[3].

MGL is a pivotal lipase that produces signaling lipid, notably hydrolyzing 2-AG (which is a known ligand of cannabinoid receptors) into arachidonic acid (AA)[9]. Given the multiple roles of the cannabinoid system in regulation of several key processes in human physiology including (but not limited to) appetite, pain and even cancer, enzymes targeting the cannabinoid catabolism are potentially interesting candidates for drug discovery and pharmaceutical development[14]. MGL is ubiquitous in the body and its expression varies greatly in an organ-specific fashion, being present in brain and in peripheral tissues such as the kidney, testis, ovary, adrenal gland, AT, and heart. At the cellular level, MGL mainly localizes in the cytoplasm as well as in the plasma membrane and in the lipid droplet[22]. Interestingly, molecular strategies exploiting genetic or pharmacological inactivation of MGL in mice resulted in a significant accumulation of MGs in several tissues demonstrating its central role in MG catabolism[9]. In diet induced obesity models, MGL ablation showed to be protective in the development of glucose intolerance and insulin resistance, although reduced MGL activity was partially reverted by hormone-sensitive lipase[23]. This phenotype was shown to be influenced by the effects of MGL on the central nervous system and derived behavioral changes triggered by the endocannabinoid pathway[23]. Importantly, MGL knockout mice (*Mgl*$^{-/-}$) showed neuroprotective properties in a parkinsonian mouse model, with consequent reduction of multiple prostaglandins and eicosanoids mediators in the brain, including prostaglandin -E2, -D2, -F2, and thromboxane B2[24]. In keeping with this parkinsonian mouse models, MGL´s network of endocannabinoid and prostaglandin regulation was also demonstrated to contribute to the pathogenesis of Alzheimer´s disease, representing a promising target for its prevention/treatment[16]. Chronic inactivation of MGL in the central nervous system

was shown to lead to a 2-AG oversupply and consecutive desensitization of cannabinoid 1 receptor (CB1r) signaling[23]. Intriguingly, central CB1r inactivation was correlated to a higher incidence of depression and several other psychiatric side effects in patients[25], which led to consequent withdrawal of the anti-obesity drug rimonabant, an inverse CB1r agonist[23]. Experiments with CB1r/MGL double-KO mice revealed that oral but not intraperitoneal lipid administration strongly suppressed the appetites of *Mgl*$^{-/-}$ and CB1r/MGL DKO mice, but not affecting wild-type and CB1r$^{-/-}$ mice[26]. In this study, appetite suppression was reversed by vagotomy, suggesting a mechanistical involvement of MGL in the gut-brain axis regulation of appetite[26]. In keeping, administration of an MGL inhibitor called MJN110, reduced food intake in rats[27]. Notably, pharmacological blockade of MGL with JZL184 caused increased systemic 2-AG levels in a mouse model of myocardial infarction[28]. This resulted in elevated cardiac C-X-C motif chemokine ligand-1, -2, and matrix metallopeptidase-9 levels as well as increased cardiac neutrophil/monocyte counts 24 h after infarction compared to vehicle-treated mice[28]. In another study, dietary supplementation of linoleic acid in a range of 1% to 8% significantly increased 2-AG in the liver and small bowel, suggesting possible dietary tools to modulate endocannabinoid ligands[29].

Of interest, a recent study characterized a unique population of human bone marrow adipocytes[30], discovering a profound downregulation of MGL expression which was shown to underlie the metabolic differences in the phenotype/lipid metabolism, also justifying bone marrow adipocytes' resistance to caloric restrictions[30]. Further studies showed that when *Mgl*$^{-/-}$ animals were challenged with high fat diet feeding, great amounts of 2-AG were detected in the brain, although affecting neither food consumption nor body weight, therefore evidencing cannabinoid receptors desensitizing effects[23]. Notably, the liver content of certain species of saturated and unsaturated MGs were highly enriched in *Mgl*$^{-/-}$, showing after 12 wk high fat diet better insulin sensitivity and glucose tolerance[31,32]; although whether adipose depots or skeletal muscle were the main players in determining this phenotype, was not thoroughly investigated. Several other works evidenced a role of MGL in tumor growth/metabolism as well as oncogenic signaling[33], being associated with gastrointestinal stromal tumors[34] and hepatocellular carcinoma (HCC); others instead showed that MGL deletion resulted into significant colorectal cancer growth inhibition[35] while also reducing ischemia/reperfusion-induced lung injury and inflammation[36,37]. Additionally, MGL was found to be part of a gene signature determining stem-like properties of cancer cells in prostate cancer[38]; this further supported a role for this enzyme in pro-tumorigenic metabolism, involving the dual control of endocannabinoid and FA pathways[38,39].

Xiang *et al*[40] elegantly showed that MGL deficiency caused lipid overload in tumor associated macrophages[40]. Intriguingly, MGL expression in macrophages was strongly decreased in cancer tissues and positively correlated with the overall survival of cancer patients[40]. Mechanistically, MGL deficiency was shown to promote CB2r/TLR4 axis and subsequent macrophage activation, which in turn suppressed the function of tumor associated CD8+ T cells. In addition, treatment with CB2r antagonist drugs delayed tumor progression in inoculated and genetic cancer models[40].

In the liver, MGL ablation was demonstrated to attenuate LPS-induced inflammation whilst whole body genetic and pharmacological inhibition protected against inflammation and liver lesions provoked by ischemia/reperfusion injury[41]. Intriguingly, hypoxia training was demonstrated to induce MGL expression and ameliorate hepatic steatosis in obese mice, showing decreased 2-AG levels and expression of CB1r[42].

2-AG accumulation in the liver has been shown to have anti-inflammatory and anti-fibrotic effects through CB2r signaling, conversely CB1r activation associates with increased liver damage and fibrosis in different models of liver injury[43] (Figure 2). Habib *et al*[43] suggested that the increased 2-AG levels following MGL blockade selectively stimulate CB2r but not CB1r, thus resulting in hepato-protective effects[43]. In their study, lack of MGL prompted fibrosis regression due to autophagy-mediated anti-inflammatory mechanisms in macrophages[43]. In details, using a mouse model lacking MGL in the myeloid lineage (*Mgl*$^{Mye-/-}$), authors demonstrated that MGL inhibition in immune cells is sufficient to reduce hepatic fibrosis and inflammation after carbon tetrachloride (CCL4) injection[43]. In line with what Cao *et al*[41] previously showed, that systemic MGL inhibition had protective effects on hepatocytes in different models of acute liver injury. These evidence was dependent on the enhanced CB2r activation and modulation of eicosanoid pathways, resulting into diminished neutrophil infiltration and neutrophil-mediated liver damage[41].

In a microarray study, the expression of MGL was shown to be enriched in HCC tumors than in matched non-tumor tissues[44]. The upregulation of MGL in HCC cells

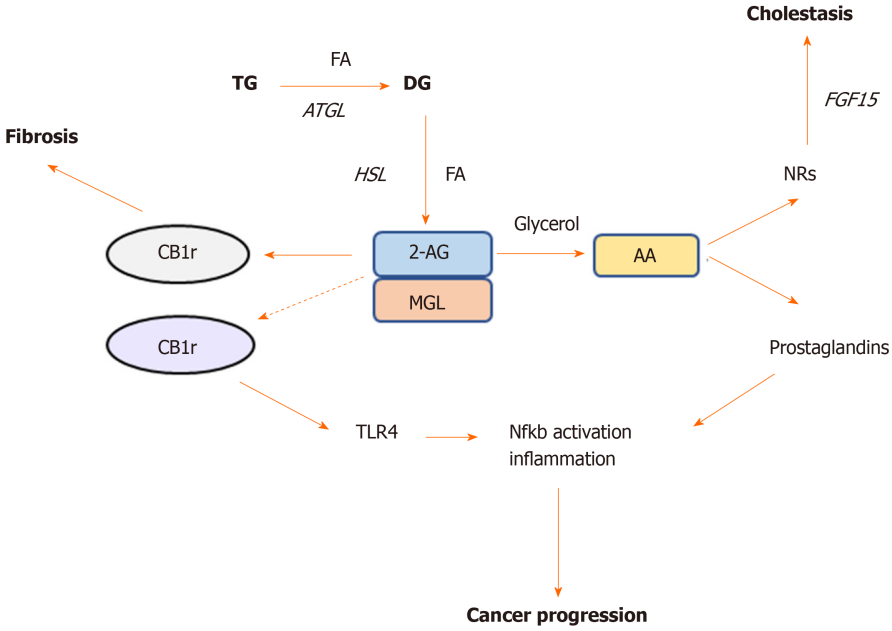

Figure 2 Monoacylglycerol lipase represent a crossroad between cannabinoid and lipid signaling pathways. Monoacylglycerol lipase is the key enzyme degrading the endogenous cannabinoid ligand 2-AG, which in turn is able to bind either cannabinoid receptor (CB) -1r or -2r. Activation of CB1r was found to promote fibrosis whereas CB2r is involved in TLR4 activation and immune cells recruitment in cancer. Monoacylglycerol lipase action further hydrolyzes 2-AG into arachidonic acid, which is a precursor of prostaglandin synthesis, the main drivers of inflammation. Arachidonic acid was also found to bind nuclear receptors such as farnesoid X receptor and peroxisome proliferator activated receptors in the intestine and ameliorate cholestatic disease. AA: Arachidonic acid; NRs: Nuclear receptors; CB: Cannabinoid; MGL: Monoacylglycerol lipase; HSL: Hormone sensitive lipase; ATGL: Adipose triglyceride lipase; TG: Triglyceride; FA: Fatty acid.

promoted cell growth and invasion through pro-tumorigenic lipid signaling[44]. Importantly, MGL was demonstrated to facilitate HCC progression *via* nuclear factor kappa light chain enhancer of activated B cells-mediated epithelial-mesenchymal transition[44]. A recent work from our group strongly demonstrated a central role of MGL inhibition in the pathophysiology of cholestatic liver disease[45]. Using total body knockout mice challenged with cholestatic diet [3,5-diethoxycarbonyl-1,4-dihydrocollidine (DDC)] and pharmacological inhibition (JZL184) of MGL in Mdr2 (Abcb4) knock out - *Mdr2*$^{-/-}$ (an established mouse model that develops spontaneous cholestasis[46]), we evidenced beneficial effects in sclerosing cholangitis development and resolution[45]. We showed that both mouse models were protected from cholestatic liver disease due to a crosstalk mechanism involving the gut-liver axis, microbiome modulation and substrate (AA) accumulation in the intestine (Figure 3). Notwithstanding that AA is a known precursor of pro-inflammatory mediators, in this study it was demonstrated to bind nuclear receptors such as peroxisome proliferator activated receptor alpha and gamma (PPAR-α, -γ) and farnesoid X receptor diminishing intestinal inflammation and consequently impacting liver bile acid synthesis *via* fibroblast growth factor 15[45]. Nevertheless, the development of tissue specific and inducible knockout models would deliver better mechanistic understanding on which organ is playing the most relevant role in the development of cholestasis and other liver diseases after MGL invalidation.

Although several pre-clinical studies showed promising/beneficial effects of MGL blockade in multiple disease models, inhibition of this key metabolic enzyme requires cautious evaluation. On the one hand, the MGL inhibitor named JZL184 (firstly characterized by Long *et al*[47]) has been shown to have low specificity and thus blocking activities of other hydrolases such as fatty acid amide hydrolase and carboxylesterases. On the other hand, another inhibitor called MJN110 was shown to have less activity towards other serine hydrolase systems, also being more effective at enhancing 2-AG levels in the brain than JZL184[48,49]. In keeping with this evidence, both inhibitors are currently used in preclinical studies and *in vitro* systems to explore the effects of MGL inhibition. In a recent work, a new candidate JNJ-42226314 was identified as a reversible and highly selective MGL inhibitor and several other approaches reported developments of positron emission tomography radioligand inhibitors for MGL such as PF-06809247[50,51].

In summary, MGL appears to serve as key metabolic hub for several pathways within chronic liver disease such as sclerosing cholangitis, non-alcoholic fatty liver

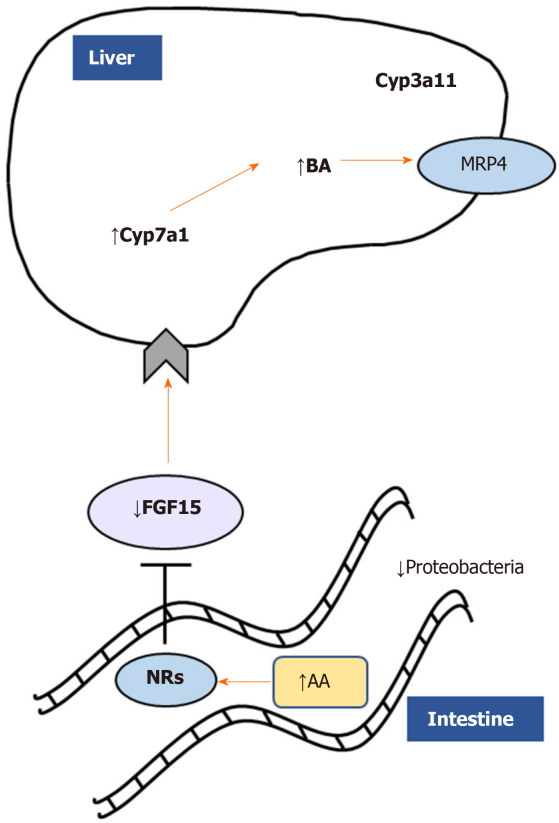

Figure 3 Monoacylglycerol lipase deletion impacts gut-liver axis *via* nuclear receptor and microbiome modulation. Monoacylglycerol lipase ablation ameliorates cholestatic liver disease induced by 3,5-diethoxycarbonyl-1,4-dihydrocollidine challenge diminishing fibrosis, inflammation, and fatty acid metabolism/oxidation in the liver. Accumulation of arachidonic acid binds nuclear receptors such as farnesoid X receptor, downregulating in turn fibroblast growth factor 15 and inducing bile acids synthesis and detoxification as shown by Cyp7a1/Cyp3a11. In addition, proinflammatory *Proteobacteria* were diminished in feces from *Mgl*$^{-/-}$ mice. AA: Arachidonic acid; NRs: Nuclear receptors; FGF15: Fibroblast growth factor 15; BA: Bile acids.

disease, fibrosis and HCC which are disorders affecting complex network of several cell types and molecular mechanisms.

CLINICAL RELEVANCE OF MONOACYLGLYCEROL LIPASE AND ITS GENETIC MUTATION

Only a handful of studies explored the clinical relevance of MGL in human patients, and those mainly focused on rare genetic variants known as single nucleotide polymorphism (SNPs), which may in turn influence determinant lipid-related traits and pathologies[52]. Intriguingly, 4 MGL SNPs named rs13076593, rs782440, rs541855, rs549662 were associated with increased LDL particle size, whilst the rs3773159 with type 2 diabetes[53]. Moreover, 20 common variants of the *MGL* gene were associated with high BMI in a cohort of 289 individuals (of which 147 controls and 142 extremely obese)[54]. Interestingly, the genotype rs604300 was shown to have protective effects against childhood abuse-related increases in cannabis dependence and was suggested to relate to epigenetic modulation of MGL expression[55]. Lastly, the variant Pro129Thr of one of the endocannabinoid inactivating enzyme called fatty acid amide hydrolase was found to significantly associate with both street drug use and problematic drug/alcohol use[56]. However, this could not be replicated in another study in which no associations were found between Pro129Thr or other MGL SNPs and alcoholism in 729 Japanese patients with alcoholism and 799 healthy controls[57].

CONCLUSION

Further work is needed to understand in detail the specific tissue/cell contribution to

the beneficial effects of MGL deletion observed in many studies and disease types. Of special interest would be unveiling the role of MGL in complex cancers such as HCC and cholangiocellular carcinoma or other liver conditions such as alcoholic liver disease, as no data are available yet. Moreover, novel therapeutic avenues may explore functional antagonism of MGL on *i.e.*, the endocannabinoid system, which could be implemented with temporary approaches such as reversible blockade, small molecules, or immuno-therapy systems to study short-term efficacy. This could ultimately lead to better speculations and understanding of the complex network of the lipid machinery involved in the development of liver disease, insulin resistance and type 2 diabetes paving the way to novel pharmacological treatments.

REFERENCES

1 **Burdge GC**, Calder PC. Introduction to fatty acids and lipids. *World Rev Nutr Diet* 2015; **112**: 1-16 [PMID: 25471798 DOI: 10.1159/000365423]
2 **Trauner M**, Arrese M, Wagner M. Fatty liver and lipotoxicity. *Biochim Biophys Acta* 2010; **1801**: 299-310 [PMID: 19857603 DOI: 10.1016/j.bbalip.2009.10.007]
3 **Zechner R**, Zimmermann R, Eichmann TO, Kohlwein SD, Haemmerle G, Lass A, Madeo F. FAT SIGNALS--lipases and lipolysis in lipid metabolism and signaling. *Cell Metab* 2012; **15**: 279-291 [PMID: 22405066 DOI: 10.1016/j.cmet.2011.12.018]
4 **Papackova Z**, Cahova M. Fatty acid signaling: the new function of intracellular lipases. *Int J Mol Sci* 2015; **16**: 3831-3855 [PMID: 25674855 DOI: 10.3390/ijms16023831]
5 **Tardelli M**, Claudel T, Bruschi FV, Trauner M. Nuclear Receptor Regulation of Aquaglyceroporins in Metabolic Organs. *Int J Mol Sci* 2018; 19 [PMID: 29914059 DOI: 10.3390/ijms19061777]
6 **Lass A**, Zimmermann R, Oberer M, Zechner R. Lipolysis - a highly regulated multi-enzyme complex mediates the catabolism of cellular fat stores. *Prog Lipid Res* 2011; **50**: 14-27 [PMID: 21087632 DOI: 10.1016/j.plipres.2010.10.004]
7 **Wakil SJ**, Abu-Elheiga LA. Fatty acid metabolism: target for metabolic syndrome. *J Lipid Res* 2009; **50** Suppl: S138-S143 [PMID: 19047759 DOI: 10.1194/jlr.R800079-JLR200]
8 **Scherer PE**. Adipose tissue: from lipid storage compartment to endocrine organ. *Diabetes* 2006; **55**: 1537-1545 [PMID: 16731815 DOI: 10.2337/db06-0263]
9 **Grabner GF**, Zimmermann R, Schicho R, Taschler U. Monoglyceride lipase as a drug target: At the crossroads of arachidonic acid metabolism and endocannabinoid signaling. *Pharmacol Ther* 2017; **175**: 35-46 [PMID: 28213089 DOI: 10.1016/j.pharmthera.2017.02.033]
10 **Yamaguchi T**, Omatsu N, Morimoto E, Nakashima H, Ueno K, Tanaka T, Satouchi K, Hirose F, Osumi T. CGI-58 facilitates lipolysis on lipid droplets but is not involved in the vesiculation of lipid droplets caused by hormonal stimulation. *J Lipid Res* 2007; **48**: 1078-1089 [PMID: 17308334 DOI: 10.1194/jlr.M600493-JLR200]
11 **Lampidonis AD**, Rogdakis E, Voutsinas GE, Stravopodis DJ. The resurgence of Hormone-Sensitive Lipase (HSL) in mammalian lipolysis. *Gene* 2011; **477**: 1-11 [PMID: 21241784 DOI: 10.1016/j.gene.2011.01.007]
12 **Tardelli M**, Bruschi FV, Trauner M. The role of metabolic lipases in the pathogenesis and management of liver disease. *Hepatology* 2020 [PMID: 32236963 DOI: 10.1002/hep.31250]
13 **Hellerbrand C**. Inhibition of monoacylglycerol lipase for the treatment of liver disease: tempting but still playing with fire. *Gut* 2019; **68**: 382-384 [PMID: 30442681 DOI: 10.1136/gutjnl-2018-317520]
14 **Fowler CJ**. Monoacylglycerol lipase - a target for drug development? *Br J Pharmacol* 2012; **166**: 1568-1585 [PMID: 22428756 DOI: 10.1111/j.1476-5381.2012.01950.x]
15 **Zhang J**, Liu Z, Lian Z, Liao R, Chen Y, Qin Y, Wang J, Jiang Q, Wang X, Gong J. Monoacylglycerol Lipase: A Novel Potential Therapeutic Target and Prognostic Indicator for Hepatocellular Carcinoma. *Sci Rep* 2016; **6**: 35784 [PMID: 27767105 DOI: 10.1038/srep35784]
16 **Chen R**, Zhang J, Wu Y, Wang D, Feng G, Tang YP, Teng Z, Chen C. Monoacylglycerol lipase is a therapeutic target for Alzheimer's disease. *Cell Rep* 2012; **2**: 1329-1339 [PMID: 23122958 DOI: 10.1016/j.celrep.2012.09.030]
17 **Poursharifi P**, Madiraju SRM, Prentki M. Monoacylglycerol signalling and ABHD6 in health and disease. *Diabetes Obes Metab* 2017; **19** Suppl 1: 76-89 [PMID: 28880480 DOI: 10.1111/dom.13008]
18 **Acuña-Aravena M**, Cohen DE. Lipoprotein Metabolism and Cholesterol Balance. In: The Liver 2020 [DOI: 10.1002/9781119436812.ch22]
19 **Goldberg IJ**, Merkel M. Lipoprotein lipase: physiology, biochemistry, and molecular biology. *Front Biosci* 2001; **6**: D388-D405 [PMID: 11229871 DOI: 10.2741/goldberg]
20 **Lowe ME**. The triglyceride lipases of the pancreas. *J Lipid Res* 2002; **43**: 2007-2016 [PMID: 12454260 DOI: 10.1194/jlr.r200012-jlr200]
21 **Shi Y**, Cheng D. Beyond triglyceride synthesis: the dynamic functional roles of MGAT and DGAT enzymes in energy metabolism. *Am J Physiol Endocrinol Metab* 2009; **297**: E10-E18 [PMID: 19116371 DOI: 10.1152/ajpendo.90949.2008]
22 **Duncan M**, Thomas AD, Cluny NL, Patel A, Patel KD, Lutz B, Piomelli D, Alexander SP, Sharkey KA. Distribution and function of monoacylglycerol lipase in the gastrointestinal tract. *Am J Physiol Gastrointest Liver Physiol* 2008; **295**: G1255-G1265 [PMID: 18948437 DOI: 10.1152/ajpgi.90500.2008]
23 **Taschler U**, Radner FP, Heier C, Schreiber R, Schweiger M, Schoiswohl G, Preiss-Landl K, Jaeger D, Reiter B, Koefeler HC, Wojciechowski J, Theussl C, Penninger JM, Lass A, Haemmerle G, Zechner R, Zimmermann R. Monoglyceride lipase deficiency in mice impairs lipolysis and attenuates diet-induced insulin resistance. *J Biol Chem* 2011; **286**: 17467-17477 [PMID: 21454566 DOI:

10.1074/jbc.M110.215434]
24 **Nomura DK**, Morrison BE, Blankman JL, Long JZ, Kinsey SG, Marcondes MC, Ward AM, Hahn YK, Lichtman AH, Conti B, Cravatt BF. Endocannabinoid hydrolysis generates brain prostaglandins that promote neuroinflammation. *Science* 2011; **334**: 809-813 [PMID: 22021672 DOI: 10.1126/science.1209200]
25 **Hillard CJ**, Liu QS. Endocannabinoid signaling in the etiology and treatment of major depressive illness. *Curr Pharm Des* 2014; **20**: 3795-3811 [PMID: 24180398 DOI: 10.2174/13816128113196660735]
26 **Yoshida K**, Kita Y, Tokuoka SM, Hamano F, Yamazaki M, Sakimura K, Kano M, Shimizu T. Monoacylglycerol lipase deficiency affects diet-induced obesity, fat absorption, and feeding behavior in CB_1 cannabinoid receptor-deficient mice. *FASEB J* 2019; **33**: 2484-2497 [PMID: 30265576 DOI: 10.1096/fj.201801203R]
27 **Sticht MA**, Lau DJ, Keenan CM, Cavin JB, Morena M, Vemuri VK, Makriyannis A, Cravatt BF, Sharkey KA, Hill MN. Endocannabinoid regulation of homeostatic feeding and stress-induced alterations in food intake in male rats. *Br J Pharmacol* 2019; **176**: 1524-1540 [PMID: 30051485 DOI: 10.1111/bph.14453]
28 **Schloss MJ**, Horckmans M, Guillamat-Prats R, Hering D, Lauer E, Lenglet S, Weber C, Thomas A, Steffens S. 2-Arachidonoylglycerol mobilizes myeloid cells and worsens heart function after acute myocardial infarction. *Cardiovasc Res* 2019; **115**: 602-613 [PMID: 30295758 DOI: 10.1093/cvr/cvy242]
29 **Ghosh S**, O'Connell JF, Carlson OD, González-Mariscal I, Kim Y, Moaddel R, Ghosh P, Egan JM. Linoleic acid in diets of mice increases total endocannabinoid levels in bowel and liver: modification by dietary glucose. *Obes Sci Pract* 2019; **5**: 383-394 [PMID: 31452923 DOI: 10.1002/osp4.344]
30 **Attané C**, Estève D, Chaoui K, Iacovoni JS, Corre J, Moutahir M, Valet P, Schiltz O, Reina N, Muller C. Human Bone Marrow Is Comprised of Adipocytes with Specific Lipid Metabolism. *Cell Rep* 2020; **30**: 949-958.e6 [PMID: 31995765 DOI: 10.1016/j.celrep.2019.12.089]
31 **Douglass JD**, Zhou YX, Wu A, Zadroga JA, Gajda AM, Lackey AI, Lang W, Chevalier KM, Sutton SW, Zhang SP, Flores CM, Connelly MA, Storch J. Erratum: Global deletion of MGL in mice delays lipid absorption and alters energy homeostasis and diet-induced obesity. *J Lipid Res* 2019; **60**: 717 [PMID: 30824679 DOI: 10.1194/jlr.M058586ERR]
32 **Tardelli M**, Bruschi FV, Claudel T, Fuchs CD, Auer N, Kunczer V, Stojakovic T, Scharnagl H, Habib A, Grabner GF, Zimmermann R, Lotersztajn S, Trauner M. Lack of monoacylglycerol lipase prevents hepatic steatosis by favoring lipid storage in adipose tissue and intestinal malabsorption. *J Lipid Res* 2019; **60**: 1284-1292 [PMID: 31048404 DOI: 10.1194/jlr.M093369]
33 **Nomura DK**, Long JZ, Niessen S, Hoover HS, Ng SW, Cravatt BF. Monoacylglycerol lipase regulates a fatty acid network that promotes cancer pathogenesis. *Cell* 2010; **140**: 49-61 [PMID: 20079333 DOI: 10.1016/j.cell.2009.11.027]
34 **Li CF**, Chuang IC, Liu TT, Chen KC, Chen YY, Fang FM, Li SH, Chen TJ, Yu SC, Lan J, Huang HY. Transcriptomic reappraisal identifies MGLL overexpression as an unfavorable prognosticator in primary gastrointestinal stromal tumors. *Oncotarget* 2016; **7**: 49986-49997 [PMID: 27366945 DOI: 10.18632/oncotarget.10304]
35 **Ye L**, Zhang B, Seviour EG, Tao KX, Liu XH, Ling Y, Chen JY, Wang GB. Monoacylglycerol lipase (MAGL) knockdown inhibits tumor cells growth in colorectal cancer. *Cancer Lett* 2011; **307**: 6-17 [PMID: 21543155 DOI: 10.1016/j.canlet.2011.03.007]
36 **Costola-de-Souza C**, Ribeiro A, Ferraz-de-Paula V, Calefi AS, Aloia TP, Gimenes-Júnior JA, de Almeida VI, Pinheiro ML, Palermo-Neto J. Monoacylglycerol lipase (MAGL) inhibition attenuates acute lung injury in mice. *PLoS One* 2013; **8**: e77706 [PMID: 24204926 DOI: 10.1371/journal.pone.0077706]
37 **Xiong Y**, Yao H, Cheng Y, Gong D, Liao X, Wang R. Effects of monoacylglycerol lipase inhibitor URB602 on lung ischemia-reperfusion injury in mice. *Biochem Biophys Res Commun* 2018; **506**: 578-584 [PMID: 30366666 DOI: 10.1016/j.bbrc.2018.10.098]
38 **Balaban S**, Nassar ZD, Zhang AY, Hosseini-Beheshti E, Centenera MM, Schreuder M, Lin HM, Aishah A, Varney B, Liu-Fu F, Lee LS, Nagarajan SR, Shearer RF, Hardie RA, Raftopulos NL, Kakani MS, Saunders DN, Holst J, Horvath LG, Butler LM, Hoy AJ. Extracellular Fatty Acids Are the Major Contributor to Lipid Synthesis in Prostate Cancer. *Mol Cancer Res* 2019; **17**: 949-962 [PMID: 30647103 DOI: 10.1158/1541-7786.MCR-18-0347]
39 **Nomura DK**, Lombardi DP, Chang JW, Niessen S, Ward AM, Long JZ, Hoover HH, Cravatt BF. Monoacylglycerol lipase exerts dual control over endocannabinoid and fatty acid pathways to support prostate cancer. *Chem Biol* 2011; **18**: 846-856 [PMID: 21802006 DOI: 10.1016/j.chembiol.2011.05.009]
40 **Xiang W**, Shi R, Kang X, Zhang X, Chen P, Zhang L, Hou A, Wang R, Zhao Y, Zhao K, Liu Y, Ma Y, Luo H, Shang S, Zhang J, He F, Yu S, Gan L, Shi C, Li Y, Yang W, Liang H, Miao H. Monoacylglycerol lipase regulates cannabinoid receptor 2-dependent macrophage activation and cancer progression. *Nat Commun* 2018; **9**: 2574 [PMID: 29968710 DOI: 10.1038/s41467-018-04999-8]
41 **Cao Z**, Mulvihill MM, Mukhopadhyay P, Xu H, Erdélyi K, Hao E, Holovac E, Haskó G, Cravatt BF, Nomura DK, Pacher P. Monoacylglycerol lipase controls endocannabinoid and eicosanoid signaling and hepatic injury in mice. *Gastroenterology* 2013; **144**: 808-817.e15 [PMID: 23295443 DOI: 10.1053/j.gastro.2012.12.028]
42 **Yang Q**, Sun S, Liu W, Liu Q, Wang J. Hypoxia training improves hepatic steatosis partly by downregulation of CB1 receptor in obese mice. *Biochem Biophys Res Commun* 2020; **525**: 639-645 [PMID: 32122652 DOI: 10.1016/j.bbrc.2020.02.134]
43 **Habib A**, Chokr D, Wan J, Hegde P, Mabire M, Siebert M, Ribeiro-Parenti L, Le Gall M, Lettéron P, Pilard N, Mansouri A, Brouillet A, Tardelli M, Weiss E, Le Faouder P, Guillou H, Cravatt BF, Moreau R, Trauner M, Lotersztajn S. Inhibition of monoacylglycerol lipase, an anti-inflammatory and antifibrogenic strategy in the liver. *Gut* 2019; **68**: 522-532 [PMID: 30301768 DOI: 10.1136/gutjnl-2018-316137]
44 **Zhu W**, Zhao Y, Zhou J, Wang X, Pan Q, Zhang N, Wang L, Wang M, Zhan D, Liu Z, He X, Ma D, Liu S, Wang L. Monoacylglycerol lipase promotes progression of hepatocellular carcinoma via NF-κB-mediated epithelial-mesenchymal transition. *J Hematol Oncol* 2016; **9**: 127 [PMID: 27884159 DOI: 10.1186/s13045-016-0361-3]

45 **Tardelli M**, Bruschi FV, Fuchs CD, Claudel T, Auer N, Kunczer V, Baumgartner M, A H O Ronda O, Verkade HJ, Stojakovic T, Scharnagl H, Habib A, Zimmermann R, Lotersztajn S, Trauner M. Monoacylglycerol Lipase Inhibition Protects From Liver Injury in Mouse Models of Sclerosing Cholangitis. *Hepatology* 2020; **71**: 1750-1765 [PMID: 31505038 DOI: 10.1002/hep.30929]

46 **Popov Y**, Patsenker E, Fickert P, Trauner M, Schuppan D. Mdr2 (Abcb4)-/- mice spontaneously develop severe biliary fibrosis via massive dysregulation of pro- and antifibrogenic genes. *J Hepatol* 2005; **43**: 1045-1054 [PMID: 16223543 DOI: 10.1016/j.jhep.2005.06.025]

47 **Long JZ**, Li W, Booker L, Burston JJ, Kinsey SG, Schlosburg JE, Pavón FJ, Serrano AM, Selley DE, Parsons LH, Lichtman AH, Cravatt BF. Selective blockade of 2-arachidonoylglycerol hydrolysis produces cannabinoid behavioral effects. *Nat Chem Biol* 2009; **5**: 37-44 [PMID: 19029917 DOI: 10.1038/nchembio.129]

48 **Long JZ**, Nomura DK, Cravatt BF. Characterization of monoacylglycerol lipase inhibition reveals differences in central and peripheral endocannabinoid metabolism. *Chem Biol* 2009; **16**: 744-753 [PMID: 19635411 DOI: 10.1016/j.chembiol.2009.05.009]

49 **Niphakis MJ**, Cognetta AB 3rd, Chang JW, Buczynski MW, Parsons LH, Byrne F, Burston JJ, Chapman V, Cravatt BF. Evaluation of NHS carbamates as a potent and selective class of endocannabinoid hydrolase inhibitors. *ACS Chem Neurosci* 2013; **4**: 1322-1332 [PMID: 23731016 DOI: 10.1021/cn400116z]

50 **Wyatt RM**, Fraser I, Welty N, Lord B, Wennerholm M, Sutton S, Ameriks MK, Dugovic C, Yun S, White A, Nguyen L, Koudriakova T, Tian G, Suarez J, Szewczuk L, Bonnette W, Ahn K, Ghosh B, Flores CM, Connolly PJ, Zhu B, Macielag MJ, Brandt MR, Chevalier K, Zhang SP, Lovenberg T, Bonaventure P. Pharmacologic Characterization of JNJ-42226314, [1-(4-Fluorophenyl)indol-5-yl]-[3-[4-(thiazole-2-carbonyl)piperazin-1-yl]azetidin-1-yl]methanone, a Reversible, Selective, and Potent Monoacylglycerol Lipase Inhibitor. *J Pharmacol Exp Ther* 2020; **372**: 339-353 [PMID: 31818916 DOI: 10.1124/jpet.119.262139]

51 **Zhang L**, Butler CR, Maresca KP, Takano A, Nag S, Jia Z, Arakawa R, Piro JR, Samad T, Smith DL, Nason DM, O'Neil S, McAllister L, Schildknegt K, Trapa P, McCarthy TJ, Villalobos A, Halldin C. Identification and Development of an Irreversible Monoacylglycerol Lipase (MAGL) Positron Emission Tomography (PET) Radioligand with High Specificity. *J Med Chem* 2019; **62**: 8532-8543 [PMID: 31483137 DOI: 10.1021/acs.jmedchem.9b00847]

52 **Bruschi FV**, Tardelli M, Claudel T, Trauner M. PNPLA3 expression and its impact on the liver: current perspectives. *Hepat Med* 2017; **9**: 55-66 [PMID: 29158695 DOI: 10.2147/HMER.S125718]

53 **Ouellette C**, Rudkowska I, Lemieux S, Lamarche B, Couture P, Vohl MC. Gene-diet interactions with polymorphisms of the MGLL gene on plasma low-density lipoprotein cholesterol and size following an omega-3 polyunsaturated fatty acid supplementation: a clinical trial. *Lipids Health Dis* 2014; **13**: 86 [PMID: 24884512 DOI: 10.1186/1476-511X-13-86]

54 **Harismendy O**, Bansal V, Bhatia G, Nakano M, Scott M, Wang X, Dib C, Turlotte E, Sipe JC, Murray SS, Deleuze JF, Bafna V, Topol EJ, Frazer KA. Population sequencing of two endocannabinoid metabolic genes identifies rare and common regulatory variants associated with extreme obesity and metabolite level. *Genome Biol* 2010; **11**: R118 [PMID: 21118518 DOI: 10.1186/gb-2010-11-11-r118]

55 **Carey CE**, Agrawal A, Zhang B, Conley ED, Degenhardt L, Heath AC, Li D, Lynskey MT, Martin NG, Montgomery GW, Wang T, Bierut LJ, Hariri AR, Nelson EC, Bogdan R. Monoacylglycerol lipase (MGLL) polymorphism rs604300 interacts with childhood adversity to predict cannabis dependence symptoms and amygdala habituation: Evidence from an endocannabinoid system-level analysis. *J Abnorm Psychol* 2015; **124**: 860-877 [PMID: 26595473 DOI: 10.1037/abn0000079]

56 **Sipe JC**, Chiang K, Gerber AL, Beutler E, Cravatt BF. A missense mutation in human fatty acid amide hydrolase associated with problem drug use. *Proc Natl Acad Sci USA* 2002; **99**: 8394-8399 [PMID: 12060782 DOI: 10.1073/pnas.082235799]

57 **Iwasaki S**, Ishiguro H, Higuchi S, Onaivi ES, Arinami T. Association study between alcoholism and endocannabinoid metabolic enzyme genes encoding fatty acid amide hydrolase and monoglyceride lipase in a Japanese population. *Psychiatr Genet* 2007; **17**: 215-220 [PMID: 17621164 DOI: 10.1097/YPG.0b013e32809913d8]

World Journal of Gastroenterology

Submit a Manuscript: https://www.f6publishing.com

World J Gastroenterol 2020 July 7; 26(25): 3586-3602

DOI: 10.3748/wjg.v26.i25.3586

ISSN 1007-9327 (print) ISSN 2219-2840 (online)

ORIGINAL ARTICLE

Basic Study

TBL1XR1 induces cell proliferation and inhibit cell apoptosis by the PI3K/AKT pathway in pancreatic ductal adenocarcinoma

Jian-Feng Gu, Wei Fu, Hai-Xin Qian, Wen-Xiu Gu, Yang Zong, Qian Chen, Long Lu

ORCID number: Jian-Feng Gu 0000-0002-8514-813X; Wei Fu 0000-0002-0153-937X; Hai-Xin Qian 0000-0003-2412-0747; Wen-Xiu Gu 0000-0003-4586-2838; Yang Zong 0000-0003-2831-4717; Qian Chen 0000-0001-7899-5552; Long Lu 0000-0001-7314-2972.

Author contributions: Gu JF and Fu W contributed equally to this work. Gu JF was involved in study concept and design, and acquisition, analysis and interpretation of data, drafted manuscript, critically revised the manuscript for important intellectual content, and provided statistical analysis and administrative, technical, or material support; Fu W performed data acquisition and drafted manuscript; Qian HX participated in data analysis and interpretation; Gu WX was involved in the drafting of the manuscript; Zong Y was involved in critically revising the manuscript for important intellectual content; Chen Q and Lu L took part in the statistical analysis.

Institutional review board statement: The study was approved by the Ethics Committee of Changshu No.1 People's Hospital.

Institutional animal care and use

Jian-Feng Gu, Wen-Xiu Gu, Yang Zong, Qian Chen, Department of General Surgery, Changshu No. 1 People's Hospital Affiliated to Soochow University, Changshu 215500, Jiangsu Province, China

Wei Fu, Long Lu, Department of Oncology, Changshu No. 1 People's Hospital Affiliated to Soochow University, Changshu 215500, Jiangsu Province, China

Hai-Xin Qian, Department of General Surgery, the First Affiliated Hospital of Soochow University, Suzhou 215006, Jiangsu Province, China

Corresponding author: Jian-Feng Gu, MD, Doctor, Department of General Surgery, Changshu No. 1 People's Hospital Affiliated to Soochow University, No.91, Yongjia Road, Changshu 215500, Jiangsu Province, China. jscsgjf@sina.cn

Abstract

BACKGROUND

Pancreatic ductal adenocarcinoma (PDAC) is one of the deadliest solid tumors. Identification of diagnostic and therapeutic biomarkers for PDAC is urgently needed. Transducin (β)-like 1 X-linked receptor 1 (TBL1XR1) has been linked to the progression of various human cancers. Nevertheless, the function and role of TBL1XR1 in pancreatic cancers are unclear.

AIM

To elucidate the function and potential mechanism of TBL1XR1 in the development of PDAC.

METHODS

Ninety patients with histologically-confirmed PDAC were included in this study. PDAC tumor samples and cell lines were used to determine the expression of TBL1XR1. CCK-8 assays and colony formation assays were carried out to assess PDAC cell viability. Flow cytometry was performed to measure the changes in the cell cycle and cell apoptosis. Changes in related protein expression were measured by western blot analysis. Animal analysis was conducted to confirm the impact of TBL1XR1 *in vivo*.

RESULTS

Patients with TBL1XR1-positive tumors had worse overall survival than those

committee statement: The animal care and use was approved by the Ethics Committee of Changshu No.1 People's Hospital.

Conflict-of-interest statement: The authors declare no conflict of interest. The authors declare that they have nothing to disclose.

Data sharing statement: No additional data are available.

ARRIVE guidelines statement: The authors have read the ARRIVE guidelines, and the manuscript was prepared and revised according to the ARRIVE guidelines.

Manuscript source: Unsolicited manuscript

Received: February 3, 2020
Peer-review started: February 3, 2020
First decision: March 24, 2020
Revised: March 26, 2020
Accepted: May 26, 2020
Article in press: May 26, 2020
Published online: July 7, 2020

P-Reviewer: Chisthi MM, Fujino Y, Gassler N, Slomiany BL, Tomizawa M
S-Editor: Yang Y
L-Editor: MedE-Ma JY
E-Editor: Ma YJ

with TBL1XR1-negative tumors. Moreover, we found that TBL1XR1 strongly promoted PDAC cell proliferation and inhibited PDAC cell apoptosis. Moreover, knockdown of TBL1XR1 induced G0/G1 phase arrest. *In vivo* animal studies confirmed that TBL1XR1 accelerated tumor cell growth. The results of western blot analysis showed that TBL1XR1 might play a key role in regulating PDAC cell proliferation and apoptosis *via* the PI3K/AKT pathway.

CONCLUSION
TBL1XR1 promoted PDAC cell progression and might be an effective diagnostic and therapeutic marker for pancreatic cancer.

Key words: Pancreatic ductal adenocarcinoma; TBL1XR1; Proliferation; PI3K/AKT pathway

Core tip: Transducin (β)-like 1 X-linked receptor 1 (TBL1XR1) has been linked to the progression of various human cancers. However, the function and role of TBL1XR1 in pancreatic cancers are unclear. Elucidation of the effect and potential molecular mechanism of TBL1XR1 in pancreatic cancer is important. This study showed that TBL1XR1 promoted pancreatic ductal adenocarcinoma (PDAC) cell proliferation, inhibited PDAC cell apoptosis and might regulate PDAC cell proliferation and apoptosis by the phosphatidylinositol 3-kinase/protein kinase B pathway. Therefore, TBL1XR1 might be a promising therapeutic marker for patients with advanced PDAC.

Citation: Gu JF, Fu W, Qian HX, Gu WX, Zong Y, Chen Q, Lu L. TBL1XR1 induces cell proliferation and inhibit cell apoptosis by the PI3K/AKT pathway in pancreatic ductal adenocarcinoma. *World J Gastroenterol* 2020; 26(25): 3586-3602
URL: https://www.wjgnet.com/1007-9327/full/v26/i25/3586.htm
DOI: https://dx.doi.org/10.3748/wjg.v26.i25.3586

INTRODUCTION

Pancreatic carcinoma is one of the deadliest solid tumors. Currently, pancreatic carcinoma is the fourth leading cause of cancer-related death in the United States, and there were approximately 48960 new cases confirmed and 40560 deaths in 2015[1,2]. The best chance for survival is early surgical detection. However, due to the lack of effective screening tests for pancreatic carcinoma, local invasion and early metastasis, only 10%–20% of patients are diagnosed at a stage amenable to resection and curative treatment[3,4]. Therefore, the overall 5-year survival rate is lower than 5%[5]. Despite decades of efforts, there has been no significant improvement in the long-term survival of pancreatic carcinoma patients[6]. Pancreatic ductal adenocarcinoma (PDAC) is the most common type of pancreatic carcinoma. Therefore, identification of efficacious early tumor markers for the early diagnosis and treatment of PDAC has clinical value and significance[7].

As a member of the TBL1 family, transducin (β)-like 1 X-linked receptor 1 (TBL1XR1) is the key element of the SMRT/N-CoR corepressor complex[8]. TBL1XR1 is located on chromosome 3 at 3q26 and has a high degree of homology to the TBL1 protein. Recently, studies have demonstrated that TBL1XR1 could react to transcriptional regulators such as nuclear receptors by switching from gene inhibition to gene activation[9]. Moreover, TBL1XR1 plays a vital role in cell growth, cell apoptosis, inflammation and transcriptional activation, which involve estrogen receptor, androgen receptor, thyroid hormone receptor β, peroxisome proliferator-activated receptor γ, nuclear factor kappa-light-chain-enhancer of activated B cells (NF-κb), Notch and β-catenin[10]. Currently, studies focus on the effect and mechanism of TBL1XR1 in carcinogenesis and tumor progression, including those of nasopharyngeal carcinoma, colon cancer, osteosarcoma cancer, prostate cancer, breast cancer, and hepatocellular carcinoma[11-16]. Nevertheless, the role and molecular mechanism of TBL1XR1 in the progression of PDAC remain unclear.

In this study, we aimed to explore the effect of TBL1XR1 in PDAC. We found that

TBL1XR1 expression was closely associated with the clinicopathologic features of PDAC, which might provide a new diagnostic and therapeutic target for PDAC.

MATERIALS AND METHODS

Patients and tissue specimens

This study was performed in 90 PDAC patients. The patients all underwent radical pancreaticoduodenectomy and were histopathologically and clinically diagnosed at Changshu No. 1 People's Hospital Affiliated with Soochow University from 2011 to 2015. Our study complied with the ethical standards of the Declaration of Helsinki and was approved by the Ethics Committee of Changshu No. 1 People's Hospital. Ninety pairs of PDAC and normal pancreatic epithelial samples were promptly fixed in 4% formalin and embedded in paraffin for immunohistochemical (IHC) staining after removal.

Immunohistochemical analysis

After obtaining fresh isolated specimens, we immediately fixed the specimens in 4% formalin and then embedded them in paraffin. Next, we cut them into 5 mm sections and mounted them on slides. IHC and HE staining were performed to examine the expression of TBL1XR1[17].

Immunohistochemical staining score

Immunohistochemical staining of TBL1XR1 expression in PDAC and normal pancreatic epithelial specimens was performed as described by Li *et al*[17]. The TBL1XR1 staining score was the summation of the staining strength and the ratio of positively stained cells. We defined TBL1XR1 staining strength as follows: 0% immunoreactive cells are scored 0; less than 5% immunoreactive cells are scored 1; 5%–50% immunoreactive cells are scored 2; and more than 50% immunoreactive cells are scored 3. Staining intensity was scored as follows: negative was scored 0; weak was scored 1; intermediate was scored 2; and strong was scored 3. For statistical convenience, we set intermediate and strong scores to be positive, and the negative and weak scores were considered to be negative[18].

Cell lines and cell cultures

The PDAC cell lines (Panc1, MiaPaCa-2, Capan1 and Aspc-1) were purchased from the Cell Bank of the Chinese Academy of Science. Panc1 and Capan1 cells were cultured in DMEM, and MiaPaCa-2 and Aspc-1 cells were cultured in RPMI-1640 medium. Streptomycin (100 μg/mL) and penicillin (100 U/ml) and 10% fetal bovine serum were added to DMEM or RPMI-1640 medium. The cells were cultivated at 37 °C in a humidified incubator with 5% CO_2.

Cell transfection

Five hundred thousand cells were inoculated into 6-well plates, and after the cells attached, we performed a cell transfection assay according to the manufacturer's instructions. In short, 50 nmol siRNA and 6 μL of Lipofectamine 2000 were added to 200 μl of Opti-MEM medium and incubated for 5 min. Then, the two suspensions were mixed and incubated for 15 min. The suspension was added to 6-well plates and incubated for 4 h. After incubation, we replaced the medium and harvested fresh culture medium every 2 d. The siRNA sequences were as follows: CTRL siRNA: 5′-TTCTCCGAACGTGTCACGT-3′;TBL1XR1: 5′-GGAGUAGACAAGACUACAA-3′.

Quantitative real-time PCR

We performed the assay using the methods described by Li *et al*[17]. Total RNA was extracted from different treated cells with TRIzol reagent (Invitrogen) in accordance with the manufacturer's instructions. The expression of TBL1XR1 and GAPDH was determined by the primers shown below: TBL1XR1: 5′-GAG GTG TTT ATT TGT GCT TGG-3′; 5′-TGC ACT TAA TAT GAA GTT GCC-3′. GAPDH: 5′-GCCGCATCTTCTTTTGCGTCGC-3′; 5′-TCCCGTTCTCAGCCTTGACGGT-3′.

The expression of TBL1XR1 was determined by normalization to the expression of the housekeeping gene GAPDH.

Lentivirus-mediated RNA interference

The lentivirus vector was constructed by the Shanghai GeneChem Company.

Lentivirus-mediated RNA interference was performed in accordance with the manufacturer's instructions. After cell adherence, a considerable volume of virus was added to the cells for 6-8 h. Then, fresh complete medium was added, and the cells were harvested for 2 d. Cells were continuously cultured and used for subsequent studies.

Cell viability assay

A CCK-8 (Beyotime, Shanghai) assay was performed to determine the viability of PDCA cells. CCK-8 is widely used in the rapid and highly sensitive detection of cell proliferation and cytotoxicity based on WST-8. PDAC cells at 1000 cells/well were inoculated into 96-well plates after the corresponding treatment and incubated for the indicated times. Then, 10 μL of CCK-8 was added to the medium and cultured for 2 h in the dark. A microplate reader (Bio-Tek, United States) was used to measure the absorbance of PDCA cells at 450 nm.

Colony formation assay

PDAC cells with different treatments (approximately 500 cells/well) were seeded in 6-well plates. The culture medium was changed every 3 d. After approximately 2 wk of culture, the cells were cleaned with PBS and fixed with 10% formalin for 20 min at ordinary temperature. Then, 0.1% crystal violet (Sigma-Aldrich) was used to stain the cells for 20 min at room temperature. After staining, the plates were washed and dried. The colonies (with more than 50 cells) were observed under a microscope (Leica, Germany).

Western blot analysis

Proteins were extracted using RIPA buffer mixed with 1% protease inhibitor cocktail (Beyotime, Shanghai, China). Ten percent sodium dodecyl sulfate polyacrylamide gel electrophoresis (SDS-PAGE) was applied to separate the cell proteins, and polyvinylidene difluoride (PVDF) membranes were used for transfer. Five percent skim milk was used to block the membranes for 2 h. Then, the membranes were incubated with primary antibodies against TBL1XR1 (Abcam, ab228940), p-AKT (CST, 9271), p-PI3K (CST, 17366) and GAPDH (Abclonal, A19056) at 4 °C overnight. The second day, secondary antibodies were added and incubated with the PVDF membranes for 1 h at room temperature. A Gel Doc 2000 system (Bio-Rad, United States) was used to detect protein expression.

Cell cycle and apoptosis analyses

For cell cycle analysis, PDAC cells with different treatments were fixed with 75% ethanol at 4°C overnight. Then, the cells were centrifuged for precipitation and incubated with 5 μL of RNase and 5 μL of PI at room temperature. For cell apoptosis analysis, PDAC cells with different treatments were resuspended with 1 × Annexin V binding buffer and Annexin V and PI at 37 °C. After incubation for half an hour, the apoptotic cell and cell cycle ratios were detected with flow cytometric analysis.

Animal study

Four- to six-week-old nu/nu nude mice were purchased from the Shanghai Laboratory Animal Centre of the Chinese Academy of Sciences (Shanghai, China). The mice were randomly divided into the Lv-shCTRL group and the Lv-shTBL1XR1 group. One hundred thousand Panc1 cells were resuspended in 0.1 mL of serum-free medium and hypodermically inoculated into the right axilla of the mice. After approximately 4 wk, the mice were sacrificed, and the subcutaneous tumors were measured and weighed. The volume of the tumors was calculated by the following formula: Volume = length (mm) × width^2 (mm^2)/2.

Statistical analysis

All experiments were repeated at least 3 times, and the results are expressed as the mean ± standard deviation unless otherwise stated. Student's *t* test was used to compare differences between the treated groups and the corresponding control groups; $P < 0.05$ was considered statistically significant.

RESULTS

Clinicopathological significance of TBL1XR1 expression in patients with PDAC

The clinicopathological features of the 90 PDAC patients are shown in Table 1. As illustrated in Table 1, the overexpression of TBL1XR1 was associated with TNM stage ($P = 0.006$) but not with patient age ($P = 0.652$), gender ($P = 1.000$), histopathological subtype ($P = 0.929$), tumor size ($P = 0.465$), tumor location ($P = 0.065$) or lymph node metastasis ($P = 0.050$). To additionally confirm the importance of TBL1XR1 in PDAC, we analyzed the overall survival (OS) of 90 patients by the Kaplan-Meier method (Table 2).Table 2 and Figure 1A show that patients with TBL1XR1-negative expression displayed a longer OS than those with TBL1XR1-positive expression ($P < 0.001$). Moreover, TNM stage ($P < 0.001$) and lymph node metastasis ($P = 0.047$) were obviously related to the average survival time. Furthermore, the Cox proportional hazards model was used in multivariate analysis. As shown in Table 3, TBL1XR1 expression, TNM stage and lymph node metastasis were found to be significant independent prognostic factors for patients with PDAC, suggesting that TBL1XR1 expression is a risk factor for PDAC.

Enhanced expression of TBL1XR1 in PDAC tissues and cell lines

To investigate the possible role of TBL1XR1 in PDAC, we used IHC staining to investigate the relationship between TBL1XR1 expression and the clinicopathological features of the patients with PDAC (Figure 1B). IHC staining revealed that TBL1XR1 was mainly localized in the PDAC cell nucleus. The positive rate of TBL1XR1 staining in the tumor cells was approximately 70% (63/90) of the PDAC patients. Only 30% (27/90) of the patients possessed positive staining in the corresponding control tissues (Figure 1C, $P < 0.001$).

To determine the expression of TBL1XR1 in the PDAC tumor tissues and the adjacent normal tissues, we performed quantitative RT-PCR (qRT-PCR) and western blot assays. As illustrated in Figure 2A and B, enhanced expression of TBL1XR1 was observed in the PDAC tissues compared with the adjacent tissues. Then, we used MiaPaCa-2, Panc1, Aspc-1, and Capan1 cell lines to evaluate the role of TBL1XR1 in PDAC cell lines. TBL1XR1 expression at the mRNA and protein levels was examined *via* qRT-PCR and western blotting . We observed that TBL1XR1 was overexpressed in the PDAC cell lines, particularly in the Aspc-1 and Panc1 lines, at the mRNA (Figure 2C) and protein (Figure 2D) levels. Taken together, these data suggest that TBL1XR1 is upregulated in PDAC.

Effects of TBL1XR1 on the proliferation and apoptosis of PDAC cells

We performed CCK-8 and colony formation assays to further evaluate the effect of TBL1XR1 on the proliferation of PDAC cells. We knocked down the expression of TBL1XR1 in the Aspc-1 and Panc1 cells, and the knockdown efficiency is shown in Figure 3A and B. The CCK-8 assay showed that the downregulation of TBL1XR1 prominently suppressed PDAC cell viability compared with that of the control cells ($P < 0.05$, Figure 3C and D). Moreover, colony formation analysis showed that the colony formation capacity was significantly reduced in the TBL1XR1-knockdown cells compared to that of the control group ($P < 0.05$, Figure 3E). These results suggested that TBL1XR1 may play a vital role in PDAC cell proliferation *in vitro*. Furthermore, we investigated whether TBL1XR1 played a role in the proliferation of PDAC cells *in vivo* using xenograft mouse models. As shown, the tumor volume and weight of the TBL1XR1-knockdown group were distinctly decreased compared to those of the control group (Figure 3F and G).

To explore the probable molecular mechanism of TBL1XR1 in PDAC cells, we detected the cell cycle and apoptotic profile of the Lv-shCTRL and Lv-shTBL1XR1 groups. As shown in Figure 4A, cell cycle analysis demonstrated that the cells treated with Lv-shTBL1XR1 exhibited cell arrest at the G0/G1 phase (Figure 4A). Moreover, we examined the protein expression of cell cycle-related regulatory genes to determine the impact of TBL1XR1 on the cell cycle by western blot assays. As depicted in Figure 4B, the protein expression levels of CDK2, CDC25A, or cyclin D1 in the Lv-shTBL1XR1 group were obviously lower than those in the control group. Therefore, we concluded that downregulation of TBL1XR1 induced PDAC cell cycle arrest at the G0/G1 phase by regulating the expression of cell cycle-related regulatory genes.

Furthermore, we performed an apoptosis assay to explore the effect of TBL1XR1 on apoptosis in PDAC cells. As shown in Figure 4C, an obvious increase in the percentage of apoptotic cells was observed in the TBL1XR1 knockdown group compared with the Lv-shCTRL group. Moreover, the knockdown of TBL1XR1 significantly enhanced the

Table 1 Association between transducin (β)-like 1 X-linked receptor 1 expression and the clinicopathological parameters of pancreatic ductal adenocarcinoma cells

Parameter	Category	Case number	TBL1XR1 expression		
			Number of positive cases, *n* (%)	χ^2	*P* value
Age (yrs)	< 60	40	27 (67.5)	0.214	0.652
	≥ 60	50	36 (72.0)		
Sex	Male	59	41 (69.5)	0.021	1.000
	Female	31	22 (71.0)		
Histopathological subtypes	High	3	2 (66.7)	0.146	0.929
	Middle	51	35 (68.6)		
	Low	36	26 (72.2)		
TNM stage	1-II	12	4 (33.3)	8.864	0.006[b]
	III-IV	78	59 (75.6)		
Tumor size	< 3 cm	60	42 (66.7)	0.952	0.465
	≥ 3 cm	30	23 (76.7)		
Tumor location	Head	37	30 (81.1)	3.674	0.065
	Body/tail	53	33 (62.3)		
Lymph node metastasis	Negative	61	44 (72.1)	0.409	0.624
	Positive	29	19 (65.5)		

[b]*P* < 0.01. TBL1XR1: Transducin (β)-like 1 X-linked receptor 1; PDAC: Pancreatic ductal adenocarcinoma; TNM: Tumor-node-metastasis.

expression of Bax and Bad and reduced the expression of Bcl-2 (Figure 4D). Taken together, these results suggest that TBL1XR1 might regulate PDAC cell apoptosis and cell cycle progression.

TBL1XR1 regulated the proliferation and apoptosis of PDAC cells via the PI3K/AKT pathway

To explore the potential mechanism by which TBL1XR1 influences proliferation and apoptosis in PDAC cells, we examined the expression changes of relevant proteins by western blotting. As shown in Figure 5A, the expression levels of p-AKT and p-PI3K were obviously reduced, while no significant effect on p-STAT3 and p-MEK was observed in the TBL1XR1 downregulation group, which indicated that TBL1XR1 might regulate PDAC cell proliferation and apoptosis *via* the phosphatidylinositol 3-kinase/protein kinase B (PI3K/AKT) pathway. To determine whether TBL1XR1 knockdown-induced inhibition of proliferation was regulated by the PI3K/AKT pathway, we assessed the effect of the presence or absence of LY294002 (a PI3K/Akt inhibitor) on the TBL1XR1-overexpressing cells. Unsurprisingly, overexpression of TBL1XR1 promoted proliferation and suppressed apoptosis in PDAC cells, which was consistent with previous results. LY294002 treatment reversed the TBL1XR1-mediated promotion of proliferation and inhibition of apoptosis (Figure 5B-D). Moreover, LY294002 inhibited the TBL1XR1 overexpression-induced increases in Bcl-2 and decreases in Bad and Bax (Figure 5E). Therefore, we deduced that TBL1XR1 induces PDAC cell proliferation, cell cycle arrest and apoptosis *via* the PI3K/AKT signaling pathway.

DISCUSSION

Although many studies have attempted to elucidate its pathogenesis, PDAC remains a deadly malignancy[19]. Hence, identification of efficacious early tumor markers for the early diagnosis and treatment of PDAC will have clinical value and significance.

TBL1XR1 (TBLR1) was first identified as a gene transcript in human CD34+CD38- cells; moreover, researchers discovered that TBL1XR1 has an F-box/WD40-repeat

Table 2 Univariate log-rank analysis of overall survival

Parameter	Category	Case number	Median survival time (mo) (95%CI)	*P* value
Age (yrs)	< 60	40	10.0 (4.8-15.2)	0.413
	≥ 60	50	9.7 (7.41–12.0)	
Sex	Male	59	9.9 (6.7-13.1)	0.983
	Female	31	9.9 (8.1-12.0)	
Histopathological subtypes	High	3	25.0 (-)	0.760
	Middle	51	10.3 (8.1–11.7)	
	Low	36	8.7 (6.0-11.4)	
TNM stage	1-II	12	25.0 (18.1-31.9)	< 0.001[c]
	III-IV	78	8.0 (5.5-10.5)	
Tumor size	< 3 cm	60	9.8 (8.6-11.0)	0.251
	≥ 3 cm	30	8.3 (4.8-11.8)	
Tumor location	Head	37	9.3 (7.0-11.7)	0.095
	Body/tail	53	11.0 (6.0-16.0)	
Lymph node metastasis	Negative	61	12.0 (7.9-16.1)	0.047[a]
	Positive	29	7.6 (5.3-9.8)	
TBL1XR1 expression	Low	27	18.9 (10.9-26.9)	< 0.001[c]
	High	63	7.0 (5.7-8.3)	

[a]$P < 0.05$,

[c]$P < 0.001$. TBL1XR1: Transducin (β)-like 1 X-linked receptor 1; CI: Confidence interval; TNM: Tumor-node-metastasis.

sequence[20]. A growing body of research has revealed that TBL1XR1 can play a vital role in tumorigenesis, invasion, metastasis, and the development of resistance to therapies[15,21]. Moreover, TBL1XR1 mRNA is highly expressed in many human tissues, such as thyroid, prostate and breast tissues[22], which indicates that TBL1XR1 may function as an oncogene. TBL1XR1 functions by activating many signal transduction pathways, such as Wnt-β-catenin, NF-κB, and Notch23. Nevertheless, it remains unclear how TBL1XR1 functions in the development of PDAC.

In this research, we discovered that the expression of TBL1XR1 was obviously enhanced in PDAC tissues compared with adjacent tissues. Moreover, we revealed that TBL1XR1 expression, TNM stage and lymph node metastasis were significant independent prognostic factors for patients with PDAC, suggesting that TBL1XR1 expression is a risk factor for PDAC. To further evaluate the function of TBL1XR1 in PDAC, we performed CCK-8 and colony formation assays, and the results showed that the downregulation of TBL1XR1 significantly suppressed PDAC cell proliferation. Moreover, we found that TBL1XR1 knockdown induced PDAC cell cycle arrest in G0/G1 phase and inhibited PDAC cell apoptosis *in vitro*. Additionally, the results of the *in vivo* animal analysis were consistent with the *in vitro* analysis, which indicated that TBL1XR1 might be a potential diagnostic target for PDAC.

The PI3K/AKT signaling pathway has a key impact on multiple cell processes, including cell growth, cell proliferation, angiopoiesis and survival, in both normal and tumor cells[23]. In our study, we found that TBL1XR1 can induce PDAC cell proliferation and inhibit PDAC cell apoptosis. However, whether the PI3K/AKT signaling pathway is involved in the TBL1XR1-induced promotion of PDAC cell proliferation and inhibition of apoptosis is unknown. Thus, we explored the potential mechanism by which TBL1XR1 influences proliferation and apoptosis in PDAC cells, and we found that inhibition of the PI3K/AKT pathway reversed the TBL1XR1 promotion of proliferation and inhibition of apoptosis, indicating that TBL1XR1 might play an important role in regulating PDAC cell proliferation and apoptosis. In addition, the activity of Akt could be regulated through S-nitrosylation at the kinase cysteine residues, and it was reported to be associated with reduced kinase

Table 3 Multivariate analysis of overall survival

Parameter	Category	Hazard ratio	95%CI	*P* value
Age (yrs)	< 60	0.139	0.907 (0.544–1.514)	0.709
	≥ 60			
Sex	Male	0.013	1.031 (0.613–1.734)	0.908
	Female			
Histopathological subtypes	High	0.536	1.184 (0.754–1.859)	0.464
	Middle			
	Low			
TNM stage	1-II	5.692	3.046 (1.220–7.604)	0.017[a]
	III-IV			
Tumor size	< 3 cm	1.297	1.378 (0.794–2.394)	0.255
	≥ 3 cm			
Tumor location	Head	3.450	1.487 (0.978–2.261)	0.063
	Body/tail			
Lymph node metastasis	Negative	7.855	2.231 (1.273–3.909)	0.005[b]
	Positive			
TBL1XR1 expression	Low	13.951	3.507 (1.815–6.774)	< 0.001[c]
	High			

[a]$P < 0.05$.

[b]$P < 0.01$.

[c]$P < 0.001$.TBL1XR1: Transducin (β)-like 1 X-linked receptor 1; CI: Confidence interval; TNM: Tumor-node-metastasis.

activity[24,25], which provides us with another research direction. Overall, we illuminated the effect and mechanism of TBL1XR1 in human PDAC, and we believe that TBL1XR1 could be a promising diagnostic and therapeutic target for treating patients with advanced PDAC. Targeted therapy is an important aspect of precision therapy. We concluded that TBL1XR1 inhibitors might be promising therapeutic measures for PDAC; however, there are no inhibitors targeting TBL1XR1, which is worth investigating in the future.

In summary, our study showed that TBL1XR1 might regulate PDAC cell proliferation and apoptosis *via* the PI3K/AKT signaling pathway. Therefore, TBL1XR1 may be a promising diagnostic and therapeutic biomarker for patients with advanced PDAC.

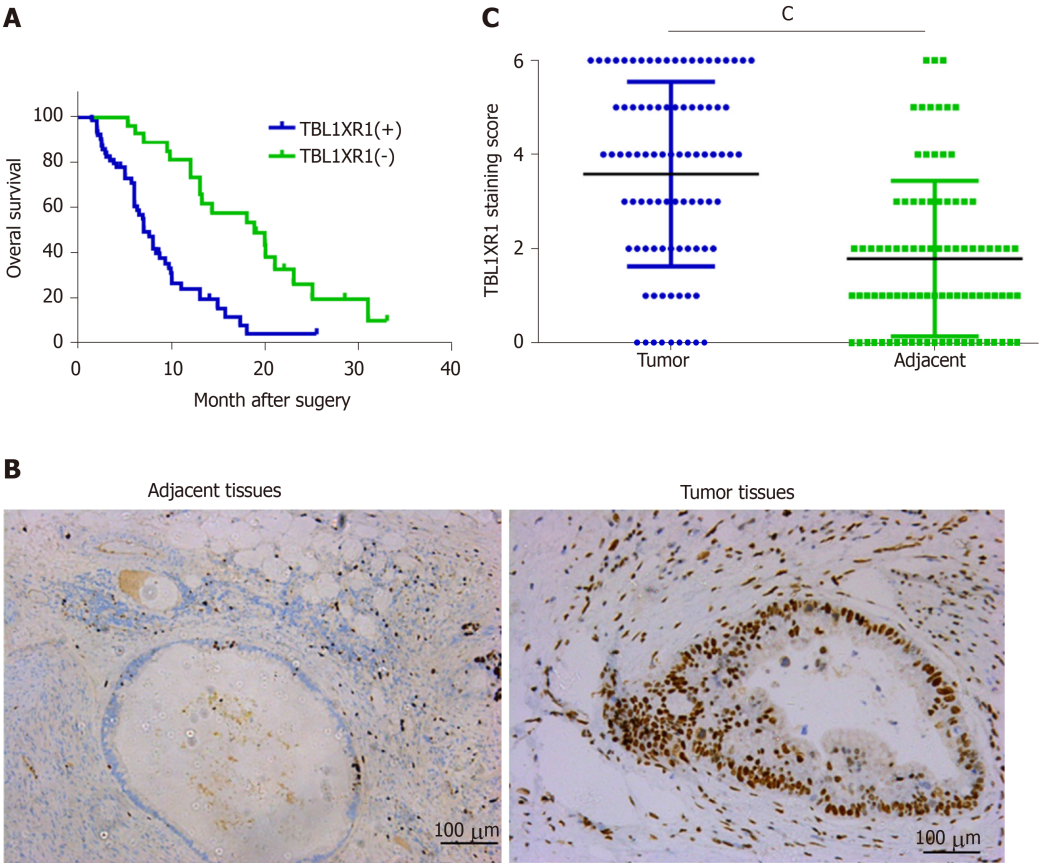

Figure 1 Clinicopathological significance of transducin (β)-like 1 X-linked receptor 1 expression in patients with pancreatic ductal adenocarcinoma. A: Kaplan–Meier plots of overall survival of pancreatic ductal adenocarcinoma (PDAC) patients with positive and negative transducin (β)-like 1 X-linked receptor 1 (TBL1XR1) expression scores; B: Negative and positive staining of TBL1XR1 in PDAC; C: The average staining scores of TBL1XR1 expression in PDAC tissues and adjacent tissues. °P < 0.001. Scale bar, 100 μm. TBL1XR1: Transducin (β)-like 1 X-linked receptor 1.

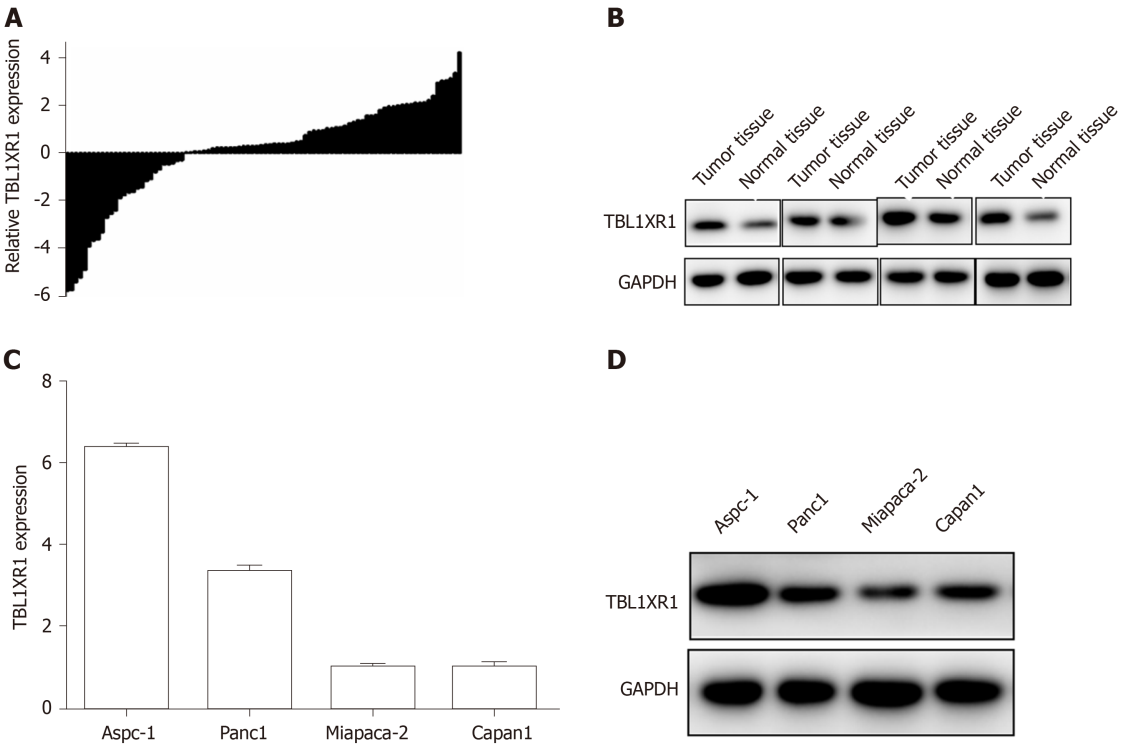

Figure 2 Enhanced expression of transducin (β)-like 1 X-linked receptor 1 in pancreatic ductal adenocarcinoma tissues and cell lines. A and B: The mRNA and protein expression of transducin (β)-like 1 X-linked receptor 1 (TBL1XR1) in pancreatic ductal adenocarcinoma tissues and adjacent nontumor tissues; C and D: The mRNA and protein expression of TBL1XR1 in pancreatic ductal adenocarcinoma cells. GAPDH: Glyceraldehyde-3-phosphate dehydrogenase; TBL1XR1: Transducin (β)-like 1 X-linked receptor 1.

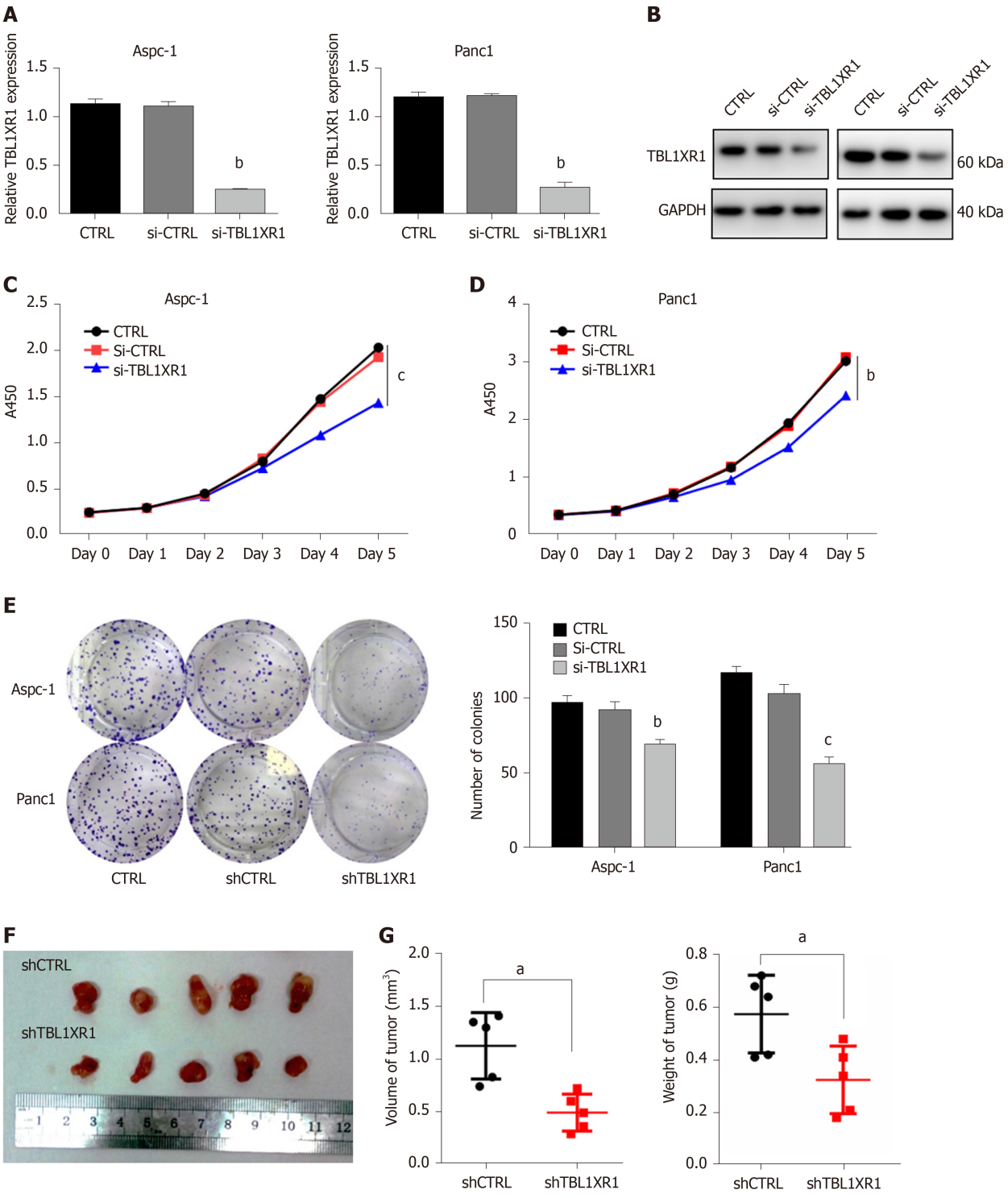

Figure 3 Transducin (β)-like 1 X-linked receptor 1 exhibited oncogenic properties in pancreatic ductal adenocarcinoma cell lines. A: The transfection efficiency of transducin (β)-like 1 X-linked receptor 1 (TBL1XR1) in pancreatic ductal adenocarcinoma (PDAC) cells by quantitative real-time PCR; B: The transfection efficiency of TBL1XR1 in PDAC cells by western blots; C and D: Cellular proliferation of untransfected or transfected Aspc-1 and Panc1 cells was measured using a CCK8 assay daily for 5 d; E: Aspc-1 and Panc1 cells were seeded at 500 cells/well, and the cells were allowed to form colonies. Colony numbers were counted and recorded; F: Mice were treated with Lv-shCTRL and Lv-shTBL1XR1 PDAC cells; G: Tumor volumes and weights were measured. $^{a}P < 0.05$, $^{b}P < 0.01$, $^{c}P < 0.001$. GAPDH: Glyceraldehyde-3-phosphate dehydrogenase; TBL1XR1: Transducin (β)-like 1 X-linked receptor 1; CTRL: Control; Si-CTRL: CTRL siRNA; Si-TBL1XR1: TBL1XR1 siRNA; ShRNA: Short hairpin RNA; ShCTRL: CTRL shRNA; ShTBL1XR1: TBL1XR1 shRNA.

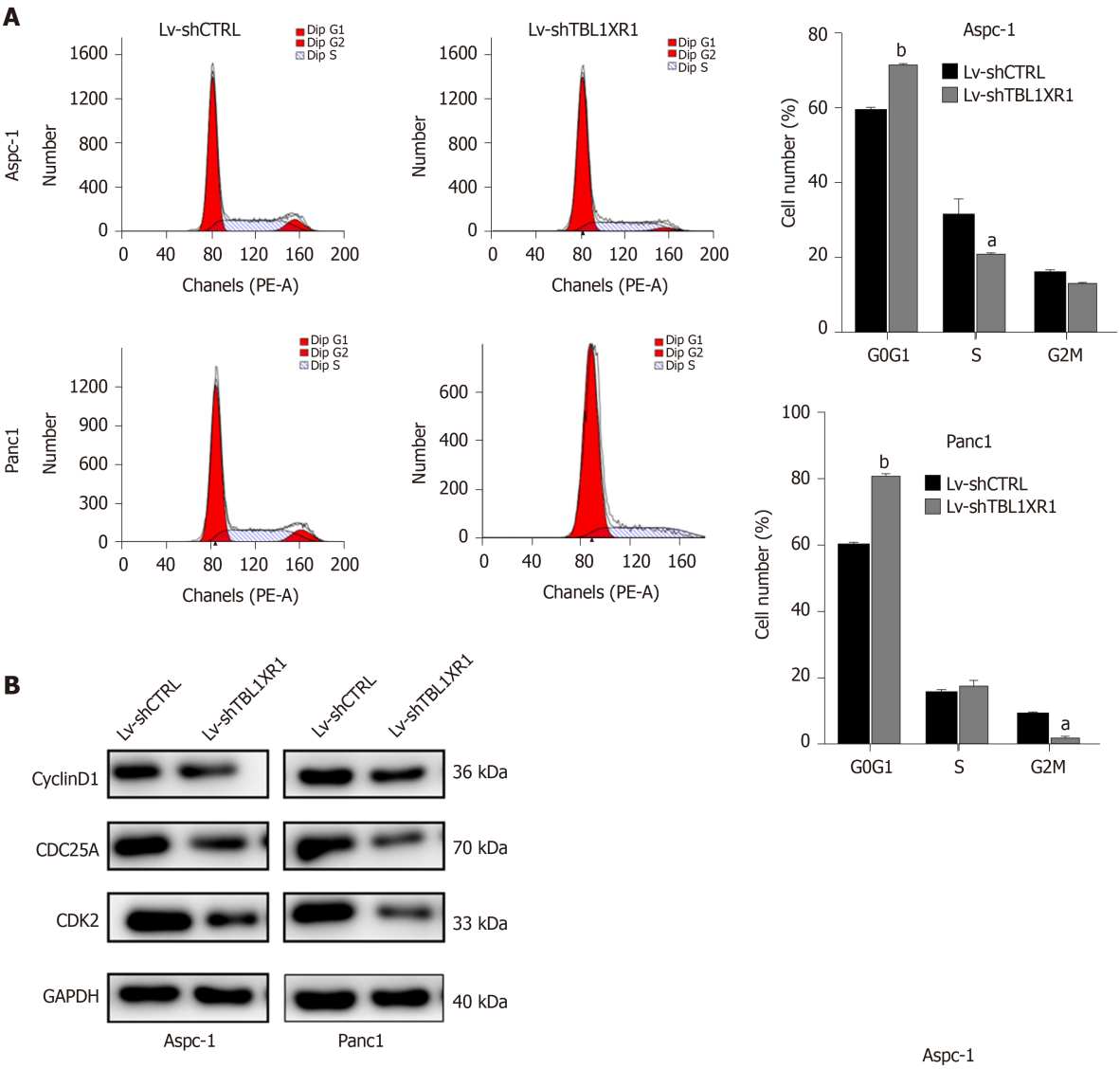
A
Lv-shCTRL
Lv-shTBL1XR1
Dip G1
Dip G2
Dip S
Aspc-1
Panc1
Number
Chanels (PE-A)
Aspc-1
Panc1
Lv-shCTRL
Lv-shTBL1XR1
Cell number (%)
G0G1
S
G2M
B
Lv-shCTRL
Lv-shTBL1XR1
CyclinD1
CDC25A
CDK2
GAPDH
36 kDa
70 kDa
33 kDa
40 kDa
Aspc-1
Panc1
C
Lv-shCTRL
Lv-shTBL1XR1
Aspc-1
Panc1
PE-A
FITC-A
Q1
Q2
Q3
Q4
Apoptosis rate (%)
Early apoptosis
Late apoptosis

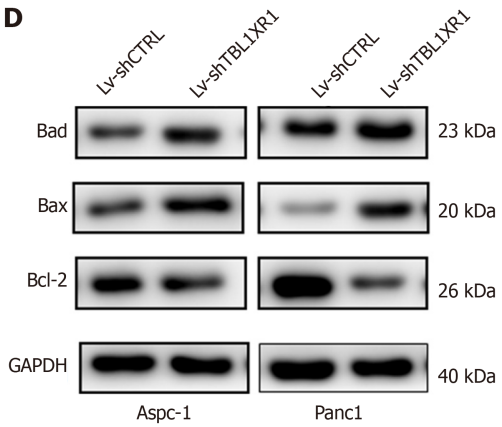

Figure 4 Effects of transducin (β)-like 1 X-linked receptor 1 silencing on cell cycle progression and apoptosis. A: The cell cycle phases of treated cells were evaluated by flow cytometry after transfection for 48 h. The X-axis indicates the different periodic distribution, and the y-axis indicates the number of cells. B: The protein levels of cell cycle regulators, such as CDK2, CDC25A and cyclinD1, were examined by western blotting analysis. C: Untransfected and transfected pancreatic ductal adenocarcinoma cells were analyzed by flow cytometry with annexin V–fluorescein 5-isothiocyanate/propidium iodide (PI) staining. The X-axis indicates annexin V-fluorescein 5-isothiocyanate, and the Y-axis indicates PI staining. Annexin V/PI+ represents necrotic cells, annexin V+/PI represents early apoptotic cells, and annexin V+/PI+ represents late apoptotic cells. D: The protein levels of bad, bax and bcl-2 were examined by western blotting analysis. $^{a}P < 0.05$, $^{b}P < 0.01$, $^{c}P < 0.001$. GAPDH: Glyceraldehyde-3-phosphate dehydrogenase; TBL1XR1: Transducin (β)-like 1 X-linked receptor 1.

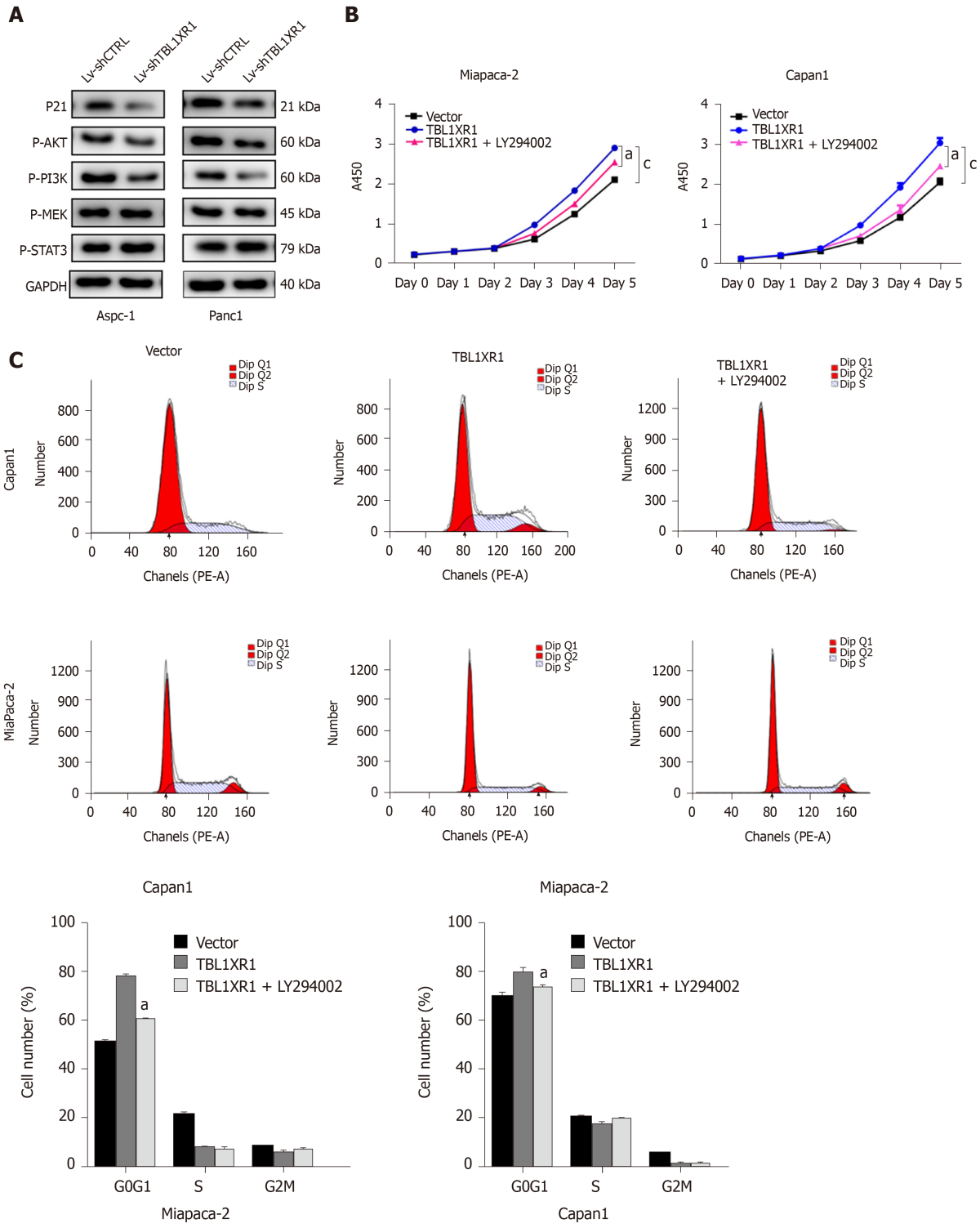
A
Lv-shCTRL
Lv-shTBL1XR1
Lv-shCTRL
Lv-shTBL1XR1
P21
P-AKT
P-PI3K
P-MEK
P-STAT3
GAPDH
21 kDa
60 kDa
60 kDa
45 kDa
79 kDa
40 kDa
Aspc-1
Panc1
B
Miapaca-2
Capan1
Vector
TBL1XR1
TBL1XR1 + LY294002
A450
Day 0 Day 1 Day 2 Day 3 Day 4 Day 5
C
Vector
TBL1XR1
TBL1XR1 + LY294002
Dip Q1
Dip Q2
Dip S
Capan1
MiaPaca-2
Number
Chanels (PE-A)
Capan1
Miapaca-2
Cell number (%)
G0G1
S
G2M
Miapaca-2
Capan1

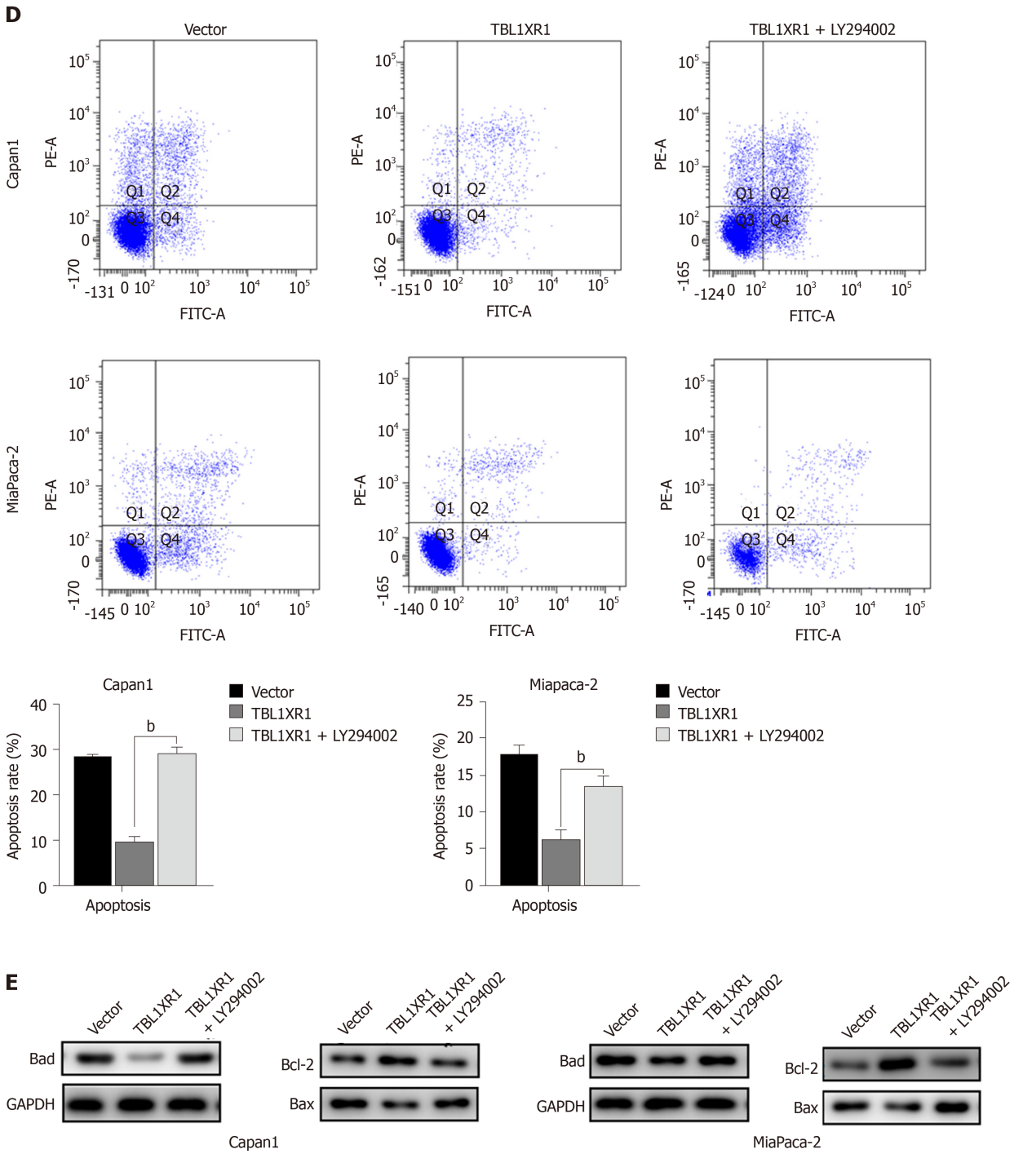

Figure 5 Transducin (β)-like 1 X-linked receptor 1 regulates phosphatidylinositol 3-kinase/protein kinase B signaling in pancreatic ductal adenocarcinoma cells. A: Western blot analysis of phosphatidylinositol 3-kinase/protein kinase B (PI3K/Akt) signaling-related proteins in both cell lines. GAPDH was used as a loading control; B: Cellular proliferation of pancreatic ductal adenocarcinoma (PDAC) cells treated with or without the PI3K/Akt pathway inhibitor LY294002 was measured using a CCK-8 assay daily for 5 d; C: Cell cycle phase analysis and apoptosis of PDAC cells treated with or without LY294002 were analyzed by flow cytometry. The X-axis indicates the different periodic distributions, and the Y-axis indicates the number of cells. D: Apoptosis analysis of PDAC cells treated with or without LY294002 was analyzed by flow cytometry. The Y-axis indicates V–fluorescein 5-isothiocyanate, and the Y-axis indicates propidium iodide (PI) staining. Annexin V/PI+ represents necrotic cells, annexin V+/PI represents early apoptotic cells, and annexin V+/PI+ represents late apoptotic cells. E: Western blot analysis of PI3K/Akt signaling-related proteins in PDAC cells treated with or without LY294002. GAPDH: Glyceraldehyde-3-phosphate dehydrogenase; TBL1XR1: Transducin (β)-like 1 X-linked receptor 1.

ARTICLE HIGHLIGHTS

Research background

Pancreatic ductal adenocarcinoma (PDAC) is one of the deadliest and most aggressive solid tumors and has a poor prognosis. Transducin (β)-like 1 X-linked receptor 1 (TBL1XR1) has been linked to the progression of various human cancers. Nevertheless, the function and role of TBL1XR1 in pancreatic cancers are unclear.

Research motivation

PDAC is one of the deadliest solid tumors. Identification of diagnostic and therapeutic biomarker of PDAC is urgently needed. TBL1XR1 has been linked to the progression of various human cancers. Nevertheless, the function and role of TBL1XR1 are unclear in pancreatic cancers.

Research objectives

To explore the potential effect and mechanism of TBL1XR1 in the development of PDAC.

Research methods

Ninety histologically confirmed PDAC patients were enrolled in this study. PDAC cancer samples and cell lines were used to determine the expression of TBL1XR1. CCK-8 assays and colony formation analysis were performed to assess the viability of PDAC cells. Flow cytometry was carried out to analyze changes in the cell cycle and apoptosis. Related protein expression changes were determined by western blot analysis. Animal analysis was performed to confirm the impact of TBL1XR1 *in vivo*.

Research results

The results showed that patients with TBL1XR1-positive tumors had worse overall survival than those with TBL1XR1-negative tumors. Moreover, we found that TBL1XR1 obviously promoted PDAC cell proliferation and inhibited PDAC cell apoptosis. Moreover, knockdown of TBL1XR1 induced G0/G1 phase arrest. *In vivo* animal studies confirmed that TBL1XR1 accelerated tumor cell growth. The results of western blot analysis showed that TBL1XR1 might play a significant role in regulating PDAC cell proliferation and apoptosis *via* the PI3K/AKT pathway.

Research conclusions

TBL1XR1 promotes PDAC cell progression and might be a probable effective diagnostic and therapeutic marker for pancreatic cancer.

Research perspectives

TBL1XR1 may be an effective diagnosis and therapeutic marker for pancreatic cancer

REFERENCES

1 **Garrido-Laguna I**, Hidalgo M. Pancreatic cancer: from state-of-the-art treatments to promising novel therapies. *Nat Rev Clin Oncol* 2015; **12**: 319-334 [PMID: 25824606 DOI: 10.1038/nrclinonc.2015.53]

2 **Siegel RL**, Miller KD, Jemal A. Cancer statistics, 2015. *CA Cancer J Clin* 2015; **65**: 5-29 [PMID: 25559415 DOI: 10.3322/caac.21254]

3 **Poruk KE**, Firpo MA, Adler DG, Mulvihill SJ. Screening for pancreatic cancer: why, how, and who? *Ann Surg* 2013; **257**: 17-26 [PMID: 22895395 DOI: 10.1097/SLA.0b013e31825ffbfb]

4 **Wolfgang CL**, Herman JM, Laheru DA, Klein AP, Erdek MA, Fishman EK, Hruban RH. Recent progress in pancreatic cancer. *CA Cancer J Clin* 2013; **63**: 318-348 [PMID: 23856911 DOI: 10.3322/caac.21190]

5 **Hidalgo M**. Pancreatic cancer. *N Engl J Med* 2010; **362**: 1605-1617 [PMID: 20427809 DOI: 10.1056/NEJMra0901557]

6 **Pérez-Mancera PA**, Rust AG, van der Weyden L, Kristiansen G, Li A, Sarver AL, Silverstein KA, Grützmann R, Aust D, Rümmele P, Knösel T, Herd C, Stemple DL, Kettleborough R, Brosnan JA, Li A, Morgan R, Knight S, Yu J, Stegeman S, Collier LS, ten Hoeve JJ, de Ridder J, Klein AP, Goggins M, Hruban RH, Chang DK, Biankin AV, Grimmond SM; Australian Pancreatic Cancer Genome Initiative, Wessels LF, Wood SA, Iacobuzio-Donahue CA, Pilarsky C, Largaespada DA, Adams DJ, Tuveson DA. The deubiquitinase USP9X suppresses pancreatic ductal adenocarcinoma. *Nature* 2012; **486**: 266-270 [PMID: 22699621 DOI: 10.1038/nature11114]

7 **Li M**, Liu F, Zhang F, Zhou W, Jiang X, Yang Y, Qu K, Wang Y, Ma Q, Wang T, Bai L, Wang Z, Song X, Zhu Y, Yuan R, Gao Y, Liu Y, Jin Y, Li H, Xiang S, Ye Y, Zhang Y, Jiang L, Hu Y, Hao Y, Lu W, Chen S, Gu J, Zhou J, Gong W, Zhang Y, Wang X, Liu X, Liu C, Liu H, Liu Y, Liu Y. Genomic *ERBB2*/*ERBB3* mutations promote PD-L1-mediated immune escape in gallbladder cancer: a whole-exome sequencing

analysis. *Gut* 2019; **68**: 1024-1033 [PMID: 29954840 DOI: 10.1136/gutjnl-2018-316039]
8 **Zhang J**, Kalkum M, Chait BT, Roeder RG. The N-CoR-HDAC3 nuclear receptor corepressor complex inhibits the JNK pathway through the integral subunit GPS2. *Mol Cell* 2002; **9**: 611-623 [PMID: 11931768 DOI: 10.1016/s1097-2765(02)00468-9]
9 **Tomita A**, Buchholz DR, Obata K, Shi YB. Fusion protein of retinoic acid receptor alpha with promyelocytic leukemia protein or promyelocytic leukemia zinc finger protein recruits N-CoR-TBLR1 corepressor complex to repress transcription in vivo. *J Biol Chem* 2003; **278**: 30788-30795 [PMID: 12794076 DOI: 10.1074/jbc.M303309200]
10 **Daniels G**, Li Y, Gellert LL, Zhou A, Melamed J, Wu X, Zhang X, Zhang D, Meruelo D, Logan SK, Basch R, Lee P. TBLR1 as an androgen receptor (AR) coactivator selectively activates AR target genes to inhibit prostate cancer growth. *Endocr Relat Cancer* 2014; **21**: 127-142 [PMID: 24243687 DOI: 10.1530/ERC-13-0293]
11 **Chen SP**, Yang Q, Wang CJ, Zhang LJ, Fang Y, Lei FY, Wu S, Song LB, Guo X, Guo L. Transducin β-like 1 X-linked receptor 1 suppresses cisplatin sensitivity in nasopharyngeal carcinoma via activation of NF-κB pathway. *Mol Cancer* 2014; **13**: 195 [PMID: 25145705 DOI: 10.1186/1476-4598-13-195]
12 **Liu H**, Liu Z, Li K, Li S, Song L, Gong Z, Shi W, Yang H, Xu Y, Ning S, Ismail S, Chen Y. TBL1XR1 predicts isolated tumor cells and micrometastasis in patients with TNM stage I/II colorectal cancer. *J Gastroenterol Hepatol* 2017; **32**: 1570-1580 [PMID: 28127799 DOI: 10.1111/jgh.13749]
13 **Liu F**, He Y, Cao Q, Liu N, Zhang W. TBL1XR1 Is Highly Expressed in Gastric Cancer and Predicts Poor Prognosis. *Dis Markers* 2016; **2016**: 2436518 [PMID: 27672238 DOI: 10.1155/2016/2436518]
14 **Cao Q**, Wang Z, Wang Y, Liu F, Dong Y, Zhang W, Wang L, Ke Z. TBL1XR1 promotes migration and invasion in osteosarcoma cells and is negatively regulated by miR-186-5p. *Am J Cancer Res* 2018; **8**: 2481-2493 [PMID: 30662805]
15 **Li X**, Liang W, Liu J, Lin C, Wu S, Song L, Yuan Z. Transducin (β)-like 1 X-linked receptor 1 promotes proliferation and tumorigenicity in human breast cancer via activation of beta-catenin signaling. *Breast Cancer Res* 2014; **16**: 465 [PMID: 25341494 DOI: 10.1186/s13058-014-0465-z]
16 **Kuang X**, Zhu J, Peng Z, Wang J, Chen Z. Transducin (Beta)-Like 1 X-Linked Receptor 1 Correlates with Clinical Prognosis and Epithelial-Mesenchymal Transition in Hepatocellular Carcinoma. *Dig Dis Sci* 2016; **61**: 489-500 [PMID: 26386862 DOI: 10.1007/s10620-015-3879-2]
17 **Li M**, Lu J, Zhang F, Li H, Zhang B, Wu X, Tan Z, Zhang L, Gao G, Mu J, Shu Y, Bao R, Ding Q, Wu W, Dong P, Gu J, Liu Y. Yes-associated protein 1 (YAP1) promotes human gallbladder tumor growth via activation of the AXL/MAPK pathway. *Cancer Lett* 2014; **355**: 201-209 [PMID: 25218593 DOI: 10.1016/j.canlet.2014.08.036]
18 **Li M**, Shen J, Wu X, Zhang B, Zhang R, Weng H, Ding Q, Tan Z, Gao G, Mu J, Yang J, Shu Y, Bao R, Ding Q, Wu W, Cao Y, Liu Y. Downregulated expression of hepatoma-derived growth factor (HDGF) reduces gallbladder cancer cell proliferation and invasion. *Med Oncol* 2013; **30**: 587 [PMID: 23609195 DOI: 10.1007/s12032-013-0587-7]
19 **Xia X**, Wu W, Huang C, Cen G, Jiang T, Cao J, Huang K, Qiu Z. SMAD4 and its role in pancreatic cancer. *Tumour Biol* 2015; **36**: 111-119 [PMID: 25464861 DOI: 10.1007/s13277-014-2883-z]
20 **Zhang X**, Dormady SP, Basch RS. Identification of four human cDNAs that are differentially expressed by early hematopoietic progenitors. *Exp Hematol* 2000; **28**: 1286-1296 [PMID: 11063877 DOI: 10.1016/s0301-472x(00)00539-7]
21 **Liu L**, Lin C, Liang W, Wu S, Liu A, Wu J, Zhang X, Ren P, Li M, Song L. TBL1XR1 promotes lymphangiogenesis and lymphatic metastasis in esophageal squamous cell carcinoma. *Gut* 2015; **64**: 26-36 [PMID: 24667177 DOI: 10.1136/gutjnl-2013-306388]
22 **Zaghlula M**, Glaze DG, Enns GM, Potocki L, Schwabe AL, Suter B. Current clinical evidence does not support a link between TBL1XR1 and Rett syndrome: Description of one patient with Rett features and a novel mutation in TBL1XR1, and a review of TBL1XR1 phenotypes. *Am J Med Genet A* 2018; **176**: 1683-1687 [PMID: 29777588 DOI: 10.1002/ajmg.a.38689]
23 **Serna-Marquez N**, Diaz-Aragon R, Reyes-Uribe E, Cortes-Reynosa P, Salazar EP. Linoleic acid induces migration and invasion through FFAR4- and PI3K-/Akt-dependent pathway in MDA-MB-231 breast cancer cells. *Med Oncol* 2017; **34**: 111 [PMID: 28456993 DOI: 10.1007/s12032-017-0969-3]
24 **Slomiany BL**, Slomiany A. Helicobacter pylori Induces Disturbances in Gastric Mucosal Akt Activation through Inducible Nitric Oxide Synthase-Dependent S-Nitrosylation: Effect of Ghrelin. *ISRN Gastroenterol* 2011; **2011**: 308727 [PMID: 21991502 DOI: 10.5402/2011/308727]
25 **Slomiany BL**, Slomiany A. Role of constitutive nitric oxide synthase S-nitrosylation in Helicobacter pylori-induced gastric mucosal cell apoptosis: effect of ghrelin. *Inflammopharmacology* 2010; **18**: 233-240 [PMID: 20596895 DOI: 10.1007/s10787-010-0051-7]

World Journal of Gastroenterology

Submit a Manuscript: https://www.f6publishing.com

World J Gastroenterol 2020 July 7; 26(25): 3603-3610

DOI: 10.3748/wjg.v26.i25.3603

ISSN 1007-9327 (print) ISSN 2219-2840 (online)

ORIGINAL ARTICLE

Basic Study

Retrievable puncture anchor traction method for endoscopic ultrasound-guided gastroenterostomy: A porcine study

Guo-Xin Wang, Kai Zhang, Si-Yu Sun

ORCID number: Guo-Xin Wang 0000-0002-5928-3370; Kai Zhang 0000-0002-0355-3415; Si-Yu Sun 0000-0002-7308-0473.

Author contributions: Wang GX and Zhang K contributed to the work equally and should be regarded as co-first authors; Wang GX, Zhang K and Sun SY conceived and designed the study; Wang GX and Zhang K analyzed and interpreted the data, drafted the article, revised the article for important intellectual content; Sun SY approved the final version of the article.

Supported by the China Postdoctoral Science Foundation, No. 2019M661174; National Natural Science Foundation of China, No. 81770655; and the Natural Science Foundation of Liaoning Province, No. 2019-MS-359.

Institutional animal care and use committee statement: The study was reviewed and approved by the Ethics Review Committee and Ethics Committee of Shengjing Hospital of China Medical University (No. 2018PS482K). All animal experiments conformed to the internationally accepted principles for the care and use of laboratory animals.

Guo-Xin Wang, Kai Zhang, Si-Yu Sun, Department of Gastroenterology, Endoscopic Center, Shengjing Hospital of China Medical University, Shenyang 110001, Liaoning Province, China

Corresponding author: Si-Yu Sun, MD, PhD, Chief Doctor, Director, Professor, Department of Gastroenterology, Endoscopic Center, Shengjing Hospital of China Medical University, No. 36, Sanhao Street, Shenyang 110004, Liaoning Province, China. sun-siyu@163.com

Abstract

BACKGROUND

Endoscopic ultrasound-guided gastroenterostomy (EUS-GE) is an alternative method for the surgical treatment of gastric outlet obstruction, but it is regarded as a challenging technique for endoscopists as the bowel is highly mobile and can tent away. Thus, the technique requires superb skill. In order to improve EUS-GE, we have developed a retrievable puncture anchor traction (RPAT) device for EUS-GE to address the issue of bowel tenting.

AIM

To evaluate the feasibility of RPAT-assisted EUS-GE using an animal model.

METHODS

Six Bama mini pigs each weighing between 15 and 20 kg underwent the RPAT-assisted EUS-GE procedure. Care was taken to ensure that the animals experienced minimal pain and discomfort. Two days prior to the procedure the animals were limited to a liquid diet. No oral intake was allowed on the day before the procedure. A fully covered metal stent was placed between the stomach and the intestine using the RPAT-assisted EUS-GE method. Infection in the animals was determined. Four weeks after the procedure, a standard gastroscope was inserted into the pig's intestine through a previously created fistula in order to check the status of the stents under anesthesia. The pig was euthanized after examination.

RESULTS

The RPAT-assisted EUS-GE method allowed placement of the stents with no complications in all six animals. All the pigs tolerated a regular diet within hours of the procedure. The animals were monitored for four weeks after the RPAT-assisted EUS-GE, during which time all of the animals exhibited normal eating behavior and no signs of infection were observed. Endoscopic imaging performed

Conflict-of-interest statement: Sun SY is a consultant for the Vedkang Company and Nanjing Microtech company. The other authors have no conflicts of interests to declare.

Data sharing statement: No additional data are available.

ARRIVE guidelines statement: The authors have read the ARRIVE guidelines, and the manuscript was prepared and revised according to the ARRIVE guidelines.

Manuscript source: Unsolicited manuscript

Received: March 3, 2020
Peer-review started: March 3, 2020
First decision: March 24, 2020
Revised: April 30, 2020
Accepted: May 27, 2020
Article in press: May 27, 2020
Published online: July 7, 2020

P-Reviewer: Altonbary Y, Kanno Y, Kozarek RA, Minaga K, Yoshinaga S
S-Editor: Dou Y
L-Editor: Webster JR
E-Editor: Zhang YL

four weeks after the RPAT-assisted EUS-GE showed that the stents remained patent and stable in all the animals. No tissue overgrowth or ingrowth was observed in any case. Each animal had a mature fistula, and the stents were removed without significant bleeding. Autopsies of all six pigs revealed complete adhesion between the intestine and the stomach wall.

CONCLUSION
The RPAT method helps reduce mobility of the bowel. Therefore, the RPAT-assisted EUS-GE method is a minimally invasive treatment modality.

Key words: Retrievable puncture anchor; Endoscopic ultrasound; Endoscopic ultrasound-guided gastroenterostomy; Gastric outlet obstruction; Gastroenterostomy; Electrocautery-enhanced delivery of lumen-apposing metal stents

Core tip: To evaluate the feasibility of retrievable puncture anchor traction (RPAT)-assisted endoscopic ultrasound-guided gastroenterostomy (EUS-GE), six Bama mini pigs underwent the RPAT-assisted EUS-GE procedure. Four weeks later, a standard gastroscope was inserted into the pig's intestine through a previously created fistula in order to check the status of the stents under anesthesia. The pigs were euthanized after examination. The results showed that the RPAT-assisted EUS-GE method allowed placement of the stents with no complications in all six animals. This study proved that the RPAT method helps reduce mobility of the bowel. Therefore, the RPAT-assisted EUS-GE method is a minimally invasive treatment modality.

Citation: Wang GX, Zhang K, Sun SY. Retrievable puncture anchor traction method for endoscopic ultrasound-guided gastroenterostomy: A porcine study. *World J Gastroenterol* 2020; 26(25): 3603-3610
URL: https://www.wjgnet.com/1007-9327/full/v26/i25/3603.htm
DOI: https://dx.doi.org/10.3748/wjg.v26.i25.3603

INTRODUCTION

Endoscopic ultrasound-guided gastroenterostomy (EUS-GE) has become an alternative to the surgical or standard endoscopic treatment methods for gastric outlet obstruction (GOO) when endoscopic stents cannot be placed. However, EUS-GE presents certain challenges and the current procedural methods have limitations. One source of difficulty during EUS-GE is the high mobility of the intestine, which can tent away during puncture with a needle or electrocautery-enhanced delivery of lumen-apposing metal stents (ECE-LAMS). In order to improve EUS-GE, we developed a retrieval puncture anchor traction (RPAT) method for EUS-GE. We evaluated the feasibility of the RPAT method using a pig model.

MATERIALS AND METHODS

Animals

Six Bama mini pigs (15-20 kg) were selected to undergo the RPAT method of EUS-GE, which consisted of placing fully covered metal stents between the animals' stomach and bowel walls. This pig model study was approved by the Ethics Review Committee and Ethics Committee of Shengjing Hospital of China Medical University (No. 2018PS482K).

Preoperative preparation

Each pig received a full liquid diet two days before the operation, and drinking water was forbidden the day before surgery. Based on the weight of each animal, propofol was intramuscularly injected for the induction of anesthesia. The pigs were placed on their left side. Venous access was established through the ear vein. The animals'

breathing was maintained by the insertion of a tracheal tube. The animals were monitored with continuous cardiopulmonary monitoring.

RPA

The RPA (Vedkang Inc., Changzhou, Jiangsu, China) is made up of two wires (Figure 1A). The direction of the anchor head can be altered by pulling the retrieval wire (Figure 1B). The anchor can be sent through the needle (Figure 1C and D)[1].

Operative procedure

RPAT method of EUS-GE: First, a gastroscope was advanced into the duodenum. A guidewire (0.035 inch/480 mm; Cook Medical Inc., Bloomington, IN, United States) was sent through the working channel of the gastroscope. A nasal biliary drainage catheter (NBDC) (7Fr; Cook Medical Inc., Limerick, Ireland) was then inserted along the guidewire. Next, the gastroscope and guidewire were removed, leaving the NBDC in place. Approximately 200 mL of saline solution containing methylene blue was injected into the bowel through the NBDC to optimally dilate the bowel and facilitate the subsequent EUS-guided puncture. Methylene blue was added to confirm bowel placement by aspirating the blue saline solution with a needle (described below) before the ECE-LAMS insertion. A longitudinal (linear) ultrasound endoscope (EG-3830-UT; Pentax Japan) was inserted into the stomach and the puncture area (*i.e.*, the closest area between the intestine and the stomach) was marked. We used color Doppler to prevent vascular damage during the puncture. A needle (19-G, Boston Scientific Corp., Massachusetts, United States) was then passed through the working channel, and the intestine was punctured under EUS guidance (Figure 2A and B). After removal of the stylet, saline solution with methylene blue was drawn out and a contrast agent was injected for endoscopy. The RPAT was then passed through the needle (Figure 2C and D) and inserted into the small intestine. The needle and the echoendoscope were removed over the wire of the RPAT. The small bowel was pulled with the anchor (Figure 2E and F). RPAT only pulls the intestinal canal during stent implantation to prevent free action, so the pulling action is gentle rather than violent. During the procedure, we did not observe the angle of the digestive tract wall due to stretching. The echoendoscope was reinserted into the stomach and the 19-G needle was advanced through the working channel. Additional saline solution with methylene blue was injected through the NBDC using multiple 50-mL syringes if the bowel expansion was insufficient. The identified small-bowel loop was punctured under EUS guidance followed by aspiration of the methylene blue solution to confirm the correct puncture site when the small bowel was pulled with the anchor. The guidewire was inserted through the needle. Next, the needle was removed, and ECE-LAMS (16 mm/30 mm; Micro-Tech/Nan Jing Co., Ltd. Nanjing, Jiangsu, China) was inserted over the guidewire and released into the small intestine until the distal flares were fully open under EUS guidance (Figure 2G and Figure H). Through endoscope monitoring, while keeping the proximal section in the field of vision, the rest of the stent was released. Finally, the stent was confirmed and leakages were excluded by EUS (Figure 3A and B). After the operation, the retrieval cord was pulled using a pair of forceps (Figure 2I and J). This changed the direction of the anchor and made it easy to remove (Figure 2K and L).

Postoperative care: Postoperatively, the pigs were observed for signs of peritonitis. Four weeks after surgery, the pigs underwent anesthesia, and a standard gastroscope was used to examine the pigs' intestines. After removing the metal stent using a pair forceps, the gastroscope was advanced into the afferent and efferent bowel loops (Figure 3C and D). X-ray examination was performed to check for the presence of free gas. All pigs were then euthanized (Figure 4).

RESULTS

All six operations were successfully performed. Each metal stent was placed successfully, and the EUS-GEs selected the body of the stomach as the puncture site in each case. All RPAs were able to be removed with no complications. No animal showed signs of peritonitis or any other complications after the procedure. Within a few hours after anesthesia, the pigs were able to tolerate a regular diet. No clinically significant adverse reactions were observed in the following weeks. Four weeks after EUS-GE, it was confirmed that the stents remained intact, in their original positions, with no hyperplastic tissue overgrowth or ingrowth in any animal. The fistulas were

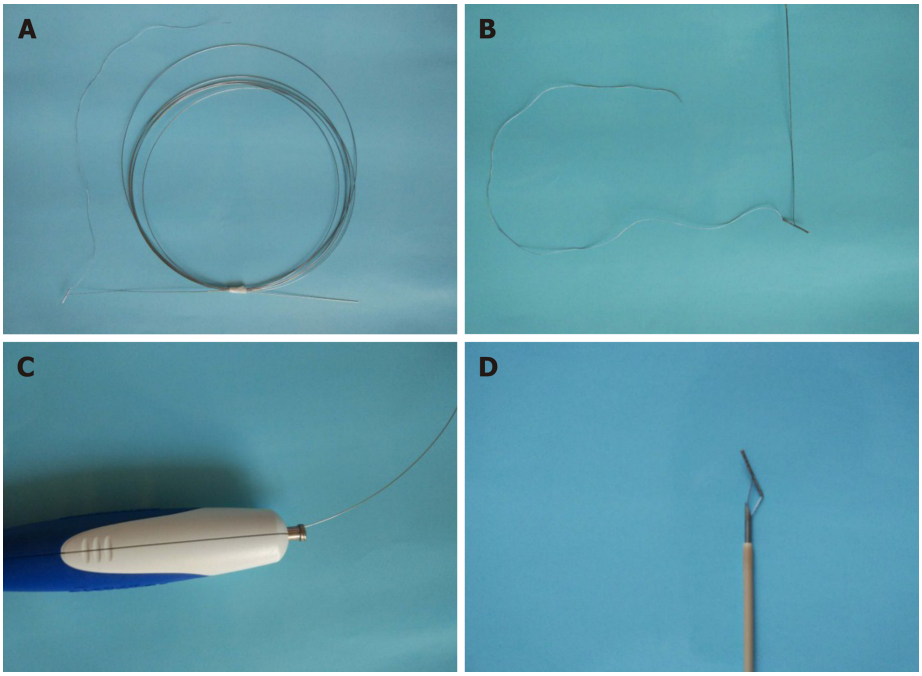

Figure 1 The retrievable puncture anchor. A: The retrievable puncture anchor (Vedkang Inc., Changzhou, Jiangsu, China) in its entirety; B: The head of the anchor; C and D: A view of the passage of the anchor along the shaft of the puncture needle.

mature in all six pigs and all the stents were easily removed using forceps without significant bleeding. On autopsy, there were no signs of bleeding, organ damage, or peritonitis, and complete adhesions of the intestines to the stomach wall were seen.

DISCUSSION

Surgical GE is a traditional choice for patients with malignant GOO. Intraluminal self-expanding metal stents (SEMS) placed through the endoscope is another method to relieve GOO[2-4]. Surgical GE is superior to endoscopic SEMS placement in terms of lumen patency[4]; however, adverse events including delayed gastric emptying, extended hospital stay, increased cost of hospitalization, and delayed treatment of cancer are not uncommon[4,5]. The main limitation of placing SEMS endoscopically is repeated occlusion of the lumen, which is mainly due to tumor ingrowth, overgrowth, or both[4]. In general, EUS-GE can provide durable lumen patency, avoid the risk of tumor overgrowth and ingrowth, and avoids the need for surgery in patients with end-stage disease[6]. In 2002, Fritscher-Ravens *et al*[7] reported the results of EUS-GE using special compression buttons in pigs. In 2012, Binmoeller *et al*[8] described the use of a new intraluminal metal stent in a porcine model that was used to invent an EUS-GE anastomosis. Recently, Itoi *et al*[9] used another endoluminal stent for EUS-GE.

The emergence of stents allows easier creation of anastomoses between the small intestine and the stomach wall. These stents are fully covered with flanges at either end to prevent leakage and migration. The EUS-GE technique using an echoendoscope is an excellent means of providing endoscopic access to the duodenal or jejunal lumen distal to obstructed intestinal segments. Various techniques have been used with EUS-GE[10], including antegrade EUS-GE (the "traditional/downstream" method and the "rendezvous method), retrograde EUS-GE, EUS-guided double-balloon-occluded GE, and direct EUS-GE[9,11-13].

One of the challenges associated with direct EUS-GE is the inability to puncture the small bowel, despite the use of an ECE-LAMS, resulting in it being pushed away rather than punctured[11]. Inadequate expansion of the small bowel or rapid dissipation of the infused contrast and methylene blue (due to peristalsis) can also be limiting factors[11]. The RPAT method for EUS-GE did not use glucagon or other antispasmodic drugs to reduce the mobility of the bowel. The RPA can pull the intestine closer to the stomach wall to reduce intestinal mobility. Compared with traditional EUS-GE, RPAT reduces the distance between the stomach and the bowel, and provides sufficient reverse tension during ECE-LAMS implantation. With sufficient opposite pulling

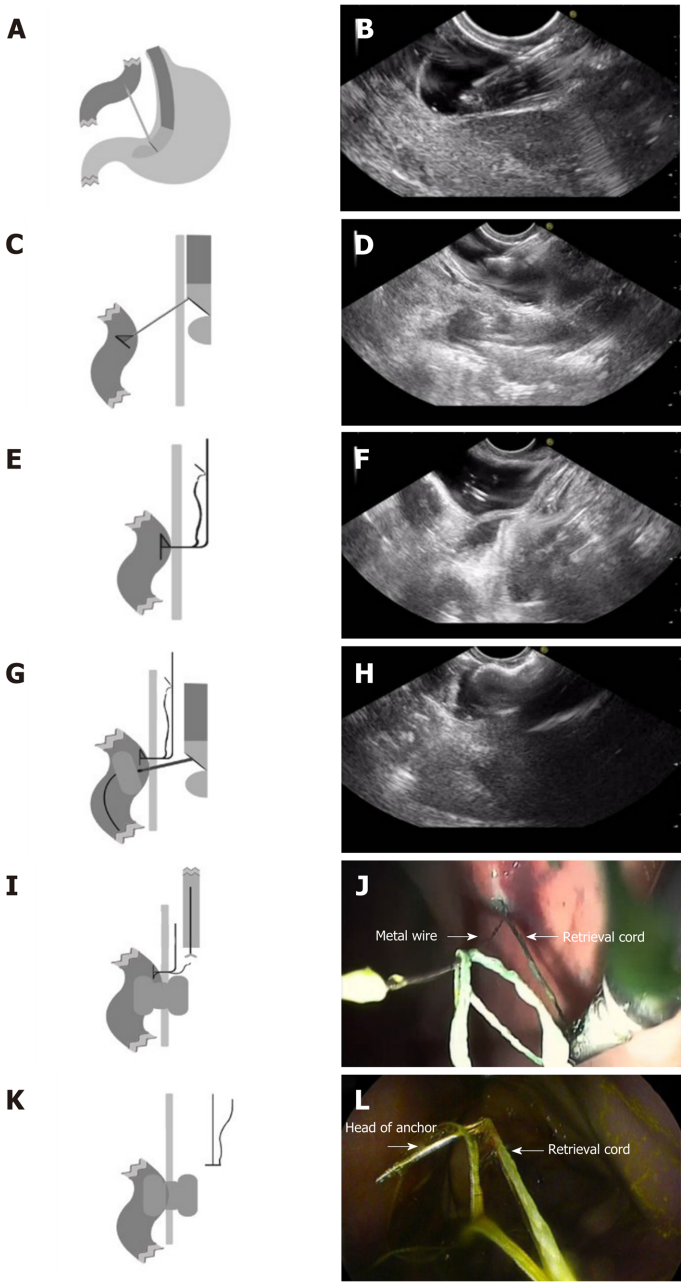

Figure 2 The retrievable puncture anchor traction method. A: Schematic diagram: The bowel is punctured under endoscopic ultrasound (EUS) guidance; B: Endoscopic ultrasound image: The bowel is punctured under EUS guidance; C: Schematic diagram: The retrievable puncture anchor is passed through the needle; D: Endoscopic ultrasound image: The anchor is inserted into the bowel; E: Schematic diagram: After pulling out the needle, the anchor attaches to the bowel; F: Endoscopic ultrasound image: After pulling out the needle, the anchor attaches to the bowel; G: Schematic diagram: The identified small-bowel loop is punctured again under EUS guidance. A guidewire is inserted through the needle. The small bowel is shown being punctured and drained using electrocautery-enhanced delivery of lumen-apposing metal stents over the guidewire; H: Endoscopic ultrasound image: The anchor-grasped bowel is shown under traction for stent implantation; I: Schematic diagram: The retrieval cord is pulled using a pair of forceps; J: Endoscopy image: The retrieval cord is pulled using a pair of forceps; K: Schematic diagram: The retrievable puncture anchor is easily removed; L: Endoscopy image: The retrievable puncture anchor is easily removed.

force, the ECE-LAMS is relatively easy to implant. The stomach wall and intestine of six experimental animals were clearly visible in the ultrasound field of view during the entire surgical procedure. We used an NBDC in the RPAT method to reduce the procedure time for EUS-GE, while avoiding the infusion of large amounts of saline into the intestine to prevent colon swelling. Prior to puncturing and guidewire insertion, a saline solution containing methylene blue was added in order to maintain the expansion of the bowel, provide a better field of view, and improve the safety of the operation.

In contrast to other techniques used with EUS-GE, the RPAT method for EUS-GE does not use a balloon, which reduces the difficulty of performing the operation as the advancement of the dilated balloon over the guidewire under fluoroscopic guidance

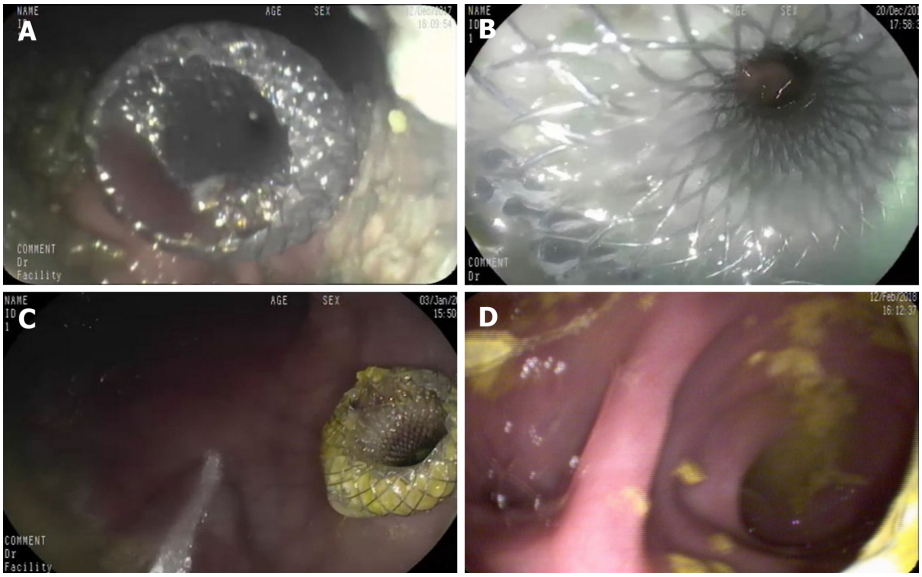

Figure 3 Endoscopic imaging of stent placement and anastomoses. A and B: Endoscopic imaging shows the well-reflected proximal flange of the stent immediately after deployment in the initial session; C: The stents were still in the same position 4 wk later and no traumatic changes were observed; D: A standard gastroscope was easily advanced through the anastomosis to observe the afferent and efferent bowel loops.

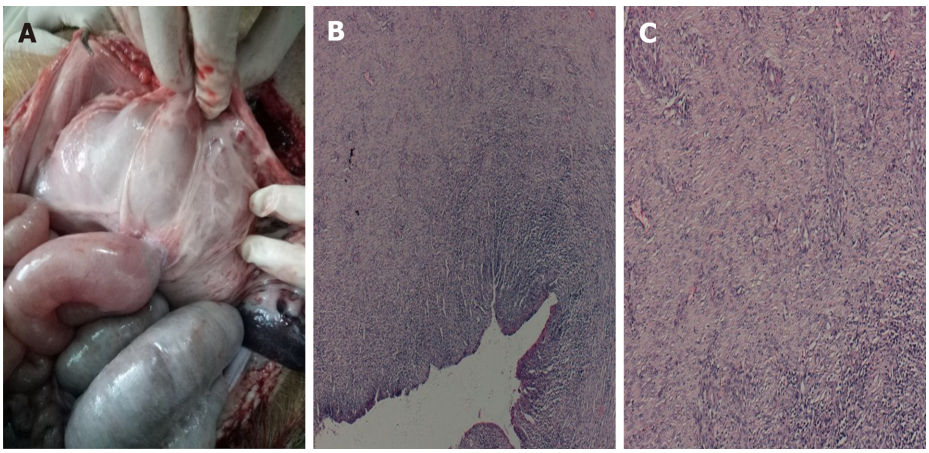

Figure 4 Autopsy and histological findings. A-C: Necropsy and histological evidence shows complete adhesion between the bowel and the stomach wall (20 ×).

can be quite challenging. Moreover, the RPAT method for EUS-GE is suitable for cases where the digestive tract is severely stenotic, allowing only the passage of liquid solution. The RPAT method for EUS-GE can help pull the intestine by pulling the anchor and can inflate the intestine by allowing the injection of saline solution through the NBDC at any time.

Although advanced EUS techniques and the availability of the proper equipment allow EUS-GE to be performed, the procedure is still in its early stages of development. This new technique is accompanied by technical issues requiring instrument modification that must be addressed prior to its clinical application[10,14-21]. Interventional EUS treatment is a newly developed method for the treatment of many diseases[9,19-22]. The small bowel has variable motility and thus tents away from the puncturing needle or the cautery tip of the ECE-LAMS. Hence, we have developed the RPAT method to improve the current EUS-GE method.

The success rate of EUS-GE using the RPAT method was 100% in our study. Remarkably, the retrievable puncture devices anchor to the bowel without causing tissue injury, and the RPA can also be removed without complications. Four weeks after the EUS-GE, it was found that all the stents remained in their original positions. Necropsy revealed complete adhesion between the intestinal wall and the stomach wall.

There are a few limitations in this study. First, the study consisted of a small

number of animals. Second, the follow-up period was four weeks, limiting the evaluation of long-term observations and results. Lastly, the procedure outcomes and findings were not compared to those of other non-EUS-guided gastrojejunostomy techniques[8]. A larger study with a longer follow-up period that compares several gastrojejunostomy techniques is needed.

In general, we proved the technical success of the RPAT method used with EUS-GE in a pig model. The RPAT method for EUS-GE is promising as a minimally invasive treatment. Clinical prospective trials are warranted to verify the efficacy of this treatment method. We are convinced that this treatment method can be widely used in EUS-GE in the future.

ARTICLE HIGHLIGHTS

Research background

Endoscopic ultrasound-guided gastroenterostomy (EUS-GE) is an alternative method for the surgical treatment of gastric outlet obstruction (GOO), but it is regarded as a challenging technique for endoscopists as the bowel is highly mobile and can tent away. Thus, the technique requires superb skill. In order to improve EUS-GE, we have developed a retrievable puncture anchor traction (RPAT) device for EUS-GE to address the issue of bowel tenting.

Research motivation

One source of difficulty in EUS-GE is the high mobility of the intestine, which can tent away during puncture with a needle or electrocautery-enhanced delivery of lumen-apposing metal stents. In order to improve EUS-GE, we developed a RPAT method for EUS-GE. We evaluated the feasibility of the RPAT method using a pig model.

Research objectives

The present study aimed to use an animal model to evaluate the feasibility of RPAT-assisted EUS-GE.

Research methods

Six Bama mini pigs each weighing between 15 and 20 kg underwent the RPAT-assisted EUS-GE procedure. Care was taken to ensure that the animals experienced minimal pain and discomfort. Two days prior to the procedure the animals were limited to a liquid diet. No oral intake was allowed on the day before the procedure. A fully covered metal stent was placed between the stomach and the intestine using the RPAT-assisted EUS-GE method. Infection in the animals was determined. Four weeks after the procedure, a standard gastroscope was inserted into the pig's intestine through a previously created fistula in order to check the status of the stents under anesthesia. The pigs were euthanized after examination.

Research results

The RPAT-assisted EUS-GE method allowed placement of the stents with no complications in all six animals. All the pigs tolerated a regular diet within hours of the procedure. The animals were monitored for four weeks after the RPAT-assisted EUS-GE, during which time all of the animals exhibited normal eating behavior and no signs of infection were observed. Endoscopic imaging performed four weeks after RPAT-assisted EUS-GE showed that the stents remained patent and stable in all the animals. No tissue overgrowth or ingrowth was observed. Each animal had a mature fistula, and the stents were removed without significant bleeding. Autopsies of all six pigs revealed complete adhesion between the intestine and the stomach wall.

Research conclusions

The RPAT method helps reduce mobility of the bowel. Therefore, the RPAT-assisted EUS-GE method is a minimally invasive treatment modality.

Research perspectives

We proved the technical success of the RPAT method used with EUS-GE in a pig model. The RPAT method for EUS-GE is promising as a minimally invasive treatment. Clinical prospective trials are warranted to verify the efficacy of this treatment method. We are convinced that this treatment method can be widely used in EUS-GE in the future.

REFERENCES

1 **Zhang K**, Sun S, Guo J, Wang S, Ge N, Liu X, Wang G. Retrievable puncture anchor traction method for EUS-guided gallbladder drainage: a porcine study. *Gastrointest Endosc* 2018; **88**: 957-963 [PMID: 30048650 DOI: 10.1016/j.gie.2018.07.019]

2 **van Hooft JE**, Uitdehaag MJ, Bruno MJ, Timmer R, Siersema PD, Dijkgraaf MG, Fockens P. Efficacy and safety of the new WallFlex enteral stent in palliative treatment of malignant gastric outlet obstruction (DUOFLEX study): a prospective multicenter study. *Gastrointest Endosc* 2009; **69**: 1059-1066 [PMID: 19152912 DOI: 10.1016/j.gie.2008.07.026]

3 **Telford JJ**, Carr-Locke DL, Baron TH, Tringali A, Parsons WG, Gabbrielli A, Costamagna G. Palliation of patients with malignant gastric outlet obstruction with the enteral Wallstent: outcomes from a multicenter study. *Gastrointest Endosc* 2004; **60**: 916-920 [PMID: 15605006 DOI: 10.1016/s0016-5107(04)02228-x]

4 **Khashab M**, Alawad AS, Shin EJ, Kim K, Bourdel N, Singh VK, Lennon AM, Hutfless S, Sharaiha RZ, Amateau S, Okolo PI, Makary MA, Wolfgang C, Canto MI, Kalloo AN. Enteral stenting versus gastrojejunostomy for palliation of malignant gastric outlet obstruction. *Surg Endosc* 2013; **27**: 2068-2075 [PMID: 23299137 DOI: 10.1007/s00464-012-2712-7]

5 **Doberneck RC**, Berndt GA. Delayed gastric emptying after palliative gastrojejunostomy for carcinoma of the pancreas. *Arch Surg* 1987; **122**: 827-829 [PMID: 2439057 DOI: 10.1001/archsurg.1987.01400190093020]

6 **Itoi T**, Ishii K, Tanaka R, Umeda J, Tonozuka R. Current status and perspective of endoscopic ultrasonography-guided gastrojejunostomy: endoscopic ultrasonography-guided double-balloon-occluded gastrojejunostomy (with videos). *J Hepatobiliary Pancreat Sci* 2015; **22**: 3-11 [PMID: 25155270 DOI: 10.1002/jhbp.148]

7 **Fritscher-Ravens A**, Mosse CA, Mills TN, Mukherjee D, Park PO, Swain P. A through-the-scope device for suturing and tissue approximation under EUS control. *Gastrointest Endosc* 2002; **56**: 737-742 [PMID: 12397289 DOI: 10.1067/mge.2002.129084]

8 **Binmoeller KF**, Shah JN. Endoscopic ultrasound-guided gastroenterostomy using novel tools designed for transluminal therapy: a porcine study. *Endoscopy* 2012; **44**: 499-503 [PMID: 22531985 DOI: 10.1055/s-0032-1309382]

9 **Itoi T**, Itokawa F, Uraoka T, Gotoda T, Horii J, Goto O, Moriyasu F, Moon JH, Kitagawa Y, Yahagi N. Novel EUS-guided gastrojejunostomy technique using a new double-balloon enteric tube and lumen-apposing metal stent (with videos). *Gastrointest Endosc* 2013; **78**: 934-939 [PMID: 24237949 DOI: 10.1016/j.gie.2013.09.025]

10 **Rimbas M**, Larghi A, Costamagna G. Endoscopic ultrasound-guided gastroenterostomy: Are we ready for prime time? *Endosc Ultrasound* 2017; **6**: 235-240 [PMID: 28820145 DOI: 10.4103/eus.eus_47_17]

11 **Irani S**, Baron TH, Itoi T, Khashab MA. Endoscopic gastroenterostomy: techniques and review. *Curr Opin Gastroenterol* 2017; **33**: 320-329 [PMID: 28767501 DOI: 10.1097/MOG.0000000000000389]

12 **Chen YI**, James TW, Agarwal A, Baron TH, Itoi T, Kunda R, Nieto J, Bukhari M, Gutierrez OB, Sanaei O, Moran R, Fayad L, Khashab MA. EUS-guided gastroenterostomy in management of benign gastric outlet obstruction. *Endosc Int Open* 2018; **6**: E363-E368 [PMID: 29527559 DOI: 10.1055/s-0043-123468]

13 **Itoi T**, Ishii K, Ikeuchi N, Sofuni A, Gotoda T, Moriyasu F, Dhir V, Teoh AY, Binmoeller KF. Prospective evaluation of endoscopic ultrasonography-guided double-balloon-occluded gastrojejunostomy bypass (EPASS) for malignant gastric outlet obstruction. *Gut* 2016; **65**: 193-195 [PMID: 26282674 DOI: 10.1136/gutjnl-2015-310348]

14 **Manvar A**, Karia K, Ho S. Endoscopic ultrasound-guided drainage of pelvic abscesses with lumen-apposing metal stents. *Endosc Ultrasound* 2017; **6**: 217-218 [PMID: 28820143 DOI: 10.4103/eus.eus_46_17]

15 **Adler DG**, Taylor LJ, Hasan R, Siddiqui AA. A retrospective study evaluating endoscopic ultrasound-guided drainage of pancreatic fluid collections using a novel lumen-apposing metal stent on an electrocautery enhanced delivery system. *Endosc Ultrasound* 2017; **6**: 389-393 [PMID: 29251273 DOI: 10.4103/eus.eus_4_17]

16 **De Cobelli F**, Marra P, Diana P, Brembilla G, Venturini M. Therapeutic EUS: Biliary drainage - The interventional radiologist's perspective. *Endosc Ultrasound* 2017; **6**: S127-S131 [PMID: 29387709 DOI: 10.4103/eus.eus_77_17]

17 **Rimbaş M**, Larghi A. Endoscopic Ultrasonography-Guided Techniques for Accessing and Draining the Biliary System and the Pancreatic Duct. *Gastrointest Endosc Clin N Am* 2017; **27**: 681-705 [PMID: 28918805 DOI: 10.1016/j.giec.2017.06.006]

18 **Saumoy M**, Arvanitakis M, Kahaleh M. Pancreatic fluid collections and necrosectomy with plastic stents *versus* lumen-apposing stents. *Endosc Ultrasound* 2017; **6**: S132-S137 [PMID: 29387710 DOI: 10.4103/eus.eus_80_17]

19 **Giovannini M**. Endoscopic ultrasound-guided pancreatic duct drainage: Ready for the prime time? *Endosc Ultrasound* 2017; **6**: 281-284 [PMID: 29063870 DOI: 10.4103/eus.eus_86_17]

20 **Itoi T**, Binmoeller KF, Shah J, Sofuni A, Itokawa F, Kurihara T, Tsuchiya T, Ishii K, Tsuji S, Ikeuchi N, Moriyasu F. Clinical evaluation of a novel lumen-apposing metal stent for endosonography-guided pancreatic pseudocyst and gallbladder drainage (with videos). *Gastrointest Endosc* 2012; **75**: 870-876 [PMID: 22301347 DOI: 10.1016/j.gie.2011.10.020]

21 **Teoh AY**, Binmoeller KF, Lau JY. Single-step EUS-guided puncture and delivery of a lumen-apposing stent for gallbladder drainage using a novel cautery-tipped stent delivery system. *Gastrointest Endosc* 2014; **80**: 1171 [PMID: 24830582 DOI: 10.1016/j.gie.2014.03.038]

22 **Binmoeller KF**, Shah J. A novel lumen-apposing stent for transluminal drainage of nonadherent extraintestinal fluid collections. *Endoscopy* 2011; **43**: 337-342 [PMID: 21264800 DOI: 10.1055/s-0030-1256127]

World Journal of Gastroenterology

Submit a Manuscript: https://www.f6publishing.com

World J Gastroenterol 2020 July 7; 26(25): 3611-3624

DOI: 10.3748/wjg.v26.i25.3611

ISSN 1007-9327 (print) ISSN 2219-2840 (online)

ORIGINAL ARTICLE

Case Control Study

Risk factors associated with inflammatory bowel disease: A multicenter case-control study in Brazil

Valéria Cristina Loureiro Salgado, Ronir Raggio Luiz, Neio Lucio Fernandes Boéchat, Isabella Sued Leão, Bianca do Carmo Schorr, José Miguel Luz Parente, Daniela Calado Lima, Eduardo Santos Silveira Júnior, Genoile Oliveira Santana Silva, Neogélia Pereira Almeida, Andrea Vieira, Maria Luiza Queiroz de Bueno, Júlio Maria Chebli, Érika Ruback Bertges, Luísa Martins da Costa Brugnara, Columbano Junqueira Neto, Stefania Burjack Gabriel Campbell, Luana Letiza Discacciati, João Paulo Silva Cézar, Tiago Nunes, Gilaad G Kaplan, Cyrla Zaltman

ORCID number: Valéria Cristina Loureiro Salgado 0000-0001-6238-5549; Ronir Raggio Luiz 0000-0002-7784-9905; Neio Lucio Fernandes Boéchat 0000-0003-4131-9635; Isabella Sued Leão 0000-0001-6618-4816; Bianca do Carmo Schorr 0000-0003-1220-7992; José Miguel Luz Parente 0000-0003-4563-2784; Daniela Calado Lima 0000-0003-3478-3528; Eduardo Santos Silveira Júnior 0000-0002-9904-725X; Genoile Oliveira Santana Silva 0000-0001-5936-9791; Neogélia Pereira Almeida 0000-0002-5812-5776; Andrea Vieira 0000-0003-1858-3446; Maria Luiza Queiroz de Bueno 0000-0002-1556-4138; Júlio Maria Chebli 0000-0003-1527-0663; Érika Ruback Bertges 0000-0002-2298-4640; Luisa Martins da Costa Brugnara 0000-0003-0052-8510; Columbano Junqueira Neto 0000-0002-3680-6722; Stefania Burjack Gabriel Campbell 0000-0002-8455-1701; Luana Letiza Discacciati 0000-0003-3061-3695; João Paulo Silva Cézar 0000-0002-2818-9920; Tiago Nunes 0000-0003-2134-4171; Gilaad G Kaplan 0000-0003-2719-0556; Cyrla Zaltman 0000-0002-5236-6501.

Author contributions: Salgado VCL, Boéchat NLF and Zaltman C designed the study; Salgado VCL,

Valéria Cristina Loureiro Salgado, Isabella Sued Leão, Bianca do Carmo Schorr, Cyrla Zaltman, Division of Gastroenterology, Department of Internal Medicine, Clementino Fraga Filho Hospital, Federal University of Rio de Janeiro, Rio de Janeiro 21940-230, Brazil

Ronir Raggio Luiz, Institute for Studies in Public Health, Federal University of Rio de Janeiro, Rio de Janeiro 21940-230, Brazil

Neio Lucio Fernandes Boéchat, Multidisciplinary Research Laboratory, Clementino Fraga Filho Hospital, Institute of Thoracic Diseases, Faculty of Medicine, Federal University of Rio de Janeiro, Rio de Janeiro 21940-230, Brazil

José Miguel Luz Parente, Daniela Calado Lima, Eduardo Santos Silveira Júnior, Division of Gastroenterology, Department of Internal Medicine, Hospital University, Faculty of Medicine, Federal University of Piauí, Piauí 64049-550, Brazil

Genoile Oliveira Santana Silva, Neogélia Pereira Almeida, Division of Gastroenterology, Inflammatory Bowel Disease Outpatient Clinic, Roberto Santos General Hospital (HGRS) of the Bahia State Department of Health, Bahia 40110-060, Brazil

Andrea Vieira, Maria Luiza Queiroz de Bueno, Division of Gastroenterology, Inflammatory Bowel Disease Outpatient Clinic, Irmandade Santa Casa da Misericórdia of São Paulo, São Paulo 01221020, Brazil

Júlio Maria Chebli, Érika Ruback Bertges, Luísa Martins da Costa Brugnara, Division of Gastroenterology, Department of Internal Medicine, Hospital University, Faculty of Medicine, Federal University of Juiz de Fora, Minas Gerais 36036-247, Brazil

Columbano Junqueira Neto, Stefania Burjack Gabriel Campbell, Luana Letiza Discacciati, João Paulo Silva Cézar, Division of Gastroenterology, Inflammatory Bowel Disease Outpatient Clinic, Federal District Base Hospital, Brasília 70330-150, Brazil

Tiago Nunes, Gastrointestinal Physiology, Institute of Nutritional Science, Nestle Research Center, Lausanne 1000, Switzerland

Zaltman C, Parente JML, Silva GOS, Vieira A, Chebli JM, Junqueira Neto C coordinated and provided the collection of all data; Salgado VCL, Leão IS, Schorr BC, Lima DC, Silveira Júnior ES, Ameilda NP, de Bueno MLQ, Bertges ÉR, Brugnara LMC, Campbell SBG, Discacciati LL and Cézar JPS made the structured interviews and collected patient's data from clinical reports; Salgado VCL and Luiz RR organized and analyzed the data; Salgado VCL, Zaltman C, Nunes T and Kaplan GG were involved in writing and editing the manuscript. All authors read and approved the final manuscript.

Supported by Carlos Chagas Filho Rio de Janeiro State Research Foundation (Faperj), No. 100.044/2011.

Institutional review board statement: The study was approved by the ethics committee of Clementino Fraga Filho University Hospital/ UFRJ (Rio de Janeiro, Brazil).

Informed consent statement: All patients gave informed consent.

Conflict-of-interest statement: No benefits in any form have been received or will be received from a commercial party related directly or indirectly to the subject of this article.

Data sharing statement: No additional data are available.

STROBE statement: The authors have read the STROBE Statement-checklist of items, and the manuscript was prepared and revised according to the STROBE Statement-checklist of items.

Gilaad G Kaplan, Departments of Medicine and Community Health Sciences, University of Calgary, Calgary T2N4Z6, Canada

Corresponding author: Cyrla Zaltman, MD, PhD, Associate Professor, Postdoc, Division of Gastroenterology, Department of Internal Medicine, Clementino Fraga Filho Hospital, Federal University of Rio de Janeiro, Rodolpho Paulo Rocco Street 255, Ilha do Fundão, Rio de Janeiro 21940-230, Brazil. c.zaltman@gmail.com

Abstract

BACKGROUND

The etiology of inflammatory bowel disease (IBD) is unknown, but it is believed to be multifactorial. The hygiene hypothesis proposes that better hygiene conditions would lead to less infectious disease during childhood and favor the development of immune-mediated diseases.

AIM

To test the hygiene hypothesis in IBD by assessing the environmental risk factors associated with IBD development in different regions of Brazil with diverse socioeconomic development indices.

METHODS

A multicenter case-control study was carried out with 548 Crohn's disease (CD) and 492 ulcerative colitis (UC) outpatients and 416 healthy controls, from six IBD centers within different Brazilian states at diverse socioeconomic development stages. A semi-structured questionnaire with 87 socioeconomic and environmental questions was applied. Logistic regression model was created to assess the odds ratio (OR) with *P* value and 95% confidence intervals (CI).

RESULTS

Predictive variables for both diseases (CD and UC) were women [odd ratios (OR) = 1.31; OR = 1.69], low monthly family income (OR = 1.78; OR = 1.57), lower number of cohabitants (OR = 1.70; OR = 1.60), absence of vaccination (OR = 3.11; OR = 2.51), previous history of bowel infections (OR = 1.78; OR = 1.49), and family history of IBD (OR = 5.26; OR = 3.33). Associated risk factors for CD were age (18-39 years) (OR = 1.73), higher educational level (OR = 2.22), absence of infectious childhood diseases (OR = 1.99). The UC predictive variables were living in an urban area (OR = 1.62), inadequate living conditions (OR = 1.48) and former smokers (OR = 3.36). Appendectomy was a risk factor for CD (OR = 1.58) with inverse association with UC (OR = 4.79). Consumption of treated and untreated water was associated with risk of CD (OR = 1.38) and UC (OR = 1.53), respectively.

CONCLUSION

This is the first examining environmental exposures as risk factors for inflammatory bowel disease in Brazil. Most of the variables associated with disease risk support the role of the hygiene hypothesis in IBD development.

Key words: Crohn's disease; Ulcerative colitis; Risk factors; Environmental factors; Hygiene hypothesis

Core tip: Brazil is a country with continental dimensions comprising an ethnically diverse population living in different regions with extreme socioeconomic differences. The country is the perfect setting to test the hygiene hypothesis in inflammatory bowel disease development. Thus, the aim of this study was to identify inflammatory bowel disease environmental risk factors across different geographical regions in Brazil and evaluate if the hygiene hypothesis might explain interregional differences in prevalence and incidence.

Manuscript source: Unsolicited manuscript

Received: December 25, 2019
Peer-review started: December 25, 2019
First decision: January 19, 2020
Revised: June 16, 2020
Accepted: June 18, 2020
Article in press: June 18, 2020
Published online: July 7, 2020

P-Reviewer: Jha AK, Leong RWL
S-Editor: Zhang L
L-Editor: A
E-Editor: Zhang YL

Citation: Salgado VCL, Luiz RR, Boéchat NLF, Leão IS, Schorr BC, Parente JML, Lima DC, Silveira Júnior ES, Silva GOS, Almeida NP, Vieira A, de Bueno MLQ, Chebli JM, Bertges ÉR, Brugnara LMC, Junqueira Neto C, Campbell SBG, Discacciati LL, Cézar JPS, Nunes T, Kaplan GG, Zaltman C. Risk factors associated with inflammatory bowel disease: A multicenter case-control study in Brazil. *World J Gastroenterol* 2020; 26(25): 3611-3624
URL: https://www.wjgnet.com/1007-9327/full/v26/i25/3611.htm
DOI: https://dx.doi.org/10.3748/wjg.v26.i25.3611

INTRODUCTION

Inflammatory bowel disease (IBD) encompasses ulcerative colitis (UC) and Crohn's disease (CD), which are recurrent immune-mediated diseases characterized by a chronic inflammatory process that involves the gastrointestinal tract[1,2]. The etiology of IBD is unknown, but it is believed to be multifactorial. Many theories have been put forward regarding IBD development; these have emphasized interactions between genetic susceptibility (genome), individual immunological factors (immunome), gut microbiota (microbiome), and environmental exposure (exposome), starting at the time of intrauterine life and going through childhood to adulthood and acting as likely triggers for the disease[3-7].

IBD was initially recognized in Europe during the industrial revolution and today has substantially higher incidence and prevalence in developed countries[1]. Although Latin America, and especially Brazil, is considered to be a region of low prevalence and incidence, its incidence has increased over the past few years[3,8]. In Brazil, an incidence increase from 0.68 cases of CD per 100000 inhabitants in 1995 to 5.5 cases in 2015[3] has been reported[4]. Regarding prevalence, Brazilian studies such as the one conducted by Parente *et al*[5] in 2015 found a prevalence of 12.8 cases per 100000 inhabitants in the northeastern region, while Lima Martins *et al*[6] reported a prevalence of 38.2 cases per 100000 inhabitants in southeastern Brazil. Until the present study, no Brazilian epidemiological study encompassing the entire national territory had been undertaken[9-11].

It has been proposed in the hygiene hypothesis that better hygiene conditions would cause less infectious disease during childhood and favor the development of immune-mediated diseases[12]. The hygiene hypothesis could be explained by the impact of the presence or absence of epitope exposure to humans in a critical phase of immune system maturation, having long-lasting effects on immunity regulation. The incidence and prevalence rates of IBD might vary between countries. This can be explained by the interplay between different gene pools and distinct environmental factor exposure[2]. Good hygiene and basic sanitation conditions, high degree of industrial development, and absence of population agglomerations have been considered risk factors for the development of IBD[13].

Brazil is a country with continental dimensions comprising an ethnically diverse population living in different regions with extreme socioeconomic differences. The country is the perfect setting to test the hygiene hypothesis in IBD development. Thus, the aim of this study was to identify IBD environmental risk factors across different geographical regions in Brazil and evaluate if the hygiene hypothesis might explain interregional differences in prevalence/incidence.

MATERIALS AND METHODS

Study design and inclusion of patients

This was a multicenter case-control study with inclusion of IBD patients from 6 outpatient clinics in different Brazilian states: Federal University of Rio de Janeiro Hospital (Rio de Janeiro), Irmandade Santa Casa da Misericórdia of São Paulo (São Paulo) and Federal University of Juiz de Fora (Minas Gerais) representing the Southeastern region; Federal University of Brasília (Distrito Federal) representing the Central-western region; Federal University of Piauí (Piauí) and Roberto Santos General Hospital (Bahia) representing the Northeastern region. Patients enrolled in the study had an established diagnosis of IBD confirmed by standard clinical, endoscopic, radiologic and histologic criteria[14,15]. Subjects were between 18-80 years of age, either sex. All patients were included in the study between May 2015 and June 2017.

The control group consisted of individuals who were accompanying the patients

seen at the various outpatient clinics of these hospitals, who were healthy and did not have any kinship with the cases. The diagnosis of psychiatric diseases or disorders that would compromise the level of consciousness or comprehension was considered to be exclusion criteria in both groups. The sample size was determined as a convenience sample, according to the number of cases registered in these outpatient units.

Data collection and definitions

The semi-structured questionnaire was a translated and modified version of a Canadian questionnaire[13]. It consisted of 87 questions regarding a priori defined risk factors for the development of IBD, such as demographic and socioeconomic characteristics (age at enrolment, age at diagnosis, sex, ethnicity, migration, educational level, monthly income, living conditions, number of cohabitants, and rural or urban origin) and exposure variables (living with domestic animals, breast-feeding for at least 6 mo, consumption of treated water (filtered or boiled), vaccination (complete childhood vaccination card), contact with infectious and parasitic diseases (through laboratory tests), appendectomy, smoking, and family history of IBD with first degree relatives. Some of the variables evaluated referred to both childhood and adulthood before the diagnosis of IBD. Age at enrollment and age at diagnosis (self-reported by the cases) was stratified as follows: 18–39 years (< 40 years) and 40–80 years (> 40 years). The individuals included were divided according to ethnicity into white and non-white. Individuals were considered to be migrants when they moved from other states or country and as non-migrants when they were originated and lived all the time in the state where they were included in the study. In the evaluation of socioeconomic level, the educational level (elementary school, high school, higher education) and monthly family income (up to 3 minimum wages, 3 to 5 minimum wages, more than 5 minimum wages; using the amounts that were currently applicable at the time of the interview) were considered. Living conditions at childhood were defined as adequate when the home was constructed using bricks, had sewage collection, and piped water supply systems; otherwise, the residence was defined as inadequate. The number of cohabitants was evaluated at two times: During the interview (up to 1 cohabitant, 2 to 3, 4 to 8) and during childhood (1 to 3 cohabitants, 4 to 6, 7 or more). According to the 2010 census of the Brazilian Institute for Geography and Statistics[16], living in an urban area was considered to refer to state capitals, smaller towns, and more isolated urban areas. If these parameters were not met, the home in childhood was considered to be in a rural area. Exposure to tobacco was characterized into three subgroups: Current smokers (individuals who had been smoking more than 1 cigarette/day for at least 6 mo before the diagnosis), former smokers (individuals who had stopped smoking more than 6 mo before the diagnosis), and non-smokers (those who had never smoked) (World Health Organization Tobacco, United States, 2012)[17]. Appendectomy was taken into account when it had been done before the diagnosis of IBD.

Ethical aspects

Free and informed consent was obtained from each participating individual, and all data were analyzed anonymously; thus, preserving the participants' privacy. The study was approved by the Research Ethics Committee of each participating center and was conducted in accordance with the Declaration of Helsinki and Ordinance No. 196/96 of the Brazilian National Health Council.

Statistical analysis

The study design was a case control study that compared cases (CD and UC separately) versus non-IBD control population. Univariate analyses using multinomial logistic regression were employed to assess the association of environmental risk factors with CD and UC and controls. The covariates assessed in univariate analyses included state of residence, age at diagnosis, sex, ethnicity, migration, educational level, family income, living conditions in childhood, cohabitants at enrollment and in childhood, rurality, exposure to domestic animals in childhood, breastfeeding, consumption of treated water at enrollment and in childhood, vaccination, infection during childhood, history of worm disease, previous bowel infection, appendectomy, and smoking status at diagnosis. All variables that met statistical significance in the univariate analyses ($P < 0.05$) were included in the multiple multinomial logistic regression and were expressed as an odds ratio (OR) and P value < 0.05. All variables without statistical significance were excluded in the multiple multinomial logistic regression and the results were expressed as an odds ratio (OR) with 95% confidence interval (CI). The data analysis was conducted using the SPSS software, version 21.

Study was conducted in accordance with the Strengthening of Reporting of Observational Studies in Epidemiology statement[18].

RESULTS

Characteristics of the study population

The study population included 1.456 individuals: 548 with CD (37%), 492 with UC (34%), and 416 controls (29%). Table 1 shows the frequencies of the CD, UC, and control groups in the different states along with the associations shown by the cases (CD and UC) and controls in relation to the various variables analyzed.

Multinomial logistic regression

In univariate multinomial analysis there was a higher predominance of CD in the southeastern region, as observed in the states of Minas Gerais [odd ratios (OR) = 3.33; $P < 0.001$], São Paulo (OR = 2.99; $P < 0.001$) and Rio de Janeiro (OR = 2.18; $P < 0.001$) in comparison to the Federal District, the only reference center of the central-western region. The results from multiple multinomial analysis showed that there was a predominance of CD in southeastern Minas Gerais (OR = 2.61; *P* value 0.001) and São Paulo (OR = 2.41; *P* value 0.002). In univariate and multiple multinomial analysis, IBD family history was associated with a higher risk for CD (OR = 5.00; $P < 0.001$/OR = 3.03; $P < 0.001$) and UC (OR = 5.26; $P < 0.001$/ OR = 3.33; $P < 0.001$). There was an inverse association for appendectomy, where presence of appendectomy was considered to be a risk factor for CD (OR = 1.78; *P* value 0.025) and a protective factor in relation to UC (OR = 3.54; *P* value 0.002). The protective factor in UC was confirmed in the multiple multinomial analysis (OR = 4.89; $P < 0.001$) (Table 2 and 3).

Final multiple multinomial analysis

After excluding the variables of ethnicity, migration, number of cohabitants during childhood, exposure to domestic animals, breast-feeding, and history of worm diseases, which were not statistically significant ($P > 0.05$) in the multiple multinomial model, some important associations were detected (Table 4). A higher risk for CD was observed in Minas Gerais (OR = 2.68; 95%CI: 1.56-4.58), São Paulo (OR = 2.52; 95%CI: 1.48-4.28) and Rio de Janeiro (OR = 1.86; 95%CI: 1.11-3.07); thus, showing higher risk of CD in the southeastern region (higher socioeconomic status) compared with the other regions analyzed.

Considering the sociodemographic characteristics, patients with CD were predominantly women, (OR = 1.31; 95%CI: 0.56-1.00) and with age at enrollment below 40 years (OR = 1.73; 95%CI: 1.25-2.39). Socioeconomic risk factors were low monthly family income (OR = 1.78; 95%CI: 0.54-1.55) and higher education (OR = 2.22; 95%CI: 0.27-0.73). In UC, there was predominance of female sex (OR = 1.69; 95%CI: 0.44-0.78) and in socioeconomic aspects there was an association with low monthly family income (OR = 1.57; 95%CI: 0.45-1.35).

Regarding the environmental exposure variables for CD, 2–3 cohabitants in adulthood (OR = 1.70, 95%CI: 1.22-2.35), absence of vaccination during childhood (OR = 3.11; 95%CI: 1.82-5.29), absence of infectious childhood diseases (OR = 1.99; 95%CI: 1.20-3.26), consumption of treated water (OR = 1.38; 95%CI: 0.51-0.98) and history of bowel infections (OR = 1.78; 95%CI: 0.42-0.73) were risk factors for disease development. For UC, inadequate living conditions (OR = 1.48; 95%CI: 1.01-2.16), 2–3 cohabitants in adulthood (OR = 1.60; 95%CI: 1.15-2.21), living in an urban area (OR = 1.62; 95%CI: 1.16-2.25), consumption of untreated water (OR = 1.53; 95%CI: 1.11-2.11), absence of vaccination during childhood (OR = 2.51; 95%CI: 1.49-4.21), and history of bowel infections (OR = 1.49; 95%CI: 0.50-0.89) were risk factors for developing UC. Regarding exposure to tobacco, an association of risk between former smokers and CD could be observed (OR = 1.81; 95%CI: 1.06-3.05), but with considerably more significant risk when associated with UC (OR = 3.36; 95%CI: 1.91-5.90). Although not statistically significant, this analysis indicated an association between the risk of development of CD and appendectomy (OR = 1.58; 95%CI: 0.36-1.09) and higher risk of UC when individuals had not undergone appendectomy (OR = 4.79; 95%CI: 2.05-11.11). Family history of IBD showed a significant association with CD (OR = 5.26; 95%CI: 0.20-1.51) and UC (OR = 3.33; 95%CI: 0.14-1.23).

Table 1 Demographic, socioeconomic and environmental aspects of the groups studied (*n* = 1.456)

Characteristics		CD (*n* = 548)		UC (*n* = 492)		Controls (*n* = 416)	
		n	%	*n*	%	*n*	%
State of Brazil	Rio de Janeiro	145	26.5	100	20.3	86	20.7
	São Paulo	102	18.6	78	15.9	44	0.6
	Minas Gerais	98	7.9	57	11.6	38	9.1
	Bahia	59	0.8	69	14.0	76	8.3
	Piauí	82	5.0	92	18.7	92	2.1
	Federal District	62	1.3	96	19.5	80	9.2
Age at enrollment (yr)	< 40	267	8.7	159	32.3	162	8.9
	> 40	281	1.3	333	67.7	254	1.1
Age at Diagnosis (yr)	< 40	462	4.3	299	60.8	Not applicable	
	> 0	86	5.7	193	39.2		
Sex	Male	227	1.4	168	34.1	208	50.0
	Female	321	8.6	324	65.9	208	50.0
Ethnicity	White	263	8.0	189	38.4	143	34.4
	Non-white	285	2.0	303	61.6	273	65.6
Migration	No	348	3.5	297	60.4	266	63.9
	Yes	200	6.5	195	39.6	150	36.1
Educational level	Elementary school	182	3.2	228	46.3	177	42.5
	High school	264	8.2	202	41.1	183	44.0
	Higher education	102	8.6	62	12.6	56	13.5
Monthly family income (minimum wages)	Up to 3	244	4.5	253	51.4	159	38.2
	3 to 5	135	4.6	113	23.0	102	24.5
	5 or more	121	2.1	89	18.1	94	22.6
	Not stated	48	8.8	37	7.5	61	14.7
Living condition	Inadequate	336	61.3	359	73.0	266	63.9
	Adequate	212	8.7	133	27.0	150	36.1
Cohabitants (*n*)[2]	Up to 1	116	1.2	110	22.4	83	20.0
	2 to 3	299	4.6	252	51.2	186	44.7
	4 to 8	133	4.3	130	26.4	147	35.3
Cohabitants (*n*)[1]	1 to 3	106	9.3	58	11.8	51	12.3
	4 to 6	220	0.1	172	35.0	161	38.7
	7 or more	222	0.5	262	53.3	204	49.0
Rural living	No	356	5.0	266	54.1	223	3.6
	Yes	192	5.0	226	45.9	193	6.4
Exposure to domestic animal[1]	No	75	3.7	64	13.0	61	14.7
	Yes	473	86.3	428	87.0	355	85.3
Breastfeeding (for at least 6 mo)	No	42	7.7	21	4.3	23	5.5
	Yes	472	86.1	421	85.6	362	87.0
	Not stated	34	6.2	50	10.2	31	7.5
Consumption of treated water[1]	No	223	40.7	316	64.2	214	51.4
	Yes	325	59.3	176	35.8	202	48.6

Vaccination	No	62	11.3	71	14.4	26	6.3
	Yes	486	88.7	421	85.6	390	93.8
Infectious diseases[1]	No	65	11.9	41	8.3	29	7.0
	Yes	483	88.1	451	91.7	387	93.0
Worm disease	No	193	35.2	141	28.7	140	33.7
	Yes	355	64.8	351	71.3	276	66.3
Bowel infection	No	225	41.1	218	44.3	229	55.0
	Yes	323	58.9	274	55.7	187	45.0
Appendectomy	No	496	90.5	484	98.4	393	94.5
	Yes	52	9.5	8	1.6	23	5.5
Exposure to tobacco at diagnosis	Never	353	64.4	273	55.5	280	67.3
	Former	145	26.5	191	38.8	91	21.9
	Current	50	9.1	28	5.7	45	0.8
Familial IBD	No	438	79.9	430	87.4	393	94.5
	Yes	80	14.6	46	9.3	14	3.4
	Not stated	30	5.5	16	3.3	09	2.2

[1]Childhood.

[2]Adulthood. IBD: Inflammatory bowel disease; CD: Crohn's disease; UC: Ulcerative colitis.

DISCUSSION

In Brazil, studies on the incidence and prevalence of inflammatory bowel diseases have been regional, and studies investigating risk factors involved in the development of IBD are lacking[19]. Historically, the incidence and prevalence of IBD in Brazil have been low as compared with Western countries in Europe, North America, and Australia. However, at the turn of the 21st century, the incidence and prevalence of IBD in Brazil have steadily risen; paralleling the incidence of IBD in the West during the second half of the 20th century[3,9,10]. Our study indicates that environmental IBD risk factors may be driving the rising incidence of IBD in Brazil, some of which share similarities to IBD in the West, whereas others are clearly different. More importantly, the results confirm that the hygiene hypothesis might explain key differences in IBD epidemiology among states with diverse socioeconomic statuses.

This was the first multicenter study in Brazil and Latin America that evaluated potential risk factors associated with IBD development in geographical regions that present very different population and socioeconomic characteristics. For example, the population in the northeastern region presents the worst socioeconomic conditions, with low human socioeconomic development indexes (HDI) compared with the southeastern and central-western regions. Piauí, a state in northeastern Brazil, presents the lowest HDI (0.646 in 2010), in comparison with the southeastern states (HDI 0.783) and central-western states (HDI 0.824)[5]. The distribution of IBD in Brazil was heterogeneous with predominance of CD in the southeastern region (Minas Gerais, São Paulo and Rio de Janeiro), compared with the northeastern states (Piauí and Bahia), and a central-western state (Federal District). Brazil is a continental country, so this can be correlated with important climatic, sociocultural, and economic variations among different geographical regions.

In the West, sex predominance varies by age at diagnosis such that males have a higher risk of CD during childhood; however, in adolescence and adulthood women are more likely to be diagnosed with CD than men. In contrast, the incidence of UC does not differ between men or women until after the age of 45 whereas men have had a higher incidence of UC than women[20]. In Brazil, female sex was a risk factor both in CD and in UC in the present study. These data are contrary to Chinese and Hungarian studies yet consistent with Latin American studies and other few Brazilian regional studies[2,9,10,21,22]. Brazil is an ethnically diverse country, which makes it a unique country to study race within Latin America and its impact on disease. For example, the Northeastern region is a geographical area where African-descendant individuals

Table 2 Significant variables obtained from the comparative univariate and multiple multinomial logistic analysis between Crohn's disease and ulcerative colitis, with healthy control as reference

Characteristics		Univariate multinomial logistic model[1]				Multiple multinomial logistic model[1]			
		CD		UC		CD		UC	
		OR	*P* value	OR	*P* value	OR	*P* value	OR	*P* value
State of Brazil	Rio de Janeiro	2.18	< 0.001	0.97	0.881	1.84	0022	0.84	0.486
	São Paulo	2.99	< 0.001	1.48	0.107	2.41	0.002	1.27	0.399
	Min Minas Gerais	3.33	< 0.001	1.25	0.388	2.61	0.001	1.28	0.400
	Bahia	1.00	0.994	0.76	0.215	0.98	0.941	0.69	0.156
	Piauí	1.15	0.539	0.83	0.388	0.92	0.736	0.81	0.376
	Federal District	1		1		1		1	
Age at enrollment (yr)	< 40	1.49	0.003	0.75	0.038	1.75	0.001	1.14	0.462
	> 40	1		1		1		1	
Sex	Male	0.71	0.008	0.52	< 0.001	0.75	0.052	0.59	< 0.001
	Female	1		1		1		1	
Ethnicity	White	1.76	< 0.001	1.19	0.208	1.21	0.227	1.08	0.620
	Non-white	1		1		1		1	
Educational level	Elementary school	0.57	0.004	1.16	0.471	0.48	0.004	0.68	0.147
	High school	0.79	0.225	1.00	0.989	0.74	0.187	0.83	0.448
	Higher education	1		1		1		1	
Monthly family income (minimum wages)	Up to 3	1.19	0.304	1.68	0.004	1.79	0.007	1.61	0.032
	3 to 5	1.03	0.884	1.17	0.435	1.25	0.311	1.13	0.587
	5 or more	1		1		1		1	
	Not stated	0.61	0.038	0.64	0.081	0.94	0.826	0.77	0.350
Living condition	Inadequate	0.89	0.404	1.52	0.004	1.17	0.411	1.47	0.046
	Adequate	1		1		1		1	
Cohabitants (*n*)[3]	Up to 1	1.55	0.020	1.50	0.032	1.07	0.764	1.20	0.400
	2 to 3	1.78	< 0.001	1.53	0.006	1.67	0.002	1.57	0.007
	4 to 8	1		1		1		1	
Cohabitants (*n*)[2]	1 a 3	1.91	0.001	0.89	0.569	1.17	0.518	0.99	0.954
	4 a 6	1.26	0.109	0.83	0.201	1.02	0.887	0.90	0.514
	7 or more	1		1		1		1	
Rural living	No	1.61	< 0.001	1.02	0.890	1.37	0.080	1.66	0.004
	Yes	1		1		1		1	
Consumption of treated water[2]	No	0.65	0.001	1.70	< 0.001	0.71	0.037	1.52	0.012
	Yes	1		1		1		1	
Vaccination	No	1.91	0.008	2.53	< 0.001	3.08	< 0.001	2.46	0.001
	Yes	1		1		1		1	
Infectious disease[2]	No	1.80	0.012	1.21	0.444	1.99	0.007	1.44	0.178
	Yes	1		1		1		1	
Bowel infection	No	0.57	< 0.001	0.65	0.001	0.56	< 0.001	0.68	0.009
	Yes	1		1		1		1	
Appendectomy	No	0.56	0.025	3.54	0.002	0.63	0.103	4.89	< 0.001

	Yes	1		1		1		1	
Exposure to tobacco	Never	1.14	0.567	1.57	0.079	1.05	0.840	1.52	0.132
	Former	1.43	0.141	3.37	< 0.001	1.75	0.039	3.40	< 0.001
	Current	1		1		1		1	
Familial IBD	No	0.20	< 0.001	0.33	< 0.001	0.19	< 0.001	0.30	< 0.001
	Yes	1		1		1		1	
	Not stated	0.58	0.259	0.54	0.234	0.55	0.248	0.41	0.106

[1]Category of reference = healthy control.

[2]Childhood.

[3]Adulthood. IBD: Inflammatory bowel disease; CD: Crohn's disease; UC: Ulcerative colitis; OR: Odd ratios.

Table 3 Non-significant variables obtained from the comparative univariate and multiple multinomial logistic analysis between Crohn's disease and ulcerative colitis, with healthy control as reference

Characteristics		Univariate multinomial logistic model[1]				Multiple multinomial logistic model[1]			
		CD		UC		CD		UC	
		OR	*P* value	OR	*P* value	OR	*P* value	OR	*P* value
Migration	No	0.98	0.888	0.86	0.269	0.83	0.258	1.04	0.802
	Yes	1		1		1		1	
Exposure to domestic animal[2]	No	0.92	0.666	0.87	0.471	0.88	0.542	0.94	0.786
	Yes	1		1		1		1	
Breastfeeding	No	1.40	0.210	0.79	0.435	1.14	0.661	0.60	0.116
	Yes	1		1		1		1	
	Not stated	0.84	0.503	1.39	0.172	0.96	0.897	1.22	0.456
History of worm disease	No	1.07	0.613	0.79	0.105	0.99	0.946	0.81	0.187
	Yes	1		1		1		1	

[1]Category of reference = healthy control.

[2]Childhood. CD: Crohn's disease; UC: Ulcerative colitis; OR: Odd ratios.

predominate. Historically, epidemiological studies have reported higher prevalence of the disease in Caucasians than in black and Asian people[23-25]. In the present study, univariate analysis showed that white individuals predominated in the CD group; thus, corroborating a previous study conducted by this team in the state of Rio de Janeiro[19]. However, the results from the multivariate analysis did not show any statistical significance for CD and UC.

A positive association between higher educational and income levels and the development of IBD has already been verified[26]. However, this association was only partially confirmed in this study. Individuals who had higher educational levels, had also higher risk of developing IBD. However, individuals with lower family monthly incomes (up to 3 minimum wages)[27] had higher risk of developing IBD. In the present study, several proxy factors of the hygiene hypothesis were associated with the development of IBD. For example, low number of cohabitants during adulthood, living in an urban area, and absence of infectious childhood diseases showed a significant positive association with the development of CD and UC. Also, consumption of treated water during both phases of life was associated with CD, but not in patients with UC. These results corroborate the hygiene hypothesis, which may explain the lower incidence of IBD in South America, Africa, and Asia compared with developed countries[12,28].

In Brazil, disease prevention and health promotion policies for the population have obtained satisfactory results, with reduction of the prevalence of infectious diseases during childhood. Reassuringly, the results from the present study showed that there

Table 4 Comparative final multiple multinomial logistic model between the Crohn's disease and ulcerative colitis groups

Characteristics		Final multiple multinomial logistic model[1]			
		CD		UC	
		OR	95%CI	OR	95%CI
State of Brazil	Rio de Janeiro	1.86	1.11-3.07	0.85	0.52-1.37
	São Paulo	2.52	1.48-4.28	1.27	0.75-2.14
	Minas Gerais	2.68	1.56-4.58	1.30	0.75-2.25
	Bahia	0.86	0.51-1.45	0.71	0.43-1.16
	Piauí	0.88	0.54-1.43	0.84	0.53-1.31
	Federal District	1		1	
Age at enrollment (yr)	18 - 39	1.73	1.25-2.39	1.09	0.78-1.52
	40 - 80	1		1	
Sex	Male	0.76	0.56-1.00	0.59	0.44-0.78
	Female	1		1	
Educational level	Elementary school	0.45	0.27-0.73	0.67	0.39-1.12
	High school	0.70	0.45-1.09	0.84	0.52-1.33
	Higher education	1		1	
Monthly family income (minimum wages)	Up to 3	1.78	0.54-1.55	1.57	0.45-1.35
	3 to 5	1.21	1.16-2.70	1.14	1.02-2.40
	5 or more	1		1	
	Not stated	0.92	0.78-1.86	0.78	0.72-1.77
Living condition	Inadequate	1.15	0.79-1.66	1.48	1.01-2.16
	Adequate	1		1	
Cohabitants (*n*)[3]	Up to 1	1.09	0.72-1.65	1.24	0.82-1.87
	2 to 3	1.70	1.22-2.35	1.60	1.15-2.21
	4 to 8	1		1	
Rural living	No	1.33	0.95-1.86	1.62	1.16-2.25
	Yes	1		1	
Consumption of treated water	No	0.72	0.51-0.98	1.53	1.11-2.11
	Yes	1		1	
Vaccination	No	3.11	1.82-5.29	2.51	1.49-4.21
	Yes	1		1	
Infectious disease[2]	No	1.99	1.20-3.26	1.37	0.80-2.32
	Yes	1		1	
Bowel infection	No	0.56	0.42-0.73	0.67	0.50-0.89
	Yes	1		1	
Appendectomy	No	0.63	0.36-1.09	4.79	2.05-11.11
	Yes	1		1	
Exposure to tobacco	Never	1.08	0.66-1.76	1.50	0.87-2.57
	Former	1.81	1.06-3.05	3.36	1.91-5.90
	Current	1		1	
Familial IBD	No	0.19	0.20 -1.51	0.30	0.14-1.23

	Yes	1		1	
	Not stated	0.56	0.10-0.34	0.42	0.16-0.56

[1]After excluding the variables that were not statistically significant ($P > 0.05$) in the multiple model (category of reference = healthy controls).

[2]Childhood.

[3]Adulthood. CD: Crohn's disease; UC: Ulcerative colitis; OR: Odd ratios.

was no association between vaccination and higher risk of developing IBD, regardless of the geographical area analyzed. These findings confirm the results from a meta-analysis on 11 studies (with 2400 IBD cases and 34000 controls), which did not show any significant increase in IBD risk after immunization against BCG, diphtheria, tetanus, varicella, pertussis, measles, mumps, and rubella[29]. Despite improvements in hygiene conditions throughout Brazil, "favelas" (slum dwellings) are still present in urban centers. These "favelas" comprise marginal communities with precarious infrastructure and basic sanitation conditions, especially those in the interior areas of some states. These places favor occurrences of infectious gastroenteritis (*Campylobacter* sp, *Salmonella* sp, *Shigella* sp, *Yersinia* sp), which are possible triggers of IBD[30]. In the present study, a strong association was detected between infectious gastroenteritis and IBD, especially in relation to CD. However, since intestinal infections are not always confirmed through diagnostic methods, these episodes might possibly represent early symptoms of IBD.

Appendectomy prior to the diagnosis and smoking are considered to be risk factors that impact CD and UC differently. Appendectomy, especially if conducted before 10 years of age, has a negative association with UC[1,12,31]. This was confirmed in the present study. It has been postulated that appendices are bacterial reservoirs that are involved in regulation of immunological responses to the hosts' microbiota, and that the presence of environmental and microbial factors would promote higher activation of the Th1 pathway, with consequent development of appendicitis. This would explain the lower risk of developing UC, because the predominating immunological pathway is Th2[32]. Regarding CD, the results from the present study showed that there was a significant positive association with appendectomy. This finding, however, could be due to interpretation bias, since a diagnosis of CD that is made during the short-term postoperative period may lead to an erroneous initial diagnosis of appendicitis in cases of CD involving the appendicular or ileocecal region[33].

Smoking is a well-established environmental risk factor for IBD in the West. Smoking increases the risk of developing CD, whereas never smokers and those who quit smoking are more likely to develop UC. Smoking may modulate the risk of IBD by promoting epigenetic alterations that modify the genic expression that occurs in innate and adaptive immune responses and in alterations to the gut microbiome composition[34]. In the present study, smoking was negatively associated with UC, with a higher association among former smokers, which is consistent with data from the West[35] and studies from Asia[36]. In contrast, former and current smokers were not associated with the development of CD. This finding is inconsistent with studies from the West; however, an environmental risk factor study from the Asia-Pacific Crohn's and Colitis Epidemiology Study also showed that smoking was not associated with CD in Asian countries[37]. Taken together smoking may not be associated with CD in newly industrialized countries outside the Western world. Future studies are necessary to corroborate these findings in other developing countries.

An inherent methodological limitation of epidemiological studies is the information bias, a common occurrence in case-control studies. In this study, however, information on the exposure to risk factors was obtained through a structured questionnaire, with data collection standardization by the researchers. These practices tend to minimize this possibility. Regarding variables related to childhood, recall bias needs to be taken into consideration. Additionally, numerous environmental risk factors were studied and thus, the findings are limited by multiple comparison errors. The study was carried out in public IBD centers located in urban areas with cases that are usually more severe and are more difficult to diagnose. These cases do not represent the totality of the population with IBD that may be undergoing treatment in the private setting, in secondary care units, and in other regions of the country that were not included.

The IBD burden in South America, including Brazil, is increasing at a rate possibly even greater than other developing regions around the world. However, there is a paucity of high-quality epidemiological studies being necessary more powerful and

representative data to further explore modifiable risk factors and disease phenotypes[38].

In conclusion, this multicenter study from the southeastern, central-western, and northeastern regions of Brazil supports the hygiene hypothesis. Interestingly, several environmental risk factors are consistent with established risk factors within the West, whereas other environmental factors have distinctly different associations. Brazil is a large heterogeneous region that differs by demography, socioeconomic status, ethnicity, and healthcare support. Therefore, future studies are necessary to confirm the risk factor associations observed in the present study.

ARTICLE HIGHLIGHTS

Research background

The etiology of inflammatory bowel disease (IBD) is unknown, but it is believed to be multifactorial. The hygiene hypothesis proposes that better hygiene conditions would lead to less infectious disease during childhood and favor the development of immune-mediated diseases.

Research motivation

Brazil is a country with continental dimensions comprising an ethnically diverse population living in different regions with extreme socioeconomic differences. The country is the perfect setting to test the hygiene hypothesis in IBD development.

Research objectives

The aim of this study was to identify IBD environmental risk factors across different geographical regions in Brazil and evaluate if the hygiene hypothesis might explain interregional differences in prevalence/incidence.

Research methods

A multicenter case-control study with 548 Crohn's disease (CD), 492 ulcerative colitis (UC) outpatients, and 416 healthy controls. A semi-structured questionnaire with 87 socioeconomic and environmental questions was applied.

Research results

Predictive variables for both diseases (CD and UC) were women [odd ratios (OR) = 1.31; OR = 1.69], low monthly family income (OR = 1.78; OR = 1.57), lower number of cohabitants (OR = 1.70; OR = 1.60), absence of vaccination (OR = 3.11; OR = 2.51), previous history of bowel infections (OR = 1.78; OR = 1.49), and family history of IBD (OR = 5.26; OR = 3.33). Associated risk factors for CD were age (18-39 years) (OR = 1.73), higher educational level (OR = 2.22), absence of infectious childhood diseases (OR = 1.99). The UC predictive variables were living in an urban area (OR = 1.62), inadequate living conditions (OR = 1.48) and former smokers (OR = 3.36). Appendectomy was a risk factor for CD (OR = 1.58) with inverse association with UC (OR = 4.79). Consumption of treated and untreated water was associated with risk of CD (OR = 1.38) and UC (OR = 1.53), respectively.

Research conclusions

Most of the variables associated with disease risk support the role of the hygiene hypothesis in IBD development.

Research perspectives

Brazil is a large heterogeneous region that differs by demography, socioeconomic status, ethnicity, and healthcare support. Therefore, future studies are necessary to confirm the risk factor associations observed in the present study.

ACKNOWLEDGEMENTS

We would like to acknowledge Professor Bernstein, who kindly provided the original questionnaire that with some modifications allow the data collection that supported this study.

REFERENCES

1 **Frolkis A**, Dieleman LA, Barkema HW, Panaccione R, Ghosh S, Fedorak RN, Madsen K, Kaplan GG; Alberta IBD Consortium. Environment and the inflammatory bowel diseases. *Can J Gastroenterol* 2013; **27**: e18-e24 [PMID: 23516681 DOI: 10.1155/2013/102859]

2 **Ponder A**, Long MD. A clinical review of recent findings in the epidemiology of inflammatory bowel disease. *Clin Epidemiol* 2013; **5**: 237-247 [PMID: 23922506 DOI: 10.2147/CLEP.S33961]

3 **Kotze PG**, Underwood FE, Damião AOMC, Ferraz JGP, Saad-Hossne R, Toro M, Iade B, Bosques-Padilla F, Teixeira FV, Juliao-Banos F, Simian D, Ghosh S, Panaccione R, Ng SC, Kaplan GG. Progression of Inflammatory Bowel Diseases Throughout Latin America and the Caribbean: A Systematic Review. *Clin Gastroenterol Hepatol* 2020; **18**: 304-312 [PMID: 31252191 DOI: 10.1016/j.cgh.2019.06.030]

4 **Victoria CR**, Sassak LY, Nunes HR. Incidence and prevalence rates of inflammatory bowel diseases, in midwestern of São Paulo State, Brazil. *Arq Gastroenterol* 2009; **46**: 20-25 [PMID: 19466305 DOI: 10.1590/S0004-28032009000100009]

5 **Parente JM**, Coy CS, Campelo V, Parente MP, Costa LA, da Silva RM, Stephan C, Zeitune JM. Inflammatory bowel disease in an underdeveloped region of Northeastern Brazil. *World J Gastroenterol* 2015; **21**: 1197-1206 [PMID: 25632193 DOI: 10.3748/wjg.v21.i4.1197]

6 **Lima Martins A**, Volpato RA, Zago-Gomes MDP. The prevalence and phenotype in Brazilian patients with inflammatory bowel disease. *BMC Gastroenterol* 2018; **18**: 87 [PMID: 29914399 DOI: 10.1186/s12876-018-0822-y]

7 **Kaplan GG**, Ng SC. Understanding and Preventing the Global Increase of Inflammatory Bowel Disease. *Gastroenterology* 2017; **152**: 313-321.e2 [PMID: 27793607 DOI: 10.1053/j.gastro.2016.10.020]

8 **Ng SC**, Shi HY, Hamidi N, Underwood FE, Tang W, Benchimol EI, Panaccione R, Ghosh S, Wu JCY, Chan FKL, Sung JJY, Kaplan GG. Worldwide incidence and prevalence of inflammatory bowel disease in the 21st century: a systematic review of population-based studies. *Lancet* 2018; **390**: 2769-2778 [PMID: 29050646 DOI: 10.1016/S0140-6736(17)32448-0]

9 **Souza MH**, Troncon LE, Rodrigues CM, Viana CF, Onofre PH, Monteiro RA, Passos AD, Martinelli AL, Meneghelli UG. [Trends in the occurrence (1980-1999) and clinical features of Crohn's disease and ulcerative colitis in a university hospital in southeastern Brazil]. *Arq Gastroenterol* 2002; **39**: 98-105 [PMID: 12612713 DOI: 10.1590/s0004-28032002000200006]

10 **Zaltman C**. Inflammatory bowel disease: how relevant for Brazil? *Cad Saude Publica* 2007; **23**: 992-993 [PMID: 17486222 DOI: 10.1590/s0102-311x2007000500001]

11 **Delmondes LM**, Nunes MO, Azevedo AR, Oliveira MM, Coelho LE, Torres-Neto JD. Clinical and Sociodemographic Aspects of Inflammatory Bowel Disease Patients. *Gastroenterology Res* 2015; **8**: 207-215 [PMID: 27785298 DOI: 10.14740/gr649w]

12 **Ye Y**, Pang Z, Chen W, Ju S, Zhou C. The epidemiology and risk factors of inflammatory bowel disease. *Int J Clin Exp Med* 2015; **8**: 22529-22542 [PMID: 26885239]

13 **Bernstein CN**, Rawsthorne P, Cheang M, Blanchard JF. A population-based case control study of potential risk factors for IBD. *Am J Gastroenterol* 2006; **101**: 993-1002 [PMID: 16696783 DOI: 10.1111/j.1572-0241.2006.00381.x]

14 **Lennard-Jones JE**. Classification of inflammatory bowel disease. *Scand J Gastroenterol Suppl* 1989; **170**: 2-6; discussion 16-9 [PMID: 2617184 DOI: 10.3109/00365528909091339]

15 **Satsangi J**, Silverberg MS, Vermeire S, Colombel JF. The Montreal classification of inflammatory bowel disease: controversies, consensus, and implications. *Gut* 2006; **55**: 749-753 [PMID: 16698746 DOI: 10.1136/gut.2005.082909]

16 **Instituto Brasileiro de Geografia e Estatística (IBGE)**. Censo 2010. Available from: http://censo2010.ibge.gov.br

17 **World Health Organization Global Youth Tobacco Survey**. USA 2012. Available from: http://www.who int/tobacco/surveillance/gyts/em/index.html

18 **Vandenbroucke JP**, von Elm E, Altman DG, Gøtzsche PC, Mulrow CD, Pocock SJ, Poole C, Schlesselman JJ, Egger M; STROBE Initiative. Strengthening the Reporting of Observational Studies in Epidemiology (STROBE): explanation and elaboration. *Epidemiology* 2007; **18**: 805-835 [PMID: 18049195 DOI: 10.1097/EDE.0b013e3181577511]

19 **Salgado VCL**, Luiz RR, Boechat N, Schorr BC, Leão IS, Nunes T, Zaltman C. Crohn's disease environmental factors in the developing world: A case-control study in a statewide catchment area in Brazil. *World J Gastroenterol* 2017; **23**: 5549-5556 [PMID: 28852314 DOI: 10.3748/wjg.v23.i30.5549]

20 **Shah SC**, Khalili H, Gower-Rousseau C, Olen O, Benchimol EI, Lynge E, Nielsen KR, Brassard P, Vutcovici M, Bitton A, Bernstein CN, Leddin D, Tamim H, Stefansson T, Loftus EV Jr, Moum B, Tang W, Ng SC, Gearry R, Sincic B, Bell S, Sands BE, Lakatos PL, Végh Z, Ott C, Kaplan GG, Burisch J, Colombel JF. Sex-Based Differences in Incidence of Inflammatory Bowel Diseases-Pooled Analysis of Population-Based Studies From Western Countries. *Gastroenterology* 2018; **155**: 1079-1089.e3 [PMID: 29958857 DOI: 10.1053/j.gastro.2018.06.043]

21 **Zeng Z**, Zhu Z, Yang Y, Ruan W, Peng X, Su Y, Peng L, Chen J, Yin Q, Zhao C, Zhou H, Yuan S, Hao Y, Qian J, Ng SC, Chen M, Hu P. Incidence and clinical characteristics of inflammatory bowel disease in a developed region of Guangdong Province, China: a prospective population-based study. *J Gastroenterol Hepatol* 2013; **28**: 1148-1153 [PMID: 23432198 DOI: 10.1111/jgh.12164]

22 **Lakatos L**, Kiss LS, David G, Pandur T, Erdelyi Z, Mester G, Balogh M, Szipocs I, Molnar C, Komaromi E, Lakatos PL. Incidence, disease phenotype at diagnosis, and early disease course in inflammatory bowel diseases in Western Hungary, 2002-2006. *Inflamm Bowel Dis* 2011; **17**: 2558-2565 [PMID: 22072315 DOI: 10.1002/ibd.21607]

23 **Cosnes J**, Gower-Rousseau C, Seksik P, Cortot A. Epidemiology and natural history of inflammatory bowel diseases. *Gastroenterology* 2011; **140**: 1785-1794 [PMID: 21530745 DOI: 10.1053/j.gastro.2011.01.055]

24 **da Silva BC**, Lyra AC, Mendes CM, Ribeiro CP, Lisboa SR, de Souza MT, Portela RC, Santana GO. The Demographic and Clinical Characteristics of Ulcerative Colitis in a Northeast Brazilian Population. *Biomed*

Res Int 2015; **2015**: 359130 [PMID: 26509150 DOI: 10.1155/2015/359130]
25 **Liu JZ**, Anderson CA. Genetic studies of Crohn's disease: past, present and future. *Best Pract Res Clin Gastroenterol* 2014; **28**: 373-386 [PMID: 24913378 DOI: 10.1016/j.bpg.2014.04.009]
26 **Dutta AK**, Chacko A. Influence of environmental factors on the onset and course of inflammatory bowel disease. *World J Gastroenterol* 2016; **22**: 1088-1100 [PMID: 26811649 DOI: 10.3748/wjg.v22.i3.1088]
27 Instituto Brasileiro de Geografia e Estatística (IBGE)/Agência de notícias/ Síntese Indicadores Sociais. 2018. Available from: http://agenciadenoticias.ibge.gov.br
28 **Vargas RD**. Epidemiology of inflammatory bowel disease (IBD): Why are there differences between North America and Latin America? *Rev Col Gastroenterol* 2010; **25**: 103-105 Available from: http://www.redalyc.org/articulo.oa? id= 3377331597001. ISSN: 0120-9957
29 **Hansen TS**, Jess T, Vind I, Elkjaer M, Nielsen MF, Gamborg M, Munkholm P. Pineton de Chambrun G. UEG Week 2015 Poster Presentations. *Unit European Gastroenterol J* 2015; **3**: 146-687 [DOI: 10.1177/2050640615601623]
30 **Ananthakrishnan AN**. Environmental risk factors for inflammatory bowel disease. *Gastroenterol Hepatol (NY)* 2013; **9**: 367-374 [PMID: 23935543]
31 **Ananthakrishnan AN**. Environmental risk factors for inflammatory bowel diseases: a review. *Dig Dis Sci* 2015; **60**: 290-298 [PMID: 25204669 DOI: 10.1007/s10620-014-3350-9]
32 **Deng P**, Wu J. Meta-analysis of the association between appendiceal orifice inflammation and appendectomy and ulcerative colitis. *Rev Esp Enferm Dig* 2016; **108**: 401-410 [PMID: 27338627 DOI: 10.17235/reed.2016.4176/2015]
33 **Kaplan GG**, Jackson T, Sands BE, Frisch M, Andersson RE, Korzenik J. The risk of developing Crohn's disease after an appendectomy: a meta-analysis. *Am J Gastroenterol* 2008; **103**: 2925-2931 [PMID: 18775018 DOI: 10.1111/j.1572-0241.2008.02118.x]
34 **Biedermann L**, Brülisauer K, Zeitz J, Frei P, Scharl M, Vavricka SR, Fried M, Loessner MJ, Rogler G, Schuppler M. Smoking cessation alters intestinal microbiota: insights from quantitative investigations on human fecal samples using FISH. *Inflamm Bowel Dis* 2014; **20**: 1496-1501 [PMID: 25072500 DOI: 10.1097/MIB.0000000000000129]
35 **Calkins BM**. A meta-analysis of the role of smoking in inflammatory bowel disease. *Dig Dis Sci* 1989; **34**: 1841-1854 [PMID: 2598752 DOI: 10.1007/bf01536701]
36 **Ng SC**, Tang W, Leong RW, Chen M, Ko Y, Studd C, Niewiadomski O, Bell S, Kamm MA, de Silva HJ, Kasturiratne A, Senanayake YU, Ooi CJ, Ling KL, Ong D, Goh KL, Hilmi I, Ouyang Q, Wang YF, Hu P, Zhu Z, Zeng Z, Wu K, Wang X, Xia B, Li J, Pisespongsa P, Manatsathit S, Aniwan S, Simadibrata M, Abdullah M, Tsang SW, Wong TC, Hui AJ, Chow CM, Yu HH, Li MF, Ng KK, Ching J, Wu JC, Chan FK, Sung JJ; Asia-Pacific Crohn's and Colitis Epidemiology Study ACCESS Group. Environmental risk factors in inflammatory bowel disease: a population-based case-control study in Asia-Pacific. *Gut* 2015; **64**: 1063-1071 [PMID: 25217388 DOI: 10.1136/gutjnl-2014-307410]
37 **Vedamurthy A**, Ananthakrishnan AN. Influence of Environmental Factors in the Development and Outcomes of Inflammatory Bowel Disease. *Gastroenterol Hepatol (N Y)* 2019; **15**: 72-82 [PMID: 31011301]
38 **Selvaratnam S**, Gullino S, Shim L, Lee E, Lee A, Paramsothy S, Leong RW. Epidemiology of inflammatory bowel disease in South America: A systematic review. *World J Gastroenterol* 2019; **25**: 6866-6875 [PMID: 31885427 DOI: 10.3748/wjg.v25.i47.6866]

World Journal of Gastroenterology

Submit a Manuscript: https://www.f6publishing.com

World J Gastroenterol 2020 July 7; 26(25): 3625-3637

DOI: 10.3748/wjg.v26.i25.3625

ISSN 1007-9327 (print) ISSN 2219-2840 (online)

ORIGINAL ARTICLE

Retrospective Cohort Study

Predictors of irreversible intestinal resection in patients with acute mesenteric venous thrombosis

Shi-Long Sun, Xin-Yu Wang, Cheng-Nan Chu, Bao-Chen Liu, Qiu-Rong Li, Wei-Wei Ding

ORCID number: Shi-Long Sun 0000-0002-2943-6655; Xin-Yu Wang 0000-0002-7605-3091; Cheng-Nan Chu 0000-0001-9986-3508; Bao-Chen Liu 0000-0002-6944-1205; Qiu-Rong Li 0000-0002-5470-3161; Wei-Wei Ding 0000-0002-5026-689X.

Author contributions: Sun SL designed the study, collected the data, and wrote the manuscript; Wang XY and Chu CN performed data collection; Liu BC and Li QR were involved in data analysis; Ding WW made substantial contributions to the conception, design, funding acquisition, and coordination of the study and gave final approval of the version to be published; all authors have read and approved the final manuscript.

Supported by National Natural Science Foundation of China, No. 81770532; Jiangsu Province Medical Foundation for Youth Talents, China, No. QNRC2016901.

Institutional review board statement: This study was approved by the Ethics Committee of the Affiliated Jinling Hospital, Medical School of Nanjing University.

Informed consent statement: All involved subjects gave their informed consent (verbal) prior to study inclusion.

Shi-Long Sun, Xin-Yu Wang, Cheng-Nan Chu, Bao-Chen Liu, Qiu-Rong Li, Wei-Wei Ding, Division of Trauma and Surgical Intensive Care Unit, Research Institute of General Surgery, Jinling Hospital, Medical School of Nanjing University, Nanjing 210002, Jiangsu Province, China

Corresponding author: Wei-Wei Ding, MD, PhD, Doctor, Division of Trauma and Surgical Intensive Care Unit, Research Institute of General Surgery, Jinling Hospital, Medical School of Nanjing University, No. 305, East Zhongshan Road, Nanjing 210002, Jiangsu Province, China. dingwei_nju@hotmail.com

Abstract

BACKGROUND

Acute mesenteric venous thrombosis (AMVT) can cause a poor prognosis. Prompt transcatheter thrombolysis (TT) can achieve early mesenteric revascularization. However, irreversible intestinal ischemia still occurs and the mechanism is still unclear.

AIM

To evaluate the clinical outcomes of and to identify predictive factors for irreversible intestinal ischemia requiring surgical resection in AMVT patients treated by TT.

METHODS

The records of consecutive patients with AMVT treated by TT from January 2010 to October 2017 were retrospectively analyzed. We compared patients who required resection of irreversible intestinal ischemia to patients who did not require.

RESULTS

Among 58 patients, prompt TT was carried out 28.5 h after admission. A total of 42 (72.4%) patients underwent arteriovenous combined thrombolysis, and 16 (27.6%) underwent arterial thrombolysis alone. The overall 30-d mortality rate was 8.6%. Irreversible intestinal ischemia was indicated in 32 (55.2%) patients, who had a higher 30-d mortality and a longer in-hospital stay than patients without resection. The significant independent predictors of irreversible intestinal ischemia were Acute Physiology and Chronic Health Evaluation (APACHE) II score (odds ratio = 2.368, 95% confidence interval: 1.047-5.357, P = 0.038) and leukocytosis (odds ratio = 2.058, 95% confidence interval: 1.085-3.903, P = 0.027).

Conflict-of-interest statement: The authors declare that they have no conflicts of interest.

Data sharing statement: The original anonymous dataset is available on request from the corresponding author at dingwei_nju@hotmail.com.

STROBE statement: The authors have read the STROBE Statement-checklist of items, and the manuscript was prepared and revised according to the STROBE Statement-checklist of items.

Manuscript source: Invited manuscript

Received: March 11, 2020
Peer-review started: March 11, 2020
First decision: April 25, 2020
Revised: May 26, 2020
Accepted: June 9, 2020
Article in press: June 9, 2020
Published online: July 7, 2020

P-Reviewer: Derikx J
S-Editor: Zhang L
L-Editor: Wang TQ
E-Editor: Wang LL

Using the receiver operating characteristic curve, the cutoff values of the APACHE II score and leukocytosis for predicting the onset of irreversible intestinal ischemia were calculated to be 8.5 and 12 × 10^9/L, respectively.

CONCLUSION
Prompt TT could achieve a favorable outcome in AMVT patients. High APACHE II score and leukocytosis can significantly predict the occurrence of irreversible intestinal ischemia. Therefore, close monitoring of these factors may help with the early identification of patients with irreversible intestinal ischemia, in whom ultimately surgical resection is required, before the initiation of TT.

Key words: Acute mesenteric venous thrombosis; Transcatheter thrombolysis; Irreversible intestinal ischemia; Surgical resection; Acute Physiology and Chronic Health Evaluation II score; Leukocytosis

Core tip: Prompt transcatheter thrombolysis (TT) can achieve early mesenteric revascularization in acute mesenteric venous thrombosis (AMVT) patients. However, irreversible intestinal ischemia still occurs in many cases. We compared AMVT patients with irreversible intestinal ischemia who underwent TT to patients with reversible intestinal ischemia. We demonstrated that the independent predictors of irreversible intestinal ischemia were Acute Physiology and Chronic Health Evaluation II score and leukocytosis and the cutoff values were 8.5 and 12 × 10^9/L, respectively. Close monitoring of these factors may help with early identification of irreversible intestinal ischemia, which requires surgical resection, before initiation of TT in AMVT patients.

Citation: Sun SL, Wang XY, Chu CN, Liu BC, Li QR, Ding WW. Predictors of irreversible intestinal resection in patients with acute mesenteric venous thrombosis. *World J Gastroenterol* 2020; 26(25): 3625-3637
URL: https://www.wjgnet.com/1007-9327/full/v26/i25/3625.htm
DOI: https://dx.doi.org/10.3748/wjg.v26.i25.3625

INTRODUCTION

Acute mesenteric venous thrombosis (AMVT) accounts for approximately 5% to 15% of cases of acute mesenteric ischemia and has a mortality of up to 10%[1-3]. AMVT is characterized by an insidious onset, rapid progression, and non-specific abdominal signs in the early stages. The occurrence of irreversible intestinal ischemia impairs the outcomes of AMVT. In the short term, AMVT can cause intestinal necrosis, which predicts a poor outcome[4]. In the long term, postischemic intestinal stenosis (delayed intestinal stricture or non-transmural necrosis) impairs the quality of life[5].

The early diagnosis of AMVT has increased because of the feasible use of abdominal computed tomography (CT), with a specificity of 100% and sensitivity of 93%[6]. The main goal of treatment is early recanalization to prevent irreversible intestinal ischemia[7]. Immediate anticoagulation is the first step and the cornerstone of management strategies. Early anticoagulation has been demonstrated to result in > 80% recanalization and to reduce mortality[8,9]. However, a previous study also showed that systemic anticoagulation was associated with 25% of cases of extrahepatic portal vein hypertension, 18% of cases of transmural bowel infarction, and an elevated risk of bleeding[10,11]. Transcatheter thrombolysis (TT) is the mainstream method used, and it is recommended when there is persistent worsening of abdominal symptoms despite systemic anticoagulation or when there is a high risk of bowel infarction at admission[12]. Prompt recanalization, salvage of additional potentially reversible segments, and decreased intestinal resection can be achieved with endovascular treatment[12,13]. The use of endovascular therapy has increased significantly in the modern era and has altered the management of ASMVT[14]. However, damage control laparotomy including intestinal resection and open abdomen may be ultimately warranted for patients with intestinal necrosis and severe sepsis[15]. Our group previously advocated the establishment of an intestinal stroke center (ISC) and a

multidisciplinary stepwise management strategy for the treatment of AMVT, which have been proven to decrease the mortality and improve the clinical outcomes[16,17].

The mortality rates associated with intestinal resection ranged between 20% and 60%, and severe disability may result from either intestinal infarction or postischemic intestinal stenosis[18,19]. Some researchers revealed that aggressive TT could improve the outcomes[13,17]. However, irreversible intestinal ischemia is still the main reason for poor prognosis. The risk factors for irreversible intestinal ischemia are unknown, especially in AMVT patients treated by TT. The present study aimed to evaluate the clinical outcomes and determine the independent clinical, laboratory, and radiologic factors that can successfully predict irreversible intestinal ischemia leading to resection according to short- and long-term outcomes in AMVT patients treated by TT. The present study also aimed to discriminate patients who develop irreversible intestinal ischemia and who are in need of operative intervention from patients who have reversible bowel ischemia.

MATERIALS AND METHODS

Patients

Prospectively maintained records of patients with AMVT admitted to the ISC during the period from January 2010 to October 2017 were retrospectively reviewed. Ethical approval of the study was obtained from the Institutional Review Board. This study was conducted in accordance with the principles of the Declaration of Helsinki.

The diagnosis of AMVT was based on the following criteria: Acute clinical onset of abdominal symptoms with a duration of less than 4 wk before admission, vascular occlusion of the superior mesenteric vein (SMV) on CT or digital subtraction angiography (DSA) portography, and intestinal wall injury on CT[5,17]. AMVT patients who were treated by TT were included in the study (Figure 1). We excluded AMVT patients (1) whose symptoms improved after anticoagulation only; (2) with contraindications to thrombolysis; (3) who underwent hybrid emergency operation upon admission without TT; (4) who underwent surgical intervention before admission; (5) who participated in follow-up for < 1 year; and (6) with incomplete records or records missing some of the vital data required for the study.

The primary outcome was the resection of irreversible intestinal ischemic injury, defined by laparotomy and/or pathology assessment of bowel necrosis/infarction and postischemic intestinal stenosis (Figure 2). Patients were divided into two groups according to primary outcomes. Patients who recovered from AMVT after TT with no need for intestinal resection after 12 mo of follow-up were considered not to have irreversible intestinal ischemic injury, considering that irreversible intestinal ischemia could be ruled out at this point in follow-up. For primary outcome assessment, patients were followed until the date of irreversible ischemia diagnosis (for patients who underwent surgery), 1 year of follow-up (for patients who did not undergo surgery), or death, whichever came first.

Treatment strategy

A multidisciplinary stepwise management strategy was followed upon admission, aiming to achieve early mesenteric recanalization as described before[17]. Immediate anticoagulation, with the initiation of an unfractionated heparin bolus followed by continuous infusion, was initiated soon after the diagnosis was made. In addition, supportive treatment included broad-spectrum antibiotics, bowel rest, microcirculation improvement, and acidosis correction. Intensive care unit (ICU) treatment, including fluid resuscitation, multi-organ function support, and early enteral nutrition, was initiated when indicated.

Endovascular treatment by transcatheter thrombolysis

Endovascular treatment approaches were chosen depending on the location of the thrombus in the portal vein and superior mesenteric vein as described before[12,17]. For patients with patent or partially patent intrahepatic portal vein branches, a percutaneous transhepatic approach or trans-jugular intrahepatic portosystemic approach was preferred for direct thrombolysis of the portal vein (PV)-SMV thrombosis, and indirect thrombolysis alone *via* the superior mesenteric artery (SMA) was also adopted. Moreover, indirect thrombolysis alone *via* the SMA was adopted for patients with a completely occluded PV or portal vein cavernous transformation associated with superior mesenteric vein thrombosis. A catheter was placed in the vein under the guidance of DSA, and the thrombi were aspirated *via* the venous catheter.

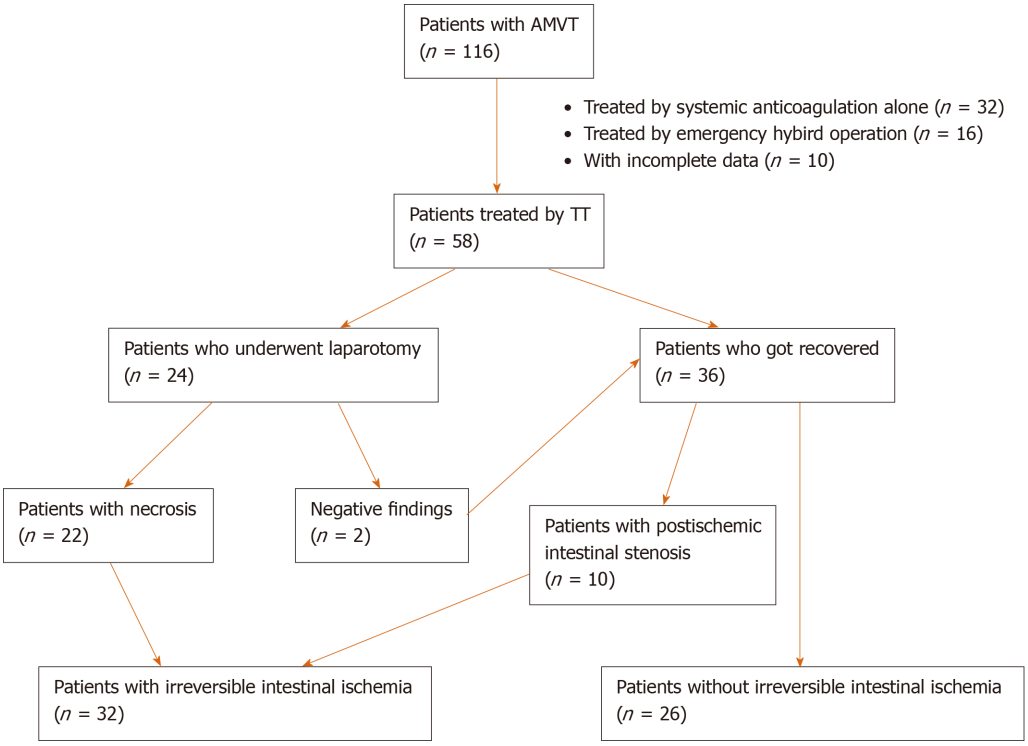

Figure 1 Flow diagram illustrating the management and outcome of patients with acute mesenteric venous thrombosis. AMVT: Acute mesenteric venous thrombosis; TT: Transcatheter thrombolysis.

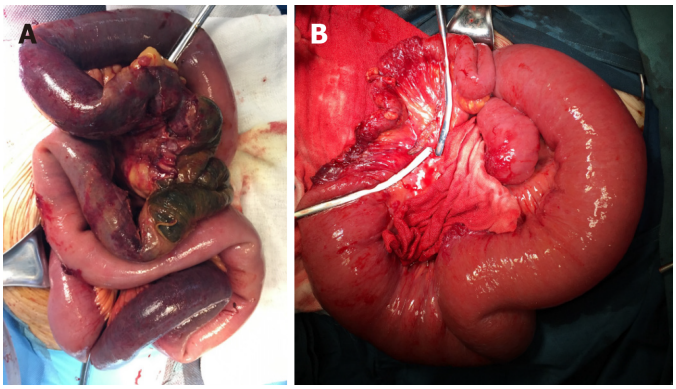

Figure 2 Operative findings of irreversible intestinal ischemia. A: Intestinal necrosis, characterized by gangrenous bowel; B: Postischemic intestinal stenosis, characterized by segmental intestinal stricture.

Low-molecular-weight heparin (4100 U/12 h) was administered as an anticoagulant. Urokinase [(40-60) × 10^4 IU/d] or recombinant tissue plasminogen activator (20 mg/d) was administered for 5 d for thrombolysis before angiography was repeated. If patients had stable vital signs and improved abdominal signs, thrombolytic treatment was continued for 1 wk. Contrast-enhanced abdominal CT and DSA were repeated to assess the abdominal and intestinal integrity. In patients who developed severe/diffuse peritonitis alongside worsening vital signs and hemodynamic instability, surgical intervention was required.

Surgical resection of irreversible intestinal ischemia

Damage control surgery was indicated during or after transcatheter thrombolytic therapy if there were signs of irreversible intestinal ischemia, including intestinal necrosis and postischemic intestinal stenosis[20,21](Figure 2).

Intestinal necrosis(Figure 2A)**:** Surgical procedures included resection of the necrotic bowel and reservation of the suspected necrotic small bowel. To determine the patency of the intestine, distal or proximal stomas were created. In the presence of

intraabdominal hypertension, the abdomen was left open. Abdominal closure was performed once the intraabdominal pressure returned to a normal range. Patients were transferred to the ICU following surgery, where patients received organ support therapy to restore homeostatic balance. A definite intestinal anastomosis was performed after the patient completely recovered from the acute phase and was on a full oral diet.

Postischemic intestinal stenosis(Figure 2B)**:** Close monitoring of postischemic intestinal stenosis was carried out in AMVT patients who got symptom alleviation after TT. Intolerance to enteral nutrition or oral diet, symptoms of ileus, and confirmed intestinal stricture by CT and enterography were used to help with the diagnosis. Close follow-up, anticoagulation, and corrections of malnutrition and water and electrolyte imbalance were initiated. Planned laparotomy was indicated, and resection of the irreversible stricture in the intestine was warranted.

Data collection

The collected data were as follows: Sex, age, thrombosis risk factors (*e.g.*, active smoking, history of thrombosis, history of abdominal surgery, and liver cirrhosis), thrombosis distribution, vital signs, hematochezia, results of abdominal examination, Acute Physiology and Chronic Health Evaluation (APACHE) II score, laboratory test values, findings of abdominal CT scanning on admission or before TT, length of stay, treatment outcomes (*i.e.*, length of resected bowel and 30-d and 1-year mortality) and complications [*i.e.*, sepsis, anastomotic or parastomal leakage, acute respiratory distress syndrome, acute kidney injury, and multiple organ dysfunction syndrome (MODS)].

Statistical analysis

Quantitative variables are expressed as the mean ± SD or median and interquartile range according to distributions after Shapiro-Wilk test. Categorical variables are expressed as absolute and relative frequencies. Comparisons between groups of independent quantitative variables were performed using Student's *t*-tests or Mann–Whitney tests. Comparisons between groups of qualitative variables were performed using the χ^2 test or Fisher's exact test when appropriate. A multivariate analysis of variables was conducted using a binary logistic regression test to determine the independent variables that predicted irreversible intestinal ischemia leading to resection, and the results are shown as odds ratios (ORs) and 95% confidence intervals (CIs). The accuracy of this model was further evaluated using a receiver operating characteristic (ROC) curve. A P value less than 0.05 was considered significant. All analyses were performed using SPSS version 17.0 software (SPSS Inc., Chicago, IL, United States).

RESULTS

Patient characteristics

From January 2010 to October 2017, a total of 58 consecutive patients [39 (67.2%) males] were included. The mean age of the patients was 45 ± 12.4 years. The patients' baseline characteristics are described in Table 1.

TT was initiated 28.5 h after systemic anticoagulation. A total of 42 (72.4%) patients underwent arteriovenous combined thrombolysis, and 16 (27.6) underwent arterial thrombolysis alone. After recanalization, exploratory laparotomies were performed in 24 patients, and 22 patients underwent resection of the infarcted intestine. In addition, planned laparotomy was also performed in 10 patients with postischemic intestinal stenosis later, and the involved stenosed bowel was resected. Eventually, 32 (55.2%) patients underwent resection of irreversible ischemic intestines, and 26 (44.8%) did not undergo resection.

There were no significant differences in age or sex between patients with and without irreversible intestinal ischemia (Table 1). Moreover, no significant difference was found in the thrombosis distribution or transcatheter thrombolytic therapy (including the initiation time, choice of thrombolytic approach, and duration of thrombolysis). Compared with patients with reversible ischemia, AMVT patients with irreversible intestinal ischemia had higher APACHE II scores (12.5 ± 3.9 *vs* 8.4 ± 3.5, $P < 0.001$). In addition, no significant difference was found in the associated morbidities or duration of symptoms from onset to admission between these two groups. In terms

Table 1 Characteristics of acute mesenteric venous thrombosis patients treated by transcatheter thrombolysis

Variable	All patients	Without resection	With resection	*P* value
	n = 58	*n* = 26	*n* = 32	
Age, yr, mean ± SD	45 ± 12.4	44.6 ± 10.4	47.6 ± 13.8	0.366
Male, *n* (%)	39 (67.2)	16 (61.5)	23 (71.9)	0.404
Location of thrombosis, *n* (%)				0.752
SMV	12 (20.7)	6 (23.1)	6 (18.8)	
SMV + PV	46 (79.3)	20 (76.9)	26 (81.3)	
Duration of anticoagulation alone before catheter-directed thrombolysis, h, median (IQR)	28.5 (22-54.8)	36 (22.8-72)	27 (18.8-48)	0.143
Thrombolytic approaches, *n* (%)				0.199
PT/TI-PV-SMV + SMA catheterization	42 (72.4)	21 (80.8)	21 (65.6)	
SMA catheterization alone	16 (27.6)	5 (19.2)	11 (34.4)	
Days of thrombolysis, d, mean ± SD	7.1 ± 2.9	6.7 ± 2.9	7.3 ± 2.8	0.421
APACHE II score, mean ± SD	10.6 ± 4.2	8.4 ± 3.5	12.5 ± 3.9	< 0.001
Associated comorbidities, *n* (%)				
Liver cirrhosis/portal hypertension	11 (19.0)	7 (26.9)	4 (12.5)	0.163
Splenectomy	10 (17.2)	7 (26.9)	3 (9.4)	0.078
History of other abdominal surgery	9 (15.5)	5 (19.2)	4 (12.5)	0.481
History of thrombosis	9 (15.5)	2 (7.7)	7 (21.9)	0.138
Active smoking	13 (22.4)	6 (23.1)	7 (21.9)	0.913
Alcohol abuse	7 (12.1)	3 (11.5)	4 (12.5)	0.911
Hypertension	6 (10.3)	2 (7.7)	4 (12.5)	0.550
Diabetes mellitus	2 (3.4)	0 (0)	2 (6.3)	0.197
Duration of symptoms from onset to admission, d, median (IQR)	7 (4-13)	7 (4-15)	7 (4-12)	0.333
Clinical presentation, *n* (%)				
Abdominal pain	53 (91.4)	23 (88.5)	30 (93.8)	0.475
Nausea and vomiting	28 (48.3)	12 (46.2)	16 (50.0)	0.771
Hematochezia	12 (20.7)	6 (23.1)	6 (18.8)	0.686
Local peritonitis	19 (32.8)	5 (19.2)	14 (43.8)	0.048

Quantitative variables are expressed as the mean ± SD or median and interquartile range (IQR). AMVT: Acute mesenteric venous thrombosis; SMV: Superior mesenteric vein; PV: Portal vein; SMA: Superior mesenteric artery; PT: Percutaneous transhepatic; TI: Trans-jugular intrahepatic; APACHE II: Acute Physiology and Chronic Health Evaluation II; IQR: Interquartile range.

of the clinical presentation, local peritonitis was significantly more often in patients with irreversible intestinal ischemia than in those with reversible ischemia (43.8% *vs* 19.2%, $P = 0.048$).

According to the results of the laboratory examinations (Table 2), patients with irreversible intestinal ischemia had significantly higher leukocyte counts as well as C-reactive protein, total bilirubin, serum albumin, serum creatinine, and arterial lactate levels than patients without resection ($P < 0.05$). The hemoglobin, platelet, procalcitonin, alanine aminotransferase, aspartate aminotransferase, and D-dimer levels were not significantly different between the groups of patients with and without irreversible intestinal ischemia. Compared to free intraperitoneal fluid, bowel dilation, bowel wall thickening, and misty mesentery, only decreased bowel wall enhancement (28.1% *vs* 7.7%, $P = 0.048$) was seen more frequently in AMVT patients with irreversible ischemia than in patients with reversible intestinal ischemia on the imaging examination.

Table 2 Laboratory and imaging examinations of acute mesenteric venous thrombosis patients treated by transcatheter thrombolysis

Variable	All patients	Without resection	With resection	*P* value
	n = 58	*n* = 26	*n* = 32	
Laboratory examination				
Total leukocyte count, × 10^9/L, mean ± SD	14.3 ± 8.9	7.1 ± 2.2	20.3 ± 7.9	< 0.001
Hemoglobin, g/L, mean ± SD	114.3 ± 29.8	117.7 ± 27.3	111.5 ± 31.9	0.451
PLT, × 10^9/L, mean ± SD	242.5 ± 160.7	287.8 ± 182.4	204.8 ± 131.4	0.056
Procalcitonin, μg/L, median (IQR)	0.25 (0.09-0.75)	0.14 (0.07-0.62)	0.42 (0.14-0.87)	0.096
CRP, mg/L, median (IQR)	59.8 (17.6-133.2)	19.0 (6.4-40.6)	120 (62.6-148.6)	< 0.001
Total bilirubin, μmol/L, mean ± SD	18.3 ± 15.5	13.6 ± 9.4	22.1 ± 18.4	0.035
ALT, U/L, median (IQR)	27 (36.3-51.9)	28 (17-43)	26 (14.5-38)	0.748
AST, U/L, median (IQR)	28 (20-38.8)	31 (21-42)	25 (19-36)	0.260
Serum albumin, g/L, mean ± SD	33.3 ± 5.2	35.8 ± 5.2	31.2 ± 4.2	0.001
D-dimer, μg/L, median (IQR)	5.6 (3.5-9.5)	3.9 (2.2-7.0)	6.5 (4.1-9.9)	0.081
Creatinine, μmol/L, mean ± SD	67.9 ± 35.6	57.3 ± 28.8	76.5 ± 38.7	0.040
Arterial lactate, mmol/L, mean ± SD	2.8 ± 0.9	2.1 ± 0.5	3.3 ± 0.8	< 0.001
Imaging Examination, *n* (%)				
Free peritoneal fluid	35 (60.3)	13 (50.0)	22 (68.8)	0.147
Bowel loop dilation	25 (43.1)	9 (34.6)	16 (50.0)	0.239
Decreased bowel wall enhancement	11 (19.0)	2 (7.7)	9 (28.1)	0.048
Bowel wall thickening	32 (55.2)	12 (45.2)	20 (62.5)	0.213
Misty mesentery	23 (39.7)	8 (30.8)	15 (46.9)	0.212

Quantitative variables are expressed as the mean ± SD or median and interquartile range (IQR). AMVT: Acute mesenteric venous thrombosis; PLT: Platelet count; CRP: C-reactive protein; ALT: Alanine aminotransferase; AST: Aspartate aminotransferase; IQR: Interquartile range.

Clinical outcomes and follow-up

The outcomes of these two groups according to the crude analysis are summarized in Table 3. Five patients died due to sepsis induced MODS during hospitalization and two died from cardiovascular accidents during follow-up. The following poor prognostic indicators demonstrated significantly higher rates in patients with intestinal resection than in those without: Sepsis and MODS ($P < 0.05$). Patients with reversible intestinal ischemia had shorter ICU stays (5.2 ± 3.9 *vs* 12.1 ± 7.7, $P < 0.001$) and hospital stays (16.6 ± 4.7 *vs* 31.9 ± 16.7, $P < 0.001$) than patients with irreversible intestinal ischemia. Although no significant difference was found in 1-year mortality, 30-d mortality showed a trend of higher mortality in patients with irreversible intestinal ischemia than in those without intestinal resection (15.6% *vs* 0; $P = 0.035$).

Predictors of irreversible intestinal ischemia leading to resection

Multivariable analysis using binary logistic regression showed that the significant independent predictors for irreversible intestinal ischemia leading to resection in AMVT patients treated by TT were leukocytosis (higher leukocyte count) (OR = 2.058, 95%CI: 1.085-3.903, $P = 0.027$) and APACHE II score (OR = 2.368, 95%CI: 1.047-5.357, $P = 0.038$) (Table 4). The overall area under the ROC curve of the model was 0.975 (95%CI: 0.936-1.000). Using the ROC curve, the cutoff values of the leukocyte count and APACHE II score for predicting the onset of irreversible intestinal ischemia were 12 × 10^9/L and 8.5, respectively (Table 5).

Table 3 Outcome and complications of acute mesenteric venous thrombosis patients treated by transcatheter thrombolysis

Variable	All patients	Without resection	With resection	*P* value
	n = 58	*n* = 26	*n* = 32	
Recanalization rate of SMV, *n* (%)				
Complete recanalization	33 (56.9)	16 (61.5)	17 (53.1)	0.520
Partial recanalization	13 (22.4)	6 (23.1)	7 (21.9)	0.913
Invalid	5 (8.6)	0 (0)	5 (15.6)	0.035
Cavernous transformation	7 (12.1)	4 (15.4)	3 (9.4)	0.485
Length of bowel resection, cm, median (IQR)	100 (60-150)	ND	100 (60-150)	ND
Short bowel syndrome, *n* (%)	1 (1.7)	0 (0)	1 (3.1)	0.552
Surgical site infection, *n* (%)	3 (5.2)	0 (0)	3 (9.4)	0.161
Sepsis, *n* (%)	9 (15.5)	1 (3.8)	8 (25.0)	0.028
Hemorrhage, *n* (%)	2 (3.4)	1 (3.8)	1 (3.1)	0.700
Anastomotic or parastomal leakage, *n* (%)	2 (3.4)	0 (0)	2 (6.3)	0.497
AKI, *n* (%)	2 (3.4)	0 (0)	2 (6.3)	0.497
ARDS, *n* (%)	2 (3.4)	0 (0)	2 (6.3)	0.497
Liver dysfunction, *n* (%)	2 (3.4)	0 (0)	2 (6.3)	0.497
MODS, *n* (%)	6 (10.3)	0 (0)	6 (18.8)	0.022
Time of ICU stay, d, mean ± SD	9.1 ± 7.2	5.2 ± 3.9	12.1 ± 7.7	< 0.001
Time of hospital stay, d, mean ± SD	25.2 ± 14.9	16.6 ± 4.7	31.9 ± 16.7	< 0.001
30-d mortality, *n* (%)	5 (8.6)	0 (0)	5 (15.6)	0.035
1-yr mortality, *n* (%)	7 (12.1)	1 (3.8)	6 (18.8)	0.090

Quantitative variables are expressed as the mean ± SD or median and interquartile range (IQR). ND: No data; AMVT: Acute mesenteric venous thrombosis; SMV: Superior mesenteric vein; AKI: Acute kidney injury; ARDS: Acute respiratory distress syndrome; MODS: Multiple organ dysfunction syndrome; ICU: Intensive care unit; IQR: Interquartile range.

Table 4 Binary logistic regression analysis of risk factors associated with irreversible intestinal ischemia leading to resection in acute mesenteric venous thrombosis patients treated by transcatheter thrombolysis

Variable	*P* value	ORs	95%CI
APACHE II score	0.038	2.368	1.047-5.357
Leukocyte count	0.027	2.058	1.085-3.903
C-reactive protein	0.875	-	-
Arterial lactate	0.661	-	-
Serum albumin	0.547	-	-

AMVT: Acute mesenteric venous thrombosis; APACHE II: Acute Physiology and Chronic Health Evaluation II; ORs: Odds ratio; CI: Confidence interval.

DISCUSSION

Acute mesenteric ischemia is an acute vascular emergency of the intestine that can also extend to involved parts of the colon[22]. Although AMVT is the least common form, accounting for 6% to 9% of acute mesenteric ischemia (AMI), mainly involving the SMV[5,23,24], the distinction between irreversible ischemia and a viable bowel is more difficult than in arterial mesenteric ischemia, and different pathophysiology is involved in these two diseases despite ultimately involving intestinal necrosis[7,21].

Table 5 Diagnostic value of the risk factors for diagnosis of irreversible intestinal ischemia in acute mesenteric venous thrombosis patients treated by transcatheter thrombolysis

Variable	AUC	Cut-off value	Sensitivity	Specificity	PPV	NPV	Youden index
APACHE II score	0.728	8.5	0.933	0.440	0.682	0.833	0.373
Leukocyte count	0.947	12×10^9	0.900	1	1	0.893	0.900

AMVT: Acute mesenteric venous thrombosis; APACHE II: Acute Physiology and Chronic Health Evaluation II; AUC: Area under curve; PPV: Positive predictive value; NPV: Negative predictive value.

Thus, the factors predictive of poor prognosis in AMVT should be distinguished from those in arterial mesenteric ischemia. However, limited to the rarity and the small number of AMI patients, predictors have often been generally analyzed in a large group of AMI patients[25-27]. Moreover, prompt treatment and early recognition of patients who need surgical intervention may help achieve a better outcome[13]. In this study, acute intestinal ischemia was reversed by TT in 26 (44.8%) patients, and the 30-d survival rate was 91.4%. Furthermore, we identified two factors from a multivariate analysis that were independent and easy to assess during the initial workup and were predictive of irreversible intestinal injury and the requirement of surgical resection (APACHE II > 8.5 and leukocytosis > 12×10^9/L). Close monitoring of these factors may help evaluate whether surgical resection of irreversible intestinal ischemia is ultimately required upon admission.

Patients with persistent symptoms, worsened abdominal pain after anticoagulation therapy, the development of signs of peritonitis, or a high risk of bowel infarction should initiate the multidisciplinary stepwise management[7,12]. According to the multidisciplinary stepwise management strategy in our ISC, initial catheter-directed thrombolysis was a preferred alternative for patients with local peritonitis[17]. A high risk of bleeding, confirmed intestinal necrosis or perforation, recent stroke, and primary or metastatic central nervous system malignancies are contraindications to thrombolysis[17]. Despite the beneficial effect of TT, emerging research has revealed the efficiency of preventing intestinal necrosis or salvaging more ischemic segments. Hollingshead *et al*[28] reported 20 patients treated by TT with symptom resolution in 85% of patients, and no patients required bowel resection[28]. In addition, in a series of pilot studies published by the intestinal stroke center in China, prompt endovascular treatment combined with damage control could improve the outcome[11,13,17]. In this research, among all AMVT patients, only those who were treated by TT were included. Although 32 (55.2%) patients, including 22 (37.9%) patients with intestinal necrosis and 10 (17.24%) with postischemic intestinal stenosis, required intestinal resection and approximately 100 cm-long segments of ischemic bowel were irreversibly resected, short bowel syndrome occurred only in 1 (1.7%) patient. Furthermore, the 30-d mortality and 1-year mortality rates were 8.6% and 12.1%, respectively.

The initiation of endovascular treatment is often suggested after 48-72 h of systemic anticoagulation[12]. The conditions of approximately 5% of AMVT patients who receive conservative treatment will deteriorate, and endovascular treatment should be initiated[29]. However, in this research, systemic anticoagulation could not improve conditions in 50% of patients, and TT was initiated 28.5 h after systemic anticoagulation. This may mainly be attributed to the severe conditions in most patients (32.8% of patients with local peritonitis). Signs of peritonitis have traditionally been considered an indication for prompt surgery[10]. However, in our research, we found that patients with local peritonitis could avoid surgical intervention. Patients with irreversible intestinal ischemia showed a significantly higher rate of peritonitis than patients with reversible intestinal injuries, but this higher rate was not independently associated with irreversible intestinal ischemia.

The APACHE II score is a severity-of-disease classification system and was designed to measure the severity of disease and predict mortality in adult patients admitted to the ICU. Fluid resuscitation, multi-organ function support, early enteral nutrition, and other special treatments in the ICU play pivotal roles in AMI treatment. In AMVT patients, the APACHE II score can also be used to evaluate the severity of illness. Wu *et al*[30] reported that a high APACHE II score was significantly associated with a poor prognosis in patients with necrotic bowel-induced hepatic portal venous gas[30]. Hsu *et al*[31] also reported that a high APACHE II score was significantly associated with a poor prognosis in AMI patients[31]. Similar findings in AMVT patients were also reported by Yang *et al*[17]. In this research, we found that a high score

was an independent predictive factor for irreversible intestinal ischemia leading to resection. Clinical awareness should be implemented in AMVT patients with a high APACHE II score (> 8.5) upon admission, even when TT is initiated; ultimately, surgical intervention may also be warranted in these patients.

In terms of the laboratory tests, patients with irreversible intestinal ischemia had higher total leukocyte counts as well as levels of C-reactive protein, total bilirubin, lactate, and creatinine. These results revealed that irreversible intestinal ischemia caused severe tissue hypoxia and that a systemic inflammatory response to irreversible ischemia and organ injury was initiated[25,27]. Moreover, intestinal dysfunction also impairs nutrition, which was reflected by decreased serum albumin levels in patients with irreversible intestinal ischemia. However, only leukocytosis independently predicted the onset of irreversible bowel ischemia in patients with AMVT treated by TT. A similar result was also reported by Emile[27]. Moreover, the onset of bowel ischemia, in general, is associated with profound leukocytosis[32], and a recent study found a total leucocyte count of more than 18000 as a cut-off point for bowel necrosis, as a significant predictor of mortality in AMI[33]. In this research, the cut-off point for irreversible intestinal ischemia was 12×10^9/L.

Although prompt TT can help achieve a better outcome, surgical intervention was still performed in 32 (55.2%) patients. Operative intervention is reserved for patients with severe and diffuse peritonitis and transmural bowel infarction or perforation[34]. In such severe cases, damage control surgery, such as bowel resection with open abdomen, is preferred over complex definitive procedures in order to reduce the second hit phenomenon[12,17,35]. In patients with intestinal necrosis, double-barrel enterostomy allows the observation of the color and vitality of the stoma, which provides an indirect assessment of the intestinal blood supply and avoids a second-look operation. Sometimes, temporary abdominal closure may be applied when there is severe bowel edema with a risk of intra-abdominal hypertension or abdominal compartment syndrome[15,36]. In the long term, AMVT can cause postischemic intestinal stenosis[37]. It tends to progressively worsen and ultimately result in total occlusion[38,39]. Correction of malnutrition and anticoagulation as well as surgical resection can be initiated in patients with postischemic intestinal stenosis[20,38,40]. In this study, 27 (84.4%) patients were discharged and the 1-year survival rate was 81.3%.

This study had some limitations. With regard to the rareness of this disease, a large randomized clinical trial seems difficult but is expected. This study, involving a total of 58 AMVT patients treated by TT, is a relatively large-scale study in the current literature. However, a multicenter prospective study is still warranted. Second, there is a lack of useful parameters that may also predict the onset of irreversible intestinal ischemia leading to resection in these patients. Third, checking for inherited or acquired thrombophilia is also warranted. For the two predictive factors, confirmation by further validation cohorts is necessary to allow clinicians and surgeons to draw generalizable conclusions.

Prompt TT can improve outcomes of AMVT. However, patients with irreversible intestinal ischemia manifest a higher risk of poor prognosis than patients with reversible injuries. The two independent predictors of irreversible intestinal ischemia leading to resection are an APACHE II score > 8.5 and a total leukocyte count > 12×10^9/L. When TT is promptly initiated, close monitoring of these factors can help discriminate AMVT patients in need of ultimately bowel resection from those who can be managed with conservative measures.

ARTICLE HIGHLIGHTS

Research background

Acute mesenteric venous thrombosis (AMVT) can cause a poor prognosis as a result of irreversible intestinal ischemia. Emerging studies revealed that prompt transcatheter thrombolysis (TT) can achieve early mesenteric revascularization and reverse early intestinal injury. However, irreversible intestinal ischemia still occurs in some cases.

Research motivation

Previous studies always involved both arterial and venous mesenteric ischemia. However, compared to arterial mesenteric ischemia, different pathophysiology is involved and it is more difficult to distinguish irreversible ischemia from viable bowels in venous mesenteric ischemia. What's more, AMVT can not only cause intestinal necrosis in the short term but also result in intestinal stenosis in the long

term, requiring intestinal resection. Limited to the rarity of AMVT, few studies have explored the predictive factors for irreversible intestinal ischemia, requiring surgical resection, in AMVT patients treated by TT.

Research objectives

This study aimed to identify predictive factors for irreversible intestinal ischemia in AMVT patients treated by TT.

Research methods

We retrospectively analyzed the data of 58 AMVT patients who underwent TT. To identify the predictive factors, AMVT patients treated by TT were divided into two groups: Patients with irreversible intestinal ischemia and those with reversible intestinal ischemia. Then, group comparisons and a multivariate binary logistic regression analysis were performed.

Research results

Thirty-two (55.2%) patients with irreversible intestinal ischemia had a higher 30-d mortality and a longer in-hospital stay than patients with reversible intestinal injuries. The significant independent predictors of irreversible intestinal ischemia were Acute Physiology and Chronic Health Evaluation (APACHE) II score (odds ratio = 2.368, 95% confidence interval: 1.047-5.357, P = 0.038) and leukocytosis (odds ratio = 2.058, 95% confidence interval: 1.085-3.903, P = 0.027). Using the receiver operating characteristic curve, the cutoff values of the APACHE II score and leukocytosis for predicting the onset of irreversible intestinal ischemia were calculated to be 8.5 and 12 × 10^9/L, respectively.

Research conclusions

Both total leukocyte count and APACHE II score are prognostic factors for irreversible intestinal ischemia in AMVT patients after initiation of TT.

Research perspectives

Both total leukocyte count and APACHE II score are common clinical parameters that are easily available to clinicians upon admission, and may be valuable predictors to discriminate AMVT patients treated by TT who will suffer from irreversible intestinal ischemia from those who can be managed with conservative measures.

REFERENCES

1 **Schoots IG**, Koffeman GI, Legemate DA, Levi M, van Gulik TM. Systematic review of survival after acute mesenteric ischaemia according to disease aetiology. *Br J Surg* 2004; **91**: 17-27 [PMID: 14716789 DOI: 10.1002/bjs.4459]

2 **Clair DG**, Beach JM. Mesenteric Ischemia. *N Engl J Med* 2016; **374**: 959-968 [PMID: 26962730 DOI: 10.1056/NEJMra1503884]

3 **Russell CE**, Wadhera RK, Piazza G. Mesenteric venous thrombosis. *Circulation* 2015; **131**: 1599-1603 [PMID: 25940967 DOI: 10.1161/CIRCULATIONAHA.114.012871]

4 **Kumar S**, Kamath PS. Acute superior mesenteric venous thrombosis: one disease or two? *Am J Gastroenterol* 2003; **98**: 1299-1304 [PMID: 12818273 DOI: 10.1111/j.1572-0241.2003.07338.x]

5 **Singal AK**, Kamath PS, Tefferi A. Mesenteric venous thrombosis. *Mayo Clin Proc* 2013; **88**: 285-294 [PMID: 23489453 DOI: 10.1016/j.mayocp.2013.01.012]

6 **Aschoff AJ**, Stuber G, Becker BW, Hoffmann MH, Schmitz BL, Schelzig H, Jaeckle T. Evaluation of acute mesenteric ischemia: accuracy of biphasic mesenteric multi-detector CT angiography. *Abdom Imaging* 2009; **34**: 345-357 [PMID: 18425546 DOI: 10.1007/s00261-008-9392-8]

7 **Björck M**, Koelemay M, Acosta S, Bastos Goncalves F, Kölbel T, Kolkman JJ, Lees T, Lefevre JH, Menyhei G, Oderich G, Esvs Guidelines Committee, Kolh P, de Borst GJ, Chakfe N, Debus S, Hinchliffe R, Kakkos S, Koncar I, Sanddal Lindholt J, Vega de Ceniga M, Vermassen F, Verzini F, Document Reviewers, Geelkerken B, Gloviczki P, Huber T, Naylor R. Editor's Choice - Management of the Diseases of Mesenteric Arteries and Veins: Clinical Practice Guidelines of the European Society of Vascular Surgery (ESVS). *Eur J Vasc Endovasc Surg* 2017; **53**: 460-510 [PMID: 28359440 DOI: 10.1016/j.ejvs.2017.01.010]

8 **Condat B**, Pessione F, Helene Denninger M, Hillaire S, Valla D. Recent portal or mesenteric venous thrombosis: increased recognition and frequent recanalization on anticoagulant therapy. *Hepatology* 2000; **32**: 466-470 [PMID: 10960436 DOI: 10.1053/jhep.2000.16597]

9 **Condat B**, Pessione F, Hillaire S, Denninger MH, Guillin MC, Poliquin M, Hadengue A, Erlinger S, Valla D. Current outcome of portal vein thrombosis in adults: risk and benefit of anticoagulant therapy. *Gastroenterology* 2001; **120**: 490-497 [PMID: 11159889 DOI: 10.1053/gast.2001.21209]

10 **Bergqvist D**, Svensson PJ. Treatment of mesenteric vein thrombosis. *Semin Vasc Surg* 2010; **23**: 65-68 [PMID: 20298951 DOI: 10.1053/j.semvascsurg.2009.12.008]

11 **Yang S**, Liu B, Ding W, He C, Wu X, Li J. Acute superior mesenteric venous thrombosis: transcatheter

thrombolysis and aspiration thrombectomy therapy by combined route of superior mesenteric vein and artery in eight patients. *Cardiovasc Intervent Radiol* 2015; **38**: 88-99 [PMID: 24934733 DOI: 10.1007/s00270-014-0896-z]

12 **Yang S**, Wu X, Li J. Transcatheter thrombolysis centered stepwise management strategy for acute superior mesenteric venous thrombosis. *Int J Surg* 2014; **12**: 442-451 [PMID: 24704749 DOI: 10.1016/j.ijsu.2014.03.015]

13 **Liu K**, Meng J, Yang S, Liu B, Ding W, Wu X, Li J. Transcatheter thrombolysis combined with damage control surgery for treatment of acute mesenteric venous thrombosis associated with bowel necrosis: a retrospective study. *World J Emerg Surg* 2015; **10**: 50 [PMID: 26516342 DOI: 10.1186/s13017-015-0045-2]

14 **Arthurs ZM**, Titus J, Bannazadeh M, Eagleton MJ, Srivastava S, Sarac TP, Clair DG. A comparison of endovascular revascularization with traditional therapy for the treatment of acute mesenteric ischemia. *J Vasc Surg* 2011; **53**: 698-704; discussion 704-5 [PMID: 21236616 DOI: 10.1016/j.jvs.2010.09.049]

15 **Ding W**, Wang K, Liu B, Fan X, Wang S, Cao J, Wu X, Li J. Open Abdomen Improves Survival in Patients With Peritonitis Secondary to Acute Superior Mesenteric Artery Occlusion. *J Clin Gastroenterol* 2017; **51**: e77-e82 [PMID: 28877534 DOI: 10.1097/MCG.0000000000000799]

16 **Corcos O**, Castier Y, Sibert A, Gaujoux S, Ronot M, Joly F, Paugam C, Bretagnol F, Abdel-Rehim M, Francis F, Bondjemah V, Ferron M, Zappa M, Amiot A, Stefanescu C, Leseche G, Marmuse JP, Belghiti J, Ruszniewski P, Vilgrain V, Panis Y, Mantz J, Bouhnik Y. Effects of a multimodal management strategy for acute mesenteric ischemia on survival and intestinal failure. *Clin Gastroenterol Hepatol* 2013; **11**: 158-65.e2 [PMID: 23103820 DOI: 10.1016/j.cgh.2012.10.027]

17 **Yang S**, Fan X, Ding W, Liu B, Meng J, Xu D, He C, Yu W, Wu X, Li J. Multidisciplinary stepwise management strategy for acute superior mesenteric venous thrombosis: an intestinal stroke center experience. *Thromb Res* 2015; **135**: 36-45 [PMID: 25466834 DOI: 10.1016/j.thromres.2014.10.018]

18 **Plessier A**, Rautou PE, Valla DC. Management of hepatic vascular diseases. *J Hepatol* 2012; **56** Suppl 1: S25-S38 [PMID: 22300463 DOI: 10.1016/S0168-8278(12)60004-X]

19 **Elkrief L**, Corcos O, Bruno O, Larroque B, Rautou PE, Zekrini K, Bretagnol F, Joly F, Francoz C, Bondjemah V, Cazals-Hatem D, Boudaoud L, De Raucourt E, Panis Y, Goria O, Hillaire S, Valla D, Plessier A. Type 2 diabetes mellitus as a risk factor for intestinal resection in patients with superior mesenteric vein thrombosis. *Liver Int* 2014; **34**: 1314-1321 [PMID: 24237969 DOI: 10.1111/liv.12386]

20 **Paraskeva P**, Akoh JA. Small bowel stricture as a late sequela of superior mesenteric vein thrombosis. *Int J Surg Case Rep* 2015; **6C**: 118-121 [PMID: 25544479 DOI: 10.1016/j.ijscr.2014.11.071]

21 **Harnik IG**, Brandt LJ. Mesenteric venous thrombosis. *Vasc Med* 2010; **15**: 407-418 [PMID: 20926500 DOI: 10.1177/1358863X10379673]

22 **Yang S**, Zhao Y, Chen J, Ni Q, Guo X, Huang X, Xue G, Zhang L. Clinical Features and Outcomes of Patients With Acute Mesenteric Ischemia and Concomitant Colon Ischemia: A Retrospective Cohort Study. *J Surg Res* 2019; **233**: 231-239 [PMID: 30502253 DOI: 10.1016/j.jss.2018.08.010]

23 **Rhee RY**, Gloviczki P. Mesenteric venous thrombosis. *Surg Clin North Am* 1997; **77**: 327-338 [PMID: 9146716 DOI: 10.1016/s0039-6109(05)70552-1]

24 **Brunaud L**, Antunes L, Collinet-Adler S, Marchal F, Ayav A, Bresler L, Boissel P. Acute mesenteric venous thrombosis: case for nonoperative management. *J Vasc Surg* 2001; **34**: 673-679 [PMID: 11668323 DOI: 10.1067/mva.2001.117331]

25 **Wang X**, Chu C, Sun S, Xie T, Duan Z, Wang K, Liu B, Fan X, Wu X, Ding W. Outcomes and clinical characteristics of transmural intestinal necrosis in acute mesenteric ischemia. *Scand J Gastroenterol* 2019; **54**: 953-959 [PMID: 31361977 DOI: 10.1080/00365521.2019.1646800]

26 **Nuzzo A**, Maggiori L, Ronot M, Becq A, Plessier A, Gault N, Joly F, Castier Y, Vilgrain V, Paugam C, Panis Y, Bouhnik Y, Cazals-Hatem D, Corcos O. Predictive Factors of Intestinal Necrosis in Acute Mesenteric Ischemia: Prospective Study from an Intestinal Stroke Center. *Am J Gastroenterol* 2017; **112**: 597-605 [PMID: 28266590 DOI: 10.1038/ajg.2017.38]

27 **Emile SH**. Predictive Factors for Intestinal Transmural Necrosis in Patients with Acute Mesenteric Ischemia. *World J Surg* 2018; **42**: 2364-2372 [PMID: 29387956 DOI: 10.1007/s00268-018-4503-3]

28 **Hollingshead M**, Burke CT, Mauro MA, Weeks SM, Dixon RG, Jaques PF. Transcatheter thrombolytic therapy for acute mesenteric and portal vein thrombosis. *J Vasc Interv Radiol* 2005; **16**: 651-661 [PMID: 15872320 DOI: 10.1097/01.RVI.0000156265.79960.86]

29 **Acosta S**, Alhadad A, Svensson P, Ekberg O. Epidemiology, risk and prognostic factors in mesenteric venous thrombosis. *Br J Surg* 2008; **95**: 1245-1251 [PMID: 18720461 DOI: 10.1002/bjs.6319]

30 **Wu JM**, Tsai MS, Lin MT, Tien YW, Lin TH. High APACHE II score and long length of bowel resection impair the outcomes in patients with necrotic bowel induced hepatic portal venous gas. *BMC Gastroenterol* 2011; **11**: 18 [PMID: 21385464 DOI: 10.1186/1471-230X-11-18]

31 **Hsu HP**, Shan YS, Hsieh YH, Sy ED, Lin PW. Impact of etiologic factors and APACHE II and POSSUM scores in management and clinical outcome of acute intestinal ischemic disorders after surgical treatment. *World J Surg* 2006; **30**: 2152-62; discussion 2163-4 [PMID: 17103101 DOI: 10.1007/s00268-005-0716-3]

32 **Sise MJ**. Mesenteric ischemia: the whole spectrum. *Scand J Surg* 2010; **99**: 106-110 [PMID: 20679047 DOI: 10.1177/145749691009900212]

33 **Akyıldız HY**, Sözüer E, Uzer H, Baykan M, Oz B. The length of necrosis and renal insufficiency predict the outcome of acute mesenteric ischemia. *Asian J Surg* 2015; **38**: 28-32 [PMID: 25183292 DOI: 10.1016/j.asjsur.2014.06.001]

34 **Riva N**, Donadini MP, Dentali F, Squizzato A, Ageno W. Clinical approach to splanchnic vein thrombosis: risk factors and treatment. *Thromb Res* 2012; **130** Suppl 1: S1-S3 [PMID: 23026649 DOI: 10.1016/j.thromres.2012.08.259]

35 **Jansen JO**, Loudon MA. Damage control surgery in a non-trauma setting. *Br J Surg* 2007; **94**: 789-790 [PMID: 17571297 DOI: 10.1002/bjs.5922]

36 **Waibel BH**, Rotondo MM. Damage control surgery: it's evolution over the last 20 years. *Rev Col Bras Cir* 2012; **39**: 314-321 [PMID: 22936231 DOI: 10.1590/s0100-69912012000400012]

37 **Eugène C**, Valla D, Wesenfelder L, Fingerhut A, Bergue A, Merrer J, Felsenheld C, Moundji A, Etienne

JC. Small intestinal stricture complicating superior mesenteric vein thrombosis. A study of three cases. *Gut* 1995; **37**: 292-295 [PMID: 7557585 DOI: 10.1136/gut.37.2.292]

38 **Takeuchi N**, Naba K. Small intestinal obstruction resulting from ischemic enteritis: a case report. *Clin J Gastroenterol* 2013; **6**: 281-286 [PMID: 23990850 DOI: 10.1007/s12328-013-0393-y]

39 **Yang XY**, Chen CX, Zhang BL, Yang LP, Su HJ, Teng LS, Li YM. Diagnostic effect of capsule endoscopy in 31 cases of subacute small bowel obstruction. *World J Gastroenterol* 2009; **15**: 2401-2405 [PMID: 19452586 DOI: 10.3748/wjg.15.2401]

40 **Nishimura N**, Yamamoto H, Yano T, Hayashi Y, Sato H, Miura Y, Shinhata H, Sunada K, Sugano K. Balloon dilation when using double-balloon enteroscopy for small-bowel strictures associated with ischemic enteritis. *Gastrointest Endosc* 2011; **74**: 1157-1161 [PMID: 21924719 DOI: 10.1016/j.gie.2011.07.024]

World Journal of Gastroenterology

Submit a Manuscript: https://www.f6publishing.com

World J Gastroenterol 2020 July 7; 26(25): 3638-3649

DOI: 10.3748/wjg.v26.i25.3638

ISSN 1007-9327 (print) ISSN 2219-2840 (online)

ORIGINAL ARTICLE

Retrospective Cohort Study

Functionality is not an independent prognostic factor for pancreatic neuroendocrine tumors

Hong-Yu Chen, Ya-Liang Zhou, Yong-Hua Chen, Xing Wang, Hao Zhang, Neng-Wen Ke, Xu-Bao Liu, Chun-Lu Tan

ORCID number: Hong-Yu Chen 0000-0003-1644-3327; Ya-Liang Zhou 0000-0002-4387-0917; Yong-Hua Chen 0000-0001-8485-0755; Xing Wang 0000-0003-3955-0686; Hao Zhang 0000-0002-0660-0117; Neng-Wen Ke 0000-0002-7135-2244; Xu-Bao Liu 0000-0002-6317-5284; Chun-Lu Tan 0000-0002-7315-1964.

Author contributions: Chen HY and Zhou YL contributed equally to this work; Liu XB, Tan CL, and Wang X designed the study; Chen HY, Zhou YL, Wang X, and Zhang H acquired the data; Chen HY, Zhou YL, and Wang X analyzed and interpreted the data; Chen HY and Zhou YL wrote the paper; Liu XB, Tan CL, and Chen YH critically revised the manuscript for important intellectual content; all authors have read and approved the version to be submitted.

Supported by 1.3.5 Project for Disciplines of Excellence, West China Hospital, Sichuan University, China, No. ZY2017302 1-3-5; and the Key Research and Development Projects of Sichuan Province, China, No. 2017SZ0132 and No. 2019YFS0042.

Institutional review board statement: This study was reviewed and approved by the West China Hospital Review

Hong-Yu Chen, Ya-Liang Zhou, Yong-Hua Chen, Xing Wang, Hao Zhang, Neng-Wen Ke, Xu-Bao Liu, Chun-Lu Tan, Department of Pancreatic Surgery, West China Hospital, Sichuan University, Chengdu 610041, Sichuan Province, China

Corresponding author: Chun-Lu Tan, MD, Associate Professor, Department of Pancreatic Surgery, West China Hospital, Sichuan University, No. 37, Guoxue Lane, Wuhou District, Chengdu 610041, Sichuan Province, China. chunlutan@163.com

Abstract

BACKGROUND

Pancreatic neuroendocrine neoplasms (pNENs) that produce hormones leading to symptoms are classified as functional tumors, while others are classified as nonfunctional tumors. The traditional view is that functionality is a factor that affects the prognosis of pNEN patients. However, as the sample sizes of studies have increased, researches in recent years have proposed new viewpoints.

AIM

To assess whether functionality is an independent factor for predicting the prognosis of pNEN patients.

METHODS

From January 2004 to December 2016, data of patients who underwent surgery at the primary site for the treatment of pNENs from the Surveillance, Epidemiology, and End Results (SEER) database and West China Hospital database were retrospectively analyzed.

RESULTS

Contemporaneous data from the two databases were analyzed separately as two cohorts and then merged as the third cohort to create a large sample that was suitable for multivariate analysis. From the SEER database, age ($P = 0.006$) and T stage ($P < 0.001$) were independent risk factors affecting the survival. From the West China Hospital database, independent prognostic factors were age ($P = 0.034$), sex ($P = 0.032$), and grade ($P = 0.039$). The result of the cohort consisting of the combined populations from the two databases showed that race ($P = 0.015$), age ($P = 0.002$), sex ($P = 0.032$) and T stage ($P < 0.001$) were independent prognostic factors. In the West China Hospital database and in the total

population, nonfunctional pNETs and other functional pNETs tended to have poorer prognoses than insulinoma. However, functionality was not associated with the survival time of patients with pNETs in the multivariate analysis.

CONCLUSION

Functionality is not associated with prognosis. Race, age, sex, and T stage are independent factors for predicting the survival of patients with pNETs.

Key words: Neuroendocrine tumors; Pancreatic neoplasms; Prognosis; Paraneoplastic endocrine syndromes; Multivariate analysis; Neoplasm staging

Core tip: Pancreatic neuroendocrine tumors (pNETs) are classified into functional and nonfunctional tumors according to the existence of hormones related symptoms or not. The traditional view is that functionality is correlated with the prognosis of pNET patients, which remains a controversial opinion. In this study, we retrospectively analyzed the clinicopathological data of 426 patients from the Surveillance, Epidemiology, and End Results database and 205 patients from the West China Hospital database. The results indicated that functionality is not associated with prognosis. Race, age, sex, and T stage are independent factors for predicting the survival of patients with pNETs.

Citation: Chen HY, Zhou YL, Chen YH, Wang X, Zhang H, Ke NW, Liu XB, Tan CL. Functionality is not an independent prognostic factor for pancreatic neuroendocrine tumors. *World J Gastroenterol* 2020; 26(25): 3638-3649
URL: https://www.wjgnet.com/1007-9327/full/v26/i25/3638.htm
DOI: https://dx.doi.org/10.3748/wjg.v26.i25.3638

INTRODUCTION

Pancreatic neuroendocrine neoplasms (pNENs) account for approximately 10% of primary pancreatic tumors and the incidence of pNENs has been increasing in recent decades[1]. Compared with pancreatic ductal adenocarcinoma, pNENs are generally considered a less aggressive tumor, which occur in relatively younger patients. Neuroendocrine neoplasms (NENs) include a heterogeneous group of neoplasms, and those which produce hormones leading to symptoms (*e.g.*, Whipple triad, Zollinger-Ellison syndrome, and carcinoid syndrome) are classified as functional tumors[2], while others that produce a series of substances without hormone related symptoms are classified as nonfunctional tumors[2,3].

The traditional view is that functionality is a factor that affects the prognosis of pNEN patients. Patients with functional tumors had a longer survival than those with nonfunctional tumors[4-6]. Tumors that secrete insulin and cause endogenous hyperinsulinemic hypoglycemia, namely, insulinomas, are believed to have a better prognosis among functional tumors, especially in the early stage[7], while patients with somatostatinoma and vipoma have been reported to have a relatively shorter survival[8].

However, as the sample sizes of studies have increased, researches in recent years have proposed new viewpoints. Due to the lack of specific symptoms, the majority of pNEN cases are diagnosed at a relatively advanced stage[1]. Therefore, nonfunctional pNENs are more likely to present with aggressive clinical manifestations[9,10], such as large diameter, increased age, high mitotic count, presence of neural invasion, extrapancreatic organ invasion or metastases, and advanced stage, which may lead to a poor prognosis[10,11]. Because of the rarity of pNENs and the low proportion of functional tumors, few studies have performed multivariate Cox regression analysis to show the effect of functionality on survival.

In the present study, we collected data from pNEN patients who underwent surgery at the primary site from the Surveillance, Epidemiology, and End Results (SEER) database and the West China Hospital database. The purpose of this study was to assess whether functionality is an independent factor to predict the prognosis of pNEN patients and explore the factors that influence the survival of these patients.

Board.

Informed consent statement: Study participants of the West China Hospital database provided written informed consent prior to study enrollment.

Conflict-of-interest statement: The authors declare no conflicts of interest.

Data sharing statement: No additional data are available.

STROBE statement: The authors have read the STROBE Statement, and the manuscript was prepared and revised according to the STROBE Statement.

Manuscript source: Unsolicited manuscript

Received: January 10, 2020
Peer-review started: January 10, 2020
First decision: March 6, 2020
Revised: May 8, 2020
Accepted: June 9, 2020
Article in press: June 9, 2020
Published online: July 7, 2020

P-Reviewer: Collin Y, Yang Z
S-Editor: Ma YJ
L-Editor: Wang TQ
E-Editor: Ma YJ

MATERIALS AND METHODS

SEER database

From January 2004 to December 2016, demographic, clinicopathological, and follow-up data of patients who underwent surgery for the treatment of pNENs were extracted from the SEER database using SEER*Stat software (version 8.3.5). The demographic data included age, race, and sex. The clinicopathological data included ICD-10 code, histology code, primary tumor location, tumor size, T, N, and M stages, pathologic grade, and surgery of the primary site. Survival data included survival months and vital status. Patients who underwent surgery other than pancreatectomy (local/partial resection, pancreaticoduodenectomy, or total pancreatectomy) were excluded.

West China Hospital database

Patients who underwent surgery with curative intent in West China Hospital between January 2004 and December 2016 with pathologically confirmed pNEN were included. Demographic, clinicopathological, and follow-up data of patients were retrospectively retrieved from the West China Hospital database. Patients with mixed neuroendocrine-non neuroendocrine neoplasms were not included. Patients were excluded if there was not enough information to determine the functionality of the tumor (n = 16). The follow-up deadline was August 2, 2019.

This study was approved by the West China Hospital Review Board under registration No. 2019 (124).

Pathologic grade and stage

The pathologic grade was evaluated using mitotic count and Ki-67 index according to the World Health Organization (WHO) 2017 classification[12]. The TNM stage of tumor was assessed following the 8th edition of the American Joint Committee on Cancer (AJCC) Cancer Staging Manual[13]. Patients with pathologic grade unavailable and patients with G3 pancreatic neuroendocrine tumors (pNETs) or pancreatic neuroendocrine carcinomas (pNECs) (mitotic count > 20, Ki-67 index > 20%, and/or previously diagnosed G3 tumor) were excluded from further analysis.

Functionality

Functionality was assessed according to whether hormone-related symptoms existed, regardless of the immunohistochemistry features. In addition to the nonfunctional pNEN group (N), functional pNENs were divided into two groups for further analysis: Insulinomas (I) and other functional pNENs (O).

Statistical analysis

SPSS version 23.0 (IBM Corporation, Chicago, IL) was employed to perform statistical analyses, and $P < 0.05$ was considered statistically significant. Continuous variables are reported in the form of the mean ± SE and were compared using the Student's t-test. Nominal data (race, primary site of tumor, sex, *etc.*) are presented as frequencies and percentages and were compared using χ^2 tests or Fisher's exact tests. The primary end point of this study was overall survival, which was measured from the date of tumor diagnosis to the date of last follow-up or death. Patients with (1) primary tumor unevaluated (Tx), (2) grade unevaluated (Gx), and/or (3) mitotic count higher than 20 or Ki-67 index higher than 20% (NET G3 or NEC) were not involved in the subsequent statistical analysis. After verification of the proportional hazard assumption, Cox proportional hazard models were constructed to identify factors that predicted the prognosis. All variables with a P value < 0.1 in the univariate analysis were used as input variables for the multivariate analysis which was performed using a forward stepwise method.

RESULTS

Patient characteristics

From the SEER database, a total of 426 patients were enrolled in this study. The baseline data are shown in Table 1. The mean age was 56.74 ± 0.67 years, and the male:female ratio was 221:205. There were 100 functional tumors (23.5%), including 52 insulinomas, 32 gastrinomas, 12 glucagonomas, 2 vipomas, and 2 somatostatinomas.

From the West China Hospital database, the mean age of the 205 patients was 48.16 ± 0.93 years. There were 88 males (42.9%) and 117 females (57.1%). One hundred and

Table 1 Characteristics of patients in the two databases, *n* (%)

Database	SEER database (*n* = 426)	West China Hospital database (*n* = 205)	*P* value
Race			NC
White	357 (83.8)	0 (0.0)	
Asian[1]	25 (5.9)	205 (100)	
Others[2]	44 (10.3)	0 (0.0)	
Tumor site			< 0.001
Head	104 (24.4)	85 (41.5)	
Body	51 (12)	55 (26.8)	
Tail	168 (39.4)	44 (21.5)	
Unknown	103 (24.2)	21 (10.2)	
Age (yr)			< 0.001
0-55	193 (45.3)	138 (67.3)	
56-	233 (54.7)	67 (32.7)	
Sex			0.035
Male	221 (51.9)	88 (42.9)	
Female	205 (48.1)	117 (57.1)	
Primary tumor			0.030[3]
T1	121 (28.4)	80 (39)	
T2	135 (31.7)	72 (35.1)	
T3	94 (22.1)	44 (21.5)	
T4	41 (9.6)	9 (4.4)	
Tx	35 (8.2)	0 (0)	
Regional lymph node metastasis			0.171[3]
N0	188 (44.1)	41 (20)	
N1	149 (35)	22 (10.7)	
Nx	89 (20.9)	142 (69.3)	
Distant metastasis			0.044[3]
M0	143 (33.6)	193 (94.1)	
M1	19 (4.5)	12 (5.9)	
Mx	264 (62)	0 (0)	
Grade			< 0.001[3]
pNET G1	229 (53.8)	90 (43.9)	
pNET G2	45 (10.6)	96 (46.8)	
pNET G3 or pNEC	16 (3.8)	9 (4.4)	
Gx	136 (31.9)	10 (4.9)	
Functionality			< 0.001
N	326 (76.5)	101 (49.3)	
I	52 (12.2)	85 (41.5)	
O	48 (11.3)	19 (9.3)	
Surgery			< 0.001[3]
Pancreaticoduodenectomy	143 (33.6)	39 (19)	

Total pancreatectomy	39 (9.2)	6 (2.9)
Partial pancreatectomy	203 (47.7)	88 (42.9)
Local excision	38 (8.9)	72 (35.1)
Other surgeries	3 (0.7)	0 (0)

[1]Consisting of Asian and Pacific Islander patients.

[2]Consisting of Black and American Indian patients and patients whose races were unknown.

[3]Rows with the title Tx, Nx, Mx, Gx, and other surgeries were not involved in the χ^2 test. SEER: Surveillance, epidemiology, and end results; NC: Not comparable; pNET: Pancreatic neuroendocrine tumor; pNEC: Pancreatic neuroendocrine carcinoma; I: Insulinoma; N: Nonfunctional pNEN; O: Other functional pNEN.

four (50.7%) patients had functional tumors including 85 insulinomas, 9 gastrinomas, 7 glucagonomas, 1 vipoma, 1 somatostatinoma, and 1 rare pNEN secreting adrenocorticotropic hormone (ACTH)[14]. Compared with the SEER database, patients in the West China Hospital database had fewer tumors of the pancreatic tail, were younger, had a lower T stage, fewer G2 tumors, and fewer distant metastases, and had more female patients ($P < 0.05$). Although the N stage was comparable in the two databases, the West China Hospital database had more patients with unevaluated N stage (Nx).

When we compared the characteristics of patients of different races (Table 2), the difference between the White and Asian populations was similar to the difference between the two datasets. In the other races, the ratio of male patients was higher, and the proportion of G3 pNETs or pNECs was higher than the respective values in the White and Asian populations. Survival curves of patients of different races from the two databases are shown in Figure 1.

Prognostic factors

Contemporaneous data from the two databases were analyzed separately as two cohorts and then merged as the third cohort to create a larger sample that was suitable for the univariate and multivariate analyses. Patients of races other than White or Asian and Pacific Islander, patients with primary tumor not assessed (Tx) or pathologic grade unevaluated (Gx), and patients who had G3 pNETs or pNECs were not enrolled in the subsequent analysis due to the limitations of the Cox regression model.

The univariate and multivariate analyses of the SEER cohort and the West China Hospital cohort are shown in Table 3. The two cohorts displayed similarities in the hazard ratios (HRs) of age, sex, T stage, regional lymph node metastasis, and distant metastasis, but showed differences in the HRs of primary site, grade, and functionality. In the multivariate analysis, the results of the SEER cohort showed that age (HR = 2.203, 95%CI: 1.249-3.884, $P = 0.006$) and T stage (HR = 2.589, 95%CI: 1.533-4.371, $P < 0.001$) were independent risk factors for predicting prognosis. The results of the West China Hospital cohort showed that age (HR = 4.558, 95%CI: 1.122-18.521, $P = 0.034$), sex (HR = 5.707, 95%CI: 1.161-28.057, $P = 0.032$), and grade (HR = 9.039, 95%CI: 1.118-73.051, $P = 0.039$) were independent prognostic factors.

In the cohort consisting of the combined populations from the two databases, factors that affected prognosis in the univariate analysis included country ($P = 0.002$), race ($P = 0.001$), age ($P < 0.001$), sex ($P = 0.005$), T stage ($P < 0.001$), regional lymph node metastasis (N1, $P = 0.036$), distant metastasis ($P < 0.001$), and functionality (nonfunctional pNETs, $P = 0.031$; other functional pNETs, $P = 0.012$). The multivariate proportional hazard model contained only race (HR = 0.438, 95%CI: 0.225-0.851, $P = 0.015$), age (HR = 2.315, 95%CI: 1.362-3.935, $P = 0.002$), sex (HR = 1.744, 95%CI: 1.049-2.899, $P = 0.032$), and T stage (HR = 2.612, 95%CI: 1.603-4.254, $P < 0.001$).

Effect of functionality on survival

In the West China Hospital database and in the total population, nonfunctional pNETs (West China Hospital database: HR = 1.473, 95%CI: 0.268-8.092, $P = 0.656$; total population: HR = 2.544, 95%CI: 1.090-5.938, $P = 0.031$) and other functional pNETs (West China Hospital database: HR = 7.913, 95%CI: 1.314-47.670, $P = 0.024$; total population: HR = 3.925, 95%CI: 1.359-11.337, $P = 0.012$) tended to have poorer prognoses than insulinoma. However, as shown in the multivariate analysis, functionality was not associated with the survival time of patients with pNETs since it was not selected into the model.

Table 2 Characteristics of patients of different races, *n* (%)

Race	White (*n* = 357)	Asian[1] (*n* = 230)	Others[2] (*n* = 44)	*P* value
Tumor site				< 0.001
Head	80 (22.4)	94 (40.9)	15 (34.1)	
Body	40 (11.2)	59 (25.7)	7 (15.9)	
Tail	153 (42.9)	48 (20.9)	11 (25)	
Unknown	84 (23.5)	29 (12.6)	11 (25)	
Age (yr)				< 0.001
0-55	156 (43.7)	150 (65.2)	25 (56.8)	
56-	201 (56.3)	80 (34.8)	19 (43.2)	
Sex				0.002
Male	162 (45.4)	130 (56.5)	30 (68.2)	
Female	195 (54.6)	100 (43.5)	14 (31.8)	
Primary tumor				0.073[3]
T1	98 (27.5)	89 (38.7)	14 (31.8)	
T2	117 (32.8)	79 (34.3)	11 (25)	
T3	79 (22.1)	51 (22.2)	8 (18.2)	
T4	35 (9.8)	10 (4.3)	5 (11.4)	
Tx	28 (7.8)	1 (0.4)	6 (13.6)	
Regional lymph node metastasis				0.094[3]
N0	157 (44)	53 (23)	19 (43.2)	
N1	128 (35.9)	25 (10.9)	18 (40.9)	
Nx	72 (20.2)	152 (66.1)	7 (15.9)	
Distant metastasis				0.054[3]
M0	119 (33.3)	202 (87.8)	15 (34.1)	
M1	16 (4.5)	12 (5.2)	3 (6.8)	
Mx	222 (62.2)	16 (7)	26 (59.1)	
Grade				< 0.001[3]
pNET G1	192 (53.8)	105 (45.7)	22 (50)	
pNET G2	42 (11.8)	98 (42.6)	1 (2.3)	
pNET G3 or pNEC	13 (3.6)	9 (3.9)	3 (6.8)	
Gx	110 (30.8)	18 (7.8)	18 (40.9)	
Functionality				< 0.001
N	277 (77.6)	117 (50.9)	33 (75)	
I	40 (11.2)	93 (40.4)	4 (9.1)	
O	40 (11.2)	20 (8.7)	7 (15.9)	
Surgery				< 0.001[3]
Pancreaticoduodenectomy	111 (31.1)	51 (22.2)	20 (45.5)	
Total pancreatectomy	33 (9.2)	7 (3)	5 (11.4)	
Partial pancreatectomy	179 (50.1)	96 (41.7)	16 (36.4)	
Local excision	31 (8.7)	76 (33)	3 (6.8)	
Other surgeries	3 (0.8)	0 (0)	0 (0)	

[1]Consisting of Asian and Pacific Islander patients.

[2]Consisting of Black and American Indian patients and patients whose races were unknown.

[3]Rows with the title Tx, Nx, Mx, Gx and other surgeries were not involved in the chi-square test. pNET: Pancreatic neuroendocrine tumor; pNEC: Pancreatic neuroendocrine carcinoma; I: Insulinoma; N: Nonfunctional pNEN; O: Other functional pNEN.

DISCUSSION

Compared with pancreatic ductal adenocarcinoma, pNETs are characterized by a lower incidence, younger age, and better prognosis[1]. According to morphological features, the WHO 2017 guidelines divide pNENs into biologically different groups, pNETs and pNECs. pNET cells have a fairly uniform, solid, trabecular, spiral or glandular patterned nucleus with pepper-salt chromatin and granular cytoplasm, while pNECs are similar to small or large cell neuroendocrine carcinomas of the lung[15]. Only pNETs can be divided into three different prognostic groups (G1, G2, and G3) according to mitotic count and Ki-67 index. Subsequently, the AJCC updated the staging system of pancreatic tumors[13]. PNET G1 and G2 are staged in a scheme that is similar to the European Neuroendocrine Tumor Society Consensus Guidelines staging system[16,17], while G3 pNETs and pNECs share the same staging system as pancreatic exocrine tumors.

pNENs were previously classified into several groups according to the existence and type of hormone related symptoms. The group, or rather, functionality was believed to be associated with the survival of patients with pNEN. Cienfuegos *et al*[4] performed a log-rank survival analysis on pNEN patients, and the results showed that the nonfunctioning tumor group had a relatively poor prognosis compared with the functioning tumor group (P = 0.052). Studies have indicated that functionality is positively related to the expression of somatostatin receptor 2[18] and negatively related to aurora kinase B[19], which may contribute to the improvement in survival. Wang *et al*[5] and Nanno *et al*[6] found that functionality is a prognostic factor affecting overall survival and disease-free survival in the results of univariate Cox regression analysis. However, the multivariate analysis was not carried out in the study by Wang *et al*[5] (due to the small sample size) and did not include functionality as a factor in the model in the study by Nanno *et al*[6] (only venous invasion and grade were used as input variables).

In recent years, studies have proposed new viewpoints. Studies[20,21] that included patients with NENs in almost all the locations suggested that functionality is not associated with progression-free survival[13] or disease-free survival[14]. However, there are differences in biological characteristics between NENs of lung origin and gastroenteropancreatic NENs: The majority of the functional NENs are carcinoid syndrome[20], while the functional tumors of gastroenteropancreatic NENs, especially pNENs, are mainly insulinomas[10].

Our results indicated that race, age, sex, and T stage were independent factors for predicting the survival of patients with pNETs. Although no significant differences were found in the effects of some factors on survival in the small sample cohorts, it does not mean that there is no relationship between these factors and survival. Only a sample that is large enough can reveal the real prognostic factor.

Functionality was correlated with survival in the univariate analysis, but was not associated with prognosis in the multivariate analysis. The prognosis of patients with nonfunctional tumors is generally considered to be poorer than that of patients with insulinoma. However, this is more likely related to the late diagnosis of patients with nonfunctional tumors, rather than the difference in biological properties between functional and nonfunctional tumors or the effect of hormones secreted by functional tumors. Hormone related syndrome is the only basis to distinguish between the nonfunctional neuroendocrine neoplasm and several types of functional neuroendocrine neoplasm. However, immunohistochemical staining also shows the expression of insulin/glucagon/gastrin/somatostatin in non-functional tumors. The reasonability of classification based on symptoms rather than gene expression needs to be further explored.

According to WHO guidelines, the assessment of grade depends on mitotic count and Ki-67 index, with a cutoff value of 2/10 high power fields and 3%, respectively. However, the cutoff values that make the most sense are still debatable. Some studies support that Ki-67 and mitotic count is correlated with prognosis[6,11], while there are also some studies that do not support this viewpoint[18]. In the Western China Hospital database, grade is an independent risk factor for prognosis. But in the SEER database, grade is not related to prognosis.

Table 3 Univariate and multivariate Cox proportional hazard regression analyses of predictors of survival in patients

Study population		SEER database		West China Hospital database			All population		
Variables		**HR (95CI)**	***P* value**	**HR (95%CI)**		***P* value**	**HR (95%CI)**		***P* value**
Univariate analysis									
Country									
United States							1.000		
China							0.326	(0.159, 0.665)	0.002
Race									
White	1.000						1.000		
Asian	0.402	(0.098, 1.652)	0.206				0.326	(0.169, 0.626)	0.001
Age (yr)									
Below 55	1.000			1.000			1.000		
Over 56	2.121	(1.204, 3.738)	0.009	4.224	(1.055, 16.919)	0.042	2.710	(1.606, 4.574)	< 0.001
Sex									
Female	1.000			1.000			1.000		
Male	1.822	(1.065, 3.119)	0.029	4.262	(0.878, 20.686)	0.072	2.067	(1.251, 3.415)	0.005
Primary site									
Head	1.000			1.000			1.000		
Body	2.077	(0.899, 4.800)	0.087	0.801	(0.146, 4.398)	0.799	1.651	(0.784, 3.479)	0.187
Tail	1.259	(0.616, 2.573)	0.527	1.193	(0.266, 5.349)	0.817	1.445	(0.769, 2.718)	0.253
Unknown	1.359	(0.598, 3.085)	0.464	0.000		0.987	1.491	(0.698, 3.187)	0.303
Primary tumor									
T1-2	1.000			1.000			1.000		
T3-4	2.515	(1.490, 4.246)	0.001	3.663	(0.980, 13.688)	0.054	2.858	(1.756, 4.651)	< 0.001
Regional lymph node metastasis									
N0	1.000			1.000			1.000		
N1	1.602	(0.918, 2.795)	0.097	2.757	(0.387, 19.630)	0.311	1.775	(1.040, 3.032)	0.036
Nx	0.911	(0.407, 2.038)	0.820	0.981	(0.186, 5.170)	0.982	0.585	(0.293, 1.167)	0.128
Distant metastasis									
M0	1.000			1.000			1.000		
M1	5.295	(1.804, 15.543)	0.002	3.423	(0.423, 27.705)	0.249	5.726	(2.269, 14.450)	< 0.001
Mx	1.993	(0.973, 4.079)	0.059				2.773	(1.551, 4.960)	0.001
Grade									
G1	1.000			1.000			1.000		
G2	1.418	(0.734, 2.739)	0.298	9.823	(1.224, 78.806)	0.032	1.266	(0.740, 2.166)	0.388
Functionality									
I	1.000			1.000			1.000		
N	1.924	(0.691, 5.353)	0.210	1.473	(0.268, 8.092)	0.656	2.544	(1.090, 5.938)	0.031
O	2.247	(0.600, 8.423)	0.230	7.913	(1.314, 47.670)	0.024	3.925	(1.359, 11.337)	0.012
Multivariate analysis									
Race									
White							1.000		
Asian							0.438	(0.225, 0.851)	0.015

Age									
Below 55	1.000			1.000			1.000		
Over 56	2.203	(1.249, 3.884)	0.006	4.558	(1.122, 18.521)	0.034	2.315	(1.362, 3.935)	0.002
Sex									
Female				1.000			1.000		
Male				5.707	(1.161, 28.057)	0.032	1.744	(1.049, 2.899)	0.032
Primary tumor									
T1-2	1.000						1.000		
T3-4	2.589	(1.533, 4.371)	< 0.001				2.612	(1.603, 4.254)	< 0.001
Grade									
G1				1.000					
G2				9.039	(1.118, 73.051)	0.039			

SEER: Surveillance, epidemiology, and end results; I: Insulinoma; N: Nonfunctional pNEN; O: Other functional pNEN.

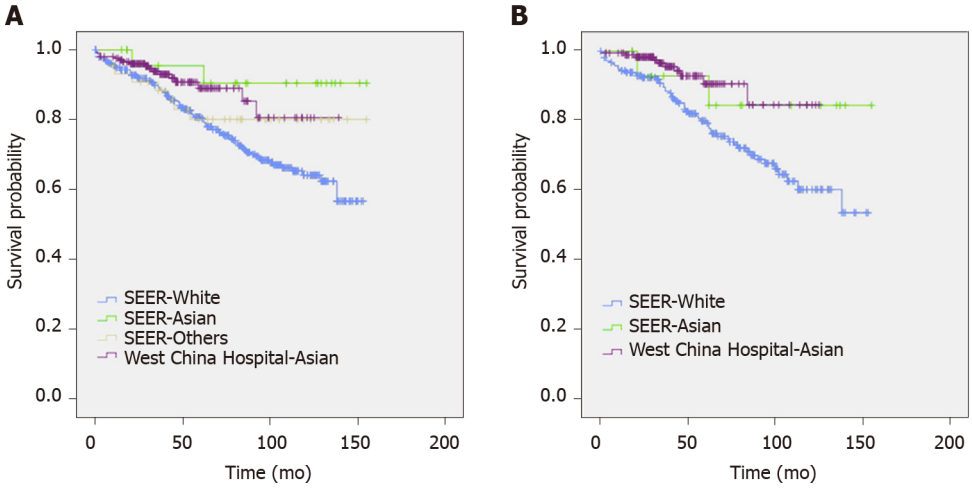

Figure 1 Survival functions of patients by database and race. A: Survival of patients enrolled; B: Survival of patients analyzed. SEER: Surveillance, epidemiology, and end results.

There was a trend of shorter survival time for patients with higher T stage in our small-sample cohort (n = 205), and T stage turned out to be an independent prognostic factor in large-sample cohorts (SEER, n = 426; total, n = 631), which is similar to the results of other studies[6,21]. On one hand, it indicated that T stage is indeed a factor that affects the prognoses of patients with pNETs; on the other hand, the results showed the importance of sample size in cohort study.

Data of the same period from the two databases were included in the analyses above. The distributions of N stage were comparable between the two datasets, but the populations from the two databases had differences in the distributions of primary tumor location, age, sex, T stage, M stage, grade, functionality, and surgery. Compared with the data in the SEER database (Table 1) and the results from other studies[4,5], the proportion of nonfunctional tumors was only approximately 50% in the West China Hospital database, indicating that some patients were not diagnosed and treated and that there is a need to advance the screening and early diagnosis of nonfunctional pNENs. Insulinomas accounted for only half of the functional tumors in the SEER database, while insulinomas accounted for the vast majority of functional pNENs in the West China Hospital database, which is similar to the results of Wang *et al*[5]. Local excision was performed more commonly in the West China Hospital database, especially before 2010, which led to a higher proportion of patients with no lymph nodes examined (Nx).

There were some limitations to this study: (1) Patients of the same time period were

enrolled from the two databases, and the inclusion/exclusion criteria were the same. However, SEER is a multicenter database, while the West China Hospital database is a single center database. The baseline data of the two datasets had differences in the distributions of some variables. Most of the data were demographic data or objective clinical data (such as tumor size and lymph node metastasis). The tumor grade depends on the mitotic count and Ki-67 index whose implementation may vary in different centers. Cox regression of the combined dataset may not represent the relationship between grade and prognosis; and (2) This study collected data from 2004 to 2016 retrospectively, and there is not sufficient information to separate poorly-differentiated pNECs from well-differentiated G3 pNETs in the SEER database. The TNM stages of G3 pNETs and pNECs may not have the same effect on survival as those of G1 and G2 tumors since they are completely different stage systems. Therefore, we excluded all tumors with mitotic counts higher than 20 or Ki-67 indexes higher than 20% (G3 pNETs and pNECs).

ARTICLE HIGHLIGHTS

Research background

Pancreatic neuroendocrine neoplasms (pNENs) that produce hormones leading to symptoms are classified as functional tumors, while others are classified as nonfunctional tumors.

Research motivation

The traditional view is that functionality affects the prognosis of pNEN patients. However, recent studies have proposed new viewpoints. Because of the rarity of pNENs and the low proportion of functional tumors, few studies have performed multivariate Cox regression to show the effect of functionality on survival.

Research objectives

To assess whether functionality is an independent factor for predicting the prognosis of pNEN patients.

Research methods

From January 2004 to December 2016, data of patients who underwent surgery at the primary site for the treatment of pNENs from the Surveillance, Epidemiology, and End Results (SEER) database and West China Hospital database were retrospectively analyzed.

Research results

From the SEER database, age and T stage were independent risk factors affecting the survival. From the West China Hospital database, independent prognostic factors were age, sex, and grade. The result of the cohort consisting of the combined populations from the two databases showed that race, age, sex, and T stage were independent prognostic factors. In the West China Hospital database and in the total population, nonfunctional pNETs and other functional pNETs tended to have poorer prognoses than insulinomas. However, functionality was not associated with the survival time of patients with pNETs in the multivariate analysis.

Research conclusions

Race, age, sex, and T stage are independent factors for predicting the survival of patients with pNETs. The results of this study do not support the opinion that hormone related syndrome is an efficacious tool to classify tumors into groups with different prognoses.

Research perspectives

Hormone related syndrome is the only basis to assess the functionality of neuroendocrine neoplasms. Nonfunctional tumors and functional tumors were reported to have different prognoses. However, they do not have much difference in pathologic feature or gene expression. Immunohistochemical staining also displays the expression of insulin/glucagon/gastrin/somatostatin in non-functional tumors. The reasonability of classification based on symptoms rather than gene expression needs to be further explored.

REFERENCES

1 **Wen J**, Chen J, Liu D, Xu X, Fan M, Zhang Z. The Eighth Edition of the American Joint Committee on Cancer Distant Metastases Stage Classification for Metastatic Pancreatic Neuroendocrine Tumors Might Be Feasible for Metastatic Pancreatic Ductal Adenocarcinomas. *Neuroendocrinology* 2020; **110**: 364-376 [PMID: 31357196 DOI: 10.1159/000502382]

2 **Jensen RT**, Cadiot G, Brandi ML, de Herder WW, Kaltsas G, Komminoth P, Scoazec JY, Salazar R, Sauvanet A, Kianmanesh R; Barcelona Consensus Conference participants. ENETS Consensus Guidelines for the management of patients with digestive neuroendocrine neoplasms: functional pancreatic endocrine tumor syndromes. *Neuroendocrinology* 2012; **95**: 98-119 [PMID: 22261919 DOI: 10.1159/000335591]

3 **Sorbye H**, Strosberg J, Baudin E, Klimstra DS, Yao JC. Gastroenteropancreatic high-grade neuroendocrine carcinoma. *Cancer* 2014; **120**: 2814-2823 [PMID: 24771552 DOI: 10.1002/cncr.28721]

4 **Cienfuegos JA**, Rotellar F, Salguero J, Ruiz-Canela M, Núñez Córdoba JM, Sola I, Benito A, Martí-Cruchaga P, Zozaya G, Pardo F, Hernández Lizoáin JL. A single institution's 21-year experience with surgically resected pancreatic neuroendocrine tumors: an analysis of survival and prognostic factors. *Rev Esp Enferm Dig* 2016; **108**: 689-696 [PMID: 27701882 DOI: 10.17235/reed.2016.4323/2016]

5 **Wang YH**, Lin Y, Xue L, Wang JH, Chen MH, Chen J. Relationship between clinical characteristics and survival of gastroenteropancreatic neuroendocrine neoplasms: A single-institution analysis (1995-2012) in South China. *BMC Endocr Disord* 2012; **12**: 30 [PMID: 23194346 DOI: 10.1186/1472-6823-12-30]

6 **Nanno Y**, Toyama H, Otani K, Asari S, Goto T, Terai S, Ajiki T, Zen Y, Fukumoto T, Ku Y. Microscopic venous invasion in patients with pancreatic neuroendocrine tumor as a potential predictor of postoperative recurrence. *Pancreatology* 2016; **16**: 882-887 [PMID: 27350059 DOI: 10.1016/j.pan.2016.06.008]

7 **de Herder WW**, Niederle B, Scoazec JY, Pauwels S, Kloppel G, Falconi M, Kwekkeboom DJ, Oberg K, Eriksson B, Wiedenmann B, Rindi G, O'Toole D, Ferone D; Frascati Consensus Conference; European Neuroendocrine Tumor Society. Well-differentiated pancreatic tumor/carcinoma: insulinoma. *Neuroendocrinology* 2006; **84**: 183-188 [PMID: 17312378 DOI: 10.1159/000098010]

8 **Peng SY**, Li JT, Liu YB, Fang HQ, Wu YL, Peng CH, Wang XB, Qian HR. Diagnosis and treatment of VIPoma in China: (case report and 31 cases review) diagnosis and treatment of VIPoma. *Pancreas* 2004; **28**: 93-97 [PMID: 14707737 DOI: 10.1097/00006676-200401000-00015]

9 **Morin E**, Cheng S, Mete O, Serra S, Araujo PB, Temple S, Cleary S, Gallinger S, Greig PD, McGilvray I, Wei A, Asa SL, Ezzat S. Hormone profiling, WHO 2010 grading, and AJCC/UICC staging in pancreatic neuroendocrine tumor behavior. *Cancer Med* 2013; **2**: 701-711 [PMID: 24403235 DOI: 10.1002/cam4.96]

10 **Han X**, Xu X, Jin D, Wang D, Ji Y, Lou W. Clinicopathological characteristics and prognosis-related factors of resectable pancreatic neuroendocrine tumors: a retrospective study of 104 cases in a single Chinese center. *Pancreas* 2014; **43**: 526-531 [PMID: 24658317 DOI: 10.1097/MPA.0000000000000065]

11 **You Y**, Jang JY, Kim SC, Yoon YS, Park JS, Cho CK, Park SJ, Yang JD, Lee WJ, Hong TH, Ahn KS, Jeong CY, Lee HK, Lee SE, Roh YH, Kim HJ, Kim H, Han IW. Validation of the 8th AJCC Cancer Staging System for Pancreas Neuroendocrine Tumors Using Korean Nationwide Surgery Database. *Cancer Res Treat* 2019; **51**: 1639-1652 [PMID: 30999719 DOI: 10.4143/crt.2019.023]

12 **Scoazec JY**, Couvelard A; Réseau TENpath. [Classification of pancreatic neuroendocrine tumours: Changes made in the 2017 WHO classification of tumours of endocrine organs and perspectives for the future]. *Ann Pathol* 2017; **37**: 444-456 [PMID: 29169836 DOI: 10.1016/j.annpat.2017.10.003]

13 **Bergsland EK**, Woltering EA, Rindi G, O'Dorisio TM, Schilsky RL, Liu EH, Kim MK, Nakakura EK, Reidy-Lagunes DL, Strosberg JR, Tang LH, Vinik AI, Wang YZ, Asare EA, Brierley JD, Bushnell DL, Jensen RT, Pommier RF, Wolin EM, Wong RKS, Klimstra DS. Amin MB. Neuroendocrine Tumors of the Pancreas. In: Amin MB. AJCC Cancer Staging Manual. 8th ed. New York: Springer-Verlag, 2016: 407-419

14 **Liu X**, Zou L, Yao W, Song B. Education and imaging. Hepatobiliary and Pancreatic: Pancreatic neuroendocrine neoplasm with pelvic metastases and ectopic ACTH production. *J Gastroenterol Hepatol* 2014; **29**: 1131 [PMID: 24832782 DOI: 10.1111/jgh.12589]

15 **Belotto M**, Crouzillard B, Araujo KO, Peixoto RD. Pancreatic Neuroendocrine Tumors: Surgical Resection. *Arq Bras Cir Dig* 2019; **32**: e1428 [PMID: 30758476 DOI: 10.1590/0102-672020180001e1428]

16 **Rindi G**, Klöppel G, Alhman H, Caplin M, Couvelard A, de Herder WW, Erikssson B, Falchetti A, Falconi M, Komminoth P, Körner M, Lopes JM, McNicol AM, Nilsson O, Perren A, Scarpa A, Scoazec JY, Wiedenmann B; all other Frascati Consensus Conference participants; European Neuroendocrine Tumor Society (ENETS). TNM staging of foregut (neuro)endocrine tumors: a consensus proposal including a grading system. *Virchows Arch* 2006; **449**: 395-401 [PMID: 16967267 DOI: 10.1007/s00428-006-0250-1]

17 **Rindi G**, Klöppel G, Couvelard A, Komminoth P, Körner M, Lopes JM, McNicol AM, Nilsson O, Perren A, Scarpa A, Scoazec JY, Wiedenmann B. TNM staging of midgut and hindgut (neuro) endocrine tumors: a consensus proposal including a grading system. *Virchows Arch* 2007; **451**: 757-762 [PMID: 17674042 DOI: 10.1007/s00428-007-0452-1]

18 **Wang Y**, Wang W, Jin K, Fang C, Lin Y, Xue L, Feng S, Zhou Z, Shao C, Chen M, Yu X, Chen J. Somatostatin receptor expression indicates improved prognosis in gastroenteropancreatic neuroendocrine neoplasm, and octreotide long-acting release is effective and safe in Chinese patients with advanced gastroenteropancreatic neuroendocrine tumors. *Oncol Lett* 2017; **13**: 1165-1174 [PMID: 28454229 DOI: 10.3892/ol.2017.5591]

19 **Briest F**, Wang Y, Arsenic R, Elezkurtaj S, Berg E, Greshake S, Lock AC, Hörsch D, Arnold CN, Hummel M, Siegmund B, Grabowski P. Immunohistochemical Study of Mitosis-regulatory Proteins in Gastroenteropancreatic Neuroendocrine Neoplasms. *Anticancer Res* 2018; **38**: 3863-3870 [PMID: 29970506 DOI: 10.21873/anticanres.12670]

20 **Baum RP**, Kulkarni HR, Singh A, Kaemmerer D, Mueller D, Prasad V, Hommann M, Robiller FC, Niepsch K, Franz H, Jochems A, Lambin P, Hörsch D. Results and adverse events of personalized peptide receptor radionuclide therapy with ^{90}Yttrium and ^{177}Lutetium in 1048 patients with neuroendocrine neoplasms. *Oncotarget* 2018; **9**: 16932-16950 [PMID: 29682195 DOI: 10.18632/oncotarget.24524]

21 **Slagter AE**, Ryder D, Chakrabarty B, Lamarca A, Hubner RA, Mansoor W, O'Reilly DA, Fulford PE,

Klümpen HJ, Valle JW, McNamara MG. Prognostic factors for disease relapse in patients with neuroendocrine tumours who underwent curative surgery. *Surg Oncol* 2016; **25**: 223-228 [PMID: 27566026 DOI: 10.1016/j.suronc.2016.05.019]

World Journal of Gastroenterology

Submit a Manuscript: https://www.f6publishing.com

World J Gastroenterol 2020 July 7; 26(25): 3650-3659

DOI: 10.3748/wjg.v26.i25.3650

ISSN 1007-9327 (print) ISSN 2219-2840 (online)

ORIGINAL ARTICLE

Retrospective Study

Chronic atrophic gastritis detection with a convolutional neural network considering stomach regions

Misaki Kanai, Ren Togo, Takahiro Ogawa, Miki Haseyama

ORCID number: Misaki Kanai 0000-0002-2227-1819; Ren Togo 0000-0002-4474-3995; Takahiro Ogawa 0000-0001-5332-8112; Miki Haseyama 0000-0003-1496-1761.

Author contributions: Kanai M and Togo R wrote the paper; Kanai M performed the majority of experiments and analyzed the data; Ogawa T and Haseyama M designed and coordinated the research.

Supported by JSPS KAKENHI Grant, No. JP17H01744.

Institutional review board statement: The study was reviewed and approved by the Institutional Review Board of The University of Tokyo Hospital.

Informed consent statement: Patients were not required to give informed consent to the study because the analysis used anonymous data that were obtained after each patient agreed to inspections by written consent.

Conflict-of-interest statement: The authors have no conflict of interest.

Data sharing statement: No additional data are available.

Misaki Kanai, Graduate School of Information Science and Technology, Hokkaido University, Sapporo 0600814, Hokkaido, Japan

Ren Togo, Education and Research Center for Mathematical and Data Science, Hokkaido University, Sapporo 0600812, Hokkaido, Japan

Takahiro Ogawa, Miki Haseyama, Faculty of Information Science and Technology, Hokkaido University, Sapporo 0600814, Hokkaido, Japan

Corresponding author: Ren Togo, Education and Research Center for Mathematical and Data Science, Hokkaido University, N-12, W-7, Kita-Ku, Sapporo 0600812, Hokkaido, Japan. togo@lmd.ist.hokudai.ac.jp

Abstract

BACKGROUND

The risk of gastric cancer increases in patients with *Helicobacter pylori*-associated chronic atrophic gastritis (CAG). X-ray examination can evaluate the condition of the stomach, and it can be used for gastric cancer mass screening. However, skilled doctors for interpretation of X-ray examination are decreasing due to the diverse of inspections.

AIM

To evaluate the effectiveness of stomach regions that are automatically estimated by a deep learning-based model for CAG detection.

METHODS

We used 815 gastric X-ray images (GXIs) obtained from 815 subjects. The ground truth of this study was the diagnostic results in X-ray and endoscopic examinations. For a part of GXIs for training, the stomach regions are manually annotated. A model for automatic estimation of the stomach regions is trained with the GXIs. For the rest of them, the stomach regions are automatically estimated. Finally, a model for automatic CAG detection is trained with all GXIs for training.

RESULTS

In the case that the stomach regions were manually annotated for only 10 GXIs and 30 GXIs, the harmonic mean of sensitivity and specificity of CAG detection

Manuscript source: Unsolicited manuscript

Received: February 10, 2020
Peer-review started: February 10, 2020
First decision: March 15, 2020
Revised: April 3, 2020
Accepted: June 18, 2020
Article in press: June 18, 2020
Published online: July 7, 2020

P-Reviewer: Abraham P, Cheng H, Vynios D
S-Editor: Zhang L
L-Editor: A
E-Editor: Ma YJ

were 0.955 ± 0.002 and 0.963 ± 0.004, respectively.

CONCLUSION
By estimating stomach regions automatically, our method contributes to the reduction of the workload of manual annotation and the accurate detection of the CAG.

Key words: Gastric cancer risk; Chronic atrophic gastritis; *Helicobacter pylori*; Gastric X-ray images; Deep learning; Convolutional neural network; Computer-aided diagnosis

Core tip: To construct a computer-aided diagnosis system, a method to detect chronic atrophic gastritis from gastric X-ray images (GXIs) with a patch-based convolutional neural network is presented in this paper. The proposed method utilizes two GXI groups for training: a manual annotation group and an automatic annotation group. The manual annotation group consists of GXIs for which we manually annotate the stomach regions, and the automatic annotation group consists of GXIs for which we automatically estimate the stomach regions. By utilizing GXIs with the stomach regions for training, the proposed method enables chronic atrophic gastritis detection that automatically eliminates the negative effect of the outside regions.

Citation: Kanai M, Togo R, Ogawa T, Haseyama M. Chronic atrophic gastritis detection with a convolutional neural network considering stomach regions. *World J Gastroenterol* 2020; 26(25): 3650-3659
URL: https://www.wjgnet.com/1007-9327/full/v26/i25/3650.htm
DOI: https://dx.doi.org/10.3748/wjg.v26.i25.3650

INTRODUCTION

Gastric cancer is the third leading cause of death in all types of malignancies behind lung cancer and colorectal cancer[1]. One of the major risk factors of gastric cancer is *Helicobacter pylori* (*H. pylori*)infection[2-4]. Chronic atrophic gastritis (CAG) induced by *H. pylori* leads to atrophic mucosa[5], which increases the risk of gastric cancer[6]. Moreover, it has been revealed that *H. pylori* eradication therapy is effective for the reduction of the risk of gastric cancer[7-9].

According to the International Agency for Research on Cancer, the number of new cases of gastric cancer in Eastern Asia accounts for more than half of those in the world. For the reduction of gastric cancer mortality, population-based screening for gastric cancer has been conducted through endoscopic and X-ray examinations in Japan[10]. Although the detection rate of early gastric cancer by endoscopic examination is higher than that by X-ray examination[11], mass screening using endoscopic examination has some problems, *e.g.*, a limit to the number of patients who can be examined[12]. Therefore, in Japan, endoscopic examination is often performed for cases in which something unusual is found by X-ray examination[13]. However, the interpretation of gastric X-ray images (GXIs) requires sufficient experience and knowledge, and there is a shortage of doctors who are skilled in diagnosis[10]. The development of computer-aided diagnosis (CAD) systems is needed to help doctors who do not have sufficient experience and knowledge.

For realizing CAD systems, researchers have been exploring methods for CAG detection from GXIs[14-17]. In early works, attempts were made to describe the visual features of CAG with mathematical models[14,15]. For more accurate detection, in the papers[16,17], we have tried to introduce convolutional neural networks (CNNs)[18] since it has been reported that CNNs outperform methods with hand-crafted features in various tasks[19-21]. We adopted a CNN that was trained on patches obtained by dividing original images, *i.e.*, a patch-based CNN, to preserve detailed textures of GXIs since they had high resolutions. In our previous investigation[17], we focused on the outside patches of the stomach since textures of these patches do not depend on the image-level ground truth (GT), *i.e.*, CAG or non-CAG. In clinical settings, GXIs generally have only the image-level GT. Therefore, we introduced manual annotation

of stomach regions for all GXIs used in training and assigned the patch-level class labels based on the image-level GT and the stomach regions. Although the previously reported method already achieved high detection performance (sensitivity: 0.986, specificity: 0.945), there remains a problem. In general, CNNs require a large number of labeled images for training to determine millions of parameters that can capture the semantic contents of images. However, manually annotating stomach regions for a large number of GXIs is time- and labor-consuming. In other words, the previous method can practically utilize only a small number of GXIs even in the case of numerous GXIs being available for training.

In this paper, we propose a novel CAG detection method that requires manual annotation of stomach regions for only a small number of GXIs. The main contribution of this paper is the effective use of stomach regions that are manually annotated for a part of GXIs used in training. We assume that distinguishing the inside and outside patches of the stomach is much easier for patch-based CNNs than distinguishing whether the patches are extracted from CAG images or non-CAG images. Therefore, we newly introduce the automatic estimation of stomach regions for non-annotated GXIs. Herewith, we can reduce the workload of manual annotation and train a patch-based CNN that considers stomach regions with all GXIs even when we manually annotate stomach regions for some of the GXIs used in training.

MATERIALS AND METHODS

The proposed method that requires manual annotation of stomach regions for only a small number of GXIs to detect CAG is presented in this section. This study was reviewed and approved by the institutional review board. Patients were not required to give informed consent to this study since the analysis used anonymous data that were obtained after each patient agreed to inspections by written consent. In this study, Kanai M from Graduate School of Information Science and Technology, Hokkaido University, Togo R from Education and Research Center for Mathematical and Data Science, Hokkaido University, Ogawa T and Haseyama M from Faculty of Information Science and Technology, Hokkaido University, took charge of the statistical analysis since they have an advanced knowledge of statistical analysis.

Study subjects

The GXIs used in this study were obtained from 815 subjects. Each subject underwent a gastric X-ray examination and an endoscopic examination at The University of Tokyo Hospital in 2010, and GXIs that had the same diagnostic results in both examinations were used in this study. Criteria for exclusion were the usage history of gastric acid suppressants, a history of *H. pylori* eradication therapy, and insufficient image data. The ground truth for this study was the diagnostic results in X-ray and endoscopic examinations. In the X-ray evaluation, subjects were classified into four categories, *i.e.*, "normal", "mild", "moderate" and "severe", based on atrophic levels[22]. It should be noted that the stomach with non-CAG has straight and fine fold distributions and fine mucosal surfaces, and the stomach with CAG has non-straight and snaked folds and coarse mucosal surfaces. X-ray examination can visualize these atrophic characteristics by barium contrast medium. We show that these differences can be trained on a chronic atrophic gastritis detection model with a small number of training images in this paper. We regarded subjects whose diagnosis results were "normal" as non-CAG subjects and the other subjects as CAG subjects. In contrast, in the endoscopic examination, subjects were classified into seven categories, *i.e.*, no atrophic change (C0), three closed types of atrophic gastritis (C1, C2, C3) and three open types of atrophic gastritis (O1, O2, O3) based on the Kimura-Takemoto seven-grade classification[23]. Since C1 is defined as the atrophic borderline, we excluded subjects whose diagnosis results were C1 from the dataset. We regarded subjects whose diagnosis results were C0 as non-CAG subjects and the other subjects as CAG subjects. As a result, we regarded 240 subjects as CAG subjects and 575 subjects as non-CAG subjects.

According to the specific condition of GXIs, the size of GXIs used in this study was 2048 × 2048 pixels with an 8-bit grayscale. Technique of fluoroscopy was a digital radiography system. Exposure was controlled by an automatic exposure control mechanism. To realize the learning of our model at the patch level, GXIs taken from the double-contrast frontal view of the stomach in the supine position were used in this study.

Preparation of dataset for training

For more accurate detection, we focus on the outside patches of the stomach since textures of these patches do not depend on the image-level GT at all. Although stomach regions can be easily determined without highly dedicated knowledge, manually annotating stomach regions for a large number of GXIs is not practical. In order to overcome this problem, we split GXIs for training into the following two groups.

(1) Manual annotation group (MAG): This group consists of GXIs for which we manually annotate the stomach regions. It is ideal for the number of GXIs in this group to be small since annotation for a large number of GXIs is time-and labor-consuming; (2) Automatic annotation group (AAG): This group consists of GXIs for which we automatically estimate the stomach regions with a CNN. By estimating the stomach regions automatically, a large number of GXIs can be used for training without the large burden of manual annotation.

An overview of the preparation of the dataset is shown in Figure 1. The preparation of the dataset for training consists of two steps. In the first step, we annotate the stomach regions for GXIs in the MAG manually and select patches for training from GXIs in the MAG. In the second step, we estimate the stomach regions for GXIs in the AAG automatically and select patches for training from GXIs in the AAG.

First step - Patch selection for training from the MAG: Each GXI in the MAG is divided into patches. To separate the inside and outside patches of the stomach, we categorize the patches with the following three kinds of patch-level class labels (P, N, U): P: inside patches of the stomach in CAG images, *i.e.*, positive patches; N: inside patches of the stomach in non-CAG images, *i.e.*, negative patches; U: outside patches of the stomach in both CAG and non-CAG images, *i.e.*, unrelated patches.

Note that if more than 80% regions within patches are included in the inside of the stomach, they were annotated as P or N. Furthermore, if less than 1% regions within patches are included in the inside of the stomach, they were annotated as U. Otherwise, we discard such patches from the training dataset. We denote a set of patches with each patch-level class label (P, N, U) as P_{MAG}, N_{MAG}, and U_{MAG}. By setting the class label U, we can train a patch-based CNN that can distinguish the inside and outside patches of the stomach.

Second step - Patch selection for training from the AAG: For estimating the stomach regions for GXIs in the AAG, we introduce a fine-tuning technique that is effective when only a small number of images for training are available[24]. First, we prepare a CNN whose weights are transferred from a CNN pre-trained for image classification with a large number of labeled natural images. The number of nodes on the last fully connected layer in the CNN is altered to the number of the patch-level class labels (P, N, U). Due to this alteration, we initialize weights of the last fully connected layer with random values sampled from a uniform distribution. Next, the CNN is fine-tuned with the patches obtained in the first step to calculate the probabilities p_c (c belong to {P,N,U}, $\sum_c p_c = 1$) of belonging to the patch-level class label c. By transferring the weights from the pre-trained CNN, accurate prediction of the patch-level class labels is realized even when the number of GXIs in the MAG is small. Second, we estimate the stomach regions for GXIs in the AAG. We divide each GXI in the AAG into patches. By inputting the patches into the fine-tuned CNN, we calculate the probabilities p_c. We can regard $p_P + p_N$ and p_U as the probability of the inside of the stomach and the probability of the outside of the stomach, respectively. Therefore, we handle the patches that satisfy $p_P + p_N \geq \alpha$ ($0.5 < \alpha \leq 1$) and the patches that satisfy $p_U \geq \alpha$ as the inside and outside patches of the stomach, respectively. Finally, we assign three kinds of patch-level class labels (P, N, U) for the patches based on the estimated results and the image-level GT. We denote a set of selected patches with patch-level class labels (P, N, U) as P_{AAG}, N_{AAG} and U_{AAG} respectively. By estimating the stomach regions for the AAG, we can add P_{AAG}, N_{AAG}, and U_{AAG} to the dataset for training even in the case of manual annotation of the stomach regions only for the MAG.

Chronic atrophic gastritis detection

With all selected patches ($P = P_{MAG} + P_{AAG}$, $N = N_{MAG} + N_{AAG}$, $U = U_{MAG} + U_{AAG}$), we retrain the fine-tuned CNN to predict the patch-level class labels. For a GXI X^{test} whose stomach regions and GT are unknown, we estimate an image-level class label y^{test} belong to {1,0} that indicates CAG or non-CAG. First, we divide the target image X^{test} into patches. We denote the patch-level class label predicted by the retrained CNN as c^{pred} belong to {P,N,U}. In order to eliminate the influence of patches outside the stomach, we select patches that satisfy c^{pred} = P or c^{pred} = N for estimating the image-

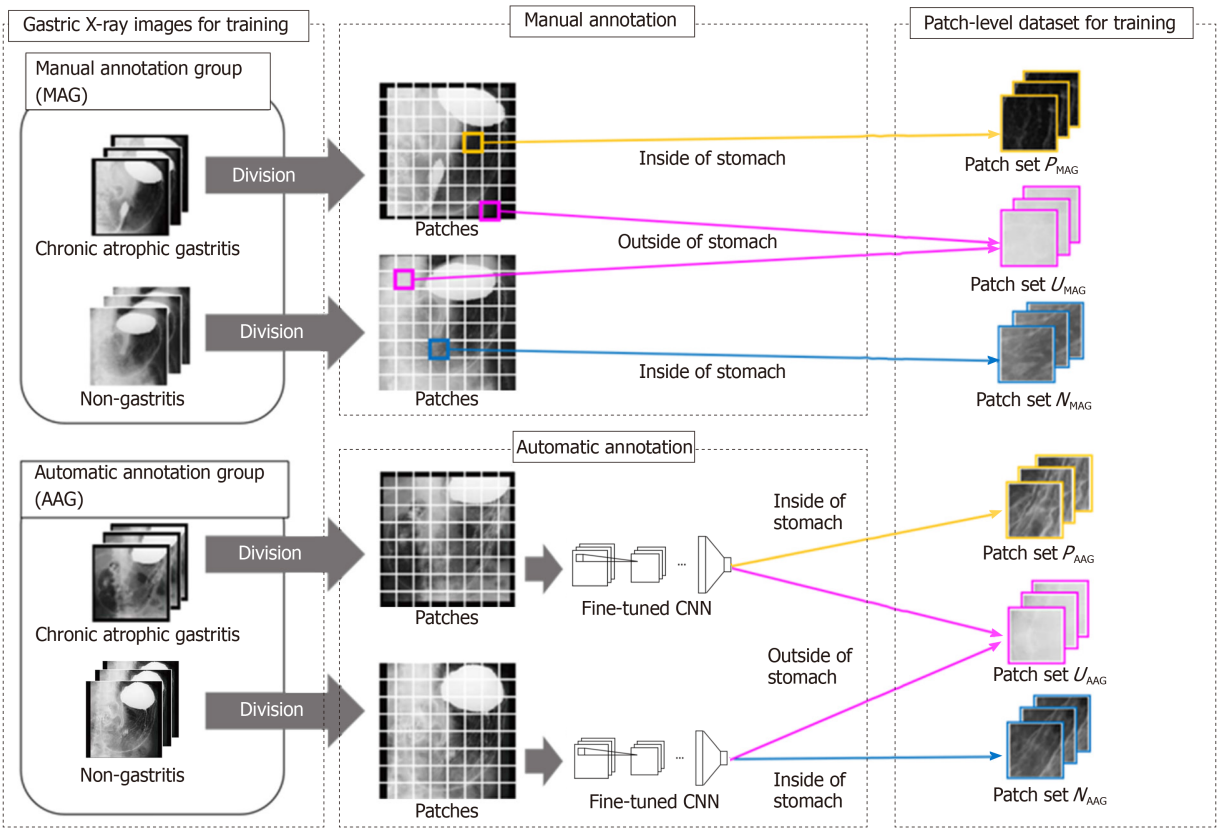

Figure 1 Overview of preparation of the dataset. CNN: Convolutional neural network; MAG: Manual annotation group; AAG: Automatic annotation group.

level class label. We calculate the ratio R with the selected patches as follows: $R = M_P/(M_P + M_N)$, where M_P and M_N are the numbers of patches that satisfy c^{pred} = P and c^{pred} = N, respectively. Finally, the image-level estimation result y^{test} for the target image X^{test} is obtained as follows: $y^{test} = 1$ if $R < \beta$, otherwise, $y^{test} = 0$, where β is a predefined threshold. By selecting patches that satisfy c^{pred} = P or c^{pred} = N, estimating the image-level class label without the negative effect of regions outside the stomach is feasible.

Evaluation of chronic atrophic gastritis detection results

A total of 815 GXIs including 200 images (100 CAG and 100 non-CAG images) for training and 615 images (140 CAG and 475 non-CAG images) for evaluation were used in this experiment. We set the number of GXIs in the MAG N_{MAG} to {10, 20,…, 50}. Note that the numbers of CAG and non-CAG images in the MAG were both set to $N_{MAG}/2$. We randomly sampled GXIs for the MAG from those for training, and the rest of them were used for the AAG. For an accurate evaluation, random sampling and calculating the performance of CAG detection were repeated five times at each N_{MAG}. It took approximately 24 h to perform each trial. Note that all networks were computed on a single NVIDIA GeForce RTX 2080 Ti GPU. In this study, we extracted patches of 299 × 299 pixels in size from GXIs at intervals of 50 pixels. The following parameters were used for training of the CNN model: Batch size = 32, learning rate = 0.0001, momentum = 0.9, and the number of epochs = 50. The threshold for estimating stomach regions α was set to 0.9.

The TensorFlow framework[25] was utilized for training CNNs. We utilized the Inception-v3[26] model with weights trained on ImageNet[27] for fine-tuning. To confirm the effectiveness of utilizing not only the MAG but also the AAG for training, we compared the proposed method utilizing only the MAG with the proposed method utilizing the MAG and AAG. Hereinafter, (MAG only) denotes the proposed method utilizing only the MAG, and (MAG + AAG) denotes the proposed method utilizing both the MAG and AAG.

The performance was measured by the following harmonic mean (HM) of sensitivity and specificity: HM = (2 × Sensitivity × Specificity)/(Sensitivity + Specificity).

Note that HM was obtained at threshold β providing the highest HM.

RESULTS

Our experimental results are shown in this section. Examples of GXIs for evaluation are shown in Figure 2. First, we evaluate the performance of the fine-tuned CNN to select patches from the AAG. Note that the fine-tuned CNN doesn't have to distinguish with high accuracy whether the patches are extracted from CAG images or non-CAG images since we utilize the fine-tuned CNN only for estimating the stomach regions. Figure 3 shows the visualization results obtained by applying the fine-tuned CNN to the CAG image shown in Figure 2A.

Specifically, the estimated patches of the inside and outside of the stomach and visualization of p_P and p_N (*i.e.*, calculated probabilities of belonging to the patch-level class labels P and N) are shown in Figure 3. It is notable that the inside and outside regions of the stomach partially overlapped since GXIs were divided into patches with the overlap in this experiment. As shown in Figure 3, regions whose probabilities p_P and p_N are high tend to increase and decrease, respectively, as N_{MAG} (*i.e.*, the number of GXIs in the MAG) increases. In contrast, the stomach regions were estimated with high accuracy and the estimated stomach regions do not depend on the change of N_{MAG}. Therefore, it is worth utilizing the fine-tuned CNN for estimating the stomach regions.

Next, we evaluate the performance of CAG detection. To confirm the effectiveness of considering stomach regions, we evaluated the detection performance of a baseline method that did not consider the stomach regions by setting patch-level class labels to the same as the image-level GT. As a result of utilizing 200 GXIs for the training, HM of the baseline method was 0.945. We show the detection performance of methods that considered the stomach regions. The detection performance of (MAG only) and that of (MAG + AAG) are shown in Figure 4. In Figure 4, HMs are shown as means ± SD of five trials. As shown in Figure 4, the mean of HM by (MAG + AAG) is higher than that by (MAG only) at each N_{MAG}. The standard deviation of HM by (MAG + AAG) is smaller than that by (MAG only) at each N_{MAG}. Therefore, the effectiveness of utilizing not only the MAG but also the AAG for the training is confirmed when the stomach regions are manually annotated for the same number of GXIs. Besides, to confirm the effect of reducing the workload of the manual annotation on detection performance, we evaluated the detection performance of a method that manually annotated the stomach regions for all GXIs used in the training (*i.e.*, $N_{MAG} = 200$). As a result, the HM of this method was 0.965. The negative effect of reducing the workload of manual annotation is small since the mean the HM of (MAG + AAG) approaches the HM of this method even when N_{MAG} is small.

DISCUSSION

This study demonstrated that highly accurate detection of CAG was feasible even when we manually annotated the stomach regions for a small number of GXIs. Figure 4 (MAG only) indicates that a larger number of GXIs with annotation of the stomach regions are required to realize highly accurate detection. In contrast, a highly accurate estimation of the stomach regions is feasible even when the number of manually annotated images is limited. Therefore, highly accurate detection of CAG and reduction of the labor required for manually annotating the stomach regions are simultaneously realized by the proposed method when a large number of GXIs with the image-level GT are available for training.

The proposed method can be applied to other tasks in the field of medical image analysis since regions outside a target organ in medical images adversely affect the performance of the tasks. With only a simple annotation of regions of the target organ for a small number of medical images, the proposed method will enable accurate analysis that excludes the effect of regions outside the target organ.

In general, endoscopic examination is superior to an X-ray examination for the evaluation of CAG in imaging inspections[28]. The endoscopic examination has been recommended for gastric cancer mass screening programs in East Asian countries in recent years. For example, South Korea has started the endoscopic examination-based gastric cancer screening program since 2002, and the proportion of individuals who underwent endoscopic examination greatly increased from 31.15% in 2002 to 72.55% in 2011[28]. Also, Japan has started the endoscopic examination-based gastric cancer mass screening program in addition to an X-ray examination since 2016. However, there remains the problem that the number of individuals who can be examined in a day is limited. Hence, X-ray examination still plays an important role in gastric cancer mass screening.

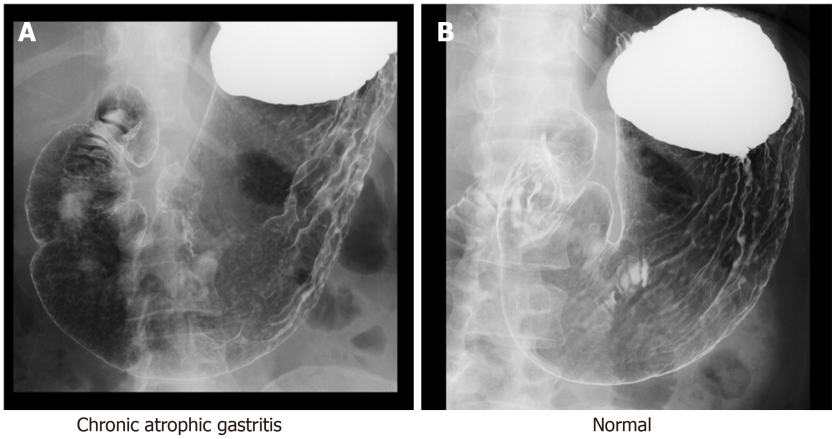

Figure 2 Examples of gastric X-ray images for evaluation.

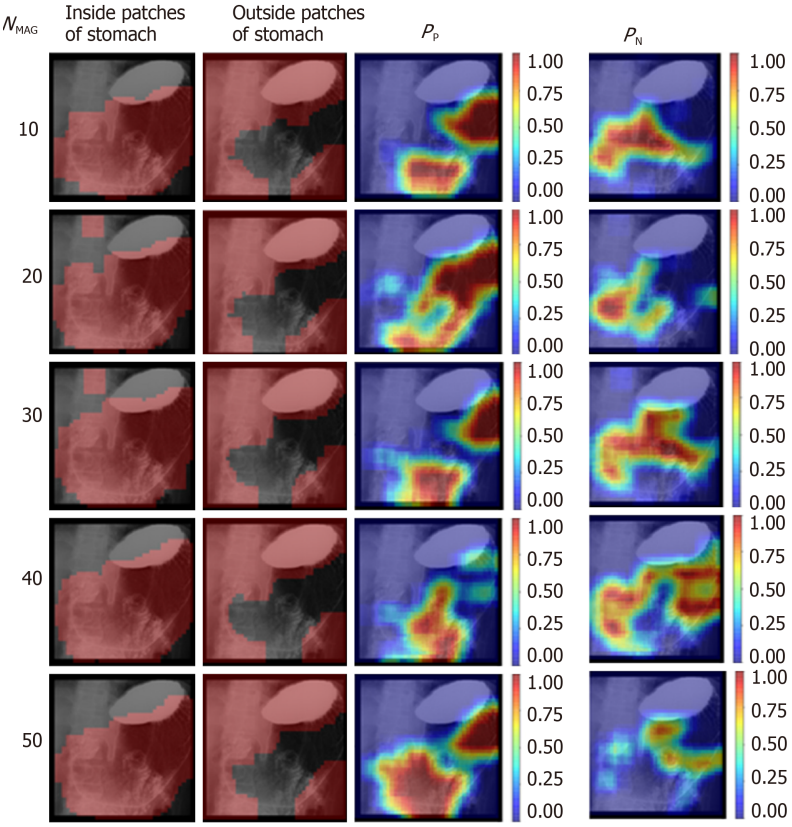

Figure 3 Visualization of the results estimated by the fine-tuned convolutional neural network to select patches from the automatic annotation group at each N_{MAG} for the chronic atrophic gastritis image shown in Figure 2A. The inside and outside regions of the stomach overlapped since gastric X-ray images were divided into patches with the overlap in this experiment.

To realize effective gastric cancer mass screening, it is crucial to narrow down individuals who need endoscopic examination by evaluating the condition of the stomach. Then CAD systems that can provide additional information to doctors will be helpful. Particularly, our approach presented in this paper realized the construction of machine learning-based CAG detection with a small number of training images. This suggests that the CAG detection method can be trained with data from a small-scale or medium-scale hospital without a large number of medical images for training.

This study has a few limitations. First, GXIs taken from only a single angle were analyzed in this study. In general X-ray examinations, GXIs are taken from multiple angles for each patient to examine the inside of the stomach thoroughly. Therefore, the detection performance will be improved by applying the proposed method to GXIs

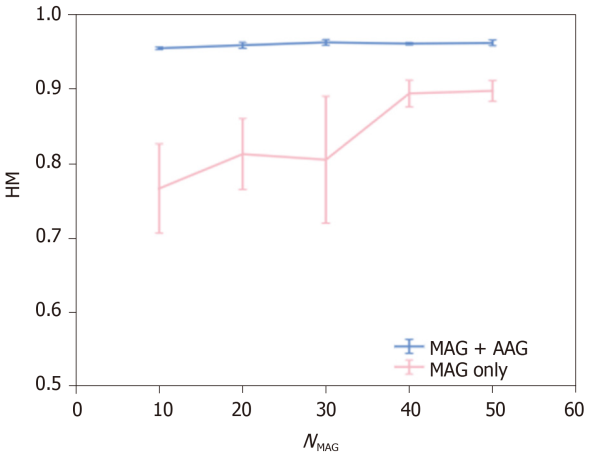

Figure 4 Harmonic mean of the detection results obtained by changing N_{MAG}. Results are shown as means ± SD of five trials. AAG: Automatic annotation group; MAG: Manual annotation group; HM: Harmonic mean.

taken from multiple angles. Furthermore, the GXIs analyzed in this study were obtained in a single medical facility. To verify versatility, the proposed method should be applied to GXIs obtained in various medical facilities.

In this paper, a method for CAG detection from GXIs is presented. In the proposed method, we manually annotate the stomach regions for some of the GXIs used in training and automatically estimate the stomach regions for the rest of the GXIs. By using GXIs with the stomach regions for training, the proposed method realizes accurate CAG detection that automatically excludes the effect of regions outside the stomach. Experimental results showed the effectiveness of the proposed method.

ARTICLE HIGHLIGHTS

Research background

It has been reported that chronic atrophic gastritis (CAG) induce by *Helicobacter pylori* infection increases the risk of gastric cancer. X-ray examination can evaluate the condition of the stomach for mass screening. On the other hand, there remains a problem that skilled doctors are decreasing.

Research motivation

Researches for the detection of CAG have been conducted, especially, deep learning-based techniques have achieved high recognition performance in general image datasets. However, early works need a large number of labeled images for training.

Research objectives

The study aimed to evaluate the effectiveness of a deep learning technique with a small number of training images with the stomach region annotation.

Research methods

A total of 815 gastric X-ray images (GXIs) were used in our analysis. The ground truth of this study was the diagnostic results in X-ray and endoscopic examinations. For a part of GXIs for training, the stomach regions are manually annotated. A deep learning model is trained with the stomach region annotations. For the rest of them, the stomach regions are automatically estimated by the learned model. Finally, a model for automatic CAG detection is trained with all GXIs for training.

Research results

In the case that the stomach regions were manually annotated for only 10 GXIs and 30 GXIs, the harmonic mean of sensitivity and specificity of CAG detection were 0.955 ± 0.002 and 0.963 ± 0.004, respectively.

Research conclusions

By estimating stomach regions automatically, our method contributes to the reduction

of the workload of manual annotation and the accurate detection of the CAG.

Research perspectives

Our CAG detection method can be trained with data from a small-scale or medium-scale hospital without medical data sharing that having the risk of leakage of personal information.

ACKNOWLEDGEMENTS

Experimental data were provided by the University of Tokyo Hospital in Japan. We express our thanks to Katsuhiro Mabe of the Junpukai Health Maintenance Center, and Nobutake Yamamichi of The University of Tokyo.

REFERENCES

1 **Bray F**, Ferlay J, Soerjomataram I, Siegel RL, Torre LA, Jemal A. Global cancer statistics 2018: GLOBOCAN estimates of incidence and mortality worldwide for 36 cancers in 185 countries. *CA Cancer J Clin* 2018; **68**: 394-424 [PMID: 30207593 DOI: 10.3322/caac.21492]

2 **Uemura N**, Okamoto S, Yamamoto S, Matsumura N, Yamaguchi S, Yamakido M, Taniyama K, Sasaki N, Schlemper RJ. Helicobacter pylori infection and the development of gastric cancer. *N Engl J Med* 2001; **345**: 784-789 [PMID: 11556297 DOI: 10.1056/NEJMoa001999]

3 **Ohata H**, Kitauchi S, Yoshimura N, Mugitani K, Iwane M, Nakamura H, Yoshikawa A, Yanaoka K, Arii K, Tamai H, Shimizu Y, Takeshita T, Mohara O, Ichinose M. Progression of chronic atrophic gastritis associated with Helicobacter pylori infection increases risk of gastric cancer. *Int J Cancer* 2004; **109**: 138-143 [PMID: 14735480 DOI: 10.1002/ijc.11680]

4 **Vannella L**, Lahner E, Annibale B. Risk for gastric neoplasias in patients with chronic atrophic gastritis: a critical reappraisal. *World J Gastroenterol* 2012; **18**: 1279-1285 [PMID: 22493541 DOI: 10.3748/wjg.v18.i12.1279]

5 **Bavi R**, Kumar R, Rampogu S, Son M, Park C, Baek A, Kim HH, Suh JK, Park SJ, Lee KW. Molecular interactions of UvrB protein and DNA from Helicobacter pylori: Insight into a molecular modeling approach. *Comput Biol Med* 2016; **75**: 181-189 [PMID: 27315565 DOI: 10.1016/j.compbiomed.2016.06.005]

6 **Kuipers EJ**, Lundell L, Klinkenberg-Knol EC, Havu N, Festen HP, Liedman B, Lamers CB, Jansen JB, Dalenback J, Snel P, Nelis GF, Meuwissen SG. Atrophic gastritis and Helicobacter pylori infection in patients with reflux esophagitis treated with omeprazole or fundoplication. *N Engl J Med* 1996; **334**: 1018-1022 [PMID: 8598839 DOI: 10.1056/NEJM199604183341603]

7 **Ma JL**, Zhang L, Brown LM, Li JY, Shen L, Pan KF, Liu WD, Hu Y, Han ZX, Crystal-Mansour S, Pee D, Blot WJ, Fraumeni JF Jr, You WC, Gail MH. Fifteen-year effects of Helicobacter pylori, garlic, and vitamin treatments on gastric cancer incidence and mortality. *J Natl Cancer Inst* 2012; **104**: 488-492 [PMID: 22271764 DOI: 10.1093/jnci/djs003]

8 **Li WQ**, Ma JL, Zhang L, Brown LM, Li JY, Shen L, Pan KF, Liu WD, Hu Y, Han ZX, Crystal-Mansour S, Pee D, Blot WJ, Fraumeni JF Jr, You WC, Gail MH. Effects of Helicobacter pylori treatment on gastric cancer incidence and mortality in subgroups. *J Natl Cancer Inst* 2014; 106 [PMID: 24925350 DOI: 10.1093/jnci/dju116]

9 **IARC Helicobacter pylori Working Group**. Helicobacter pylori eradication as strategy for preventing gastric cancer. Lyon, Fr Int Agency Res Cancer (IARC Work Gr Reports, No 8). 2014

10 **Sugano K**. Screening of gastric cancer in Asia. *Best Pract Res Clin Gastroenterol* 2015; **29**: 895-905 [PMID: 26651251 DOI: 10.1016/j.bpg.2015.09.013]

11 **Tashiro A**, Sano M, Kinameri K, Fujita K, Takeuchi Y. Comparing mass screening techniques for gastric cancer in Japan. *World J Gastroenterol* 2006; **12**: 4873-4874 [PMID: 16937471 DOI: 10.3748/wjg.v12.i30.4873]

12 **Kato M**, Asaka M. Recent development of gastric cancer prevention. *Jpn J Clin Oncol* 2012; **42**: 987-994 [PMID: 23018579 DOI: 10.1093/jjco/hys151]

13 **Yuan Y**. A survey and evaluation of population-based screening for gastric cancer. *Cancer Biol Med* 2013; **10**: 72-80 [PMID: 23882421 DOI: 10.7497/j.issn.2095-3941.2013.02.002]

14 **Abe K**, Miura D, Minami M. Features for discriminating helicobacter pylori infection from gastric X-ray images. In: Proc Int Conf Signal Processing Systems (ICSPS) 2016: 31-35 [DOI: 10.1145/3015166.3015190]

15 **Ishihara K**, Ogawa T, Haseyama M. Helicobacter Pylori infection detection from gastric X-ray images based on feature fusion and decision fusion. *Comput Biol Med* 2017; **84**: 69-78 [PMID: 28346875 DOI: 10.1016/j.compbiomed.2017.03.007]

16 **Ishihara K**, Ogawa T, Haseyama M. Detection of gastric cancer risk from X-ray images via patch-based convolutional neural network. In: Proc IEEE Int Conf Image Processing (ICIP) 2017: 2055-2259 [DOI: 10.1109/ICIP.2017.8296643]

17 **Kanai M**, Togo R, Ogawa T, Haseyama M. Gastritis detection from gastric X-ray images via fine-tuning of patch-based deep convolutional neural network. In: Proc IEEE Int Conf Image Processing (ICIP) 2019: 1371-1375 [DOI: 10.1109/ICIP.2019.8803705]

18 **LeCun Y**, Bottou L, Bengio Y, Haffner P. Gradient-based learning applied to document recognition. In: Proc the IEEE 1998: 2278-2324 [DOI:

10.1109/5.726791]

19 **Krizhevsky A**, Sulskever Ii, Hinton GE. ImageNet Classification with Deep Convolutional Neural Networks. In: Proc Int Conf Adv Neural Inf Process Syst 2012: 1-9 [DOI: 10.1145/3065386]

20 **Mai L**, Jin H, Liu F. Composition-preserving deep photo aesthetics assessment. In: Proc IEEE Conf Computer Vision and Pattern Recognition (CVPR) 2016: 497-506 [DOI: 10.1109/CVPR.2016.60]

21 **Litjens G**, Kooi T, Bejnordi BE, Setio AAA, Ciompi F, Ghafoorian M, van der Laak JAWM, van Ginneken B, Sánchez CI. A survey on deep learning in medical image analysis. *Med Image Anal* 2017; **42**: 60-88 [PMID: 28778026 DOI: 10.1016/j.media.2017.07.005]

22 **Yamamichi N**, Hirano C, Ichinose M, Takahashi Y, Minatsuki C, Matsuda R, Nakayama C, Shimamoto T, Kodashima S, Ono S, Tsuji Y, Niimi K, Sakaguchi Y, Kataoka Y, Saito I, Asada-Hirayama I, Takeuchi C, Yakabi S, Kaikimoto H, Matsumoto Y, Yamaguchi D, Kageyama-Yahara N, Fujishiro M, Wada R, Mitsushima T, Koike K. Atrophic gastritis and enlarged gastric folds diagnosed by double-contrast upper gastrointestinal barium X-ray radiography are useful to predict future gastric cancer development based on the 3-year prospective observation. *Gastric Cancer* 2016; **19**: 1016-1022 [PMID: 26486508 DOI: 10.1007/s10120-015-0558-0]

23 **Quach DT**, Hiyama T. Assessment of Endoscopic Gastric Atrophy according to the Kimura-Takemoto Classification and Its Potential Application in Daily Practice. *Clin Endosc* 2019; **52**: 321-327 [PMID: 31327182 DOI: 10.5946/ce.2019.072]

24 **Tajbakhsh N**, Shin JY, Gurudu SR, Hurst RT, Kendall CB, Gotway MB, Jianming Liang. Convolutional Neural Networks for Medical Image Analysis: Full Training or Fine Tuning? *IEEE Trans Med Imaging* 2016; **35**: 1299-1312 [PMID: 26978662 DOI: 10.1109/TMI.2016.2535302]

25 **Mart' A**, Ashish A, Paul B, Eugene B, Zhifeng C, Craig C, Greg SC, Andy D, Jeffrey D, Matthieu D, Sanjay G, Ian G, Andrew H, Geoffrey I, Michael I, Yangqing J, Rafal J, Lukasz K, Manjunath K, Josh L, Dan M, Rajat M, Sherry M, Derek M, Chris O, Mike S, Jonathon S, Benoit S, Ilya S, Kunal T, Paul T, Vincent V, Vijay V, Fernanda V, Oriol V, Pete W, Martin W, Martin W, Yuan Y, Xiaoqiang Z. TensorFlow: Large-Scale Machine Learning on Heterogeneous Systems, 2015

26 **Szegedy C**, Vanhoucke V, Ioffe S, Shlens J, Wojna Z. Rethinking the inception architecture for computer vision. In: Proc IEEE Conf Computer Vision and Pattern Recognition (CVPR) 2016: 2818-2826

27 **Russakovsky O**, Deng J, Su H, Krause J, Satheesh S, Ma S, Huang Z, Karpathy A, Khosla A, Bernstein M, Berg C A, Fei-Fei L. ImageNet large scale visual recognition challenge. *Int J Comput Vis* 2015; **115**: 211–52 [DOI: 10.1007/s11263-015-0816-y]

28 **Lee S**, Jun JK, Suh M, Park B, Noh DK, Jung KW, Choi KS. Gastric cancer screening uptake trends in Korea: results for the National Cancer Screening Program from 2002 to 2011: a prospective cross-sectional study. *Medicine (Baltimore)* 2015; **94**: e533 [PMID: 25715251 DOI: 10.1097/MD.0000000000000533]

World Journal of Gastroenterology

Submit a Manuscript: https://www.f6publishing.com

World J Gastroenterol 2020 July 7; 26(25): 3660-3672

DOI: 10.3748/wjg.v26.i25.3660

ISSN 1007-9327 (print) ISSN 2219-2840 (online)

ORIGINAL ARTICLE

Retrospective Study

Multiphase convolutional dense network for the classification of focal liver lesions on dynamic contrast-enhanced computed tomography

Su-E Cao, Lin-Qi Zhang, Si-Chi Kuang, Wen-Qi Shi, Bing Hu, Si-Dong Xie, Yi-Nan Chen, Hui Liu, Si-Min Chen, Ting Jiang, Meng Ye, Han-Xi Zhang, Jin Wang

ORCID number: Su-E Cao 0000-0002-0756-1957; Lin-Qi Zhang 0000-0002-0607-6300; Si-Chi Kuang 0000-0003-3674-651X; Wen-Qi Shi 0000-0003-2497-3299; Bing Hu 0000-0002-8270-433X; Si-Dong Xie 0000-0003-1280-5706; Yi-Nan Chen 0000-0003-0858-2087; Hui Liu 0000-0001-6218-8123; Si-Min Chen 0000-0001-7073-1472; Ting Jiang 0000-0002-6630-3392; Meng Ye 0000-0003-2210-3396; Han-Xi Zhang 0000-0001-9489-3062; Jin Wang 0000-0002-7956-9579.

Author contributions: Cao SE, Zhang LQ, Shi WQ, Chen YN, Liu H, and Ye M contributed to the conception and design of the study; Cao SE, Kuang SC, Shi WQ, Hu B, Jiang T, Chen SM, and Zhang HX collected the patient data, analyzed and interpreted the data; Cao SE wrote original draft and revised the manuscript; Wang J contributed to the conception of the study and provided final approval of the version to be submitted and any revised versions.

Supported by National Natural Science Foundation of China, No. 91959118; Science and Technology Program of Guangzhou, China, No. 201704020016; SKY Radiology Department International Medical

Su-E Cao, Lin-Qi Zhang, Si-Chi Kuang, Wen-Qi Shi, Bing Hu, Si-Dong Xie, Si-Min Chen, Ting Jiang, Han-Xi Zhang, Jin Wang, Department of Radiology, The Third Affiliated Hospital, Sun Yat-Sen University, Guangzhou 510630, Guangdong Province, China

Yi-Nan Chen, Hui Liu, Meng Ye, Department of Scientific and Technological Research, 12 Sigma Technologies, Beijing 100102, China

Corresponding author: Jin Wang, MD, Doctor, Professor, Department of Radiology, The Third Affiliated Hospital, Sun Yat-Sen University, No. 600, Tianhe Road, Tianhe District, Guangzhou 510630, Guangdong Province, China. wangjin3@mail.sysu.edu.cn

Abstract

BACKGROUND

The accurate classification of focal liver lesions (FLLs) is essential to properly guide treatment options and predict prognosis. Dynamic contrast-enhanced computed tomography (DCE-CT) is still the cornerstone in the exact classification of FLLs due to its noninvasive nature, high scanning speed, and high-density resolution. Since their recent development, convolutional neural network-based deep learning techniques has been recognized to have high potential for image recognition tasks.

AIM

To develop and evaluate an automated multiphase convolutional dense network (MP-CDN) to classify FLLs on multiphase CT.

METHODS

A total of 517 FLLs scanned on a 320-detector CT scanner using a four-phase DCE-CT imaging protocol (including precontrast phase, arterial phase, portal venous phase, and delayed phase) from 2012 to 2017 were retrospectively enrolled. FLLs were classified into four categories: Category A, hepatocellular carcinoma (HCC); category B, liver metastases; category C, benign non-inflammatory FLLs including hemangiomas, focal nodular hyperplasias and adenomas; and category D, hepatic abscesses. Each category was split into a training set and test set in an

Research Foundation of China, No. Z-2014-07-1912-15; and Clinical Research Foundation of the 3rd Affiliated Hospital of Sun Yat-Sen University, No. YHJH201901.

Institutional review board statement: The study was reviewed and approved for publication by our Institutional Reviewer.

Informed consent statement: All study participants or their legal guardian provided informed written consent about personal and medical data collection prior to study enrolment.

Conflict-of-interest statement: All the Authors have no conflict of interest related to the manuscript.

Data sharing statement: The original anonymous dataset is available on request from the corresponding author at wangjin3@mail.sysu.edu.cn.

Manuscript source: Unsolicited manuscript

Received: March 16, 2020
Peer-review started: March 16, 2020
First decision: April 25, 2020
Revised: May 8, 2020
Accepted: June 4, 2020
Article in press: June 4, 2020
Published online: July 7, 2020

P-Reviewer: Jennane R
S-Editor: Dou Y
L-Editor: Filipodia
E-Editor: Zhang YL

approximate 8:2 ratio. An MP-CDN classifier with a sequential input of the four-phase CT images was developed to automatically classify FLLs. The classification performance of the model was evaluated on the test set; the accuracy and specificity were calculated from the confusion matrix, and the area under the receiver operating characteristic curve (AUC) was calculated from the SoftMax probability outputted from the last layer of the MP-CDN.

RESULTS

A total of 410 FLLs were used for training and 107 FLLs were used for testing. The mean classification accuracy of the test set was 81.3% (87/107). The accuracy/specificity of distinguishing each category from the others were 0.916/0.964, 0.925/0.905, 0.860/0.918, and 0.925/0.963 for HCC, metastases, benign non-inflammatory FLLs, and abscesses on the test set, respectively. The AUC (95% confidence interval) for differentiating each category from the others was 0.92 (0.837-0.992), 0.99 (0.967-1.00), 0.88 (0.795-0.955) and 0.96 (0.914-0.996) for HCC, metastases, benign non-inflammatory FLLs, and abscesses on the test set, respectively.

CONCLUSION

MP-CDN accurately classified FLLs detected on four-phase CT as HCC, metastases, benign non-inflammatory FLLs and hepatic abscesses and may assist radiologists in identifying the different types of FLLs.

Key words: Deep learning; Convolutional neural networks; Focal liver lesions; Classification; Multiphase computed tomography; Dynamic enhancement pattern

Core tip: We developed and evaluated a deep learning-based convolutional neural network (CNN) to classify focal liver lesions (FLLs) on multiphase computed tomography. The most important highlight of the current study is that, to the best of our knowledge, this study is the first to employ four-channel input data to preserve the dynamic enhancement properties. The combination of the lesion's dynamic enhancement pattern with a CNN can imitate the image diagnosis of radiologists and is expected to improve diagnostic accuracy. It was interesting to note that the accuracy and specificity of differentiating each category from others were high. This model may become an efficient tool to assist radiologists in the classification of FLLs.

Citation: Cao SE, Zhang LQ, Kuang SC, Shi WQ, Hu B, Xie SD, Chen YN, Liu H, Chen SM, Jiang T, Ye M, Zhang HX, Wang J. Multiphase convolutional dense network for the classification of focal liver lesions on dynamic contrast-enhanced computed tomography. *World J Gastroenterol* 2020; 26(25): 3660-3672
URL: https://www.wjgnet.com/1007-9327/full/v26/i25/3660.htm
DOI: https://dx.doi.org/10.3748/wjg.v26.i25.3660

INTRODUCTION

The frequency of detection of focal liver lesions (FLLs) has increased due to the widespread application of imaging techniques[1,2]. Because the treatment of FLLs depends on the nature of the lesion, the ability to accurately distinguish the types of FLLs is an important step in the management of these patients. Currently, dynamic contrast-enhanced computed tomography (DCE-CT) is commonly used for the noninvasive detection and characterization of FLLs due to its high scanning speed and high-density resolution[3,4]. The appearances, especially the dynamic enhancement patterns of FLLs on CT imaging, are essential for categorizing lesions. With the careful evaluation of CT images, diagnosis with a relatively high accuracy can be achieved for most liver lesions. However, in current clinical practice, the evaluation of CT images is mainly performed by radiologists. The results are influenced by the radiologist's experience and are generally subjective. Radiologists have began investigating the potential of computer-aided diagnostic systems to overcome these limitations. Rather

than using qualitative reasoning, artificial intelligence (AI) conducts quantitative assessments by automatically identifying imaging information[5]. Therefore, AI can assist radiologists in making more accurate imaging diagnoses and substantially reduces the radiologists' workload.

Traditional machine learning algorithms need features to be predefined and require the placement of complexly shaped regions of interest (ROIs) on images[6-8]. The predefined features are applied in various combinations to effectively determine the diagnosis using traditional machine learning algorithms, but the combinations are usually incomprehensive and result in low accuracy. Today, deep learning-based algorithms are widely used due to their automatic feature generation and image classification abilities[9,10]. A convolutional neural network (CNN) is considered the first truly successful deep-learning method based on a multilayer hierarchical network, and shows high performance in the image analysis field[9-11]. CNN has been successfully applied to analyze the medical images of patients with many diseases such as pulmonary tuberculosis, breast cancer, brain tumors, and some hepatic diseases[12-19]. However, few studies have attempted to apply CNN in the differential diagnosis of FLLs, and these studies have limited value. The dynamic enhancement pattern of FLLs is essential for making differential diagnoses and may have a complementary role to CNN in the diagnostic workup of FLLs.

Hence, we developed and evaluated an automated multiphase convolutional dense network (MP-CDN) that uses four channels of input data to classify FLLs on four-phase CT.

MATERIALS AND METHODS

Patients

The retrospective study was reviewed and approved by our institutional review board, and written informed consent was obtained from the patients whose data were analyzed. Two radiologists (Cao SE and Shi WQ, both with 5 years of experience in imaging diagnosis) searched for patients with FLLs in the picture archiving and communication system (PACS). The images of patients who underwent a four-phase DCE-CT examination and for whom FLLs were confirmed by histopathological evaluation or were diagnosed based on a combination of clinical and radiological findings with follow-up were collected for further screening. The exclusion criteria were as follows: Lesions larger than 10 cm; images with prominent artifacts; and prior local-regional therapy prior to the CT examination.

Standard of classification

The lesions were classified into four categories according to different pathological types and treatment decisions. (1) Category A was hepatocellular carcinoma (HCC), which was confirmed by histopathologic evaluation after surgery or biopsy. (2) Category B represents liver metastases derived from different primary sites such as colorectal cancer, gastric carcinoma, breast cancer, lung cancer, thyroid cancer, malignant jejunal stromal tumor, duodenal papillary carcinoma, and laryngocarcinoma. The primary lesions were confirmed by a pathological examination, but the metastatic lesions were diagnosed based on the clinical data, patient history, other follow-up CT, magnetic resonance imaging, and positron emission tomography/CT scans. For liver metastases, the follow-up time was 60 d to 1230 d, and the median was 300 d. (3) Category C was defined as benign non-inflammatory FLLs, including hemangiomas, focal nodular hyperplasias (FNHs), and adenomas. A total of 27 lesions, including all adenomas, were confirmed by a histopathological evaluation after surgery, while the remaining 135 lesions were diagnosed based on imaging diagnostic criteria from the CT scan in combination with the clinical information and follow-up MRI; the follow-up time was 90 d to 1800 d, and the median was 330 d. And (4) Category D was hepatic abscesses. The diagnosis of hepatic abscess was based on typical imaging findings, clinical aspects, laboratory findings, and microbiology on blood or aspirate culture results. While all patients received early empirical antibiotic treatment, 37% patients underwent percutaneous or surgical drainage. A longer follow-up with a median time of 100 d (range, 60-365 d) confirmed the remission or absence of signs and symptoms together with imaging studies without findings compatible with hepatic abscess after treatment.

Finally, a total of 375 patients with 517 lesions were enrolled in this study from 2012 to 2017. Each category was split into a training set and test set. Patients who underwent CT scan before June 2016 were used for training, while those after June

2016 were used for testing. The ratio between training set and test set was approximately 8:2.

Basic information about the patients was obtained from the hospital information system, including gender, age, surgical and pathological reports, lesion size, and follow-up time.

Input data: CT imaging protocol

A 320-detector CT scanner (Aquilion ONE; Toshiba Medical Systems, Otawara, Japan) was used to acquire four-phase DCE-CT imaging protocols including precontrast phase (PP), arterial phase (AP), portal venous phase (PVP), and delayed phase (DP). The following scan parameters were used: A peak tube voltage of 120 kV, a tube rotation time of 0.5 s per rotation, a pitch factor of 0.828, a field of view of 35 cm × 35 cm, a matrix of 512 × 512, and automatic tube current modulation.

The first phase was PP to cover the whole liver. The next three phases were contrast-enhanced phases with the same scanning range after the intravenous injection of low osmolar nonionic contrast medium (Ioversol-350; Tyco Healthcare, Montreal, Quebec, Canada and Isovue-370, Bracco Diagnostics, Guangzhou, China) into the right antecubital vein at an injection rate of 3 mL/s and a dose of 1.5 mL/kg body weight, followed by a 20-mL saline chaser.

The AP was acquired by performing a bolus tracking technique. The AP was scanned 15 s after CT attenuation of the aorta at the level of the diaphragm had reached 200 Hounsfield Units. For the PVP, images were acquired 30 s after the AP. The DP was scanned 45 s after the PVP. All images were reconstructed in the axial plane with a slice thickness of 5 mm and interval of 5 mm using a kernel for the evaluation of soft tissues (FC19) and then sent to the PACS.

Input data: CT imaging annotation

The CT imaging annotation was manually and independently performed by four radiologists (all had at least 4 years of imaging experience), and the results were reviewed by a radiologist with 20 years of imaging experience. For each patient, the four-phase CT images were manually loaded into 3D Slicer (https://www.slicer.org). The boundary of each lesion was manually drawn slice-by-slice along the visible borders of the lesion using the annotation module available in 3D Slicer. The classification of the type of each lesion was manually annotated using a home-developed lesion annotation module in 3D Slicer.

Input data: CT imaging processing pipeline

The four phases were organized in a sequence according to the acquisition time and fed into the image processing pipeline, as shown in Figure 1. The inner-phase registration and normalization were used to achieve volume-wise processing. The inner-phase registration was performed by using a nonrigid registration module implemented in Elastix (http://elastix.isi.uu.nl) with PVP as the reference phase, and then each phase was linearly normalized to (-1, 1) with a corresponding HU of (0, 300). Cropping and resizing were performed for lesion-wise processing using the Python library scikit-image 0.15.0 (https://scikit-image.org/scikit-image 0.15.0). For each lesion, a three-dimensional bounding box was generated to cover the lesion boundary and extended with a spare boundary of 10 mm along each direction. After extracting the bounding box of the lesion, ROIs were cropped from the PVP. The ROI was a square on each axial plane, the length of the side was 1.5 times the value of the longest side of the bounding box on the axial plane, and the center point was the projection of the center point of the bounding box on each axial plane. Then the bounding boxes were propagated on other phases to crop the lesion. Following lesion cropping, each cropped ROI was resized into an identical shape in the size of 128 × 128. ROIs from five slices centered at the lesion were extracted and stacked together to form a (128, 128, 5) tensor as the input data for each phase.

Deep convolutional network architecture

The deep convolutional network was designed following the concept of the automatic extraction of useful features from each phase and then the sequential combination of each phase's features to achieve classification, as detailed in Figure 2. Each phase's automatic feature extraction was implemented using a densely connected stack of two-dimensional convolutional, center-cropping and max-pooling layers, where the convolutional kernel size was 3 × 3; the cropping and pooling size was 2 × 2; and the activation layer used the "ReLU" activation function. Then, the four-phase convolutional layers were flattened and sequentially connected to the last dense layer

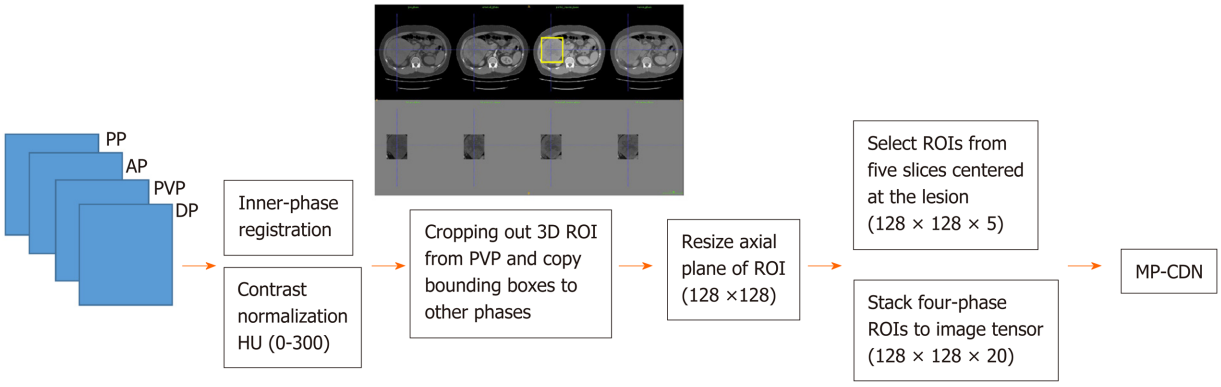

Figure 1 Four-phase images processing pipeline for multiphase convolutional dense network. AP: Arterial phase; DP: Delayed phase; HU: Hounsfield unit; MD-CDN: Multiphase convolutional dense network; PP: Precontrast phase; PVP: Portal venous phase; ROI: Region of interest.

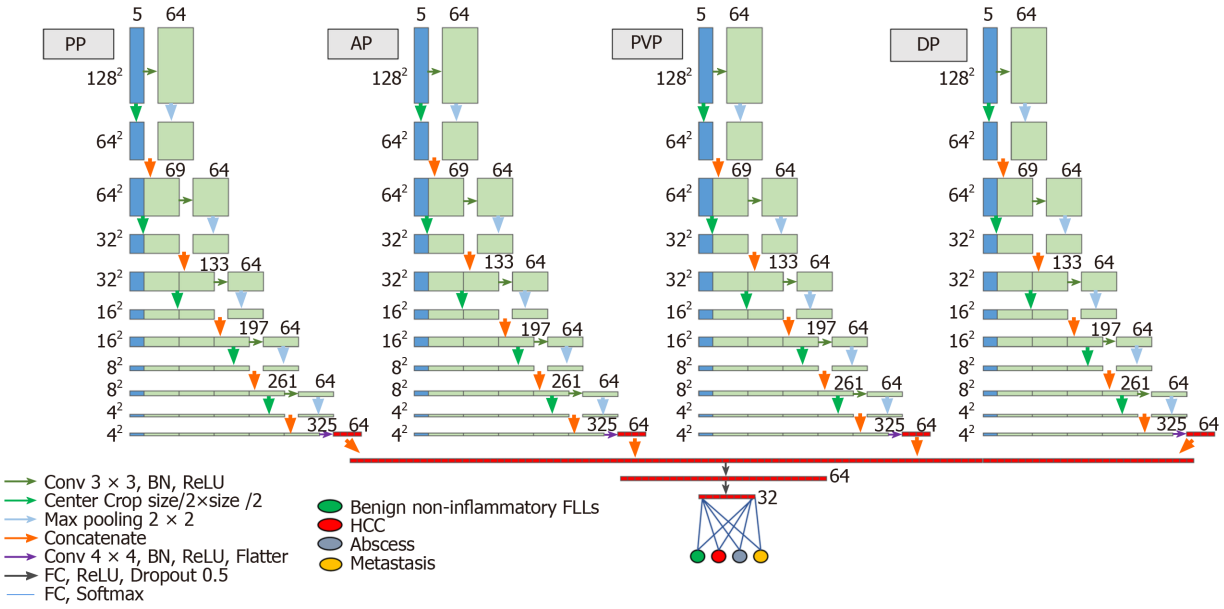

Figure 2 Architecture of the proposed multiphase convolutional dense network. AP: Arterial phase; DP: Delayed phase; FLLs: Focal liver lesions; HCC: Hepatocellular carcinoma; PP: Precontrast phase; PVP: Portal venous phase.

with SoftMax activation for classification purposes. The sequential connection of each phase's CNN network block was designed to preserve the dynamic enhancement properties.

The deep convolutional network was a 2.5 D MP-CDN with the four phases of resized multichannel images as the input (the slice was used as the channel dimension in this network). The classification tasks consisted of training and testing, in which the training task was performed with a batch size of 100 and the test task was performed once for each lesion.

Training and evaluation

For the training set, data augmentation options, which include scaling and rotation, were applied to each ROI. An augmented training dataset with a size 21 times greater than the raw dataset was used to train the model. The test set without augmentation was directly used to assess the model.

During the training phase, the category label was converted to 0.0 or 1.0 as the SoftMax probability to train the model. During the testing phase, the category label included the binary label and probability label, where the binary label was 1.0 or 0.0 corresponding to the class with the largest or non-largest probability from the SoftMax layer. In terms of probability label, the result was derived from the SoftMax probability outputted from the last layer of the MP-CDN.

Model implementation

The model was programmed using Python3.7 (https://www.python.org/) under the deep learning model development framework of Keras (https://keras.io) with the TensorFlow (https://www.tensorflow.org) backend. The network weights were optimized using the Adam optimizer, the learning rate was 0.00001 and the loss function was categorical cross-entropy. A graphics processing unit (GPU) (NVIDIA Titian 1080Ti) was used to accelerate the model training and testing phases.

Statistics

The distributions of age, sex, and lesion size in each of the sets (training and test sets) were compared using SPSS 17.0 software (SPSS Inc., Chicago, IL, United States). Quantitative variables were compared using the Wilcoxon rank sum test or *t*-test, and qualitative variables were compared using the chi-squared test.

The classification performance of the model was assessed on the test set: The accuracy, specificity, and sensitivity for differentiating each category from the others were calculated from the confusion matrix from the confusion matrix, and the area under the receiver operating characteristic (ROC) curve (AUC) was calculated from the SoftMax probability outputted from the last layer of the MP-CDN using SPSS 17.0 Software.

The model was further evaluated by applying a "phase cheating" experiment on the test set. The "phase cheating" experiment was implemented by eliminating one or more phases from the four phases and replacing it with the wrong phase(s) before feeding it into the model. The design idea of this experiment was based on the following concepts: (1) The liver lesion's dynamic enhancement pattern is vital in differential diagnosis; (2) Our model was designed to accommodate the correct sequence of four phases, which preserved the dynamic enhancement properties; and (3) The "phase cheating" experiment was used to test whether our model had learned this important dynamic enhancement pattern. If the phases were replaced by a certain phase (the so-called "phase cheating" experiment), its dynamic enhancement pattern might be different and may result in an incorrect category prediction. We re-evaluated the classification performance by comparing the AUCs between the model in the normal set and that in the "phase cheating" sets by using MedCalc Software (version 11.4.2 for Windows, MedCalc Software bvba).

Statistical significance was defined as $P < 0.05$.

RESULTS

Of the 15680 patients with FLLs treated at our hospital from 2012 to 2017, 375 patients with 517 lesions met the inclusion criteria. Of the 517 FLLs, 410 FLLs (88 HCCs, 89 metastases, 128 benign non-inflammatory FLLs, and 105 abscesses) were used for training, and 107 FLLs (23 HCCs, 23 metastases, 34 benign non-inflammatory FLLs, and 27 abscesses) were used for testing. Table 1 presents the basic and detailed information of each dataset.

The confusion matrix analysis on the test set is shown in Table 2. Of the 23 HCCs, 17 lesions were correctly classified, 4 lesions were misclassified as benign non-inflammatory FLLs, and the remaining 2 lesions were misclassified as metastases. It was interesting to note that all metastases (23 lesions) were correctly classified. Of the 34 benign non-inflammatory FLLs, 25 lesions were correctly classified, 3 lesions were misclassified as HCC, 3 lesions were misclassified as metastases, and the remaining 3 lesions were misclassified as hepatic abscesses. Of the 27 hepatic abscesses, 22 lesions were correctly classified, 3 lesions were misclassified as metastases, and the remaining 2 lesions were misclassified as benign non-inflammatory FLLs. The representative correctly classified and misclassified examples of each category are shown in Figure 3. The accuracy/specificity/sensitivity of differentiating each category from others were 0.916/0.964/0.739, 0.925/0.905/1.0, 0.860/0.918/0.735 and 0.925/0.963/0.815 for HCC, metastases, benign non-inflammatory FLLs, and abscesses, respectively.

ROC analysis was performed on the test set. The AUC (95% confidence interval [CI]) for differentiating each category from the others was 0.92 (0.837-0.992), 0.99 (0.967-1.00), 0.88 (0.795-0.955) and 0.96 (0.914-0.996) for HCC, metastases, benign non-inflammatory FLLs, and abscesses, respectively (Figure 4A). The model's classification probability was calibrated for each category, as shown in Figure 4B, and the Brier scores were 0.104, 0.080, 0.124, and 0.074 for HCC, metastases, benign non-inflammatory FLLs, and hepatic abscesses, respectively.

Table 3 shows the AUC and *P* value when using the "phase cheating" sets

Table 1 The basic information and detail distribution of each dataset

		Training set	Test set	*P* value
Category A: HCC	No. of lesions/No. of patients	88/79	23/22	
	Age (median [range]) in yr	49 (24-81)	49.5 (33-70)	0.726
	Sex (percentage of women)	6/79 (7.6%)	5/22 (22.7%)	0.044
	Size of lesion (mean ± SD) in mm	60.6 ± 36.3	63.0 ± 45.4	0.789
	Histopathologic diagnosis (No. of lesions/No. of patients)			
	Surgery	79/70	20/19	
	Biopsy	9/9	3/3	
Category B: Metastases	No. of lesions/No. of patients	89/34	23/14	
	Age (Median [range]) (yr)	58.5 (23-79)	58 (23-79)	0.937
	Sex (Percentage of women)	8/34 (23.5%)	6/14 (42.9%)	0.181
	Size of lesion (mean ± SD) in mm	23.0 ± 13.9	22.7 ± 11.5	0.937
	Primary tumors (No. of lesions/No. of patients)			
	Colorectal cancer	40/20	10/6	
	Gastric carcinoma	13/3	3/2	
	Breast cancer	2/1	0/0	
	Lung cancer	14/4	4/2	
	Thyroid cancer	16/4	4/2	
	Malignant jejunal stromal tumor	2/1	1/1	
	Duodenal papillary carcinoma	0/0	1/1	
	Laryngocarcinoma	2/1	0/0	
Category C: Benign non-inflammatory FLLs	No. of lesions/No. of patients	128/97	34/32	
	Age (median [range]) in yr	34 (17-82)	34 (10-74)	0.729
	Sex (percentage of women)	52/97 (53.6%)	16/32 (50.0%)	0.723
	Size of lesion (mean ± SD) in mm	41.9 ± 30.5	52.9 ± 28.4	0.060
	Histological type (No. of lesions/No. of patients)			
	Hemangioma	55/35	15/15	
	FNH	67/58	17/15	
	Adenoma	6/4	2/2	
Category D: Hepatic abscesses	No. of lesions/No. of patients	105/77	27/20	
	Age (median [range]) in yr	54 (4-82)	55 (25-82)	0.936
	Sex (percentage of women)	24/77 (31.2%)	7/20 (35.0%)	0.743
	Size of lesion (mean ± SD) in mm	64.5 ± 34.9	63.8 ± 24.2	0.916

FLLs: Focal liver lesions; FNH: Focal nodular hyperplasias.

compared to the normal set. The AUCs were lower for the "phase cheating" set with eliminating AP and/or PVP than for the normal set in differentiating HCC from the others ($P < 0.05$). When we replaced PP with AP, there was no significant difference between the AUCs of the normal set and "phase cheating" sets in differentiating HCC from the others ($P > 0.05$). Figure 5 shows the heatmaps of the predicted category when using the "phase cheating" sets compared to the normal set.

Table 2 The confusion matrix analysis on test set

		Ground truth				Positive predictive value
		Benign non-inflammatory FLLs	Metastases	HCCs	Hepatic abscesses	
Prediction	Benign non-inflammatory FLLs	25	0	4	2	0.806
	Metastases	3	23	2	3	0.742
	HCCs	3	0	17	0	0.85
	Hepatic abscesses	3	0	0	22	0.88
	Sensitivity	0.735	1	0.739	0.815	
	Specificity	0.918	0.905	0.964	0.963	
	Accuracy	0.86	0.925	0.916	0.925	
	Mean accuracy	0.813				

HCCs: Hepatocellular carcinomas; FLLs: Focal liver lesions.

Table 3 The model's performance comparison between the normal set and "phase cheating" sets

Policy	HCCs (AUC [95%CI]/*P* value)	Metastases (AUC [95%CI]/*P* value)	Benign non-inflammatory (AUC [95%CI]/*P* value)	Hepatic Abscesses (AUC [95%CI]/*P* value)
PP + AP + PVP + DP	0.92 (0.837-0.992)	0.99 (0.967-1.00)	0.88 (0.795-0.955)	0.96 (0.914-0.996)
AP + AP + PVP + DP	0.820 (0.705-0.905)/0.0699	0.901 (0.805- 0.960)/0.0289	0.893 (0.809-0.949)/0.2502	0.924 (0.823-0.977)/0.3387
PP + PVP + PVP + DP	0.704 (0.565-0.821)/0.0017	0.930 (0.832- 0.981)/0.2573	0.799 (0.701- 0.877)/0.0924	0.938 (0.846-0.984)/0.4317
PP + AP + AP + DP	0.768 (0.643-0.866)/0.0013	0.833 (0.714 -0.916)/0.0120	0.864 (0.774-0.929)/0.9720	0.935 (0.846-0.981)/0.4047
PP + AP+ PVP + PVP	0.911 (0.815-0.967)/0.6404	0.959 (0.882- 0.992)/0.4066	0.913 (0.832-0.963)/0.7877	0.831 (00.716- 0.914)/0.0184
PP + AP + AP + AP	0.672 (0.542-0.785)/< 0.0001	0.758 (0.692- 0.909)/0.0079	0.863 (0.773-0.927)/0.3188	0.806 (0.690- 0.893)/0.0475
PP + PVP + PVP + PVP	0.721 (0.584-0.834)/0.0019	0.913 (0.807-0.972)/0.1165	0.775 (0.675-0.857)/ 0.0247	0.900 (0.796- 0.962)/0.7491
PP + DP+ DP+ DP	0.652 (0.513-0.774)/0.0002	0.818 (0.692-0.909)/0.0079	0.790 (0.688-0.870)/0.0356	0.904 (0.802-0.964)/0.7911
AP + AP + AP + AP	0.573 (0.443- 0.696)/< 0.0001	0.674 (0.548-0.785)/< 0.0001	0.833 (0.739- 0.904)/0.3375	0.697 (0.567- 0.807)/0.0019
PVP + PVP + PVP+ PVP	0.697 (0.554-0.817)/0.0029	0.859 (0.748- 0.934)/0.0101	0.794 (0.693- 0.874)/0.1144	0.782 (0.650-0.882)/0.0278
DP + DP + DP + DP	0.697 (0.562-0.811)/0.0007	0.787 (0.666- 0.880)/0.0008	0.751 (0.646-0.838)/0.0387	0.873 (0.760-0.946)/0.1805

AP: Arterial phase; AUC: Area under the receiver operating characteristic curve; CI: Confidence interval; DP: Delayed phase; FLLs: Focal liver lesions; HCC: Hepatocellular carcinoma; PP: Precontrast phase; PVP: Portal venous phase.

DISCUSSION

The correct diagnosis of liver lesions before treatment is of great significance. In our study, a classification system was proposed based on the features derived from the four-phase DCE-CT images. The AUC (95%CI) for differentiating each category from the others was 0.92 (0.837-0.992), 0.99 (0.967-1.00), 0.88 (0.795-0.955), and 0.96 (0.914-0.996) for HCC, metastases, benign non-inflammatory FLLs, and hepatic abscesses, respectively, indicating that the classification system is highly capable of distinguishing one lesion type from the others.

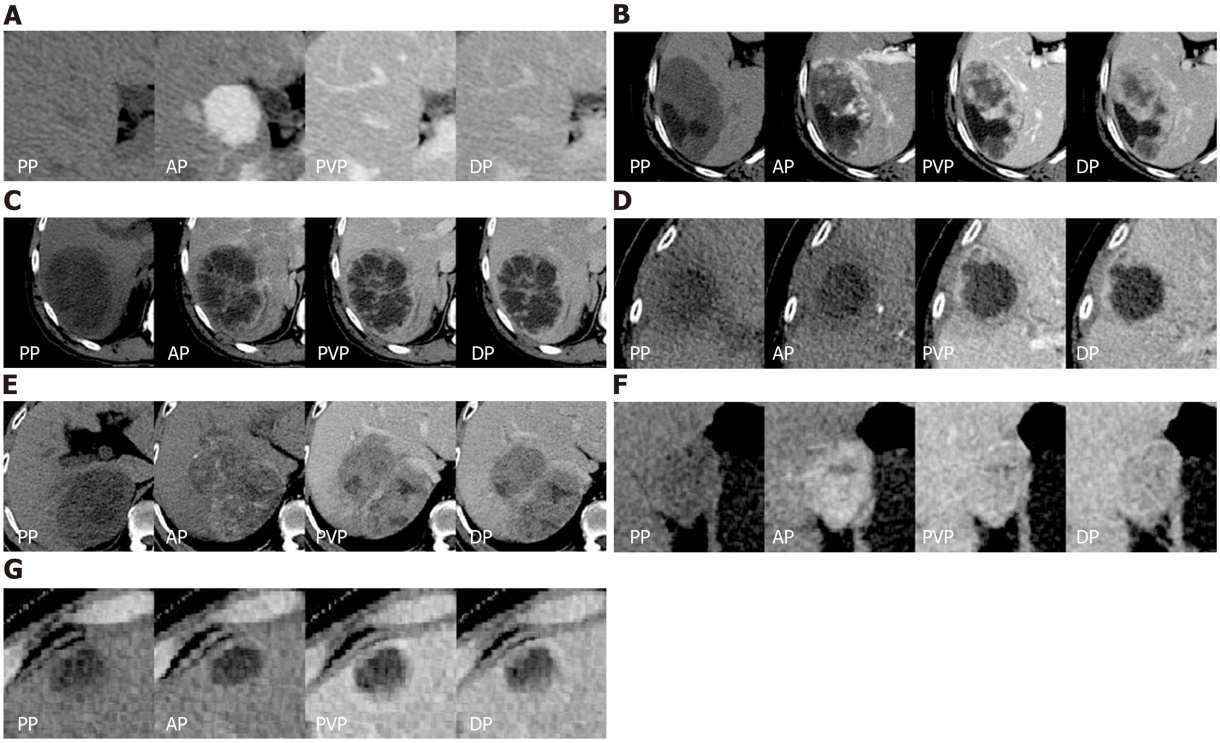

Figure 3 The representative correctly classified and misclassified categories. For each patient, axial four-phase (PP, AP, PVP, DP) computed tomography images were obtained and focal liver lesions were diagnosed by histopathologic evaluation after biopsy or surgery. A: A 33-year-old man with focal nodular hyperplasia was correctly classified as category C; B: A 54-year-old woman with hemangioma was misclassified as category D; C: A 52-year-old man with hepatic abscess was correctly classified as category D; D: An 82-year-old woman with hepatic abscess was misclassified as category B; E: A 55-year-old man with HCC was correctly classified as category A; F: A 38-year-old woman with HCC was misclassified as category C; G: A 75-year-old man with liver metastases derived from colorectal cancer was correctly classified as category B. And there was no misclassification for the metastasis group. AP: Arterial phase; DP: Delayed phase; PP: Precontrast phase; PVP: Portal venous phase.

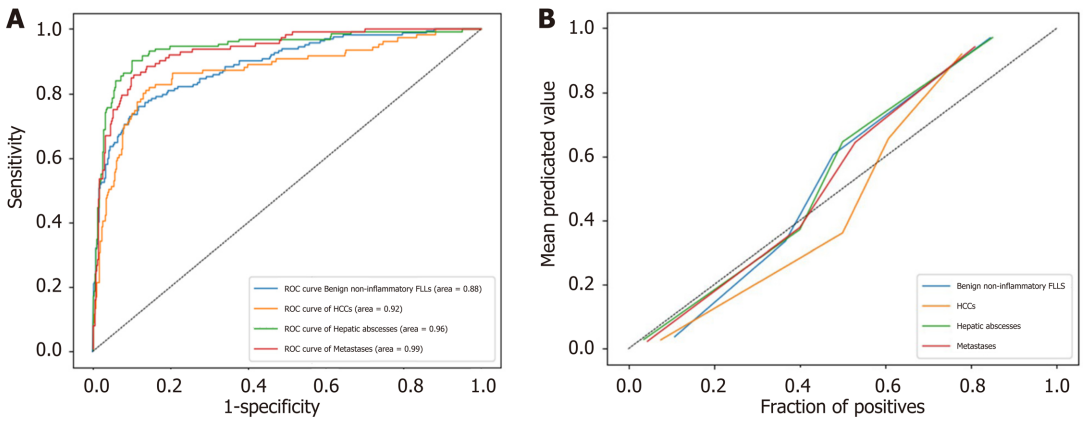

Figure 4 The receiver operating characteristic analysis of model's classification performance on test set and calibration curve of model's classification probability for each category. A: The receiver operating characteristic analysis of model's classification performance on test set; B: Calibration curve of model's classification probability for each category. FLLs: Focal liver lesions; HCC: Hepatocellular carcinoma; ROC: Receiver operating characteristic.

Since the different types of FLLs have different outcomes and require different clinical interventions, the current challenge in determining an accurate diagnosis involves not only effectively differentiating between benign and malignant FLLs according to the medical image but also accurately recognizing the different types of FLLs. A previous study[20] proposed a novel two-stage multiview learning framework for the ultrasound-based computer-aided diagnosis of benign and malignant liver tumors. Although both HCC and metastases are malignant liver tumors, their treatment strategies are completely different; thus, more accurate classification is

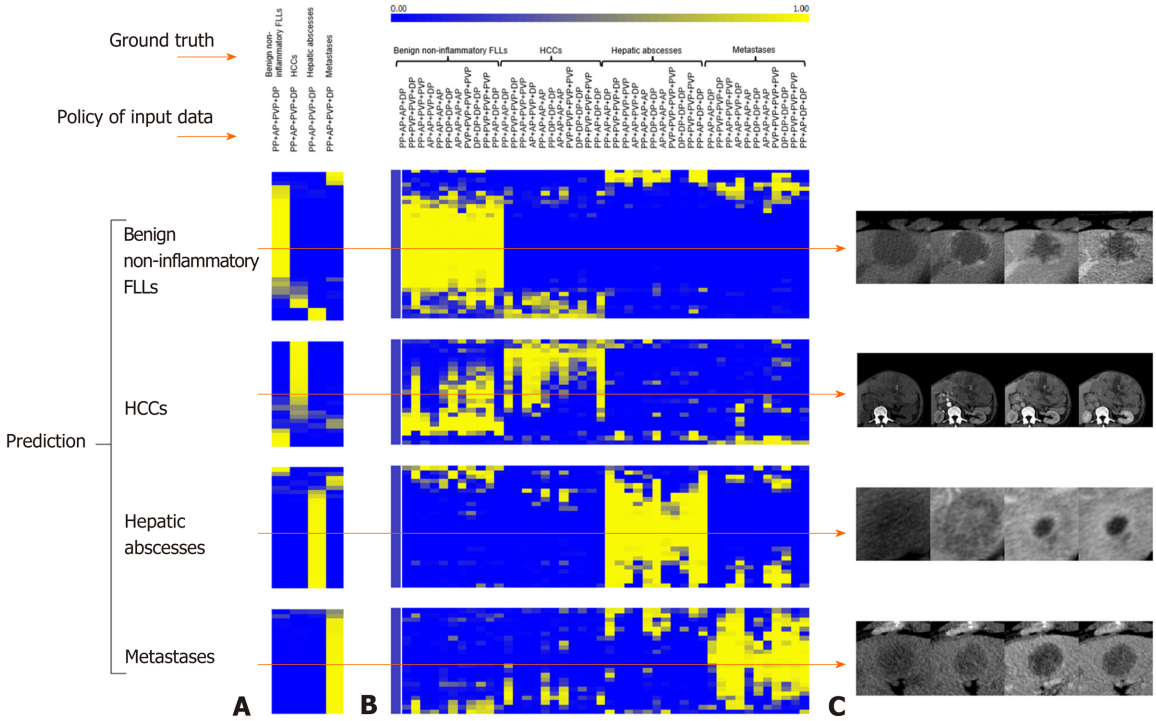

Figure 5 Predicted probability heatmaps. The top color bar represents the classification probability of the model from 0 to 1, which corresponds to dark blue to bright yellow. A: Shows the results from normal four-phase input; B: Shows the results from different "phase cheating" sets as indicated in the policy of input data; C: Shows the representative examples. AP: Arterial phase; DP: Delayed phase; PP: Precontrast phase; PVP: Portal venous phase.

needed. Yasaka *et al*[15] investigated the feasibility of applying deep learning models for liver lesion classification using CT images and showed good model performance. However, their standard of classification was based on the radiologic features. HCC is treated differently from metastases, as are abscesses and FNHs. In our study, the category label obtained from the combination of contemporaneous histology and treatment decisions should have more practically applicable value.

Notably, the sensitivity for distinguishing HCC was not high (0.739) in our study, similar to that of previous studies. The range of sensitivities reported in the literature for the detection of HCC on DCE-CT is 50%-75%[21-24]. However, the diagnosis of the lesions may vary depending on the imaging modality. Hamm *et al*[18] developed a CNN model based on MRI images for liver lesion classification, demonstrating high sensitivity. Previous studies[24,25] also reported the superiority of MRI over CT. However, in clinical practice, CT is more accessible and more inexpensive than MRI. Those patients who have a contraindication for MRI due to a comprehensive past history and clinical evaluation are candidates for the CT examination. Our model should be made available to these patients.

The interpretation of how neural networks, particularly deep neural networks, obtain the conclusion is difficult, and these networks are criticized as black boxes[26]. To evaluate whether our model correctly learned useful features from the four-phase CT images, we applied a "phase cheating" experiment on the test set. Compared to the normal set, the performance of the deep-learning network in differentiating HCC from others was dramatically degraded once the placeholder on AP and/or PVP was occluded ($P < 0.05$). This finding probably indicates that the networks make decisions by using accurate distinguishing features, AP hypervascularity and washout in the PVP, which is consistent with the clinical diagnostic criteria for HCC[26]. However, there was no significant difference in the AUCs for differentiating HCC from others between the normal set and the "phase cheating" set when PP was replaced by AP. This result was likely because most lesions are hypodense in the PP[27,28] and the normal hepatic parenchyma shows only minimal enhancement during the AP. The degree of enhancement of lesions in the AP was obtained by comparing the normal hepatic parenchyma around the lesions. In addition, the enhanced scans and the PP have the same value in the diagnosis of calcium, necrosis and gas in the lesion.

One issue for supervised learning is overfitting[29], which normally shows good fit on training data but performs poorly on unseen test data. When the size of training set

is small, this phenomenon becomes more apparent. To avoid overfitting, we applied various regulation techniques in the model during training, such as adding normalization layers to generalize the model, applying L2 regulation to the filters, adding a dropout layer, and augmenting the data to accommodate data variation. The Brier scores for HCCs, metastases, benign non-inflammatory FLLs and hepatic abscesses also suggest that our model is accurate and reasonable.

Our study had several limitations. First, we only evaluated the four-phase CT images and did not consider the clinical information, such as an increased alpha-fetoprotein level and a history of hepatitis B, C infection or liver cirrhosis, which might suggest HCC[29]. Second, we only trained and evaluated the model in a single center setting using a single CT scanner, where there might be a data bias that may lead to model bias. The model should display better generality if more variable data are analyzed. Third, the sample size of the test set was relatively small. Therefore, a larger sample is needed for further studies. Finally, we did not include lesions larger than 10 cm due to the balance among network depth, input matrix size, receptive field size, and memory load. For larger lesions, a higher matrix input size and a deeper network depth are needed, causing a rapid increase in memory requirement, which exceeds the capacity of the current GPUs.

In conclusion, the MP-CDN showed a high differential diagnostic performance for classifying FLLs as HCC, metastases, benign non-inflammatory FLLs and hepatic abscesses in four-phase CT images. If trained on a larger sample or a diverse cohort imaged with a variety of CT scanners, the MP-CDN could become an efficient tool to assist radiologists in accurate identification of the different types of FLLs. However, further evaluation of this model in a multicenter setting is necessary to evaluate its clinical utility.

ARTICLE HIGHLIGHTS

Research background

The accurate classification of focal liver lesions (FLLs) is essential to properly guide treatment options and predict prognosis. Dynamic contrast-enhanced computed tomography (DCE-CT) is commonly used for the noninvasive detection and exact classification of FLLs due to its high scanning speed and high-density resolution. Since their recent development, convolutional neural network (CNN)-based deep learning techniques have been recognized to have high potential for image recognition tasks.

Research motivation

Since the different types of FLLs have different outcomes and require different clinical interventions, the current challenge in determining an accurate diagnosis involves not only effectively differentiating between benign and malignant FLLs according to the medical image but also accurately recognizing the different types of FLLs. Our purpose was to develop and evaluate a deep learning-based CNN to classify FLLs on multiphase CT. Our CNN model is expected to become an efficient tool to assist radiologists in accurately identifying the different types of FLLs.

Research objectives

The appearances, especially the dynamic enhancement patterns of FLLs on CT imaging, are essential for categorizing lesions. We employed a four-channel input data to preserve the dynamic enhancement properties. The combination of the lesion's dynamic enhancement pattern with a CNN can imitate the image diagnosis of radiologists and is expected to improve diagnostic accuracy.

Research methods

A total of 517 FLLs scanned on a 320-detector CT scanner using a four-phase DCE-CT imaging protocol (including precontrast phase, arterial phase, portal venous phase, and delayed phase) from 2012 to 2017 were retrospectively enrolled. FLLs were classified into four categories: Category A, hepatocellular carcinoma (HCC); category B, liver metastases; category C, benign non-inflammatory FLLs including hemangiomas, focal nodular hyperplasias and adenomas; and category D, hepatic abscesses. Each category was split into a training set and test set in an approximately 8:2 ratio. The CNN model with a sequential input of the four-phase CT images was developed to automatically classify FLLs. The classification performance of CNN model was evaluated on the test set: The accuracy, specificity and sensitivity were

calculated from the confusion matrix, and the area under the receiver operating characteristic curve (AUC) was calculated from the SoftMax probability outputted from the last layer of the CNN model.

Research results

A total of 410 FLLs were used for training and 107 FLLs were used for testing. The accuracy/specificity/sensitivity of differentiating each category from others were 0.916/0.964/0.739, 0.925/0.905/1.0, 0.860/0.918/0.735 and 0.925/0.963/0.815 for HCC, metastases, benign non-inflammatory FLLs, and abscesses on the test set, respectively. The AUC (95% confidence interval) for differentiating each category from others was 0.92 (0.837-0.992), 0.99 (0.967-1.00), 0.88 (0.795-0.955) and 0.96 (0.914-0.996) for HCC, metastases, benign non-inflammatory FLLs, and abscesses on the test set, respectively. Also, for this study, we only trained and evaluated the CNN model in a single center setting using a single CT scanner, where there might be a data bias that may lead to model bias. Further evaluation of this model in a multicenter setting is needed to evaluate its clinical utility.

Research conclusions

Overall, our CNN model showed a high differential diagnostic performance for classification FLLs as HCC, metastases, benign non-inflammatory FLLs and hepatic abscesses in four-phase CT image and could become an efficient tool to assist radiologists in accurate identification of the different types of FLLs.

Research perspectives

Further multicenter studies are necessary to evaluate the clinical utility of our CNN model. In addition, it's worth to evaluate the clinical information whether can further improve the perform of CNN model.

REFERENCES

1 **Horta G**, López M, Dotte A, Cordero J, Chesta C, Castro A, Palavecino P, Poniachik J. [Benign focal liver lesions detected by computed tomography: Review of 1,184 examinations]. *Rev Med Chil* 2015; **143**: 197-202 [PMID: 25860362 DOI: 10.4067/S0034-98872015000200007]

2 **Kaltenbach TE**, Engler P, Kratzer W, Oeztuerk S, Seufferlein T, Haenle MM, Graeter T. Prevalence of benign focal liver lesions: ultrasound investigation of 45,319 hospital patients. *Abdom Radiol (NY)* 2016; **41**: 25-32 [PMID: 26830608 DOI: 10.1007/s00261-015-0605-7]

3 **Heimbach JK**, Kulik LM, Finn RS, Sirlin CB, Abecassis MM, Roberts LR, Zhu AX, Murad MH, Marrero JA. AASLD guidelines for the treatment of hepatocellular carcinoma. *Hepatology* 2018; **67**: 358-380 [PMID: 28130846 DOI: 10.1002/hep.29086]

4 **The American College of Radiology**. CT/MRI LI-RADS® v2018 CORE. Available from: https://www.acr.org/Clinical-Resources/Reporting-and-Data-Systems/LI-RADS/CT-MRI-LI-RADS-v2018

5 **Ambinder EP**. A history of the shift toward full computerization of medicine. *J Oncol Pract* 2005; **1**: 54-56 [PMID: 20871680 DOI: 10.1200/JOP.2005.1.2.54]

6 **Gletsos M**, Mougiakakou SG, Matsopoulos GK, Nikita KS, Nikita AS, Kelekis D. A computer-aided diagnostic system to characterize CT focal liver lesions: design and optimization of a neural network classifier. *IEEE Trans Inf Technol Biomed* 2003; **7**: 153-162 [PMID: 14518728 DOI: 10.1109/titb.2003.813793]

7 **Huang YL**, Chen JH, Shen WC. Diagnosis of hepatic tumors with texture analysis in nonenhanced computed tomography images. *Acad Radiol* 2006; **13**: 713-720 [PMID: 16679273 DOI: 10.1016/j.acra.2005.07.014]

8 **Mougiakakou SG**, Valavanis IK, Nikita A, Nikita KS. Differential diagnosis of CT focal liver lesions using texture features, feature selection and ensemble driven classifiers. *Artif Intell Med* 2007; **41**: 25-37 [PMID: 17624744 DOI: 10.1016/j.artmed.2007.05.002]

9 **Lakhani P**, Gray DL, Pett CR, Nagy P, Shih G. Hello World Deep Learning in Medical Imaging. *J Digit Imaging* 2018; **31**: 283-289 [PMID: 29725961 DOI: 10.1007/s10278-018-0079-6]

10 **Biswas M**, Kuppili V, Saba L, Edla DR, Suri HS, Cuadrado-Godia E, Laird JR, Marinhoe RT, Sanches JM, Nicolaides A, Suri JS. State-of-the-art review on deep learning in medical imaging. *Front Biosci (Landmark Ed)* 2019; **24**: 392-426 [PMID: 30468663]

11 **Litjens G**, Kooi T, Bejnordi BE, Setio AAA, Ciompi F, Ghafoorian M, van der Laak JAWM, van Ginneken B, Sánchez CI. A survey on deep learning in medical image analysis. *Med Image Anal* 2017; **42**: 60-88 [PMID: 28778026 DOI: 10.1016/j.media.2017.07.005]

12 **Shen W**, Zhou M, Yang F, Yang C, Tian J. Multi-scale Convolutional Neural Networks for Lung Nodule Classification. *Inf Process Med Imaging* 2015; **24**: 588-599 [PMID: 26221705 DOI: 10.1007/978-3-319-19992-4_46]

13 **Yasaka K**, Akai H, Kunimatsu A, Abe O, Kiryu S. Liver Fibrosis: Deep Convolutional Neural Network for Staging by Using Gadoxetic Acid-enhanced Hepatobiliary Phase MR Images. *Radiology* 2018; **287**: 146-155 [PMID: 29239710 DOI: 10.1148/radiol.2017171928]

14 **Kermany DS**, Goldbaum M, Cai W, Valentim CCS, Liang H, Baxter SL, McKeown A, Yang G, Wu X,

Yan F, Dong J, Prasadha MK, Pei J, Ting MYL, Zhu J, Li C, Hewett S, Dong J, Ziyar I, Shi A, Zhang R, Zheng L, Hou R, Shi W, Fu X, Duan Y, Huu VAN, Wen C, Zhang ED, Zhang CL, Li O, Wang X, Singer MA, Sun X, Xu J, Tafreshi A, Lewis MA, Xia H, Zhang K. Identifying Medical Diagnoses and Treatable Diseases by Image-Based Deep Learning. *Cell* 2018; **172**: 1122-1131.e9 [PMID: 29474911 DOI: 10.1016/j.cell.2018.02.010]

15 **Yasaka K**, Akai H, Abe O, Kiryu S. Deep Learning with Convolutional Neural Network for Differentiation of Liver Masses at Dynamic Contrast-enhanced CT: A Preliminary Study. *Radiology* 2018; **286**: 887-896 [PMID: 29059036 DOI: 10.1148/radiol.2017170706]

16 **Lakhani P**, Sundaram B. Deep Learning at Chest Radiography: Automated Classification of Pulmonary Tuberculosis by Using Convolutional Neural Networks. *Radiology* 2017; **284**: 574-582 [PMID: 28436741 DOI: 10.1148/radiol.2017162326]

17 **Albarqouni S**, Baur C, Achilles F, Belagiannis V, Demirci S, Navab N. AggNet: Deep Learning From Crowds for Mitosis Detection in Breast Cancer Histology Images. *IEEE Trans Med Imaging* 2016; **35**: 1313-1321 [PMID: 26891484 DOI: 10.1109/TMI.2016.2528120]

18 **Hamm CA**, Wang CJ, Savic LJ, Ferrante M, Schobert I, Schlachter T, Lin M, Duncan JS, Weinreb JC, Chapiro J, Letzen B. Deep learning for liver tumor diagnosis part I: development of a convolutional neural network classifier for multi-phasic MRI. *Eur Radiol* 2019; **29**: 3338-3347 [PMID: 31016442 DOI: 10.1007/s00330-019-06205-9]

19 **Kutlu H**, Avcı E. A Novel Method for Classifying Liver and Brain Tumors Using Convolutional Neural Networks, Discrete Wavelet Transform and Long Short-Term Memory Networks. *Sensors (Basel)* 2019; 19 [PMID: 31035406 DOI: 10.3390/s19091992]

20 **Guo LH**, Wang D, Qian YY, Zheng X, Zhao CK, Li XL, Bo XW, Yue WW, Zhang Q, Shi J, Xu HX. A two-stage multi-view learning framework based computer-aided diagnosis of liver tumors with contrast enhanced ultrasound images. *Clin Hemorheol Microcirc* 2018; **69**: 343-354 [PMID: 29630528 DOI: 10.3233/CH-170275]

21 **Addley HC**, Griffin N, Shaw AS, Mannelli L, Parker RA, Aitken S, Wood H, Davies S, Alexander GJ, Lomas DJ. Accuracy of hepatocellular carcinoma detection on multidetector CT in a transplant liver population with explant liver correlation. *Clin Radiol* 2011; **66**: 349-356 [PMID: 21295772 DOI: 10.1016/j.crad.2010.11.012]

22 **Libbrecht L**, Bielen D, Verslype C, Vanbeckevoort D, Pirenne J, Nevens F, Desmet V, Roskams T. Focal lesions in cirrhotic explant livers: pathological evaluation and accuracy of pretransplantation imaging examinations. *Liver Transpl* 2002; **8**: 749-761 [PMID: 12200773 DOI: 10.1053/jlts.2002.34922]

23 **Ladd LM**, Tirkes T, Tann M, Agarwal DM, Johnson MS, Tahir B, Sandrasegaran K. Comparison of hepatic MDCT, MRI, and DSA to explant pathology for the detection and treatment planning of hepatocellular carcinoma. *Clin Mol Hepatol* 2016; **22**: 450-457 [PMID: 27987537 DOI: 10.3350/cmh.2016.0036]

24 **Burrel M**, Llovet JM, Ayuso C, Iglesias C, Sala M, Miquel R, Caralt T, Ayuso JR, Solé M, Sanchez M, Brú C, Bruix J; Barcelona Clínic Liver Cancer Group. MRI angiography is superior to helical CT for detection of HCC prior to liver transplantation: an explant correlation. *Hepatology* 2003; **38**: 1034-1042 [PMID: 14512891 DOI: 10.1053/jhep.2003.50409]

25 **Kim BR**, Lee JM, Lee DH, Yoon JH, Hur BY, Suh KS, Yi NJ, Lee KB, Han JK. Diagnostic Performance of Gadoxetic Acid-enhanced Liver MR Imaging versus Multidetector CT in the Detection of Dysplastic Nodules and Early Hepatocellular Carcinoma. *Radiology* 2017; **285**: 134-146 [PMID: 28609205 DOI: 10.1148/radiol.2017162080]

26 **Zhang Z**, Beck MW, Winkler DA, Huang B, Sibanda W, Goyal H; written on behalf of AME Big-Data Clinical Trial Collaborative Group. Opening the black box of neural networks: methods for interpreting neural network models in clinical applications. *Ann Transl Med* 2018; **6**: 216 [PMID: 30023379 DOI: 10.21037/atm.2018.05.32]

27 **Ma Y**, Zhang XL, Li XY, Zhang L, Su HH, Zhan CY. [Value of computed tomography and magnetic resonance imaging in diagnosis and differential diagnosis of small hepatocellular carcinoma]. *Nan Fang Yi Ke Da Xue Xue Bao* 2008; **28**: 2235-2238 [PMID: 19114368]

28 **Li CS**, Chen RC, Tu HY, Shih LS, Zhang TA, Lii JM, Chen WT, Duh SJ, Chiang LC. Imaging well-differentiated hepatocellular carcinoma with dynamic triple-phase helical computed tomography. *Br J Radiol* 2006; **79**: 659-665 [PMID: 16641423 DOI: 10.1259/bjr/12699987]

29 **Cook JA**, Ranstam J. Overfitting. *Br J Surg* 2016; **103**: 1814 [PMID: 27901280 DOI: 10.1002/bjs.10244]

30 **Bruix J**, Sherman M; Practice Guidelines Committee, American Association for the Study of Liver Diseases. Management of hepatocellular carcinoma. *Hepatology* 2005; **42**: 1208-1236 [PMID: 16250051 DOI: 10.1002/hep.20933]

31 **Yeh MM**, Daniel HD, Torbenson M. Hepatitis C-associated hepatocellular carcinomas in non-cirrhotic livers. *Mod Pathol* 2010; **23**: 276-283 [PMID: 19935643 DOI: 10.1038/modpathol.2009.174]

World Journal of Gastroenterology

Submit a Manuscript: https://www.f6publishing.com

World J Gastroenterol 2020 July 7; 26(25): 3673-3685

DOI: 10.3748/wjg.v26.i25.3673

ISSN 1007-9327 (print) ISSN 2219-2840 (online)

ORIGINAL ARTICLE

Observational Study

Type I and type II *Helicobacter pylori* infection status and their impact on gastrin and pepsinogen level in a gastric cancer prevalent area

Lin Yuan, Jun-Bo Zhao, Ying-Lei Zhou, Ya-Bin Qi, Qiong-Ya Guo, Hai-Hui Zhang, Muhammad Noman Khan, Ling Lan, Chang-He Jia, Yan-Rui Zhang, Song-Ze Ding

ORCID number: Lin Yuan 0000-0003-3816-6551; Jun-Bo Zhao 0000-0002-3299-7955; Ying-Lei Zhou 0000-0003-4270-6709; Ya-Bin Qi 0000-0002-7736-4043; Qiong-Ya Guo 0000-0002-1615-6005; Hai-Hui Zhang 0000-0003-3436-7997; Muhammad Noman Khan 0000-0003-4817-7768; Ling Lan 0000-0001-9744-4545; Chang-He Jia 0000-0001-7262-7708; Yan-Rui Zhang 0000-0003-4401-4183; Song-Ze Ding 0000-0002-4589-6942.

Author contributions: Yuan L, Lan L, Zhang YR and Ding SZ designed the research; Yuan L, Zhao JB, Zhou YL, Qi YB, Guo QY, Zhang HY, Khan MN and Jia CH collected clinical data and performed experiments; Yuan L analyzed the data; Yuan L and Ding SZ wrote the paper; Ding SZ revised the article; All authors have approved the final version of the manuscript.

Supported by National Natural Science Foundation of China, No. U1604174; Henan Provincial Government-Health and Family Planning Commission, No. 20170123; Henan Provincial Government-Health and Family Planning Commission Research Innovative Talents Project, No. 51282; and Henan Provincial Government-Science and

Lin Yuan, Jun-Bo Zhao, Ying-Lei Zhou, Ya-Bin Qi, Qiong-Ya Guo, Hai-Hui Zhang, Muhammad Noman Khan, Ling Lan, Chang-He Jia, Yan-Rui Zhang, Song-Ze Ding, Department of Gastroenterology and Hepatology, People's Hospital of Zhengzhou University, Henan Province, China

Lin Yuan, Jun-Bo Zhao, Ying-Lei Zhou, Ya-Bin Qi, Qiong-Ya Guo, Hai-Hui Zhang, Muhammad Noman Khan, Ling Lan, Chang-He Jia, Yan-Rui Zhang, Song-Ze Ding, Henan Provincial People's Hospital, Henan Province, China

Ying-Lei Zhou, Ya-Bin Qi, Qiong-Ya Guo, Hai-Hui Zhang, Muhammad Noman Khan, Ling Lan, Chang-He Jia, Yan-Rui Zhang, Song-Ze Ding, Henan University School of Medicine, Zhengzhou 450003, Henan Province, China

Corresponding author: Song-Ze Ding, MD, PhD, Chief Doctor, Professor, Department of Gastroenterology and Hepatology, People's Hospital of Zhengzhou University, No. 7 Weiwu Road, Jinshui District, Zhengzhou 450003, Henan Province, China. dingsongze@hotmail.com

Abstract

BACKGROUND

Type I *Helicobacter pylori* (*H. pylori*) infection causes severe gastric inflammation and is a predisposing factor for gastric carcinogenesis. However, its infection status in stepwise gastric disease progression in this gastric cancer prevalent area has not been evaluated; it is also not known its impact on commonly used epidemiological gastric cancer risk markers such as gastrin-17 (G-17) and pepsinogens (PGs) during clinical practice.

AIM

To explore the prevalence of type I and type II *H. pylori* infection status and their impact on G-17 and PG levels in clinical practice.

METHODS

Thirty-five hundred and seventy-two hospital admitted patients with upper gastrointestinal symptoms were examined, and 523 patients were enrolled in this study. *H. pylori* infection was confirmed by both ^{13}C-urea breath test and

Technology Bureau, No. 142300410050.

Institutional review board statement: This study was approved by the Ethics Committee of People's Hospital of Zhengzhou University (ID: 2019-KY-No. 10), Zhengzhou, China.

Conflict-of-interest statement: Authors declare no competing interests.

Data sharing statement: No additional data are available.

STROBE statement: The authors have read the STROBE Statement, and the manuscript was prepared and revised according to the STROBE Statement.

Manuscript source: Unsolicited manuscript

Received: January 4, 2020
Peer-review started: February 24, 2020
First decision: March 27, 2020
Revised: April 8, 2020
Accepted: June 4, 2020
Article in press: June 4, 2020
Published online: July 7, 2020

P-Reviewer: Jeon CH, Kishikawa H, Link A
S-Editor: Ma YJ
L-Editor: Filipodia
E-Editor: Ma YJ

serological assay. Patients were divided into non-atrophic gastritis (NAG), non-atrophic gastritis with erosion (NAGE), chronic atrophic gastritis (CAG), peptic ulcers (PU) and gastric cancer (GC) groups. Their serological G-17, PG I and PG II values and PG I/PG II ratio were also measured.

RESULTS

A total *H. pylori* infection rate of 3572 examined patients was 75.9%, the infection rate of 523 enrolled patients was 76.9%, among which type I *H. pylori* infection accounted for 72.4% (291/402) and type II was 27.6%; 88.4% of GC patients were *H. pylori* positive, and 84.2% of them were type I infection, only 11.6% of GC patients were *H. pylori* negative. Infection rates of type I *H. pylori* in NAG, NAGE, CAG, PU and GC groups were 67.9%, 62.7%, 79.7%, 77.6% and 84.2%, respectively. *H. pylori* infection resulted in significantly higher G-17 and PG II values and decreased PG I/PG II ratio. Both types of *H. pylori* induced higher G-17 level, but type I strain infection resulted in an increased PG II level and decreased PG I/PG II ratio in NAG, NAGE and CAG groups over uninfected controls. Overall PG I levels showed no difference among all disease groups and in the presence or absence of *H. pylori;* in stratified analysis, its level was increased in GC and PU patients in *H. pylori* and type I *H. pylori*-positive groups.

CONCLUSION

Type I *H. pylori* infection is the major form of infection in this geographic region, and a very low percentage (11.6%) of GC patients are not infected by *H. pylori*. Both types of *H. pylori* induce an increase in G-17 level, while type I *H. pylori* is the major strain that affects PG I and PG IIs level and PG I/PG II ratio in stepwise chronic gastric disease. The data provide insights into *H. pylori* infection status and indicate the necessity and urgency for bacteria eradication and disease prevention in clinical practice.

Key words: *Helicobacter pylori*; Chronic gastric diseases; Gastrin-17; Pepsinogen; Gastric cancer

Core tip: Type I and type II *Helicobacter pylori* (*H. pylori*) infection status and their impact on gastrin-17 and pepsinogen level in chronic gastric diseases have not been studied in this high gastric cancer risk area. Our results show that type I *H. pylori* infection is the major form of infection, and a very low percentage (11.6%) of gastric cancer patients are not infected by *H. pylori*. Both type I and type II *H. pylori* induce an increase in gastrin-17 level, while type I *H. pylori* is the major strain that affects pepsinogen (PG) I, PG II level and PG I/PG II ratio in stepwise gastric disease in this geographic area.

Citation: Yuan L, Zhao JB, Zhou YL, Qi YB, Guo QY, Zhang HH, Khan MN, Lan L, Jia CH, Zhang YR, Ding SZ. Type I and type II *Helicobacter pylori* infection status and their impact on gastrin and pepsinogen level in a gastric cancer prevalent area. *World J Gastroenterol* 2020; 26(25): 3673-3685
URL: https://www.wjgnet.com/1007-9327/full/v26/i25/3673.htm
DOI: https://dx.doi.org/10.3748/wjg.v26.i25.3673

INTRODUCTION

Helicobacter pylori (*H. pylori*) infection is the major cause of chronic gastritis, peptic ulcers, gastric cancer and mucosa-associated lymphoid tissue lymphoma, it is also associated with many extra gastrointestinal diseases[1-3]. *H. pylori* cytotoxin CagA and VacA are major virulence factors and molecular basis for disease pathogenesis. *H. pylori* strains that carry *cag*PAI with CagA-, VacA-positive cause severe gastric inflammation, which contributes to either tissue damage or neoplastic transformation, are high-risk strains of gastric cancer, and the role of CagA protein is critical in these processes[4]. Studies have shown that there is both genotypic and geographic diversity of *H. pylori* infection, which can trigger different inflammatory processes and result in

various degrees of pathological consequences[4-6].

Type I *H. pylori* expresses CagA and VacA protein; type II strain does not express CagA and VacA[7]. CagA-, VacA-positive strains are the major forms of *H. pylori* infection in many areas globally, corresponding to their high prevalence in pre-cancerous lesions and gastric cancer incidences[4]. However, their infection status and roles in the stepwise gastric disease progression in this high gastric cancer prevalent area has not been studied[8].

Serological detection of pepsinogen (PG) I, II, PG I/PG II ratio and gastrin-17 (G-17) provide valuable information on the status of gastric mucosa, and they have been used as epidemiological markers for gastric cancer risk investigation[9-12]. Studies have indicated that low concentrations of PG I and PG I/PG II ratios are indicators of gastric atrophy, which are linked with elevated gastric cancer risk[9,10]. However, others have indicated that the results are not consistent and not sensitive enough to replace endoscopy[11,12]. PG I/PG II ratio also should not be used as a biomarker of gastric neoplasia as recommended[1]. It is therefore uncertain if they might be suitable to evaluate stepwise gastric disease progression and development of mucosal precancerous conditions in the presence or absence of *H. pylori* infection in clinical practice.

In the present study, we investigated the prevalence of type I and type II *H. pylori* infection in stepwise chronic gastric diseases and the clinical implications. Their impact on G-17 and PGs levels was also evaluated. The results indicated that there is a stepwise increase in type I *H. pylori* infection rate as disease progress from chronic gastritis to gastric cancer. Both types of *H. pylori* induce an increase in G-17 level, while type I *H. pylori* is the major strains that affects PG I, PG II levels and PG I/PG II ratio in chronic gastric diseases in this geographic region. The results provide insight on the subtypes of *H. pylori* infection status and their impact on G-17 and PGs, which will be helpful to guide *H. pylori* eradication and application of G-17 and PGs assay in clinical practice.

MATERIALS AND METHODS

Study population

This cross-section study was conducted at the Department of Gastroenterology, People's Hospital of Zhengzhou University, Zhengzhou, Henan, China. From March 2018 to March 2019, a total of 3572 consecutively ward admitted patients with upper gastrointestinal symptoms were examined. Exclusion criteria were as follows: (1) Taking proton pump inhibitors, bismuth salts, H_2-receptor blockers or other medications that could affect test results over the past 2 wk, taking antibiotics over the past 1 mo; (2) Severe concomitant diseases such as liver, kidney, nervous system or cardiac dysfunction; (3) People with active upper gastrointestinal bleeding; (4) Patients with a history of gastrointestinal surgery for gastric cancer, esophageal cancer or gastric adenoma; and (5) People with mental illness or severe neurosis, affecting correct expression or study. The study finally enrolled 523 patients, the flow chart of patient screening is summarized in Figure 1.

All 523 enrolled patients were examined by upper-endoscopy to get pathological confirmation. Based on histopathologic types, subjects were categorized into five groups: Non-atrophic gastritis (NAG), non-atrophic gastritis with erosion (NAGE), chronic atrophic gastritis (CAG), peptic ulcers (PU) and gastric cancer (GC). Demographic data of patients including age and gender were recorded, and *H. pylori* CagA, VacA status, G-17, PG I, II levels and PG I/PG II ratio were analyzed. The research protocol was approved by the Ethics Committee of People's Hospital of Zhengzhou University (2019-KY-No. 10); informed consents were obtained from all participating patients.

Measurement of H. pylori infection

The status of *H. pylori* infection was confirmed by both ^{13}C-urea breath test (UBT) and serological *H. pylori* antibody test, patients were considered not infected when both tests were negative; when patients were either ^{13}C-UBT or serological *H. pylori* antibody positive, but not both, they were not enrolled to avoid false-positive or -negative results. ^{13}C-UBT was performed after overnight fasting, a baseline breath sample was obtained by blowing gas into a bag container, and a powder capsule containing 50 mg of ^{13}C-urea was given to patients with 80-100 mL water. The second breath sample was collected after 30 min of meditation. Patients were considered *H. pylori* positive if the difference between baseline sample and 30-min sample exceeded

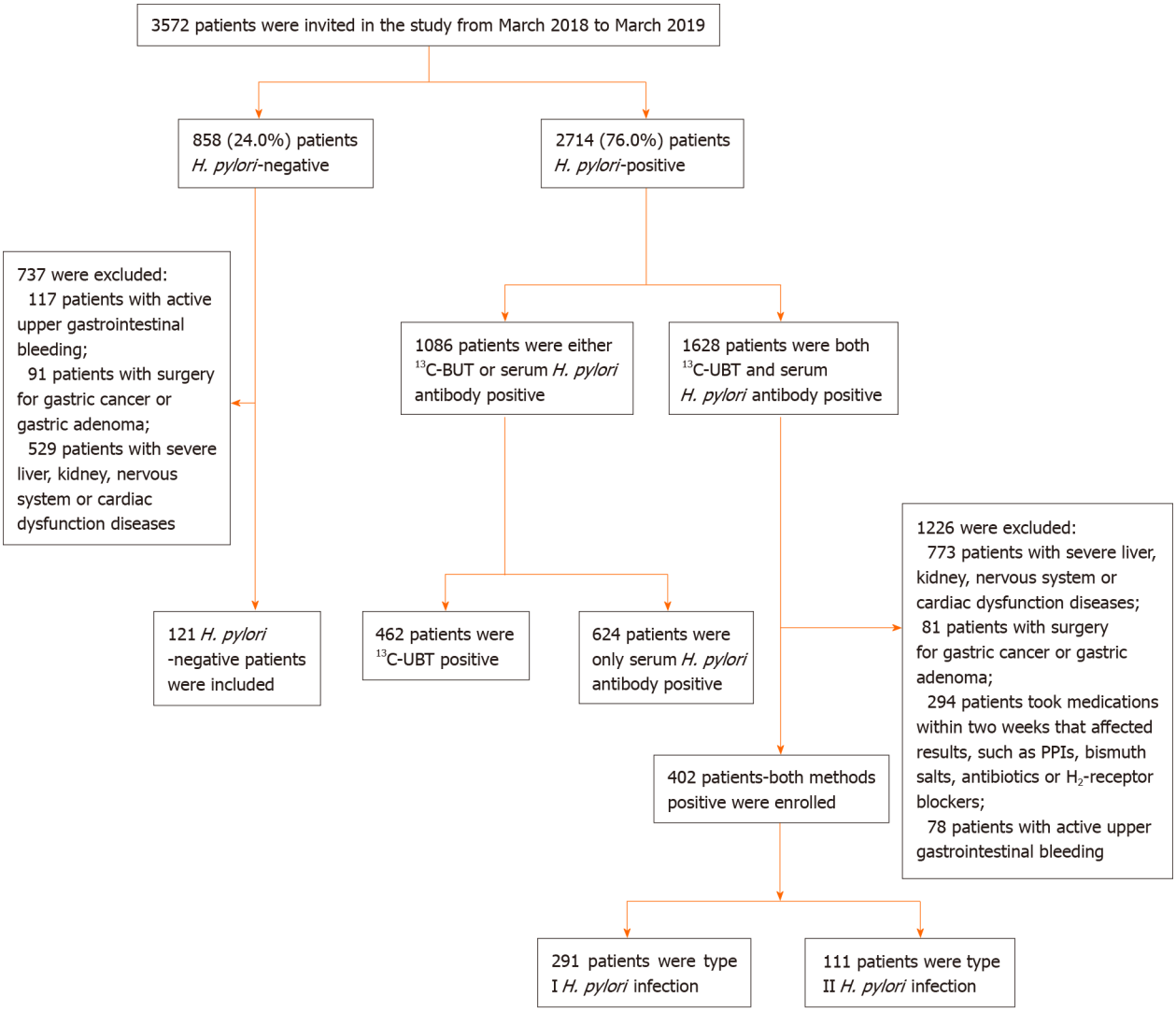

Figure 1 Flowchart of enrolled patients–screening program.*H. pylori*: *Helicobacter pylori*.

4.0 arbitrary units by ^{13}C-breath test (HY-IREXC 16 channel; Huayou Mingkang Photoelectric Technology Co., Ltd, Guangzhou, China).

Serological measurements of H. pylori antibody, G-17 and PGs

Five milliliters of fasting venous blood sample was collected from each participant. All samples were centrifuged at 1500 × *g* for 5 min and analyzed within 2 h of blood collection. Serum anti-*H. pylori* antibody, G-17, PG I, PG II levels, and PG I/PG II ratio were measured by enzyme-linked immunosorbent assay (ELISA) kit (*Helicobacter pylori* ELISA kit, Blot Biotech Co., Ltd, Shenzhen, China; PG I, PG II, G-17 ELISA kits, Biohit Biotechnology Co., Ltd. Anhui, China). The procedure followed manufacturers' instructions; quality control analysis showed that the coefficient of variation in intra-batch and inter-batch sample tests was less than 10%.

Determination of *H. pylori* positivity from blood samples: (1) Type I *H. pylori* antibody positive: either or both CagA and VacA bands were present; (2) Type II *H. pylori* antibody positive: only one of urease (Ure) A and UreB bands or both appeared, no CagA, VacA bands were present; and (3) *H. pylori* antibody negative: Only control band appeared in the color-developing zone, and no positive zone was observed. Representative *H. pylori* serological test blot pictures are provided in Supplementary Figure 1.

Endoscopic and histopathological evaluation

Histopathological diagnosis was available in all enrolled 523 patients. Two pieces of biopsy specimen were obtained from the lesion area, antrum and angulus during endoscopic examination. The biopsies were oriented, fixed in formalin, embedded in

paraffin blocks and then sectioned and stained with hematoxylin and eosin for histopathological analysis. For histologic sections where there was initial disagreement on histopathologic interpretation, the final results were determined through adjudication among two pathologists and a third pathologist.

Statistical analysis

Data were analyzed using SPSS for Windows Version 22 (Armonk, NY, United States). Continuous variables were described as mean ± standard deviation, while categorical variables were described as percentages or frequencies. All data were tested for normal distribution by Kolmogorov-Smirnov test and homogeneity of variances by Levene's test. Data of normal distribution and similar variances were tested by Student's "t" test for two independent samples comparison, and analysis of variance for multiple comparisons among different groups. A comparison of ratios was made by the χ^2 test. A P value less than 0.05 was considered statistically significant, which was derived from two-tailed tests. Receiver operating characteristic (ROC) curves were used to calculate the overall diagnostic performance of G-17, PG I, PG II, and PG I/PG II ratio in PU, CAG and GC patients to determine the best cutoff values, sensitivity and specificity.

RESULTS

Overall H. pylori infection status of patients

H. pylori infection status of 3572 patients is presented in Figure 1. Among which, 2714 (76.0%) patients were positive either by UBT test, serological test or both, and 858 (24.0%) patients were negative. Among *H. pylori*-positive patients, 1226 were excluded due to either surgery, medication or bleeding reasons, and 1086 patients were excluded due to either only ^{13}C-BUT or serum antibody test positive but not both; the final enrolled patient number was 402 with both tests being positive. In 858 *H. pylori*-negative patients, 737 patients were excluded either due to bleeding, surgery or severe organ diseases; this resulted in only 121 patients being enrolled with both tests being negative. Interestingly, we noticed almost identical *H. pylori* infection rates when comparing the prior- and post-excluded non-enrolled patients. The infection rates of the final enrolled patients were 76.9% positive and 23.1% negative (Figure 1).

Patient clinical data and H. pylori infection status

Among the 523 enrolled patients, 305 were male and 218 were female, with an average age of 53.4 ± 11.6 years (range from 28 to 79). Their clinical characteristics and *H. pylori* infection status are presented in Table 1. Patients in 51-60 and 61-80 years age groups had the highest *H. pylori* infection rates of 78.5% (150/191) and 78.4% (116/148), respectively. The average age of patients in the GC group was significantly higher than that in NAG, NAGE and PU groups ($P < 0.05$). The mean age of the CAG group was higher than that in the NAG group ($P < 0.001$). There was no significant difference in *H. pylori* infection status between male and female gender. *H. pylori* infection in male and female genders were mainly type I *H. pylori* strains (54.8%, 56.9% respectively), which were significantly higher than that of type II and *H. pylori* negative patient groups (range from 20.2%-23.3%). There was a significant male dominance in CAG, PU and GC groups ($P < 0.05$). Among 77 CAG patients, 48 (62.3%) patients were antrum atrophic gastritis and 29 (33.8%) were corpus atrophic gastritis, and all 43 gastric cancer patients were intestinal type.

Prevalence of Type I and Type II H. pylori infection in stepwise chronic gastric diseases

Total *H. pylori* infection rate of 523 patients was 76.9% (402/523), of which type I *H. pylori* infection rate was 72.4% (291/402), and type II infection rate was 27.6% (111/402). Overall, 88.4% of GC patients were *H. pylori* positive, and 84.2% of them were type I infection, only 11.6% of GC were *H. pylori* negative. As the disease progressed, *H. pylori* infection rate was gradually increased in NAG, NAGE, PU, CAG and GC groups; among which *H. pylori*-positive rate reached the highest level in PU group, accounting for 90.4% (85/94) of the patients. Infection rates of type I *H. pylori* in NAG, NAGE, PU, CAG and GC groups were 67.9%, 62.7%, 77.6%, 79.7%, 84.2%, respectively; and was significantly higher than the corresponding type II *H. pylori* groups; and type I *H. pylori* infection rates were also higher in PU, CAG, and GC groups when compared with the NAG group (Table 2).

Table 1 Patient clinical data and *Helicobacter pylori* infection status

Groups	Total patients, *n* = 523	NAG, *n* = 213	NAGE, *n* = 96	PU, *n* = 94	CAG, *n* = 77	GC, *n* = 43	*Hp* (+),*n* = 402	Type I *Hp*(+),*n* = 291	Type II *Hp*(+),*n* = 111	*Hp* (-), *n* = 121
Age in yr										
mean ± SD	53.4 ± 11.6	50.3 ± 11.3[a]	53.7 ± 11.3	53.5 ± 13.1	58.0 ± 9.4[a]	59.6 ± 7.8[c]	53.7 ± 11.4	53.6 ± 11.3	53.9 ± 11.7	52.5 ± 12.1
28-40	76	57 (26.8%)	13 (13.5%)	16 (17.0%)	4 (5.2%)	0	57 (75.0%)	43 (56.6%)[e]	15 (19.7%)	18 (23.7%)
41-50	108	71 (33.3%)	21 (21.9%)	17 (18.1%)	7 (9.1%)	6 (14.0%)	78 (72.2%)	55 (50.9%)[e]	23 (21.3%)	30 (27.8%)
51-60	191	54 (25.3%)	36 (37.5%)	30 (31.9%)	32 (41.6%)	21 (48.8%)	150 (78.5%)	108 (56.5%)[e]	42 (22.0%)	41 (21.5%)
61-80	148	31 (14.6%)	26 (27.1%)	31 (33.0%)	34 (44.2%)	16 (37.2%)	116 (78.4%)	85 (57.5%)[e]	31 (20.9%)	32 (21.6%)
Gender										
Male	305	105 (49.3%)	52 (54.2%)	68 (70.2%)[g]	53 (68.8%)[g]	27 (58.3%)[g]	234 (76.7%)	167 (54.8%)[i]	67 (22.0%)	71 (23.3%)
Female	218	108 (50.7%)	44 (45.8%)	26 (27.7%)	24 (31.2%)	16 (37.3%)	168 (77.1%)	124 (56.9%)[i]	44 (20.2%)	50 (22.9%)

Data are presented as *n* (%), unless otherwise indicted.

[a]$P < 0.05$, mean age in CAG group was compared with NAG group;

[c]$P < 0.05$, mean age in GC group was compared with NAG, NAGE groups;

[e]$P < 0.05$, infection rate of type I *H. pylori* patients was compared with type II and *H. pylori*-negative patients in the same age groups;

[g]$P < 0.05$, percentage in male groups was compared with female groups among PU, CAG, and GC groups;

[i]$P < 0.05$, infection rate of type I *H. pylori* patients was compare with type II and Hp-negative patients in the same gender groups. CAG: Chronic atrophic gastritis; GC: Gastric cancer; *H. pylori*: *Helicobacter pylori*; NAG: Non-atrophic gastritis; NAGE: Non-atrophic gastritis with erosion; PU: Peptic ulcer; SD: Standard deviation.

Table 2 Infection rates of type I and type II *Helicobacter pylori* in stepwise chronic gastric diseases

Groups	Total	*H. pylori* (+)	*H. pylori* (-)	Type I*H. pylori* (+)	Type II*H. pylori* (+)
NAG	213	140 (65.7)	73 (34.3)	95 (67.9)[a]	45 (32.1)
NAGE	96	75 (78.1)[c]	21 (21.9)	47 (62.7)[a]	28 (37.3)
PU	94	85 (90.4)[c]	9 (9.6)	66 (77.6)[ae]	19 (22.4)
CAG	77	64 (83.1)[c]	13 (16.9)	51 (79.7)[ae]	13 (20.3)
GC	43	38 (88.4)[c]	5 (11.6)	32 (84.2)[ae]	6 (15.8)
Total	523	402 (76.9)	121 (23.1)	291 (72.4)	111 (27.6)

Data are presented as *n* (%).

[a]$P < 0.05$, when type I *H. pylori* infection rate was compared with type II *H. pylori* infection rate in the same disease groups;

[c]$P < 0.05$, when *H. pylori* infection rate was compared with the rate of control [non-atrophic gastritis (NAG)] group;

[e]$P < 0.05$, when type I *H. pylori* infection rate was compared with the rate of NAG group. CAG: Chronic atrophic gastritis; GC: Gastric cancer; *H. pylori* : *Helicobacter pylori*; NAG: Non-atrophic gastritis; NAGE: Non-atrophic gastritis with erosion; PU: Peptic ulcer.

Distribution of H. pylori CagA, VacA, UreA and UreB in stepwise chronic gastric diseases

Positive rates of CagA, VacA, UreA and UreB antibodies are described in Table 3. In 402 infected samples, the percentage of CagA, VacA, UreA and UreB were 70.1%, 61.9%, 70.6% and 98.8%, respectively. CagA antibody was detected in 63.3%, 60.0%, 76.5%, 79.7% and 84.2% in NAG, NAGE, PU, CAG and GC groups, respectively. The positive rates of CagA and VacA were highest in GC group and lowest in NAGE group. UreB antibodies were present in 98.8% of patients with *H. pylori* infection, and there was no statistical differences between disease groups ($P > 0.05$).

Effects of H. pylori infection on overall G-17, PG I, PG II levels and PG I/PG II ratio

Overall serum G-17, PG I, PG II values and PG I/PG II ratio at different *H. pylori* infection status are shown in Table 4. G-17 and PG II values in *H. pylori* infected

Table 3 Distribution of CagA, VacA, UreA and UreB serological antibodies in stepwise chronic gastric disease

Groups	CagA	VacA	UreA	UreB
NAG, *n* = 140	89 (63.6)	82 (55.6)	93 (66.4)	138 (98.6)
NAGE, *n* = 75	45 (60.0)	36 (48.0)	44 (58.7)	74 (98.7)
PU, *n* = 85	65 (76.5)	57 (67.0)	67 (78.8)	83 (97.6)
CAG, *n* = 64	51 (79.7)	43 (67.2)	49 (76.6)	64 (100.0)
GC, *n* = 38	32 (84.2)	28 (73.7)	31 (81.6)	38 (100.0)
Total, *n* = 402	282 (70.1)	249 (61.9)	284 (70.6)	397 (98.8)

Data are presented as *n* (%). CAG: Chronic atrophic gastritis; GC: Gastric cancer; NAG: Non-atrophic gastritis; NAGE: Non-atrophic gastritis with erosion; PU: Peptic ulcer.

Table 4 Effects of *Helicobacter pylori* infection on gastric gastrin-17, pepsinogen I, pepsinogen II levels and pepsinogen I/II ratios

H. pylori status	*n*	G-17, pmol/L	PG I, μg/L	PG II, μg/L	PG I/PG II
H. pylori (+)	402	7.9 ± 8.9[a]	131.4 ± 86.6	17.3 ±13.2[a]	8.4 ± 4.8[a]
H. pylori (-)	121	3.6 ± 5.2	117.0 ± 76.7	10.5 ± 9.2	12.8 ± 6.5
Type I *H. pylori* (+)	291	8.5 ± 9.5[ac]	134.2 ± 86.4	18.7 ± 13.7[ac]	7.7± 4.2[ac]
Type II *H. pylori* (+)	111	6.1 ± 6.5[a]	123.9 ± 86.9	13.9 ± 11.0	10.5 ± 5.6[a]

Data are presented as mean ± standard deviation.

[a]$P < 0.05$, when compared with *H. pylori*-negative group;

[c]$P < 0.05$, when compared between type I and type II *H. pylori*-infected groups. G-17: Gastrin-17; *H. pylori*: *Helicobacter pylori*; PG I: Pepsinogen I; PG I/PG II : Pepsinogen I/II ratio; PG II: Pepsinogen II.

groups were significantly higher and PG I/PG II ratio were lower than those in *H. pylori*-negative patients ($P < 0.05$); while PG I level was not different between *H. pylori*-positive and -negative groups ($P > 0.05$). There was also no significant difference in PG I levels between type I and II *H. pylori*-infected patients. G-17 and PG II levels were significantly increased and PG I/PG II ratio were decreased only in patients with type I *H. pylori* infection when compared with type II and *H. pylori*-negative patients ($P < 0.05$).

Receiver operating characteristic curves for G-17, PG I, PG II and PG I / PG II in the prediction of CAG, PU and GC patients

Figure 2 shows ROC curves for G-17, PG I, PG II and PG I/PG II in the prediction of CAG, PU and GC patients. ROC curves for predicting PU based on G-17, PG I, PG II and PG I/PG II ratio are listed in Figure 2 a1-2. Area under the receiver operating characteristic curves (AUROC) were 0.579 (95%confidence interval (CI): 0.514-0.643), 0.663 (95%CI: 0.599-0.729) and 0.653 (95%CI: 0.593-0.713), and 0.529 (95%CI: 0.460-0.598); cut-off values of Youden index were 5.91 pmol/L, 146.20 μg/L, 13.31 μg/L and 9.49, respectively; the sensitivity was 45.7%, 52.1%, 62.8% and 55.3%, respectively; and specificity was 69.4%, 76.9%, 64.5% and 54.0%, respectively.

ROC curves for predicting CAG based on G-17, PG I, PG II and PG I/PG II ratio are listed in Figure 2 b1-2. AUROC were 0.550 (95%CI: 0.474-0.626), 0.531 (95%CI: 0.455-0.607), 0.610 (95%CI: 0.535-0.684) and 0.623 (95%CI: 0.552-0.694), respectively; the cut-off values of Youden index were 4.63 pmol/L, 110.7 μg/L, 7.41 μg/L and 9.37, respectively; the sensitivity was 71.4%, 68.8%, 50.5% and 68.8%, respectively; and specificity was 39.4%, 46.0%, 70.9% and 49.8%, respectively.

ROC curves for predicting GC based on G-17, PG I, PG II and PG I/PG II ratio are listed in Figure 2 c1-2, AUROC were 0.786 (95%CI: 0.737-0.834), 0.634 (95%CI: 0.533-0.735), 0.719 (95%CI: 0.646-0.792) and 0.760 (95%CI: 0.684-0.836), respectively; cut-off values of Youden index: 6.21pmol/L, 174.49 μg/L, 14.83 μg/L and 6.47, respectively; the sensitivity was 88.4%, 53.5%, 68.8% and 67.4%, respectively; and specificity was 68.3%, 81.0%, 64.4% and 72.7%, respectively.

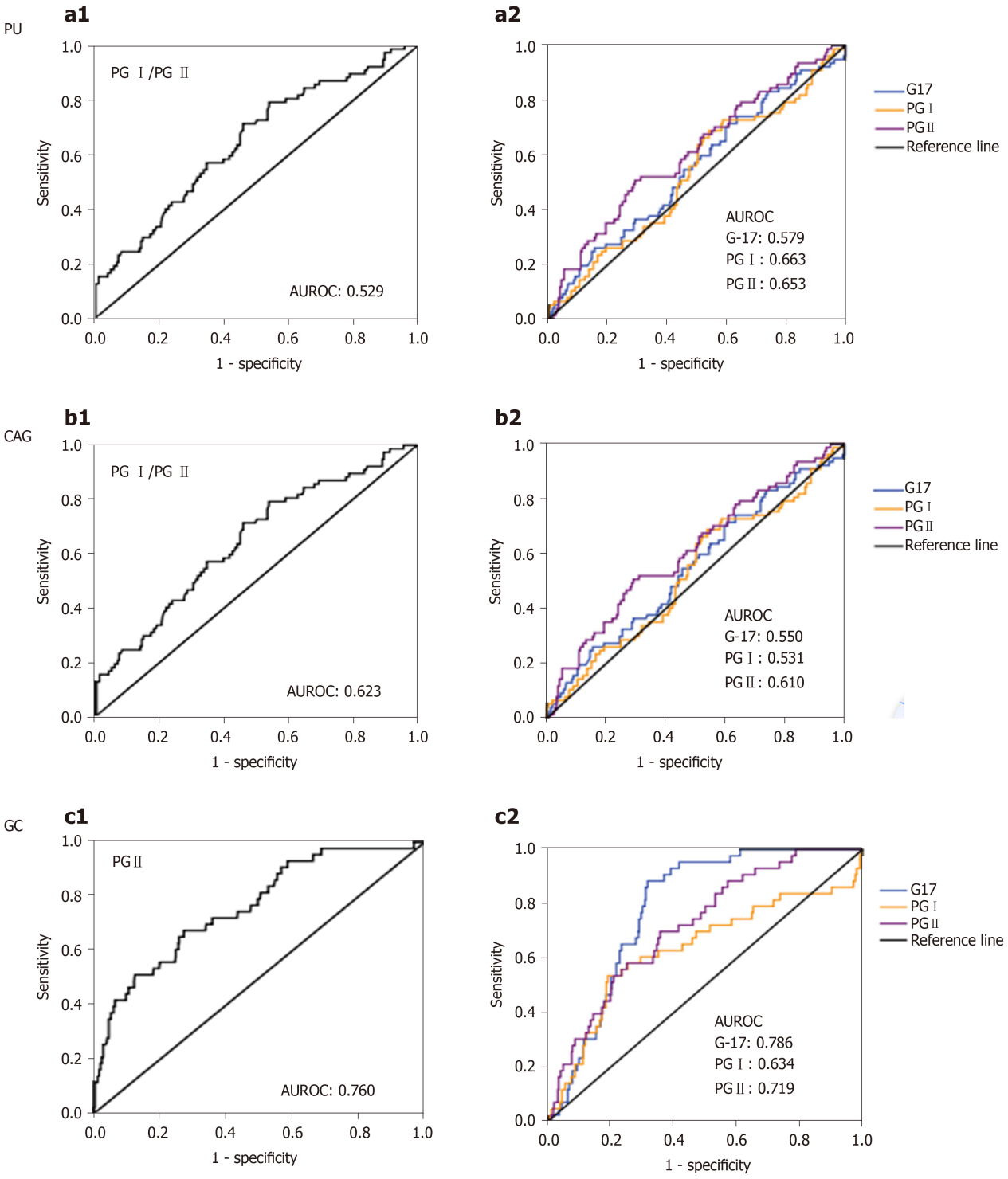

Figure 2 Receiver operating characteristic curves for gastrin-17, pepsinogen I, pepsinogen II and pepsinogen I / pepsinogen II in prediction of chronic atrophic gastritis, peptic ulcers and gastric cancer patients. Receiver operating characteristic (ROC) curves of gastrin-17 (G-17), pepsinogen (PG) I, PG II level and PG I/PG II ratio in predicting chronic atrophic gastritis (CAG), peptic ulcers (PU) and gastric cancer (GC) patients. a1-2: ROC curves of PG I/PG II ratio, G-17, PG I and PG II values for predicting PU; b1-2: ROC of PG I/PG II ratio, G-17, PG I and PG II values for predicting CAG; c1-2: ROC of PG I/PG II ratio, G-17, PG I and PG II values for predicting GC. PG: Pepsinogen; PU: Peptic ulcers; AUROC: Area under receiver operating characteristic curve; CAG: Chronic atrophic gastritis; G-17: Gastrin-17; GC: Gastric cancer.

Effects of type I and type II H. pylori infection on G-17, PG I, PG II levels and PG I/PG II ratio in gastric diseases

Table 5 shows the stratified disease group analysis results. G-17 levels in NAG, NAGE and GC groups in *H. pylori*-infected patients were significantly higher than that of *H. pylori*-negative patients ($P < 0.05$), and this effect was mostly from type I infection, as type II *H. pylori* infection and *H. pylori*-negative group did not show a difference across

Table 5 Effects of *Helicobacter pylori* infection on gastric gastrin 17, pepsinogens levels in stepwise chronic gastric diseases

	NAG	NAGE	PU	CAG	GC
G-17 pmol/L level in different groups,					
mean ± SD	5.6 ± 6.2[a]	6.7 ± 8.3[a]	9.1 ± 12.2	5.1 ± 6.5[a]	12.2 ± 7.6
H. pylori (+)	6.9 ± 6.5[ac]	7.5 ± 8.5[ac]	9.5 ± 12.6	5.2 ± 6.8[a]	13.0 ± 7.6[c]
H. pylori (-)	3.0 ± 4.6	3.9 ± 6.6	5.5 ± 7.4	4.4 ± 5.5	6.0 ± 2.5
Type I *H. pylori* (+)	7.3 ± 6.7[ac]	7.6 ± 8.4[ac]	10.9 ± 13.8[e]	25.3 ± 7.4[a]	13.8 ± 7.9[c]
Type II *H. pylori* (+)	6.0 ± 6.2[c]	7.3 ± 9.0	4.6 ± 4.9	4.8 ± 3.2	8.9 ± 4.5
PG I μg/L level in different groups,					
mean ± SD	116.5 ± 72.4[ag]	116.0 ± 74.2[ag]	168.7 ± 103.7	103.1 ± 60.2[ag]	168.6 ± 103.5
H. pylori (+)	117.0 ± 69.8[g]	117.5 ± 74.8[g]	172.9 ± 105.0	101.4 ± 64.4[ag]	169.4 ± 104.9
H. pylori (-)	115.4 ± 77.6	110.7 ± 73.6	128.8 ± 86.2	110.3 ± 64.3	162.0 ± 103.7
Type I *H. pylori* (+)	118.4 ± 67.5[ag]	113.9 ± 62.6[ag]	178.1 ± 109.6	100.6 ± 65.0[ag]	170.8 ± 96.3
Type II *H. pylori* (+)	114.0 ± 75.1	123.4 ± 92.9	154.9 ± 87.2	105.9 ± 78.6	162.1 ± 154.5
PG II μg/L level in different groups,					
mean ± SD	13.7 ± 11.2[ag]	14.4 ± 12.1[a]	19.5 ± 14.3	13.8 ± 10.1[ag]	24.5 ± 15.9
H. pylori (+)	15.3 ± 11.3[ac]	15.9 ± 13.0[ac]	20.4 ± 14.7[c]	14.8 ± 11.0[ac]	25.1 ± 15.9
H. pylori (-)	10.5 ± 10.2	8.9 ± 5.5	10.8 ± 4.8	8.7 ± 4.3	20.6 ± 16.5
Type I *H. pylori* (+)	17.1 ± 12.0[ce]	16.5 ± 11.3[c]	21.9 ± 16.0[ce]	14.7 ± 11.3[ac]	25.5 ± 16.3
Type II *H. pylori* (+)	11.5 ± 8.6	14.9 ± 15.5	15.1 ± 6.8	15.4 ± 9.6[c]	22.8 ± 15.3
PG I/PG II ratios in different groups,					
mean ± SD	10.6 ± 6.3[ai]	9.6 ± 5.4[a]	9.7 ± 4.3[a]	7.9 ± 4.4[a]	5.6 ± 3.8
H. pylori (+)	9.3 ± 5.6[aci]	8.7 ± 4.6[ac]	9.5 ± 4.4[ai]	6.8 ± 3.3[c]	5.1 ± 3.0
H. pylori (-)	13.2 ± 7.0	13.1 ± 6.7	11.8 ± 3.7	12.8 ± 4.7	9.1 ± 7.3
Type I *H. pylori* (+)	8.2 ± 4.9[ace]	7.8 ± 3.3[ace]	9.2 ± 4.2[a]	6.5 ± 3.2[c]	4.7 ± 2.9[c]
Type II *H. pylori* (+)	11.4 ± 6.3	10.3 ± 5.9	10.7 ± 4.9	8.8 ± 3.4[c]	7.6 ± 2.1

[a]$P < 0.05$, *vs* gastric cancer patients;
[c]$P < 0.05$, *vs H. pylori*-negative patients in the same disease groups;
[e]$P < 0.05$, type I and type II *H. pylori*-positive patients were compared in the same disease groups;
[g]$P < 0.05$, *vs* peptic ulcer patients;
[i]$P < 0.05$, *vs* chronic atrophic gastritis patients. CAG: Chronic atrophic gastritis; G-17: Gastrin 17; GC: Gastric cancer; *H. pylori*: *Helicobacter pylori*; NAG: Non-atrophic gastritis; NAGE: Non-atrophic gastritis with erosion; PU: Peptic ulcer; PG I: Pepsinogen I; PG II: Pepsinogen II; PG I/PG II: Pepsinogen I /pepsinogen II ratio.

disease groups. In PU patients, the level of G-17 in type I *H. pylori*-positive patients was significantly higher than that in type II *H. pylori*-infected patients (P<0.05). G-17 levels in the GC group were significantly higher when compared with NAG, NAGE and CAG groups in both *H. pylori*- and type I *H. pylori*-infected patients.

PG I levels in type II *H. pylori*-positive and *H. pylori*-negative patients showed no difference among all disease groups, while PG I level in GC group was significantly higher when compared with NAG, NAGE and CAG groups only in both type I and *H. pylori*-positive patients (P<0.05).

PG II levels in *H. pylori*- and type I *H. pylori*-infected patients were significantly higher in NAG, NAGE, PU and CAG groups when compared with *H. pylori*-negative patients ($P < 0.05$) except in the GC group, which showed no difference. PG II levels in *H. pylori*-negative and type II *H. pylori*-infected patients had no difference among all disease groups. In *H. pylori*-infected patients, PG II level was significantly higher in the GC group than that in NAG, NAGE and CAG groups. PG II level was also higher in the GC group over the CAG group in type I *H. pylori*-infected patients.

PG I/PG II ratios of *H. pylori*- and type I *H. pylori*-positive patients were lower when

compared with *H. pylori*-negative patients in NAG, NAGE and CAG groups ($P < 0.05$). Except for the CAG group, PG I/PG II ratios in type II *H. pylori*-infected groups were not significantly different from those in *H. pylori*-negative groups ($P > 0.05$). In type II and *H. pylori*-negative patients, PG I/PG II ratios showed no difference across different disease groups ($P > 0.05$); while PG I/PG II ratio of both *H. pylori*- and type I *H. pylori*-positive patients was significantly lower in the GC group when compared with the NAG, NAGE and PU groups ($P < 0.05$) (Table 5).

DISCUSSION

H. pylori cytotoxins CagA and VacA are major virulence factors and pathogenic mechanisms. Virulent strains are associated with increased risk of gastroduodenal disorders, but virulence varied among different strains of *H. pylori*[4-6,13]. Clinical relevance of type I *H. pylori* infection in gastric disease and gastric cancer has been very well defined, but the mechanism of type II *H. pylori*-induced gastric disease needs further exploration. The present results have demonstrated that type I *H. pylori* is the major form of infection in stepwise gastric diseases in present region, which is a high gastric cancer risk area[8].

Meta-analyses[4,14] have shown that CagA seropositivity are correlated with the occurrence of gastric cancer among *H. pylori*-infected patients. Sheikh *et al*[15] examined 201 patients infected by *H. pylori* and found that *cag*A gene was detected in 66.7% of the isolates; positive rates of *cagA* gene in gastric cancer and peptic ulcer patients were 68.2% and 71%, respectively. Kim *et al*[16] found that *H. pylori* infection in South Koreans was closely related to highly virulent strains [*vacA s1/i1/m1, cagA* (+), *iceA1* (+), *and oipA* (+)] and has an intimate association with the progression of peptic ulcer diseases. A recent survey of the high gastric cancer incidence area in Shandong Province, China showed[17] that seroprevalences of CagA, VacA antibodies in 573 *H. pylori*-infected patients were 83.9%, 38.9%, respectively; suggesting that CagA-positive strains are the dominant form of infection in Chinese population and are associated with progression of gastric mucosal lesions.

Here, we noted a high infection rate of *H. pylori* in GC patients, where 88.4% of GC are *H. pylori* positive, 84.2% of them are type I infection, and only 11.6% of GC are *H. pylori* negative. Such a high rate of *H. pylori* infection in GC patients has not been reported in this area previously. A Japanese study in 2011 indicated that *H. pylori* negative gastric cancers are rare in Japan[18], and both intestinal type and diffuse type of gastric cancer are closely related to *H. pylori*infection[19]. The current results are in line with these results, and indicate an important role of type I *H. pylori* in the development of upper gastrointestinal diseases and gastric cancer. It is also worth exploring further the mechanism of *H. pylori*-negative and type II *H. pylori*-infected GC patients.

PG I is produced by chief cells and mucosal neck cells in the fundic glands, whereas PG II is produced in fundic glands, pyloric glands and Brunner's glands. Gastric inflammation can lead to increased release of both pepsinogens into the bloodstream, with a greater increase in PG II than in PG I[20]. Other previous studies[8,9,21] have reported that low PG I levels and/or low PG I/PG II ratios are associated with increased risk of gastric cancer. PG I < 70 μg/L and PG I/PG II ratio < 3.0 have been frequently applied as the thresholds for defining population with high-risk of gastric cancer. *H. pylori* infection causes chronic inflammation of gastric mucosa[22] and affects the secretion of PGs and gastrin, but very few studies have explored the different effects of type I and type II *H. pylori* on G-17 and PGs levels.

In this study, *H. pylori*-positive patients have high levels serum PG II and G-17 and lower levels of PG I/PG II ratio when compared with *H. pylori*-negative patients. The results are in agreement with previous reports[20,23]. Our study further found that type I *H. pylori* infection result in a significant increase in PG II levels and a marked decline of PG I/PG II ratios when compared with type II *H. pylori* infection, which is an effect that has not been shown previously. We also noted that PG I levels have no difference in *H. pylori*-negative and type II *H. pylori*-positive patients across different disease groups. PG I levels were significantly increased in GC and PU patients in *H. pylori*- and type I *H. pylori*-infected group over the NAG, NAGE and CAG group patients. The results differ from previous reports that found low PG I level is associated with GC risk[24], probably due to different analysis methods or patients population involved. Further research is needed to explore the effect of *H. pylori* on PG I level in different gastric diseases.

Hypergastrinemia is more common in patients with *H. pylori*-infected

gastroduodenal diseases, which may be one cause of precancerous lesions or gastric cancer[25,26]. Gastrin is synthesized and secreted from antral G-cells. *H. pylori*-associated gastritis tends to raise serum gastrin levels, which is possibly due to hyperplasia of antral G-cells and an acid-suppressive effect of chronic gastritis when the corpus mucosa is involved. Our study shows a significant increase in G-17 in *H. pylori*-positive patients, which is consistent with previous results[25,26], and we further find that the levels of G-17 in type I *H. pylori* infected patients are significantly higher than that in type II *H. pylori*-infected patients ($P < 0.05$). The response of G-17 to *H. pylori* appears to be disease stage dependent, as in PU and CAG patients; there is no difference when compared with *H. pylori*-negative controls. Further studies are required to elucidate its pathogenesis in *H. pylori*-induced carcinogenesis.

In the current study, as the disease progresses, the levels of G-17, PG I, PG II and PG I/PG II ratios do not show differences in all *H. pylori*-negative and type II *H. pylori*-positive groups. In contrast, in type I *H. pylori*-positive groups, G-17, PG I and PG II levels are significantly higher and PG I/PG II ratios are lower in GC patients when compared with NAG, NAGE and CAG patients. The explanation of the results is probably due to the presence of CagA-, VacA-proteins, which are major *H. pylori* virulence factors that cause greater epithelial injury and mucosal inflammation, including the release of inflammatory mediators or cytokines that affect epithelial cell homeostasis, therefore resulting in disturbed secretion of PGs and gastrin[27,28].

Application of G-17, PG I, PG II levels and PG I/PG II ratios in gastric cancer epidemiology study have been reported extensively, although their predicative values in stepwise gastric disease in clinical studies have not been very well defined. Previous investigations have generated inconsistent conclusions[9-12], and our results using AUROC analysis (Figure 2) indicated relatively low predictive value range from 0.529-0.786 for PU, CAG and GC patients, and type I *H. pylori* infection is the major factor that affects their levels as the disease progresses. These data provide insight to evaluate their application during clinical practice and are helpful in explaining the results.

In CAG patients, we also noticed that our PGI level and PG I/PG II ratios are slightly higher when compared with other reports[9-12], and as all the CAG patients have histological confirmation, we therefore consider this effect could be due to patient population- or region-based variations, or might be due to variations from the degrees of atrophy itself. Future studies are required to explain these discrepancies.

Results of this study also show that *H. pylori* infection rate in our hospitalized patients is 76.9%, which is higher than that in the general population[1,2]. This could be because all patients enrolled in this study have gastrointestinal symptoms, so the infection rate of *H. pylori* is reasonably higher. One important difference between the current investigation and previous studies is that screening criteria for patients with *H. pylori* infection is more strict, as patients with only both ^{13}C-BUT and serological *H. pylori* antibody positive were enrolled. This selection makes our research results more accurate and reliable, allowing for the true status of *H. pylori* infection and reducing the possibility of false-positives and -negatives. Moreover, the fact that the proportions of *H. pylori* infection rates prior- and post-patient selections are almost identical indicates that the data analyses are reliable and not biased.

In conclusion, the present study evaluated type I and type II *H. pylori* infection status in chronic gastric disease and their impact on commonly used gastric cancer risk markers, such as PG I and PG II levels and PG I/PG II ratio in this high gastric cancer risk area. We noted that *H. pylori* infection rate is high in our gastric cancer patients, and only about 11.6% of gastric cancers were *H. pylori* negative. Type I *H. pylori* was the major form of infection. Our results also reveal that the effects of *H. pylori* on PG I, PG II and PG I/PG II ratio are mostly from type I strain infection and not from type II strain infection. The data provide insight in *H. pylori*-induced carcinogenesis and will be helpful to guide clinical practice for *H. pylori* eradication, to explain G-17 and PGs clinical results and for disease prevention.

ARTICLE HIGHLIGHTS

Research background

Type I *Helicobacter pylori* (*H. pylori*) is the major form of *H. pylori* infection in many areas globally. However, its infection status and role in stepwise gastric disease in this gastric cancer prevalent area have not been studied. Its impact on the commonly used gastric cancer risk markers such as gastrin-17 (G-17) and pepsinogens (PGs) is also not known.

Research objectives

We investigated the prevalence of type I and type II *H. pylori* infection in stepwise gastric diseases and the clinical implications; their impact on G-17 and PGs levels during routine clinical practice were also evaluated.

Research methods

Five hundred and twenty-three hospital admitted patients were enrolled in this study. *H. pylori* infection was confirmed by both ^{13}C-urea breath test and serological assay. Their serological G-17, PG I, PG II values and PG I/PG II ratio were also measured. Receiver operating characteristic curves were used to calculate the overall diagnostic performance of G-17, PG I, PG II and PG I/PG II ratio in peptic ulcers (PU), chronic atrophic gastritis (CAG) and gastric cancer (GC) patients to determine the best cutoff values, sensitivity and specificity.

Research results

The infection rate of 523 enrolled patients was 76.9%, among which type I *H. pylori* infection accounted for 72.4%, and type II was 27.6%. Overall, 88.4% of GC patients were *H. pylori* positive, 84.2% of them were type I infection, and only 11.6% of GC patients were *H. pylori* negative. *H. pylori* infection resulted in significantly higher G-17 and PG II values and decreased PG I/PG II ratio. Both types of *H. pylori* induced higher G-17 level, but type I strain infection resulted in an increased PG II level and decreased PG I/PG II ratio in NAG, NAGE and CAG patients. PG I levels showed no difference among disease groups, and only showed a difference in stratified analysis in GC and PU patients. The diagnostic performance of G-17, PG I, PG II and PG I/PG II ratio in PU, CAG and GC patients indicated relatively low predictive value.

Research conclusions

Type I *H. pylori* infection is the major form of infection in this geographic region, and a very low percentage (11.6%) of GC patients are not infected by *H. pylori*. Both types of *H. pylori* induce an increased G-17 level, while type I *H. pylori* is the major strain that affects PG I, PG II levels and PG I/PG II ratio in stepwise chronic gastric diseases.

Research perspectives

The results provide insight on *H. pylori* infection status in hospital admitted patients, and their impact on G-17 and PGs levels, which will be helpful to guide *H. pylori* eradication and explain G-17 and PGs assay results in clinical practice.

ACKNOWLEDGEMENTS

Authors are grateful to the staff of the Department of Gastroenterology and Hepatology, People's Hospital of Zhengzhou University for their valuable assistance in this work.

REFERENCES

1 **Malfertheiner P**, Megraud F, O'Morain CA, Gisbert JP, Kuipers EJ, Axon AT, Bazzoli F, Gasbarrini A, Atherton J, Graham DY, Hunt R, Moayyedi P, Rokkas T, Rugge M, Selgrad M, Suerbaum S, Sugano K, El-Omar EM; European Helicobacter and Microbiota Study Group and Consensus panel. Management of *Helicobacter pylori* infection-the Maastricht V/Florence Consensus Report. *Gut* 2017; **66**: 6-30 [PMID: 27707777 DOI: 10.1136/gutjnl-2016-312288]

2 **Liu WZ**, Xie Y, Lu H, Cheng H, Zeng ZR, Zhou LY, Chen Y, Wang JB, Du YQ, Lu NH; Chinese Society of Gastroenterology, Chinese Study Group on Helicobacter pylori and Peptic Ulcer. Fifth Chinese National Consensus Report on the management of Helicobacter pylori infection. *Helicobacter* 2018; **23**: e12475 [PMID: 29512258 DOI: 10.1111/hel.12475]

3 **Banić M**, Franceschi F, Babić Z, Gasbarrini A. Extragastric manifestations of *Helicobacter pylori* infection. *Helicobacter* 2012; **17** Suppl 1: 49-55 [PMID: 22958156 DOI: 10.1111/j.1523-5378.2012.00983.x]

4 **Matos JI**, de Sousa HA, Marcos-Pinto R, Dinis-Ribeiro M. *Helicobacter pylori* CagA and VacA genotypes and gastric phenotype: a meta-analysis. *Eur J Gastroenterol Hepatol* 2013; **25**: 1431-1441 [PMID: 23929249 DOI: 10.1097/MEG.0b013e328364b53e]

5 **Jones KR**, Whitmire JM, Merrell DS. A Tale of Two Toxins: *Helicobacter pylori* CagA and VacA Modulate Host Pathways that Impact Disease. *Front Microbiol* 2010; **1**: 115 [PMID: 21687723 DOI: 10.3389/fmicb.2010.00115]

6 **Rick JR**, Goldman M, Semino-Mora C, Liu H, Olsen C, Rueda-Pedraza E, Sullivan C, Dubois A. In situ expression of cagA and risk of gastroduodenal disease in *Helicobacter pylori*-infected children. *J Pediatr*

Gastroenterol Nutr 2010; **50**: 167-172 [PMID: 20038850 DOI: 10.1097/MPG.0b013e3181bab326]
7 **Xiang Z**, Censini S, Bayeli PF, Telford JL, Figura N, Rappuoli R, Covacci A. Analysis of expression of CagA and VacA virulence factors in 43 strains of *Helicobacter pylori* reveals that clinical isolates can be divided into two major types and that CagA is not necessary for expression of the vacuolating cytotoxin. *Infect Immun* 1995; **63**: 94-98 [PMID: 7806390 DOI: 10.0000/PMID7806390]
8 **Liu S**, Chen Q, Quan P, Zhang M, Zhang S, Guo L, Sun X, Wang C. Cancer incidence and mortality in Henan province, 2012. *Chin J Cancer Res* 2016; **28**: 275-285 [PMID: 27478313 DOI: 10.21147/j.issn.1000-9604.2016.03.02]
9 **Chiang TH**, Chiu SY, Chen SL, Yen AM, Fann JC, Liu CY, Chou CK, Chiu HM, Shun CT, Wu MS, Lin JT, Lee YC, Chen TH, Lin MW. Serum Pepsinogen as a Predictor for Gastric Cancer Death: A 16-Year Community-based Cohort Study. *J Clin Gastroenterol* 2019; **53**: e186-e193 [PMID: 29369241 DOI: 10.1097/MCG.0000000000000992]
10 **Kudo T**, Kakizaki S, Sohara N, Onozato Y, Okamura S, Inui Y, Mori M. Analysis of ABC (D) stratification for screening patients with gastric cancer. *World J Gastroenterol* 2011; **17**: 4793-4798 [PMID: 22147980 DOI: 10.3748/wjg.v17.i43.4793]
11 **McNicholl AG**, Forné M, Barrio J, De la Coba C, González B, Rivera R, Esteve M, Fernandez-Bañares F, Madrigal B, Gras-Miralles B, Perez-Aisa A, Viver-Pi-Sunyer JM, Bory F, Rosinach M, Loras C, Esteban C, Santolaria S, Gomollon F, Valle J, Gisbert JP; Helicobacter pylori Study Group of Asociación Española de Gastroenterología (AEG). Accuracy of GastroPanel for the diagnosis of atrophic gastritis. *Eur J Gastroenterol Hepatol* 2014; **26**: 941-948 [PMID: 25014624 DOI: 10.1097/MEG.0000000000000132]
12 **Koivusalo AI**, Pakarinen MP, Kolho KL. Is GastroPanel serum assay useful in the diagnosis of *Helicobacter pylori* infection and associated gastritis in children? *Diagn Microbiol Infect Dis* 2007; **57**: 35-38 [PMID: 16949782 DOI: 10.1016/j.diagmicrobio.2006.06.022]
13 **Ding SZ**, Goldberg JB, Hatakeyama M. *Helicobacter pylori* infection, oncogenic pathways and epigenetic mechanisms in gastric carcinogenesis. *Future Oncol* 2010; **6**: 851-862 [PMID: 20465395 DOI: 10.2217/fon.10.37]
14 **Shiota S**, Matsunari O, Watada M, Yamaoka Y. Serum *Helicobacter pylori* CagA antibody as a biomarker for gastric cancer in east-Asian countries. *Future Microbiol* 2010; **5**: 1885-1893 [PMID: 21155667 DOI: 10.2217/fmb.10.135]
15 **Sheikh AF**, Yadyad MJ, Goodarzi H, Hashemi SJ, Aslani S, Assarzadegan MA, Ranjbar R. CagA and vacA allelic combination of *Helicobacter pylori* in gastroduodenal disorders. *Microb Pathog* 2018; **122**: 144-150 [PMID: 29908307 DOI: 10.1016/j.micpath.2018.06.023]
16 **Kim JY**, Kim N, Nam RH, Suh JH, Chang H, Lee JW, Kim YS, Kim JM, Choi JW, Park JG, Lee YS, Lee DH, Jung HC. Association of polymorphisms in virulence factor of *Helicobacter pylori* and gastroduodenal diseases in South Korea. *J Gastroenterol Hepatol* 2014; **29**: 984-991 [PMID: 24372834 DOI: 10.1111/jgh.12509]
17 **Pan KF**, Formichella L, Zhang L, Zhang Y, Ma JL, Li ZX, Liu C, Wang YM, Goettner G, Ulm K, Classen M, You WC, Gerhard M. *Helicobacter pylori* antibody responses and evolution of precancerous gastric lesions in a Chinese population. *Int J Cancer* 2014; **134**: 2118-2125 [PMID: 24155048 DOI: 10.1002/ijc.28560]
18 **Matsuo T**, Ito M, Takata S, Tanaka S, Yoshihara M, Chayama K. Low prevalence of *Helicobacter pylori*-negative gastric cancer among Japanese. *Helicobacter* 2011; **16**: 415-419 [PMID: 22059391 DOI: 10.1111/j.1523-5378.2011.00889.x]
19 **Uemura N**, Okamoto S, Yamamoto S, Matsumura N, Yamaguchi S, Yamakido M, Taniyama K, Sasaki N, Schlemper RJ. *Helicobacter pylori* infection and the development of gastric cancer. *N Engl J Med* 2001; **345**: 784-789 [PMID: 11556297 DOI: 10.1056/NEJMoa001999]
20 **Tu H**, Sun L, Dong X, Gong Y, Xu Q, Jing J, Yuan Y. Serum anti-*Helicobacter pylori* immunoglobulin G titer correlates with grade of histological gastritis, mucosal bacterial density, and levels of serum biomarkers. *Scand J Gastroenterol* 2014; **49**: 259-266 [PMID: 24329006 DOI: 10.3109/00365521.2013.869352]
21 **Huang YK**, Yu JC, Kang WM, Ma ZQ, Ye X, Tian SB, Yan C. Significance of Serum Pepsinogens as a Biomarker for Gastric Cancer and Atrophic Gastritis Screening: A Systematic Review and Meta-Analysis. *PLoS One* 2015; **10**: e0142080 [PMID: 26556485 DOI: 10.1371/journal.pone.0142080]
22 **Adamu MA**, Weck MN, Rothenbacher D, Brenner H. Incidence and risk factors for the development of chronic atrophic gastritis: five year follow-up of a population-based cohort study. *Int J Cancer* 2011; **128**: 1652-1658 [PMID: 20503273 DOI: 10.1002/ijc.25476]
23 **Shan JH**, Bai XJ, Han LL, Yuan Y, Sun XF. Changes with aging in gastric biomarkers levels and in biochemical factors associated with *Helicobacter pylori* infection in asymptomatic Chinese population. *World J Gastroenterol* 2017; **23**: 5945-5953 [PMID: 28932086 DOI: 10.3748/wjg.v23.i32.5945]
24 **Bornschein J**, Selgrad M, Wex T, Kuester D, Malfertheiner P. Serological assessment of gastric mucosal atrophy in gastric cancer. *BMC Gastroenterol* 2012; **12**: 10 [PMID: 22289789 DOI: 10.1186/1471-230X-12-10]
25 **Malfertheiner P**. The intriguing relationship of *Helicobacter pylori* infection and acid secretion in peptic ulcer disease and gastric cancer. *Dig Dis* 2011; **29**: 459-464 [PMID: 22095010 DOI: 10.1159/000332213]
26 **Sun L**, Tu H, Liu J, Gong Y, Xu Q, Jing J, Dong N, Yuan Y. A comprehensive evaluation of fasting serum gastrin-17 as a predictor of diseased stomach in Chinese population. *Scand J Gastroenterol* 2014; **49**: 1164-1172 [PMID: 25157583 DOI: 10.3109/00365521.2014.950693]
27 **Di Mario F**, Cavallaro LG, Moussa AM, Caruana P, Merli R, Maini A, Bertolini S, Dal Bó N, Rugge M, Cavestro GM, Aragona G, Plebani M, Franzé A, Nervi G. Usefulness of serum pepsinogens in *Helicobacter pylori* chronic gastritis: relationship with inflammation, activity, and density of the bacterium. *Dig Dis Sci* 2006; **51**: 1791-1795 [PMID: 17203556 DOI: 10.1007/s10620-006-9206-1]
28 **Hatakeyama M**. *Helicobacter pylori* CagA and gastric cancer: a paradigm for hit-and-run carcinogenesis. *Cell Host Microbe* 2014; **15**: 306-316 [PMID: 24629337 DOI: 10.1016/j.chom.2014.02.008]

World Journal of Gastroenterology

Submit a Manuscript: https://www.f6publishing.com

World J Gastroenterol 2020 July 7; 26(25): 3686-3711

DOI: 10.3748/wjg.v26.i25.3686

ISSN 1007-9327 (print) ISSN 2219-2840 (online)

SYSTEMATIC REVIEWS

Quality of life in patients with gastroenteropancreatic tumours: A systematic literature review

Catherine Watson, Craig William Tallentire, John K Ramage, Rajaventhan Srirajaskanthan, Oscar R Leeuwenkamp, Donna Fountain

ORCID number: Catherine Watson 0000-0001-8752-0081; Craig William Tallentire 0000-0003-2172-7244; John K Ramage 0000-0003-4824-6600; Rajaventhan Srirajaskanthan 0000-0001-9835-8681; Oscar R Leeuwenkamp 0000-0002-4447-7404; Donna Fountain 0000-0003-4216-1147.

Author contributions: Watson C and Tallentire CW performed the research and analysed the data; they contributed to the manuscript equally; Ramage JK has reviewed the manuscript and offered invaluable contribution based on his disease expertise; Srirajaskanthan R also provided disease expertise; Leeuwenkamp OR and Fountain D designed and supervised the research. All authors contributed to writing the manuscript; all authors read and approved the final manuscript.

Conflict-of-interest statement: All the authors declare that they have no competing interests.

PRISMA 2009 Checklist statement: This study followed PRISMA guidelines.

Catherine Watson, Craig William Tallentire, Donna Fountain, PHMR Health Economics, Pricing and Reimbursement, London NW1 8XY, United Kingdom

John K Ramage, Rajaventhan Srirajaskanthan, Kings Health Partners NET centre, Kings College Hospital London, London SE5 9RS, United Kingdom

Oscar R Leeuwenkamp, Advanced Accelerator Applications, Geneva 1204, Switzerland

Corresponding author: Donna Fountain, PhD, Research Scientist, PHMR Health Economics, Pricing and Reimbursement, PHMR Head Office, London NW1 8XY, United Kingdom. donnafountain@phmr.com

Abstract

BACKGROUND

Gastroenteropancreatic neuroendocrine tumours (GEP-NETs) are slow-growing cancers that arise from diffuse endocrine cells in the gastrointestinal tract (GI-NETs) or the pancreas (P-NETs). They are relatively uncommon, accounting for 2% of all gastrointestinal malignancies. The usual treatment options in advanced GEP-NET patients with metastatic disease include chemotherapy, biological therapies, and peptide receptor radionuclide therapy. Understanding the impact of treatment on GEP-NET patients is paramount given the nature of the disease. Health-related quality of life (HRQoL) is increasingly important as a concept reflecting the patients' perspective in conjunction with the disease presentation, severity and treatment.

AIM

To conduct a systematic literature review to identify literature reporting HRQoL data in patients with GEP-NETs between January 1985 and November 2019.

METHODS

The PRISMA guiding principles were applied. MEDLINE, Embase and the Cochrane library were searched. Data extracted from the publications included type of study, patient population data (mid-gut/hind-gut/GI-NET/P-NET), sample size, intervention/comparators, HRQoL instruments, average and data spread of overall and sub-scores, and follow-up time for data collection.

RESULTS

Manuscript source: Unsolicited manuscript

Received: March 9, 2020
Peer-review started: March 9, 2020
First decision: March 31, 2020
Revised: June 4, 2020
Accepted: June 17, 2020
Article in press: June 17, 2020
Published online: July 7, 2020

P-Reviewer: Karaivazoglou K, Moschovi MA, Wang ZJ
S-Editor: Zhang L
L-Editor: A
E-Editor: Ma YJ

Forty-three publications met the inclusion criteria. The heterogeneous nature of the different study populations was evident; the percentage of female participants ranged between 30%-60%, whilst average age ranged from 53.8 to 67.0 years. Eight studies investigated GI-NET patients only, six studies focused exclusively on P-NET patients and the remaining studies involved both patient populations or did not report the location of the primary tumour. The most commonly used instrument was the European Organisation for Research and Treatment of Cancer Quality of Life Questionnaire-C30 (n = 28) with consistent results across studies; the GI-NET-specific module Quality of Life Questionnaire-GINET21 was used in six of these studies. A number of randomised trials demonstrated no HRQoL changes between active treatment and placebo arms. The Phase III NETTER-1 study provides the best data available for advanced GEP-NET patients; it shows that peptide receptor radionuclide therapy can significantly improve GEP-NET patients' HRQoL.

CONCLUSION
HRQoL instruments offer a means to monitor patients' general disease condition, disease progression and their physical and mental well-being. Instruments including the commonly used European Organisation for Research and Treatment of Cancer Quality of Life Questionnaire-C30 and GINET21 lack, however, validation and a defined minimal clinical important difference specifically for GI-NET and P-NET patients.

Key words: Gastroenteropancreatic neuroendocrine tumours; Health-related quality of life; Systematic literature review; Chemotherapy; Biological therapies; Peptide receptor radionuclide therapy

Core tip: Gastroenteropancreatic neuroendocrine tumours (GEP-NETs) are slow-growing cancers that arise from diffuse endocrine cells in the gastrointestinal tract and pancreas. An increased emphasis has been placed on health-related quality of life assessment in clinical studies, using reliable and validated patient-reported outcome instruments. Long-term therapeutic options provide symptomatic relief for patients with GEP-NETs, and can slow down or stabilise disease progression, but are not curative. Thus, understanding the impact of the long-term treatment options is particularly important. The aim of this study was to perform a systematic review to assess health-related quality of life focusing on patients with inoperable metastatic GEP-NETs undergoing different treatments in order to uncover areas for future research.

Citation: Watson C, Tallentire CW, Ramage JK, Srirajaskanthan R, Leeuwenkamp OR, Fountain D. Quality of life in patients with gastroenteropancreatic tumours: A systematic literature review. *World J Gastroenterol* 2020; 26(25): 3686-3711
URL: https://www.wjgnet.com/1007-9327/full/v26/i25/3686.htm
DOI: https://dx.doi.org/10.3748/wjg.v26.i25.3686

INTRODUCTION

Gastroenteropancreatic tumours (GEP-NETs) account for 2% of all gastrointestinal malignancies, with a United Kingdom age-standardised incidence rate of 8.6/100000/year[1]. GEP-NETs tend to be slow-growing cancers arising from diffuse endocrine cells in the gastrointestinal tract (GI-NETs) or pancreas (P-NETs). GEP-NETs are categorised as "functioning" or "non-functioning". Functioning tumours cause symptoms due to the hypersecretion of peptides and hormones[2,3], whilst non-functioning tumours have no hormone-related clinical features. Specific symptoms vary by primary tumour location[4,5]. Around 3 in 10 patients with GI-NET develop symptoms of diarrhoea, abdominal pain and flushing due to increased serotonin production[6], known as carcinoid syndrome (CS). P-NETs can produce a variety of hormones, the most common of which are insulin and gastrin. Other abnormal

hormone production associated with GEP-NETs include glucagon, vasoactive intestinal peptide, adrenocorticotropic hormone, somatostatin, and parathyroid hormone-related protein[7].

Surgery is the only curative treatment for GEP-NETs and can be performed when tumours are localised and resectable. The majority of GEP-NET patients, however, are diagnosed with metastatic disease requiring systemic treatment[8,9], including chemotherapy, biological therapies, and peptide receptor radionuclide therapy (PRRT)[10]. These long-term therapeutic options provide symptomatic relief, and can slow down or stabilise disease progression, but are not curative. The 5-year survival rate for patients with metastatic GI-NETs is approximately 75% and the 5-year survival rate for patient with metastatic P-NETs is > 60%, whilst the prevalence of GEP-NETs has been on the rise in the recent decades[2,11]. For instance, the median overall time of survival from the date of diagnosis of distant metastatic disease was reported to be 103 mo (8.5 years) in patients with metastatic midgut GI-NETs[12]. It is therefore vital to assess the patient's health-related quality of life (HRQoL) in general and related to the disease whilst taking treatments which can have a marked impact on well-being.

In oncology, an increased emphasis has been placed on HRQoL assessment as a secondary endpoint in clinical studies, using reliable and thoroughly validated patient-reported outcome (PRO) instruments for which the minimal important difference for improvement/worsening has been defined[13-17]. High-quality information on HRQoL serves a variety of purposes such as the development of targeted interventions, informed decision making about treatment options and allocation of healthcare resources[18]. Indeed, the United States Food and Drug Administration and European Medicines Agency have published guidance on the use of PRO measures in oncology studies emphasising the value of patient perspective when evaluating medicinal products[19,20].

To date, systematic assessments of HRQoL in patients with GEP-NETs have been performed to a limited extent. In the past, where the literature was systematically evaluated, the review focused on the methodological quality of the identified studies[18]. To our knowledge, there has been no systematic literature review published to provide a comprehensive overview of the different treatment options and associated impact on the patients' HRQoL. The aim of our study was to perform a systematic review to assess HRQoL focusing on patients with inoperable metastatic GEP-NETs undergoing different treatments in order to uncover areas for future research.

MATERIALS AND METHODS

Search strategy and study selection

This systematic review adheres to the established international guidelines for conducting systematic reviews, such as those provided by the Preferred Reporting Items for Systematic Reviews and Meta-Analyses report (PRISMA Statement[21]), and the Cochrane Handbook for Systematic Reviews of Interventions[22]. Methods of analysis and inclusion criteria were defined in advance and outlined in a designated protocol.

An extensive search of MEDLINE, Embase and the Cochrane library was performed by an experienced information specialist to identify relevant studies. We examined articles published in English between January 1985 and November 2019. The protocol outlined the electronic search strategy in full; searches were supplemented by manual searches of relevant review journals.

After de-duplication, article titles and abstracts were independently reviewed by two analysts, with discrepancies resolved *via* discussion with a third reviewer. Full-text articles were then obtained for records that met the inclusion criteria to re-evaluate eligibility.

Eligibility criteria

Eligibility for this systematic review was defined according to the PICOS[21]. Participants were adult patients (≥ 18 years) with inoperable GEP-NETs. Outcome measures included HRQoL, PROs, utility estimates, validity, and minimally important difference. The study design incorporated studies reporting utility estimates and HRQoL data, including economic evaluations, observational studies, and relevant randomised control trials. Cross-sectional studies were included, as they can provide useful HRQoL data at a specific point in time, although not providing longitudinal changes due to treatment over time. Studies were also required to report at least one relevant outcome for ≥ 15 patients. There were no limits defined in terms of

intervention or comparator PICOS elements.

Articles were excluded if patients were diagnosed with neuroendocrine tumours that did not originate in the gastrointestinal tract or the pancreas, and when the HRQoL data for patients with GEP-NETs were not separated by sub-analysis (*e.g.*, the population included patients with lung and/or thyroid neuroendocrine tumours). Studies indexed as case reports, case series, editorials and letters, conference abstracts, systematic reviews and non-human studies were also excluded. Finally, studies where the treatment applied did not target the malignancies specifically, such as psychotherapeutic interventions, were excluded.

Data extraction

A dedicated data extraction sheet was devised to capture all relevant data, including publication details, study design, country, intervention(s), comparator(s), eligibility, population description (including any specific sub-groups), sample size, age (average and range), sex ratio, tumour location, description of HRQoL measure (including valuation technique, method of elicitation, timepoints, follow-up duration, response rates), utility tool assessment (including disease state, timepoint, average utility) and HRQoL assessment (including scale domain where relevant, timepoint, average score, data spread). Disagreements were resolved by discussion between the two reviewers, with third reviewer involvement as required.

Quality assessment

The quality and relevance of HRQoL studies were assessed based on the key criteria described by Papaioannou *et al*[23] and Brazier *et al*[24], where applicable. Papers reporting insufficient information to assess study methods and populate the data extraction sheet were considered lower quality and were excluded on this basis.

RESULTS

Identified literature

A total of 42 studies published between 1985 and 2019 met the inclusion criteria of this study, of which 32 were found electronically and 10 were found by handsearching the reference lists of relevant articles (Figure 1). Of these studies, 6 can be classed as cross-sectional studies. There was a combined total of 3552 participants in the 42 studies, excluding healthy participants used for comparisons and the duplicate patients taken from the same data, with study sample sizes ranging from 17 to 253 patients. The heterogeneous nature of the different study populations was evident; the percentage of female participants ranged between 30%-60%, whilst average age ranged from 53.8 to 67.0 years (Table 1). In terms of disease location, 8 studies focused on GI-NET patients only and 6 studies focused on P-NET patients; the remaining studies were either a combination of both populations or did not report the specific disease location.

Of the total studies, 14 included somatostatin analogues as the intervention, including octreotide (n = 7), lanreotide (n = 3), pasireotide (n = 1), and undefined (n = 3). Such treatments slow down the production of hormones, such as serotonin, and thus reduce the symptoms of CS. In two studies, somatostatin analogues were combined with immunotherapy drugs such as interferon[25,26]. Three studies compared somatostatin analogues with placebos, allocated within the context of a randomised controlled trial[16,27,28]. Five studies used somatostatin analogues as comparators for an alternative somatostatin therapy, ^{177}Lu-DOTATATE or octreotide combined with interferon alpha[17,29-32].

In PRRT, a radioactive substance can be combined with a relevant peptide (or its analogue), such as somatostatin, so that it preferentially binds with a high affinity to the tumour. Nine studies considered PRRT as the intervention: ^{225}Ac-DOTATATE (n = 1), ^{177}Lu-DOTATATE (n = 5), ^{90}Y-DOTATOC (n = 2) and/or ^{177}Lu-DOTATOC (n = 3) (Table 1).^{177}Lu-DOTATATE was compared with octreotide administered at a high dose in one prospective study[17]. One retrospective study considered PRRT as the comparator[33], with somatostatin analogues or interferon therapy as the intervention.

Everolimus, sunitinib and erythropoietin were studied as interventions in three, three and one studies, respectively. Two studies compared sunitinib with a placebo within the context of randomised control trials[34,35]. Sunitinib was investigated as a comparator of everolimus in an additional study[36]. In some studies, interferon was used within the populations[25,31,33,37,38], but this was not applied to a specific subgroup.

Six studies used chemotherapy as the intervention: These combined bevacizumab with 5-FU/streptozocin (n = 2), capecitabine and streptozocin plus cisplatin (n = 1),

Table 1 Extracted literature

Ref.	Intervention	Comparator(s)	Study design, "Open" Label / "Blinded" / "Double blinded"	Total sample size	Patient sub-group	Pt sub-group sample size	Sex (% female)	Average age (yr)	Mean/median	Total GI-NET, %	P-NET, %	Functioning /Non-functioning, "function"	Additional information about disease[1]: "Stage (TNM)" "progressive" "stable", ("advanced" "metastatic/metastases" "spread") ("grow" "grade" "differentiated")
Zandee *et al*[58], 2019	^{177}Lu-DOTATATE	NA	Retrospective study	34	NA	NA	50	59	Mean	NA	100	Functioning (100%)	Grade 1 or 2 tumours with metastases (stage IV). Metastatic disease sites: Liver (97%), bone (21%), lung (6%)
Ramage *et al*[54], 2019	Everolimus	NA	Phase IV, open	48	All Patients	46	30	64.3	Median	NR	100	NR	Advanced and/or metastatic, well-differentiated, grade 1 and 2
					Continuing treatment at month 6	30	NR	NR	NR	NR	NR		
Ballal *et al*[8], 2019	^{225}Ac-DOTATATE	NA	Prospective study, open	21	NA	NA	57	54	Median	38	57	NR	Metastatic GEP-NETs with stable disease after completing ^{177}Lu-PRRT (57%) or progressive disease on ^{177}Lu-PRRT (43%). Grades 1 (n = 9), 2 (n = 11), and 3 (n = 1). Metastatic disease sites: Liver (86%), lymph node (71%), bone (33%)
Marinova *et al*[61], 2019	^{177}Lu-DOTATATE	NA	Retrospective study	70	NA	NA	44.3	64.2	Mean	100	NR	Functioning (83%), non-functioning (17%)	Metastatic. Grade 1 (50%), grade 2 (35.7%), unknown (14.3%). Morphological or clinical progression prior to 1st cycle PRRT (78.6%)
Rinke *et al*[16], 2019	Long-acting octreotide	Placebo (sodium chloride)	Clinical trial (RCT), Phase IIIb trial, double blind, placebo controlled	85	Long-acting octreotide	42	49.4	62.4	Mean	NR	NR	Functioning (39%), non-functioning (61%)	Metastatic, liver metastases (86%)
					Placebo	43		60.3	Mean	NR	NR		
					NA	NA		NR	NA	NR	NR		
Martini *et al*[59], 2018	DOTATATE or ^{90}Y-DOTATOC	General population norms	Retrospective study	61	Small intestine NET patients	37	40.5	62.8	Mean	100	0	NR	No brain metastases; otherwise not defined
					P-NET patients	24	37.5	61.0	Mean	0	100		
Lewis *et al*[3], 2018	Not defined	Patients with CS *vs* patients without CS	Prospective study	50	Without CS (CS)	25	48.0	62.0	Median	60.0	40.0	NR	Advanced, well-differentiated, with liver metastases
					With CS (CS)	25	36.0	67.0	Median	96.0	4.0	NR	

Strosberg *et al*[17], 2018	^{177}Lu-DOTATATE	High-dose octreotide	Clinical trial (RCT), phase III, open	231	^{177}Lu-DOTATATE	117	NR	NR	NR	100	NR	NR	Advanced, progressive, low- or intermediate-grade
					octreotide LAR	114	NR	NR	NR	100	NR		
Karppinen *et al*[46], 2018	NA	Control population	Cross-sectional	134	Impaired excretion	87	55	66.8	Mean	100	NR	Flushing (31%), diarrhoea (63%)	Locally advanced or metastatic disease (91%), grade 1 (54.1%), grade 2 (45.9%)
Cella *et al*[44], 2018	Telotristat ethyl	Placebo	Clinical trial (RCT), phase III trial, double blind	135	NA	135	48.1	63.6	Mean	NR	NR	NR	Well-differentiated, metastatic NETs and CS inadequately controlled by somatostatin analogues (for ≥ 3 mo)
					Durable responders (DR)	48	52.1	63.4	Mean	NR	NR		
					Non-durable responders (DR)	87	46	63.6	Mean	NR	NR		
Meng *et al*[28], 2017	Somatostatin analogue lanreotide	Placebo	Clinical trial (RCT), phase III trial, double blind	204	Lanreotide	101	48	62.1	Mean	NR	NR	Non-functioning	Advanced, well-differentiated or moderately differentiated, somatostatin receptor-positive NETs of grade 1 or 2
					Placebo	103				NR	NR		
					Overall	204				NR	NR		
Vinik *et al*[35], 2016	Sunitinib plus best supportive care	Placebo plus best supportive care	Clinical trial (RCT), phase III trial, double blind	171	NA	NA	NR	NR	NR	NA	100	NR	Advanced and/or metastatic, pathologically confirmed, well-differentiated P-NETs with disease progression as assessed by RECIST
Haugland *et al*[9], 2016	None	None	Cross-sectional	196	None	NA	50.5	65.0	Mean	100.0	0.0	NR	NR
Pavel *et al*[56], 2016	Everolimus	NA	Clinical trial, Phase IIIb, open, expanded access study	246	P-NET	126	46	61	Median	NR	100	Functioning (n = 38), non-functioning (n = 88)	Metastatic, well differentiated (n = 81), moderately differentiated (n = 26), poorly differentiated (n = 1), unknown (n = 16), missing (n = 2)
					Non P-NET	120	50.8	66	Median	NR	0	Functioning (n = 66), non-functioning (n = 55)	Metastatic, well differentiated (n = 65), moderately differentiated (n = 34), poorly differentiated (n = 2), unknown (n = 19)
Delpassand *et al*[66], 2014	^{177}Lu-DOTATATE	NA	Clinical trial, phase II, open	37	Patients with available data participated in quality of life questionnaire	27	56.8	63.4	Mean	43.2	37.8	NR	Grade 1 and grade 2, disseminated, progressive, somatostatin receptor-positive. Multiple metastases in the liver: grade 2 (n = 4), grade 3 (n = 26), grade 4 (n = 7). Metastatic disease sites: Liver (n = 34), lymph nodes (n = 16), bone (n = 11), pancreas (n = 8), lung (n = 3)
Ducreux *et al*[41], 2014	Bevacizumab combined with 5-FU/ streptozocin (Mitry *et al*[40]	Capecitabine plus bevacizumab	Clinical trial, phase II, open	34	NA	NA	35	55	Median	NR	100	Functioning (n = 7): CS (n = 3), Zollinger–Ellison syndrome (n = 1), other	Progressive, metastatic disease. Metastatic disease sites: Liver (n = 33), lymph node (n = 14), peritoneum (n = 2), lung (n = 3),

	2014)											(*n* = 3)	bone (*n* = 2), other (*n* = 2)
Mitry *et al*[40], 2014	Bevacizumab combined with 5-FU/ streptozocin (reported in a companion paper focusing on P-NET patients (Ducreux *et al*[41], 2014)	Capecitabine plus bevacizumab	Clinical trial, phase II, open	49	NA	NA	47	60	Median	100	NA	NR	Progressive, metastatic well-differentiated. Metastatic disease sites: Liver (*n* = 46), lymph node (*n* = 24), peritoneum (*n* = 23), lung (*n* = 7), bone (*n* = 7), other (*n* = 5)
Meyer *et al*[42], 2014	Capecitabine and streptozocin plus cisplatin (stratified)	Capecitabine and streptozocin (stratified)	Clinical trial (RCT), Phase II	86	Capecitabine and streptozocin	44	39	57	Median	21	46.0	Functioning (*n* = 31; 36%)	Advanced and/or metastatic. Metastatic disease sites: Local/regional (*n* = 2), distant (*n* = 42), liver (included in distant; *n* = 41)
					Capecitabine and streptozocin plus cisplatin	42	45	59	Median	19	50.0		
Yadegarfar *et al*[33], 2013	Somatostatin analogues or interferon therapy (88 patients)	Peptide-receptor radiotherapy (102 patients), chemotherapy (23 patients), surgery (20 patients) or ablative/ other therapies (20 patients)	Phase IV, open	253	P-NET	70	NR	NR	NR	NR	NR	Functioning: Secreting 5-hydroxy-indoloacetic acid (*n* = 111), gastrin (*n* = 4), glucagon (*n* = 3), insulin (*n* = 5), vasoactive intestinal peptide (*n* = 1). Non-functioning (secreting only chromogranin-A; *n* = 124)	Any gut-primary with metastases, lung-primary with liver/abdominal metastases and pancreas with/without metastases
Casciano *et al*[36], 2012	Everolimus (Afinitor)	Sunitinib (Sutent)	Economic analysis of phase III studies	NA	NA	NA	NA	NA	NA	NA	NA	NR	Advanced, progressive
Kvols *et al*[29], 2012	Pasireotide	Octreotide	Prospective study, phase II, open	44	Pasireotide responders	12 (Baseline), 12 (Month 1), 10 (Month 2), 11 (Month 3)	44	61	Mean	NR	NR	NR	Advanced, metastatic (symptoms refractory or resistant to octreotide LAR therapy). Metastatic disease sites: Liver (87%), lymph node (*n* = 16), peritoneum (*n* = 8), lung (*n* = 5), bone (*n* = 3), abdomen (*n* = 3), pleura (*n* = 3), retroperitoneal (*n* = 2), pancreas (*n* = 2), kidney (*n* = 1)
					Pasireotide non responders	13 (Baseline), 13 (Month 1), 13 (Month 2), 13 (Month 3)				NR	NR		
					Patients who discontinued treatment before	19 (Baseline), 15 (Month				NR	NR		

					3 mo	1), 8 (Month 2)							
Raymond *et al*[34], 2011	Sunitinib plus Best Supportive Care	Placebo plus Best Supportive Care	Clinical trial (RCT), phase III, double blind	171	sunitinib	86	51	56	Median	NR	100	Sunitinib Arm: Functioning: Gastrinoma (*n* = 9), glucagonoma (*n* = 3), insulinoma (*n* = 2), somatostatinoma (*n* = 1), other, multisecretory, or unknown (*n* = 10). Non-functioning (*n* = 42)	Advanced and/or metastatic, progressive, well-differentiated
					Placebo	85	53	57	Median	NR	100	Placebo Arm: Functioning: Gastrinoma (*n* = 10), glucagonoma (*n* = 2), insulinoma (*n* = 2), vasoactive intestinal peptide–secreting tumour (*n* = 2), other, multisecretory, or unknown (*n* = 5). Non-functioning (*n* = 44)	
Pezzilli *et al*[49], 2009	NA	NA	Prospective study	51	NA	NA	58.8	61	Mean	NR	100	NR	Advanced disease (lymph node involvement/liver metastases) (*n* = 22)
Rinke *et al*[27], 2009	Octreotide LAR	Placebo	Clinical trial (RCT), phase IIIb, double blind	85	Octreotide LAR	42	52.4	63.5	Median	100	NR	Octreotide LAR arm: Functioning: CS (*n* = 17) 40.5%	Well-differentiated, metastatic. Metastatic disease sites: Liver (*n* = 73), regional lymph node involvement (*n* = 6)
					Placebo	43	46.5	61	Median	100	NR	Placebo arm: Functioning: CS (*n* = 16) 37.2%	
Korse *et al*[30], 2009	Long-acting sandostatin LAR	Short-acting Sandostatin	Clinical trial, phase II	39	NA	NA	51.3	61	Mean	51.3	NR	Functioning: CS (*n* = 39)	Metastatic: Liver metastases (*n* = 35)
van der Horst-Schrivers *et al*[67] , 2009	NA	NA	Prospective study	43	NA	NA	37.2	60.6	Mean	NR	NR	NR	Metastatic midgut carcinoid tumours: Liver metastases (*n* = 37)
Haugland *et al*[47], 2009	NA	NA	Cross-sectional	5341	NET patients	189	50	65	Mean	100	NR	NR	GI-NET patients (excluded radical surgery that may have been curative), otherwise undefined
					General population	5152	48.8	NR	NR	NA	NA		
Larsson and Janson[50],	Erythropoietin	None	Pilot study	18	None	NA	50.0	63.0	Mean	100	NR	NR	NR

2008													
Kulke *et al*[55], 2008	Sunitinib	NA	Clinical trial, phase II, open	107	NA	NA	40.2	Carcinoid tumour = 58, P-NET= 56	Median	37.3	61.7	P-NET: Functioning: Gastrinoma *n* = 5 (7.6%), insulinoma *n* = 3 (4.5%), VIPoma *n* = 2 (3.0%), glucagonoma *n* = 4 (6.1%), other *n* = 5 (7.6%). Non-functioning *n* = 46 (69.7%)	Advanced carcinoid or P-NET
Fröjd *et al*[37] , 2007	Various included	None	Longitudinal, prospective, comparative study	59	T1-T4 successful	36	47.0	60.0	Mean	NR	NR	NR	Metastatic (70% metastatic at start; 78% metastatic at end)
Davies *et al*[68], 2006	NA	NA	Cross-sectional, open	50	Patients	35	42.9	60	Mean	NR	NR	NR	Metastatic
					Healthcare workers	15	NR	NR	NR	NA	NA		
Frilling *et al*[48], 2006	^{90}Y-DOTATOC then ^{177}Lu-DOTATOC	NA	Prospective study	20	Excluding pt (no 3) with Paraganglioma-neck	19	30	53.8	Median	NR	NR	NR	Advanced, progressive, and metastatic
Arnold *et al*[31], 2005	Octreotide plus interferon alpha	Octreotide monotherapy	Clinical trial (RCT), open	114	Octreotide monotherapy	51	47.1	58	Median	NR	NR	Octreotide: Functioning (*n* = 23), non-functioning (*n* = 28). Octreotide plus Interferon-alpha: functioning (*n* = 24), non-functioning (*n* = 30)	Metastatic or locally advanced disease without curative therapeutic option
					Octreotide plus interferon alpha	54	44.4	57	Median	NR	NR		
					Nonrandomised	9	33.3	60	Median	NR	NR		
Teunissen *et al*[62], 2004	^{177}Lu-DOTATOC	None	Clinical trial	50	None	NA	56.0	58.3	Mean	NR	26.0	NR	Metastatic
Pasieka *et al*[43], 2004	I-MIBG	NA	Clinical trial, open	19	I-MIBG	10	40	59	Mean	90	10	NR	Progressive
					Octreotide	9	55.6	55.6	Mean	66.6	33.3		
Kwekkeboom *et al*[60], 2003	Somatostatin analogue ^{177}Lu-DOTATOC	NA	Clinical trial, open	35	None	NA	60	54	Mean	NR	NR	NR	Metastatic
Larsson *et al*[25], 2001	Interferon, somatostatin analogue, interferon, and a somatostatin	None	Prospective study	24	None	NA	42.0	62.0	Median	100	NR	NR	NR
O'Toole	Octreotide	Lanreotide	Clinical trial	33	Patients received	16	50	63	NR	62.5	0		

et al[32], 2000	followed by lanreotide	followed by octreotide	(RTC), double blind		octreotide followed by Lanreotide								
					Patients received lanreotide followed by octreotide	17	53	64	NR	76	5.9	NR	NR
Wymenga *et al*[57], 1999	Lanreotide prolonged release	NA	Clinical trial, phase II, open	55	NA	NA	49.1	59.7	Mean	NR	5.5	NR	Advanced (Stage IV), metastatic. Metastatic disease sites: Lymph nodes (n = 39), distant organs (n = 44)
Larsson *et al*[26], 1999	Ongoing treatment: interferon and octreotide, other	NA	Cross-sectional	119	Patients with carcinoid tumours	64	43.7	64	Median	53.8	NA	NR	NR
					Patients with EPT	55	37.5	54	Median	NR	46.20		
					Overall	119	43.7	61	Median	53.8	46.20		
Larsson *et al*[38] , 1999	Interferon and/or a somatostatin analogue	NA	Clinical trial	99	NA	NA	39.4	59	Mean	NR	NR	NR	Stage = not terminal, no other status provided.
					HADS Anxiety (cases)	19	NR	NR	NR	NR	NR		
					HADS Depression (cases)	13	NR	NR	NR	NR	NR		
Larsson *et al*[69], 1998	Interferon and/or a somatostatin analogue	NA	Cross-sectional	17	NA	NA	47	58	Mean	NR	NR	NR	NR

[1]Disease description provided in each reference. NA: Not available; P-NET: Pancreas-neuroendocrine tumours; CS: Carcinoid syndrome; NR: Not relevant; HADS: Hospital Anxiety and Depression Scale; PRRT: Peptide receptor radionuclide therapy.

and bevacizumab plus capecitabine (n = 1). Two studies followed patients with various ongoing treatments[37,39]. Three studies used chemotherapy treatments as the comparators to chemotherapeutic interventions; two studies combined capecitabine with the anti-angiogenic drug bevacizumab and used the same population data[40,41], whilst one study combined capecitabine and streptozocin as the comparator[42].

Two additional studies identified within the scope of this review focused on meta-iodobenzylguanidine (MIBG) therapy and telotristat ethyl[43,44], respectively. MIBG is a radiometabolic therapy with limited antitumor effect on GEP-NETs. Telotristat ethyl is used to inhibit L-tryptophan hydroxylases TPH-1 and TPH-2 and reduce the production of serotonin, thereby alleviating CS symptoms[44]; this was assessed in the context of a randomised controlled trial, randomised 1:1:1 to receive 250 mg TID, 500 mg TID, and placebo.

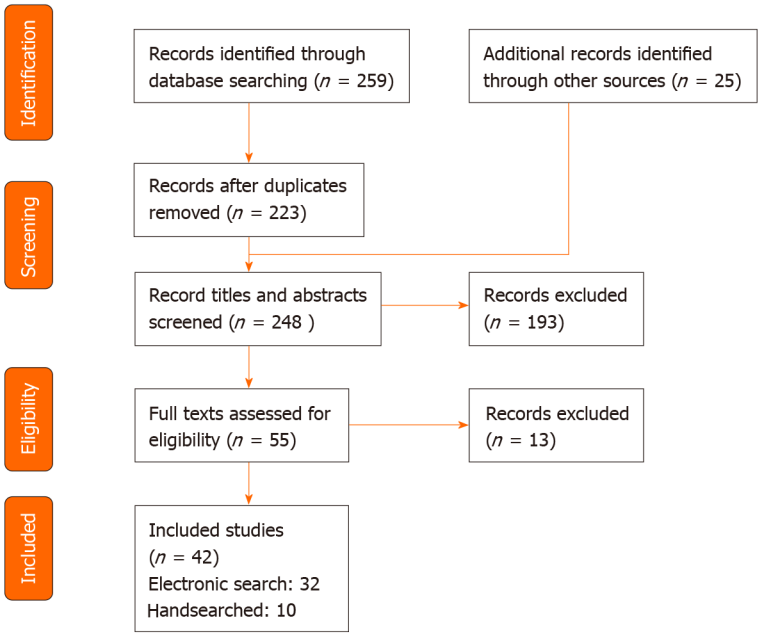

Figure 1 PRISMA diagram of included and excluded studies; the number of studies propagating to each stage of the process are included.

HRQoL assessment

In total, 30 studies employed a version of the European Organisation for Research and Treatment of Cancer Quality of Life Questionnaire (EORTC QLQ), in which linear transformation is used to standardise the raw score, so that scores range from 0 to 100. The majority of these studies utilised the EORTC QLQ-C30 HRQoL measure (n = 28). One study developed a disease-specific quality of life score questionnaire for patients with GI-NETs to supplement EORTC QLQ-C30. Six studies employed the GI-NET specific module QLQ-GI.NET21, of which one study apparently did not use the HRQoL measure in conjunction with EORTC QLQ-C30[8], thus will not show valid data. Others administered the EQ-5D or EQ-VAS to assess patient utilities and/or the Hospital Anxiety and Depression Scale (HADS) (Although HADS is not strictly a HRQoL measure, it provides insight into the anxiety and depressive symptoms of GEP-NET patients' underlying HRQoL) in addition to the EORTC measures (n = 5)[45]. Larsson *et al*[25] reported mean baseline HADS anxiety and depression scores of 4.6 (SD: 4.0) and 3.2 (SD: 2.7), respectively. Four studies applied the Short Form-36 (SF-36) questionnaire[9,46-48], three of which were cross-sectional studies. Other measures used include the SF-12[49], the Functional Assessment of Cancer Therapy-Anaemia[50] and the Functional Assessment of Chronic Illness Therapy-Diarrhoea (FACIT-D). Pezzilli *et al*[49] reported no significant difference between P-NET patients and a sample of age- and sex-matched subjects in terms of physical domain (44.7 ± 11.0 *vs* 46.1 ± 9.9, P = 0.610), but a significantly lower mental score in the same patients compared to the normative population (42.4 ± 13.0 *vs* 48.2 ± 9.8, P = 0.036).

The average HRQoL global health score at baseline and at different timepoints during each trial, obtained by asking patients to rate their overall health, have been reported for the EORTC QLQ-C30 (Table 2). A higher score represents a higher ("better") level of functioning, including the global health score. This particular tool became the primary focus of this manuscript, as EORTC QLQ-C30 was the single most commonly cited HRQoL dimension (n = 24), with global health score providing a single HRQoL dimension for comparison between studies. The average value for the baseline global health score had a range of 56–70. A higher score for symptoms represents a "worse" level of symptoms. Lowest average score ranges were observed for baseline EORTC QLQ-C30 scores in the following symptoms: nausea and vomiting (4.1–20), insomnia (11.0–38.6), appetite loss (9.2–27.8), constipation (0–24.4) and financial difficulties (6–23.6). Diarrhoea demonstrated a wide range of mean values (16.7–78.3), which can be attributed to the heterogeneity of disease symptoms in GI-NET and P-NET patients, indicating that diarrhoea in GEP-NET patients is multifactorial and very variable. Considering disease location, the average baseline global health scores were comparable, ranging from 56–68 for GI-NETs (4 studies) and

Table 2 Literature reporting scores for health-related quality of life average global health score for gastroenteropancreatic neuroendocrine tumours patients using European Organisation for Research and Treatment of Cancer Quality of Life Questionnaire-C30

Ref.	Intervention/comparator	Time point	Global health score	Statistical analysis and *P* values, as presented in the literature
Arnold *et al*[31], 2005	Octreotide plus interferon alpha	Baseline	57.9	0.04 (between treatment arms at 3 mo)
		3 mo	51.2	
	Octreotide monotherapy	Baseline	63	
		3 mo	74.4	
Cella *et al*[44], 2018	Telotristat ethyl	-	Overall: 55.4; Durable responders: 40; Non-durable responders: 66	NR (NS)
Fröjd *et al*[37], 2007	Various (*i.e.* interferon, octreotide, chemotherapy and other)	Timepoint 1	58	NR
		Timepoint 2	61	NR
		Timepoint 3	58	NR
		Timepoint 4	58	NR
van der Horst-Schrivers *et al*[67], 2009	NA	-	61.8	NR
Korse *et al*[30], 2009	Long-acting sandostatin LAR	Baseline	70	0.275 (repeated measurement analysis using mixed linear models)
		3 mo	71	
		6 mo	67	
		9 mo	68	
		12 mo	64	
Larsson *et al*[50], 2008	Erythropoietin	Baseline	56	NR (NS)
		4 mo	55	
		8 mo	66	
		2 yr	70	
Larsson *et al*[25], 2001	Interferon, somatostatin analogue, interferon, and a somatostatin.	Baseline	68	NR (NS)
		3 mo	59	
		6 mo	58	
		9 mo	50	

		12 mo	63	
Larsson *et al*[26], 1999	Interferon and/or a somatostatin analogue for at least 4 weeks - Five patients were treated with interferon, three with a somatostatin analogue, and nine with a combination	-	64.71	NR
Larsson *et al*[38], 1999	Interferon and/or a somatostatin analogue	-	Overall: 66.7; HADS Anxiety (cases): 46; HADS Anxiety (non-cases): 71.6; HADS Depression (cases): 43; HADS Depression (non-cases): 70.2	< 0.001 between HADS anxiety "cases" (n = 19) and "non-cases" (n = 80) and 0.001 between HADS depression "cases" (n = 13) and "non-cases" (n = 86)
Larsson *et al*[69], 1998	Interferon and/or a somatostatin analogue and/or a combination	-	64.71	NR
Lewis *et al*[3], 2018	NA	-	Without CS: 63.0; With CS: 61.7	0.04 (between subpopulations)
Marinova *et al*[61], 2019	^{177}Lu-DOTATATE	Baseline	62.6	
		3 mo	66.7	< 0.05 (compared to baseline using mixed longitudinal model)
		6 mo	69.6	< 0.01 (compared to baseline using mixed longitudinal model)
		9 mo	69.4	< 0.01 (compared to baseline using mixed longitudinal model)
Meyer *et al*[42], 2014	Capecitabine and streptozocin plus cisplatin.	Baseline	69.3	
		≤ 9 wk - after 3 × 3 weekly cycles	52.2	0.052 (compared to baseline)
		6 mo	56	0.68 (compared to baseline)
	Capecitabine and streptozocin	Baseline	67	
		≤ 9 wk - after 3 × 3 weekly cycles	62.2	0.5 (compared to baseline)
		6 mo	68.9	0.75 (compared to baseline)
Mitry *et al*[40], 2014	Bevacizumab plus capecitabine	Baseline	67	
		6 mo	63	NR (NS)
		12 mo	71	NR (NS)
Pavel *et al*[56], 2016	Everolimus	End of treatment (compared to baseline)	P-NET: -3.9; non P-NET: -13	NR
Ramage *et al*[54], 2019	Everolimus	1 mo	FAS Population (paired scores baseline and 1 m): 58	NR (NS)
			Continuing tx at 6m (paired scores baseline and 1 m): 56.9	NR (NS)

		2 mo	FAS Population (paired scores baseline and 2 m): 57.6	NR (NS)
			Continuing tx at 6m (paired scores baseline and 2 m): 56.9	NR (NS)
		3 mo	FAS Population (paired scores baseline and 3 m): 56.7	NR (NS)
			Continuing tx at 6m (paired scores baseline and 3 m): 56.3	NR (NS)
		4 mo	FAS Population (paired scores baseline and 4 m): 56	NR (NS)
			Continuing tx at 6 m (paired scores baseline and 4 m): 56.8	NR (NS)
		5 mo	FAS Population (paired scores baseline and 5 m): 56.6	NR (NS)
			Continuing tx at 6 m (paired scores baseline and 5 m): 58.6	NR (NS)
		6 mo	FAS Population (paired scores baseline and 6 m): 56.9	NR (NS)
			Continuing tx at 6 m (paired scores baseline and 6 m): 56.9	NR (NS)
Raymond *et al*[34], 2011	Sunitinib	Baseline	67	
		"post-baseline"	62.4	NR
	Placebo	Baseline	64	
		"post-baseline"	61.3	NR
Rinke *et al*[16], 2019	Long-acting octreotide	Baseline	64	
	Placebo	Baseline	65.7	
		12 wk	+4.13 (difference in global health score compared to placebo)	NR
		24 wk	+5.05 (difference in global health score compared to placebo)	NR
		36 wk	+1.85 (difference in global health score compared to placebo)	NR
Strosberg *et al*[17], 2018	^{177}Lu-DOTATATE	Baseline	67	NR
	High-dose octreotide	Baseline	64	NR
Teunissen *et al*[62], 2004	^{177}Lu-DOTATOC	Baseline	69	
		6 wk	78.2	< 0.01 (Analysis of variance (two-sided) compared to baseline)

Vinik *et al*[35], 2016	Sunitinib	Baseline	67	NR (NS difference between arms)
		Up to cycle 10 (about 9 mo)	60.4	
	Placebo	Baseline	64	NR (NS difference between arms)
		Up to cycle 10 (about 9 mo)	61.3	
Wymenga *et al*[57], 1999	Lanreotide prolonged release	Baseline	60.4	
		1 mo	69.7	0.001 (compared to baseline using t tests or Wilcoxon signed rank)
		End of treatment	65.5	NR (NS)
Yadegarfar *et al*[33], 2013	Somatostatin analogues or interferon therapy	Baseline	61	
		3 mo	67	NR
		6 mo	67	NR
Zandee *et al*[58], 2019	^{177}Lu-DOTATATE	Baseline	61.7	
		3 mo (after final PRRT cycle)	79.5	0.002 (compared to baseline using paired *t* test)

NA: Not available; NET: Neuroendocrine tumours; CS: Carcinoid syndrome; NR: Not relevant; PRRT: Peptide receptor radionuclide therapy; NS: Not significant.

56–67 for P-NETs (5 studies).

Whilst the most popular HRQoL measure was EORTC QLQ-C30, studies that employed the QLQ-GI.NET21 module provided domain scores specific to the disease that is the focus of this report, including: endocrine systems, gastrointestinal systems, disease-related worries, bone/muscle pain *etc*. Table 3 presents the scores given for these domains. The average HRQoL score ranges for body image (13.3–29.1), weight gain (9-27.8) information/communication (1.1–16.0) and treatment-related symptoms (6.5–26.24) showed that these were only minor problems experienced by patients with GI-NETS. Other domains displayed a wide range of scores, *e.g*. sexual function (28.2–68.4), social function (30.0–72.9) and disease-related worries (37.6–84.2), making these some of the most important problems experienced by many patients. The QLQ-GI.NET21 module has been validated as a responsive tool for assessing HRQoL of patients with GEP-NETs[33], although it is accepted that numbers were too small for a proper validation in patients with P-NETs alone. This is of relevance, as P-NET patients often present with a more aggressive disease and concomitant treatments may be used.

In addition, a 10-point change in an EORTC domain score is frequently considered a minimal clinically important difference and, using Kaplan-Meier methodology, time to

Table 3 The specific domain scores reported in the literature for gastroenteropancreatic neuroendocrine tumours patients using QLQ-GI.NET21

Ref.	Intervention/ comparator	Time point	Endocrine Symptoms	Gastrointestinal Symptoms	Social function	Disease related worries	Muscle/bone pain symptom	Weight gain	Information/Communication function	Body Image	Sexual function	Treatment related symptoms scale
Ramage *et al*[54], 2019	Everolimus	Baseline (paired scores with 3 mo)	14.8	24.4	44.1	51.1	35.2	NR	1.9	25.9	37	NA
		3 mo	12.3	20.2	42.6	44.8	35.2	NR	4.6	24.1	42.6	22
		Baseline (paired scores with 6 mo)	14.4	25.8	44.8	50.9	33.3	NR	1.1	20	35.6	NA
		6 mo	12.6	21.8	34.4	43.7	30	NR	1.1	21.1	37.8	14.1
Lewis *et al*[3], 2018	NA	Single timepoint (patients without CS)	16.7	18.9	60.0	56.9	41.3	18.7	10.7	15.3	60.8	17.5
		Single timepoint (patients with CS)	28.4	24.0	68.4	38.7	46.7	13.3	16.0	13.3	68.4	10.1
Yadegarfar *et al*[33], 2013	Various	Baseline (P-NETs)	22	26	39	56	25	11	10	25	32	18
		3 mo (P-NETs)	16	18	33	44	31	9	4	21	31	22
		6 mo (P-NETs)	18	22	30	50	32	13	10	19	31	23
Ballal *et al*[8], 2019	^{225}Ac-DOTATATE TAT	Baseline	21.4	40.2	64.3	61.2	38.8	25	NR	28.8	40	6.53
		End of assessment	3.57	22.8	72.9	84.2	26.8	27.8	NR	15.6	45	26.24
Strosberg *et al*[17], 2018	^{177}Lu-DOTATATE	Baseline	NR	22.8	33.4	43.7	29	NR	5.4	20	30.6	11.6
	High-dose octreotide	Baseline	NR	23.8	37.1	43.8	34.6	NR	12.3	20.3	28.2	11.9
Cella *et al*[44], 2018	Telotristat ethyl	Baseline (Durable responders)	37.8	33.8	46.7	41.1	35	NR	5	29.1	47.2	18.1
		Baseline (Nondurable responders)	29.5	28.5	38.5	37.6	30.3	NR	7	26.9	32.6	12.8
		Difference in change from baseline between subpopulations	-1.9	-9.6	-2.8	1.9	-4.5	NR	3.9	1	-1.6	-3.4

NA: Not available; P-NET: Pancreas-neuroendocrine tumours; CS: Carcinoid syndrome; NR: Not relevant.

deterioration (TTD) can be measured using a 10-point decline in analogy with time to event curves[51,52]. Two studies identified in the literature search applied the use of minimal important difference in the change in HRQoL domains as a means of assessing the impact of interventions using TTD, and time until definitive deterioration (TUDD), *i.e.* ≥ 10 point worsening of a HRQoL domain score from baseline without further improvement[16,17].

The SF-36 measures eight dimensions of HRQoL, where item scores are linearly transformed into scales ranging from 0 to 100, with higher scores indicating better HRQoL. In cross-sectional studies, HRQoL has been shown to be significantly reduced in patients with GEP-NETs compared to the general population in every SF-36 dimension[46,47]: 77.9 *vs* 70.0 for physical functioning, 65.0 *vs* 40.2 for role physical, 69.1 *vs* 64.3 for bodily pain, 74.3 *vs* 54.8 for general health, 60.9 *vs* 49.5 for vitality, 83.9 *vs* 75.5 for social functioning, 77.4 *vs* 64.4 for role emotional and 80.6 *vs* 74.9 for mental health. Mean scores for each scale were consistently worse in a sub-population of patients with impaired bowel/bladder function, which was strongly correlated with high scores for diarrhoea[46], a symptom of CS which reduces patient HRQoL. Elsewhere, Haugland *et al*[9] reported only the physical component (39.6) and the mental component (45.9) scores; these were similar to baseline scores previously reported[53]. Frilling *et al*[48] reported improved HRQoL (assessed using SF-36) in 50% of patients in their prospective study of ^{90}Y-DOTATOC therapy followed by ^{177}Lu-DOTATOC, but sample size was low (n = 20).

Various studies used other HRQoL tools to evaluate HRQoL in GEP-NET patients; direct comparisons between these studies were limited by the small number of studies using each tool ($n \leq 2$) and the heterogenous population and treatment interventions. Pezzilli *et al*[49] was the only identified publication to use SF-12 in a population of P-NET patients, reporting a good physical HRQoL that was not significantly different to the normative population (44.7 ± 11.0 *vs* 46.1 ± 9.9, P = 0.610), but a significantly impaired mental component (42.4 ± 13.0 *vs* 48.2 ± 9.8, P = 0.036). Pezzilli *et al*[49] was also the only study to employ the Beck Depression Inventory and State Anxiety Inventory Y-1; 8 patients (18.2%) identified with moderate depression, 9 patients (20.5%) with mild moderate depression, and 27 patients (61.4%) with no depression. Anxiety results were similar in the patients and in the normative population. Ramage *et al*[54] used the EQ-5D-5L (in addition to EORTC QLQ-C30 and GINET21), with no significant difference for the composite health index or self-rated (global) health score noted between baseline and 6-mo treatment with everolimus. The EQ-5D VAS was employed in two studies: Kulke *et al*[55] examined patients receiving repeated 6-weekly cycles of oral sunitinib, noting no significant difference in VAS scores over the study period, whilst Pavel *et al*[56] reported a reduced mean VAS from baseline to end of treatment with oral everolimus (10 mg daily, in 28-d cycles) in non-P-NET patients (63.9 ± 19.0 *vs* 55.3 ± 23.0, respectively) compared to P-NET patients (68.8 ± 19.9 *vs* 66.5

± 20.6, respectively). The FACIT-D measure is a symptom-specific measure used by Kvols *et al*[29] in a Phase II, open-label, multicentre prospective study of self-administered pasireotide. Clinical responders were noted to have improved mean scores at the end of treatment compared to baseline. Kulke *et al*[55] reported that the mean FACIT-fatigue score remained stable for each treatment cycle of sunitinib with a "modest" score increase during the dosing period. Elsewhere, Larsson *et al*[50] used the Functional Assessment of Cancer Therapy-Anaemia measure to assess the HRQoL of GEP-NET patients with anaemia being treated with erythropoietin; no significant changes were observed over the study period. Finally, O'Toole *et al*[32] showed no significant difference in HRQoL scores between lanreotide and octreotide using the Index de Santé Perceptuel de Nottingham measure. These studies provide a basis for future randomised control trials to test whether interventions improve HRQoL for patients with GEP-NETs.

All studies included in this review reported the HRQoL of patients with inoperable tumours; the majority of which described the disease as metastatic and/or advanced (Table 1), and thus the disease could be categorised as stage IV. Out of these studies, only two provided explicit information regarding disease stage for the entire study population[57,58]. Notably, no studies investigated how disease stage and tumour functionality affect HRQoL in GEP-NET patients, with HRQoL data most often presented according to treatment comparator.

Treatment impact on HRQoL

Few studies reported a significant difference ($P < 0.05$) in the patients' global health score between baseline and after a period of treatment (Table 2).

HRQoL was maintained with few deteriorations in patients receiving long-acting octreotide compared to the deterioration observed in patients who received a placebo[16,27]. Octreotide improved HRQoL scores for the clinically important GEP-NET symptoms such as fatigue, insomnia, diarrhoea and pain; whereas significantly earlier TUDD was observed in the placebo arm for fatigue, pain and insomnia in patients with GI-NETs than those treated with long-acting octreotide ($P < 0.05$)[16]. An improvement in the EORTC global health score was shown after 3 mo on octreotide but not when octreotide was combined with interferon alpha[31]. Flushing was shown to be reduced significantly following 12 mo of treatment with long-acting octreotide[30]. Further studies are deemed necessary to assess the HRQoL of GEP-NET patients treated with pasireotide, who are refractory or resistant to octreotide; symptom-specific scores and total FACIT-D assessments showed some variability and no clear trends but sample size was small ($n = 30$)[29].

Another somatostatin analogue shown to bring about significant improvement in the global health score of GEP-NET patients was prolonged-release lanreotide[57], possibly driven by improvements in symptom scales or single-term measures such as fatigue, pain, nausea/vomiting, sleeping problems, appetite, constipation, diarrhoea and financial problems; although dyspnoea became more severe during the 6-mo treatment period. O'Toole *et al*[32] found no significant HRQoL differences between lanreotide and octreotide, although most patients prefer lanreotide due to its simplified mode of administration. However, examining evidence from the CLARINET study, and mapping EORTC QLQ-C30 to EQ-5D-based utility values, no significant differences in HRQoL were noted between the lanreotide and placebo arms[28].

PRRT treatment for GEP-NETs has been shown to result in stable HRQoL scores during and after a 3-mo treatment period, compared to baseline levels using the EORTC QLQ-C30 measure[59,60]. In more recent studies, treatment with ^{177}Lu-DOTATATE was shown to be a safe and effective therapy in the treatment of functioning P-NETs[58] leading to a significant increase in the global health score observed at follow-up compared to baseline (79.5 *vs* 61.7, $P = 0.002$). Furthermore, significant improvements in the physical functioning, role functioning, emotional functioning, and social functioning were reported. Of all symptom scales, only "fatigue" was found to have significantly decreased (27.3 *vs* 17.2, $P = 0.02$). These results are consistent with a recent retrospective analysis study conducted by Marinova[61]; HRQoL was significantly improved in GI-NET patients receiving ^{177}Lu-DOTATATE compared to baseline, revealing an increased global health score (3 mo after 1st, 2nd, and 3rd treatment cycle $P = 0.049$, $P = 0.004$, and $P = 0.041$, respectively).

In the Phase III NETTER-1 study, 231 patients were recruited with 117 randomised to the ^{177}Lu-DOTATATE arm (200 mCi every 8 wk for four treatments) and 114 to the high-dose octreotide long-acting repeatable arm (60 mg every 4 wk)[17]. HRQoL analysis, conducted on an intention-to-treat basis, demonstrated that ^{177}Lu-DOTATATE provides a significant and clinically robust HRQoL benefit for patients

with progressive GI-NETs (compared to high-dose octreotide). TTD, defined as the time from randomisation to first HRQoL deterioration of ≥ 10 points from baseline score, was significantly longer in the ^{177}Lu-DOTATATE arm ($P < 0.001$); the hazard ratio was 0.406 for global health status, 0.518 for physical functioning, 0.580 for role functioning, 0.621 for fatigue, 0.566 for pain, 0.473 for diarrhoea, 0.425 for body image and 0.572 for disease-related worries. Differences in median TTD were clinically significant in several domains: 28.8 mo *vs* 6.1 mo for global health status, and 25.2 mo *vs* 11.5 mo for physical functioning. Significant improvements in TUDD were also observed for the global health score ($P < 0.001$), as well as for physical functioning ($P = 0.002$), role functioning ($P < 0.001$), emotional functioning ($P = 0.020$), social functioning ($P = 0.001$), pain ($P = 0.002$), insomnia ($P = 0.026$), appetite loss ($P = 0.009$), constipation ($P = 0.042$), diarrhoea ($P = 0.001$), GI scale ($P = 0.005$), treatment scale ($P = 0.002$), social function scale ($P = 0.011$), disease-related worries scale ($P = 0.001$), and body image ($P = 0.002$).

Other PRRT interventions included the use of ^{177}Lu-DOTATOC[62], ^{90}Y-DOTATOC[59] and ^{225}Ac-DOTATATE[8]. ^{177}Lu-DOTATOC treatment improved functional scales and most single item scores in GEP-NET patients, whilst symptom scale scores for fatigue and pain decreased significantly from 31.9 to 22.8 ($P < 0.01$) and 23.3 to 15.0 ($P < 0.05$), respectively[62]. Martini *et al*[59] examined HRQoL following 4–6 cycles of ^{177}Lu-DOTATATE or ^{90}Y-DOTATOC. The most significant domain change for GI-NETs was noted for diarrhoea (-16.3 points, $P = 0.008$). Compared to ^{90}Y-DOTATOC, ^{177}Lu-DOTATATE demonstrated a reduced score for fatigue (-27.7 points, $P = 0.020$) and better physical functioning (+22.4 points, $P = 0.050$), cognitive functioning (+23.1 points, $P = 0.003$) and global health score (+17.3 points, $P = 0.029$) in P-NET patients. ^{225}Ac-DOTATATE therapy has the potential to overcome the resistance of GEP-NET to ^{177}Lu-DOTATATE beta therapy and promote remission with minimal or transient toxicity, whilst reducing endocrine ($P = 0.001$) and gastrointestinal symptoms ($P < 0.001$), although treatment-related symptoms were worsened by the end of the assessment ($P = 0.001$)[8].

A significant difference in the EORTC QLQ-C30 physical functioning scale was noted by Ramage *et al*[54] following 6-mo treatment with everolimus, but no other significant differences were noted during this treatment period; in line with what was also shown by analysis conducted in conjunction with the RADIANT trial[56]. Likewise, sunitinib has no significant impact on global health score of EORTC QLQ-C30, but it has been shown to improve the HRQoL symptom scores of insomnia and diarrhoea compared to placebo in P-NETs[34,35]. In another study[55], there was no significant difference in EQ-VAS scores over 6 treatment cycles of sunitinib. There was no significant impact on the HRQoL of patients with GI-NETs when treated with erythropoietin for the anaemia associated with interferon therapy[50].

Chemotherapy in the BETTER trial was chosen based on NET location; GI-NETs were treated with capecitabine and bevacizumab, whilst P-NETs patients received 5-fluorouracil/streptozocin with bevacizumab. Differences in the EORTC QLQ-C30 global health score between baseline, 3-mo, 6-mo and 12-mo follow-up assessments were not significant[40,41]. The NET01 trial suggested that the addition of cisplatin to the combined capecitabine and streptozocin regimen worsened HRQoL[42]. After three cycles, the mean global health score was 67.0 *vs* 62.2 ($P = 0.5$) in the capecitabine and streptozocin arm and 69.3 *vs* 52.2 ($P = 0.052$) in the capecitabine and streptozocin plus cisplatin arm. After 6 cycles, mean global health score remained virtually unchanged in the capecitabine and streptozocin arm from 66.7 *vs* 68.9 ($P = 0.75$) and 59.8 *vs* 56.0 ($P = 0.68$) in the capecitabine and streptozocin plus cisplatin arm. All three studies were based on small HRQoL sample sizes (less than 100).

Of the remaining treatments identified within the scope of this study, the HRQoL was improved or remained the same in all GEP-NET patients treated with MIBG therapy. Three studies used more than one treatment in the populations studied without breaking down HRQoL results into treatment categories[26,37,38]. Using HADS, Larsson *et al*[25] noted a lower anxiety rating at 12 mo ($P < 0.05$) following treatment with interferon, somatostatin analogue or a combination of both, whilst the depression score was significantly higher at 9 mo ($P < 0.01$) when compared to baseline. The study by Fröjd *et al*[37] suggested a slight increase in HADS anxiety over time (timepoints unspecified) in a longitudinal study of octreotide and/or interferon or chemotherapy or no treatment, but sample size was small and significance was not reported. Finally, telotristat ethyl therapy was not shown to be associated with any measurable short-term HRQoL benefits when assessed using the EORTC QLQ-30 measure, beyond diarrhoea[44].

DISCUSSION

Given the indolent nature and slow progression of disease in most GEP-NET patients, assessment of HRQoL is vital for monitoring impact of treatment. The lack of conclusive data on outcomes in GEP-NETs can be attributed, in part, to the small sample size of clinical trials involving GEP-NETs that makes it difficult to capture clinically meaningful changes or a significant benefit in terms of HRQoL[6]. Moreover, the work by Martini *et al*[18] showed that a transfer of HRQoL results into clinical practice is hindered by the scarcity of robust studies and the quality of HRQoL assessment[18]. To our knowledge, our study is the first to report a systematic review investigating the impact of treatments on the HRQoL of GEP-NET patients and the development status of instruments used in terms of validation and minimal important difference.

Martini *et al*[18] performed a systematic review examining methodological robustness of HRQoL studies of patients with GEP-NETs. They concluded that heterogeneity and limited methodological quality of considered studies did not permit them to draw conclusions regarding the impact of HRQoL in clinical practice. In agreement, our review confirmed heterogeneity of studies and patient characteristics, including variety in intervention or comparator treatment, disease severity and location of primary tumour, age, gender and other symptoms or comorbidities. Sample size for studies considered eligible for inclusion ranged from 17 to 253 patients, with a median of 57, highlighting the usual small number of study participants. A similar median value of 51 (range 9–663 patients) was reported by Martini *et al*[18]. Further, where comparator groups were used, HRQoL scores were sometimes reported for the entire study population and not for the respective treatment groups in the study[29,33,40,41,44]. Due to the wide range of comparators identified and the significant heterogeneity across the studies included in this review, which would violate the assumptions of meta-analysis, HRQoL related to various GEP-NET treatments was assessed in a qualitative manner rather than quantitative (*e.g.* meta-analysis).

In line with Martini *et al*[18], we identified the well-validated EORTC QLQ-C30 as the most commonly used HRQoL instrument in GEP-NET patients. The EORTC instrument has been used in 30 out of 43 published studies; however, validation and definition of minimal important difference have not been reported to date specifically for GEP-NET patients. The EORTC QLQ-GINET21 module (n = 6) and the SF-12/36 tools (n = 5) have occasionally been used, with other instruments used in two or less publications.

Where change in the EORTC QLQ-C30 global health score could be calculated from baseline scores (Table 2), six studies demonstrated a trend towards an improved score, three showed a decline, with the remaining studies presenting mixed or inconsistent responses depending on intervention and/or follow-up time point. However, results should be interpreted with caution for the reasons given above. The mixed HRQoL trends are comparable to those reported by Jimenez-Fonseca *et al*[63], who highlighted the existing evidence for improved treatment efficacy, safety or toxicity for a range of therapies, including somatostatin analogues, sunitinib and everolimus, but with mixed HRQoL response. Jimenez-Fonseca *et al*[63] suggested the generic EORTC QLQ-C30 has not been developed specifically for GEP-NET patients and, therefore, may lack the sensitivity to detect subtle HRQoL changes in association with disease items that are relevant to GEP-NET patients.

Given the potentially long treatment duration in GEP-NET patients, one challenge of HRQoL analysis is taking the potential occurrence of a response shift into consideration. This can occur as self-assessment of HRQoL is inherently subjective; patients can adapt to their disease and the treatment toxicities resulting in changing standards of HRQoL over time[51]. Thus, the choice of the reference score to qualify a change such as deterioration is a major concern. With this in mind, it is difficult to determine the change in HRQoL over time in most studies identified in this systematic review. One approach that deals with response shift effect as a concept is evaluation of TTD, making use of minimal important difference as a criterion for signalling deterioration. In the Phase III trial NETTER-1, it was shown that adjusting for significant covariates (HRQoL baseline values, OctreoScan maximum tumour uptake score, and/or age), the impact of treatment remained statistically significant for global health score, physical functioning, diarrhoea, and body image domains[17]. Osoba *et al*[52] rated patients' perceived change in EORTC QLQ-C30 in breast cancer or small-cell lung cancer patients, concluding a "moderate" change equated to a 10–20 change in mean scores. Use of a minimal important difference of at least 10 points as a criterion for deterioration yielded TTD curves with a time course similar to that of the curves for centrally reviewed radiological progression[17]. It should be noted, however,

that the "minimal important difference" was not defined specifically for patients with midgut NETs participating in the NETTER-1 study. Moreover, the TTD and TUDD criterion of a drop in ≥ 10 points in a domain score was used to show more than half of the EORTC QLQ-30 domains improved for patients treated with ^{177}Lu-DOTATATE compared to a control arm; the same TUDD criterion was also applied by Rinke *et al*[16], who showed long-acting octreotide significantly extended TUDD for fatigue, pain and insomnia HRQoL domains compared to a placebo.

Treatment of GEP-NETs with ^{177}Lu-DOTATATE consistently improved global health score compared to baseline[58,61,62] and increased TTD. The Phase III NETTER-1 study provides the best information available regarding HRQoL in patients with advanced progressive GEP-NETs not only in terms of benefit but also in terms of TTD[17]. However, the minimal important difference (and clinically meaningful thresholds) for improvement/worsening has not been defined yet for the EORTC QLQ-C30 specifically in GEP-NET patients, although it has for a number of other common cancers[64,65]. It is conceivable that the abbreviated version of the EORTC QLQ-C30 (possibly combined with GINET21 and computer adaptive testing) can be developed especially for use in clinical practice. Thus, there is scope for further research in this area and exploration of HRQoL as a potential tool for monitoring disease progression. Longitudinal studies with a long-term follow-up and involving clinical practice patients may provide further insight into the potential role of HRQoL in patient monitoring and management.

In conclusion, study and patient heterogeneity, small sample sizes and limited methodological quality in terms of assessing HRQoL has impaired definitive statements being made regarding the impact of the various treatment options for GEP-NETs in terms of HRQoL[66-69]. A number of randomised trials demonstrated only small or no HRQoL changes between active treatment and placebo arms. The Phase III NETTER-1 is the only study to have shown more significant and robust differences between active and placebo groups. It demonstrated that PRRT can delay the time to worsening of HRQoL in GEP-NET patients. However, validation of QLQ-C30 and GINET21 specifically for GI-NET and P-NET patients, and definition of minimal important difference and clinical thresholds, are still lacking for these patients. As such, further research is necessary in order to offer a benchmark for interpreting the clinical importance of differences in HRQoL domain scores between groups or changes in these scores over time in conjunction with different treatment modalities.

ARTICLE HIGHLIGHTS

Research background

Gastroenteropancreatic neuroendocrine tumours (GEP-NETs) are slow-growing cancers that arise from diffuse endocrine cells in the gastrointestinal tract (GI-NETs) and pancreas (P-NETs). The majority of patients who are diagnosed with GEP-NETs have metastatic disease. Despite this, systemic therapies provide a 5-year survival rate of about 75% for patients with GI-NETs and > 60% for patients with P-NETs.

Research motivation

Health related quality of life (HRQoL) is an increasingly important concept, reflecting the patients' perspective in conjunction with the disease presentation, severity, and treatment. Although not curative, long-term therapeutic options are available for patients with GEP-NETs to provide symptomatic relief, and these can even slow down and stabilise disease for multiple years. Since patients can live many years by managing their disease in this way, understanding the impact of treatment on GEP-NETs patients' HRQoL is paramount especially given the indolent course the disease may take in patients.

Research objectives

The aim of this study was to perform a systematic review to assess the HRQoL of patients with inoperable metastatic GEP-NETs undergoing various treatments in order to uncover areas for future research. This systematic literature review is a response to the increased importanceof assessing HRQoL with validated patient-reported outcome instruments for which the minimal important difference has been defined.

Research methods

The systematic review performed here adhered to the established international

guidelines for conducting systematic reviews. A search strategy was developed and refined to recover relevant publications reporting HRQoL data for adult patients with GEP-NETs. Data were extracted from every record returned by the literature search that met the inclusion criteria of the study.

Research results

A total of 42 studies met the inclusion criteria of the study. The EORTC QLQ-C30 and gastrointestinal GI-NET module (QLQ-GI.NET21) were the most used HRQoL instruments, exhibiting a range of outcomes compared to baseline for the specific interventions.

The worst HRQoL observed at baseline were related to the following symptoms: Nausea and vomiting (4.1–20.0), insomnia (11.0–38.6), appetite loss (9.2–27.8), constipation (0–24.4) and financial difficulties (6.0–23.6). Diarrhoea demonstrated a wide range of mean values (16.7–78.3), which can be attributed to the heterogeneity of involved GEP-NET patients.

The average value for the baseline global health score had a range of 56–70. Where change in the EORTC QLQ-C30 global health score could be calculated from baseline scores, five studies demonstrated a significant trend towards an improved score. Treatment of GEP-NETs with ^{177}Lu-DOTATATE consistently improved global health score compared to baseline and increased time-to-deterioration, *i.e.* time until HRQoL worsens by at least 10 points for each domain (*e.g.* global health, physical functioning). The Phase III NETTER-1 study resulted in time-to-deterioration curves consistent with the curves for progression free survival for ^{177}Lu-DOTATATE. However, the EORTC QLQ-C30 and QLQ-GINET21 have not been validated, and the minimal important differences have not yet been defined, specifically for GI-NET and P-NET patients.

Research conclusions

Study and patient heterogeneity, small sample sizes and limited methodological quality in terms of assessing HRQoL has impaired definitive statements being made regarding the impact of the various treatment options for GEP-NETs in terms of HRQoL. A notable finding was that PRRT can delay the time to worsening of HRQoL in GEP-NET patients. However, validation of EORTC QLQ-C30 and GINET21 specifically for GI-NET and P-NET patients and the definitions of minimal important difference and clinical thresholds are still lacking for these patients. As such, further research is necessary in order to offer a benchmark for interpreting the clinical importance of differences in HRQoL domain scores between treatment groups or changes in these scores over time in conjunction with different treatment modalities.

Research perspectives

Further research is necessary in order to offer a benchmark for interpreting the clinical importance of differences in HRQoL domain scores over time and between treatment groups.

ACKNOWLEDGEMENTS

We would like to acknowledge Dr Persefoni Ioannou for providing editorial support and guiding the research from the outset of this project.

REFERENCES

1 **Genus TSE**, Bouvier C, Wong KF, Srirajaskanthan R, Rous BA, Talbot DC, Valle JW, Khan M, Pearce N, Elshafie M, Reed NS, Morgan E, Deas A, White C, Huws D, Ramage J. Impact of neuroendocrine morphology on cancer outcomes and stage at diagnosis: a UK nationwide cohort study 2013-2015. *Br J Cancer* 2019; **121**: 966-972 [PMID: 31649320 DOI: 10.1038/s41416-019-0606-3]

2 **Öberg K**, Knigge U, Kwekkeboom D, Perren A; ESMO Guidelines Working Group. Neuroendocrine gastro-entero-pancreatic tumors: ESMO Clinical Practice Guidelines for diagnosis, treatment and follow-up. *Ann Oncol* 2012; **23** Suppl 7: vii124-vii130 [PMID: 22997445 DOI: 10.1093/annonc/mds295]

3 **Lewis AR**, Wang X, Magdalani L, D'Arienzo P, Bashir C, Mansoor W, Hubner R, Valle JW, McNamara MG. Health-related quality of life, anxiety, depression and impulsivity in patients with advanced gastroenteropancreatic neuroendocrine tumours. *World J Gastroenterol* 2018; **24**: 671-679 [PMID: 29456406 DOI: 10.3748/wjg.v24.i6.671]

4 **Wilander E**, Lundqvist M, Oberg K. Gastrointestinal carcinoid tumours. Histogenetic, histochemical, immunohistochemical, clinical and therapeutic aspects. *Prog Histochem Cytochem* 1989; **19**: 1-88 [PMID: 2662260 DOI:

10.1016/S0079-6336(89)80012-9]
5 **Ahlman H**, Wängberg B, Jansson S, Stenqvist O, Geterud K, Tylén U, Caidahl K, Scherstén T, Tisell LE. Management of disseminated midgut carcinoid tumours. *Digestion* 1991; **49**: 78-96 [PMID: 1724766 DOI: 10.1159/000200707]
6 **Gelhorn HL**, Kulke MH, O'Dorisio T, Yang QM, Jackson J, Jackson S, Boehm KA, Law L, Kostelec J, Auguste P, Lapuerta P. Patient-reported Symptom Experiences in Patients With Carcinoid Syndrome After Participation in a Study of Telotristat Etiprate: A Qualitative Interview Approach. *Clin Ther* 2016; **38**: 759-768 [PMID: 27041406 DOI: 10.1016/j.clinthera.2016.03.002]
7 **Jacobsen MB**, Hanssen LE. Clinical effects of octreotide compared to placebo in patients with gastrointestinal neuroendocrine tumours. Report on a double-blind, randomized trial. *J Intern Med* 1995; **237**: 269-275 [PMID: 7534331 DOI: 10.1111/j.1365-2796.1995.tb01175.x]
8 **Ballal S**, Yadav MP, Bal C, Sahoo RK, Tripathi M. Broadening horizons with ^{225}Ac-DOTATATE targeted alpha therapy for gastroenteropancreatic neuroendocrine tumour patients stable or refractory to ^{177}Lu-DOTATATE PRRT: first clinical experience on the efficacy and safety. *Eur J Nucl Med Mol Imaging* 2020; **47**: 934-946 [PMID: 31707430 DOI: 10.1007/s00259-019-04567-2]
9 **Haugland T**, Wahl AK, Hofoss D, DeVon HA. Association between general self-efficacy, social support, cancer-related stress and physical health-related quality of life: a path model study in patients with neuroendocrine tumors. *Health Qual Life Outcomes* 2016; **14**: 11 [PMID: 26787226 DOI: 10.1186/s12955-016-0413-y]
10 **Uri I**, Grozinsky-Glasberg S. Current treatment strategies for patients with advanced gastroenteropancreatic neuroendocrine tumors (GEP-NETs). *Clin Diabetes Endocrinol* 2018; **4**: 16 [PMID: 30009041 DOI: 10.1186/s40842-018-0066-3]
11 **Kane A**, Thorpe MP, Morse MA, Howard BA, Oldan JD, Zhu J, Wong TZ, Petry NA, Reiman R Jr, Borges-Neto S. Predictors of Survival in 211 Patients with Stage IV Pulmonary and Gastroenteropancreatic MIBG-Positive Neuroendocrine Tumors Treated with ^{131}I-MIBG. *J Nucl Med* 2018; **59**: 1708-1713 [PMID: 29777005 DOI: 10.2967/jnumed.117.202150]
12 **Strosberg J**, Gardner N, Kvols L. Survival and prognostic factor analysis of 146 metastatic neuroendocrine tumors of the mid-gut. *Neuroendocrinology* 2009; **89**: 471-476 [PMID: 19174605 DOI: 10.1159/000197899]
13 **Brundage M**, Blazeby J, Revicki D, Bass B, de Vet H, Duffy H, Efficace F, King M, Lam CL, Moher D, Scott J, Sloan J, Snyder C, Yount S, Calvert M. Patient-reported outcomes in randomized clinical trials: development of ISOQOL reporting standards. *Qual Life Res* 2013; **22**: 1161-1175 [PMID: 22987144 DOI: 10.1007/s11136-012-0252-1]
14 **Efficace F**, Rees J, Fayers P, Pusic A, Taphoorn M, Greimel E, Reijneveld J, Whale K, Blazeby J; European Organization for Research and Treatment of Cancer (EORTC) Quality of Life Group. Overcoming barriers to the implementation of patient-reported outcomes in cancer clinical trials: the PROMOTION Registry. *Health Qual Life Outcomes* 2014; **12**: 86 [PMID: 24902767 DOI: 10.1186/1477-7525-12-86]
15 **Reeve BB**, Mitchell SA, Dueck AC, Basch E, Cella D, Reilly CM, Minasian LM, Denicoff AM, O'Mara AM, Fisch MJ, Chauhan C, Aaronson NK, Coens C, Bruner DW. Recommended patient-reported core set of symptoms to measure in adult cancer treatment trials. *J Natl Cancer Inst* 2014; 106 [PMID: 25006191 DOI: 10.1093/jnci/dju129]
16 **Rinke A**, Neary MP, Eriksson J, Hunger M, Doan T, Karli D, Arnold R. Health-Related Quality of Life for Long-Acting Octreotide versus Placebo in Patients with Metastatic Midgut Neuroendocrine Tumors in the Phase 3 PROMID Trial. *Neuroendocrinology* 2019; **109**: 141-151 [PMID: 30852564 DOI: 10.1159/000499469]
17 **Strosberg J**, Wolin E, Chasen B, Kulke M, Bushnell D, Caplin M, Baum RP, Kunz P, Hobday T, Hendifar A, Oberg K, Sierra ML, Thevenet T, Margalet I, Ruszniewski P, Krenning E; NETTER-1 Study Group. Health-Related Quality of Life in Patients With Progressive Midgut Neuroendocrine Tumors Treated With ^{177}Lu-Dotatate in the Phase III NETTER-1 Trial. *J Clin Oncol* 2018; **36**: 2578-2584 [PMID: 29878866 DOI: 10.1200/JCO.2018.78.5865]
18 **Martini C**, Gamper EM, Wintner L, Nilica B, Sperner-Unterweger B, Holzner B, Virgolini I. Systematic review reveals lack of quality in reporting health-related quality of life in patients with gastroenteropancreatic neuroendocrine tumours. *Health Qual Life Outcomes* 2016; **14**: 127 [PMID: 27614762 DOI: 10.1186/s12955-016-0527-2]
19 **United States Food and Drug Administration**. Value and use of patient-reported outcomes (PROs) in assessing effects of medical devices. CDRH strategic priorities 2016-2017
20 **European Medicines Agency**. Integrating patients' views in clinical studies of anticancer medicines 2016. Available from: https://www.ema.europa.eu/en/news/integrating-patients-views-clinical-studies-anticancer-medicines
21 **Liberati A**, Altman DG, Tetzlaff J, Mulrow C, Gøtzsche PC, Ioannidis JP, Clarke M, Devereaux PJ, Kleijnen J, Moher D. The PRISMA statement for reporting systematic reviews and meta-analyses of studies that evaluate healthcare interventions: explanation and elaboration. *BMJ* 2009; **339**: b2700 [PMID: 19622552 DOI: 10.1136/bmj.b2700]
22 **Higgins JP**, Thomas J, Chandler J, Cumpston M, Li T, Page MJ, Welch VA. Cochrane handbook for systematic reviews of interventions. 2nd Edition. Chichester (UK): John Wiley and Sons, 2019. Available from: https://training.cochrane.org/handbook
23 **Papaioannou D**, Brazier J, Paisley S. NICE DSU Technical Support Document 9: The Identification, Review and Synthesis of Health State Utility Values from the Literature [Internet]. London: National Institute for Health and Care Excellence (NICE) 2010. Available from: https://www.ncbi.nlm.nih.gov/books/NBK425822/?term=collection-id_nicedsutsd%5BAttribute%5D
24 **Brazier J**, Ara R, Azzabi I, Busschbach J, Chevrou-Séverac H, Crawford B, Cruz L, Karnon J, Lloyd A, Paisley S, Pickard AS. Identification, Review, and Use of Health State Utilities in Cost-Effectiveness Models: An ISPOR Good Practices for Outcomes Research Task Force Report. *Value Health* 2019; **22**: 267-275 [PMID: 30832964 DOI: 10.1016/j.jval.2019.01.004]
25 **Larsson G**, Sjödén PO, Oberg K, Eriksson B, von Essen L. Health-related quality of life, anxiety and

depression in patients with midgut carcinoid tumours. *Acta Oncol* 2001; **40**: 825-831 [PMID: 11859981 DOI: 10.1080/02841860152703445]

26 **Larsson G**, Sjödén PO, Oberg K, von Essen L. Importance-satisfaction discrepancies are associated with health-related quality of life in five-year survivors of endocrine gastrointestinal tumours. *Ann Oncol* 1999; **10**: 1321-1327 [PMID: 10631460 DOI: 10.1023/a:1008360718646]

27 **Rinke A**, Müller HH, Schade-Brittinger C, Klose KJ, Barth P, Wied M, Mayer C, Aminossadati B, Pape UF, Bläker M, Harder J, Arnold C, Gress T, Arnold R; PROMID Study Group. Placebo-controlled, double-blind, prospective, randomized study on the effect of octreotide LAR in the control of tumor growth in patients with metastatic neuroendocrine midgut tumors: a report from the PROMID Study Group. *J Clin Oncol* 2009; **27**: 4656-4663 [PMID: 19704057 DOI: 10.1200/JCO.2009.22.8510]

28 **Meng Y**, McCarthy G, Berthon A, Dinet J. Patient-reported health state utilities in metastatic gastroenteropancreatic neuroendocrine tumours - an analysis based on the CLARINET study. *Health Qual Life Outcomes* 2017; **15**: 131 [PMID: 28662673 DOI: 10.1186/s12955-017-0711-z]

29 **Kvols LK**, Oberg KE, O'Dorisio TM, Mohideen P, de Herder WW, Arnold R, Hu K, Zhang Y, Hughes G, Anthony L, Wiedenmann B. Pasireotide (SOM230) shows efficacy and tolerability in the treatment of patients with advanced neuroendocrine tumors refractory or resistant to octreotide LAR: results from a phase II study. *Endocr Relat Cancer* 2012; **19**: 657-666 [PMID: 22807497 DOI: 10.1530/ERC-11-0367]

30 **Korse CM**, Bonfrer JM, Aaronson NK, Hart AA, Taal BG. Chromogranin A as an alternative to 5-hydroxyindoleacetic acid in the evaluation of symptoms during treatment of patients with neuroendocrine Tumors. *Neuroendocrinology* 2009; **89**: 296-301 [PMID: 18840995 DOI: 10.1159/000162876]

31 **Arnold R**, Rinke A, Klose KJ, Müller HH, Wied M, Zamzow K, Schmidt C, Schade-Brittinger C, Barth P, Moll R, Koller M, Unterhalt M, Hiddemann W, Schmidt-Lauber M, Pavel M, Arnold CN. Octreotide versus octreotide plus interferon-alpha in endocrine gastroenteropancreatic tumors: a randomized trial. *Clin Gastroenterol Hepatol* 2005; **3**: 761-771 [PMID: 16234004 DOI: 10.1016/s1542-3565(05)00481-7]

32 **O'Toole D**, Ducreux M, Bommelaer G, Wemeau JL, Bouché O, Catus F, Blumberg J, Ruszniewski P. Treatment of carcinoid syndrome: a prospective crossover evaluation of lanreotide versus octreotide in terms of efficacy, patient acceptability, and tolerance. *Cancer* 2000; **88**: 770-776 [PMID: 10679645 DOI: 10.1002/(sici)1097-0142(20000215)88:4<770::aid-cncr6>3.0.co;2-0]

33 **Yadegarfar G**, Friend L, Jones L, Plum LM, Ardill J, Taal B, Larsson G, Jeziorski K, Kwekkeboom D, Ramage JK; EORTC Quality of Life Group. Validation of the EORTC QLQ-GINET21 questionnaire for assessing quality of life of patients with gastrointestinal neuroendocrine tumours. *Br J Cancer* 2013; **108**: 301-310 [PMID: 23322194 DOI: 10.1038/bjc.2012.560]

34 **Raymond E**, Dahan L, Raoul JL, Bang YJ, Borbath I, Lombard-Bohas C, Valle J, Metrakos P, Smith D, Vinik A, Chen JS, Hörsch D, Hammel P, Wiedenmann B, Van Cutsem E, Patyna S, Lu DR, Blanckmeister C, Chao R, Ruszniewski P. Sunitinib malate for the treatment of pancreatic neuroendocrine tumors. *N Engl J Med* 2011; **364**: 501-513 [PMID: 21306237 DOI: 10.1056/NEJMoa1003825]

35 **Vinik A**, Bottomley A, Korytowsky B, Bang YJ, Raoul JL, Valle JW, Metrakos P, Hörsch D, Mundayat R, Reisman A, Wang Z, Chao RC, Raymond E. Patient-Reported Outcomes and Quality of Life with Sunitinib Versus Placebo for Pancreatic Neuroendocrine Tumors: Results From an International Phase III Trial. *Target Oncol* 2016; **11**: 815-824 [PMID: 27924459 DOI: 10.1007/s11523-016-0462-5]

36 **Casciano R**, Chulikavit M, Perrin A, Liu Z, Wang X, Garrison LP. Cost-effectiveness of everolimus vs sunitinib in treating patients with advanced, progressive pancreatic neuroendocrine tumors in the United States. *J Med Econ* 2012; **15** Suppl 1: 55-64 [PMID: 22881362 DOI: 10.3111/13696998.2012.720319]

37 **Fröjd C**, Larsson G, Lampic C, von Essen L. Health related quality of life and psychosocial function among patients with carcinoid tumours. A longitudinal, prospective, and comparative study. *Health Qual Life Outcomes* 2007; **5**: 18 [PMID: 17428340 DOI: 10.1186/1477-7525-5-18]

38 **Larsson G**, von Essen L, Sjödén PO. Health-related quality of life in patients with endocrine tumours of the gastrointestinal tract. *Acta Oncol* 1999; **38**: 481-490 [PMID: 10418716 DOI: 10.1080/028418699432022]

39 **Ramage J**, Yadegarfar G, Friend L, Jones L, Plum L, Ardill J, Taal B, Larsson G, Jesiorski K. Clinical and psychometric validation of the disease-specific questionnaire module (EORTC qlqgiNET21) in assessing quality of life of patients with neuroendocrine tumors. 9th Annual ENETS Conference (2012). Available from: https://www.enets.org/clinical-and-psychometric-validation-of-the-disease-specific-questionnaire-module-eortc-qlq-ginet21-in-assessing-quality-of-life-of-patients-with-neuroendocrine-tumors.html

40 **Mitry E**, Walter T, Baudin E, Kurtz JE, Ruszniewski P, Dominguez-Tinajero S, Bengrine-Lefevre L, Cadiot G, Dromain C, Farace F, Rougier P, Ducreux M. Bevacizumab plus capecitabine in patients with progressive advanced well-differentiated neuroendocrine tumors of the gastro-intestinal (GI-NETs) tract (BETTER trial)--a phase II non-randomised trial. *Eur J Cancer* 2014; **50**: 3107-3115 [PMID: 25454413 DOI: 10.1016/j.ejca.2014.10.001]

41 **Ducreux M**, Dahan L, Smith D, O'Toole D, Lepère C, Dromain C, Vilgrain V, Baudin E, Lombard-Bohas C, Scoazec JY, Seitz JF, Bitoun L, Koné S, Mitry E. Bevacizumab combined with 5-FU/streptozocin in patients with progressive metastatic well-differentiated pancreatic endocrine tumours (BETTER trial)--a phase II non-randomised trial. *Eur J Cancer* 2014; **50**: 3098-3106 [PMID: 25454412 DOI: 10.1016/j.ejca.2014.10.002]

42 **Meyer T**, Qian W, Caplin ME, Armstrong G, Lao-Sirieix SH, Hardy R, Valle JW, Talbot DC, Cunningham D, Reed N, Shaw A, Navalkissoor S, Luong TV, Corrie PG. Capecitabine and streptozocin ± cisplatin in advanced gastroenteropancreatic neuroendocrine tumours. *Eur J Cancer* 2014; **50**: 902-911 [PMID: 24445147 DOI: 10.1016/j.ejca.2013.12.011]

43 **Pasieka JL**, McEwan AJ, Rorstad O. The palliative role of 131I-MIBG and 111In-octreotide therapy in patients with metastatic progressive neuroendocrine neoplasms. *Surgery* 2004; **136**: 1218-1226 [PMID: 15657579 DOI: 10.1016/j.surg.2004.06.050]

44 **Cella D**, Beaumont JL, Hudgens S, Marteau F, Feuilly M, Houchard A, Lapuerta P, Ramage J, Pavel M, Hörsch D, Kulke MH. Relationship Between Symptoms and Health-related Quality-of-life Benefits in Patients With Carcinoid Syndrome: Post Hoc Analyses From TELESTAR. *Clin Ther* 2018; **40**: 2006-2020.e2 [PMID: 30477789 DOI:

10.1016/j.clinthera.2018.10.008]
45 **Zigmond AS**, Snaith RP. The hospital anxiety and depression scale. *Acta Psychiatr Scand* 1983; **67**: 361-370 [PMID: 6880820 DOI: 10.1111/j.1600-0447.1983.tb09716.x]
46 **Karppinen N**, Lindén R, Sintonen H, Tarkkanen M, Roine R, Heiskanen I, Matikainen N, Schalin-Jäntti C. Health-Related Quality of Life in Patients with Small Intestine Neuroendocrine Tumors. *Neuroendocrinology* 2018; **107**: 366-374 [PMID: 30293074 DOI: 10.1159/000494293]
47 **Haugland T**, Vatn MH, Veenstra M, Wahl AK, Natvig GK. Health related quality of life in patients with neuroendocrine tumors compared with the general Norwegian population. *Qual Life Res* 2009; **18**: 719-726 [PMID: 19479341 DOI: 10.1007/s11136-009-9487-x]
48 **Frilling A**, Weber F, Saner F, Bockisch A, Hofmann M, Mueller-Brand J, Broelsch CE. Treatment with (90)Y- and (177)Lu-DOTATOC in patients with metastatic neuroendocrine tumors. *Surgery* 2006; **140**: 968-76; discussion 976-7 [PMID: 17188146 DOI: 10.1016/j.surg.2006.07.030]
49 **Pezzilli R**, Campana D, Morselli-Labate AM, Fabbri MC, Brocchi E, Tomassetti P. Patient-reported outcomes in subjects with neuroendocrine tumors of the pancreas. *World J Gastroenterol* 2009; **15**: 5067-5073 [PMID: 19860000 DOI: 10.3748/wjg.15.5067]
50 **Larsson G**, Janson ET. Anemia in patients with midgut carcinoid, treated with alpha interferon: effects by erythropoietin treatment on the perceived quality of life. *Eur J Cancer Care (Engl)* 2008; **17**: 200-204 [PMID: 18302658 DOI: 10.1111/j.1365-2354.2007.00844.x]
51 **Anota A**, Hamidou Z, Paget-Bailly S, Chibaudel B, Bascoul-Mollevi C, Auquier P, Westeel V, Fiteni F, Borg C, Bonnetain F. Time to health-related quality of life score deterioration as a modality of longitudinal analysis for health-related quality of life studies in oncology: do we need RECIST for quality of life to achieve standardization? *Qual Life Res* 2015; **24**: 5-18 [PMID: 24277234 DOI: 10.1007/s11136-013-0583-6]
52 **Osoba D**, Rodrigues G, Myles J, Zee B, Pater J. Interpreting the significance of changes in health-related quality-of-life scores. *J Clin Oncol* 1998; **16**: 139-144 [PMID: 9440735 DOI: 10.1200/JCO.1998.16.1.139]
53 **Haugland T**, Veenstra M, Vatn MH, Wahl AK. Improvement in Stress, General Self-Efficacy, and Health Related Quality of Life following Patient Education for Patients with Neuroendocrine Tumors: A Pilot Study. *Nurs Res Pract* 2013; **2013**: 695820 [PMID: 23738063 DOI: 10.1155/2013/695820]
54 **Ramage JK**, Punia P, Faluyi O, Frilling A, Meyer T, Saharan R, Valle JW. Observational Study to Assess Quality of Life in Patients with Pancreatic Neuroendocrine Tumors Receiving Treatment with Everolimus: The OBLIQUE Study (UK Phase IV Trial). *Neuroendocrinology* 2019; **108**: 317-327 [PMID: 30699423 DOI: 10.1159/000497330]
55 **Kulke MH**, Lenz HJ, Meropol NJ, Posey J, Ryan DP, Picus J, Bergsland E, Stuart K, Tye L, Huang X, Li JZ, Baum CM, Fuchs CS. Activity of sunitinib in patients with advanced neuroendocrine tumors. *J Clin Oncol* 2008; **26**: 3403-3410 [PMID: 18612155 DOI: 10.1200/JCO.2007.15.9020]
56 **Pavel M**, Unger N, Borbath I, Ricci S, Hwang TL, Brechenmacher T, Park J, Herbst F, Beaumont JL, Bechter O. Safety and QOL in Patients with Advanced NET in a Phase 3b Expanded Access Study of Everolimus. *Target Oncol* 2016; **11**: 667-675 [PMID: 27193465 DOI: 10.1007/s11523-016-0440-y]
57 **Wymenga AN**, Eriksson B, Salmela PI, Jacobsen MB, Van Cutsem EJ, Fiasse RH, Välimäki MJ, Renstrup J, de Vries EG, Oberg KE. Efficacy and safety of prolonged-release lanreotide in patients with gastrointestinal neuroendocrine tumors and hormone-related symptoms. *J Clin Oncol* 1999; **17**: 1111 [PMID: 10561168 DOI: 10.1200/JCO.1999.17.4.1111]
58 **Zandee WT**, Brabander T, Blazevic A, Kam BLR, Teunissen JJM, Feelders RA, Hofland J, De Herder WW. Symptomatic and radiological response to 177Lu-DOTATATE for the treatment of functioning pancreatic neuroendocrine tumors. *J Clin Endocrinol Metab* 2019; **104**: 1336-1344 [[DOI: 10.1210/jc.2018-01991]
59 **Martini C**, Buxbaum S, Rodrigues M, Nilica B, Scarpa L, Holzner B, Virgolini I, Gamper EM. Quality of Life in Patients with Metastatic Gastroenteropancreatic Neuroendocrine Tumors Receiving Peptide Receptor Radionuclide Therapy: Information from a Monitoring Program in Clinical Routine. *J Nucl Med* 2018; **59**: 1566-1573 [PMID: 30042164 DOI: 10.2967/jnumed.117.204834]
60 **Kwekkeboom DJ**, Bakker WH, Kam BL, Teunissen JJ, Kooij PP, de Herder WW, Feelders RA, van Eijck CH, de Jong M, Srinivasan A, Erion JL, Krenning EP. Treatment of patients with gastro-entero-pancreatic (GEP) tumours with the novel radiolabelled somatostatin analogue [177Lu-DOTA(0),Tyr3]octreotate. *Eur J Nucl Med Mol Imaging* 2003; **30**: 417-422 [PMID: 12634971 DOI: 10.1007/s00259-002-1050-8]
61 **Marinova M**, Mücke M, Fischer F, Essler M, Cuhls H, Radbruch L, Ghaei S, Conrad R, Ahmadzadehfar H. Quality of life in patients with midgut NET following peptide receptor radionuclide therapy. *Eur J Nucl Med Mol Imaging* 2019; **46**: 2252-2259 [PMID: 31338547 DOI: 10.1007/s00259-019-04431-3]
62 **Teunissen JJ**, Kwekkeboom DJ, Krenning EP. Quality of life in patients with gastroenteropancreatic tumors treated with [177Lu-DOTA0,Tyr3]octreotate. *J Clin Oncol* 2004; **22**: 2724-2729 [PMID: 15226340 DOI: 10.1200/JCO.2004.10.016]
63 **Jiménez-Fonseca P**, Carmona-Bayonas A, Martín-Pérez E, Crespo G, Serrano R, Llanos M, Villabona C, García-Carbonero R, Aller J, Capdevila J, Grande E; Spanish Neuroendocrine Tumor Group (GETNE). Health-related quality of life in well-differentiated metastatic gastroenteropancreatic neuroendocrine tumors. *Cancer Metastasis Rev* 2015; **34**: 381-400 [PMID: 26245646 DOI: 10.1007/s10555-015-9573-1]
64 **Giesinger JM**, Loth FLC, Aaronson NK, Arraras JI, Caocci G, Efficace F, Groenvold M, van Leeuwen M, Petersen MA, Ramage J, Tomaszewski KA, Young T, Holzner B; EORTC Quality of Life Group. Thresholds for clinical importance were established to improve interpretation of the EORTC QLQ-C30 in clinical practice and research. *J Clin Epidemiol* 2020; **118**: 1-8 [PMID: 31639445 DOI: 10.1016/j.jclinepi.2019.10.003]
65 **Cocks K**, King MT, Velikova G, de Castro G Jr, Martyn St-James M, Fayers PM, Brown JM. Evidence-based guidelines for interpreting change scores for the European Organisation for the Research and Treatment of Cancer Quality of Life Questionnaire Core 30. *Eur J Cancer* 2012; **48**: 1713-1721 [PMID: 22418017 DOI: 10.1016/j.ejca.2012.02.059]
66 **Delpassand ES**, Samarghandi A, Zamanian S, Wolin EM, Hamiditabar M, Espenan GD, Erion JL,

O'Dorisio TM, Kvols LK, Simon J, Wolfangel R, Camp A, Krenning EP, Mojtahedi A. Peptide receptor radionuclide therapy with 177Lu-DOTATATE for patients with somatostatin receptor-expressing neuroendocrine tumors: the first US phase 2 experience. *Pancreas* 2014; **43**: 518-525 [PMID: 24632546 DOI: 10.1097/MPA.0000000000000113]

67 **van der Horst-Schrivers AN**, van Ieperen E, Wymenga AN, Boezen HM, Weijmar-Schultz WC, Kema IP, Meijer WG, de Herder WW, Willemse PH, Links TP, de Vries EG. Sexual function in patients with metastatic midgut carcinoid tumours. *Neuroendocrinology* 2009; **89**: 231-236 [PMID: 19033719 DOI: 10.1159/000178754]

68 **Davies AH**, Larsson G, Ardill J, Friend E, Jones L, Falconi M, Bettini R, Koller M, Sezer O, Fleissner C, Taal B, Blazeby JM, Ramage JK; EORTC Quality of Life Group. Development of a disease-specific Quality of Life questionnaire module for patients with gastrointestinal neuroendocrine tumours. *Eur J Cancer* 2006; **42**: 477-484 [PMID: 16412628 DOI: 10.1016/j.ejca.2005.10.025]

69 **Larsson G**, von Essen L, Sjödén PO. Quality of life in patients with endocrine tumors of the gastrointestinal tract: patient and staff perceptions. *Cancer Nurs* 1998; **21**: 411-420 [PMID: 9848999 DOI: 10.1097/00002820-199812000-00005]

Published by **Baishideng Publishing Group Inc**
7041 Koll Center Parkway, Suite 160, Pleasanton, CA 94566, USA
Telephone: +1-925-3991568
E-mail: bpgoffice@wjgnet.com
Help Desk: https://www.f6publishing.com/helpdesk
https://www.wjgnet.com